
Dokuz Eylül University
Faculty of Engineering
Department of Textile Engineering

ITTC 7th | international technical textiles congress

# ITTC 7th | international technical textiles congress

10-12 October 2018 - İzmir

# PROCEEDINGS BOOK

*10 - 12 October 2018*

*İzmir / TURKEY*

ITTC 7th | international technical textiles congress

Dokuz Eylül University
Faculty of Engineering
Department of Textile Engineering

# 7th INTERNATIONAL TECHNICAL TEXTILES CONGRESS

**10-12 October 2018**
**Izmir / TURKEY**

**Editors**
Assoc. Prof. Dr. Tuba ALPYILDIZ
Res. Assist. Gizem Ceylan TÜRKOĞLU

7th International Technical Textiles Congress

10-12 October 2018, İzmir, Turkey

**Cover Design**
Assist. Prof. Dr. Rahşan AKGÜL
Assist. Prof. Dr. Ali Serkan SOYDAN



Publisher: Meta Basım Press

metabasim@gmail.com

Tel: +90 232 3436454

# PREFACE

Technical textiles have attracted more and more attention in recent years. These high-performance materials are widely used in civil engineering, electrical engineering and electronics, agriculture, medical and automotive industries in addition to protective and military clothing.

Developed countries have focused their strategy on technical textiles to carry forward their competitive advantage and to control technical textiles market and consequently have held the global technical textiles market.

7th International Technical Textiles Congress is held in Izmir on 10-12 October 2018, where it started with 1st International Technical Textiles Congress in 2002. The congress targets to gather all the players of the industry; the experts and the researchers with the manufacturers, the consumers and the investors from Turkey and abroad. 7th International Technical Textiles Congress provides the possibility to share the industrial experiences and scientific investigations, which have very important contributions to the development of the sector.

We would like to thank to all sponsor companies, to all authors and participants for their supports. We hope that this international event will also generate an occasion to create new opportunities.

We are happy to welcome you.

Organizing Committee

# ORGANIZING COMMITTEE

- Prof. Dr. Merih SARIIŞIK
- Assoc. Prof. Dr. Tuba ALPYILDIZ
- Res. Assist. Gizem Ceylan TÜRKOĞLU
- Res. Assist. Gülşah Ekin KARTAL

# ADVISORY BOARD

# SCIENTIFIC COMMITTEE

# CONTRIBUTORS OF THE CONGRESS

- Aegean Exporters' Union / Ege İhracatçı Birlikleri
- Aygenteks Dış Ticaret ve Tekstil Sanayi Ltd. Şti.
- AzoLab Laboratuvar Hizmetleri A.Ş.
- Baldwin Technology GmbH
- Can Tekstil Entegre Tesisleri ve Tarım Ürünleri Sanayi Ticaret A.Ş
- Çalık Denim Tekstil San.ve Tic.A.Ş.
- Ekoteks Laboratuvar Gözetim Hizmetleri Ltd. Şti.
- Filidea Tekstil Sanayi ve Tic.A.Ş.
- Gamateks Tekstil San. ve Tic. A.Ş.
- Kıvanç Kimya San. ve Tic. A.Ş.
- Matesa Tekstil A.Ş.
- Mesdan S.p.A.
- Roteks Tekstil İhracat San.ve Tic.A.Ş.
- Rudolf Duraner Kimyevi Maddeleri San.Tic.A.Ş.
- Sun Tekstil Ar-Ge Merkezi
- Turkey Textile Industry Employers' Association / Türkiye Tekstil Sanayii İşverenleri Sendikası
- Turkey Textile Finishing Industrialist' Association / Türkiye Tekstil Terbiye Sanayicileri Derneği
- Uğurlular Tekstil San ve Tic. A.Ş.
- Üniteks Gıda Tekstil Motorlu Araçlar San. ve Tic. A.Ş.
- Yünsa Yünlü Sanayi ve Tic. A.Ş.

**Confirmed companies until 03 October 2018.*

*Names of the companies are listed alphabetically.*

# CONTENTS



## PROCEEDINGS

## 11 October 2018 Thursday

## Invited Speakers



## Session I: Functional Fibers

## Session II: Smart and Interactive Textiles

## Session III: Transportation Textiles



## Session IV: Protective Textiles



## Session V: Ecological Aspects for Technical Textiles

## Session VI: Functional Textiles

# 12 October 2018 Friday

## Invited Speakers



## Session I: Composites

## Session II: Medical Textiles



## Session III: Sportive Textiles

## Session IV: Medical Textiles



## Session V: Technical Designs

## Session VI: Nano Technical Textiles

# POSTER PRESENTATIONS

# 11 OCTOBER 2018

# ORAL PRESENTATIONS

# FUTURE OF NATURAL FIBRES, NEW TRENDS IN THEIR PRODUCTION, PROCESSING AND APPLICATIONS ESPECIALLY IN SCOPE OF TECHNICAL TEXTILES AND THEIR COMPETITION WITH MAN-MADE FIBRES IN XXI. CENTURY

**Ryszard KOZLOWSKI**

Institute of Natural Fibres and Medical Plants, Poland

Corresponding author: rkscience.biuro@gmail.com

**Abstract:** *The fibrous lignocellulosic raw materials like cotton, jute, kenaf, flax, hemp, sisal, ramie, abaca, curaua, pineapple, bamboo, coir, and also protein fibres like wool and silk can be extracted, processed, modified, functionalized and used in production of textiles: woven, knitted, nonwoven technical and 3D textiles and also used as reinforcement of more friendly biocomposites. Functionalization and special treatment such as plasma, corona, enzymatic, liquid ammonia, UV, providing flame retardancy and protection against bio deterioration contributes to new promising future and properties of all these fibres. From these fibrous resources it is possible to obtain textiles, and biopolymers, including food, fodder and fuel (ethanol and buthanol) and also commodity chemicals like surfactants, lubricants, agro-fine-chemicals by combining knowledge in scope of chemistry, material engineering, power and heat technologies. Key words: Natural fibres, functionalization, biopolymers, flame retardancy, biocomposites*

## 1. INTRODUCTION

Fibrous plants were well known to mankind more than 7 000 BC.

The fibrous plants can grow from Northern to Southern arctic circle. Now this is especially very important fact, that fibrous plants are completely sustainable, renewable, biodegradable and they recycle the carbon dioxide ($CO_2$).

Different parts of lignocellulosic plants are valuable sources of lignocellulosic fibres used in textiles and eco-friendly composites, sources of human food, nutrients, animal feed, agro-fine-chemicals for cosmetics and other area of application. The natural fibres are classified as follows:

Bast (flax, hemp, jute, kenaf, ramie etc.), and Leaf (sisal, abaca, etc.), Seeds (cotton, kapok, etc.), and Fruit (coir, African palm, luffa, etc.), Grass (bamboo,

totora), Wood (hardwood and softwood), Animal Fibers (wool, silk, hair etc.), Mineral Fibers - Asbestos, basalt, volastonite etc.

## 2. PROPERTIES OF NATURAL FIBRES

Generally natural fibres are miniature composites, formed from a ”reinforcement” of cellulose embedded in a ”matrix” of lignin and other polysaccharides e.g. hemicellulose. Cellulose molecules of lignocellulosic fibre have a hydrophilic nature due to its hydroxyl group. It is worth to underline, that pectin is a natural polymer present in plants, and as all natural polymers has biodegradation properties. Chemically pectin is a polysaccharide composed of a linear chain of 1-4 linked galacturonic acids which is etherified with methanol at 80%.

Natural fibres and derived products have very important properties like: excellent air permeability, high hygroscopicity, high heat absorption, no release of substances harmful for health, they not cause allergy effect (connected with higher histamine level in human blood), as well as safer behaviour in flame and fire combustion versus man-made fibres.

## 3. PRODUCTION AND PROCESSING OF NATURAL FIBRES

Global fibre production: 95.6 million tonnes, while the total production of all natural fibres is expected at the level about 40 million tons/year. The total fiber production is expected to increase by 3.7% per year by 2025. The per-capita fiber consumption increased to 10.3 kg / person. Demand for fibre in 2018: 85.3 million metric tons. Special treatment and functionalization of these fibres like plasma, corona, mercerization, liquid ammonia, encapsulation, ultrasound (US), modification with dendrimers, treatment by POMs (polyoxometalates), MOFs (Metal-organic frameworks), and other provide new promising features and expected new properties of these fibres and new area of their application.

## 4. POTENTIAL OF APPLICATION OF NATURAL FIBRES

Natural fibres can be processed for production of woven goods, knitting, nonwoven, technical and 3D textiles, also as the reinforcement of more friendly composites. One of the newest development deals with spunlace nonwoven made from bast fibres e.g. flax. Flax makes it possible to manufacture nonwovens with exceptional characteristics: extreme tear-resistance, durability and robustness, at a relatively low production cost. Through their natural elastic (e-) module, their minimal mass in comparison to carbon and glass fibres, their vibration dampening features and their UV resistance, flax fibres have many advantages when compared to synthetic fibres.

Spunlace nonwoven are introduced on the market for making e.g. flax window shades, fun board, roof construction etc. www.avroline.de, avr Spec.Issue1/2013avr - Allgemeiner Vliesstoff-Report 4/2008,

In case of those hydroentangled nonwoven, bast fibres are completely clean by removing dust, pectin, waxes and partially chemicellulose. Norafin reports that it has successfully qualified its 100% flax, lightweight spunlaced nonwovens as the complementary reinforcement material for surfboard construction via the contact vacuum moulding composites process. Surfboards employing the material are now commercially available from French manufacturer Notox Green Wave SAS.

These whole plants and woody parts (shives) and fibres (retted or green decorticated) can be used for production of special pulp and paper and some other by-products of these fibrous plants for obtaining the agro-fine-chemicals. The whole plants, with high yield of lignocellulosic materials (like cotton, jute, kenaf, flax, hemp, abaca) can be also explored as source of energy by burning (combusting) or by transforming to bioethanol or biobuthanol.

Some of these bast fibrous plants like flax and hemp could be explored for reclaiming the soil polluted by heavy metals thanks to their ability to extract cadmium (Cd), lead (Pb), copper (Cu) and zinc (Zn).

The new emerging method of genetic modification (GM) of fibrous plants provides promising performance e.g. higher level of cellulose, possibility of creating polyhydroxy-alcanate (PHA) for example polyhydroxy butyrate – natural polyester “in statu nascendi”.

Such GM plants are resistant to special herbicides, better resistant to drought also with controlled level of lignin and pectin. It is being considered to apply GM to increase the biomass of bast plants as well as for higher oil content in plant (using Rubisco promotor for gene expression). The idea of novel fibrous plants containing the nano-fibres is another alternative attracting considerable scientific attention and making it possible to incorporate phosphate groups into cellulose in order to obtain modified cellulose with higher thermal resistance.

## 5. COEXISTENCE AND COMPETITION WITH MAN-MADE FIBRES IN XXI CENTURY, FUTURE TRENDS

In 21st century the and competition between man-made and natural fibres is stabilized, especially in area of quality, sustainability and economy of their production. Natural fibres conduct heat, can be dyed well, resist mildew and have natural antibacterial properties, block UV and are easy to make them flame retardant. This makes them ideal for the production of comfortable healthy clothing that provide UV protection for the body, decrease of oxidative stress and muscle tension, increase of the level of alpha-globulin thus improving the wellbeing of users.

The facts mentioned above influence the position of natural fibres and stable the level of their production thanks to the growing area of their application, not only in textiles (woven, knitting, non-woven, technical textiles), but also in more eco-friendly composites, agro-fine-chemicals used in nutrients, pharmaceuticals and cosmetics as well as reasonable blends with man-made fibres.

It should be stated that production and application of man-made fibres is also important – we can observe tremendous development of new multifunctional man-made fibres.

Bio-silk, especially spider silk, fibres on base of polylactic acid and some other emerging new fibres for example those based on fibroin and chitin are also very interesting things in area of natural fibres

The report “European Technology Platform for Sustainable Chemistry – a Vision for 2025. Industrial Biotechnology and White. A Driver of Sustainable Growth in Europe” assumed that 30% of raw materials for industry of the textile, biochemical and chemical industry will be derived from renewable raw materials and biomass will constitute 30% of energy resources.

## REFERENCES

1. Handbook of Natural Fibres, Vol. 1, Ed. Ryszard Kozlowski, Woodhead Publishing, Cambridge, UK, 2012
2. Handbook of Natural Fibres, Vol. 2, Ed. Ryszard Kozlowski, Woodhead Publishing, Cambridge, UK, 2012
3. Smart Fibres, Fabrics and Clothing. Ed. Xiaoming Tao, Woodhead Publishing 2001
4. Akbari S., The Application of Dendritic Materials in Textile Engineering. Scientific Bulletin of ESCORENA, Vol. 7, 2013.
5. Natural Polymers and Composites, Ed. L.H. Capparelli Mattoso, A. Leao, E. Frolini, 14-17 May 2000, Sao Pedro, Brazil.
6. Renewable Resources, Obtaining, Processing and Applying, Ed. R. Kozlowski, G. Zaikov, F. Pudel 2009, Nova Science Publisher Inc. New York.
7. Biodegradable, and Sustainable fibres, Ed. R.S. Blackburn, WoodHead Publishing in Textiles, 2005, Cambridge, UK
8. Interior textiles: Design and Developments. Ed. T. Rove, WoodHead Publishing in Textiles, 2009, Oxford, Cambridge, New Delhi.
9. Textiles - Special Century Issue 2010, No ¾
10. Natural Fibers: Properties, Mechanical Behavior, Functionalization and Applications, eds. Ryszard M. Kozlowski R.M., Muzyczek M., Nova Publishers, USA, 2017, ISBN: 978-1-53612-071-4 (available online from July 12, 2017), Kozlowski R.M., Muzyczek M., Chapter 2. A New Challenge for Flax and Hemp Bast Fibers, pp 19-44, Kozlowski

# PRODUCTION OF MELT-SPUN POLY (Ε-CAPROLACTONE) FIBERS

**Figen SELLI[1,2], Edith PERRET[1], Ümit Halis ERDOGAN[2], Rudolf HUFENUS[2]**

[1]Dokuz Eylul University, Department of Textile Engineering, Turkey
[2]EMPA, Laboratory of Advanced Fibers, Switzerland

Corresponding author: figen.selli@empa.ch

**Abstract:** Poly (ε-caprolactone) (PCL), a member of biodegradable polyesters, has gained a notable interest as a biomaterial in medical applications such as sutures, drug delivery systems and scaffolds. As a commercial biomaterial, the main attention is on PCL blends with biodegradable polymers like polyglycolic acid (PGA), and poly-L-lactide (PLLA). Numerous studies have applied electrospinning, wet spinning and melt spinning techniques for processing PCL and its copolymers. However, to the best of our knowledge, there are no melt-spun PCL fibers on the market. Several research studies have investigated the production of PCL fibers via melt spinning, which is the most cost-effective fiber production method. Still, the production parameters and fiber properties so far are not compatible with large-scale production. Therefore, the aim of our study is to develop pure PCL melt-spun fibers with an economic process and to improve the properties of melt-spun PCL filaments.

Since PCL is thermoplastic in nature, melt-spinning under common conditions is feasible. In this study, PCL monofilaments were produced on a pilot-scale melt-spinning plant. As a semi-crystalline polymer with extension-thinning behaviour, PCL shows necking (ductile failure) during drawing in the spinline. This abrupt and drastic decrease in the cross-sectional area produces oscillations in the filament tension (draw resonance) which impede melt-spinning. We could overcome this draw instability using a modified drawing setup that takes the extensibility of this polymer into account. With this setup, stable drawing of monofilaments was successfully performed. Tensile test results suggest that PCL can be melt-spun into filaments with decent mechanical properties, with a process that is applicable to large-scale production.

**Key Words**: *Poly (ε-caprolactone), melt spinning, biodegradable fiber*

## 1. INTRODUCTION

The production of fibres from synthetic biopolymers is a niche market in the application range of biopolymers. Nevertheless, starting in the 21st century, due to the environmental concerns, there is an increasing interest in the development of bio-based and biodegradable fibres in the world. Besides, there is also a special interest on resorbable and biocompatible polymers mainly for medical applications. The synthetic biopolymer polycaprolactone (PCL) is either prepared by ring opening polymerization of ε-caprolactone using a catalyst (Figure 1) or the polycondensation of a hydroxycarboxylic acid: 6-hydroxyhexanoic acid [1].

This biodegradable aliphatic polyester is one of the earliest polymers which first synthesized in 1934 [2]. As a commercial biomaterial, in order to improve the degradation rate the main attention is on PCL blends with biodegradable polymers such as polyglycolic acid (PGA), and poly-L-lactide (PLLA) [3].

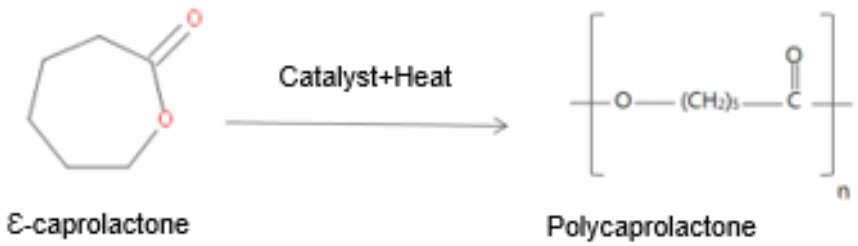


**Figure 1.** Ring opening polymerization of PCL using a catalyst

PCL has a low melting temperature ($T_m$=60 °C) which makes it a good candidate for processing with additives that are thermally sensitive. Numerous studies have applied electrospinning, wet spinning and melt spinning technique for PCL and its copolymers [4]. Regarding melt spinning, production parameters and fiber properties are still not compatible with industrial-scale production. Moreover, the end-use of PCL is limited to medical applications [5].

The goal of this study is to provide a basis for industrial-scale production of biodegradable PCL monofilaments using melt spinning method and therefore to decrease the high production costs and expand the field of PCL application. The study also aims to characterize these filaments. In consequence, the ultimate goal of our study is to develop biodegradable polyester fibers with an economic process and to improve the properties of melt-spun PCL filaments.

## 2. EXPERIMENTAL PART

### 2.1. Melt spinning and offline drawing of PCL fibers

PCL polymer Capa™ 6500, the average molecular weight of $M_w$=50 000 Dalton and particle size <600 µm was provided by Perstorp/UK. Melt spinning of undrawn and online drawn PCL filaments was carried out on a pilot-scale melt spinning plant (Fourné Polymertechnik, Germany) at Empa/St. Gallen. This pilot plant enables the spinning of fibers with various materials in different cross-sections.

Following the melt spinning of undrawn fibers, offline drawing of monofilaments was carried out by a custom-made drawing and winding machine (SSM, Switzerland).

## 2.2. Characterization

Mechanical testing of the filaments was performed with a tensile testing machine Textechno Statimat ME+. The load-strain behaviour of the filaments was evaluated with a 100 N load cell in reference to the standard ASTM D 2256 [6]. Filament tests were performed with 50 mm long test samples at a rate of extension of 100 mm/min.

Thermal properties of the PCL polymer were characterized using differential scanning calorimetry (DSC) and thermogravimetric analysis (TGA). In DSC, measurements were performed in nitrogen (N2) atmosphere (40 mL/min) using standard Al crucibles and the following heating/cooling program: 1st heating from 0 ºC to 120 ºC, followed by a cooling step to -50 ºC and then second heating back to 120 ºC. The heating/cooling rate was set to 10 K/min. TGA analysis was performed with a NETZSCH TG 209F1 device, under nitrogen (N2) and between 25-600 ºC.

Wide-angle x-ray diffraction (WAXD) was applied to determine crystallinity, crystal sizes and degree of orientation of crystals in the polymer fibers. In this method, the scattered intensity is plotted as a function of the 2θ angle. When x-rays hit a crystalline sample, they create an interference pattern. Wide-angle x-ray diffraction (WAXD) patterns were recorded on a Bruker Nanostar U diffractometer (Bruker AXS, Karlsruhe, Germany) with a Cu Kα radiation λ = 1.5419 Å and a VÅNTEC-2000 MikroGap area detection system.

## 3. RESULTS AND DISCUSSION

### 3.1. Thermal properties of the PCL polymer

According to DSC results, the melting temperature upon second heating was determined to be ≈ 58 ºC and the crystallization temperature upon cooling ≈ 18 ºC (Figure 2). The melting temperature of the polymer coincides with the datasheet of the manufacturer.

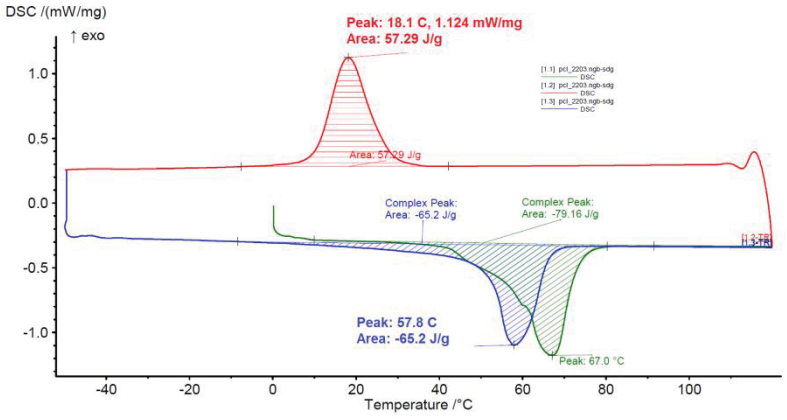


**Figure 2.** 1st heating, 2nd heating and cooling curves of PCL Capa™ 6506 obtained from DSC data.

The crystallinity of the polymer was estimated according to the following equation:

$$\% \text{ Crystallinity} = (\Delta H_{melt} - \Delta H_{cc}) / \Delta H_{literature} \times 100\% \quad [7]$$

in which $\Delta H_{melt}$ the enthalpy of heating, $\Delta H_{cc}$ the cold crystallization enthalpy and $\Delta H_{literature}$, the enthalpy of heating of an ideal crystal (PCL,139,5 J/g ref [8]. Since no cold crystallization peak was observed during the measurement, the enthalpy of this peak was taken to be zero and the crystallinity of the PCL polymer was estimated to be 47 %.

Thermal degradation of PCL was studied by determining the weight loss of a sample using TGA. Figure 3 shows the temperature dependence of the PCL weight loss. The TGA curve displays one main degradation with an inflection point at 385 ºC.

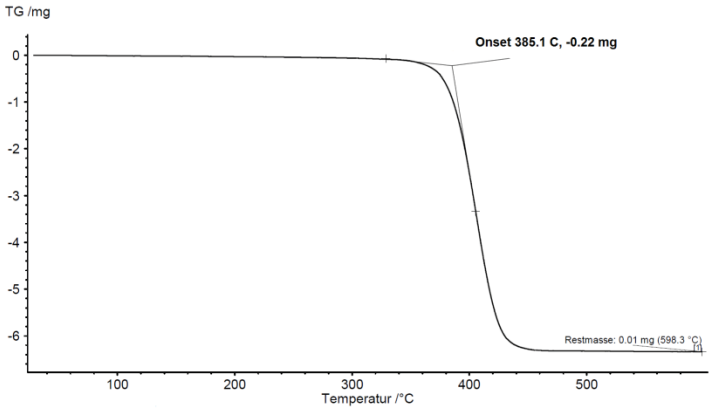


**Figure 3.** TGA curve of PCL polymer, heating rate 10 K.min$^{-1}$

### 3.2. Fiber melt spinning and drawing of pure PCL monofilaments

Melt spinning is the most commonly used fiber production method for commercial synthetic fibers. Here, the processing temperature was chosen based on thermal characterization test results of the polymer and PCL was melted and pressurized using a single screw extruder with a diameter of 13 mm. Extruder temperatures were varied between 60-100 ºC, whereas spin pack temperatures ranged between 90-100 ºC and godet temperatures between 20-30 ºC. The circular monofilament die had a diameter of 0.5 mm and a capillary length to diameter ratio of 4. The draw ratio was set to 6, with final winding speeds between 300-600 m/min. In addition to standard godets, both in the online and offline drawing, filaments were directed over an additional godet that revolved reversely to the running direction of the filament in order to impose friction that steadies the necking point (Figure 4). Four different filaments; undrawn (1319) and drawn with ratio 6 (1697, 1698 and 1699) were produced whereas the sample 1319D4 was offline drawn from as-spun 1319 with draw ratio 7. In the production, the take-up

speed was altered in order to get finer filaments (1699). A temperature decrease in the spin pack did not cause a significant difference in the properties of the filaments (Table 1). Table 1 summarizes the production parameters of the different spinning and drawing trials performed in this study.

**Table 1.** Production parameters of PCL monofilaments

| Sample | Drawing | Extruder Temp.(ºC) | | | Spin pack Temp.(ºC) | Take-up Speed (m/min) | Winder Speed (m/min) | Draw Ratio |
|---|---|---|---|---|---|---|---|---|
| 1319 | Undrawn | 80 | 100 | 100 | 100 | 50 | 50 | 1 |
| 1319D4 | Offline Drawing | 80 | 100 | 100 | 100 | 6 | 42 | 7 |
| 1697 | Online Drawing | 60 | 100 | 100 | 100 | 50 | 300 | 6 |
| 1698 | Online Drawing | 60 | 100 | 100 | 90 | 50 | 300 | 6 |
| 1699 | Online Drawing | 60 | 100 | 100 | 90 | 100 | 600 | 6 |

In order to draw the as-spun fiber 1319 fiber (offline draw ratio 7) first and third godets were held at room temperature whereas the second godet was set to 35.5 ºC. A heat chamber was placed between the first and second godet in order to get a thorough heating of the filament. The filament was directed over that second godet which revolved reversely to the running direction of the filament (Figure 4).

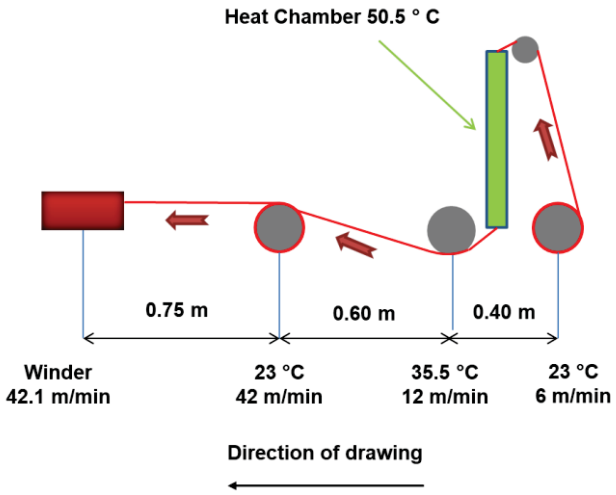


**Figure 4.** Schematic assembly of offline drawing. Red colour shows the winding of the filament on the godets

### 3.3. Mechanical properties of PCL fibres

Mechanical properties of PCL fibers were evaluated in terms of yarn count, diameter and draw ratio of filaments. The test revealed that the specific stress and strain are in a range of 27-41 cN/tex and 68-88 %, respectively. Mechanical properties are evaluated in terms of yarn count, diameter and draw ratio of filaments. The filament properties are summarized in Table 2.

**Table 2.** Properties of undrawn, online drawn and offline drawn PCL filaments

| Sample | Drawing | Draw Ratio [a] | Yarn Count [b] (tex) | Diameter [c] (μm) | Specific Stress (cN/tex) [d] | Elongation at Break (%) [e] |
|---|---|---|---|---|---|---|
| 1319 | Undrawn | 1 | 41.2±3.5 | 221.9±4.7 | 6.05±11.7 | 1368±6.7 |
| 1319D4 | Offline Drawing | 7 | 6.43±4.0 | 90.5±6.1 | 41.5±11.4 | 68.5±18.6 |
| 1697 | Online Drawing | 6 | 7.65±0.5 | 93.1±0.9 | 27.4±6.35 | 88.5±5.0 |
| 1698 | Online Drawing | 6 | 7.65±0.3 | 87.4±0.7 | 29.3±7.32 | 88.3±8.0 |
| 1699 | Online Drawing | 6 | 3.79±1.2 | 69.7±1.0 | 31.5±5.80 | 72.9±8.5 |

a, draw ratio: winding speed divided by take-up speed
b, d and e depict averages and standard deviation of 10 measurement
c, depicts average and standard deviation of 15 readings with an optical microscope

According to tensile measurements, offline drawn PCL 1319D4 has the highest specific stress (41.5 cN/tex) whereas online drawn PCL 1697 has the lowest (27.4 cN/tex). Specific stress-strain results are given in Figure 5. Sample 1699 which is the finest filament with a diameter of ≈70 μm has the highest specific stress value among online drawn filaments. Elongation at break results suggest that online drawn 1697 and 1698 have the same elongation due to their similar yarn counts and diameter. As-spun 1319 fiber (not shown in Figure 5) has the lowest specific stress, which is due to the low molecular orientation of this fiber. It is well-known that the molecular orientation increases with increasing draw ratio and therefore drawn fibers have a higher specific stress.

### 3.4 WAXD patterns of PCL fibres

PCL is a semi-crystalline polymer. Every crystalline material has a unique WAXD pattern which represents a fingerprint of its crystal structure. Figure 6 shows the WAXD patterns of samples 1319 (a) and 1697 (b), the PCL fiber which was drawn with a draw ratio of 6. The rings in Figure 4a indicate that the PCL crystallites are randomly oriented. Upon drawing the crystallites orient themselves and clear diffraction peaks are observed (Figure 4b). The indexing of the peaks to specific lattice planes is performed by comparing the peak positions with previously published WAXD data of PCL [9]. The most intense peaks come from the (110) and the (200) planes with a corresponding d-spacing of 4.145 Å and 3.748 Å, respectively.

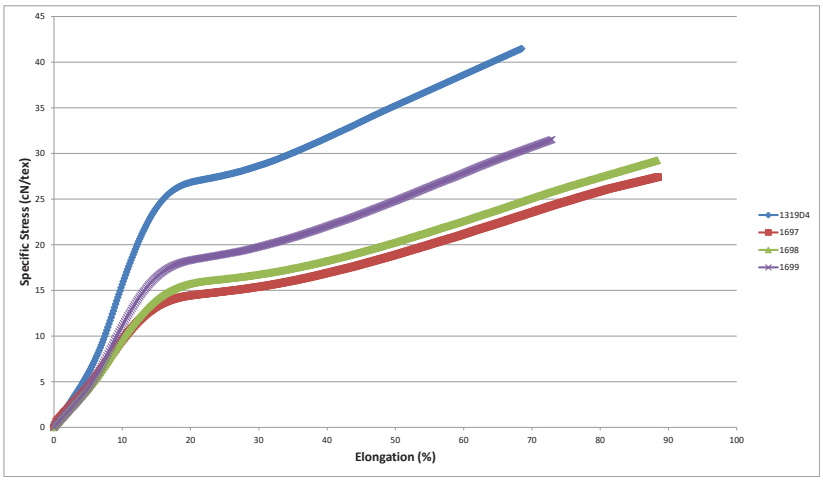


**Figure 5.** Specific stress-strain curves of PCL filaments. Specific stress vs elongation for four different PCL melt spun and online drawn fiber yarns. Online draw ratio (DR) =6, Offline draw ratio (DR) =7

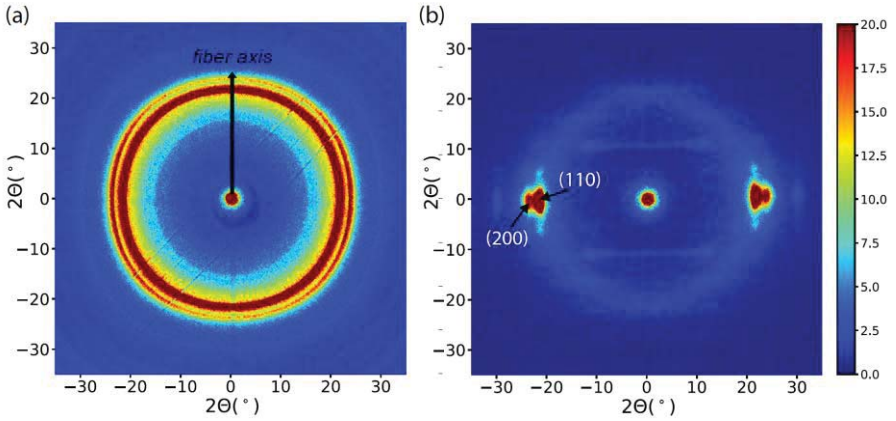


**Figure 6.** WAXD Patterns of as-spun fiber 1319 (a) and fiber 1697 drawn with draw ratio 6 (b)

## 4. CONCLUSION

Undrawn and drawn PCL monofilaments with decent mechanical properties have been produced by means of melt spinning. Modification in the drawing system, by running the filament over the second godet in reverse direction, enabled to prevent ductile failure of the fiber. It was shown that the PCL polymer was well processable without thermal degradation. The achieved mechanical properties revealed that the offline drawn filament had higher specific stress values. WAXD patterns showed distinct diffraction peaks for the drawn fibers which indicate oriented crystallites.

## ACKNOWLEDGEMENTS

The work was supported by The Scientific and Technological Research Council of Turkey (TÜBİTAK 2214A to Figen Selli). Authors would like to thank Benno Wüst for operating the spinning plant and Markus Hilber for operating the SSM winding machine.

## REFERENCES

1. Labet, M. and W. Thielemans, Synthesis of polycaprolactone: a review. Chem Soc Rev, 2009. **38**(12): p. 3484-3504.
2. Natta, F.J.V., J.W. Hill, and W.H. Carothers, Studies of Polymerization and Ring Formation. XXIII.1 e-Caprolactone and its Polymers. 1934. **56**(2): p. 455-457.
3. Azimi, B., et al., Poly (ε-caprolactone) Fiber: An Overview. Journal of Engineered Fibers and Fabrics, 2014. **9**(3): p. 74-90.
4. Woodruff, M.A. and D.W. Hutmacher, The return of a forgotten polymer—Polycaprolactone in the 21st century. Progress in Polymer Science, 2010. **35**(10): p. 1217-1256.
5. Handbook of Biodegradable Polymers.pdf. 2011: WILEY-VCH.
6. ASTM, Standard Test Method for Tensile Properties of Yarns by the Single-Strand Method. 2015.
7. Perkin Elmer Instruments, DSC as Problem Solving Tool Measurement of Percent Crystallinity of Thermoplastics, 2000.
8. Pal, J., et al., Control on molecular weight reduction of poly(epsilon-caprolactone) during melt spinning--a way to produce high strength biodegradable fibers. Mater Sci Eng C Mater Biol Appl, 2013. **33**(7): p. 4213-20.
9. Bittiger, H. and R.H. Marchessaul, Crystal Structure of Poly Ɛ-caprolactone.pdf. Acta Cryst, 1970. **B26**: p. 1923-1927.

# ANTIOXIDANT CAROTENOIDS-CYLODEXTRIN INCLUSION COMPLEX NANOFIBERS VIA ELECTROSPINNING

**Zehra Irem YILDIZ[1], Fuat TOPUZ[1], Bhushan PATİL[1], Mehmet Emin KİLİC[1], Engin DURGUN[1], Tamer UYAR[1]**

[1]Bilkent University, UNAM-Institute of Materials Science & Nanotechnology, Turkey

Corresponding author: tamer@unam.bilkent.edu.tr

***Abstract:*** *Carotenoids, substances giving color to vegetables and fruits, are frequently used in many fields due to their special properties like being vitamins, being used as colorants and being antioxidants. However, the application of carotenoids are limited because of their low stability against light, heat, air, etc., and their low water solubility. In this study, the main aim is to remove or reduce these restrictions by encapsulating two carotenoids, lycopene and β-carotene, into cyclodextrins (CDs) and then turn these cyclodextrin-inclusion complexes (CD-ICs) into nanofibrous web structure via electrospinning. As a result, it is expected to increase the heat and light stability, increase water solubility and antioxidant activity of lycopene and β-carotene in nanofibers. In addition to all these advantages, the use of such functional nanofibrous web with high surface area will be promising in textile/food/pharmacy/cosmetic.*

***Keywords****: Carotenoids, cyclodextrin inclusion complexes, electrospinning, nanofibers, antioxidant*

## 1. INTRODUCTION

Carotenoids are naturally occurring fat-soluble pigments found in plants. They are used as colorants, and furthermore, they are widely used as food supplements due to their antioxidant activity and health related benefits like reducing the risk of many chronic and degenerative diseases such as cardiovascular disease, arthrosclerosis, eye problems, some types of cancer and developing the immune system [1]. Lycopene, known as antioxidant, and β-carotene, which is provitamin A and antioxidant, are among the main carotenoids (Figure 1a.). However, they are highly susceptible to external factors such as light, heat, air, etc., and they are slightly soluble in water which restrict their applications.

Cyclodextrins (CDs) are cyclic oligosaccharides produced from enzymatic conversion of starch [2]. CDs with their truncated cone shape structure are capable of forming noncovalent host-guest inclusion complexes (IC) with variety of molecules due to their relatively hydrophobic cavity [3]. CDs consist of either six (α-cyclodextrin), seven (β-cyclodextrin) or eight (γ-cyclodextrin) glucopyranose units. These native CDs can be modified by substitution of some functional groups like hydroxypropyl for some of the hydroxyl groups of the native CDs to provide enhanced water solubility (Figure 1a.).

Electrospun nanofibers are promising materials used in many applications thanks to their remarkable properties such as large surface area-to-volume ratio, nanoporous structure, lightweight and design flexibility. In general, electrospinning requires polymers with high molecular weight and high concentration to fabricate nanofibers. Nonetheless, it has been shown that the fabrication of functional nanofibers from cyclodextrin inclusion complexes (CD-IC) without using any carrier polymeric matrix [4,5].

In this study, we fabricate electrospun nanofibers from the inclusion complexes of Lycopene and β-carotene with two modified CDs, hydroxypropyl-β-cyclodextrin (HPβCD) and hydroxypropyl-γ-cyclodextrin (HPγCD). With this study, it is expected to increase the low water solubility of carotenoids, and reduce their susceptibility to external factors such as heat and light which severely limit their applications.

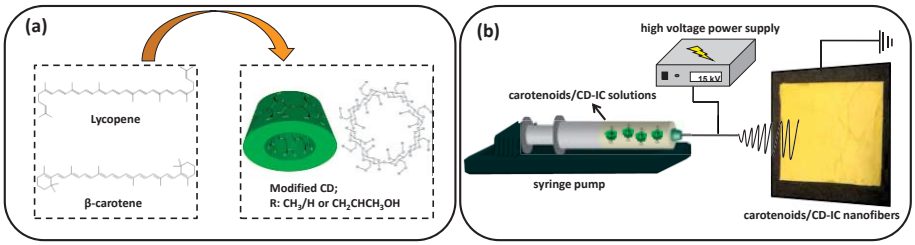


**Figure 1.** (a) The chemical structure of carotenoids and CD and (b) electrospinning of nanofibers from carotenoids/CD-IC solution.

## 2. MATERIAL AND METHOD

### 2.1. Preparation and electrospinning of IC solutions

For the preparation of carotenoids/CD-ICs solutions, firstly, carotenoids were dispersed in a solvent system, then, CDs were added. These dispersions were stirred overnight at room temperature. At the end, the solutions of carotenoids/CD-ICs were obtained. Then, the solutions of carotenoids/CD-ICs were electrospun at optimized conditions to obtain carotenoids/CD-ICs nanofibers by electrospinning.

### 2.2. Characterization of Carotenoids/CD-IC nanofibers

The complexation mechanism of carotenoids/CD-ICs systems, interaction energies, structural properties and water solubility are performed by ab initio computational modeling. Morphological analyses of nanofibers were performed by scanning electron microscope (SEM). The average fiber diameter (AFD) was calculated from the SEM image and the diameter of 100 fibers were measured. The presence of carotenoids in nanofibers were analyzed by proton nuclear magnetic resonance ($^1$H NMR). Fourier transform infrared spectrometer (FTIR) was used for structural characterizations of nanofibers. The X-ray diffraction (XRD) data was taken to see crystalline structures of nanofibers. Differential scanning calorimetry (DSC) and thermogravimetric analyzer (TGA) were used to

investigate thermal properties of nanofibers. The fast-dissolving character and water-solubility enhancement were studied.

## 3. RESULTS AND DISCUSSION

The solutions of carotenoids/CD-ICs were electrospun at optimized parameters to get bead-free, free-standing nanofibers (Figure 2). The AFD was calculated as 1455±585 nm for β-carotene/CD-IC NFs (Figure 2). The presence of carotenoids in nanofibers were confirmed by $^{1}$H-NMR and FTIR. The formation of ICs were suggested by XRD and DSC data. TGA data showed the change in thermal stability of carotenoids after CD-IC nanofibers formation. Fast-dissolving character of nanofibers and water-solubility enhancement of carotenoids was proved. The characterizations on antioxidant activity and light stability of nanofibers are performed.

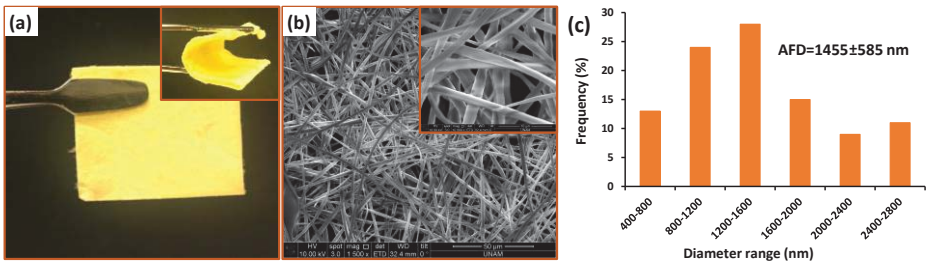


**Figure 2.** (a) The photographs, (b) SEM images and (c) the fiber diameter distribution with average fiber diameter (AFD) of β-carotene/CD-IC NFs.

## 4. CONCLUSION

Fast-dissolving, free-standing carotenoids/CD-ICs nanofibers of lycopene and β-carotene were fabricated. By the fabrication of carotenoids/CD-ICs nanofibers, the use of these carotenoids, which have many useful properties, will be possible in a more efficient manner in the required fields. In addition, the use of electrospun nanofibrous webs will gain a new field of application.

**ACKNOWLEDGMENT:** The authors acknowledges The Scientific and Technological Research Council of Turkey (TUBITAK)-Turkey (Project # 117Z535) for funding this research

## REFERENCES

1. Peinado I., Mason M., Romano A., Biasioli F., Scampicchio M.: Stability of β-carotene in polyethylene oxide electrospun nanofibers. 2016. Appl Surf Sci, 370, 111-116.
2. Szejtli J.: Introduction and general overview of cyclodextrin chemistry. 1998 Chem. Rev. 98 (5), 1743e1753.
3. Del Valle E.M.M.: Cyclodextrins and their uses: a review. 2004. Process Biochem. 39 (9), 1033e1046.
4. Aytac Z., Yildiz Z.I., Kayaci-Senirmak F., San-Keskin N.O., Kusku S.I., Durgun E., Tekinay T., Uyar T.: Fast-Dissolving, Prolonged Release, and Antibacterial Cyclodextrin/Limonene-Inclusion Complex Nanofibrous Webs via Polymer-Free Electrospinning. 2016. J Agric Food Chem. 64(39): 7325-7334.
5. Celebioglu A., Uyar T.: Electrospinning of polymer-free nanofibers from cyclodextrin inclusion complexes. 2011. Langmuir. 27(10): 6218-6226.

# INVESTIGATION OF THE PERMEABILITY PROPERTIES KNITTED FABRICS PRODUCED FROM ISLANDS IN THE SEA TYPE MICROFILAMENT YARNS

**Nimet KÖLEOĞLU[1], Hatice Kübra KAYNAK[1]**

[1] Gaziantep University, Department of Textile Engineering, Turkey

Corresponding author: nimetkoleoglu@gmail.com

***Abstract:*** *Island in the sea type is an important type of microfilament. Since, it allows producing finer filaments than those of produced by direct spinning technique. In the scope of this study, the performance properties of single jersey knitted fabrics produced from island in the sea type microfilament yarns are investigated. For this purpose three knitted fabric samples are produced as single jersey structure with three different fabric densities (loose, medium, tight). Air and water vapour permeability properties of these samples are tested as permeability properties, since this type of fabrics are in the market as high value added thermally comfortable products. Also bursting strength of the samples is determined as a basic durability property.*

***Keywords:*** *island in the sea, microfilament, knitted fabric, air permeability, water vapour permeability, bursting strength*

## 1. INTRODUCTION

Synthetic fiber industry has been enforced to make developments due to the increasing performance demand from textile products. One of the most important developments in synthetic fiber industry, is absolutely producing extremely fine fibers which are named as microfibers and nanofibers. Until today, there is no exact definition for microfibers. But common opinion is defining a fiber finer than 1 dtex or 1 denier as microfiber. 1 dtex polyester fiber has a fiber diameter of approximately 10 μm [1]. There are various methods of producing microfibers. All three conventional spinning methods, namely melt spinning, wet spinning, and dry spinning can be employed to manufacture microfibers. Although, it is possible to produce microfibers through conventional melt spinning, to create such fine filaments requires very strict process controls and a uniformly high quality of polymer. Ultra-fine fibers are classified into two types: filament type, and staple type. Recent developments in the field of ultra-fine fibers have focused on the filament type. In islands in the sea method, a number of continuous very fine filaments are extruded in a matrix of another polymer. In the spinneret a number of bi-component sheath-core polymer flows are combined into a single flow and extruded. The islands in the sea fiber is then quenched and drawn in the usual way [2]. Island microfibers are obtained after dissolving the sea component. In the literature there are some studies on optimum parameters to obtain island in the sea type microfilaments [3-6]. On the other hand, microfibers offer a great

variety of applications in sportswear owing to their extra softness, full handle, drape, comfort and easy care properties. One general point that should be mentioned is that the desired properties (i.e. sophisticated handle, pleasant silky appearance, leather lookalike, good filtration properties, etc.) are only obtained when a suitable fabric construction is produced. As well as fineness, the material combination, cross-section of the elementary filaments and their effect when used in combinations are extremely important and can offset negative parameters (i.e. proneness to creasing, somewhat lower absolute tenacity) [2]. In the context of this study, the permeability properties of knitted fabrics produced from island in the sea type microfilament yarns are investigated.

## 2. MATERIAL AND METHODS

In this study, it is aimed to investigate the structural and performance properties of knitted fabrics produced from island in the sea microfilament yarns. Island in the sea type microfilament yarns are exposed to alkali treatment to dissolve sea component and to obtain microfilament island components in yarn structure. In this study, Teijin brand polyester, island in the sea type microfilament yarn (Figure 1) (Nanofront) is used. The manufacturer twist this yarn with a regular yarn to obtain durability then the twisted yarn is exposed to alkali treatment by the manufacturer and sea component is dissolved. So there is no need to additional wet process for the buyers.

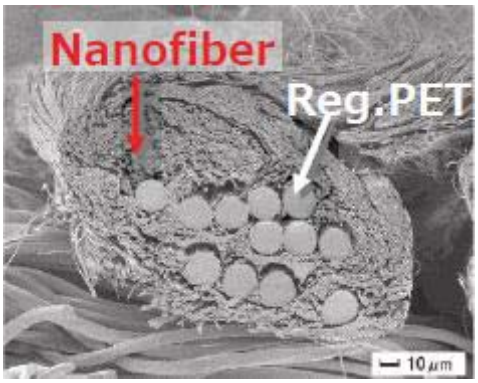


**Figure 1.** Cross-sectional view of Nanofront yarn from TEIJIN

Before dissolving process linear density of yarn is 56 dtex and 10 filaments in cross section. After dissolving process yarn linear density is 39 dtex and 8360 filaments in cross section providing 700 nm filament diameter. As mentioned earlier, the alkali treatment for dissolving the sea component is done by the manufacturer. The cross sectional SEM view of the yarn is given in Figure 2.

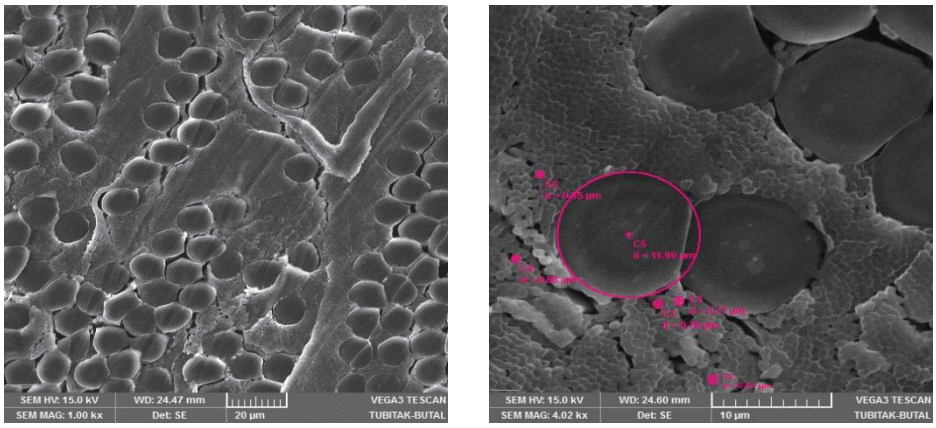


**Figure 2.** Cross-sectional SEM views of Nanofront yarn, left 1000X magnification, right 4000X magnification

Three knitted fabric samples are produced with different levels of fabric density as loose, medium and tight. Knitted fabric samples are produced as single jersey structure, by a 3.5" gauge, 22 fein and one feeder sample circular knitting machine at 20±2 rev/min production speed. Surface views of the fabric samples are given in Figure 3.

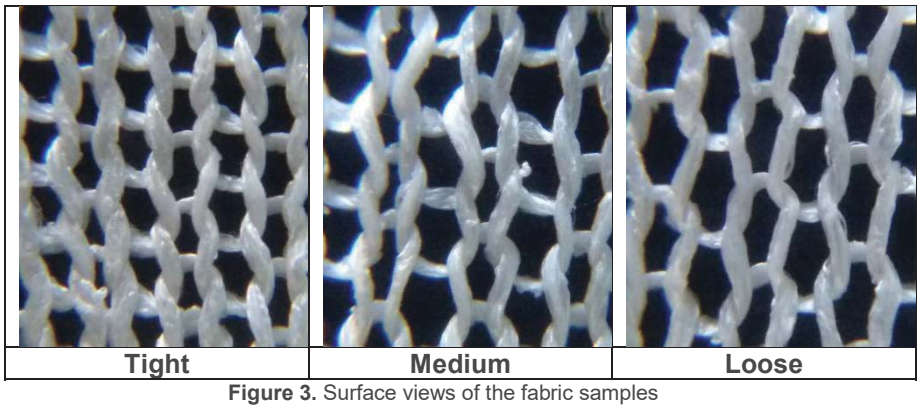


**Figure 3.** Surface views of the fabric samples

All fabric samples are conditioned according to TS EN ISO 139 [7] before the tests and the tests are performed in the standard atmosphere of 20±2ºC and 65±4% relative humidity. Fabric mass, thickness, loop density and loop length properties of samples are determined according to TS EN 12127:1999 [8], TS 7128 EN ISO 5048:1998 [9], TS EN 14971:2006 [10] and TS EN 14970:2006 [11], respectively. The results are given in Table 1.

**Table 2.** Structural properties fabric samples

| | Thickness, mm | Loop density, loops/cm² | Loop length, mm |
|---|---|---|---|
| **Loose** | 0.45 | 80 | 4.6 |
| **Medium** | 0.43 | 99 | 4.2 |
| **Tight** | 0.42 | 130 | 3.8 |

Then, air permeability, water vapour permeability properties of the samples are determined. Air permeability test is done according to TS 391 EN ISO 9237:1999 [12] with digital air permeability test device at 100 Pa pressure drop and 20 cm² test area. The air permeability tests are performed over ten measurements for each fabric sample. Water vapour permeability test is done according to evaporative dish method and BS 7209:1990 from three measurement of each fabric sample [13]. Three test specimens are mounted over the test dishes containing distilled water at 20±2ºC. These dishes are placed on a rotating turntable. The samples are rotated with turntable for one hour to establish equilibrium of water vapor pressure gradient across the sample. Then, the mass of the dishes are determined. The turntable with dishes is then rotated for a further period of 5 hour. The mass of the dishes is weighed after this period. The weight difference is found. The water vapor permeability (*WVP*) in *g/m²/day* is given by the equation:

$$WVP = \frac{24M}{At} \quad (1)$$

Where,

**M =** loss in mass of the dish over the time period in grams

**t =** time between successive weighing of the assembly in hours

**A =** area of the exposed sample, $5.41 \times 10^{-3}$ m²

In order to obtain bursting strength and bursting distension values, the knitted fabric samples are applied bursting strength test in accordance with TS EN ISO 13938-2 [14]. Truburst pneumatic bursting strength test device is used at 7.3 cm² test area. The bursting strength and distension are measured. The measurements are repeated five times from different parts of the samples. After five bursting measurements are completed, diaphragm correction procedure is applied. In this procedure, the diaphragm is distended without the presence of the specimen with the same test area and same rate of increase in volume to burst the previous specimen tests. Then, the pressure at this distension is noted as diaphragm pressure and subtracted from the initial pressure values.

## 3. RESULTS AND DISCUSSION

In this study, air permeability and water vapor permeability tests are applied to the sample fabrics for determination of thermal comfort and the results are given in Figures 4 and 5, respectively. Also, bursting strength test is applied for assessing the durability and bursting strength and bursting distension results are given in Figures 6.

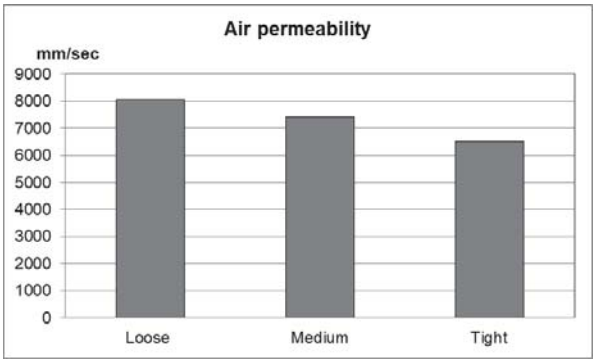


**Figure 4.** Air permeability of the samples

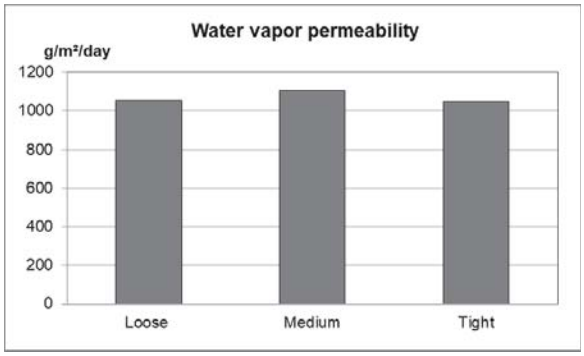


**Figure 5.** Water vapor permeability of the samples

As it is seen from Figures 4 and 5, the samples used in this study have high level of air permeability. On the other hand, it is seen that as the fabric tightness increases the air permeability decreases. This is an expected result because the increase in fabric tightness means increase in fiber material in unit area of the fabric. By this way total pore structure decreases. During air passage through the fabric, air passes through the pores between the fibers and between the yarns. So, the air permeability is expected to decrease as the total porosity of the fabric decreases. Besides, it should be noted that the decrease in air permeability due to the fabric tightness is not a considerable change since the air permeability is

still high. With respect to water vapour permeability, it is seen that all three fabric samples have good level of water vapor permeability. The lowest value belongs to the tight samples as 1051 g/m²/day. This value means that a sport shirt made from nearly 1 m² of this fabric will permit 1051 grams of water vapor passage during one day under 20±2ºC and 65±4% relative humidity conditions. Also it should be considered that this value will increase with higher temperature and relative humidity owing to higher vapor pressure in real use conditions. Besides, there is no regular tendency of decrease or increase in water vapor permeability owing to fabric tightness or in other words total porosity.

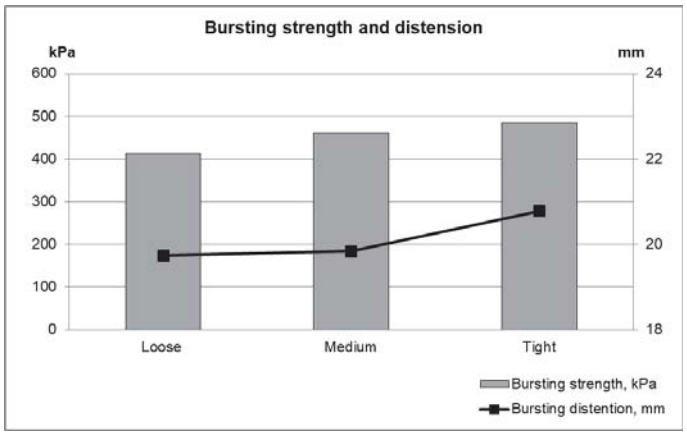


**Figure 6.** Bursting strength and distension

Figure 6 exhibits the bursting strength and distension of the samples used in this study. As it is seen, the bursting strength of the samples increases with the increase in fabric tightness regularly. This is an expected result because as the fabric tightness increases the loop density (loops/cm$^2$) of the fabric increase. This situation cause more number of loops per unit area that resists the bursting forces on the sample. So the bursting strength increases. On the other hand, a regular increase in bursting distension is also observed. This is a positive behavior of knitted fabric under bursting forces. Since a reverse situation is generally observed in textile materials as increase in strength generally result in decrease in elongation. But the samples in this study produced from islands in the sea type microfilament yarns provide higher bursting strength and distension with the increase in fabric tightness.

## 4. CONLUSION

In this study, knitted fabric samples were produced from only one type of commercially available island in the sea type microfilament yarn. As a result of air and water vapour permeability tests it is seen that all three fabric types provide

good air and water vapour permeability providing a good level of thermal comfort. On the other hand, as an expected result air permeability values of the fabrics decrease from loose to tight fabric type. But there is no similar trend for water vapor permeability. Also, bursting strength property was determined as a durability assessment that a good level of bursting strength was obtained all three samples. There is a minor increase in bursting strength and bursting distension of the samples as the fabric tightness increase. Consequently, it is seen that the knitted fabric samples produced from this yarn can be used as value added products considering the thermal comfort and durability. On the other hand, for further studies different properties of these products may be determined such as surface roughness and wet moisture management. Also, performance properties of woven fabric samples may be determined for different technical uses. In addition it may be beneficial to compare commercially available yarns for different usage areas.

## REFERENCES


1. Kaynak H.K., Çelik H.İ. (2016), Investigation of Performance Properties of Knitted Fabrics Produced from Splittable Microfilament Yarns, Tekstil ve Mühendis, 23: 104, 238-246.
2. Kaynak, H.K., Babaarslan, O., (2012), Polyester Microfilament Woven Fabrics, Woven Fabrics, Prof. Han-Yong Jeon (Ed.), ISBN: 978-953-51-0607-4, InTech, Available from: http://www.intechopen.com/books/woven-fabrics/polyester-microfilamentwoven- fabrics.
3. Kim H., Kim H.S., Park Y.K., Lee J.J., (2015), Alkaline dissolution and dyeing properties of sea-island type polyethylene terephthalate ultramicrofiber knitted fabrics, *Fibers and Polymers*, 16, 9, 1995-2002.
4. Park Y.K., Jo A.R., Lee J.J., (2015), Weight Reduction and Dyeing Properties of Sea-island-type Polyethylene Terephthalate Ultramicrofiber Fabric, *Textile Science and Engineering*, 52, 5, (344).
5. Koh J., (2004), Alkaline dissolution monitoring of sea–island type polyester microfibre fabrics by a cationic dye staining method, *Coloration Technology*, 120, (80-86).
6. Kabir S.M.M., Koh J., (2017), Alkaline weight reduction and dyeing properties of black dope-dyed poly(ethylene terephthalate) microfibre fabrics, *Coloration Technology*, 133, 3, (209-217).
7. TS EN ISO 139: 2008 Textiles-Standard atmospheres for conditioning and testing.
8. TS EN 12127: 1999 Textiles- Fabrics - Determination of mass per unit area using small samples.
9. TS 7128 EN ISO 5048:1998-Textiles - Determination of thickness of textiles and textile products
10. TS EN 14971:2006 Textiles - Knitted fabrics - Determination of number of stitches per unit length and unit area.
11. TS EN 14970:2006 Textiles – Knitted fabrics - Determination of stitch length and yarn linear density in weft knitted fabrics.
12. TS 391 EN ISO 9237:1999Textiles-Determination of permeability of fabrics to air.
13. BS 7209:1990 Specification for water vapour permeable apparel fabrics.
14. TS EN ISO 13938-2 Textiles – Bursting properties of fabrics – Part 2: Pneumatic method for determination of bursting strength and bursting distention.

# POLI LACTIC ACID FILAMENT (PLA) YARN AND WOVEN FABRIC CHARACTERIZATION

**Onur ÇELEN[1], Hasan Basri KOÇER[2], Olcay TOK[3]**

[1]KORTEKS Mensucat San. A.Ş.
[2]Bursa Technical Unıversity, Turkey [3]ZORLUTEKS A.S

Corresponding author: hasan.kocer@btu.edu.tr

***Abstract :*** *Bio-based polymers have become increasingly important both in the protection of the environment and in the themes of sustainability. Poly lactic acid (PLA) is an innovative renewable polymer that incorporates mechanical properties and is inherently sustainable in biocompatibility with the end result of end use.*

*The fast crystallization behavior of the PLA polymer gives hard and brittle form, occuring difficulties in filament yarn spinning and texturising. (unstabil melt , yarn breakages and filamentations) In this study, PLA filament yarn spinning and texturising processes were enhanced by R&D trials. 68-300 denier Pre Oriented Yarn (POY) ,Fully Drawn Yarn (FDY) and Texturising yarns were developed successfully. Phsycial, chemical and thermal properties were gained by characterization methodes.*

*Enhanced PLA yarns will be weaved at plain, twill and satin constructions. Tensile and tear strengh and abrasion tests will be performed for determining fabric characterization with comparative Polyethylenetaphthalate (PET) fabric.*

**Key words:** PLA, sustainability, spinning, textile, characterization

## 1. INTRODUCTION

Environmental, economic, and safety challenges have provoked packaging scientists and producers to partially substitute petrochemical-based polymers with biodegradable ones. Biopolymers are produced from natural resources and crude oil.

In comparison to other biopolymers, the production of PLA has numerous advantages including: (a) production of the lactidemonomer from lactic acid, which is produced by fermentationof a renewable agricultural source corn; (b) fixation of significant quantities of carbon dioxide via corn (maize) production by thecorn plant; (c) significant energy savings; (d) the ability to recycleback to lactic acid by hydrolysis or alcoholysis; (e) the capability ofproducing hybrid paper-plastic packaging that is compostable; (f)reduction of landfill volumes; (g) improvement of the agricultural economy; and (h) the all-important ability to tailor physical properties through material modifications [1].

Briefly, PLA is based on agricultural (crop growing), biological (fermentation), and chemical (polymerization) sciences and technologies. It is classified as generally recognized as safe (GRAS) by the United State Food and Drug Administration (FDA) and is safe for all food packaging applications. [2]

PLA is rigid thermoplastic and aliphatic polymers with semi-crystalline or amorphous structure. It has unique properties as it has both PET and Polypropylene (PP) polymer characteristics. [1-2] PLA production begins with the removal of starch from plants such as corn, sugar cane . Starch is then converted into sugars (such as glucose and dextrose) that can be fermented by enzymatic hydrolysis. By microorganism fermentation sugar is broken into small fractions known as lactic acid. Lactic acid is then polycondensated and genareted in PLA form. [3] Polycondensation is divided into two: direct polycondensation which produces low molecular weight PLA and ring opening polycondensation which produces high molecular weight PLA. Figure 1 shows the polymerisation mechanisms.

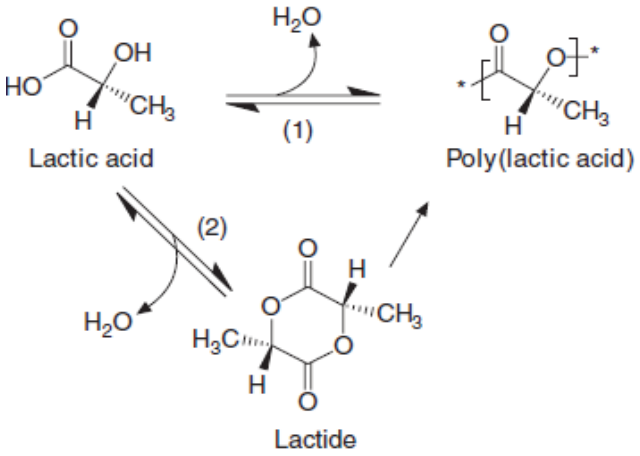


**Figure 1.** PLA formation methodes

PLA has unique bio-degradation and bio-compostable properties after use life so contributes to the natural cycle by making contributions rather than creating waste after being produced from natural sources. PLA is FDA approved for use in the food industry and other packaging applications because it is non-volatile and odorless. It has functional properties such as low flammability and smoke formation, UV resistance property. Good moisture management, easy drying and comfort features are other benefits [4].

## 2. MATERIAL AND METHOD

The PLA polymer to were supplied from the supplier abroad. The thermal behavior of PLA chip is given in figure 2.

PLA POY filament yarn were produced by melt spinning technology. Experimental design is started with trials at Spinboy machine. This machine is the most complex and big spinning machine. The Spinboy machine trials shows

the spinability of PLA yarn. Also the mechanical properties are satisfactory to be used in textile applications. Next, trials are continued with commercial spinning and texturising machines. In this technology firstly chips are dried and cristialized then melted in extruder and finaly occur in filament yarn form by cooling the polymer melt and subsequently winding processes. POY yarns were converted into texturized yarn by heat, drawing and false twisting parameters. Tensile strength and breaking elongation analyzes were carried out according to DIN EN ISO 2062 / STATIMAT, evenness (DIN 53817/Uster) and other physical tests KORTEKS in house methods. Thermal characterization analyzes were performed with DSC instrument. Enhanced PLA texturized yarns will be turned into fabric form by weaving process. Plain weave, twill and satin weaving constructions will be used at fabrics. Tensile strength (ISO 13934-1), breaking strength (ISO 13937-1), and abrasion test (ISO 12947-1999, 20.000 cycle) will be carried out with reference PET (Poly Ethylene Teraftalate) fabrics.

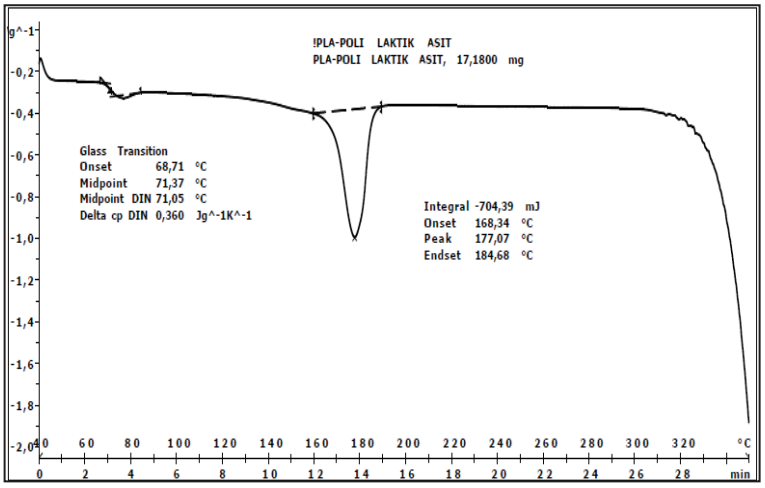


**Figure 2.** DSC graphic of PLA polymer

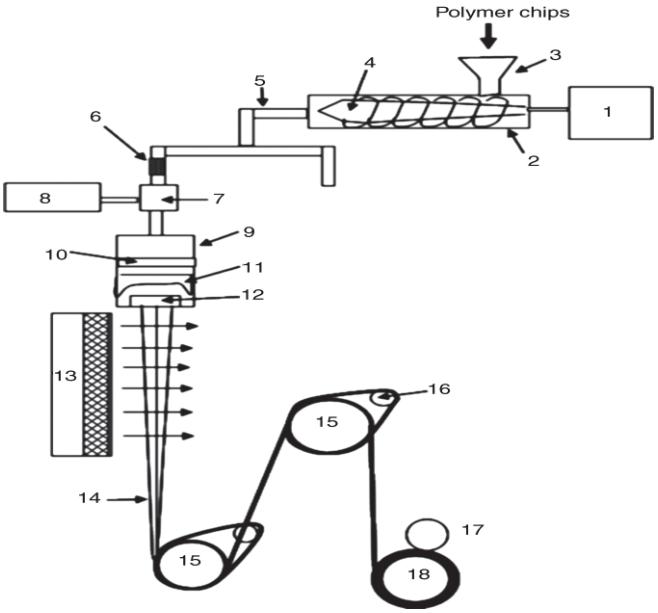


**Figure 3.** Melt Spinning Technology schema [7]

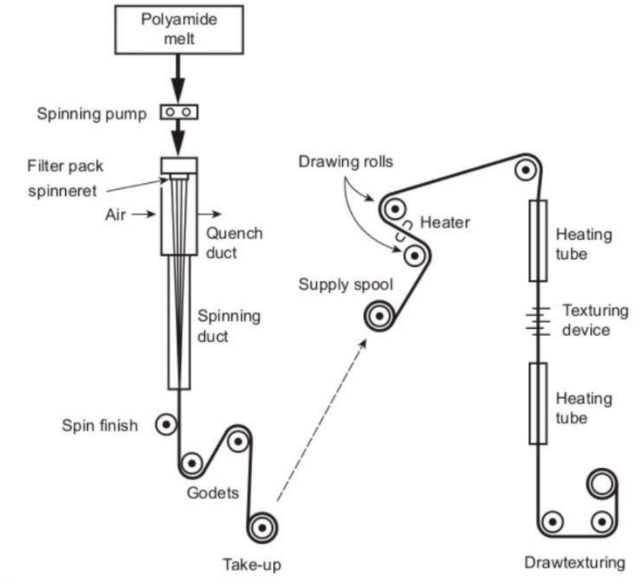


**Figure 4.** Texturising Process Technology schema [8]

## 3. RESULTS AND DISCUSSION

PLA filament yarn are produced and developed by R&D trials. Starting from 68 denier upto 300 denier POY and FDY Super Bright yarns are produced. The trials perfomed successfully to ocur commercail PLA yarn product. Mechanical properties of yarns are stabil and enough to be used in woven and knitted fabrics.

**Table 1**. PLA POY and FDY pyhsical analyses

| Yarn Property | Tenacity (cn/dtex) | Elongation at break (%) | Uster (%um) | Shrinkage at boiling water (%) |
|---|---|---|---|---|
| PLA 150 denier 36 filament Round POY | 1,93 | 83 | 0,89 | 71 |
| PLA 150 denier 36 filament Round FDY | 3,7 | 30 | 0,63 | 9 |

150 denier 36 filament Texturised yarns are chosen to design fabric construction. Plain, twill and sateen constructions are applied in weaving process. All fabrics performed satisfactory performance in warping and weaving process. Tensile strength (ISO 13934-1), breaking strength (ISO 13937-1), and abrasion test (ISO 12947-1999, 20.000 cycle) will be carried out with reference PET (Poly Ethylene Teraftalate) fabrics.

**Table 1.** PLA Fabric Constructions

| Sample Code | Weft Yarn | Warp Yarn | Yarn Density | Construction |
|---|---|---|---|---|
| 1 | 150/36 Round Strong Intermingled Texturised | 150/36 Round Strong Intermingled Texturised | 30/29 | Plain weave |
| 2 | 150/36 Round Strong Intermingled Texturised | 150/36 Round Strong Intermingled Texturised | 30/29 | 3/2 twill |
| 3 | 150/36 Round Strong Intermingled Texturised | 150/36 Round Strong Intermingled Texturised | 30/29 | 5 sateen |
| 4 | 150/36 Round Strong Intermingled Texturised | 150/36 Round Strong Intermingled Texturised | 30/29 | 3/2 twill |
| 5 | 150/36 Round Strong Intermingled Texturised | 150/36 Round Strong Intermingled Texturised | 30/29 | 5 sateen |
| 6 | 150/36 Round Strong Intermingled Texturised | 150/36 Round Strong Intermingled Texturised | 30/29 | Plain weave |

## 4. CONCLUSION

PLA is a special material from renewable sources that has biodegradation and biocompostable property after use life. Its features give highlight to its importance at sustainabiity. In this study Different PLA filament yarns are produced and physical and thermally characterized. Future works will focus on to developing new commercial PLA filament yarn types with new R&D trials. In addition biodegradation and biocompast tests will also be performed.

## REFERENCES

1. Dorgan JR, Lehermeier H, Mang M.. Thermal and rheological properties of commercial-grade poly(lactic acids)s. J Polym Environ 8:1–9., 2000
2. CONN RE, Kolstad JJ, Borzelleca JF, Dixler DS, Filer LJ, LaDu BN, Pariza MW."Safety assessment of polylactide (PLA) for use as a food-contact polymer". Food Chem Toxicol 33:273–83, V
3. HENTON David .E.,GRUBER Patrick., LUNT Jim And RANDALL Jed., (2005)" Natural fibers,Biopolymers and biocomposites / Polylactic acid Technologhy book chapter 16 .
4. B Gupta, N Revagade, J Hilborn - Progress in polymer science, 2007 - Elsevier
5. Doç.Dr. Hüseyin Aksel EREN , Y.Doç.Dr. Osman Ozan AVDİNÇ, "Ozonun Polilaktik Asit (PLA) Liflerine Etkisi ve PLA Terbiyesinde Ozon Kullanımı" 2010, BAP Proje No: 109M266,
6. Ebru TEKTEMUR, POLİ (LAKTİK ASİT) ÜRETİMİNE İŞLETME PARAMETRELERİNİN ETKİSİ, 2011, yüksek lisans tezi, Ankara Üniversitesi
7. https://www.google.com.tr/search?q=CERT%C4%B0F%C4%B0CAT%C4%B0ON&rlz=1C1RLNS_trTR802TR802&source=lnms&tbm=isch&sa=X&ved=0ahUKEwiWwo-FueTcAhVQ3aQKHQqqDbAQ_AUICigB#imgrc=zKuHIt35-oZt9M:
8. C.Lawrance, Fibre To Yarn: Filament Yarn Spinning, 2015

# IMPLEMENTATION OF DIGITAL TECHTEX MANUFACTURING CONCEPTS – INTERDISCIPLINARY ANALYSIS OF BENEFITS, RISKS AND REQUIREMENTS

**Jan Vincent JORDAN[1], Robert PETERS[2], Philip MARSCHALL[3], Thomas GRIES[1]**

[1] Aachen University, Institut für Textiltechnik of RWTH, Germany
[2] Aachen University, Research Unit for Economics and Social History and History of Technology of RWTH, Germany
[3] Aachen University, Chair of Economic Geography of RWTH, Germany

Corresponding author: jan.jordan@ita.rwth-aachen.de

***Abstract:*** *The term "Industry 4.0" is a subject of intense discussions, especially among experts in the textile manufacturing sector. On one hand it is seen as a new paradigm of industrial production in which digital processes, real-time data and cyber-physical production systems are being deployed to increase quality and overall efficiency. On the other hand it is decried as a synthetic, made-up technological revolution which only serves for marketing uses. Whatever attitude we have towards the concepts that surround the term "Industry 4.0", we can assume that digital manufacturing technologies will have a strong impact on the quality of manufacturing processes, products and the working conditions of the affected employees.*

*Profound changes are predicted across all industry branches and along entire value chains. Not least in the textile industry, where an increase of digital transformation is already becoming increasingly apparent in the production of technologically advanced technical textiles. Implications of this change are estimated to be far-reaching and require concepts beyond the technical engineering sphere to understand the consequences both for industry and society and to provide a sustainable diffusion of Industry 4.0. In present work an overview will be given over the implementation of digital manufacturing concepts in the field of technical textiles. The benefits, needs and requirements for an implementation have to be evaluated from case to case as the correct "digital strategy differs with regard to the product portfolio and the structure and philosophy of every company.*

***Key Words****: Digitalization, Industry 4.0, Quality Control 4.0, Implementation, Requirements*

## 1. INTRODUCTION

According to [1], approximately 120,000 employees were employed in the textile and clothing industry throughout Germany in 2015. In 1975 there were still about 1.1 million employees working in this industry throughout Germany [2, 3]. The significant decline in employment figures (see Figure 1) is closely connected to the structural changes that the industry went through as manufacturing of

traditional textiles (e.g. home textiles and apparel) was more and more outsourced to low-wage countries.

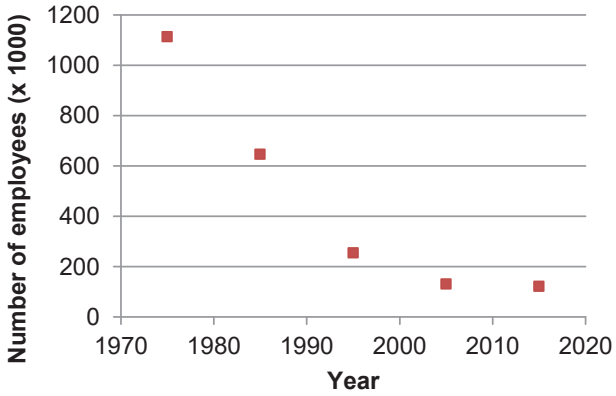


**Figure 1.** Decline of employment figures from 1975 till 2015 according to the statistical yearbooks of the Federal Republic of Germany (from 1990 on) as well as the statistical yearbooks of the German Democratic Republic (before 1990) [1 – 7]

Mostly a focus on technical textiles led to a stabilization of the employment numbers and a market with a significant growth could be established [8]. Nevertheless a number of manufacturers of traditional textiles still persists. Reasons for their ability to sustain can be that they include technical textiles in their pproduct portfolio or that they provide traditional textiles with unique features (e.g. outstanding quality, flexibility with regard to quickly changing customer demands and short delivery times). The concepts that are linked to the term „Industry 4.0" are ment to support the industry to be „ready for the future" [9]. Hence the textile „Industry 4.0" should apply to manufacturers of technical textiles as well as to manufacturers of traditional textiles. Nevertheless „Industry 4.0" is still a very abstract term to many stakeholders in the textile industry. Due to their heterogeneity with regard to production processes and product portfolio as well as the historically grown infrastructure of production at their sites companies may not expect to be offered the one digital solution that is suitable to fulfill every company's needs. The digital transformation is a process which has to be given time and which has to be implemented step by step. Therefore a thorough analysis of an individual company's manufacturing structure has to be applied, to ensure that the transformation is carried out according to the companies' philosophy and values. The transformation can only be successful, if the employees are open towards the process of change and hence are willing to participate in the implementation changes.

Present work outlines and discusses an explorative, interdisciplinary research project analyzing the requirements and potential effects of Industry 4.0 transition in three traditional German textile clusters. The project team develops a holistic model for explaining technology-driven impacts on the textile production system by providing a historical, spatial/network as well as an engineering perspective

within the conceptual framework. The aim of the project is to provide an increased level of awareness towards the changes that are to be borne by the textile industry and the society due to the “digital transformation”. Furthermore, the applicability of tools is investigated that are intended to support companies in defining their digital road map and to determine their next steps towards digital transformation.

Embedded in this interdisciplinary research approach, the working group Economic Geography concentrates on possible structural changes of Industry 4.0 within the textile value chain and their representation on a regional, national and global level. The focus of this study is on three traditionally grown and highly innovative tech textile clusters in Germany: Aachen-Niederrhein, Münsterland-Ostwestfalen-Lippe and Western Saxony. Stakeholders within the textile value chain are investigated with regard to their interaction with other regional, national and international textile and non-textile stakeholders. It is examined how the interaction between different stakeholders is or will be affected by Industry 4.0 concepts and which barriers can be identified that slow down the establishment of Industry 4.0 across companies and industries.

Within the presented project the Institute for Economic and Social History and History of Technology focuses on the importance of tradition. Furthermore it is investigated to which extent a company that has already lived through one or more technological revolutions can enhance its readiness with regard to coping with the digital transformation.

The Institut für Textiltechnik (ITA) investigates selected companies from a textile engineering perspective with regard to their „Digital Roadmap”. Fields of this in-depth investigation consequently include the manufacturing process and its organisational infrastructure, the current and target product portfolio as well as the relevant stakeholders within the manufacturing process. The aim of this investigation is to determine how companies are currently experiencing the topic „Industry 4.0”, how they are currently set up with regard to their digital transformation process and in which field of digitalization they want to put a stronger focus. As the digital transformation is widely perceived as a rather abstract technological phenomenon that has to be interpreted by every single company individually for itself [10] one crucial information for the decision-takers is to determine what next steps in the implementation of digitalization concepts will make the most sense to them. Special attention is hence paid to the implementation requirements that have to be met in order to allow the relevant stakeholders in the company to participate in the transformation process so that they can shape the change and are able sustain it.

The results of the above mentioned investigations are in a second phase of the project considered to build up a basis for the creation of different scenarios (Figure 2). These scenarios shall describe possible states of the textile industry due to the impact of the digital transformation in a time-line of 15 years. The impact of digital transformation is evaluated focusing on various transmission channels as described in [11]. These transmission channels hence are linked to

the potential social, technological, economical, political, legislative and environmental impact of the digital transformation.

From these scenarios suggestions for the industry, politics and economy shall be derived, to support a most beneficial scenario for the affected stakeholders.

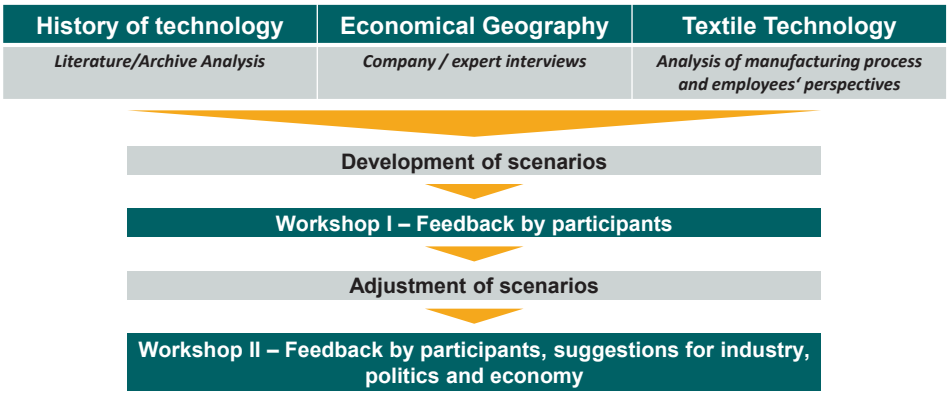


**Figure 2**. Project structure

## 2. METHODOLOGY & EMPIRICAL DESIGN

The in-depth investigation of ITA is based on the use of three tools. These tools are described in the following.

### 2.1 Semi-structured interview and digital maturity

The first tool is a semi-structured company interview designed by the working group Economic Geography, which supports the participants to broaden their view on digital transformation and to bring this term in connection with their own company. This interview includes a set of questions dealing with the interviewed company's tradition and experience with technological revolutions from the past. The interview has a further set of questions with a focus on the textile engineering perspective.

When the focus is put on the textile engineering perspective, the second tool is used which is an investigation of the current digital state of the company. Hence questions are asked to determine what has been described by [12] as the company's "Industry 4.0 Maturity Index". This assessment is the basis for the digital roadmap of the company. It is most important to take the digital maturity into account as a company with an already well-established digitalization of the manufacturing process requires a completely different set of action compared to a company which is just at the beginning of digital transformation.

### 2.2 Guideline for the implementation of Smart Factory concepts

To determine in detail, the first steps that are to be taken to bring the company's digital transformation forward the third tool is applied. This tool is the "Guideline

for the implementation of Smart Factory concepts“which has been developed by ITA’s Arash Rezaey et. al. in the German research project “Smart Factory” of the “futureTEX” project framework [13]. The Guideline for the implementation of Smart Factory concepts aims at analyzing the manufacturing process and to determine the most critical failures that may occur. An excerpt of the guideline is displayed in Figure 3.

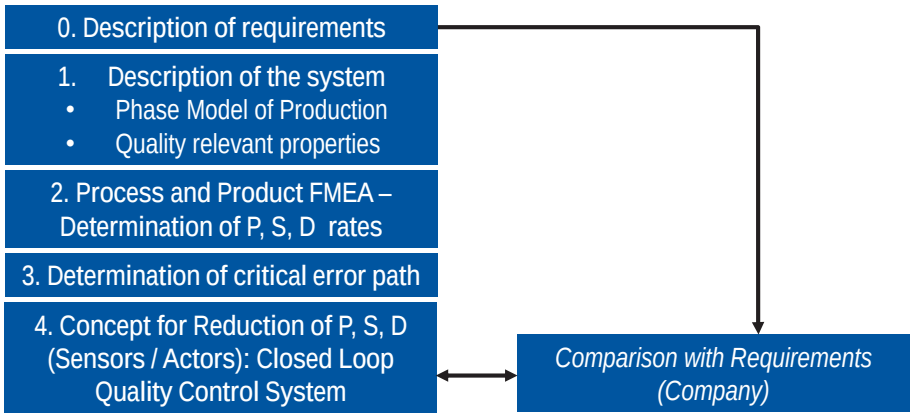


**Figure 3**. Guideline for the implementation of Smart Factory concepts [14]

The Guideline suggests starting with a description of the company’s implementation requirements for digitalization concepts from the CEO’s perspective. These requirements consequently are determined in a discussion with the company’s management level. This assessment of requirements includes e.g. a definition of maximum implementation costs and duration as well as the definition of the project team.

In a further conversation (“1. Description of the system”) in which the company’s project team participates, the manufacturing process with its organizational structure and the relevant stakeholders is discussed.

Consequently a product and process FMEA according to [15] is carried out for a selected article. Hence failures that have occurred in the manufacturing process are identified. Every failure is evaluated with regard to its criticality. This criticality is expressed by the risk priority number (*RPN*). The *RPN* is a dimensionless size and it is a function of a selected failure’s probability of occurrence (*P*), its severity (*S*) and its likelihood to be detected (*D*). Usually the dimensions *P*, *S* and *D* are assigned values in the range of 1 to 10. The (*RPN*) is then calculated to $RPN = P \times S \times D$.

In the next step the failures with the highest *RPN* are (in a discussion with the project team) tracked throughout the manufacturing process. Hence the critical failure path is determined as every failure has at least one origin and one

consequence in the manufacturing process. The origin can be e.g. an irregular set of processing material characteristics, defect of machine parts, environmental disturbances or human failure. The consequences may e.g. be reduced product quality, production stop or in the worst case the injury of employees.

Consequently it is determined how the values of *P*, *S* and *D* of the selected error can be reduced. Characteristics which indicate the occurrence of a failure e.g. can be detected via an external sensor system. This would enhance its likelihood of detection (and thus decrease the value *D*). Furthermore actuation concepts for the compensation of severity of failure consequences are identified. In this way a set of sensor and actuation concepts is established which can be evaluated with regard to the fulfillment of the pre-stated company's implementation requirements.

A suitable concept would then be selected for a validation test. After a successful validation test the criticality of the selected failure is reduced and the digital maturity of the company is expected to have increased.

### 2.3 Requirements for the establishment of an ideal smart factory

As costs induced by failures rise significantly with increasing time till detection, a goal is to obtain data relevant for product and process quality as early as possible. The most sophisticated goal is to obtain real-time data which can be used to predict process instabilities and hence completely prevent the occurrence of failure. This ideal situation requires the permanent acquisition and automatic interpretation of data ("Big Data"). Furthermore a precise model of the interdependencies of material, machine and process data is required to predict the effect that a deviation of a target input value has on a target output value. This sophisticated approach is only applicable for manufacturing systems with thoroughly defined system borders and well understood interdependencies of material, machine and process data. Hence such a sophisticated approach is expected to be applicable only to a small number of companies and their manufacturing processes.

## 3. IN-DEPTH INVESTIGATION OF INDIVIDUAL COMPANIES

A number of up to 6 companies from the selected regional textile clusters are investigated with regard to expected benefits, potentials and risks of digital transformation as well as requirements for a successful implementation of Industry 4.0 concepts. In the following the first results gathered in the investigation of the selected participating companies are presented.

### 3.1 Results of the semi-structured interview and the estimation of the digital maturity

Whilst carrying out the semi-structured interview which is used for the preparation of the in-depth analysis a number of insights were obtained:

- The term "Industry 4.0" is widely regarded as a marketing term rather than a new paradigm of production technology

- "Industry 4.0" is perceived as a trend that "*the whole industry seems to participate in*"
- A number of apparent benefits that the digital transformation offers are understood
- The inability of implementation of digital concepts is perceived as a risk, especially as the digital maturity of competitors is unknown
- The companies are concerned about their own "digital maturity" and seek to determine how digitally mature they are compared to their competitors
- "Industry 4.0" is a very abstract complex of technologies which are difficult to be understood and brought into a reasonable relation with the own company
- The questions that the companies are asked during the interview result in a better understanding of the concepts surrounding "Industry 4.0"
- Digitalization is understood in very different ways
- Out of the complex set of "Industry 4.0" concepts very specific approaches are regarded beneficial for the company

Hence only by being confronted with questions with regard to Industry 4.0 and what this term means for the respective company, the understanding of the digital transformation already is enhanced.

As the companies were introduced to the "Industry 4.0 Maturity Index" the companies were able to assign their manufacturing process one of the six levels of digital maturity. It became evident that specific parts of the manufacturing process had a higher degree of digital maturity than other parts of the process of the respective company. Consequently, most of the participating companies already use Enterprise Resource Planning (ERP) software. Nevertheless, information that stakeholders within the process chain rely on to carry out their tasks is transferred via paper sheets. This results in inconsistencies in the flow of information and is hence a significant source of failures.

### 3.2 Lessons learned by the application of the Guideline for the implementation of Smart Factory concepts

The participating stakeholders of the respective manufacturing processes had in a number of cases an insight into how failures in "their" process step affect down-stream process steps and the product quality. The understanding of the importance of the failures that occur in the "own" process step could be enhanced by a digital solution, visualizing origin and effect of typical failures. Such a digital solution was broadly accepted by the participants.

The implementation requirements of digital concepts will be most challenging with regard to technology acceptance of the employees. Especially if workers are used to rely on a system of documentation and transfer of information based on paper sheets for decades, instructions transferred via ERP systems are not likely to be implemented. Only if the employees witness the benefits of a digital system (e.g.

increased handling comfort and availability of relevant information), it will be accepted.

Stakeholders throughout the manufacturing process wish to obtain real-time data of up-stream and down-stream process steps. Nevertheless the set of data that a specific stakeholder is interested in is not comprehensive. ERP software basically grants this real-time availability of relevant information. Nevertheless many of the available ERP systems still do not provide the complete sets of data and interfaces that manufacturers with a wide product portfolio and heterogeneous machinery ask for. Especially real-time data which should be directly transferred from machines to the ERP system is not available as the machine manufacturers do not provide access to their machine data. In other cases old machinery was not intended to be linked to a software system at all and hence lacks the necessary interfaces.

The participating companies welcomed the application of the presented guideline as it in 80% of cases led to the identification of further steps towards digital transformation. The suggested actions are in every case customized with regard to the companies needs and its digital maturity.

## 4. CONCLUSIONS

As the future of production cannot clearly be foreseen, the presented project aims at giving the affected industry and society an insight of how change will evolve and how to be prepared. Especially for the manufacturing of technical textiles the presented project is of significant relevance, as a number of 50 companies (most of which are active in the field of manufacturing of technical textiles) contributed to the project. Tools such as the presented Guideline on the implementation of Smart Factory concepts have shown to reduce the perceived degree of complexity of Industry 4.0. As stakeholders have the chance to express their own view on which degree of digitalization is suitable to be implemented in a selected range of their manufacturing process an important benefit is achieved. The stakeholders are not only affected by the change, they rather participate in designing it. Hence the willingness of employees to accept and use the new digital technologies increases significantly. This is expected to result in a reduced time for implementation as well as in a persistent positive impact of the implemented technology on employee satisfaction and hence product and process quality.

## ACKNOWLEDGMENTS

This work has been carried out in the project “Wirtschaftsräumliche Implikationen von Industrie 4.0 in relationaler Perspektive: Innovation, Evolution, Organisation und Interaktion; untersucht am Beispiel der deutschen Textilindustrie (WiSoTex 4.0)” funded by the Deutsche Forschungsgemeinschaft (DFG) of Germany. The authors would like to express their gratitude to the companies and experts that contributed to the research.

## REFERENCES


1. NN: Statistisches Jahrbuch 2017, Statistisches Bundesamt, Berlin (2017)
2. NN: Statistisches Jahrbuch für die Bundesrepublik Deutschland - 1976, Bundesrepublik Deutschland und West-Berlin; Statistisches Bundesamt, Berlin (1976)
3. NN: Statistisches Jahrbuch der Deutschen Demokratischen Republik 1976
4. NN: Statistisches Jahrbuch für die Bundesrepublik Deutschland - 1986, Bundesrepublik Deutschland und West-Berlin; Statistisches Bundesamt, Berlin (1986)
5. NN: Statistisches Jahrbuch der Deutschen Demokratischen Republik 1986
6. NN: Statistisches Jahrbuch für die Bundesrepublik Deutschland - 1997, Bundesrepublik Deutschland; Statistisches Bundesamt, Berlin (1997)
7. NN: Statistisches Jahrbuch 2007, Statistisches Bundesamt, Berlin (2007)
8. NN: Technische Textilien – Branchenreport – Corporate Sector Report, Commerzbank AG, Frankfurt (2014)
9. Dorst, W. (Editor): Umsetzungsstrategie Industrie 4.0 - Ergebnisbericht der Plattform Industrie 4.0; Berlin, Frankfurt (2014)
10. Giebeler, M.; Jansen, K.; Spiesecke, H.: INDUSTRIE 4.0 IN DER TEXTIL- UND MODEPRODUKTION – Tagungsbericht, Gesamtverband der deutschen Textil- und Modeindustrie (Editor), Berlin (2016)
11. Peters, Robert, Labour Market Regulation and Its Commercial and Economic Impact - A Preindustrial Case Study, WST Working Paper Series 2/2017, SSRN ID 3082826, 2017
12. Schuh, G.; Anderl, R.; Gausemeir, J. ten Hompel, M; Wahlster, W.: Industrie 4.0 Maturity Index - Die digitale Transformation von Unternehmen gestalten; (acatech STUDIE), München: Herbert Utz Verlag (2017)
13. Rezaey, A. Jordan, J.; Gloy, Y.-S.: Ermittlung kritischer Prozessgrößen und Beschreibung einer Maschinenkommunikationsstrategie für Webereien; In: Technische Universität Chemnitz / Institut für Betriebswissenschaften und Fabriksysteme (Editor): futureTEX Basisvorhaben Smart Factory - Entwicklung von Prozessen und Strukturen für den Aufbau von Smart Factories in der Textilindustrie und Ableitung von typischen Industrie 4.0 Anwendungen: Schlussbericht. - Chemnitz: Technische Universität Chemnitz, 2017, pp. 39-50
14. Rezaey, A.; Jordan, J.; Dangel, R.; Gries, T.: PPE manufacturing 4.0 : supporting manufacturers in implementing the new EU PPE regulation; In: Citeve Technologia Textil (Ed): Abstracts / 8th European Conference on Protective Clothing ; Upcoming Generation, 7th to 9th of May 2018, Porto, Portugal. - Vila Nova de Famalicão : Citeve, 2018, pp. 102-104
15. NN: DIN EN 60812 - Analysis techniques for system reliability – Procedure for failure mode and effects analysis (FMEA) (IEC 60812:2006);

# AN INVESTIGATION ON CONDUCTIVITY OF POLYETHYLENE TERAPHTALATE FABRICS MODIFIED WITH METHYL-TRI-N-BUTYLAMMONIUM METHYL SULFATE

**Yasemin SEKİ**

Dokuz Eylul University, Department of Textile Engineering, Turkey

Corresponding author: yasemin.seki@deu.edu.tr

***Abstract:*** This work attempts to enhance electrical conductivity of polyethylene teraphtalete fabrics (PET) via ionic liquid modification. The PET fabrics were modified with methyl-tri-n-butylammonium methyl sulfate in ethanol at 10, 15 and 20% concentrations. After modifications, surface resistivity and thermal conductivity of the PET fabrics were measured. Additively, functional groups and surface morphology of the fabrics were investigated by fourier infrared spectroscopy and scanning electron microscopy, respectively. Under the lights of the test results, surface resistivity of the PET fabrics dramatically decreased with ionic liquid modification. In other words, electrically conductive performance of PET fabrics enhanced by the use of ionic liquid. Thermal insulation of the PET fabrics enhanced after modification at low concentration of the ionic liquid. New functional groups were introduced on PET fabric after modification. SEM photographs confirmed the existence of ionic liquid both in the gaps and on the surface fabrics and also adhesion to PET.

***Keywords:*** *polyethylene teraphlatate, ionic liquid, electrical conductivity, PET*

## 1.INTRODUCTION

Polyethylene teraphtalate (PET) is a most commonly used man made fibers in textile industry. Great potential as usability in apparel, home and technical textiles with their superior thermal and mechanical properties, their high electrical resistance restricted their applications. In accordance with the related literature, many attemptions were performed to improve conductivity of PET [1-5]. To our best knowledge, no study was found to investigate the effect of ionic liquid on conductivity of PET fabrics.

Ionic liquids are generally stated as liquids composed of ions. The ionic liquids which are also determined as molten salts exhibit properties change with aqueous and organic solvents for chemical processes. Ionic liquids are also known as green solvents and commonly used in chemistry and industry for chemical stability, ionic conductivity, non-flammability, thermal stability and so on [6,7]. Ionic liquids (ILs) can add value to many chemical processes as well. Many of ionic liquids are related with its unique character of molten salts at room temperature which existed as conductive liquids (Vila et al., 2006). 8

This current study aims to modify polyethylene teraphtalate fabrics with methyl-tri-n-butylammonium methyl sulphate to enhance conductivity performance. For this purpose, PET fabrics were modified with methyl-tri-n-butylammonium methyl sulfate with different concentrations and surface resistivity and thermal conductivity measurements were handled. Additively, functional groups and surface morphology of the PET fabrics were observed by fourier transform infrared spectroscopy and scanning electron microscopy, respectively.

## 2.MATERIALS AND METHODS

PET knitted fabric was used in this study. The ionic liquid, methyl-tri-n-butylammonium methyl sulfate, was provided from Sigma-Aldrich Corp.

BIL was dissolved in ethanol in 10, 15, 20 w/v% concentrations and continuously stirred via magnetic stirrer until totally dissolved. PET fabrics were treated with the EIL solutions for 5min at ambient temperature and after removing the excessive solution from the fabric samples, PET fabrics were dried at room temperature. Table 1 gives sample codes of the PET fabrics.

**Table 1.** Sample codes of the PET fabrics

| Fabric code | Concentration |
|---|---|
| **F** | Untreated |
| **F10** | 10% ionic liquid treated |
| **F15** | 15% ionic liquid treated |
| **F20** | 20% ionic liquid treated |

Surface resistivity tests of the PET fabrics were carried out according to ASTM D 257-9 using 6517B/E Keithley Electrometer/High Resistance Meter. Thermal conductivity performance of the PET fabric samples was determined by using C-Therm TCI Thermal Conductivity Analyzer. Thermal degradation of the PET fabrics was determined by thermogravimetric analysis. Thermogravimetric analysis (TGA) was carried out by Perkin Elmer STA 8000 TG/DTA by heating from room temperature to 700$^{o}$C by a heating rate of 10oC/min under N2 atmosphere to avoid oxidation effects. Surface morphology of the PET fabrics was optically viewed by using JEOL-JJM 6060 model scanning electron microscopy (SEM) operated at 5kV. The samples were coated with gold by plasma sputtering method.

## 3. RESULTS AND DISCUSSION

Surface resistivity of the unmodified PET fabrics was obtained to be $7.45x10^{11}$ ohm/sq. After 10, 15 and 20% ionic liquid modification, the surface resistivity of the PET fabrics noticably decreased to $3.62x10^{6}$ ohm/sq, $1.60x10^{6}$ ohm/sq and

$1.38x10^6$ ohm/sq, respectively. This can be due to the high electrical conductivity performance of the ionic liquids [9].

Table 2 gives the thermal conductivity and effusivity values of PET fabrics. It is noticeable that ionic liquid treatment decreased thermal conductivity of the PET fabrics clearly at low concentrations. However thermal conductivity increased after 15% concentration. It is probable to reveal that there can be an optimum point for ionic liquid concentration to enhance thermal insulation of PET fabrics. Thermal conductivity of the ionic liquids depends on their chemical structure [10].

**Table 2.** Thermal conductivity and effusivity values of the PET fabrics

| | Thermal conductivity k (W/mK) | Thermal effusivity (Ws½/m²K) |
|---|---|---|
| **F** | 0.30±0.05 | $6.71 \times 10^{14}$±0.58 $x10^{14}$ |
| **F10** | 0.21±0.03 | $5.54 \times 10^{14}$±0.37 $x10^{14}$ |
| **F15** | 0.17±0.01 | $5.11 \times 10^{14}$±0.18 $x10^{14}$ |
| **F20** | 0.29±0.05 | $5.73 \times 10^{14}$±0.23 $x10^{14}$ |

TGA data of the PET fabrics are listed in Table 3. TGA was performed to determine the effect of ionic liquid treatment on thermal stability of the fabrics. The mass loss at 120°C is due to the dehydration of PET. It is notable that moisture content of PET fabrics decreased with increasing ionic liquid concentration. The temperatures at which 10% and 50% mass losses are occurred decrased after treatments. Therefore, it may be probable to state that thermal stability of the PET fabrics deteriorated after treatments. This may be due to the low thermal stability of the ionic liquids.

**Table 3.** TGA data of the PET fabrics

| | Mass loss at 120°C (%) | $T_{10\%}$ (°C) | $T_{50\%}$ (°C) | Char yield (%) |
|---|---|---|---|---|
| **F** | 0.21 | 411.99 | 439.87 | 18.16 |
| **F10** | 0.79 | 307.15 | 427.77 | 12.37 |
| **F15** | 1.73 | 302.20 | 418.74 | 12.14 |
| **F20** | 1.98 | 298.17 | 414.57 | 10.99 |

* $T_{10\%}$ (°C) and $T_{50\%}$ (°C) are the temperatures at which 10% and 50% mass losses occurred, respectively.

The surface morphology of the unmodified and modified PET fabrics was investigated by means of SEM. Figure 1 presents SEM images of the PET fabrics. It is observable that there is a coating layer both on the surface and in the gaps of the fibers. This can reveal that both of the ionic liquids have adhesion on the PET fabrics. Coating layer gets more prominent with increasing concentration of the ionic liquid.

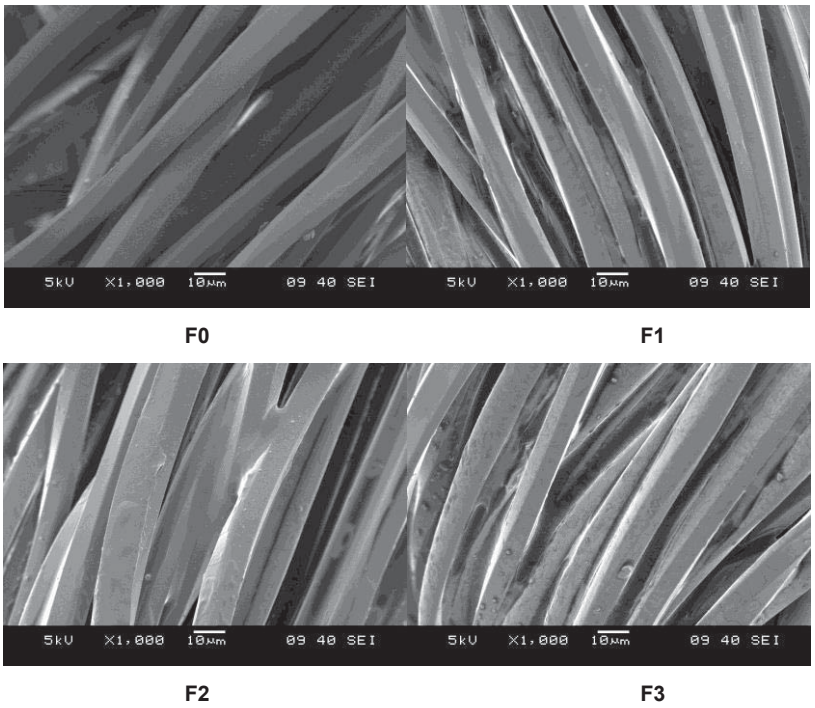


**Figure 1.** SEM imges of the PET fabrics

*F0: unmodified PET fabric; F1: 10% ionic liquid modification; F1: 15% ionic liquid modification; F1: 20% ionic liquid modification

## 4.CONCLUSION

In this study, PET fabrics were modified with methyl-tri-n-butylammonium methyl sulfate with different concentrations to enhance conductivity. Surface resistivity of the PET fabrics dropped of after ionic liquid measurement. This is related to the high electrical conductivity of ionic liquid. Concentrations in ionic liquid slightly affected the surface resistivity. There is an optimum point to enhance thermal insulation of the PET fabrics. Ionic liquid treatment decreased moisture content and deteriorated of PET fabrics. SEM observations confirmed the existence of ionic liquid both in the gaps of the fibers and on the surface of the fabric. Consequently, the ionic liquids can be good alternative to enhance electrical conductivity of the man-made fibers.

## REFERENCES


1. Lu, J.; Yan, F.; Texter, J. Advanced applications of ionic liquids in polymer science. Progress in Polymer Science 2009, 34 (5), 431-448.
2. Seki, Y.; Seki, Y. Development of Conductivity of Acrylic Polymer Using Ionic Liquids Incorporated with Zinc Oxide Nanoparticles, Polymer Plastics Technology and Engineering 2017, 56 (18), 1942-1948.
3. Steinert, B.W.; Dean, D.R. Magnetic field alignment and electrical properties of solution cast PET–carbon nanotube composite films, Polymer 2009, 50 (3), 898-904.
4. Mazinani, S.; Ajji, A.; Dubois, C. Fundamental study of crystallization, orientation, and electrical conductivity of electrospun PET/carbon nanotube nanofibers, Journal of Polymer Science Part B: Polymer Physics 2010, 48 (19), 2052-2064.
5. Xin, F.; Li, L.; Chan, S.H.; Zhao, J. Influences of carbon fillers on electrical conductivity and crystallinity of polyethylene terephthalate, Journal of Composite Materials 2012, 46 (9), 1091-1099.
6. Cruz-Delgado, V.J. et al. Carbon nanotube surface-induced crystallization of polyethylene terephthalate (PET), Polymer 2014, 55 (2), 642-650.
7. Mehmood, T.; Dai, X.J.; Kaynak, A.; Kouzani, A. Improved Bonding and Conductivity of Polypyrrole on Polyester by Gaseous Plasma Treatment, Plasma Processes and Polymers 2012, 9 (10), 1006-1014.
8. Vila, J., Gines, P., Rilo, E., Cabeza, O., Varela, L.M. (2006). Great increase of the electrical conductivity of ionic liquids in aqueous solutions, Fluid Phase Equilibria, 247(12), 32–39. 8
9. Zhang, Q.C.; Sun, S.S.; Pitula, S.; Liu, Q.S.; Welz-Biermann, U.; Zhang, J.J. Electrical conductivity of solutions of ionic liquids with methanol, ethanol, acetonitrile, and propylene carbonate. Journal of Chemical & Engineering Data 2011, 56, 4659 –4664.
10. Albert, J. And Müler, K. (2014). Thermal conductivity of Ionic liquids: An estimation approach, Chemical Engineering Science, 119, 109-113.

# INVESTIGATION ELECTRICAL PROPERTIES OF FABRICS COATED WITH BARIUM TITANATE AND GRAPHENE

**Gizem MANASOĞLU[1], Rumeysa ÇELEN[1], Mehmet KANIK[1], Yusuf ULCAY[1]**

[1]Uludağ University, Turkey

Corresponding author: gmanas@uludag.edu.tr

***Abstract:*** *The aim of the study is to investigate electrical conductivity of fabrics coated with barium titanate and graphene at different concentrations (50 and 100 g/kg). It is aimed to use coated fabrics for electrical conductivity and electromagnetic shielding applications. Pre-treated 100% polyester woven fabrics were used as substrat. Barium titanate ($BaTiO_3$) and graphene which have nano particle sizes were used as coating materials. Woven fabrics were coated by knife coating technique. The effect of material type and coating concentrations on electrical resistivity properties were examined.*

***Key Words****: Coating, graphene, barium titanate, electrical resistivity*

## 1. INTRODUCTION

Conductive textile surfaces play a major role in the production of products such as sensors, electromagnetic shielding, dust and bacteria prevention, static charge discharge [1]. Textiles can gain electrical conductivity with different methods such as using conductive polymers, conductive yarns or conductive coatings [2]. Most of the commercially available electromagnetic shielding fabrics are produced by coating technologies and have very homogeneous and closed structures thus exhibiting extremely high electromagnetic shielding capabilities [3].

Barium titanate is an inorganic compound which has the chemical formula $ABO_3$ ($BaTiO_3$) depending on the perovskite family. It is one of the most important ferro electrical materials studied in large scale. One-dimensional (1D) barium titanate nano materials such as nano fibers, nano tubes and nano strips attract attention due to their improvable properties and their potential applications in nano devices [4].

Graphene, which is composed of carbon atoms, is a two-dimensional material and has extraordinary properties in terms of mechanical, electrical, thermal and optical properties [5]. Grafen is a nano material which is the subject of many application fields and whose usage area is expanding [6]. In the literature, there are a lot of studies about fiber, yarn and composite structures added barium titanate and graphene in electrical conductivity and electromagnetic shielding

applications. However, in the literature, barium titanate has not been found to be used in fabric coatings.

## 2. MATERIAL AND METHOD

### 2.1. Material

Properties of woven fabrics were given in Table 1. Barium titanate ($BaTiO_3$) and graphene which have nano particle sizes were used as coating materials. Materials were supplied from Grafen Chemical Industries (Grafen Co.).

**Table 1.** Properties of woven fabric

| Property | Warp | Weft |
|---|---|---|
| Raw material | Polyester | Polyester |
| Density (1/cm) | 30 | 18 |
| Fabric structure | Plain weave | |

**Table 2.** Properties of graphene and barium titanate

| Property | Graphene | Barium Titanate |
|---|---|---|
| Particle size (nm) | 50-100 | 100 |
| Purity (%) | 96-99 | 99.9 |
| Surface area ($m^2/g$) | 13-15 | 10-11 |

### 2.2 Method

Pre-treated 100 % polyester woven fabrics were coated at 50 and 100 g/kg concentration rates. Coatings were made according to knife over roll principle and sharp pointed knife was used. The distance between the knife and fabric were arranged as 0.5 mm. Samples were dried at 100˚C for 10 minutes and they were fixed at 160˚C for 3 minutes on a laboratory type steamer (Rapid H-TS-3). For each material and concentration group, five pieces of fabric were coated and one of them was reserved for wet coating weight. Measurements were carried out by selecting the three most uniform samples among the remaining samples.


**Figure 1:** Ataç GK 40 RKL laboratory type coating machine

Thickness measurements of coated fabrics were made according to TS 7128 EN ISO 5084 standard with James Heal's R & B Cloth thickness tester.

The measurement of the fabric weights (g/m$^2$) was carried out in accordance with the TS 251 standard.

Surface resistance measurements of coated fabrics were made according to ASTM D 257 standard with Keithley 8009 Resistivity Test Fixture.

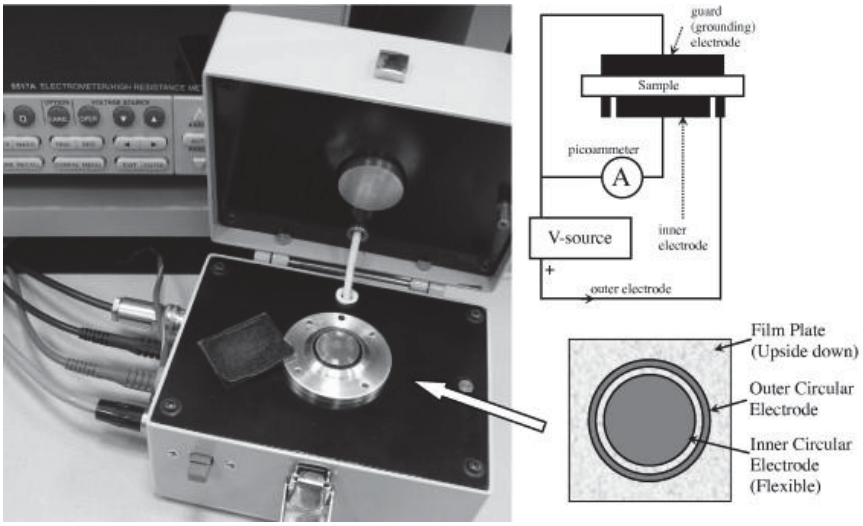


**Figure 2.** Keithley 8009 Resistivity Test Fixture

## 3. RESULTS AND DISCUSSION

### 3.1. Physical Test Results

Weight and thickness measurement results of the fabrics coated with graphene and barium titanate at two different concentrations (50 and 100 g/kg) were given in Table 3. As the concentration of the filler (the ratio of the solid content in the paste) increased, the fabric weight and the thickness increased.

**Table 3.** Fabric weight and thickness results of fabrics

| Sample Code | Concentration (g/kg) | Fabric Weight (g/m$^2$) | Fabric Thickness (mm) |
|---|---|---|---|
| **$R_1$** | - | 169 | 0.34 |
| **$R_2$** | - | 275.5 | 0.37 |
| **GR 50** | 50 | 292.16 | 0.39 |
| **GR 100** | 100 | 324.16 | 0.41 |
| **BT 50** | 50 | 290 | 0.39 |
| **BT 100** | 100 | 341.5 | 0.49 |

*$R_1$: Raw fabric *$R_2$: Coated fabric which has not filler material (graphene, barium titanate)

### 3.2. Coating Add-on Amounts

Add-on amounts of coated fabrics were given in Table 4. The amount of the substance transferred to the fabric increased in direct proportion to the increase in the concentration of the filler.

**Table 4.** Coating add-on amounts

| Sample Code | Concentration (g/kg) | Coating Add-on |
|---|---|---|
| **GR 50** | 50 | 123.16 |
| **GR 100** | 100 | 155.16 |
| **BT 50** | 50 | 121 |
| **BT 100** | 100 | 172.5 |

### 3.3. Electrical Resistivity Test Results

Table 5 shows that surface resistivity results depending on concentration rates. Increasing with graphene concentration, surface resistivity values decreased. The highest surface resistivity value ($1.36\times10^5$ Ω/sq ) was obtained at 100 g/kg graphene concentration rate. Electromagnetic shielding and heating textiles call relatively low resistivity levels less than $10^3$ Ω/sq [7,8], while the materials for electrostatic dissipative protective clothing should have the performance of around $10^9$ Ω/sq [9]. Electrical resistivity of barium titanate coated fabrics was not decreased. They have nearly same values with reference fabric.

**Table 5.** Surface resistivity test results of fabrics

| Sample Code | Concentration (g/kg) | Surface Resistivity (Ω / sq) |
|---|---|---|
| **$R_2$** | - | $2.61\times10^9$ |
| **GR 50** | 50 | $5.29\times10^7$ |
| **GR 100** | 100 | $1.36\times10^5$ |
| **BT 50** | 50 | $2.1\times10^9$ |
| **BT100** | 100 | $2.7\times10^9$ |

*$R_2$: Coated fabric which has not filler material (graphene, barium titanate)

## 4. CONCLUSIONS

This paper describes nano graphene and nano barium titanate coated fabrics by knife over roll technique. Thickness, fabric weight (g/m$^2$), surface resistivity measurements were performed.

As expected, according to reference fabric ($R_2$), surface resistivity values were decreased with increased graphene concentration ratios. Graphene coating has positive effect on electrical conductivity properties. In barium titanate coatings, some revisions will be tried for better results. In future works, alternative conductive materials will be studied and electromagnetic shielding effectiveness of coated fabrics will be measured. Different concentrations and processes will be studied.

## ACKNOWLEDGMENTS

The authors thanks to Res. Assist. Yasin ALTIN for support in electrical resistivity measurements.

## REFERENCES

1. Bedeloğlu A, Sünter N & Bozkurt Y: Electrically conductive textiles, production methods and usage areas. 2010. Journal of Textiles and Engineer, 17, 79.
2. Kilic G, Ortlek H.G, Saracoglu G.Ö: Electromagnetic pollution and textile barriers for protection from electromagnetic pollution. 2007. Journal of Textiles and Engineer, 14, 67.
3. Bonaldi, R. R, Siores, E, & Shah, T: Characterization of electromagnetic shielding fabrics obtained from carbon nanotube composite coatings. 2014. Synthetic Metals, 187, 1-8.
4. Zhuang Y, et al.: Fabrication and piezoelectric property of BaTiO 3 panofibers.2014. Journal of the American Ceramic Society, 97(9): 2725-2730.
5. Yıldırım H, Çakmak S: Electronic properties of buckled graphene. 2016. Suleyman Demirel University Journal of Science, 11(2), 102-108.
6. Bedeloğlu A, Taş M: Graphene and its production methods. 2016. AKU Journal of Science and Engineering. 16, 544-554.
7. Textiles for Protection, in: R.A. Scott (Ed.), Woodhead Publishing in Textiles, 2005, p. 784.
8. Intelligent Textiles and Clothing, in: H.R. Mattila (Ed.), Woodhead Publishing in Textiles, 2006, p. 528.

# WEARABLE SENSOR PRODUCTION FOR ECG MONITORING

**Hidayet KÖSE[1], Suat ÇETİNER[1], Gökhan TANDOĞAN[2]**

[1]Kahramanmaraş Sütçü İmam University, Turkey
[2]ISKUR Tekstil Ar-Ge Merkezi

Corresponding author: suatcetiner@ksu.edu.tr

***Abstract:*** *Electrocardiography (ECG) is a non-invasive method to monitor cardiac activity and can reveal vital information on cardiovascular disorders, including heart rhythm abnormalities, collectively known as arrhythmias or dysrhythmias. Modern biomedical systems allow the incorporation of high-performance ambulatory monitoring devices in commonly used elements such as clothing. These elements are known as wearable systems and belong to a strategic trend of technological devices that seek the improvement of the health care promotion. They have enabled continuous wearable monitoring of several physiological signals at a low cost, easily manufacturability and comfort. This study was conducted to develop diffirent methods for the fabrication of textile electrodes and analyse their characteristic features for use as electrocardiography (ECG) signal sensors. The conductivity of the textile substrate can also be modified by treating the textile with a polymer, thereby avoiding the use of metallic components in contact with the skin.*

***Key Words****: ECG, conductive polymer, conductive textile**, wearable sensors*

## 1.INTRODUCTION

Continuous health monitoring is an essential tool for accessing vital physiological functions. In 2012, cardiovascular diseases constituted about 42.8% of all noncommunicable deaths. One of the most important techniques used for monitoring physiological function is electrocardiography (ECG) [1].

In the past years, several groups have been working on the development of conductive textiles with different fabrication approaches, mainly exploiting either finished textiles, woven or stitched with fine metal wires, or silver coated synthetic fibers. Compared to the former, the latter achieve better mechanical flexibility but still suffer the presence of a metallic material in contact with the skin. With the development of stable and highly conductive polymers, it is now possible to transform any finished non-conductive yarn into flexible conductors that can be used, either dry or wet, as a biosensor for electrophysiological signals [2]. Electronically conducting polymers (ECPs) are a new class of conducting polymers (CPs) with high intrinsic conductivity and p-conjugated structure that possess the electrical, electronic, magnetic, and optical properties of metals or semiconductors while retain attractive mechanical properties and processing advantages of conventional organic polymers [3].

A new approach to highly conductive textile materials is the use of intrinsically conductive polymers. An interesting alternative is to create the conductive polymers by polymerization of monomers on the textile. Methods for in situ polymerization are well known for polypyrrole (PPy), polyaniline (PANI) and poly(3,4-ethylene dioxythiophene) (PEDOT). Recently, polymers derived from alkoxythiophenes like 3,4 ethylenedioxythiophene (EDOT) yielding poly(3,4-ethylene dioxythiophene) (PEDOT) find increasing interest [4].

In this study, we present the evaluation of novel wearable textile electrodes based on woven fabrics treated with conductive monomer 3,4-ethylenedioxythiophene. The electrical activity of the human heart was sensed by PET-PEDOT conductive polymeric fabric sensor on a smart garment [5].

## 2. MATERIAL AND METHOD

### 2.1 Material

A conductive monomer, Edot (97%), iron(III) chloride ($FeCl_3$) and *p*-toluensulfonic acid monohydrate (*p*-TSA) were used without further purification. All reagents were supplied from Sigma-Aldrich. Methanol, acetonitrile, acetone and ethanol were supplied from Merck and were used as received. A scoured and undyed 100% polyester (PET) woven fabric with a 256 gr/$m^2$ was selected.

### 2.2 Method

In this study,the *in situ* polymerization mechanism was given in Figure 1. PEDOT coated PET fabrics were produced by *in-situ* chemical oxidative polymerization method. The iron(III) chloride and *p*-toluensulfonic acid monohydrate were mixtured at room temperature with a magnetic stirrer for ½ h in a 50 mL of acetonitrile.The PET fabric was rinsed in acetone and distilled water to remove the contaminations of oilresidues and was dried in an oven at 80°C. Then PET fabric was wetted in acetonitrile which contains dissolved of iron(III) chloride and *p*-toluensulfonic acid monohydrate. The calculated amount of EDOT was added drop by drop to the acetonitrile-PET solution and mixtured for 3 hours with a magnetic stirrer. At the end of the polymerization, the PEDOT coated conductive PET fabric was rinsed with methanol, ethanol and distilled water for 15 minutes to remove the unpolymerized particles [5].

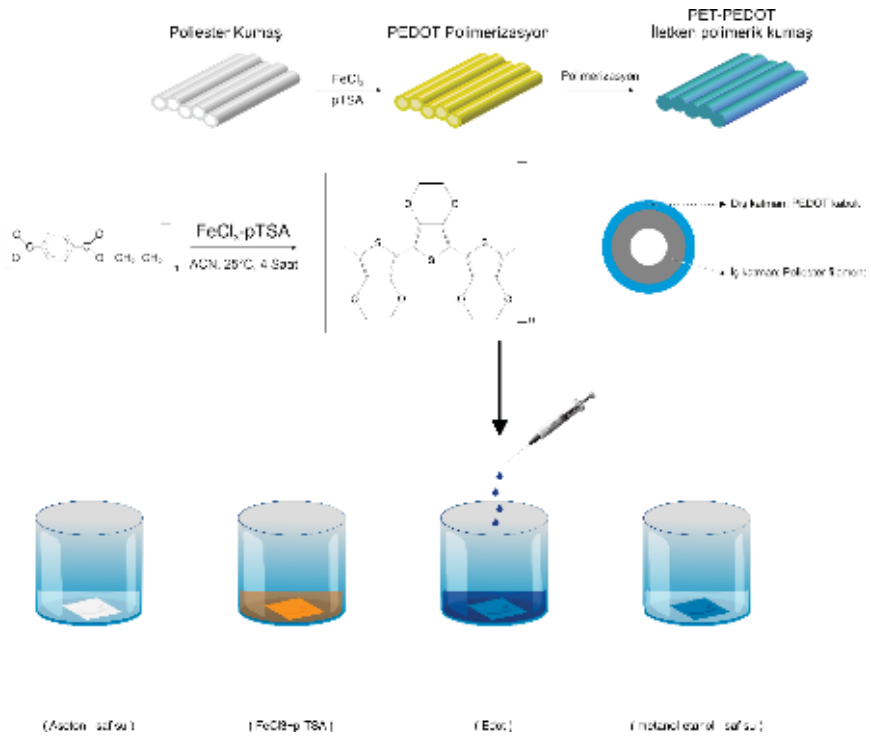


**Figure 1.** The Procedure of in situ chemical polymerization

## 3. RESULTS AND DISCUSSION

### 3.1 Analysis

Fourier Transform-Infrared (FT-IR) analysis for PEDOT coated polyester fabrics was performed using a Perkin Elmer Spectrum One. Scanning electron microscopy (SEM) analysis was carried out using a ZEISS/EVO LS10. Four point probe surface resistivity measurement was carried out using a ENTEK Electronics FPP 510.

#### 3.1.1. FTIR Spectrophotometric Analysis of PET-PEDOT Fabrics

Figure 2 presents the IR spectrum of the uncoated PET fabric and PEDOT coated PET fabric.

In the absence of PEDOT; a strong absorption band at 1712 $cm^{-1}$ is attributed to C=O stretching vibrations of PET. Other absorption peaks of polyester fabrics are aromatic ring stretching (1408 $cm^{-1}$), carboxylic ester or anhydride (1338 $cm^{-1}$), O=C–O–C or secondary alcohol (1090 and 1015 $cm^{-1}$), C=C stretching (969 $cm^{-1}$), five substituted H in benzene (871 $cm^{-1}$), two neighboring H in benzene (847 $cm^{-1}$) and heterocyclic aromatic ring stretching (722 $cm^{-1}$) [5,6].

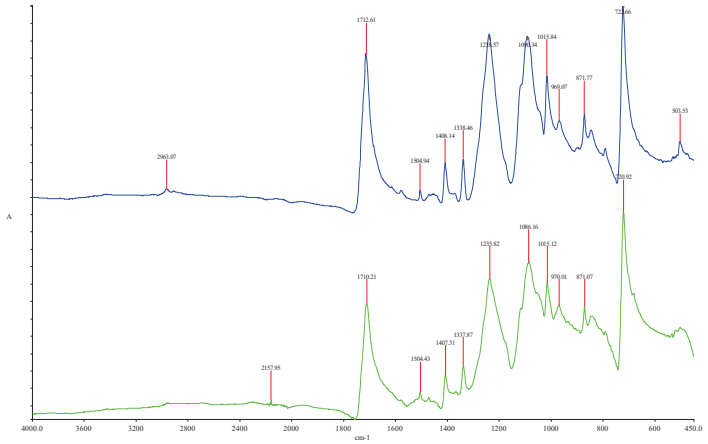


**Figure 2.** Fourier Transform Infrared Spectra of (a) PET Fabric, (b) PET-PEDOT Fabric [5]

In the presence of PET-PEDOT composite fabric, the absorption peak at 1,710 $cm^{-1}$ is usually associated with the doped state of PEDOT. An absorption band appeared at 1504 $cm^{-1}$ is assigned to asymmetric stretching mode of C = C that correspond to thiophene rings of PEDOT. Vibrations at 1407 and 1337 $cm^{-1}$ are attributed to the stretching modes C–C in the thiophene ring. The vibration peaks of the C–S bond in the thiophene ring can be seen at 970, 871 and 842 $cm^{-1}$. The bands at 1235 and 1086 $cm^{-1}$ are assigned to the stretching vibrations of the ethylenedioxy group [7,8].

So these results showed that the PEDOT formation could be followed by FTIR measurements in PET-PEDOT composite fabric structures.

### 3.1.2. Surface Morphology of PET-PEDOT Fabrics

Figure 3 shows the surface morphology of uncoated and (% 0,8 v/v) PEDOT coated PET fabrics.

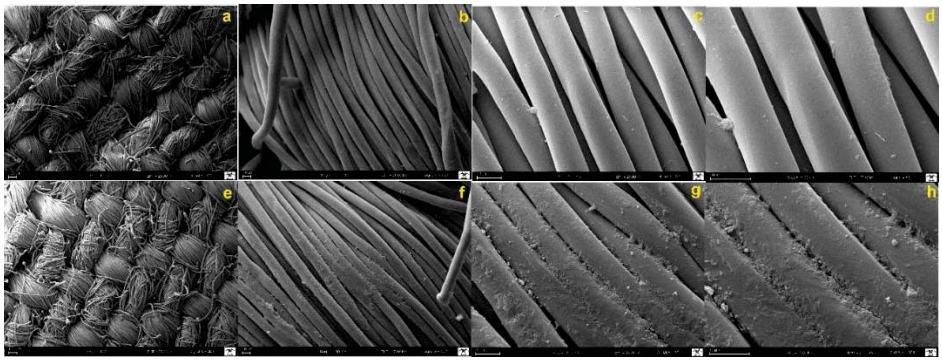


**Figure 3.** Surface Morphologies of Pristine PET Fabric (a,b,c,d) and PET-(% 0,8 v/v) PEDOT Fabric (e,f,g,h)

When the uncoated PET fabric had a quite smooth surface, a significant change on the surface of PET fabric was occurred after PEDOT coating. The homogeneously distributed PEDOT nanoparticle formations were observed on the PET-PEDOT fabric structures by scanning electron microscope. The SEM images of PET-PEDOT composite fabric surface was coated uniformly by PEDOT layers. The SEM results showed that the *in-situ* polymerization process could change the surface morphology of PET fabric effectively and confirmed the conductive polymeric coatings on fabric surfaces was a remarkable effects that could be used for modifying the microstructure of the polyester fabrics [5].

### 3.1.3. Four Point Probe Surface Resistivity Measurement of PET-PEDOT Fabrics

Figure 4 shows the four-point probe surface resistivity and thickness measurement of uncoated and PEDOT coated PET fabrics.

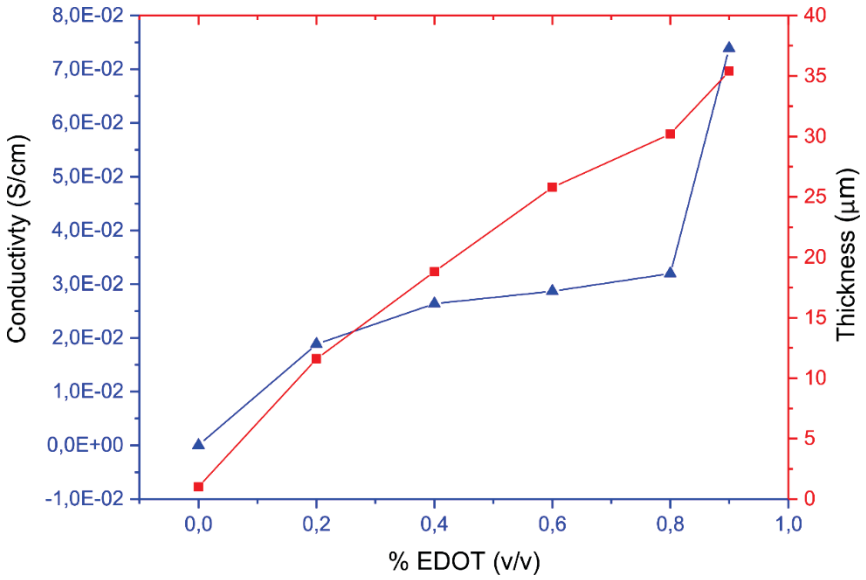


**Figure 4.** The four point probe surface resistivity and thickness measurement of uncoated and PEDOT coated PET fabrics.

When the amount of edot used in different ratios increased in PEDOT coated PET fabrics, the conductivity value increased with their coating thickness, as shown in Fig.4.

## 4. CONCLUSION

The aim of this study is to present a conductive polymer-based wearable sensors to detect the electrical activity of a human heart for electrocardiogram (ECG)

monitoring. For this purpose a textile based sensor was produced by in-situ polymerization of 3,4-ethylenedioxythiophene on polyethylene terephthalate woven fabrics.

## REFERENCES

1. Sinha S. K., Noh Y., Reljin N., Treich G. M., Mohammadalipour S. H., Guo Y., Chon K. H., Sotzing G. A., Screen-Printed PEDOT:PSS Electrodes on Commercial Finished Textiles for Electrocardiography. 2017. *ACS Appl. Mater. Interfaces*, vol. 9, no. 43, pp. 37524–37528.

2. Pani D., Dessi A., Gusai E., Cogollo J. F. S., Barabino G., Fraboni B., Bonfiglio A., Evaluation of Novel Textile Electrodes for ECG Signals Monitoring Based on PEDOT : PSS-Treated Woven Fabrics. 2015. *Embc 2015*, pp. 3197–3200.

3. Wen Y., Xu J., Scientific Importance of Water-Processable PEDOT–PSS and Preparation, Challenge and New Application in Sensors of Its Film Electrode: A Review. 2017.*J. Polym. Sci. Part A Polym. Chem.*, vol. 55, no. 7, pp. 1121–1150.

4. Knittel, D., and Eckhard Schollmeyer. 2009. Electrically High-Conductive Textiles. *Synthetic Metals* 159(14): 1433–37.

5. Cetiner S., Gol B., Kose H., Development of Flexible Smart Fabric Sensor for Wearable Electrocardiogram. 2017. KSU. Journal of Engineering Sciences, 20(3), 10-15.

6. Li, L., Frey, M., Browning, K.J. 2010. Biodegradability Study on Cotton and Polyester Fabrics. *Journal of Engineered Fibers and Fabrics*, 5, 42–53.

7. Selvaganesh, S.V., Mathiyarasu, V., Phani, K.L.N., Yegnaraman, V. 2007. Chemical Synthesis of PEDOT-Au Nanocomposite, *Nanoscale Research Letters,* 2, 546–549.

8. Wu, J. 2011. Morphology of Poly (3, 4-Ethylene dioxythiophene)(PEDOT) Thin Films, Crystals, Cubic Phases, Fibers and Tubes. PhD Thesis, University of Michigan, Macromolecular Science and Engineering, Michigan.

# DESIGN AND ANALYSIS OF NONWOVENS WITH SOUND ABSORPTION PROPERTIES

**Handan PALAK[1], Burçak KARAGÜZEL KAYAOĞLU[1]**

[1]Istanbul Technical University, Turkey

Corresponding author: bkayaoglu@itu.edu.tr

**Abstract:** In this study, acoustic performance of needle punched and thermal bonded nonwovens is reported. Nonwoven samples were produced from polyester (PET) fibers having various cross sections such as hollow, round and hexaflower (with hexagonal petal shape cross section and hollow cavity) which were blended with a low melt PET (LMPET) fiber at different ratios i.e., 50/50, 65/35 and 80/20. Areal density values of samples were selected as 300, 450 and 650 g/m$^2$. After the carding stage, one set of samples was bonded by needle punching (with 200 punch cm$^2$) while the other set of samples was thermally bonded. Design points of experiments were set up with Taguchi experimental design method. Sound absorption coefficients of samples were measured using an impedance tube equipped with two microphones. Minitab software was used to analyze the sound absorption ability of the samples and relationships between independent variables (web bonding method, fiber cross section, blend ratio and areal density) and dependent varible (sound absorption performance). Results indicated that web bonding method and areal density independent varibles have significant effects on sound absorption coefficient values of nonwoven samples. In addition, areal density was found to be the most effective factor affecting sound absorption coefficients of the samples. It was concluded that blend ratio and fiber cross section were less effective compared to web bonding and areal density; therefore these variables were found to be statistically insignificant on sound absorption performance.

***Keywords:*** *nonwoven, sound absorption, acoustic, Taguchi, PET fiber*

## 1. INTRODUCTION

Noise is an undesired, loud sound, which cause discomfort on people in many ways. Population growth, strict regulations in construction of new buildings, increased environmental concerns result in a demand for noise control applications [1]. There are several application areas of acoustic materials in buildings and construction; transportation; and industry. Most preferred sound absorbers for noise control applications are nonwoven materials because of their high porosity as well as short production process and competitive price.

Many studies have been carried out to investigate the sound absorption properties of textile materials including their physical properties, raw material properties, production method parameters, or sound absorption measurement conditions. Kucuk et al. [2] investigated the relationship between physical parameters and sound absorption performance of natural fiber blended nonwoven fabrics. They concluded that sound absorption performance improved as thickness increased and air permeability decreased. Lee et al. [3] examined

the relationship between the acoustic absorption values of the recycled polyester nonwovens and the nonwoven process parameters including fiber and web properties. Ghorbani et al. [4] investigated the effects of variables such as initial carded web mass, needle penetration depth, punch density, and the frequency on transmission of sound through PP needle-punched nonwovens. They concluded that initial carded web mass was the most effective factor affecting sound transmission through the samples. Tascan and Vaughn [5] produced five different vertically lapped nonwoven fabrics that were used with three different fiber shapes (4DG, round and trilobal) and two different fiber deniers (3 and 15 denier). They concluded that the vertically lapped nonwoven fabrics made from 4DG and trilobal fibers had better sound insulation results than nonwoven fabrics made from round fibers. In another study [6], it was reported that thermally bonded samples with octolobal PET fiber showed better sound insulation compared to trilobal and round PET fiber based samples. Suvari et al. [7] investigated sound absorption properties of spunbonded nonwovens made from fibrillated islands-in-the-sea bicomponent filaments. They concluded that sound absorption increased with an increase in the number of islands. It was also shown that multi-layer 108 islands nonwovens absorbed more acoustic energy at some frequency ranges compared to a 300 gsm air-though thermal bonded, high loft nonwoven made from 85% PET and 15% PP with 5 mm thickness. Yang et al. [8] studied sound absorption and thermal properties as well as the relationship between these two performances of struto nonwovens with varying thicknesses and areal density (gsm) values. The results indicated that fabric thickness, fiber fineness and fabric gsm have a significant positive effect on the sound absorption performance of struto nonwovens. They also observed that sound absorption had an insignificant correlation with thermal conductivity, while they were strongly correlated with thermal resistance.

Only limited recent studies [5,6] have been carried out on the effect of fiber cross section on the acoustic performance of nonwovens. In this study, the acoustic performance of nonwoven samples produced from PET fibers having various cross sections such as hollow, round and hexaflower (with hexagonal petal shape cross section and hollow cavity) blended with a low melt PET fiber at different ratios was reported. To the best our knowledge, there is no previous study in the literature that shows the acoustic performance of a fiber with both hexagonal petal shape cross sectional and hollow cavity. Moreover, the sound absorption of samples bonded with needle punching and thermal bonding were compared. Statistical analyses was performed with a Minitab statistical software to determine the regression coefficients and coefficient of determination (R-squared). In additon, an ANOVA analysis was performed to compare the significance level (α) with probability value (p-value) of chosen parameters in the experimantal design.

## 2. MATERIALS AND METHODS

### 2.1 Materials

In the study, PET fibers having various cross sections as hollow (6 denier), round (6 denier) and hexaflower (4 denier) were used. A low melt PET fiber (LMPET) (4 denier) with a round cross section was used as a binder. The hollow, round and LMPET fibers were supplied from Sasa Inc. (Adana/ Turkey) and hexaflower fiber was supplied from Huvis Inc. (South Korea).

### 2.2 Design of Experiments

Design of experiments was set up based on a Taguchi experimental design method. Independent variables were chosen as cross section of fibers, blend ratios with LMPET, areal density of samples and web bonding method. The levels of independent variables can be seen in Table 1. A proper Taguchi orthogonal array, L18 (2*1,3*3), was determined in which the variables; cross section, blend ratio and areal density had three levels and the variable web bonding had just two levels. The array which contains variation levels of independent variables can be seen in Table 2.

**Table 1.** Independent variables and levels

| Independent Variables | Levels | | |
|---|---|---|---|
| | 1 | 2 | 3 |
| Cross section | Hollow | Round | Hexaflower |
| Blend ratio (PET/LM PET) | 50/50 | 65/35 | 80/20 |
| Areal Density (g/m$^2$) | 300 | 450 | 650 |
| Web Bonding | Needlepunch | Thermal | X |

**Table 2.** Experimental design Taguchi L18

| Sample Number | Web Bonding Method | Fiber Cross Section | Blend Ratio (PET/ LMPET) | Areal Density (g/m$^2$) |
|---|---|---|---|---|
| 1 | Needlepunch | Hollow | 50/50 | 300 |
| 2 | Needlepunch | Hollow | 65/35 | 450 |
| 3 | Needlepunch | Hollow | 80/20 | 650 |
| 4 | Needlepunch | Round | 50/50 | 300 |
| 5 | Needlepunch | Round | 65/35 | 450 |
| 6 | Needlepunch | Round | 80/20 | 650 |
| 7 | Needlepunch | Hexa | 50/50 | 450 |
| 8 | Needlepunch | Hexa | 65/35 | 650 |
| 9 | Needlepunch | Hexa | 80/20 | 300 |
| 10 | Thermal | Hollow | 50/50 | 650 |
| 11 | Thermal | Hollow | 65/35 | 300 |
| 12 | Thermal | Hollow | 80/20 | 450 |
| 13 | Thermal | Round | 50/50 | 450 |
| 14 | Thermal | Round | 65/35 | 650 |
| 15 | Thermal | Round | 80/20 | 300 |
| 16 | Thermal | Hexa | 50/50 | 650 |
| 17 | Thermal | Hexa | 65/35 | 300 |
| 18 | Thermal | Hexa | 80/20 | 450 |

### 2.3 Sample preparation

According to the selected blend ratios and areal density values, PET fibers (hollow, round and hexa) and LMPET fiber were weighed and prepared. After fiber preparation based on design arrays, all samples were opened with a sample carding machine. After carding stage, according to the experimental design (L18), samples were needle punched using 200 punches/cm$^2$ (for three needling passes as 50/75/75 punches/cm$^2$ with 11/12/6 mm needling depths). Thermal bonded samples were bonded with a through-air bonding oven at 200$^o$ with a 3 m/min conveyor belt speed and 1800 rpm fan speed. Edges were removed and samples were sized as A4 paper (0.21m*0.29m) with a cutter machine to obtain more homogenous nonwoven samples.

### 2.4 Methods

Sound absorption coefficients were measured with a Bias Engineering TestSENS impedance tube based on ASTM 1050-12 [9]. This standard method uses an impedance tube equipped with two microphones, and a digital frequency analyzer for sound absorption coefficient (SAC) measurement. A sound source is mounted at one end of the impedance tube, and a sample of the material is placed at the other end. The sound source generates broadband sound waves which propagate as plane waves in the tube. The sound waves then hit the sample and reflect. It is possible to determine the sound absorption coefficient of the material measuring the sound pressure at two fixed locations and calculating the complex transfer function using a two-channel digital frequency analyzer. To measure SAC values, nonwoven samples were cut in circular shapes with 50 mm diameter to place into impedance tube. Measurements were performed between 100 Hz and 4000 Hz frequency range. Nine different measurements were performed for each sample; then average SAC values were calculated.

Minitab statistical software was used to calculate the regression coefficients to compare the effects of independent variables on dependent variables. ANOVA analysis was performed for comparing the significance level (α) with probability value (p-value) of all chosen parameters in the experimental design. Then R-squared value was investigated to determine the strength of the statistical model in which SAC was explained as a function of web bonding, cross section, blend ratio and areal density. SAC measurements were performed between 100 Hz and 4000 Hz frequency range; however, statistical analysis was conducted based on SAC values at 2000 Hz as a middle frequency because porous materials show inadequate acoustic performance at low frequencies while they show very good performance at high frequencies [1].

A 95% confidence interval (α=0.05) was selected for the analysis; therefore, p values of independent variables were compared with 0.05.

In Taguchi method, analysis was performed based on the ratio of signal to noise (S/N), which compares the level of a desired signal with the level of background noise. S/N ratio implies the amount of noise in the output of a specified process. Three standard S/N equations for classification of the objective function includes ‘larger the better’, ‘smaller the better’, or ‘nominal the best’. In this study, larger

sound absorption coefficient was desired; therefore, 'larger is better' function, which was shown in Eq 1 was used [10].

$$S/N = -10 \log\left(\frac{1}{n}\sum_{k=1}^{n} {}^{1}/_{y_k^2}\right) \qquad (2)$$

where; n is the number of tests, $y_k$, the experimental value of the $k^{th}$ quality characteristic.

The level of an independent variable with the highest sound and noise S/N ratio (S/N) implies the optimum level for this variable. Taguchi analysis aims to obtain the optimum levels of each independent variable. Therefore, S/N ratio values were also investigated to represent optimum combination of parameters and their levels.

## 3. RESULTS AND DISCUSSION

L18 design and corresponded SAC values can be seen in Table 3.

**Table 3.** SAC values at 2000 Hz

| Web Bonding | Crosssection | Blend Ratio | Areal Density | SAC (@2000Hz) |
|---|---|---|---|---|
| Needlepunch | Hollow | 50/50 | 300 | 0.15 |
| Needlepunch | Hollow | 65/35 | 450 | 0.29 |
| Needlepunch | Hollow | 80/20 | 650 | 0.36 |
| Needlepunch | Round | 50/50 | 300 | 0.15 |
| Needlepunch | Round | 65/35 | 450 | 0.23 |
| Needlepunch | Round | 80/20 | 650 | 0.31 |
| Needlepunch | Hexa | 50/50 | 450 | 0.28 |
| Needlepunch | Hexa | 65/35 | 650 | 0.35 |
| Needlepunch | Hexa | 80/20 | 300 | 0.26 |
| Thermal | Hollow | 50/50 | 650 | 0,48 |
| Thermal | Hollow | 65/35 | 300 | 0.31 |
| Thermal | Hollow | 80/20 | 450 | 0.33 |
| Thermal | Round | 50/50 | 450 | 0.25 |
| Thermal | Round | 65/35 | 650 | 0.50 |
| Thermal | Round | 80/20 | 300 | 0.36 |
| Thermal | Hexa | 50/50 | 650 | 0.50 |
| Thermal | Hexa | 65/35 | 300 | 0.31 |
| Thermal | Hexa | 80/20 | 450 | 0.33 |

As seen in ANOVA analysis (Table 4), p-values of web bonding and areal density variables were less than 0.05. Therefore, web bonding and areal density variables were statistically significant for SAC values. On the other hand, p-values of blend ratio and cross section variables were obtained higher than 0.05. Thus,

blend ratio and cross section variables were statistically insignificant for SAC values.

Table 5 shows the S/N ratios in association with the selected independent parameters and their variation levels. Delta value was used as an index, which is the difference between the highest and the lowest S/N ratios of each variable that shows the effect of the independent variables on SAC values of the nonwoven samples. Independent variables were listed based on their delta values as seen in Table 5. It was observed that areal density was the most important parameter with the highest delta value (4.595). The second effective variable was the web bonding with a 3.214 delta value. They were followed by blend ratio variable as the third and cross section variable as the fourth variable.

**Table 4.** Analysis of variance for SN ratios

| Source | DF | Seq SS | Adj SS | Adj MS | F | P |
|---|---|---|---|---|---|---|
| Web Bonding | 1 | 46.479 | 46.479 | 46.479 | 22.71 | 0.001 |
| Cross Section | 2 | 6.492 | 6.492 | 3.246 | 1.59 | 0.252 |
| Blend Ratio | 2 | 11.058 | 11.058 | 5.529 | 2.70 | 0.115 |
| Areal Density | 2 | 67.513 | 67.513 | 33.756 | 16.50 | 0.001 |
| Residual Error | 10 | 20.464 | 20.464 | 2.046 | | |
| Total | 17 | 152.006 | | | | |

**Table 5.** Response table for signal to noise ratio

| Level | Web Bonding | Cross Section | Blend Ratio | Areal Density |
|---|---|---|---|---|
| 1 | -12.020 | -10.454 | -11.520 | -12.369 |
| 2 | -8.806 | -11.127 | -9.906 | -11.094 |
| 3 | | -9.657 | -9.812 | -7.775 |
| Delta | 3.214 | 1.469 | 1.708 | 4.595 |
| Rank | 2 | 4 | 3 | 1 |

A regression equation (Eq. 2) was formed based on coefficients obtained from general regression analysis. Coefficient of determination ($R^2$) and adjusted coefficient of determination (adj-$R^2$) were obtained as 86.7% and 77.4%, respectively. These coefficients indicate how well the model fits the data.

SAC= 0.317779 -0.055557*'Web Bond Needlepunch'-0.000158*'Cross Section Hollow'-0.018731*'Cross Section Round'-0.018968*'Blend Ratio 5050'+ 0.011747*'Blend Ratio 6535'-0.062063*'Areal Density 300'-0.036350*'Areal Density 450' (2)

Based on the response table (Table 5), the main effects plot was drawn as seen in Figure 1, showing the main effect of independent variables on the SAC value. The slope of the plot refers to the effectiveness of an independent variable. In other words, if a variable's slope is higher, it implies that it is more effective than the other independent variables.

### 3.1. Web Bonding Effect

Thermal bonded nonwoven samples were not compressed; they were bonded with melting of LMPET fiber by hot air. Needlepunched samples became more compact because of the punching effect whereas thermal bonded samples were thicker and bulkier. A bulkier material provides a larger volume for sound waves to propagate and absorb better compared to compact materials as also shown in the main effect plot (Figure 1). S/N ratio difference between needlepunch bonding and thermal bonding method was approximately 3.214; and there is a dramatic increase in the slope from needlepunch method to thermal bond method. Thus, thermal bonding method was the optimum level for web bonding independent variable.

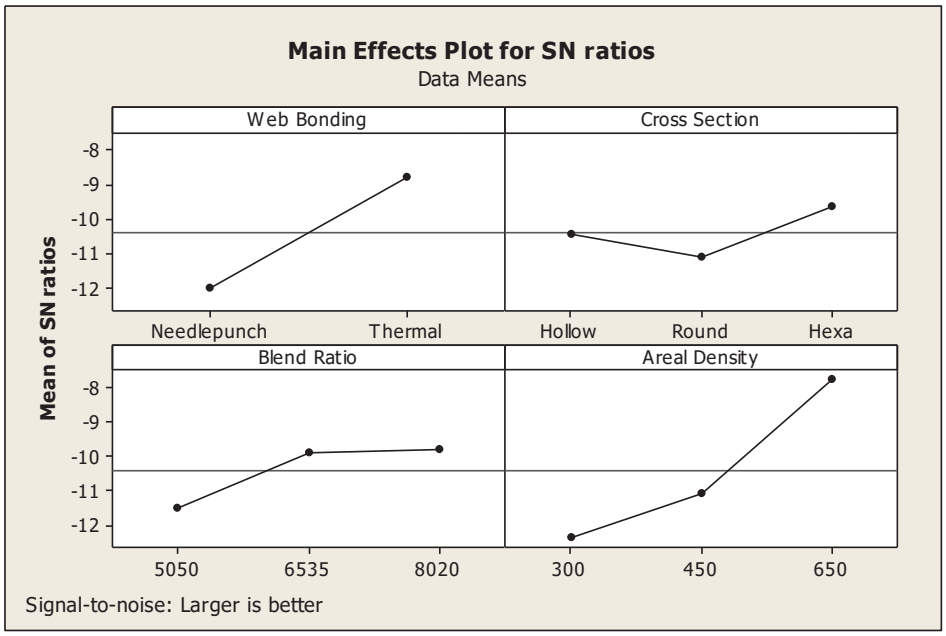


**Figure 1.** Main effect plot

### 3.2. Areal Density Effect

As seen in Figure 1, the main effect plot of areal density showed the highest slope indicating its significance. Increasing the areal density effectively resulted in a higher number of fibers and, thus, increased the air/fiber boundaries within the

nonwoven structure [1,4]. This eventually resulted in reduction of sound wave energy and higher sound absorption coefficient. S/N ratio difference between 300 g/m$^2$ and 650 g/m$^2$ samples was approximately 4.595; therefore, the slope of main effect graphic line of areal density was the highest one, which referred to the most significant independent variable among other variables. Thus, 650g/m$^2$ was the optimum level for areal density independent variable.

### 3.3. Fiber Cross Section Effect

The denier and cross-section shape directly affect the surface area of a fiber. Thus, the fiber cross section shape can be a parameter that affects the acoustic performance of the fiber and the material consequently. Figure 1 indicated that hollow and hexa PET fiber based nonwoven samples showed better acoustic performance compared to round PET fiber based nonwoven samples. This can be the result of having a hollow cavity, which allowed easier sound propagation. According to Figure 1 and Table 5, S/N ratios of hollow and hexa PET fiber were close to each other with just a 0.7 S/N ratio difference. This difference may occur because the hexa PET fiber had larger surface area compared to hollow PET fiber due to its hexagonal petal cross section shape. However, delta value of the fiber cross section (1.469) and the slope of cross section effect plot was quite low, which indicated that the cross-section independent variable was the least effective on SAC values.

### 3.4. Blend Ratio Effect

As seen in Figure 1, the increase in the PET fiber weight ratio of the blend affected the sound absorption positively. When the weight ratio of PET fiber increased from 50% to 65%, acoustic performance was affected dramatically whereas increasing the ratio to 80% was not making a remarkable change on acoustic performance for both needlepunch bonded and thermal bonded samples. On the other hand, as seen in Figure 1 and Table 5, delta value of blend ratio independent variable (1.708) and the slope of the plot was rather low, which implied that the effect of blend ratio was quite low which may even be negligible.

## 4. CONCLUSION

Sound absorption properties of needle punch bonded and air-through thermal bonded nonwovens made from PET fibers having various cross sections such as hollow, round and hexaflower blended with LMPET fibers at different ratios were investigated. It was shown that areal density had the most significant effect on the sound absorption coefficient. The second significant independent variable was found as web bonding method which directly affected the thickness of nonwoven materials and sound absorption performance consequently. Increasing PET fiber ratio in nonwoven material affected sound absorption performance positively; however, this effect was statisticaly insignificant with a 0.115 p-value. It was also found that hexa and hollow PET fiber based materials had better acoustic performance compared to round PET fiber based materials; however, this effect was also statistically insignificant with a 0.252 p-value. As a

result, web bonding method (i.e. thickness and bulkiness of a material) and areal density together explained sound absorption performance of a nonwoven material with a 77.4% $R^2$ adjusted value. Air-through thermally bonded nonwoven materials with 650 g/$m^2$ areal density value reached to a 0.5 SAC value at 2000 Hz indicating that these samples may be suitable to use for acoustic applications in the automotive industry.

## ACKNOWLEDGEMENT

The authors acknowledge Istanbul Technical University Scientific Research Projects Fund under Grant No. BAP 40892 for the financial support and Hassan Company for the support in the production of nonwoven samples.

## REFERENCES

1. Nayak, R.& Padhye, R. (2016). Acoustic textiles: An introduction. In R. Nayak (Ed.) & R. Padhye (Ed.), *Acoustic Textiles* (pp. 1-32). Singapore: Springer.
2. Küçük, M., Korkmaz, Y., (2012). The effect of physical parameters on sound absorption properties of natural fiber mixed nonwoven composites, *Textile Research Journal*, 82(20) 2043–2053
3. Y. Lee, C. Joo, Sound absorption properties of recycled polyester fibrous assembly absorbers, AUTEX Res. J. 3 (2003) 78-84
4. Ghorbani, K., Hasani, H., Zarrebini, M., Saghafi, R. (2016). An investigation into sound transmission loss by polypropylene needle-punched nonwovens, *Alexandria Engineering Journal*, 55, 907–914
5. Tascan, M., Vaughn, E., (2008). Effects of Fiber Denier, Fiber Cross-Sectional Shape and Fabric Density on Acoustical Behavior of Vertically Lapped Nonwoven Fabrics, *Journal of Engineered Fibers and Fabrics, Volume 3, Issue 2*
6. Tascan, M., Vaughn, E.,Stevens, K.A., Brown, P.J. (2011). Effects of total surface area and fabric density on the acoustical behavior of traditional thermal-bonded highloft nonwoven fabrics, *The Journal of The Textile Institute,* 102:9, 746-751
7. Suvari, F., Ulcay, Y., Maze, B. & Pourdeyhimi, B., (2013). Acoustical absorptive properties of spunbonded nonwovens made from islands-in-the-sea bicomponent filaments, *Journal of The Textile Institute, 104:4*, 438-445
8. Yang, T., Xiong, X.,, Mishra, R., Nova, J., Militky, J., (2016). Acoustic evaluation of Struto nonwovens and their relationship with thermal properties, *Textile Research Journal*, 0(00) 1–12
9. ASTM E1050-12. Standard Test Method for Impedance and Absorption of Acoustical Materials Using a Tube, Two Microphones and a Digital Frequency Analysis System.
10. Minitab16 Software Manual, 2013.

# AN INVESTIGATION ON THE USE OF SPACER FABRICS IN OFFICE CHAIRS

**Münire Sibel ÇETİN[1], Gülseren KURUMER[2], Gülseren KARABAY[2], Hasan ÖZTÜRK[3]**

[1] Dokuz Eylül University, The Graduate School of Natural and Applied Sciences, Turkey
[2] Dokuz Eylül University, Department of Textile Engineering, Turkey
[3] Dokuz Eylül University, Department of Mechanical Engineering, Turkey

Corresponding author: muniresibelcetin@outlook.com

***Abstract:*** *Nowadays, sitting hours at the offices are increasing because of reason that the number of jobs based on computer usage in offices increased. Therefore, the anthropometric suitability and comfort properties of office chairs used in these types of work are becoming progressively important. For those who sit for a long time, the tendency to muscle aches are increasing due to the fact that sweating and sweat which can not be removed from their body. For this reason, anti-allergic and sweat absorbent/breathable fabrics should be selected to improve the office chairs' ease of use and sitting comfort of office workers. In this study, the possibilities of using spacer fabrics instead of traditional materials on office chairs in terms of textile comfort features were investigated. For this purpose, the moisture management and air permeability properties of three types of traditional materials and six types of spacer fabrics were compared.*

***Key Words****: spacer fabrics, office chairs, moisture management, air permeability, textile comfort properties*

## 1. INTRODUCTION

There are many components of comfort perception in the human-sitting system. However, it is important to evaluate the human-sitting system in terms of textile comfort. When you look at the chair, the first thing that attracts your attention, is the aesthetic features such as fabric, structure and color. When you first touch the chair, you feel the surface features. Another important point is the type of fabric. For those who sit for a long time, the tendency to muscle aches are increasing due to the fact that sweating and sweat which can not be removed from their body. For this reason, anti-allergic and sweat absorbent/breathable fabrics should be selected to improve the office chairs' ease of use and sitting comfort of office workers [1].

Padding materials commonly used in chairs are polyurethane based foams [3]. Their thermophysiological properties, compressibility and flexibility properties are poor, they lose these kinds of their properties over time, their washing and drying properties are insufficient and they are flammable [2]. Because of such disadvantages, the ease of use comfort of the user is affected negatively.

Due to these disadvantages, alternative materials to polyurethane based foams are becoming important. Warp knit spacer fabrics offer a better option over polyurethane foam in car seats owing to their advantages such as better recovery to compression, thermal properties and breathability [4].

Yip and Sun-Pui (2008) were investigated the characteristics of different spacer fabrics including low-stress mechanical properties, air permeability and thermal conductivity. It is found that both air permeability and thermal conductivity are closely related to the fabric density. It is believed that the fabric characteristics of spacer fabric show a very significant effect on the air permeability, thermal conductivity and mechanical properties of spacer fabric [5].

Liu and Hu (2011) were investigated the compression properties and air permeability of twenty weft-knitted spacer fabrics. Spacer fabrics compression property and air permeability were tested with the Kawabata Evaluation System for Fabrics (KES-F). Among the different factors affecting the air permeability of the fabric, such as the knitted structure and the outer and spacer layer characteristics, it has been found that the fabric structure shows the most significant effect [6].

Ye, et al. (2007) were investigated the application of warp-knitted spacer fabrics as cushion in car seats. The results show that, relatively to polyurethane foam, warp-knitted spacer fabrics demonstrate better recovery to compression, thermal properties and breathability [7].

Pamuk (2006) were investigated the physical properties of the fabrics used for automotive seat covers. Some tests such as tensile strength, tear strength, abrasion resistance, air permeability and UV resistance, which are the mostly important for automotive seat cover manufacturers, were applied to the fabrics. It has been found that there is a positive correlation between the air permeability and the weight of the fabric, even though there is a negative correlation between the air permeability of the automobile seat upholstery fabrics used in this study and the fabric thickness [8].

There are studies in the literature investigating the air permeability and / or thermal properties of spacer fabrics. There are also studies comparing compression and air permeability properties of polyurethane sponges with spacer fabrics. Unlike the literature air permeability and moisture management properties of spacer fabrics and polyurethane sponges were evaluated and compared in this study.

In this study, the physical properties of spacer fabrics which are tought to have a low possibility of sweating and which have a high air permeability due to their porous structure as an alternative to polyurethane foams have been investigated. Three types of traditional materials and six kinds of spacer fabrics were compared in terms of their textile comfort properties.

## 2. MATERIAL AND METHOD

The materials used in the study are gray foam, yellow foam and six different spacer materials. Figure 1 shows the surface images of the spacer fabrics.

Spacer material is coded as 1,2,3,4,5 and 6. Table 1 shows the properties of the materials used in this study.

| TABLO 1. MATERIAL PROPERTIES | | |
|---|---|---|
| **Material Name** | **Material Properties** | **Mesh Density (courses/wales) (1/cm)** |
| Yellow polyurethane foam | Thickness: 3 cm; Density: 23 kg/m3 | |
| Grey polyurethane foam | Thickness: 3 cm; Density: 32 kg/m3 | |
| Spacer-1 | 100% polyester warp knitted fabric of both faces open structure | 6.5/2 |
| Spacer-2 | 100% polyester warp knitted fabric of both faces closed structure | 8/6 |
| Spacer-3 | 100% polyester warp knitted fabric of both faces open structure | 6.25/6 |
| Spacer-4 | 100% polyester warp knitted fabric of one face open and other face closed structure | 5.5/4 |
| Spacer-5 | 100% polyester warp knitted fabric of one face open and other face closed structure | 6.25/4 |
| Spacer-6 | 100% polyester warp knitted fabric of both faces closed structure | 7/5 |

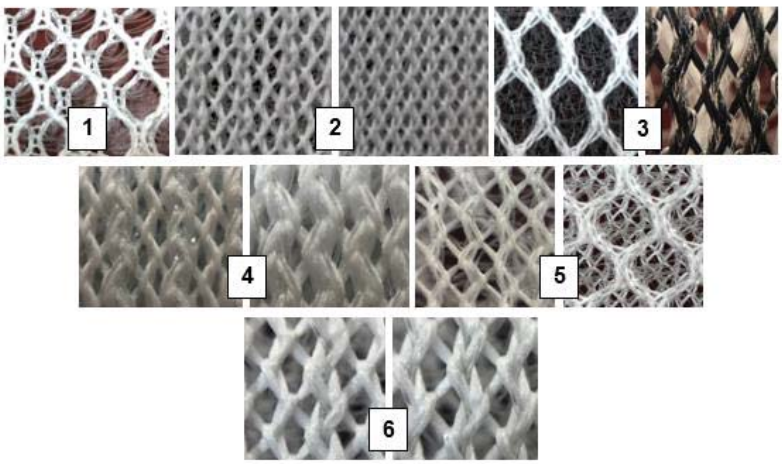


**Figure 1.** The surface images of the spacer fabrics (from left to right and from top to bottom; 1, 2 front-back, 3 front-back, 4 front-back, 5 front-back, 6 front-back)

Moisture management behavior is a vital factor in evaluating thermal and physiological comfort of functional textiles. spacer fabrics can be used to absorb a user's sweat, to reduce the humidity and improve user's thermal comfort [9].

All materials are tested to determine air permeability and moisture transmission properties. Air permeability test is made according to TS 391 EN ISO 9237 “Textiles-Determination of permeability of fabrics to air” standard with Textest FX 3300 Air Permeability Tester III. This test was carried out under pressure of 200 Pa with 10 repetitions and using a 20 cm2 apparatus.

Moisture management properties are determined according to AATCC 195 "Liquid Moisture Management Properties of Textile Fabrics" standard with Moisture Management Tester. This test was carried out with 6 repetitions.

## 3. RESULTS AND DISCUSSION

Table 2 shows the values of air permeability and moisture management properties.

**Table 2.** Results of Moisture Managemet Test Applied to Padding Materials

| | | | Moisture Management Properties Values and Grades | | | |
|---|---|---|---|---|---|---|
| | | Air Permeability | Wetting time (top surface) | Absorption rate (top surface) | Maximum wetted radius (top surface) | Spreading speed (top surface) |
| **Material Name** | **Material Properties** | **l/m2/sec** | **sec** | **%/sec** | **mm** | **mm/s** |
| Yellow polyurethane foam | Thickness: 3 cm; Density: 23 kg/m3 | 869 | 9.25 (3) | 261.4613 (5) | 5 (1) | 0.549 (1) |
| Grey polyurethane foam | Thickness: 3 cm; Density: 32 kg/m3 | 427 | 7.2603 (3) | 69.9942 (4) | 15 (3) | 1.4506 (2) |
| Spacer-1 | 100% polyester warp knitted fabric of both faces open structure | - | 21.4637 (2) | 24.4065 (2) | 16.6667 (3) | 7.7695 (5) |
| Spacer-2 | 100% polyester warp knitted fabric of both faces closed structure | 4332 | 2.231 (5) | 25.0325 (2) | 20 (4) | 8.4619 (5) |
| Spacer-3 | 100% polyester warp knitted fabric of both faces open structure | 3804 | 2.453 (5) | 26.0718 (2) | 20 (4) | 8.3283 (5) |
| Spacer-4 | 100% polyester warp knitted fabric of one face open and other face closed structure | 7261 | 1.6513 (5) | 42.1984 (3) | 20 (4) | 13.6484 (5) |
| Spacer-5 | 100% polyester warp knitted fabric of one face open and other face closed structure | 6841 | 2.6384 (5) | 27.1501 (2) | 16,4286 (3) | 8.0701 (5) |
| Spacer-6 | 100% polyester warp knitted fabric of both faces closed structure | - | 2.5702 (5) | 22.0043 (2) | 20 (4) | 7.4354 (5) |
| The grades of moisture management properties are taken from the AATCC 195 standard. | | | | | | |

The moisture management properties test results were evaluated according to the scale in Table 3.

**Table 3.** The grades of moisture management properties [10]

| Index | | Grade | | | | |
|---|---|---|---|---|---|---|
| | | 1 | 2 | 3 | 4 | 5 |
| Wetting time (sec | Top | ≥ 120 | 20–119 | 5–19 | 3–5 | <3 |
| | | No wetting | Slow | Medium | Fast | Very Fast |
| | Bottom | ≥ 120 | 20–119 | 5–19 | 3–5 | <3 |
| | | No wetting | Slow | Medium | Fast | Very Fast |
| Absorption rate (%/sec) | Top | 0– 9 | 10–29 | 30–49 | 50–100 | > 100 |
| | | Very slow | Slow | Medium | Fast | Very Fast |
| | Bottom | 0– 9 | 10–29 | 30–49 | 50–100 | > 100 |
| | | Very slow | Slow | Medium | Fast | Very Fast |
| Max wetted radius (mm) | Top | 0– 7 | 8–12 | 13–17 | 18–22 | >22 |
| | | No wetting | Small | Medium | Large | Very Large |
| | Bottom | 0– 7 | 8–12 | 13–17 | 18–22 | >22 |
| | | No wetting | Small | Medium | Large | Very Large |
| Spreading speed (mm/sec) | Top | 0.0– 0.9 | 1.0 – 1.9 | 2.0 – 2.9 | 3.0 – 4.0 | >4.0 |
| | | Very slow | Slow | Medium | Fast | Very Fast |
| | Bottom | 0.0– 0.9 | 1.0 – 1.9 | 2.0 – 2.9 | 3.0 – 4.0 | >4.0 |
| | | Very slow | Slow | Medium | Fast | Very Fast |
| One-way transport capability (OWTC) | | <-50 | -50–99 | 100 – 199 | 200 – 400 | > 400 |
| | | Poor | Fair | Good | Very good | Excellent |
| Overall Moisture Management Capability (OMMC) | | 0.00– 0.19 | 0.20 – 0.39 | 0.40 – 0.59 | 0.60 – 0.80 | > 0.80 |
| | | Poor | Fair | Good | Very good | Excellent |

The padding materials' air permeability values are aligned from the best to the worst as spacer-4, spacer-5, spacer-2, spacer-3, yellow polyurethane foam and grey polyurethane foam. Due to the very large pore structure of the spacer-1 and spacer-6 no values could be recorded by the air permeability tester. According to the wetting time grading, spacer-1's grade is 2, yellow and grey polyurethane foam's 3 and the other padding materials grade are 5. With regard to the absorption rate grading, yellow polyurethane foam's grade is 5, grey polyurethane foam's 4, spacer-4's 3 and the other padding materials grade are 2. In accordance with the maximum wetted radius grading, spacer-2, spacer-3, spacer-4 and spacer-6's grade are 4, spacer-1, spacer-5 and grey polyurethane

foam's 3 and yellow polyurethane foam's grade is 1. With respect to the spreading speed grading, yellow polyurethane foam's grade is 1, grey polyurethane foam's 2 and the other padding materials grade are 5 (Table 2).

Since the padding materials do not directly contact the body, there will be no fluid moisture on the surface of the padding material. Therefore, the most important of these properties are the wetting time and the absorption rate. The padding materials will absorb the moisture that is transferred to the bottom surface of the upholstery fabric. As the absorption rate increases, the speed of transfer of the moisture to the lower surface of the padding material will increase. So, the feeling of humidity on the surface will be the least. The shorter the wetting time, the material will absorb liquid more quickly and easily. According to the wetting time and the absorption rate values, the padding material having the best performance (having the shortest wetting time and the highest absorption rate) is the spacer-4. Spacer-4 is followed by spacer-5 and spacer-3.

## 4. CONCLUSIONS

It has been determined that polyurethane based foams used in office chairs are weak in terms of air permeability and moisture management properties. On the contrary, it has been determined that the performance of the spacer fabrics is good in terms of these properties due to their porous structure. As a result, the use of spacer fabrics will have positive effects on the textile comfort of office chairs.

## ACKNOWLEDGMENTS

This study was supported by SAN-TEZ program of T.C. Ministry of Science, Industry, and Technology (Project No.: 0185.ST.2013-1). We thank to the Ermetal Group of Companies for their support within the Industrial Thesis Supporting Program (SAN-TEZ).

## REFERENCES

1. Çetin, M. S. Design of ergonomic office chair which textile comfort properties optimised. 2018. Dokuz Eylül University, The Graduate School of Natural and Applied Science, Unpublished PhD Thesis, İzmir.
2. Gopalakrishnan, D. Knitted Fabrics for Industrial Applications. 2014. Sardar Vallabhbhai Patel Institute of Textile Management.
3. Kim, W. J., & Chang, M. A comparison of the average sitting pressures and symmetry indexes between air-adjustale and foam cushions. 2013. Journal of physical therapy science, 25(9), 1185-1187.
4. Gokarneshan, N., Velumani, K. Some Significant Advances in Spacer Fabric Technology for Newer Areas of Applications. 2018. Journal of Textile Science & Engineering, 8: 339. 8:1.
5. Yip, J., & Ng, S. P. Study of three-dimensional spacer fabrics: Physical and mechanical properties. 2008. Journal of materials processing technology, 206(1-3), 359-364.

6. Liu, Y., & Hu, H. Compression property and air permeability of weft-knitted spacer fabrics. 2011. The Journal of the Textile Institute, 102(4), 366-372.
7. Ye, X., Fangueiro, R., Hu, H., & Araújo, M. D. Application of warp-knitted spacer fabrics in car seats. 2007. Journal of the Textile Institute, 98(4), 337-344.
8. Pamuk, G. The Properties of Fabrics Used For Automotive Seat Covers. 2006. Dokuz Eylül University, The Graduate School of Natural and Applied Science, Master of Science Thesis, İzmir.
9. Bagherzadeh, R., Gorji, M., Latifi, M., Payvandy, P., & Kong, L. X. Evolution of moisture management behavior of high-wicking 3D warp knitted spacer fabrics. 2012. Fibers and Polymers, 13(4), 529-534.
10. AATCC, T. 195: 2009 Liquid moisture management properties of textile fabrics. 2009. American Association of Textile Chemists and Colourists.

# DETERMINATION OF TOXIC COMBUSTION GASES IN RAILWAY TRIM MATERIALS BY A NOVEL METHOD

**Fatma Filiz YILDIRIM[1,3], Elif KAYNAK URAZ[2], Fatma Nur PARIN[3], Kenan YILDIRIM[3]**

[1] TÜBİTAK BUTAL, Bursa Test and Analysis Laboratory, Turkey
[2] Eskişehir Technical University, Department of Chemical Engineering, Turkey
[3] Bursa Technical University, Fiber and Polymer Engineering Department, Turkey

Department*Corresponding author: filiz.yildirim@tubitak.gov.tr

***Abstract:*** *Determination of toxic gases released from materials used in railway products when they are burned is an important issue as it is vital in a fire. There is a quantitative method in the standard of EN ISO 45545-2 Annex C by using a smoke chamber and FTIR sampling system. It is possible to analyze the eight gas components: $CO_2$, CO, HF, HCl, HBr, HCN, $SO_2$ and $NO_x$ by using this method. Because the investment and analysis cost of this system are very high, looking for cheaper analysis methods is required. This research focuses on the development a cheaper method based on combustion emission analyzer that can determine $CO_2$, CO, $NO_x$, $SO_2$. After establishing of the new method test assembly, the power of this system was tested on one upholstery fabric and three different rubbers. It was observed that this system is useful to determine the toxic gas emissions from burning materials.*

***Keywords:*** *Railway vehicles, combustion gases, textile fabrics, portable combustion & emission analyzer, EN ISO 45545-2 Annex C.*

## 1. INTRODUCTION

Rolling stocks for passenger and goods have a variety of fire risks, dependent on the type of train, materials used in train construction and operating conditions. Fire risk analysis is based on the design of fire scenario concept. Design of fire scenario represents a chronological chain of events from the fire ignition to the finalization of the evacuation of people on trains. Each event has been described and evaluated with respect to fire standards. In this respect, European Community have determined to use EN 45545 standard for fire safety in railway vehicles. EN 45545 is a harmonic standard for fire safety in the railway systems and composed of seven parts. According to the standard, the burning behavior of materials and components are classified for different hazard systems based on operation and the vehicle design categories in EN 45545-2 part. This standard include classification, standardization and test/analysis methods for exterior and interior materials. Standardization of the materials is based on the fire behavior, toxicity, smoke and energy emission parameters.

Toxicity of materials is measured by using two devices one of them is smoke chamber for fire materials according to ISO 5659-2. The other is FT-IR

spectrometry for gas analysis according to EN 45545-2 Annex C. Standardization of materials based on the toxicity is made with $CO_2$, CO, HBr, HCl, HCN, HF, $NO_x$, $SO_2$ gases. During this test smoke density parameter is also measured via the attenuation of a white light beam by the effluent gases/smoke [1-3]. Due to the high instrument and analysis costs of this system, other techniques which enable the determination of combustion mechanism and identification of toxic gaseous products are required. The aim of this study is to reveal the applicability of a new method that is absolutely cheaper, to determine the combustion mechanism and toxic gas emissions from railway trim materials by combustion&emission and TG-FTIR analysis.

## 2. MATERIAL AND METHOD

In this study one upholstery 100 % polyester velvet fabrics and three different rubber materials were used. Both types of materials are flammable. Rubber materials are silicone (VMQ 50/XGR 50-05), NBR (shore A 70) and NR (shore A 60). The fabric was produced by EPENGLE company and rubbers were produced by LASPAR company. NBR and NR rubbers are sulphur based vulcanized rubbers.

### 2.1 Test Assembly

The test assembly consists of two main parts; the combustion chamber (Govmark Horizontal Burning Chamber) defined in ISO 3795 and portable combustion & emission analyzer (Testo 350XL). The combustion chamber was chosen because it simulates the real combustion condition.

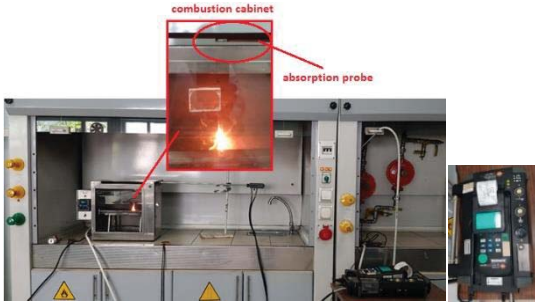


**Figure 1.a.**Test assembly for determining combustion gases. **b.** Testo portable combustion & emission analyzer.

### 2.2 TGA-FTIR Analysis

TGA-FTIR analysis system was chosen to determine the combustion gases of samples as another gas analysis system. Approximately 5 mg of sample was heated up to 700°C at a heating rate of 10°C/min under air flow (100ml/min) in SDT (Q600, TA Instruments). The real time spectra of the evolved gases were collected by a FTIR, Cary 600 (Agilent Technologies, USA) coupled to SDT with a heated transfer line. DTG curve and Gram-Schmidt curve obtained by FTIR

analysis, were superimposed and the time required for the transfer of evolved gases from SDT to FTIR was calculated for each sample.

## 3. RESULTS AND DISCUSSION

This research focuses on establishing a new test method as an alternative to EN 45545. The first main result is that the material should be flammable and should produce combustion gases that could be detected by this analyzer during burning. Some certain gases (CO2, CO, NOx, $SO_2$) released by the combustion of flammable materials could be successfully detected quantitatively by portable combustion & emission analyzer. However it is required to validate this method by EN 45545 standard test method. After validation this new developed and cheaper method can be used as an alternative method for EN 45545 standard method. It can be possible to measure quantitative gas analysis which is defined in EN 45545 standard by using this new developed analysis method.

By TGA-FTIR system combustion gases of every type of material can be determine but calibration should be carried out for quantitative determination of each combustion gas before measurement.

**Table 1.** Combustion & emission gases results

| No | Types of Materials | Measurement No & Time | O2 (%) | CO (ppm) | NO (ppm) | NO2 (ppm) | NOX (ppm) | CO2 (%) | SO2 (ppm) | Pump (l/min) | Air Temp. (°C) | Chamber Temp. (°C) |
|---|---|---|---|---|---|---|---|---|---|---|---|---|
| 1 | Silicone (VMQ 50 / XGR50-05) | 1. | 19,99 | 57 | 3 | 2,1 | 5 | 1,23 | 0 | 0,91 | 29,2 | 49,8 |
| | | 2.(+18s) | 19,79 | 64 | 3 | 1,9 | 5 | 1,47 | 0 | 0,63 | 29,2 | 54 |
| | | 3.(+30s) | 19,76 | 65 | 3 | 2,3 | 5 | 1,5 | 1 | 0,37 | 29,2 | 55,3 |
| 2 | NBR 70 (N7007) | 1. | 19,86 | 74 | 58 | 2,8 | 61 | 1,39 | 18 | 0,9 | 29 | 47,8 |
| | | 2.(+8s) | 19,68 | 101 | 62 | 3 | 65 | 1,6 | 32 | 0,27 | 29 | 47,8 |
| | | 3.(+25s) | 19,56 | 116 | 75 | 2,3 | 77 | 1,75 | 31 | 0,87 | 29 | 60,6 |
| | | 4.(+85s) | 17,81 | 770 | 166 | 5,8 | 172 | 3,88 | 163 | 0,9 | 29,1 | 113,5 |
| | | 5.(+205s) | 18,1 | 912 | 149 | 4,7 | 154 | 3,52 | 194 | 0,89 | 29,2 | 128,3 |
| 3 | NR 60 | 1. | 19,92 | 131 | 15 | 1,1 | 16 | 1,31 | 27 | 0,9 | 29,4 | 50 |
| | | 2.(+13s) | 19,94 | 143 | 14 | 1,1 | 15 | 1,29 | 29 | 0,89 | 29,3 | 50,7 |
| | | 3.(+26s) | 19,88 | 131 | 15 | 0,9 | 16 | 1,36 | 29 | 0,64 | 29,5 | 51,2 |
| | | 4.(+35s) | 19,89 | 100 | 15 | 0,9 | 16 | 1,34 | 28 | 0,89 | 29,5 | 51,7 |
| 4 | 100% Polyester (pile part) | 1.240 s | 19,92 | 199 | 3 | 1,1 | 4 | 1,42 | 5 | 0,93 | 25,7 | 63,8 |
| | | 2.480 s | 19,99 | 199 | 3 | 1,1 | 4 | 1,43 | 6 | 0,92 | 25,5 | 81,3 |

After establishing test assembly, fabric and rubber trim materials were tested by this new method. According to analysis results, combustion gases of fabric mainly CO and $CO_2$, and trace amount of $NO_x$, $SO_2$ gases. The combustion gases of sulphur based vulcanized rubbers are CO, $CO_2$, $NO_x$ and $SO_2$. But the combustion gases of the silicone rubber are only CO and $CO_2$ (Table 1).

NO, $NO_2$, $NO_x$ and $SO_2$ gases from combustion of fabric were related to dyestuff. $SO_2$ gas from NBR and NR rubbers was associated to the sulphur based vulcanization agent. NO, $NO_2$ and $NO_x$ gases from combustion of NBR rubber was related to nitrile group of the rubber composition. CO and $CO_2$ gases were related to carbonyl group in the macromolecule structure of the polymer. By FTIR, the major gases detected were $CO_2$ (2358/2310 $cm^{-1}$), CO (2180/2109 $cm^{-1}$) and $H_2O$ (1514 $cm^{-1}$) for NBR70. CO and $CO_2$ were detected or PES100% where DTG peaks occur (Figure 2).

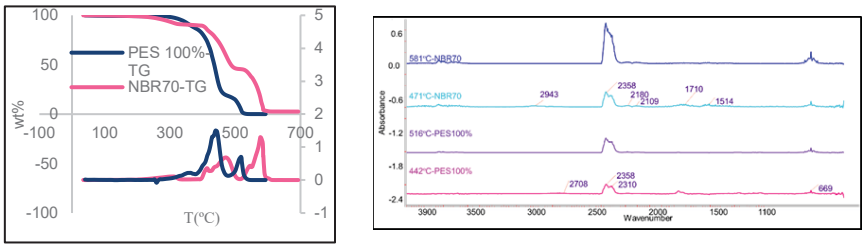


**Figure 2.a.** Results of the thermal analysis**. b.** Evolved gas analysis

## 4. CONCLUSION

The new test assembly for determining toxic gases can be used to measure the toxic gases from combustion of interior and exterior materials in railway vehicles. The variation of the amount of NO, $NO_X$ and $SO_2$ gases from four different types of materials shows that this method can be applicable for measuring toxicity according to EN 45455-2. $SO_2$ and NOx gas concentrations change according to sulphure and nitrogen content in the materials. Further studies required to investigate data correlations between the present technique and EN 45455-2. Detailed results will be presented in future studies.

**This study was supported by Bursa Technical University Scientific Research Projects (Project No: 171N1).**

## REFERENCES

1. EN 45545-2: Railway applications - Fire protection on railway vehicles – Part 2: Requirements for fire behavior of materials and components.
2. http://www.lsfire.it/cosa/pdf/transfeu/20130822_134449_11798_Transfeu_Final_Report.pdf .
3. http://atena.ikolej.pl/images/PDF/160_3.pdf.

# DEVELOPMENT OF HIGH PERFORMANCE FABRICS WITH GRAPHENE

**Nazlı ÇAĞLAR CİNPERİ[1], Duygu YAVUZKASAP AYAKTA[1]**

[1]YÜNSA Yünlü Sanayi ve Ticaret A.Ş.

Corresponding author: ncinperi@yunsa.com

***Abstract:*** *Graphene, with its unique nano scale, is a material that has been investigated and started to use in various research fields in many areas that carry many functional features together. Graphene which has two-dimensional, unique in atomic thickness and strong bond structure gives very good electrical, electrochemical, optical, thermal and mechanical properties. In this study, pyhsical tests of 4 different yarns which content poliamid-graphene/cotton and viscon-graphene/cotton were carried out. Their dyeability has been tested. Absorbancy, drying rate, UV protection, antibacterial (gram +, gram -), blade cut resistance, abrasion, pilling, tear strength, breaking strength and air permeability tests were performed on fabrics woven with these yarns. It has been proved that high performance products can be used both in terms of handle and physical properties.*

***Key Words****: graphene, high performance fabrics, multifunctional fabrics, UV protection, blade cut resistance*

## 1. INTRODUCTION

Graphene is the most famous allotrope of carbon, which has a long history of many applications because it is the lightest, thinnest, hardest and most robust materials. The graphene, which has the name of the strongest material ever measured up to now, is a two-dimensional (atom-thickness) carbon allotropic with a hexagonal honeycomb lattice. Excellent mechanical strength and considerable flexibility are among the striking features of graphene [1].

Graphene has many special functions such as antibacterial, anti-mite, heat and cold resistant, cut resistant, anti-static, UV resistant. These functions can be used in many different fields of textile products such as clothing, knitting, home textiles and etc [1-5].

## 2. MATERIAL AND METHOD

Firstly, the purchase of blends with cotton yarns of polyamide-graphene and viscose-graphene yarns was provided in the properties specified at Table 1. The structure which the graphene is attached was produced with a technology that makes graphene covalent bond with various chemical reactions with the aid of grafene oxide. The functionalization of covalent bonds of graphene provides the use of the resulting functional fibers in a wide range of applications.

In Table 1, the yarns specified by 2 and 4 are folded with the 721S, 800S twist respectively to obtain the appropriate thickness. The dyeability of the obtained yarns has been tested. The prepared yarns were slashed and woven as 2/2 twill weave with the same conditions (Table 2).

Woven fabrics were singed, washed at 50 °C, dried at 120 °C dry steam with 30 m/min, fixed in dry steam machine respectively. The finished fabrics were subjected to absorbancy tests according to AATCC 79 standard, drying rate tests according to AATCC 201 standard, UV protection tests according to AS/NZS 4399:1996 standard, antibacterial tests (Gram +, Gram-) according to AATCC 100 standard, blade cut resistance tests according to EN-388:2016 standard, abrasion tests according to ISO 12947-2 standard and pilling tests according to ISO 12945 – 2 standard, tear stregth -Elmendorf tests according to ISO 13937-1 standard, breaking strength-strip method tests according to ISO 13934-1 standardand air permeability tests according to TS 391 EN ISO 9237 standard.

**Table 1.** Properties of yarns

| Yarn Sample Number | Raw Material Content | Yarn Count (Nm) | Breaking Time (s) | Breaking Strength (cN) | Elongation (%) | Strength (cN/tex) | U % |
|---|---|---|---|---|---|---|---|
| 1 | 50%polyamide-graphene/ 50%cotton | 53 | 0.80 | 251.4 | 13.24 | 13.52 | 9.88 |
| 2 | 50%polyamide-graphene/ 50%cotton | 60 | 0.58 | 193.3 | 9.50 | 12.72 | 10.82 |
| 3 | 50%viscose-graphene/ 50%cotton | 34 | 0.43 | 583.7 | 7.13 | 19.26 | 7.99 |
| 4 | 50%viscose-graphene/ 50%cotton | 80 | 0.36 | 217.0 | 6.03 | 18.08 | 10.16 |

**Table 2.** Technical properties of sample fabrics

| Fabric Code | Fabric Composition | Warp Yarn Count (Nm) | Reed Number | Weft Yarn Count (Nm) | Weft Density | Average Weigth (g/m2) |
|---|---|---|---|---|---|---|
| 1 | 50%polyamide-graphene/ 50%cotton | 60/2 | 72/4 | 53/1 | 38,0 | 210,0 |
| 2 | | 60/2 | 72/4 | 60/2 | 28,0 | 217,7 |
| 3 | 50%viscose-graphene/ 50%cotton | 80/2 | 80/4 | 34/1 | 27,5 | 196,7 |
| 4 | | 80/2 | 80/4 | 80/2 | 30,0 | 186,7 |

## 3. RESULTS AND DISCUSSION

The finished fabrics passed the handle and visual controls made in the quality control department. Physical properties of the fabrics were given at Table 3.

The results of this work showed that the abrasion cycle at break on 1 and 2 numbered fabrics with 50% polyamide-graphene/50% cotton content was higher than 1.000.000. While 20,000 cycles were enough in the standard, the output was at an excellent level. Whereas samples with 50% viscose-graphene/50% cotton showed lower values. It is thought that this result arises because of the viscous material obtained from short fibers. The images obtained after 1.000.000 are shown in Figure 1.

It was found that the samples had high performance (as high as 4 times compared to conventional worsted fabrics) in terms of tear strength and tear strength. In the tests made on woven fabrics, it was seen that the air permeability values of 50% polyamide-graphene/ 50% cotton contented fabrics (1 and 2 samples) were better than 50% viscose-graphene/ 50% cotton fabrics. Pilling and abrasion values were lower than expected. The reason for this is thought to be the tendency of the carbon in the structure to be caused by the friction effect. Blade cut resistance results showed that all samples passed the test with performance level 1.

**Table 3.**Physical properties of the fabrics

| Fabric Code | Average of Air Permability (mm/s) | Average of Tear Strength (kgf) | | Average of Breaking Strength (daN) | | Pilling (2000 cycle) | Abrasion |
|---|---|---|---|---|---|---|---|
| | | Warp Direction | Weft Direction | Warp Direction | Weft Direction | | Cycle at break |
| **1** | 46,4 | 3733,7 | 3190,7 | 91,00 | 61,7 | 3/4,3/4, 3 | >1.000.000 |
| **2** | 52,3 | 3929,0 | 4073,3 | 84,33 | 79,3 | 3,3,3/4 | >1.000.000 |
| **3** | 90,6 | 4999,7 | 4544,0 | 85,00 | 79,7 | 3,3/4, 3/4 | 55.000 |
| **4** | 86,8 | 3380,0 | 2752,3 | 88,00 | 73,7 | 3/4,3/4, 3/4 | 40.000 |

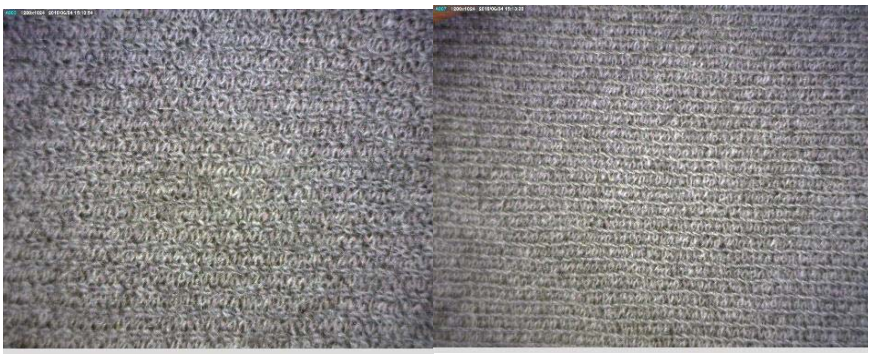

**Figure 1.** The images of the sample 1 and 2 after 1.000.000 cycles

**Table 4.** Functional properties of the fabrics

| Fabric Code | Drying Rate (ml/hours) | Absorbency (sec) Face/ Back | Solar UV Protective Properties | | | | Antibacterial Tests (Reduction %R) | |
|---|---|---|---|---|---|---|---|---|
| | | | UVA Transmittance (315-400 nm) (%) | UVB Transmittance (290-315 nm) (%) | Measurement of UV Protection Factor (290-400 nm UPF) (%) | UPF Rate | S.aureus ATCC 6538 | K.pneumonie ATCC 4352 |
| **1** | No absorption | >60/>60 | 0,35 | 0,12 | 754,35 | 580 | 72,50 | 90,00 |
| **2** | No absorption | >60/>60 | 0,19 | 0,07 | 1306,3 | 475 | 89,47 | 72,72 |
| **3** | 1,13 | >60/>60 | 0,86 | 0,25 | 312,8 | 265 | 90,00 | 67,50 |
| **4** | 1,14 | >60/>60 | 1,16 | 0,29 | 249,05 | 185 | 60,00 | 72,22 |

Functional properties of the fabrics such as antibacterial, UV protection, absorbancy, drying rate were given at Table 4.

Drying rate of the fabrics consisting of 50% polyamide-graphene/50% cotton could not be tested because they did not absorp water on them at the test which was maden according to heated plated method. Rapid drying was observed in samples 3 and 4 consisting of 50% viscose-graphene / 50% cotton. According to the results of the absorption, all of the fabrics gave values higher than 60 seconds. If the fabrics are to be used for fast drying purposes, hydrophilic finishing will be required. The UV protection results in Table 4 were evaluated according to the classification system in Table 5. All the fabrics showed very high UV protection. 50% polyamide-graphene/50% cotton samples were found to have 2-3 times higher values than 50% viscose-graphene/50% cotton samples. Furthermore, it was shown that the obtained fabrics had antibacterial properties between 60 and 90 against S. aureus bacteria and between 67.5 and 90 against K. pneumoniae bacteria.

**Table 5.** Functional properties of the fabrics

| UPF Range | UVR Protection Category | Effective UVR Transmision (%) | UPF Ratings |
|---|---|---|---|
| 15 to 24 | Good Protection | 6,7 to 4,2 | 15, 20 |
| 25 to 39 | Very Good Protection | 4,1 to 2,6 | 25, 30, 35 |
| 40 to 50, 50+ | Excellent Protection | ≤2,5 | 40, 45, 50, 50 + |

## 4. CONCLUSIONS

It has been proved that high performance products can be used both in terms of handle and physical properties. According to the results obtained, it was seen that the fabrics produced can be used both as suits and uniforms. It is predicted that in case of high pilling, it can be achieved by improving the finishing conditions.

The pilling values were seen at the limit values because graphene in the fibers affected the friction on the fabric surface negatively. If the use of fabrics, such as trousers, where there is a lot of rubbing is preferred, it will require improvement with finishing conditions.

All fabrics that exhibited antibacterial properties without application of finish showed very high UV protection. It is foreseen that these level performances can only be obtained in coated fabrics, and they can be easily preferred as uniforms. The abrasion cycle break in fabrics 1 and 2 with 50% polyamide-graphene/50% cotton content is the reason why two groups of fabrics are preferred due to their higher than 1,000,000 value.

It is clearly seen that the fabrics they can be easily used on surfaces that are exposed to abrasion resistant to outdoor conditions that require UV protection, especially in transport upholstery, uniform clothes with various designs.

## ACKNOWLEDGMENTS

This work has been supported by Yünsa Worsted & Woolen Production and Trading Co. as an R&D project.

## REFERENCES

1. Taghioskoui, M., Trends in graphene research, Materials Today, 2009, vol 12, issue 10, pp. 34-37.
2. Hu, W., Peng, C., Luo, W., Lv, M., Li, X., Li, D., Huang, Q., Fan, C., Graphene-based antibacterial paper, ACS Nano, 2010, vol 4, pp.4317–4323.
3. Akhavan, O., Ghaderi, E., Toxicity of graphene and graphene oxide nanowalls against bacteria, ACS Nano, 2010, vol.4, pp. 5731–5736.
4. Zhao, J., Deng, B., Lv, M., Li, J., Zhang, Y., Jiang, H., Peng, C., Li, J., Shi, J., Huang, Q., Fan, C., Graphene oxide-based antibacterial cotton fabrics, Adv. Healthcare Mater., 2013, vol 2, pp.1259–1266.
5. Azimi, S., Behin, J., Abiri, R., Rajabi, L., Derakhshan, A.A., Karimnezhad, H., Synthesis, characterization and antibacterial activity of chlorophyllin functionalized graphene oxide nanostructures, Sci. Adv. Mater., 2014, vol. 6 , pp.771–781.
6. Krishnamoorthy, K., Navaneethaiyer, U., Mohan, R., Lee, J., Kim, S.-J., Graphene oxide nanostructures modified multifunctional cotton fabrics, Appl. Nanosci., 2011, vol 2, pp. 119–126.

# SMART TEXTILE SOLUTIONS FOR THE PREVENTION OF VECTOR-BORNE DISEASES

**Lisandra VİLAÇA**

Smart Inovation

Corresponding author: lisandra.vilaca@smartinovation.com

***Abstract:*** *Mosquitoes are considered one of the deadliest animals in the world. Most*

***Abstract:*** *Mosquitoes are considered one of the deadliest animals in the world. Most species are vectors of diseases, such as Malaria, Dengue, Yellow Fever and Chikungunya, causing millions of deaths every year. The World Health Organization (WHO) has been highlighting measures for the prevention and control of vector-borne diseases (VBDs). It is in this strategy that Smart Inovation presents the Si Repel Mosquito solutions.*

*This work aimed to demonstrate the effectiveness and safety of the Si Repel Mosquito solutions, thus ensuring maximum protection against mosquitoes and therefore reducing the transmission of these diseases to civilians and the military.*

***Keywords:*** *Si Repel Mosquito, vector-borne diseases, innovative technology, mosquito repellency*

## 1. INTRODUCTION

There are many products and technologies designed to prevent bites from arthropods and to reduce the risk for transmission of vector-borne pathogens. Indoor residual spraying and long-lasting insecticidal bed nets are the two most important vector control measures that protect humans from the bite of carrier mosquitoes. Currently only one class of insecticides – pyrethroids – is recommended for use in bed nets, but resistance to pyrethroid insecticides has been increasing over the recent years and now threatens the success of control programs [1]. Alternatively, we have insect repellents, which do not kill insects, but keep them away from the target, and this is where the *Si Repel Mosquito* solution is effective [2, 3].

*Si Repel Mosquito* solution uses the active ingredient 3-(N-acetyl-N-butyl) aminopropionic acid ethyl ester (IR3535), a synthetic insect repellent, whose structure is related to β-alanine, having as chemical formula $C_{11}H_{21}NO_3$. This substance is FDA, EPA and WHO approved [4].

*Smart Inovation* has a unique and innovative technology, which consists of a matrix of particles that allows the transport of active substances. This matrix can bind to various materials giving them new properties and characteristics. Through

this technology, IR3535 can be fixed to several substrates, products and materials, producing an extremely effective, nontoxic, odorless, safe and ecofriendly repellent effect for the prevention of diseases caused by insect bites.

## 2. MATERIAL AND METHOD

Several samples of fabric were impregnated with *Si Repel Mosquito Textile Finish* by padding process, and then cycled to 50, 80 and 100 washes. In the padding process, 30g of *Smart Fix with softener* solution and 80g of the *Si Repel Mosquito Textile Finish* solution per litre of water, were applied. To determine the effectiveness % of the samples, they were submitted to the mouse feed method, in *Siri Life India*, and *IHTM* of Lisbon. This test is used to measure the effectiveness of washed textiles treated with insect repellent active ingredients, to protect against insect bites. To perform this test, 100 mosquitoes *Aedes aegypti* were used. This method was conducted according to the following guidelines: Documentation issued the European Commission; Technical Notes for Guidance. Product Type 18- Insecticides, acaricides and products to control other arthropods and product type 19- repellents and attractants (only concerning arthropods); USA EPA (USA Environment Protection Agency), EPA Product performance test guidelines OPPTS 810-3700: insect repellents to be applied on human skin, July 7, 2010; WHO Guidelines for efficacy testing of mosquito repellents for human skin (WHO/CDS/NTS/WHOPES/2009.4).

In order to test the *Si Repel Mosquito Laundry Additive* solution, we proceeded as follows: 10mL of *Si Repel Mosquito Laundry Additive* solution for every kg of textile. To determine the efficacy of the solution, the fabrics were submitted to the "*arm in cage"* method, in *Siri Life India*. "*Arm in cage*" method is used to evaluate the 'fabric samples' by comparing the number of landings / bites done by mosquitoes during the 5 minutes exposure on to the forearm of volunteers wrapped with insecticide impregnated cloth and a cloth without any insecticide (control) in a cage containing 100 female *Aedes aegypti* mosquitoes. Forearms of the volunteers without any fabric were also inserted for 1 minute to check propensity for biting of the mosquitoes and to use the data to extrapolate number of bites for 5 minutes exposure. Percentage protection offered by the fabric sample was calculated based on reduction in number of bites per experiment.

## 3. RESULTS AND DISCUSSION

No landing or probing was observed on the fabric with 50, 80 and 100 washes, only on the exposed area of the mouse (table 1). The test concludes that fabric sample showed excellent mosquito repellency.

**Table 1** - % efficacy of fabrics impregnated with the solution *Repel Mosquito Si Textile Finish*, after 50, 80 and 100 washes.

| Sample type | % Efficacy | |
|---|---|---|
| | On fabric | On exposed area |
| **50 wash** | 100% | 89,70% |
| **80 wash** | 100% | 83,82% |
| **100 wash** | 100% | 75% |

Another solution was tested, *Si Repel Mosquito Laundry Additive*, which can be use in laundry machine or in handwashing. To determine the efficacy of this solution, the fabrics were submitted to the arm in cage method, in *Siri Life India*.

**Table 2** - % efficacy of fabrics impregnated with the solution *Si Repel Mosquito Laundry Additive*, after 20 washes

| | Treated w/ hand wash softener | | | Treated w/washing machine softener | | |
|---|---|---|---|---|---|---|
| **Washes** | 0 wash | 10 wash | 20 wash | 0 wash | 10 wash | 20 wash |
| **% Efficacy** | 99,5 | 98,52 | 98,06 | 99,02 | 98,52 | 98,06 |

It was observed that for washing by hand, after 20 washes we still had 98,06% efficacy, the same value was found in the washing machine (table 2). We believe that the method of application does not interfere with the effectiveness, since after 20 washes an excellent repellency is obtained.

## 4. CONCLUSION

It is concluded that the technology invented and commercialized by *Smart Inovation*, in these applications and areas, ensures that the release of the active ingredient is done in a controlled and regular way, ensuring high effectiveness after several washes and, therefore, better performance and more durability.

## REFERENCES

1. World Health Organization. “A global brief on vector-borne diseases.” 2014.
2. Ethyl Butylacetylaminopropionate.” 2006.Cilek, J. E., J. L. Petersen, e C. E. Hallmon . “Comparative efficacy of IR3535 and deet as repellents against adult Aedes aegypti and Culex quinquefasciatus.” *American Mosquito Control Association* 20 (2004): 299-304.
3. Lupi, E., C. Hatz, e P. Schlagenhauf. “The efficacy of repellents against Aedes, Anopheles, Culex and Ixodes spp. - a literature review.” *Travel Medicine and Infectious Disease* 11 (2013): 374-411.
4. Unites States Environmental Protection Agency. “3-[N-Butyl-N-acetyl]-aminopropionic acid, ethyl ester (IR3535) (113509) Fact Sheet .” 1999.

# HIGH PERFORMANCE AND BLADE CUT RESISTANT YET SOFT APPAREL FABRICS PRODUCED BY HARD-CORE SPUN YARNS IN WORSTED SYSTEM

**Duygu YAVUZKASAP AYAKTA[1], Fatma GÖKTEPE[2]**

[1] YÜNSA Yünlü Sanayi ve Ticaret A.Ş. Arge Merkezi
[2]Namık Kemal University, Department of Textile Engineering, Turkey

Corresponding author: dayakta@yunsa.com

***Abstract:*** *There has been an increasing trend in personal protective clothing, however providing desired handle and comfort properties along with protection and strength have been the main challenge. In this work high performance and cut-resistant fabrics were developed including composite worsted yarns with core filaments, while soft touch of the fabrics was preserved due to wool fibres at the sheath part of the yarns. In this respect, four types of yarns were produced on ring siro spinning machine and yarn properties were analysed. Then, eight different fabric samples were woven including two different fibre blend ratio, two different core filament linear density and three different dyeing processes, to evaluate the effect of these parameters on blade cut resistance and other fabric physical properties. The analysis of the results show that these fabrics have high performance (approximately as high as 3 times compare to conventional worsted fabrics) and blade cut resistance yet they have soft handle, therefore can be used for men's suit without any compromise in user comfort.*

***Key Words****: Blade cut resistance, worsted fabrics, High performance fabrics*

## 1. INTRODUCTION

Protective clothing has an increasing market in textiles and there is a demand for clothing with cut/stab resistance. A recent survey show that 40% of attacks have been in main parts of the human body while 60% is on the neck and head [1]. There are various works aiming for development of stab and cut resistant clothing in this respect, mainly for knitted products [2-4] while works for woven fabrics seem to be very limited [5]. There are attempts for developing multi-layer knitted structures as well [6]. Cut resistance of single fibres [7] and high strength yarns were also studied [8]. However, maintaining soft handle and comfort properties is the key issue in development of these high performance fabrics. A recent study presents a comprehensive work on deformable stab-resistant fabrics for body protective clothing by using triaxial weave fabrics in comparison with other types of constructions such as plain weave and single jersey knitted fabrics [9]. However, it is difficult to comment on unit weight and comfort properties of developed fabrics as there was no further detail regarding these. Different from these works above, we aim to develop high performance and cut-resistant woven fabrics with light-weight suitable for men's suiting in worsted sector providing a soft touch and comfort.

## 2. MATERIAL AND METHOD

In this work, composite yarns were produced on ring siro-spinning machine by using high tenacity polyamide 6.6 filament as the core. Then, by using these yarns at both weft and warp direction, eight different fabric samples (2/1 twill weaving construction) were woven including two different sheath blend ratios (B1:100% wool and B2: 60%wool/40% Polyester), two different core filament linear density (33 and 50 dtex) and three different dyeing processes (L:loose stock dyeing, Y: bobbin dyeing and P: piece dyeing) as summarised in Table 1 to evaluate the effect of these parameters on blade cut resistance of high performance worsted fabrics produced in this work.

Following fabric production, performance tests were applied to each fabric type. The fabric samples were conditioned at standard atmospheric conditions for 24 hours before the tests. Physical performance of the fabrics, such as breaking strength, tear strength, abrasion, seam slippage, pilling and air permeability, were analysed. All tests were repeated three times. Regarding cut resistance performance, the fabrics were tested according to EN-388:2016 (Figure 1) as suggested by a previous work [10] that provides a comparative evaluation of blade cut resistance between EN-ISO13997 and EN-388:2016.

**Table 1**. Fabric samples produced in this work

| **Composite yarn properties** | | **Blend 1 (Sheath: 100% wool Core: HT PA) Nm 76/2 750 t/m S** | | **Blend 2 (Sheath: 60%wool/40% Polyester Core: HT PA) Nm 80/2 750 t/m S** | |
|---|---|---|---|---|---|
| **Core filament linear density (dtex)** | | 33 | 50 | 33 | 50 |
| **Weft density (ends/dm)** | | 270 | 270 | 280 | 280 |
| **Warp density (ends/dm)** | | 285 | 285 | 285 | 285 |
| **Dyeing process** | **Loose (fiber) dyed** | B1L33 | _ | B2L33 | _ |
| | **Yarn (bobbin) dyed** | B1Y33 | _ | B2Y33 | _ |
| | **Piece (fabric) dyed** | B1P33 | B1P50 | B2P33 | B2P50 |

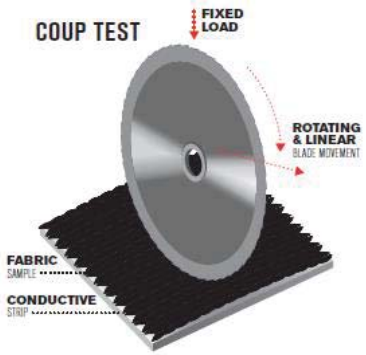


**Figure 1.** Coup test in accordiance with EN 388

## 3. RESULTS AND DISCUSSION

### 3.1. Analysis of yarn properties

In this part, core filament tenacity properties were analysed first. Following this, tenacity and breaking elongation of composite yarns produced by ring siro-spinning were also analysed. These results are given below in Table 2

**Table 2**. Tenacity and breaking elongation values of yarns

| Yarns | | | | Tenacity (cN) | % Breaking Elongation |
|---|---|---|---|---|---|
| **Core Filament** | **Polyamide 6.6** | *c1: 33 dtex* | Average | 249,7 | 24,8 |
| | | | % CV | 3,1 | 2,4 |
| | | *c2: 50 dtex* | Average | 317,6 | 22,3 |
| | | | % CV | 5,09 | 8,6 |
| **Composite yarn (Nm 76/2)** | **Sheath: 100%Wool (Blend 1)** | *core c1* | Average | 395,5 | 22,6 |
| | | | % CV | 7,8 | 12,7 |
| | | *core c2* | Average | 528,5 | 27,4 |
| | | | % CV | 2,5 | 0,3 |
| **Composite yarn (Nm 80/2)** | **Sheath: 60%wool/40% Polyester (Blend 2)** | *core c1* | Average | 610,3 | 27,3 |
| | | | % CV | 5,2 | 8,4 |
| | | *core c2* | Average | 653,5 | 26,8 |
| | | | % CV | 9,2 | 0,4 |

### 3.2. Analysis of fabric properties

When we evaluate the overall results summarised in Table 3, it is clearly seen that the fabrics have high performance and blade cut resistance, therefore they can be used for suitings as protective clothing in worsted fabric sector. The results of this work were also analysed considering the effect of three different parameters on fabric performance, i.e.the effect of core filament linear density, blend ratio for sheath part of the yarns and dyeing type applied during fabric production. Regarding the effect of core filament linear density, both fabrics produced by core filaments with higher linear densities (B1P50 and B2P50) pass the blade cut resistance test while there was no difference between performance of these fabrics in terms of cut resistance level. However, the breaking strength, abrasion resistance and pilling performance of the fabrics with 50 dtex core yarns were lower in general compare to the fabrics produced by 33 dtex core yarns, probably due to the less coverage by sheath fibers. When we analyse the effect of blend ratio, there is a clear increase in performance of fabrics with polyester fibres due to the contribution of better physical performance of these fibres. The results regarding the type of dyeing process show that when loose stock dyeing process was applied, the strength of fabrics improves compare to the fabrics produced by bobbin dyed yarns.

Fabric breaking strength results were given in Figure 2. When these results were examined, it is clearly seen that the fabrics that include polyester fibers have higher breaking strength values as expected. Also, the breaking strength values of the fabrics in warp direction are higher than values in weft direction.

**Table 3**. Physical properties of high performance fabrics

| Fabrics | | Blend 1 | | | | Blend 2 | | | |
|---|---|---|---|---|---|---|---|---|---|
| | | B1L33 | B1Y33 | B1P33 | B1P50 | B2L33 | B2Y33 | B2P33 | B2P50 |
| Weft density | | 27 | 27 | 27 | 27 | 28 | 28 | 28 | 28 |
| Breaking Strength (daN) | Warp direction | 60,7 | 55,0 | 59,7 | 57,7 | 91,0 | 75,0 | 86,7 | 84,0 |
| | Weft direction | 56,3 | 48,7 | 57,0 | 46,0 | 86,3 | 59,0 | 81,0 | 72,3 |
| Tear Strength (N) | Warp direction | 29,7 | 28,5 | 31,9 | 42,7 | 50,0 | 40,9 | 43,5 | 53,1 |
| | Weft direction | 27,8 | 26,7 | 29,2 | 37,2 | 46,8 | 35,7 | 43,6 | 50,8 |
| Abrasion (cycle) | | 43.000 | 40.000 | 43.300 | 39.000 | 70.000 | 86.667 | 70.333 | 73.000 |
| Seam slippage (kgf) | | >20 | >20 | >20 | >20 | >20 | >20 | >20 | >20 |
| Pilling Martindale (2000 cycle) | | 4-5 | 4-5 | 5 | 4-5 | 4-5 | 4-5 | 4-5 | 4-5 |
| Blade cut resistance performance | | pass | pass | pass | pass | pass | pass | pass | pass |
| Air Permability (l/m²/s) | | 126,0 | 91,0 | 187,0 | 120,0 | 216,3 | 181,7 | 93,8 | 135,3 |

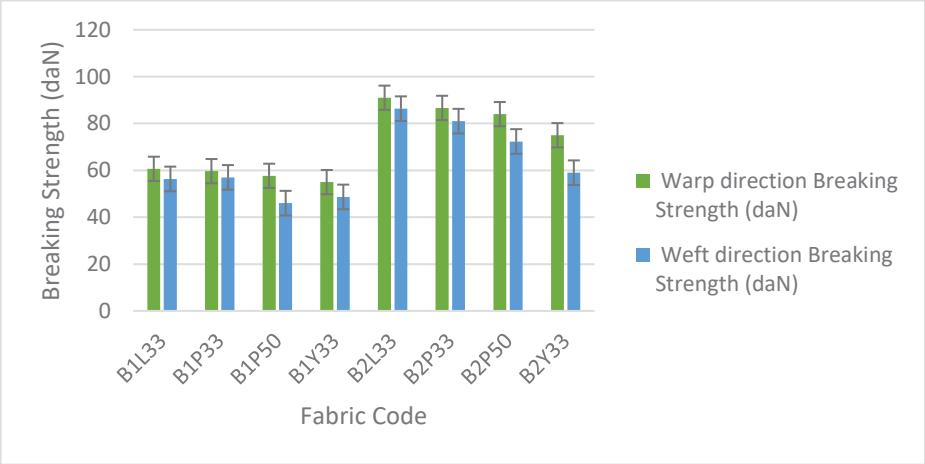


**Figure 2.** Breaking strength values of high performance fabrics

Tear strength results for developed fabrics were given in Figure 3. When results were examined, it is clearly seen that the high performance having polyester have higher tear strength values. The tear strength values of the fabrics with 50 dtex core yarns were higher than the fabrics with 33 dtex core yarns at the same fiber blending.

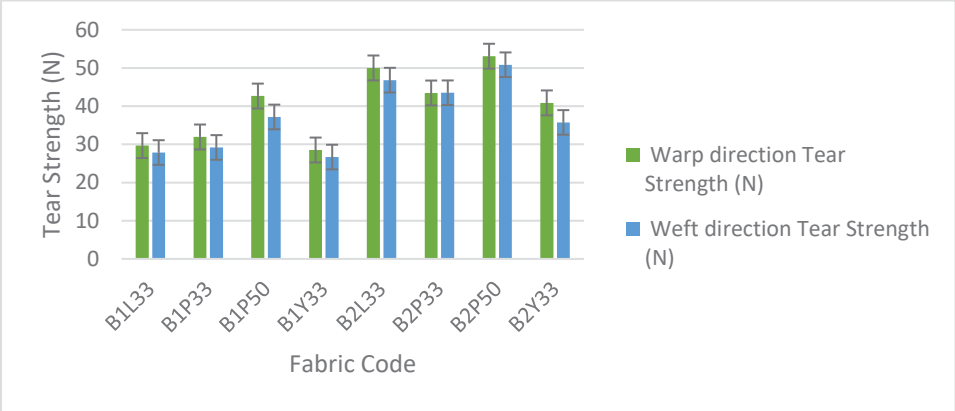


**Figure 3.** Tear strength values of high performance fabrics

Air permability has a significant influence on the moisture and heat transfer properties of protective clothing, and these results were given in Figure 4. As seen in Figure 4, the fabrics with 50 dtex core yarns have lower air permeability than the fabrics with 33 dtex core yarns.

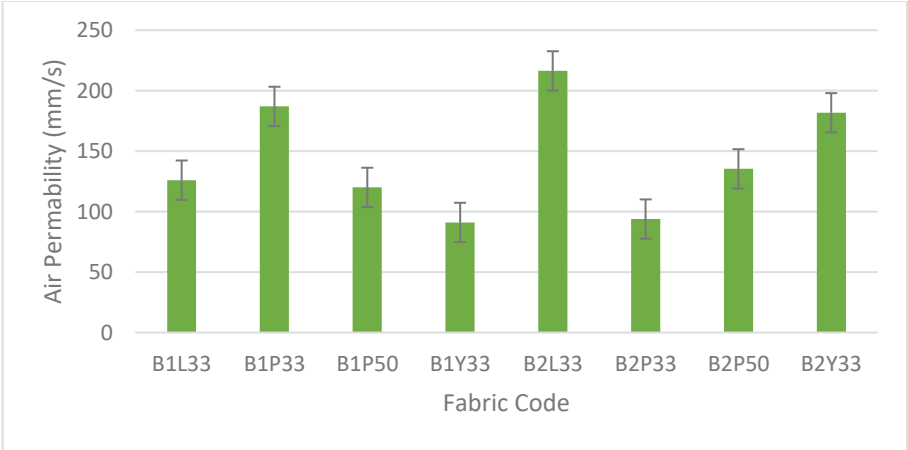


**Figure 4.** Air permability values of high performance fabrics

The results of Martindale abrasion at 9 KPa are expected greater than 20.000 or equal, and the results of abrasion resistance values of the fabrics have varied between 38.000-88.000 cycles. Fabric abrasion cycles at break results were shown in Figure 5. When results wereexamined, it is clearly seen that the fabrics with polyester fiber have higher abrasion cycles.

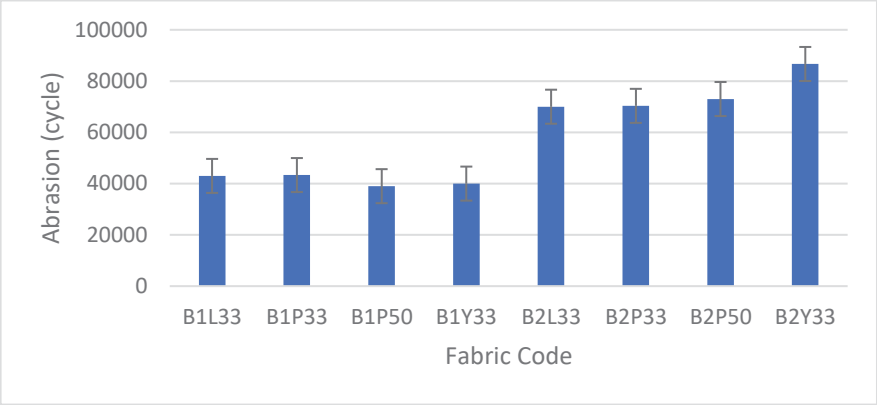


**Figure 5.** Abrasion cycles at break of high performance fabrics

## 4. CONCLUSIONS

This work was carried out following demands for protective clothing in light-weight apparel fabrics in worsted fabric sector. In this regard, four types of composite yarns were produced on ring siro-spinning system. Then, eight different fabrics were woven by using these yarns in weft and warp direction and fabric performance was evaluated in terms of general physical properties as well as their blade cut resistance, which was the main aim of this work. The results of this work show that worsted fabrics with high performance (as high as 3 times compare to conventional worsted fabrics) and blade cut resistance yet soft handle can be developed suitable for men's suit without any compromise in user comfort.

The findings also show that linear density of core filament has no effect on cut resistance performance. On the other hand, there is a clear increase in performance of fabrics with polyester fibres compare to the fabrics with 100% wool fibres in sheath part of the yarns. The results also show that when loose stock dyeing process was applied during fabric production instead of bobbin dyeing or piece dyeing process, the performance of fabrics improves further.

## ACKNOWLEDGMENTS

This work has been supported by TUBITAK-Teydeb project no: 3171019

## REFERENCES

1. Govarhanam K.K, Anand S.C., Rajendran S.: Technical textiles for knife and slash resistance, Handbook of Technical Textiles, 193-236.
2. Alpyıldız T., Rochery M., Kurbak A., Flambard X.: Stab and cut resistance of knitted structure: a comparative study. 2011. Textile Research Journal, 81(2), 205-214.
3. Ertekin M.: Kaplamanın koruyucu performans özelliklerine etkisi. 2017. Tekstil ve Mühendis, 24 (107), 172-180.

4. Anand SC, Kathick KG., Rajendran S., Tracey A.: Development of an advanced personal protection equipment garment for protection against slashes. 2011. International Congress of Innovative Textiles Icontex, 428-437.
5. Kothari V.K, Das A., Sreedevi R.: Cut resistance of textile fabrics: A theoretical and an experimental approach. 2007. Indian Journal of Fibre & Textile Research, 32, 306-311.
6. Thilagavathi G., Rajendrakumar K., Kannaian T.: Development of textile laminates for improved cut resistance. 2010. Journal of Engineered Fibers and Fabrics, 5(2), 40-44.
7. Mayo JB JR., Wetzel ED.: Cut resistance and failure of high performance single fibres. 2014. Textile Research Journal, 84(12), 1233-1246.
8. Shin H.S., Erlich D.C., Simons J.W., Shockey D.A.: Cut resistance of high-strength yarns. 2006. Textile Research Journal, 76(8), 607-613.
9. Mesiry M.E, Eltahan E.: Stab resistance of triaxial woven fabric for soft body armour. 2016. Journal of Industrial Textiles. 45(5) 1062-1082.
10. Irzmanska E., Stafko A.: Comparative evaluation of test methods for cut resistance of protective gloves according Polish standards. 2012. Fibres&Textiles in Eastern Europe, 20, 5(94), 99-103.

# FABRICATION OF CONDUCTIVE COMPOSITE YARN LOADED WITH SILVER NANOPARTICLES VIA "GREEN APPROACH"

**Şeyma KANARA[1], Suat ÇETİNER[1], Neslihan BOZAN[2]**

[1] Kahramanmaraş Sütçü İmam University, Turkey
[2] Karacasu Tekstil Tic ve San A.Ş.

Corresponding author: suatcetiner@ksu.edu.tr

***Abstract:*** *In this study, we presented a facile, environmentally-friendly and cost-effective method for the synthesis of silver nanoparticles (AgNPs) using carboxymethyl starch (CMS). Silver nitrate was reduced on the surface of the polyamide (PA) yarn which allowed formation of silver nanoparticles. Efficiency of composite yarns loaded with silver nanoparticles (AgNPs) was studied which were developed by "green process" using natural reducing agents. Scanning electron microscopy (SEM) studies confirmed the presence of silver nanoparticles on the composite yarns and electrical conductivity was changed from 1.206x10$^{-6}$ to 6.120x10$^{-5}$S/cm. The effect of silver nitrate on the morphological, electrical and spectrophometeric properties was investigated.*

***Keywords:*** *Silver nanoparticle, polyamide yarn, conductive textile, green chemistry*

## 1.INTRODUCTION

Nowadays special focus on "green chemistry" by researchers is strongly created as a result of increasing awareness about the environment. Utilization of nontoxic chemicals, environmentally be solvents and renewable materials are some of the key issues that merit important consideration in a green synthesis strategy [1]. Silver nanoparticles (AgNPs) are increasingly used in various fields; such as medical, food, health care, consumer, textiles and industrial purposes, due to their unique physical and chemical properties. These include optical, electrical, thermal, high electrical conductivity, and biological properties [2]. Recently, biologically-mediated synthesis of nanoparticles have been shown to be simple, cost effective, dependable, and environmentally friendly approaches. Several studies reported the synthesis of AgNPs using green, cost effective, and biocompatible methods without the use of toxic chemicals in biological methods. Compared to chemical methods, biological methods allow for more ease in the control of shape, size, and distribution of the produced nanoparticles by optimization of the synthesis methods, including the amount of precursors, temperature, pH, and the amount of reducing and stabilizing parameters [2]. In this paper, a texturized multifilament polyamide yarn was used. In situ synthesis of nano-silver on polyamide yarn has been introduced through a biological reduction method in order to create a thin layer of silver nanoparticles on

polyamide yarn. The advantage of this method is preparing of AgNPs without any organic solvents or other chemical reducing agents.

## 2. MATERIAL AND METHOD

### 2.1. Preparation of silver nanoparticles

Initially, the carboxymethyl strach (CMS) solution was stirred by a magnetic stirrer for 3 h at room temperature. Then, PA multifilament yarn was treated with CMS solution at 25 °C for 1 h. Meanwhile $AgNO_3$ solution was prepared by magnetic stirrer at 25 °C. $AgNO_3$ solution was added dropwise to CMS solution and PA yarn was treated with that solution at 25 °C for 3 h to obtain a thin silver nanolayer formation on the fiber surface. The color of the solution turned yellow and dark brown depending of the concentration of the reduced silver ions. After the reducing process, the composite PA yarns were rinsed with distilled water and dried in an oven at 60 °C.


**Scheme 1.** Preparation of silver loaded PA composite yarn

The effect of process parameters such as $AgNO_3$ concentration and time was investigated and optimum conditions have been determined for these yarns.

**Figure 1.** Images of pristine yarn (a) and composite yarn (b)

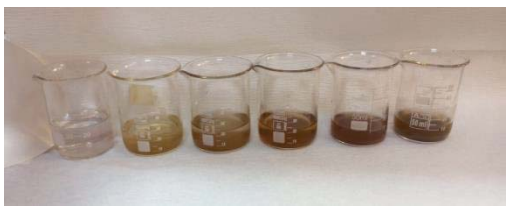

**Figure 2** .Silver nitrate solutions (distilled water, 0,5 wt %, 1 wt %, 2 wt %, 4 wt %, 10 wt %)

### 2.2. Characterization of silver nanoparticles

The morphological characteristics of AgNPs were determined by a Carl Zeiss Evo LS10 high resolution scanning electron microscope (SEM). The samples were gold coated and placed on the aluminum stub and observed under vacuum in SEM-EDX. The electrical conductivity of composite yarns was measured by four-point probe technique.

## 3. RESULTS AND DISCUSSION

### 3.1. Morphology of Composite Yarns

Figure 3 shows the surface morphology of PA multifilament yarn containing 1%wt reduced silver nanoparticles. When the uncoated PA yarn has a smooth surface, a thin coating layer was observed which indicates the formation of AgNPs on the fiber surface. This is consistent with the previous observations incorporating nanoparticles into polymeric materials [3,4].

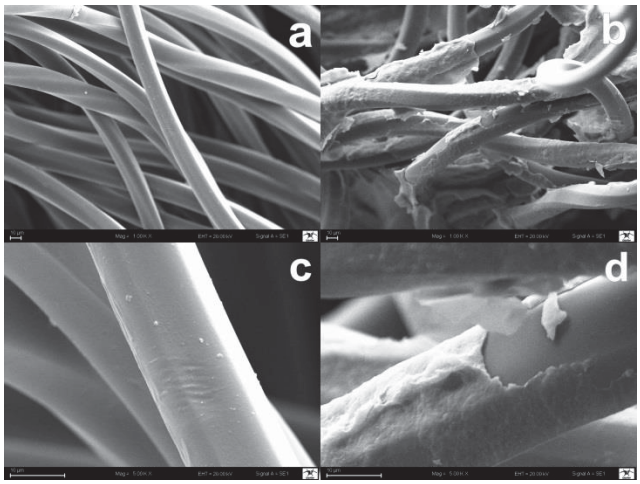


**Figure 3.** SEM images of pristine PA yarn (a,c) and coated PA yarns with 1% wt AgNPs (b,d) [Magnification: 1.00KX (a,b), 5.00KX (c,d)]

Figure 4 presents the Energy dispersive X-ray analysis (EDX) results of multifilament PA composite yarns. According to the SEM-EDX analysis, the presence of AgNPs with 8.42 at% was measured which confirm the AgNPs formation on multifilament PA composite yarn structure (Figure 4).

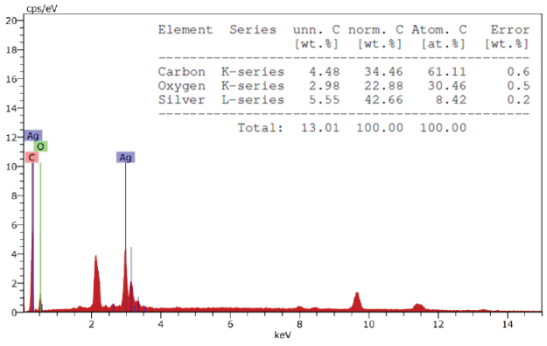


**Figure 4.** EDX measurements

### 3.2. DC Conductivity of Composite Yarns

Electrical conductivity measurements were conducted using the standard four point probe technique. The system has four probes at equally spaced. A constant current is passed between the two external probes. Conductivity is measured using Van der Pauw equation [5,6].

$$\sigma\ (S/cm) = (\ln(2) i) / (\pi\ d\ V)$$

d:Thick V:Volt I: Amper

The electrical conductivity of composite yarns was changed from $1.206x10^{-6}$ *to* $6.120x10^{-5}$ *S/cm.* Conductivity of AgNPs composite samples *(0,5 wt %, 1 wt %, 2 wt %, 4 wt %, 10 wt %)* was determined as in the table.

**Table 1**. Conductivity of AgNPs composite samples

| YARN | THICKNESS | % RATE | DC CONDUCTIVITY |
|---|---|---|---|
| **0,5 ( wt %)** | 0,603 | 1,1 | $1.206x10^{-6}$ |
| **1 (wt %)** | 0,617 | 2,5 | $2.638x10^{-6}$ |
| **2 (wt %)** | 0,621 | 2,9 | $1.385x10^{-5}$ |
| **4 (wt %)** | 0,631 | 3,9 | $1.900x10^{-5}$ |
| **10 (wt %)** | 0,634 | 4,2 | $6.120x10^{-5}$ |

The effect of silver nitrate concentration on electrical conductivity was investigated and the electrical conductivity increased with increasing concentration.

### 3.3. UV-Vis Measurement Result of Composite Yarns

Analysis UV–vis spectra were recorded on a U-3900 HITACHI UV–vis spectrophotometer. The UV-vis absortion spectra were measured at room

temperature by placing the sample in a 1 cm quartz cuvette over wavelength 200-800 nm.

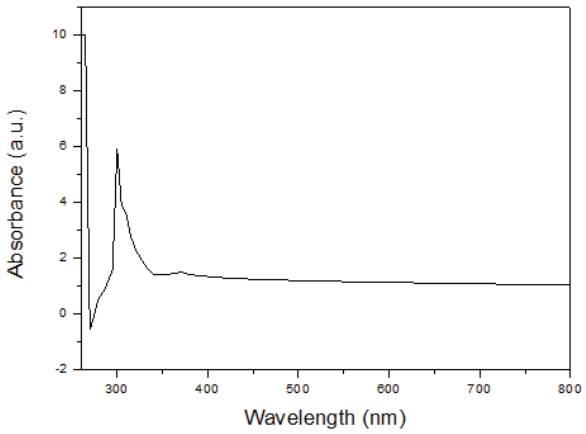


**Figure 5.** UV measurement of % 1 AgNP solution

Fig. 5 represents the UV–vis spectral data of % 1 wt AgNP solution, for the synthesized silver nanoparticles by use of CMS. All the solutions exhibited characteristic silver surface plasmon resonance (SPR) typically located in between 280–340 nm. [7].

It seemed that the AgNPs absorbed radiation in the visible regions of 280–340 nm [8,9]. At this concentration of AgNO3, the maximum absorption wavelength gives rise to a blue shift, meaning a decrease in the particles size [10].

## 4. CONCLUSION

The silver nanoparticles were successfully synthesized on the PA multifilament yarn to obtain a conductive functional textile by in situ green synthesis approach. This strategy is expected to become an effective method for the fabrication of conductive functional textiles.

## REFERENCES

1. El-Rafie M.H,. El-Naggar M.E, Ramadan M.A., Fouda M. M.G., Salem S., Al-Deyab., Hebeish A., 2011, Environmental synthesis of silver nanoparticles using hydroxypropyl starch and their characterization
2. Zhang X.F., Liu Z.G, Shen W., Gurunathan S., 2016, Silver Nanoparticles: Synthesis, Characterization, Properties, Applications, and Therapeutic Approaches, College of Biological and Pharmaceutical Engineering,Wuhan Polytechnic University, Wuhan 430023, China.
3. Alshehri S. M., Aldalbahi A., Baker Al-hajji A., Chaudhary A.A., Panhuis M., Alhokbany N., Ahamad T.,2016, Development of carboxymethyl cellulose-based hydrogel andnanosilver composite as antimicrobial agents for UTI pathogens, 2015, Carbohydrate Polymers 138 -2016-229–236.

4. Xue, C.H., Chen J., Yin W., Tian Jia S., J. Zhong Ma, Superhydrophobic conductive textiles with antibacterial property by coating fibers with silver nanoparticles a College of Resource and Environment Chemistry and Technology for Light Chemical Industry, Ministry of Education, Shaanxi University of Science and Technology.
5. Madl, C. M., Kariuki P. N., Gendron, J., Piper, L. F.J., Jones W. E., 2011, Vapor Phase Polymerization of Poly (3,4-ethylenedioxythiophene) on Flexible Substrates for Enhanced Transparent Electrodes, *Synthetic Metals,* 161, 1159– 1165.
6. Performing van der Pauw Sheet Resistance Measurements Using the Keithley S530 Parametric Tester, Number 3180.
7. M. A., Saad, Aldalbahia A., Al-hajjia A. B.,. Chaudharyb A. A , Panhuis M., , Ahamada, T. Alhokbanya N., Development of carboxymethyl cellulose-based hydrogel andnanosilver composite as antimicrobial agents for UTI pathogens, Carbohydrate Polymers 138 (2016) 229–236.
8. Hebeish A., Hashem M., Abd El-Hady M.M., Sharaf S., 2013, Development of CMC hydrogels loaded with silver nano-particles for
9. medical applications, Carbohydrate Polymers 92 (2013) 407– 413.
10. Kanmani P., Taik Lim S., Synthesis and characterization of pullulan-mediated silver nanoparticles and its antimicrobial activities, Carbohydrate Polymers 97 (2013) 421– 428.
11. Hebeish A.,. El-Rafie M. H, El-Sheikh M. A.,. El-Naggar M. E, 2013 , Nanostructural Features of Silver Nanoparticles Powder Synthesized through Concurrent Formation of the Nanosized Particles of Both Starch and Silver, ournal of Nanotechnology Volume 2013, Article ID 201057, 10 pages http://dx.doi.org/10.1155/2013/201057

# EVALUATION OF MECHANICAL AND DISPERSIBLE PROPERTIES OF FLUSHABLE NONWOVENS

**Hande Gül ATASAĞUN[1], Gajanan BHAT[2]**

[1] Dokuz Eylül University, Turkey
[2] The University of Georgia, USA

Corresponding author: handegul.yuksel@deu.edu.tr

***Abstract:*** *Flushable nonwoven wipes have become popular in recent years thanks to an increase in environmental consciousness of consumers. It is important that flushable wipes are compatible with water treatment systems. In addition, they should be biodegradable and dispersible to remove their harmful effects on the environment. The dispersion of these nonwovens is associated with their wet strengths, which are needed during the storage and use of wipes, and the increase in the strength might prevent the dispersibility of webs. Therefore, the aim of this study was to investigate the mechanical and dispersibility performances of commercially available flushable wipes. The production system had a significant effect on both the strength and dispersible properties of the nonwovens. The findings of the study are useful for understanding the dispersion mechanisms of different flushable nonwovens.*

***Keywords****: dispersibility, extension, flushable wipes, maximum load*

## 1. INTRODUCTION

Flushable wipes are nonwovens that can be broken up into small pieces, dispersed quickly and transferred from the toilet bowl to sewer systems. They can be used for different purposes such as moist toilet tissues, baby wipes, and bathroom cleaning wipes. The flushable wipe market is developing rapidly because of the ease-of-use of these wipes and the increase in consumers' environmental perception. The sales are expected to double to $2.7 billion in the world through 2020 [1].

A truly flushable wipe should not float, should quickly submerge to the bottom of the toilet bowl and should be removed by the sludge. Moreover, it should disintegrate under agitation in water, and eventually not damage the sewer system [2, 3]. Namely, a flushable wipe should be compatible with sewer and water treatment systems and not lead to any pollution. These can be achieved using biodegradable and dispersible materials and by selecting appropriate production techniques and process parameters [2, 4]. Short fiber length is a significant factor in the dispersibility of nonwovens because the structures made of conventional staple fibers might not completely break up into the individual fibers in the water [5]. Zhang et al. [6] reported that as the content and the length-to-diameter ratio of the Danufil fiber used in wetlace nonwovens increased, their dispersion performance decreased and the tensile and tearing strengths increased. Zhang and Jin [7] observed that the basis weight of wetlace

nonwovens affected the dispersibility performance when the hydroentanglement pressure sum was above 135 bars.

Flushable wipes should be weak enough to disintegrate in sewer systems. On the other hand, it is also crucial that they have the adequate wet strength during storage, converting processes and usage. The improvement in their mechanical strength might decrease the dispersibility performance of these nonwovens [8]. These properties should be balanced during the production of flushable wipes. In this study, we aimed to examine the structure, dispersibility and mechanical properties of various commercially available flushable wipes. The results can help develop new flushable wipes, which are appropriate for sanitary and other applications.

## 2. MATERIAL AND METHODS

Six different commercially available nonwoven wet wipes were used in this study. Their production systems are wetlaid/hydroentanglement and airlaid/triggerable binder. While wetlace products consisted of wood pulp and viscose fiber, ion-triggered airlaid nonwovens were made of wood pulp only. The constructional parameters of these nonwovens are given in Table 1.

**Table 1.** The constructional parameters of nonwovens used in the study

| Sample code | Laying / Bonding | Mass per unit area ($g/m^2$) | Fabric thickness (mm) | Fabric bulk density ($g/cm^3$) |
|---|---|---|---|---|
| W1 | Wetlaid/ Hydroentanglement | 61.96 (2.11) | 0.40 (0.02) | 0.156 |
| W2 | | 61.04 (2.42) | 0.40 (0.02) | 0.155 |
| W3 | | 63.00 (1.81) | 0.41 (0.01) | 0.154 |
| A1 | Airlaid/ Ion-triggered binder | 83.09 (4.50) | 0.42 (0.02) | 0.197 |
| A2 | | 83.15 (4.05) | 0.45 (0.01) | 0.184 |
| A3 | | 81.44 (2.03) | 0.43 (0.02) | 0.190 |

Structural characteristics of the products were determined by using the field emission scanning electron microscope (FE-SEM) (FEI Teneo, FEI, Inc., Hillsboro, OR, USA) at the magnification of 500.

Tensile properties were determined along the machine direction (MD) and cross-machine direction (CD) of nonwovens according to the ASTM D 5035-11 standard. An Instron tensile tester (Instron 4400R, Norwood, MA, USA) equipped with a 50 N load cell was used to measure the maximum load and the extension at this load. The specimen dimensions were 25 x 125 $mm^2$. The test speed was 25 mm/min, and the gage length was 50 mm. Five specimens were tested in the dry state and wet states (in-use and post-use). Pre-moistened wipes, which are in their packages, simulated the in-use condition. Besides, they were soaked into tap water for 15 minutes to mimic the post-use condition.

Dispersible properties of the nonwovens were evaluated in compliance with the UKWIR Flushability Protocol- Sewer disintegration test method (Figure 1) [3]. Three samples were dried at 105°C for 3 hours, and the average dry weight of each sample was determined. A 2-liter conical flask, which includes 1 liter of tap water and a wet wipe, was mounted on the orbital shaker at a test speed of 150 rpm for 6 hours. At the end of this test, the content of the flask was poured onto a perforated plate sieve. A showerhead with a flow rate of 4 l/min was used to rinse the residuals on the sieve for 1 min, and then they were dried and weighed. The percentage of the product weight passed through the sieve (PPW) was based on the equation below, with the dry weight of the retained residuals (DWR) and control samples (DW). Statistical analyses were conducted with SPSS 22.0 statistical software package (IBM, Armonk, NY, USA).

$$\text{PPW}\ (\%) = \left[1 - \left(\frac{\text{DWR}}{\text{DW}}\right)\right] \text{x}\ 100 \qquad (1)$$

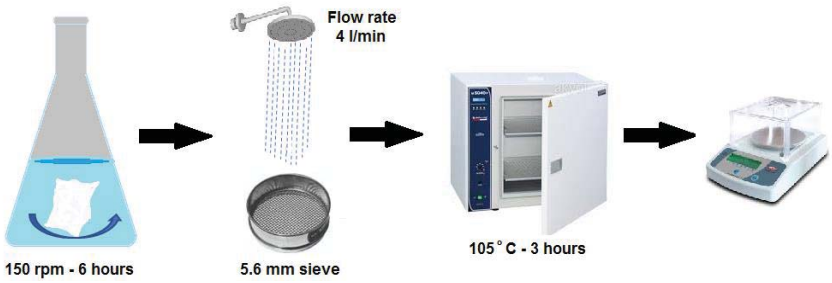


**Figure 1.** Schematic of the sewer disintegration test.

## 3. RESULTS AND DISCUSSION

### 3.1 Morphological characteristics

The structure of nonwoven specimens was analyzed with the FE-SEM. SEM photographs in Figure 2 show the morphology of the wetlace (W1) and airlaid (A1) products. As can be seen in Figure 2a, the wood pulp and viscose fibers were interlaced by the hydroentanglement process. Fiber entanglements and cohesions were observed in the sample structure. The flexural rigidity of the wood pulp is lower as compared to that of the viscose fibers [6]. Therefore, viscose fibers could not be entangled as easily as the wood pulps. On the other hand, the fibers formed U-shape entanglements in order to be interlocked in the structure. When examining the image of the airlaid sample (Figure 2b), it was determined that the wood pulps were arranged cross to each other, and any binder particles were not observed on their surface.

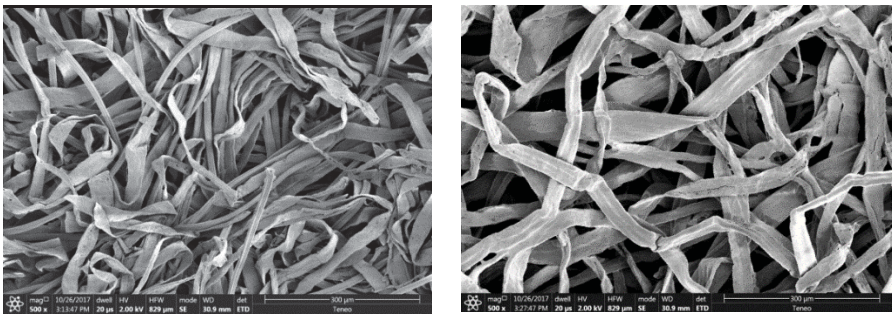

**(a)** **(b)**

**Figure 2.** SEM images of the **(a)** W1 and **(b)** A1 samples.

### 3.2 Mechanical properties

Maximum load and the extension at maximum load for the nonwovens used in this study are shown in Figure 3. It was determined that the MD maximum load of nonwovens, particularly airlaid products (A1-A3), was generally higher as compared to the CD ones. In addition, as the samples got wet, the measured maximum loads generally decreased in both directions. While the airlaid nonwovens had a higher strength in the dry state as compared to wetlace products (W1-W3), their maximum load values were the lowest under the in-use and post-use conditions. This may be owing to the triggerable binder, which is used to hold the fibrous materials together. When the product is submerged in tap water, the binder becomes water-soluble due to the triggerable polymer in its structure, and accordingly, the wet strength decreases [9]. The maximum load of the wetlace nonwovens was slightly reduced when the conditions were changed from the dry state to the wet state. This decrease might be due to the viscose fiber strength because the dry strength of viscose fibers is higher than their wet strength [10]. Also, the reduction in the friction coefficient between fibers in wet conditions might decrease the strength of the webs [11]. The statistical analyses showed that the dry-wet condition was a statistically significant factor on the maximum load measured for these products ($p<0.05$).

The extension of airlaid samples had almost similar values in both directions. However, the extension measured for the CD of wetlace nonwovens was higher than that in the MD. The reason could be the predominant fiber orientation leading to the formation of ribbon-like structures extending along the MD of these nonwovens. Viscose fibers might be separated from the ribbons during the extension in the CD, and therefore, resulting in relatively higher elongation in the CD than that observed in the MD [12]. The extension of wetlace products showed a significant increase in the wet conditions as compared to the dry state ($p<0.05$). This is likely owing to the viscose fiber, which has higher wet elongation than the dry elongation [10]. The extension of airlaid samples slightly decreased from the dry state to the post-use condition.

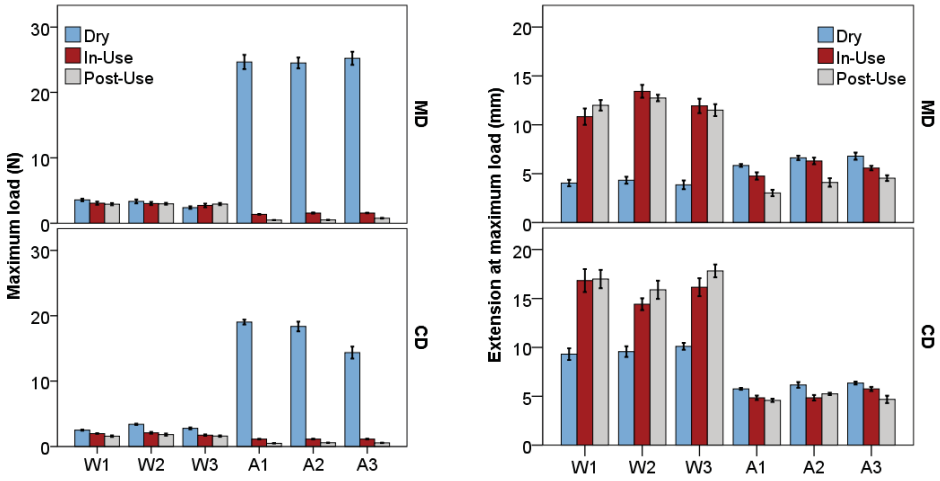


**Figure 3.** Tensile properties of the nonwovens used in the study. Data are shown as mean values with error bars indicating "1" standard error

### 3.3. Dispersible properties

Dispersion is a disintegration process in which the tested product breaks up into small pieces, which separate from each other and distribute in water [13]. The disintegration percentages measured for wetlace products were around 18%, and there was no statistically significant difference among the wetlace nonwovens used in the study ($p<0.05$). These values were between 57.4% and 84.1% in the airlaid products. These nonwovens might be disintegrated quickly under agitation thanks to the triggerable binder dissolving in water. Also, strong negative correlations were observed between the disintegration percentage and wet strength of samples (in-use, $R$=-0.963; post-use, $R$=-0.974).

The SEM images of nonwovens were re-taken after the disintegration test (Figure 4) in order to determine their structural changes. As can be seen, the wood pulps were damaged under agitation in the water. Also, the stacked fibers in the wetlace sample started to disentangle at the end of the disintegration test. This may be due to the fiber-fiber and water-fiber frictions and the shear stress caused by turbulence in the water during this test.

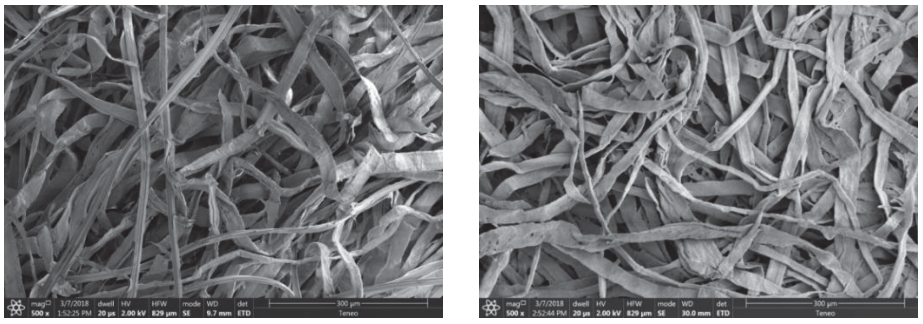

**(a)** **(b)**

**Figure 4.** SEM images of the **(a)** W1 and **(b)** A1 samples after the disintegration test

## 4. CONCLUSIONS

In this study, the mechanical and dispersible properties of commercially available flushable nonwovens were investigated. The disintegration of nonwovens was related mainly to their wet strength, and the increased strength caused a simultaneous decrease in their disintegration percentage. Moreover, the findings revealed that the production system used to make the wipes was an effective factor on these properties. The results will contribute to developing new flushable products, which are compatible with sewer systems. Further studies will focus on the biodegradability of flushable nonwovens.

## ACKNOWLEDGMENTS

This study was supported by the Scientific and Technological Research Council of Turkey (TÜBİTAK) - 2219 International Post-Doctoral Research Fellowship Programme. The authors would like to thank Shuangyan Wu for her support with some of the disintegration tests.

## REFERENCES

1. Smithers Pira (2015). New dispersible nonwovens capacity to outstrip demand by at least 200%. Available: http://www.smitherspira.com/news/2015/december/dispersible-nonwovens-capacity-to-outstrip-demand
2. Rengasamy R.S.: Composite nonwovens in wipes in Composite Nonwoven Materials: Structure, Materials and Applications, 2014. D. Das and B. Pourdeyhimi (eds.), Woodhead Publishing, Cambridge, 89-120.
3. Drinkwater A., Galleti S., Moy F., et al.: Test protocol to determine the flushability of disposable products, Report for the UK Water Industry Research, 2012, Report no.WM07G202, London, UK,
4. Kim M.J., Hergeth H.H.: Technology roadmap for flushable nonwoven wipes. 2012. J Text Inst v. 103(2), 200-209.
5. Scholz R., Sigmund I.: Steering of dispersibility of spunlaced nonwovens with fibre properties and spunlacing parameters. 2012. Lenzinger Berichte v. 90, 72-75.

6. Zhang Y., Zhao Y., Latifi M., et al.: Investigation of the mechanical and dispersible properties of wood pulp/Danufil wetlaid nonwovens with/without hydroentanglement. 2018. J Text Inst v. 109(5), 647-655.
7. Zhang Y., Jin X.: The influence of pressure sum, fiber blend ratio, and basis weight on wet strength and dispersibility of wood pulp/Lyocell wetlaid/spunlace nonwovens. 2018, J Wood Sci v. 64(3), 256-263.
8. Bhat G., Parikh D.V.: Biodegradable materials for nonwovens in Applications of Nonwovens in Technical Textiles, 2010. R.A. Chapman (ed.), Woodhead Publishing, Cambridge, 46-62.
9. Zwick K.J., Zhang J., Johnson K.D., et al.: Dispersible wet wipes constructed with a plurality of layers having different densities and methods of manufacturing, Patent US 8,603,297 B2, USA, 2013.
10. Yan Y.: Developments in fibers for technical nonwovens in Advances in Technical Nonwovens, 2016. G. Kellie (ed.), Woodhead Publishing, Cambridge, 19-96.
11. Zhang Y., Deng C., Qu B., et al.: A study on wet and dry tensile properties of wood pulp/lyocell wetlace nonwovens in IOP Conference Series: Materials science and engineering, 2017. IOP Publishing v. 241(1), 1-4.
12. Zhang Y., Deng C., Wang Y., et al.: A new dispersible moist wipe from wetlaid/spunlace nonwoven: Development and characterization. 2018, J Ind Text, DOI: 10.1177/1528083718757524.
13. INDA & EDANA. Guidelines for Assessing the Flushability of Disposable Nonwoven Products, 3rd ed. 2013.

# PERFORMANCE OF THE DOUBLE FACE LIGHTWEIGHT WOVEN FABRICS FROM SUSTAINABLE YARNS

**Duygu YAVUZKASAP AYAKTA[1], Vildan SÜLAR[2], Eren ÖNER[3]**

[1]YÜNSA Yünlü San. ve Tic.A.Ş.
[2]Dokuz Eylul University, Department of Textile Engineering, Turkey
[3]Uşak University, Department of Textile Engineering, Turkey

Corresponding author: vildan.sular@deu.edu.tr

***Abstract:*** *In this study, the effects of raw material and weft density on the performance properties of the double face woven fabrics, which are used for many different purposes, were researched. In this concept, double face lightweight woven fabrics were produced from different raw materials as cotton, Promodal, Tencel and kapok fibres. Three density levels as tight, medium and loose were used for technical design of the double face fabric production. Basic structural parameters of the fabrics systematically produced were tested and some performance properties as breaking strength, abrasion resistance, air permeability and contact angle were examined. According to findings, the effect of fibre type in weft yarn and the effect of fabric density were evaluated.*

***Key Words****: Tencel, Promodal, kapok, double face, lightweight, woven fabric, performance*

## 1. INTRODUCTION

In parallel with the development of the technology, the existing methods for the weaving production have been found unsatisfactory, and novel weaving methods have been researched. Based on fabric construction, woven fabrics provide different properties which are achieved to satisfy consumer demands for specific end-use.

At this point, double face woven fabrics are taken attention with their visual effects, different construction and some important physical properties. Double face woven fabrics consist of two warp and two weft systems, the first weft and warp systems produce the upper surface of the fabric and the second weft and warp systems produce the lower surface. Double face woven fabrics may be considered under the following heads; the relative proportions and thickness of the face and backing threads, the origination or the selection of the face and backing weaves, the construction of the design, the beaming, the drafting and the contruction of the pegging plan [1]. Thanks to this production technique, different properties can be given to the different face of the fabric. Double face fabrics have been used for improving heat insulation in winter garments, preventing water penetration in rain coats, giving tensile strength in industrial textiles.

In addition to this, double fabrics are also produced to give different features to textile garments without increasing to fabric weight excessively. With the use of double fabrics, it is tried to provide many features to garment in one fabric structure instead of creating heavy structure with the use of more than one fabric type. At this point, lightweight fabric structure increases this advantage of double fabrics with low density. The lightweight double fabric has become more attracted with advances in textile technology and garment construction.

Many researchers focused on the measurement of some properties of double face fabrics [2-9]. Although there are many studies on the double layer knitted fabrics, there are limited published papers which investigate the properties of double woven fabrics experimentally [10,11]. In this research it is decided to investigate the possibility of constructing double layer woven fabrics which offer lightweight structures with good performance properties. Usually double woven fabrics are used for thicker fabrics with good thermal isolation properties. The chosen fabric parameters with thin and sustainable yarns enables to produce the double fabrics suitable for suiting fabrics without any requirement for linings. Thus, this study aims to design a special construction which is 30-50% lighter than common suit fabrics, double face, does not sweat and smell with its natural antibacterial and soft characteristics. In addition to this, it is aimed to produce a suit fabric which can be used for four seasons, will eliminate the need of lining, will provide lightness and comfort.

Different fiber types and fabric constructions should be experimented in order to produce different fabric types while lightening double fabrics. In this research wool, cotton, cotton/kapok Promodal, Tencel yarns were chosen to achieve the purposes of the study by using sustainable yarns. Wool fibers have long been associated with thick and lofty structures with good thermal resistance and may therefore be used for overcoat clothing [12]. However, wool fibers can be produced with other light density fibers in fine, lightweight double face weaves and may be utilized for clothing in different climates. Wool is an all-natural, renewable fibre, grown on sheep. Good absorbing moisture properties and reducing sweat on the body reduces the amount of resulting body odour, caused by sweat and its contact with any bacteria on the skin [13]. As a type of renewable natural plant fiber, kapok fiber is abundant, biocompatible and biodegradable, and its full exploration and potential application have received increasing attention in both academic and industrial fields. Kapok is a natural, cellulosic fiber which has many unique properties for textile industry. Fiber is as single cell fiber having very highly extreme hollowness (80-90%) [14]. Short in length, smooth surface and low density are the properties of this fiber making difficulties in yarn spinning. So, this fiber generally is used in yarn blends especially with cotton fibre. Regenerated biodegradable fiber types are introduced to the textile markets favoring their natural raw material backgrounds. They are produced from renewable cellulosic plants such as beech trees, pine trees, and bamboo. The most known regenerated fiber production technologies are viscose rayon—the first-generation technology, modal—the second-generation technology, and

lyocell—the third-generation technology [15]. In this reseach, Tencel and Promodal yarns were chosen as regenerated biodegradable fibers.

## 2. MATERIAL AND METHOD

Twelve types of double face woven fabrics with three different weft density levels were designed and produced from four different weft yarns having different fibre types. Face weft yarns were changed systematically, and the other face and back warp and weft yarns were kept constant. 100% Wool yarns were utilized for face warp, while 100% cotton yarns were used for back warp and weft. The basic properties of the face weft yarns used in the study are given in Table 1.

**Table 1**. Properties of all yarns used for the production of double face woven fabrics

| Yarn Sample Code | Raw Material Content | Yarn Count | Twist (T/m) | Yarn Tenacity (cN/tex) | Breaking Elongation (%) |
|---|---|---|---|---|---|
| Face warp | 100% Wool | 2x10tex (Nm 100/2) | 919 | 9.0 | 21.40 |
| Face weft 1 | 85% Cotton / 15% Kapok | 16.7 tex (Nm 60) | 951 | 15.7 | 6.40 |
| Face weft 2 | 100% Promodal | 20 tex (Nm50) | 812 | 23.0 | 11.04 |
| Face weft 3 | 100%Tencel | 20 tex (Nm50) | 810 | 26.6 | 9.74 |
| Face weft 4 | 100% Cotton | 20 tex (Nm50) | 880 | 21.0 | 6.54 |
| Back warp | 100% Cotton | 2x10tex (Nm 100/2) | 781 | 26.8 | 6.50 |
| Back weft | 100% Cotton | 20 tex (Nm50) | 880 | 21.0 | 6.54 |

All fabrics were produced on Dobby weaving by Dornier HTV6/SD machine rapier picking mechanism at the same machine set up to handle self-stitching double fabrics. Same weave unit were used for all of the fabrics, and same finishing routine was applied.

The finishing routine of the fabrics was washing, dyring, softening in foulard, decatizing and fixing with vacuum from inside to outside of the fabrics and reverse of this operation. The production plan of the fabrics, which were coded according to the changing weft yarns, is shown in Table 2. Besides, a sample photograph of the double face woven fabric can be seen in Figure 1.

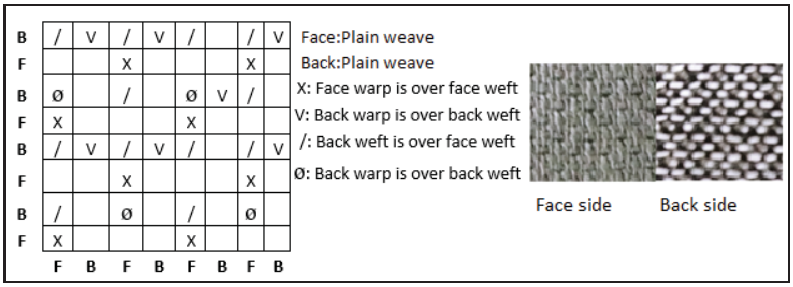


**Figure 1.** Weave design and a sample photograph of produced double woven fabrics (face and back side of CK2)

**Table 2.** Production plan of lightweight double woven fabrics

| Fabric no | Fabric code | Face warp | Face weft | Back warp | Back weft | Total warp density (thread/cm) 1Face:1 Back | Total weft density (thread/cm) 1Face:1 Back | Mass per unit area (g/cm$^2$) |
|---|---|---|---|---|---|---|---|---|
| 1<br>2<br>3 | CK1<br>CK2<br>CK3 | 100% Wool | 85% Cotton/ 15% Kapok | 100% Cotton | 100% Cotton | 40<br>40<br>40 | 33<br>37<br>39 | 159<br>166<br>170 |
| 4<br>5<br>6 | P1<br>P2<br>P3 | 100% Wool | 100% Promodal | 100% Cotton | 100% Cotton | 40<br>40<br>40 | 33<br>37<br>39 | 164<br>172<br>177 |
| 7<br>8<br>9 | T1<br>T2<br>T3 | 100% Wool | 100% Tencel | 100% Cotton | 100% Cotton | 40<br>40<br>40 | 33<br>37<br>39 | 155<br>171<br>176 |
| 10<br>11<br>12 | C1<br>C2<br>C3 | 100% Wool | 100% Cotton | 100% Cotton | 100% Cotton | 40<br>40<br>40 | 33<br>37<br>39 | 162<br>171<br>173 |

## 3. RESULTS

Mass per unit area, air permeability, breaking strength, breaking elongation, abrasion resistance and contact angle were determined to compare the performance properties of the double woven fabrics. Besides mechanical properties, contact angle performance was examined to have a better understanding of wetting properties of the fabrics. Wetting property of the fabrics plays an important role in many industrial processes, such as oil recovery, dirt-repellence, lubrication, liquid coating, printing etc., and daily uses, such as water absorbing, sweat transport etc.

Before all other performance tests, fabric handle, mass per unit area and fabric air permeability values were tested because the customers first check fabric handle and try to sense fabric weight. Besides, fabric air permeability is one of the critical properties for a fabric which is produced for the purpose of clothing. In Figure 2, mass per unit area values were illustrated before and after finishing process. As seen in Figure 2, increments in mass per unit area values close to 10% were determined after finishing. The highest increments were obtained for the fabrics having Tencel and Promodal weft yarns while the lowest was obtained for cotton fabrics.

Air permeability also has a significant influence on the moisture and heat transfer properties of clothes and is primarily determined by their structures, such as warp and weft densities, while the fiber types and yarn structures have less influence in comparison to the other structural proeperties [16]. There are several parameters affecting air permeability, such as yarns (looseness, twist and count), fabric structure, cover factor, warp and weft density. For example, an increase in warp and weft density results in a decrease of pore size in fabrics and then a lower air permeability. As seen in Figure 3, there is a relation between air permeability and fabric density. Increments in fabric density values cause decrements in fabric air permeability results as it is expected. The attractive point is dramatically decreasing air permeability values after finishing process. After finishing process, air permeability values decreased by 78% on values ranging from 72% to 83%. This condition once again

emphasizes the need to make very careful choices in the design phase in such fabrics, which are considered to be suits.

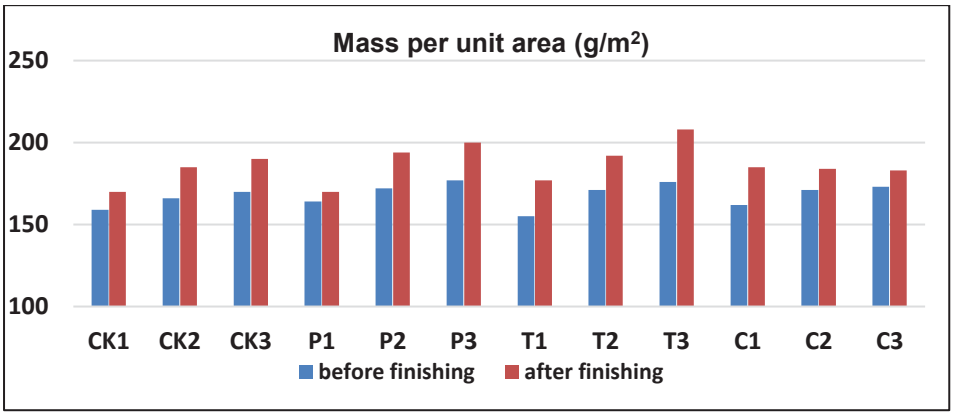


**Figure 2.** Change in mass per unit area values before and after finishing process

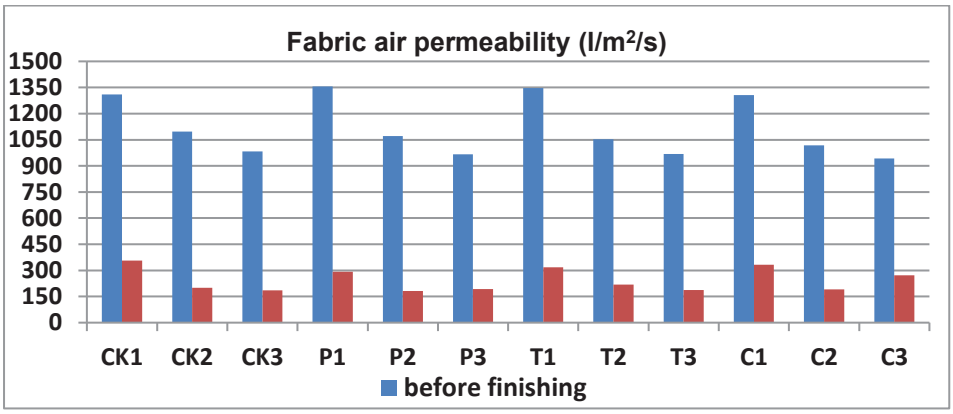


**Figure 3.** Change in fabric air permeability values before and after finishing process

Breaking strength and elongation results were given in Figure 4 and Figure 5, respectively. When results were examined, it is clearly seen that the double fabrics having Tencel ve Promodal weft yarns on face side have higher breaking strength and elongation values. In spite of that, double fabrics having cotton and kapok weft yarns have generally low breaking strength values. The breaking strength values of the fabrics in warp direction are higher than values in weft direction, while the elongation values in warp direction are lower than values in weft direction.

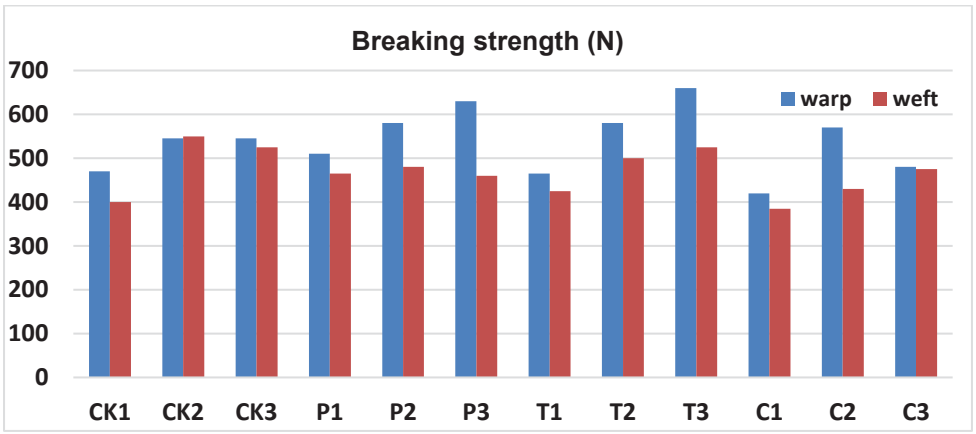


**Figure 4.** Breaking strength of lightweight double fabrics

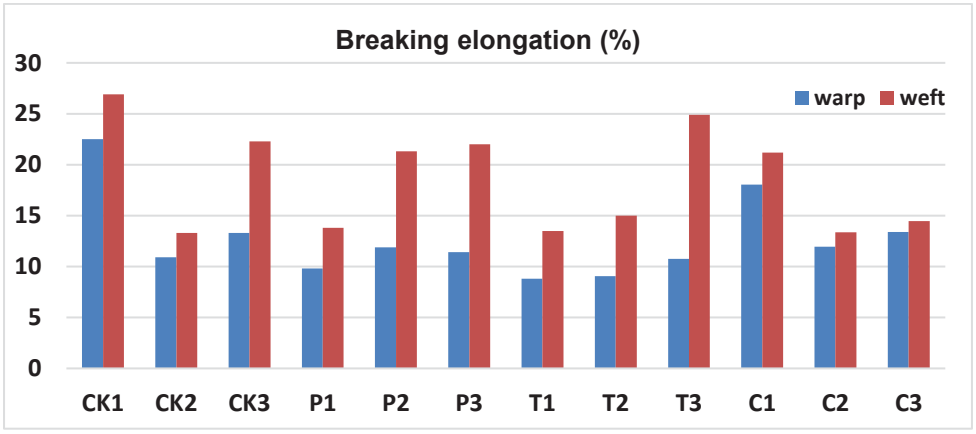


**Figure 5.** Breaking elongation of lightweight double fabrics

Fabric abrasion results were calculated by using weight loss values after 10.000 abrasion cycles and were illustrated in Figure 6. As seen in Figure 6, the highest fabric abrasion values were determined for the double fabrics having cotton yarns on face weft. When the porperties of the yarn used in these fabrics are examined, the lowest tenacity and breaking elongation values were found for cotton yarns, and it may be result of this the lowest abrasion resistance values are observed in double fabrics having cotton weft yarns (C1, C2, C3). On the other hand, the highest abrasion resistance values are found in the double fabrics having Tencel weft yarns (T1, T2, T3). Although Tencel fibers have fibrillation degree, the double fabrics having Tencel produced in this study have shown high abrasion resistance. This finding may be related with high yarn tenacity values of the Tencel yarns. Low weight loss values are also observed in double fabrics having cotton/kapok blends on face (CK1, CK2,

CK3). Cotton/kapok yarns are not only good in tensile properties compared to other yarns used in the study, but also have high twist level. It can be said that, better abrasion resistance values are obtained in these fabrics since the high yarn twist makes difficult the fiber exit from yarn structure.

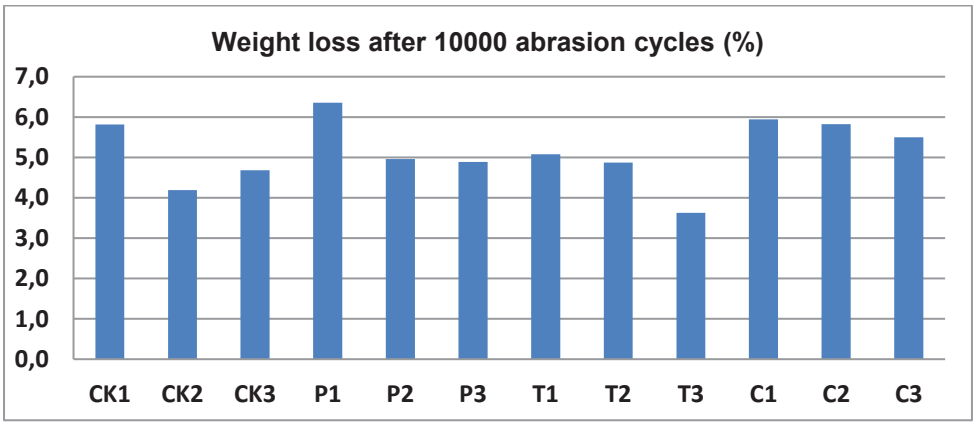


**Figure 6.** Weight loss values (%) of lightweight double fabrics after 10000 abrasion cycles

The contact angle results are shown in Figure 7. The contact angle values of the fabrics have been found greater than 90° meaning that they have hidrofobic properties. This result means that wetting of the surface is unfavourable in terms of moisture management. However, this finding may be valuable in terms of water and oil repellence properties. Except the double fabrics having Tencel weft yarns, contact angle values increased with the increments in weft density. Kapok fibre is well known its water retention properties but in this study, it was used as cotton/Kapok blended yarn and the amount of fibre in fabric content is less according to the other fibres. In further studies it is possible to check the effect of Kapok fibre content on contact angle properties. The contact angles for all fabrics were similar, although yarns having different sustainable yarns were used for all the fabrics. The double woven fabrics exhibited unique behaviour when water was placed on the surface of the fabric, with higher contact angle values. Especially double fabrics having Tencel weft yarns (T1, T2, T3) have the lowest contact angle values. Also in other studies in the literature, Tencel fabrics were found to have high liquid moisture management capacity [16, 17], it can be reason for the lowest contact angle values of these fabrics in this study.

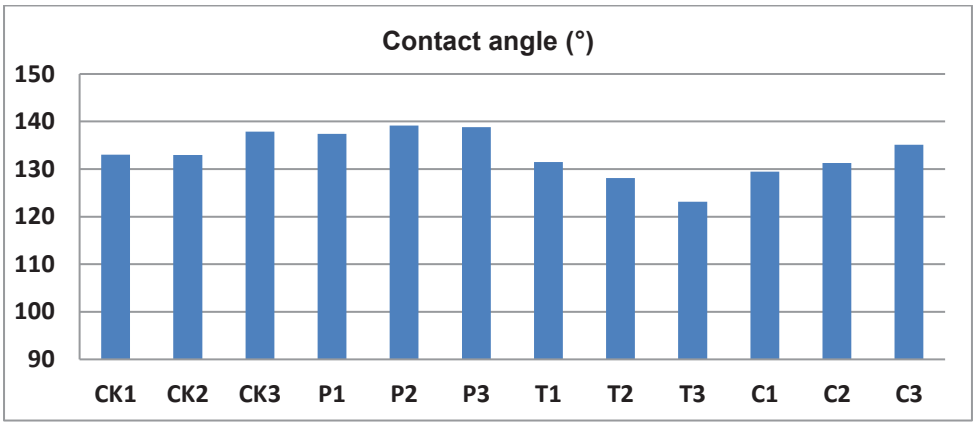


**Figure 7.** Contact angle values (°) of lightweight double fabrics

## 4. CONCLUSIONS

According to the research objective, four different sustainable yarns were used in weft direction to produce lightweight and double layer woven fabrics. 3/1 twill and plain weaves were used for face and back sides respectively. Three different weft settings were chosen, and warp setting was kept constant. Since only the warp was kept constant, the effect of weft setting, and the effect of fiber type were evaluated according to the findings.

The test results have revealed the durability and performance of the designed double face fabrics having sustainable yarns. Satisfactory high breaking strength values have been obtained for the test fabrics. Promodal and cotton double fabrics have shown the highest abrasion values in comparison to the other fabrics. The contact angles of the fabrics have been found greater than 90°, in general. These fabrics may be useful for outdoor wearing with their high repellence abilities. These technical designs can provide pleasing results both for customers and garment manufacturers because of time and cost consuming during garment production. Besides using sustainable yarns helps to reduce environmental impact of production company and it can be accepted as necessary processess in the research and development of textiles.

For further studies, production and testing the performance of double fabrics having sustainable yarns in different contents are planned. Especially clothing comfort of lightweight double structures will be interesting besides examination of other performance properties.

## REFERENCES


1. Watson W 1913 Advanced textile design, Longsman Green and Co. London 24-63.
2. Supuren, G, Oglakcioglu, N, Ozdil, N and Marmarali, A. 2011 Moisture management and thermal absorptivity properties of double-face knitted fabrics, Textile Research Journal **81(13)** 1320-1330.
3. Tokura, H, Sasase, A, Hashimoto, S and Midorikawa, T. 1989 Thermophysiological studies of double-face knitted fabrics under cycle ambient temperatures, Descente Sport Science, **10**, 203-208.
4. Hebeish, A A, Elgamel, M A, Abdelhady, R A and Abdelaziz, A. 2008 Factors affecting the performance of the radar absorbant textile materials of different types and structus, Progress in Electromagnetics Research, **3**, 219-226
5. Ng, M C F and Zhou, J 2009 A study on figured double-face jacquard fabric with full-color effect, Textile Research Journal, **79(10)**, 930-936.
6. Wilbik-Halgas, B, Danych, R, Wiecek, B and Kowalski, K 2006 Air and water vapour permeability in double-layered knitted fabrics with different raw materials, Fibres and Textiles in Eastern Europe, **14(3)**, 77-84
7. Suganthi, T and Senthilkumar, P. 2018 Comfort properties of double face knitted fabrics for tennis sportswear, Indian Journal of Fibre & Textile Research, **43(1)**, 9-19
8. Elnashar, E A and Dubrovski, P D 2008 The influence of the weave and the method of stitching on selected mechanical properties of woven double fabrics. Autex Research Journal, **8(2)**,12-19
9. Park, S W and Hwang, Y G 1999. Measuring and fuzzy predicting total handle from selected mechanical properties of double weft-knitted fabrics, Textile Research Journal, **69(1)**, 19-24
10. Urbas R., Kostanjs˘ek, K., Dimitrovski, K. 2011 Impact of structure and yarn colour on UV properties and air permeability of multilayer cotton woven fabrics, Textile Research Journal, 81(18) 1916–1925
11. Zhu, L., Naebem., Blanchonette, I., Wang X., 2017 Heat transfer properties of bifacial fabrics, Textile Research Journal Vol. 87(19) 2307–2313
12. Ukponmwan J O 1993 The thermal-insulation properties of fabrics, Textile Progress 24(4) 13-23.
13. https://www.iwto.org/sustainability, 15.08.2018
14. Jinjiang Yan , Guangbiao Xua and Fumei Wang 2013 A study on the quality of kapok blended yarns through different processing methods, The Journal of The Textile Institute, 2013 Vol. 104, No. 7, 675–681
15. Palamutcu S. (2017) Sustainable Textile Technologies. In: Muthu S. (eds) Textiles and Clothing Sustainability. Textile Science and Clothing Technology. Springer, Singapore
16. Oner, E. and Okur, A. 2015 Thermophysiological comfort properties of selected knitted fabrics and design of T-shirts. The Journal of The Textile Institute, 106(12), 1403-1414.
17. Oner, E., Atasağun, H. G., Okur, A., Beden, A. R. and Durur, G. 2013. Evaluation of moisture management properties on knitted fabrics. Journal of the Textile Institute, 104(7), 699-707.

# ASSESSING CARBON FOOTPRINT OF PROCESS EFFICIENCY IMPROVEMENT OPTION FOR FLAME RETARDANT FABRICS BASED ON SOL-GEL METHOD

**Yeşim ÜNVAR[1], Aysun AKŞİT[1], Evren SERGİN[1], Eylem KILIÇ[2]**

[1] Dokuz Eylul University, Department of Textile Engineering, Turkey
[2] Usak University, Department of Material Science and Nanotechnology Engineering, Turkey

Corresponding author: aysun.cireli@deu.edu.tr

***Abstract:*** *In recent years, sol-gel technique has gained more attention that enable efficient flame retardant applications on condition of synergistic effect. Within a study it was proved that the limited oxygen index value of the cotton fabrics can be reached up to the 60% via sol-gel technology. Although this is an essential improvement, process efficiency of sol-gel technique needs further developments and improvement options should be evaluated both in terms of flame retardancy efficiency and sustainable production of flame retardant textile materials. Preliminary results showed that some opportunities lie in case of modifications of drying step of fabric. In this perspective, carbon emission of an improvement option for process efficiency was evaluated to support decision-making process while evaluating different improvement options.*

***Keywords:*** *Sol-gel technique, flame retardancy, cotton fabric, carbon emission, process parameters.*

## 1. INTRODUCTION

In 2016, over 3 million fires occurred and caused to approximately 18,000 deaths and 58,000 injuries in the worldwide [1]. Today, flame retardancy is an essential need due to losses of life and property resulting from fires involving polymeric materials. Textile products used in many places have high risk in terms of causing or spreading fire, therefore it is vital to impart flame retardant (FR) properties to them [2].

While the worldwide consumption of flame retardants (FRs) has increased with the obvious reason [3], concerns regarding toxicity and potential hazards of FRs have risen and stricter sanctions were needed to be applied by environmental related authorities. For instance, some halogen containing FRs were banned, and some others were allowed limited use [4]. Hence, use of halogen free FRs has become widespread [5]. Among these, phosphorus and nitrogen compounds are prominent especially for the textile sector. Besides, their synergistic effect has led to performing lots of practice. The synergistic effect between nitrogen and phosphorus compounds as already recognized [6-9], however, a wide number of studies compromised that the phosphorus compounds showed even better flame

retardancy at the presence of silicon (Si) in addition to the nitrogen [10-15]. One of the latest studies proved that the sol-gel technique is a proper and effective method to obtain high FR performance cotton fabrics as they increased the Limited Oxygen Index (LOI) value of cotton fabric from 18.2% to 60% [16]. In this perspective, the sol-gel technology is one of the best candidates for improved flame retardancy effect [17].

On the other hand, environmental impacts caused by production of FR textiles needs to be controlled and mitigated. Because the application of FRs, somehow involves toxic chemical procedures and leads to deposition of these harmful chemicals in the environment. This turn to high $CO_2$ emissions corresponding to global warming potential (GWP) [3]. Apart from the material usage, environmental impacts strongly depend on the dynamics of processes such as drying and fixation conditions due to high-energy consumption [18]. Since, mostly energy has come from non-renewable sources, it is quite important carrying out any modification that can decrease the energy consumption.

Today, many sectors are obliged to take responsibility of the consequences of their industrial activities on human and environment [19]. In this regard, the methods providing holistic approach such as life cycle analysis (LCA) come to the fore. LCA is a quantitative indicator for determining the sustainability of products and production processes [20]. Therefore, LCA is a valuable decision-making tool [21] for practitioners and decision makers, especially for the ones that are seeking novel and alternative production methods like sol-gel technique.

## 2. MATERIAL AND METHOD

### 2.1 Goal and Scope Definition

The objective of this study is to determine the effect of process modification on FR performance and quantify the carbon footprint of the FR cotton fabrics. As a result, it is to reveal effect of the process modification within the comparative assessment to support decision making process while evaluating different improvement options.

### 2.2 Description of Analyzed System

Sol-gel treatment consists of nanosol preparation, nano coating (dip-coating), drying and fixation processes. In the previous study was done by Aksit et al. [6] scoured and bleached 100% plain-weave cotton fabrics (120 g/m$^2$ weight, 26 picks/cm, 36 ends/cm) were impregnated with prepared nanosol solutions via sol-gel method according to the procedure described. After impregnation, fabric was squeezed for approximately 90% pick up rate (IN) at 1.8 bar of nip pressure using a fulard machine (ATC-F350, Ataç, Turkey). After that, the cotton fabrics were dried at 100°C for 10 min in an incubator (EN 500, Nüve, Turkey) and cured at 140°C for 3 min in a laboratory scale stenter (H-TS-3, Rapid, Taiwan), respectively. Nano coating, drying and fixation processes were carried out three times which resulted in more energy consumption for FR fabric, but also means to higher LOI values due to increase in add-on (%). Eventually, this process leads to increase in carbon footprint as expected [17]. Considering this, in the first part

we employed abovementioned processes as a single step to reveal the effect of minimum conditions to the FR efficiency and the carbon emission performance. In the second part, we applied a modification to aforementioned sol-gel treatment. For this, while one set of cotton fabrics were exposed the pre-drying process until loss of moisture by 4% of the initial weight of the fabrics. The pre-drying process carried out in a laboratory scale stenter at 130°C for 5 minutes. The remaining processes were kept same except for pick up rate which was determined based on pressure of squeezing roller. In this comparative assessment in terms of carbon footprint, we called that the first part of this study is 'sol-gel process' (SG) and the second part is 'modified sol-gel process' (M-SG).

### 2.3 Functional Unit and System Boundaries

Functional unit was chosen as the production of 1 kg of FR cotton fabric using the sol-gel method (SG and M-SG). System boundaries for SG are composed of 4-unit processes which are nanosol preparation, dip-coating (nano coating), drying and fixation as depicted in Figure 1a. M-SG is composed of 5-unit processes together with pre-drying process as depicted Figure 1b.

### 2.4 Inventory Analysis and Assumptions

A part of the inventory data is achieved from a previous study [16] which is pending for patent, and data for process improvement were obtained from laboratory experiments. For this reason, substances and the related details were kept confidential, but they were included in life cycle analysis. The exact procedure cannot be expressed; however, it was indicated that the guanidine phosphate monobasic was the main FR and the (3-aminopropyl) triethoxysilane and (3-glycidyloxypropyl) trimethoxysilane were the epoxysilane precursors in that sol-gel study. The inputs involved in LCA were calculated according to pick up rate of each sol-gel process. The excessive nanosol flowing/dropping throughout the dip-coating process was taken out from the bath and reused. Due to lack of inventory data related to several chemicals which are specific to sol-gel process used in nanosol preparation, some assumptions were made. Some chemicals were not included in impact assessment of presented processes since use rate is less than 1%.

### 2.5 Life Cycle Impact Assessment

The LCA was carried out using GaBi 6 (Thinkstep) software and database. The carbon footprint was calculated using characterization factors developed by Centre of Environmental Science of Leiden (CML 2001). Impact assessment was included the Global Warming Potential (GWP 100 years), excl biogenic carbon [kg $CO_2$-Equivalent].

### 2.6 Flammability Assessment with LOI Test

With respect to textiles, LOI test is mainly used to identify tendency of textile fabric sustainability to flame. And it is a simple way to compare the effects of different FR finishes, varying add-on values or synergism of FR compounds [22].

## 3. RESULTS AND DISCUSSION

Results of the sol-gel process (SG) and modified sol-gel process (M-SG) are given in Figure 2. Figure 2 a, b and c has showed that Impregnated Nanosol (IN %), Add-on Percent (Add-on %) and Limited Oxygen Index Value (LOI, respectively. According to the results, pre-drying process before the dip-coating has increased loading of FR additive onto the fabrics. It was recognized that increased available space in the fabric after pre-drying process resulted in higher quantities of impregnated nanosol from 91% to 107% and add-on from 13.5% to 19.3%. For the same fabric structure, LOI value has increased simultaneously with the increasing percent add-on however; increase in LOI value was not linear. Thus, pre-dried samples have higher LOI value due to simple replacement of water with FR agents present in the nanosol.

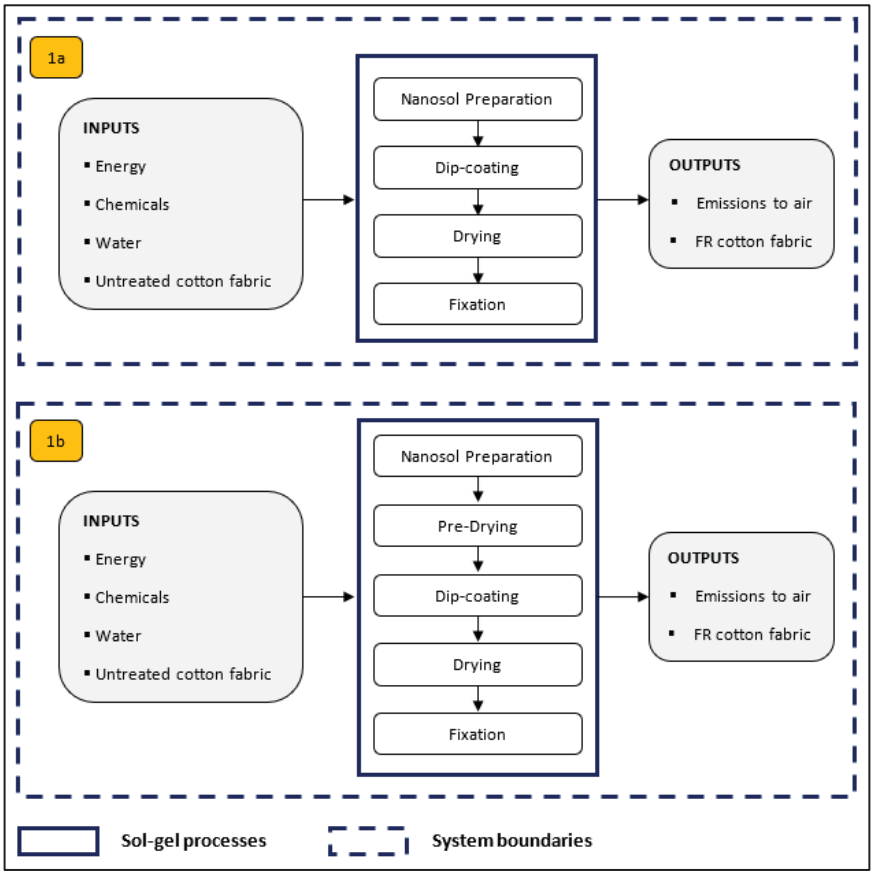


**Figure 1** System Boundaries for **(1a)** sol-gel process (SG) and **(1b)** modified sol-gel process with pre-drying process (M-SG)

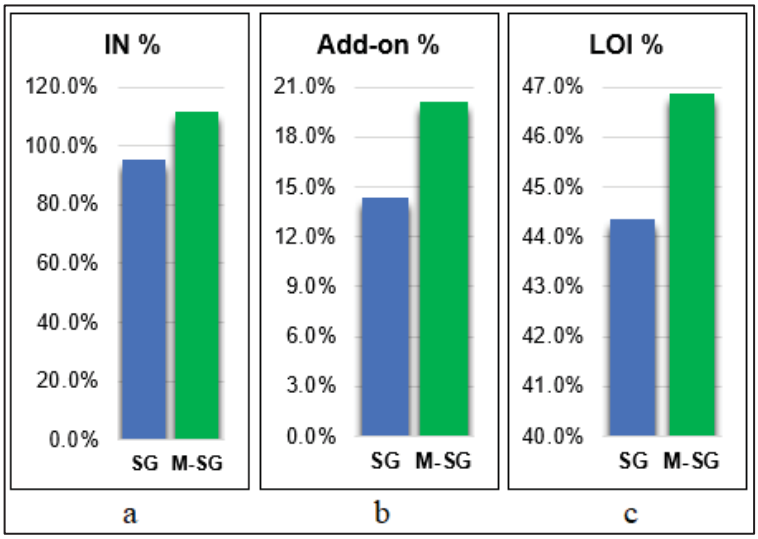


**Figure 2** (a) Amounts of impregnated nanosol, (b) add-on percentages and (c) LOI values

Global warming potential for SG and M-SG processes is given in Figure 3. Global warming potential for SG and M-SG processes is given in Figure 3. Carbon footprint of the processes SG and M-SG was found as 0.87 and 1.17 kg $CO_2$ equivalent, respectively. Besides, nanosol preparation, dip-coating, drying, pre-drying and fixation were also showed separately in the Figure 3 as percentage.

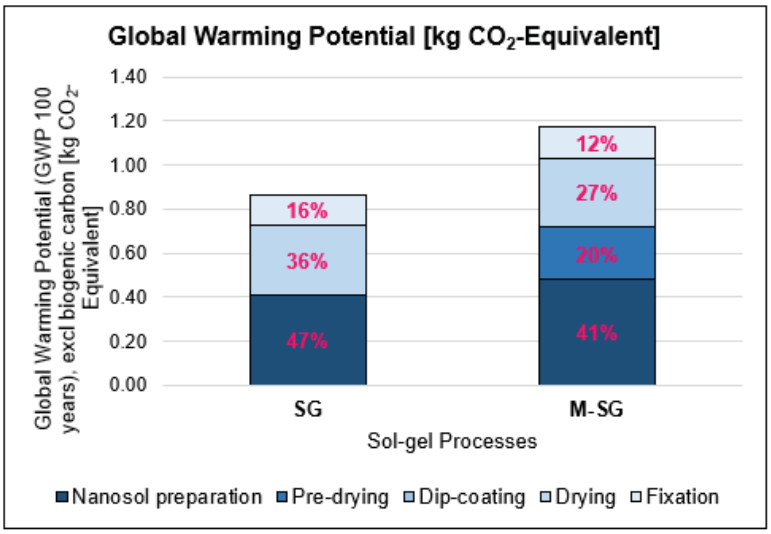


**Figure 3** GWPs of SG and M-SG processes

This LCA study has revealed that increase in LOI value (%) caused an increase in GWP by 7% in the case of M-SG process. As seen in Figure 3, carbon footprints of SG and M-SG processes mainly have arisen from energy dominant processes such as pre-drying, drying and fixation. The second considerable contribution to GWP comes up with solvent (ethanol) use in which nanosol preparation. However, considering change between SG and M-SG processes, it was found that increasing GWP of pre-dried samples was related to mostly increasing energy inputs rather than mass of nanosol.

## 4. CONCLUSION

A simple modification in the sol-gel process by pre-drying within the scope of this study has led to increase in uptake of FRs to cotton fabrics, which in turn has enhanced the LOI value from 44.1% to 46.6%. Indeed, based on higher energy consumption carbon footprint value has also increased due to the additional pre-drying process in the case of single-layer coating. It is revealed that different processing options have emerged corresponding to the level of fire protection and environmental impacts. The best available option should be determined according to demand for FR specification, considering the sufficient FR performance and having least global warming potential. Consequently, this study has drawn attention to an alternative process in terms of efficiency and carbon emission which were evaluated to support decision-making process.

## ACKNOWLEDGEMENT

We appreciate kind support of Prof. Dr. Nurdan Buyukkamaci for providing GaBi 6 software (Thinkstep).

## REFERENCES

1. Brushlinsky, N. N., Ahrens, M., Sokolov, S. V., & Wagner, P. (2018). *World Fire Statistics*. Center of Fire Statistics of CTIF, International Association of Fire and Rescue Services. Reports No. 23. Retrieved May 7, 2018, from https://www.ctif.org/sites/default/files/2018-04/CTIF_Report23_World_Fire_statistcs_2018.pdf.
2. Horrocks, A. R., & Price, D. (Eds.). (2008). *Advances in fire retardant materials*. England: Woodhead Publishing Limited.
3. Yasin, S., Behary, N., Curti, M., & Rovero, G. (2016). Global consumption of flame retardants and related environmental concerns: A study on possible mechanical recycling of flame retardant textiles. *Fibers*, *4*(2), 16.
4. Abelkop, A. D., Graham, J. D., & Royer, T. V. (2016). *Persistent, bioaccumulative, and toxic (PBT) chemicals: technical aspects, policies, and practices*. Boca Raton: CRC Press.
5. Morgan, A. B. ve Wilkie, C. A. (Eds.). (2014). *Non-halogenated flame retardant handbook*. New Jersey: Scrivener Publishing LLC.
6. Aksit, A., Onar, N., Kutlu, B., Sergin, E., & Yakin, I. (2016). Synergistic effect of phosphorus, nitrogen and silicon on flame retardancy properties of cotton fabric treated by sol-gel process. *International Journal of Clothing Science and Technology*, *28*(3), 319-327.

7. Alongi, J., & Frache, A. (2010). Flame retardancy properties of α-zirconium phosphate based composites. *Polymer Degradation and Stability*, *95*(9), 1928-1933.
8. Cheng, X., & Yang, C. Q. (2009). Flame retardant finishing of cotton fleece fabric: Part V. Phosphorus-containing maleic acid oligomers. *Fire and Materials*, *33*(8), 365-375.
9. Wu, W., & Yang, C. Q. (2007). Comparison of different reactive organophosphorus flame retardant agents for cotton. Part II: Fabric flame resistant performance and physical properties. *Polymer Degradation and Stability*, *92*(3), 363-369.
10. Liu, Y. L., & Chou, C. I. (2005). The effect of silicon sources on the mechanism of phosphorus–silicon synergism of flame retardation of epoxy resins. *Polymer Degradation and Stability*, *90*(3), 515-522.
11. Hsiue, G. H., Liu, Y. L., & Tsiao, J. (2000). Phosphorus-containing epoxy resins for flame retardancy V: Synergistic effect of phosphorus–silicon on flame retardancy. *Journal of Applied Polymer Science*, *78*(1), 1-7.
12. Hsiue, G. H., Liu, Y. L., & Liao, H. H. (2001). Flame-retardant epoxy resins: An approach from organic–inorganic hybrid nanocomposites. *Journal of Polymer Science Part A: Polymer Chemistry*, *39*(7), 986-996.
13. Wu, C. S., Liu, Y. L., & Chiu, Y. S. (2002). Epoxy resins possessing flame retardant elements from silicon incorporated epoxy compounds cured with phosphorus or nitrogen containing curing agents. *Polymer*, *43*(15), 4277-4284.
14. Yang, Z., Fei, B., Wang, X., & Xin, J. H. (2012). A novel halogen-free and formaldehyde-free flame retardant for cotton fabrics. *Fire and materials*, *36*(1), 31-39.
15. Zhao, X. (2010). Synthesis and application of a durable phosphorus/silicon flame-retardant for cotton. *The Journal of The Textile Institute*, *101*(6), 538-546.
16. Sergin, E. (2017). *Developing flame retardant hybrid textile coating materials which are durable to washing and environmental with sol-gel method*. (Unpublished Master's Thesis). Dokuz Eylul University, Graduate School of Natural and Applied Sciences, Izmir, Turkey.
17. Unvar, Y., Aksit, A., & Kilic, E. (2017). *Carbon footprint of antibacterial cotton fabric produced with sol-gel method*. Paper presented at the 16th International The Recent Progress Symposium on Textile Technology and Chemistry (pp. 294-301), Bursa, Turkey.
18. Alongi, J., & Malucelli, G. (2012). State of the art and perspectives on sol–gel derived hybrid architectures for flame retardancy of textiles. *Journal of Materials Chemi*stry, *22*(41), 21805-21809.
19. Parisi, M. L., Fatarella, E., Spinelli, D., Pogni, R., & Basosi, R. (2015). Environmental impact assessment of an eco-efficient production for coloured textiles. *Journal of Cleaner Production*, *108*, 514-524.
20. Consoli, F., Allen, D., Boustead, I., Fava, J., Franklin, W., Jensen, A. A., De Oude, N., Parrish, D., Perriman, R., Postlethwaite, D., Quay, B., Siéguin, J., & Vigon, B. (Eds.) (1994). Guidelines for Life-Cycle Assessment: A 'Code of Practice' from the workshop held at Sesimbra, Portugal, 31 March – 3 April 1993 Society of Environmental Toxicology and Chemistry (SETAC), *Environmental Science and Pollution Research*, *1*(1), 55.
21. Kilic, E., Puig, R., Baquero, G., Font, J., Colak, S., & Gürler, D. (2011). Environmental optimization of chromium recovery from tannery sludge using a life cycle assessment approach. *Journal of hazardous materials*, *192*(1), 393-401.
22. Horrocks, A. R., Tune, M., & Cegielka, L. (1988). The burning behaviour of textiles and its assessment by oxygen-index methods. *Textile Progress*, *18*(1-3), 1-186.

# SOIL DEGRADATION BEHAVIOUR OF DIFFERENT TEXTILE FIBERS: VISUAL, MORPHOLOGICAL AND STRUCTURAL PROPERTIES

**Gökberk DEVRİM[1], Vildan SÜLAR[2]**

[1] Dokuz Eylul University, The Graduate School of Natural and Applied Sciences, Turkey
[2] Dokuz Eylul University, Department of Textile Engineering, Turkey

Corresponding author: vildan.sular@deu.edu.tr

***Abstract:*** *The biodegradation of fabrics having various types of fibers (Modal, Tencel, polylactic acid (PLA) and polyethylene teraphtalate (PET)) under the attack of microorganisms were studied by using soil burial method for two different burial intervals (1month and 4 months. Visual observations, weight losses, Fourier transform infrared spectroscopy (FTIR) and scanning electron microscopy (SEM) were used to examine the biodegradation behaviour. The study revealed that the regenerated cellulosic fabric samples changed physically and chemically even after 1 month. Weight losses of Modal fabric were close to 90% showing the high degradation whereas Tencel fiber had 60% for 4 months burial interval. Within the synthetic fabrics, only PLA fabric lost its weight. The degradation behaviour of these different polymers was discussed by the characterization tests.*

***Key Words****: biodegradation, SEM, FT-IR, PLA, soil burial test*

## 1. INTRODUCTION

Textile wastes can be classified as either pre-consumer or post-consumer waste. Pre-consumer waste consists of by product materials from the textile, fibre, and cotton industries that are remanufactured for the automotive, aeronautic, home building, furniture, mattress, coarse yarn, home furnishings, paper, apparel and other industries[1]. Post-consumer waste is defined as any type of garment or household article made from manufactured textiles that the owner no longer needs and decides to discard. These articles are discarded either because they are worn out, damaged, outgrown, or have gone out of fashion [1]. The U.S. EPA estimates that Textile waste occupies nearly 5% of all landfill space [2]. A discarded textile item may be a reason for environmental pollution. Therefore, the concept of biodegradation has started to be used widely because of the increasing efforts to prevent environmental pollution. Biodegradation can be visualized as the method used by nature to recycle waste and to break down organic materials into compounds which can be used as nutrients by other organisms [3]. During biodegradation, numerous microorganisms such as fungi, bacteria, worms, and many other species have attack on materials. Biodegradability is considerable for materials particularly utilized in any part of daily life. Biodegradability behavior of the polymers is depended on some physical and chemical properties. Hydrophilic character, crystalline and

amorphous structures, linearity or branching of the polymers, molecular compositions and chemical bonds are chemical bonds are determinative elements on biodegradability of the polymeric materials [3, 4]. Due to their primarily ease of processing, high weathering resistance and strength, the production and consumption mass of synthetic fibers increase steadily. However, these fibers exhibit high resistance to microbial degradation. In the related literature, there are some researches on biodegradation of textile materials such as cotton, jute, linen, wool, viscose, polyester and recently polylactic acid fibers [3-13]. In this research, biodegradation of fabrics composed of various different raw materials (i.e. cellulose based and synthetic) were studied by using soil burial test. The test fabrics were visually observed after two different soil burial intervals and the weight losses were calculated. The biodegradation tendency of the fabrics was examined by Fourier transform infrared spectroscopy and scanning electron microscopy.

## 2. MATERIAL AND METHOD

### 2.1 Materials

In the experimental study, four knitted fabrics having similar structural parameters (Table 1) and consisting different fibres were used. No finishing and dyeing treatment were applied to the fabrics before tests.

**Table 1.** Basic structural parameters of the fabrics

| Fabric Code | Raw Material | Courses (/cm) | Wales (/cm) | Mass per unit area ($g/m^2$) | Fabric thickness(mm) (pressure:5$g/cm^2$) |
|---|---|---|---|---|---|
| CMD | 100% Modal | 12.0 | 8.5 | 118.9 | 0.65 |
| CLY | 100% Tencel | 12.0 | 8.5 | 118.2 | 0.77 |
| PLA | 100% Poly (lactic acid) | 12.0 | 9.0 | 139.6 | 0.88 |
| PET | 100%Polyethylene teraphtalate | 12.0 | 9.0 | 132.8 | 0.76 |

### 2.2 Methods

#### 2.2.1 Soil Burial Testing

A test equipment having boxes was prepared for soil burial testing. Two different burial periods simulating a short and a comparatively longer interval were selected such as “1 month and 4 months”. The soil burial test carried out in accordance with ISO 11721-1:2001 [10]. The unburied fabric samples of each fabric were called as control fabrics and were used for comparisons. Three replicates were conducted for each fabric type for each burial interval. The temperature and relative humidity in soil were controlled regularly and held constant during the experiment by spraying with water.

The test samples were cut in square shape for each fabric type and weighed in a textile testing laboratory before burying under standard atmosphere conditions. Figure 1 presents test equipment after burying the fabric samples.

**Figure 1.** Test equipment after burying the fabric samples

The temperature and relative humidity of the soil were controlled periodically and kept constant as 25±5°C and higher than 90% during burial intervals. The fabric samples were removed from soil after 1 month and 4 months intervals. The fabric samples removed from soil were lightly rinsed with ethanol/water solution for two times, sieved carefully by using a filter paper, then dried in ambient temperature. After this stage; weight losses were determined and characterization analyses were conducted. Table 2 lists the sample codes of the test fabrics.

**Table 2.** The sample codes of the test fabrics

| Fabric Code | Raw Material | Control sample (not buried, 0 month) | Buried sample for 1 month | Buried sample for 4 month |
|---|---|---|---|---|
| CMD | 100% Modal | CMD0 | CMD1 | CMD4 |
| CLY | 100% Tencel | CLY0 | CLY1 | CLY4 |
| PLA | 100% Poly (lactic acid) | PLA0 | PLA1 | PLA4 |
| PET | 100%Polyethylene teraphtalate | PET0 | PET1 | PET4 |

### 2.2.2 Determination of Weight Loss After Soil Burial

After rinsing with ethanol and drying in ambient temperature, the test fabrics were conditioned for 24 hours in a textile testing laboratory having standard atmosphere conditions. A balance having four digit sensitivity (0.0001g) was used to weigh the test fabrics. The weights of buried and control fabrics were compared and weight loss percentage was calculated via following formula to evaluate biodegradation:

$$\text{Weight loss } (\%) = \frac{W1 - W2}{W1} x100$$

where W1 and W2 are corresponded to the initial weight and the weight after being buried in soil, respectively.

### 2.2.3 Morphology Study

The control and buried samples were viewed by JEOL-JJM 6060 model scanning electron microscope (SEM). SEM images were obtained with an accelerating voltage of 5 kV and magnification of 500X. The test samples were prepared by coating gold.

### 2.2.4 FTIR Analysis

FTIR spectra of the fabric samples were recorded using a Fourier Transform Infrared Spectrometer (Perkin Elmer Spectrum BX). Each spectrum was recorded in the range of 600– 4.000cm-1 with a resolution of 2$cm^{-1}$. Spectra of the samples were obtained from 25 scans.

## 3. RESULTS AND DISCUSSION

### 3.1.Visual observation

Biodegradation of materials such as fibres, films or textiles can be assessed firstly by their physical appearances. The changes in physical appearances can be observed by naked eyes. The appearances of fabrics before and after soil degradation are exhibited in between Figure 2 by photographs and SEM micrographs. In general, the buried fabrics were evaluated thinner and more brittle than control fabrics.

SEM images show the changes of the test fabrics. After 4 months burial period, Modal and Tencel fabrics noticeably degraded and the integrity and structure of the fabrics are nearly collapsed. The fibre breakages of the Tencel fabrics are prominent and it is noteworthy that the Modal fibres seem to be inseparable from the soil after 4 months' burial period. The significant changes in the cellulosic fabrics may be due to their hydrophilic character. In case of PET fabric, minor changes in comparison to the other fibers was observed. This may be due to the high resistance of these polymers based on its chemical composition. When photographs of PLA fabrics was examined, it was seen that the fabric sample had taken water inside of fabric because the line of drawing pencil around the sample was spread to inner side of sample.

### 3.2 Weight Loss

Change in weight is a direct way to measure the biodegradability of polymers [11]. The weight loss of the fabrics after 1 month and 4 months are given in Figure 3. The weight losses for the regenerated cellulosic fibres are higher in comparison with synthetic fibres as expected. The higher moisture and water uptake in other words higher hydrophilicity causes more deterioration by means of biodegradability [11]. The microorganisms in soil caused reduction in weight of the fabrics. Further, the breakage and deterioration of the samples facilitate the colonization of the microorganism into the fabric[12]. At the end of 4 months, it is hard to see Modal fabric particles in soil. PET fiber due to aromatic structure has excellent physical and mechanical properties compared to aliphatic structures, but their strong resistance to bacterial or fungal attack results in low degradability

under the environmental conditions [13]. No weight loss was determined after 4 months burial period in accordance with the findings of Chen et al. When PLA fibre was examined, although there was a little degradation (1.2% weight loss) after 4 months burial period, it was clear that biodegradation will not be easy under soil burial conditions applied in the study. This result is in accordance with the review of Karamanlioglu [9] explaining that no degradation was determined by weight loss of the PLA film when it was buried in soil for 120 days at 25°C.

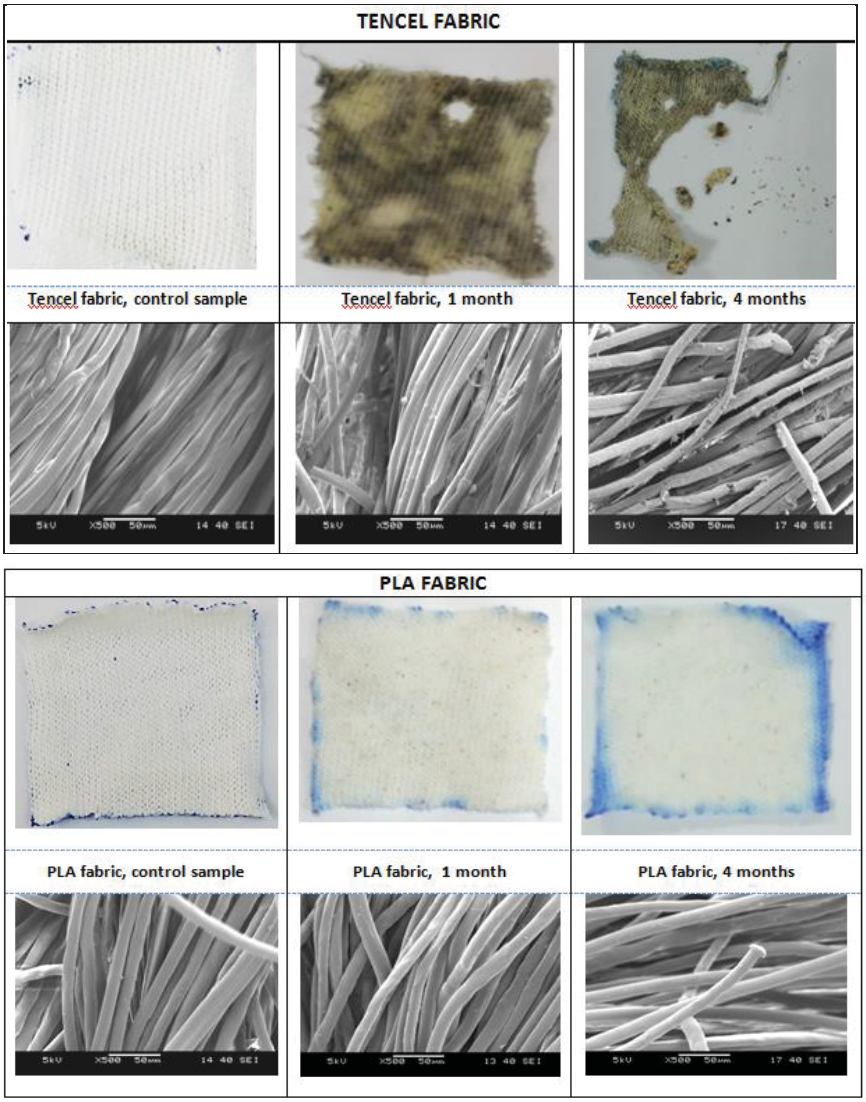


**Figure 2.** Photographs and SEM micrographs (X500) of the Tencel and PLA fabrics for different soil burial intervals

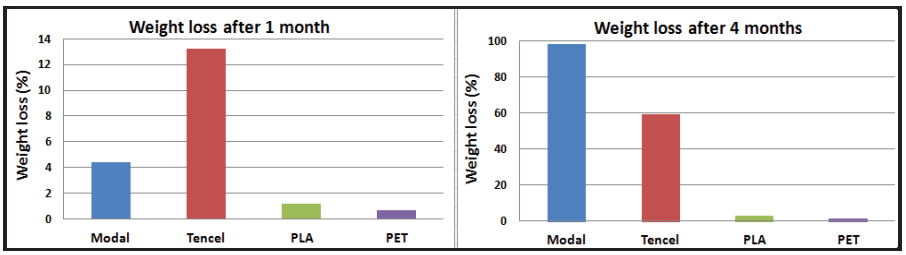


**Figure 3.** Weight loss of the fabrics for different soil burial intervals

### 3.3. FTIR Analysis

FTIR analysis was performed to examine the effect of burial test on chemical structure of the fabrics. FTIR spectra of the control and buried Tencel, Modal and PLA fabric samples are presented in Figure 4-6.

Regenerated cellulose fibers (Tencell and Modal) the main peaks at app. 3330 and 2900cm$^{-1}$ absorption bands can be attributed to -OH stretching and C-H stretching viration of cellulose, respectively [14]. OH of water absorbed from cellulose is centered at around 1640cm$^{-1}$ [15]. The band at 1370cm$^{-1}$ is corresponded to CH bending. The strong absorption peak at 1020cm$^{-1}$ can be indicative of C-O stretching of cellulose. The smaller peaks at 1200, 1155 and 895 cm$^{-1}$ absorption bands can be assigned to ‑OH in plane bending, C-O-C asymmetric stretching and C1 group frequency, respectively [16].

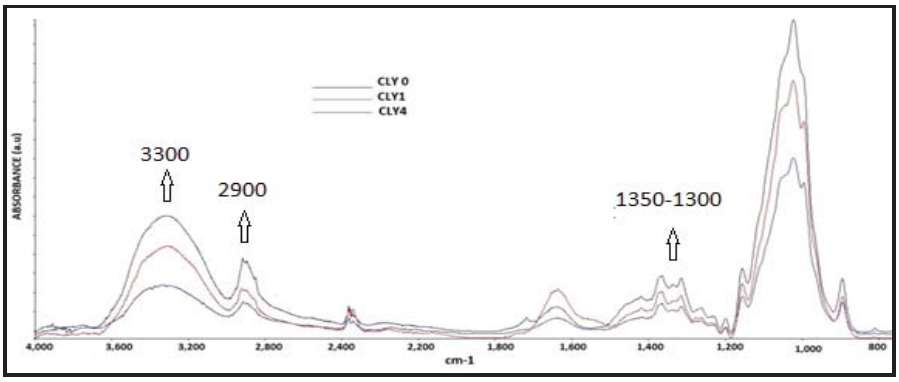


**Figure 4.** FTIR spectra of the control and buried Tencel fabric samples

FTIR spectra the control and buried PLA fibres are given in Figure 6. The band located at 1745cm-1 can be corresponded to C=O stretching. The absorption peaks detected between 1050-1250cm-1 can be attributed to C–O and C–O–C stretching vibrations. The symmetric and asymmetric deformational vibrations of C-H in CH3 groups are exhibited in the ranges between at 1300-1500cm-1 [17]. Although the control and buried PLA samples give resembling FTIR spectra, the intensities of the functional groups were exposed to change after burial testing.

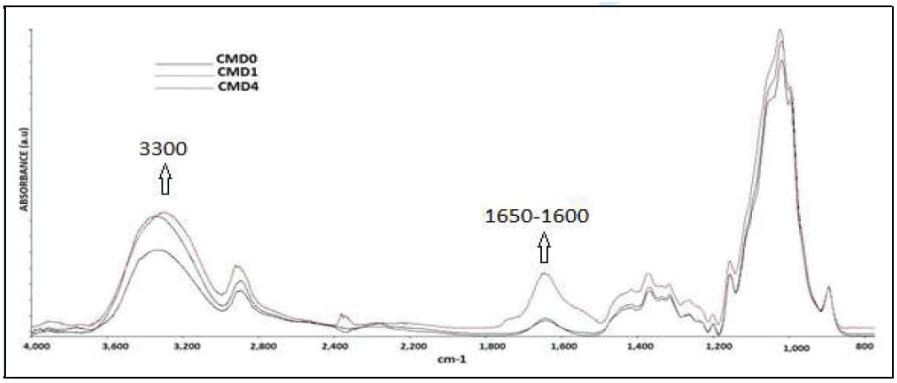


**Figure 5.** FTIR spectra of the control and buried Modal fabric samples

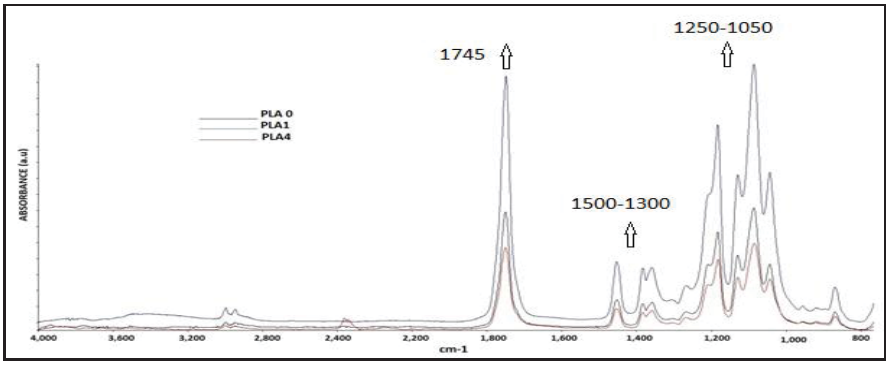


**Figure 6.** FTIR spectra of the control and buried PLA fabric samples

## 4. CONCLUSION

In this study, the biodegradability behaviour of knitted fabrics having similar structural parameters and consisting common fiber types such as Modal, Tencel, polylactic acid (PLA) and polyethylene teraphtalate(PET) were studied by soil burial tests. Three common fiber types and one biodegradable synthetic fiber (PLA) were compared by evaluating the changes of the fabrics.

Morphological characterization and visual observations indicated that the major portion of biodegradation can be attributed to the regenerated cellulosic fibers while synthetic fibers stayed generally undamaged for defined burial periods. Morphological observations revealed that the cellulosic fibers began to disintegrate in varying portions whereas the synthetic fibers kept their original status at the end of 4 months burial period. The biodegradation results of cellulosic fibers show that it is possible to dispose of these materials by burying because of their high biodegradation. Biodegradation is important for a sustainable environment but the production technologies of fibers, amount of

used chemicals and pollution occurred during fibre production are also important as much as the level of biodegradation.

## ACKNOWLEDGMENT

The authors are thankful to Dokuz Eylul University (Scientific Research Projects Coordination Unit) for financial support of this research as a scientific project (2017.KB.FEN.034).

## REFERENCES

1. Yogita Agrawal, Shyam Barhanpurkar and Ajay Joshi, Recycle Textiles Waste, p:1-9 https://static.fibre2fashion.com/ArticleResources/PdfFiles/68/6798.pdf, June 2018
2. Council for Textile Recycling, www.weardonaterecycle.org.index.html, June 2018
3. Rana, S., Pichandi, S., Parveen, S., Fangueiro, R. Biodegradation Studies of Textiles and Clothing Products, Roadmap to Sustainable Textiles and Clothing, edited by Muthu, S.S., Textile Science and Clothing Technology, (2014) DOI: 10.1007/978-981-287-110-7_4.
4. Arutchelvi J, Sudhakar M, Arkatkar A et al.,odegradation of polyethylene and polypropylene. Indian J Biotechnol 7 (2008) 9-22
5. Li, L., Frey, M., Browning, K.J., Biodegradability Study on Cotton and Polyester Fabrics, Journal of Engineered Fibers and Fabrics, 5(4) (2010) 42-53.
6. Solazzo, C., Dyer, J.M., Clerens, S., Plowman, J., Peacock, E.E., Collins, M.J. Proteomic evaluation of the biodegradation of wool fabrics in experimental burials, International Biodeterioration & Biodegradation, 80, (2013) 48-59.
7. Weng, Y.X., Jin, Y.J., Meng, Q.Y., Wang, L., Zhang, M., Wang, Y.Z. Biodegradation behavior of poly(butylene adipate-co terephthalate) (PBAT), poly(lactic acid) (PLA), and their blend under soil conditions, Polymer Testing, 32(5), (2013) 918-926.
8. Arshad, K., Skifvars, M., Vera, V., Julija, V. Biodegradation of natural textile materials in soil, Tekstilec, 57(2) (2014) 118-132.
9. Karamanlioglu, M., Preziosi, R., Robson, G.D. Abiotic and biotic environmental degradation of the bioplastic polymer poly (lactic acid): A review, Vol:37, (2017) 122-130
10. ISO 11721-1:2001 Textiles -- Determination of resistance of cellulose-containing textiles to micro-organisms -- Soil burial test -- Part 1: Assessment of rot-retardant finishing
11. Yaacob, N.D., Ismail, H. And Ting, S.S, Soil Burial of Polylactic acid/Paddy straw powder biocomposite, Bioresources, 11(1) (2016) 1255-1269.
12. Luckachan, G.E. and Pillai, C.K.S. Biodegradable Polymers- A Review on Recent Trends and Emerging Perspectives, Journal of Polymers and the Environment, 19(3) (2011) 637-676.
13. Yiwang Chen; Licheng Tan; Lie Chen; Yan Yang; Xiaofeng Wang, Study on biodegradable aromatic/aliphatic copolyesters, Braz. J. Chem. Eng. Vol.25 No.2 São Paulo (2008) http://dx.doi.org/10.1590/S0104-66322008000200011
14. Kılınç, A.Ç., Atagür, M., Ozdemir, O., Sen, I., Kuçukdoğan, N., Sever, K., Sarıkanat, M., Seki, Y. Manufacturing and characterization of vine stem reinforced high density polyethylene composites, Composites Part B, 91 (2016) 267-274.
15. Carillo, F., Colom, X., Sunol, J.J., Saurino, J. Structural FTIR analysis and thermal characterisation of lyocell and viscose-type fibres, European Polymer Journal, 40(9) (2004). 2229-2234.

16. Seki, Y.,Seki, Y., Sarıkanat, M., Sever, K., Durmuşkahya, C. and Bozacı, E. Evaluation of linden fibre as a potential reinforcement material for polymer composites, Journal of Industrial Textiles, 45(6) (2016) 1221-1238.
17. Pamula, E., Blazewicz, M., Paluszkiewicz, C., Dobrzynski, P. FTIR study of degradation products of aliphatic polyesters–carbon fibres composites, Journal of Molecular Structure, 596(1-3), (2001) 69-75.

# DETERMINATION OF THE IN - PLANE WATER VAPOUR RESISTANCE OF SELECTED FABRICS

**Lubos HES[1], Vladimir BAJZIK[1]**

[1] Technical University of Liberec, Faculty of Textile Engineering, Czech Republic

Corresponding author: lubos.hes@gmail.com

***Abstract:*** *In the study, a new method of determination of the in-plane evaporation resistance of fabrics is described. It is based on a special application of the non-destructive PERMETEST Skin model, which enables fast determination of the evaporation resistance of e. g. car seats, furniture, antiballistic vests etc. In the second part of the paper, principle of water vapour transfer in the plane direction of a fabric is outlined, and first in-plane water vapour resistance values of selected knitted fabrics were experimentally determined.*

***Keywords:*** *in-plane water vapour resistance, textiles, measurement*

## 1. INTRODUCTION

In many applications, water vapour evaporated from the human skin cannot escape directly through the clothing into the environmental air, as the outer fabric surface is not free, like at sitting on a chair or wearing an impermeable antiballistic body armour or vest, tightly fixed to the body. Here, water vapour keeps accumulated on the garment system and stepwise causes the wearing discomfort. That is why contact fabrics of some recent car seats contain distant knits, in order to conduct the gaseous moisture out of the seated body by the in-plane conduction (diffusion) toward the free edge of the seat. Unfortunately, there is still no measuring method published, which could quantitatively determine the in-plane evaporation resistance of these porous fabrics [1]. In the study, a new method of determination of the in-plane evaporation resistance of fabrics is described and experimentally verified. It is based on a special application of the non-destructive PERMETEST Skin model. This instrument is displayed on the Fig.1. On the next Fig. 2 is in the upper position outlined the standard measuring PERMETEST procedure. Heat power sensor is placed in the middle of the heated block covered by a wetted porous sheet. The tested sample is placed over this porous sheet, just above the sensor. Then, water in the porous sheet starts to evaporate and water vapour passes through the tested fabric. The sensor then records the total evaporation heat $q_{evap}$ of the transformed water [2,3]. When testing the in-plane evaporation resistance of the tested fabric, then the surface of the tested sample should be covered by a thin circular impermeable foil – see the bottom figure. Water vapour then needs to find other way to escape, and had to pass through the in-plane pores in the fabric, until it reaches the edge of the circular cover. Here, the total evaporation resistance Ret [$m^2Pa/W$] values determined according to the standard ISO 11092 procedure are much larger then in case of the direct water vapour diffusion.


**Figure 1.** Non- destructive tester of thermal and evaporation resistance of textile fabrics PERMETEST and its operation display figured on any external computer (see in www.sensora.eu)

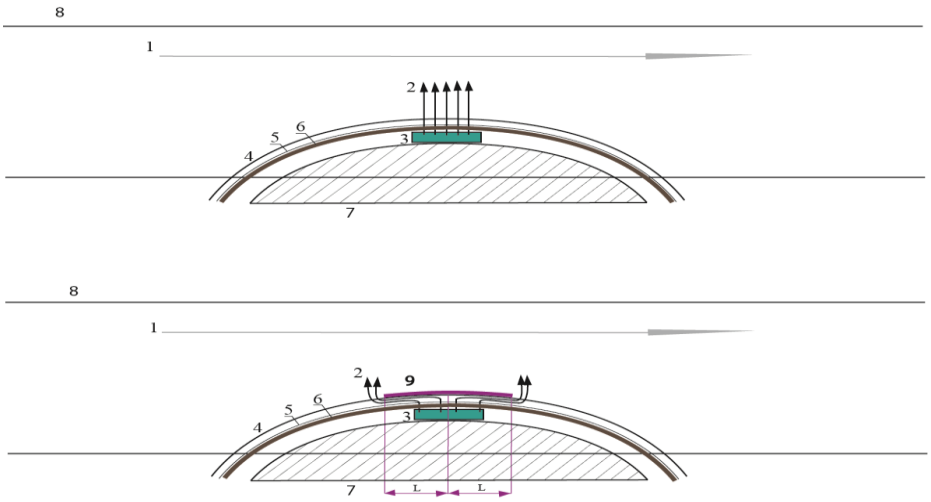


**Figure 2.** Trajectory of the water vapour molecule in case of the through thickness diffusion and in case of the in-plane diffusion through a fabric

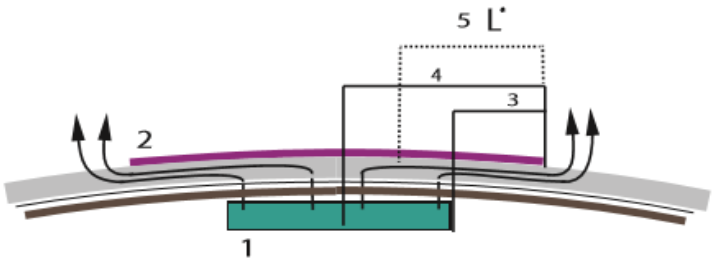


**Figure 3.** Mean trajectory of the water vapour molecule between the cooling power sensor and the outside air flow

## 2. THEORY OF THE WATER VAPOUR TRANSFER IN THE IN-PLANE DIRECTION IN A FABRIC

The amount of the water vapour **m*** transferred in steady state through a fabric in a skin model by diffusion and convection is proportional to the driving force, which is the difference of water vapour concentration or (in our case) difference of partial pressures of water vapour $\Delta p_{wv}$ on both sides of the fabric, and indirectly proportional to the evaporation resistance $R_{evap,f}$ of the fabric and the evaporation resistance of the adhered boundary layer $R_{evap,bl}$, as follows (**E** means heat of evaporation, about 2 500 000 J/kg):

$$m^* = \Delta p_{wv} / (R_{evap,f} + R_{evap,bl}) \qquad q_{evap} = \Delta p_{wv} E /(R_{evap,f} + R_{evap,bl}) \tag{1}$$

In the case of the in-plane diffusion through a fabric, the in-plane evaporation resistance $R_{evap,f,\ in\text{-}pl}$ will be much higher then the $R_{evap,f}$. The level of the the in-plane evaporation resistance $R_{evap,f\ in\text{-}pl}$ will depend on the length of the effective average water vapour (wv) trajectory **L*** and the effective average section porosity **ε*** of the studied fabric, and it will be indirectly proportional to the coefficient of water vapour diffusion $D_p$ in the moist air present in the pores, as follows:

$$R_{par,\ sed} = L^* /(\varepsilon^* . D_p) \tag{2}$$

The boundary layer) evaporation resistance $R_{evap,bl}$ is given by the equation

$$R_{evap,bl} = (1/\beta) \tag{3}$$

where the parameter **β** is the convection mass transfer coefficient – see in [4,5]. This coefficient **β** can be determined by means of the dimensionless Sherwood Sh, Schmidt Sc and Reynolds Re numbers defined by the next relations (b is the dimension, v is the viscosity of the humid air):

$$Sh = \beta\, b/D_p,\ \beta = Sh\, D_p/v,\ Sh = 0{,}664\, Re^{1/2}.Sc^{1/3} \text{ (for a flow parallel to a plane)},$$
$$Re = uD/v \tag{4}$$

In the PERMETEST instrument, where the velocity u of the air parallel flow reaches 1 m/s, the Re = 5700, which confirms the presence of the turbulent flow. As the Schmidt number for air is 0,60, the determined Sherwood number was 39,5. Thus, the reference (100%) cooling flow present in the PERMETEST instrument under standard conditions and without any sample has the level of about 1200 W/m$^2$, when considering the uniform distribution of moisture in the porous plate which in the Skin model simulates the wetted human skin. As in a human body the sweating coefficient mostly does not exceed 30%, the calculated cooling flow seems realistic.

## 3. EXPERIMENTAL PART

13 woven samples and distant knits consisting of cotton, polypropylene and polyester with square mass ranging from 0.138 to 0,696 kg/m$^2$. The diameter of the thin covering aluminium disc was 25 mm, 35 mm and 45 mm. The mean trajectories of water vapour molecules were 7,5 mm, 12,5 mm and 17,5 mm [6].

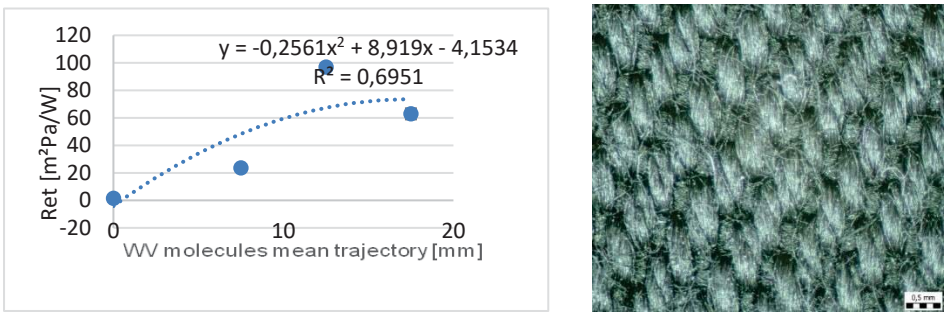


**Figure 4.** Effect of the water vapour molecules trajectory in woven a fabric No 5 (PES 50%, cotton, twill, 228 g/m$^2$) on the experimentally determined evaporation resistance

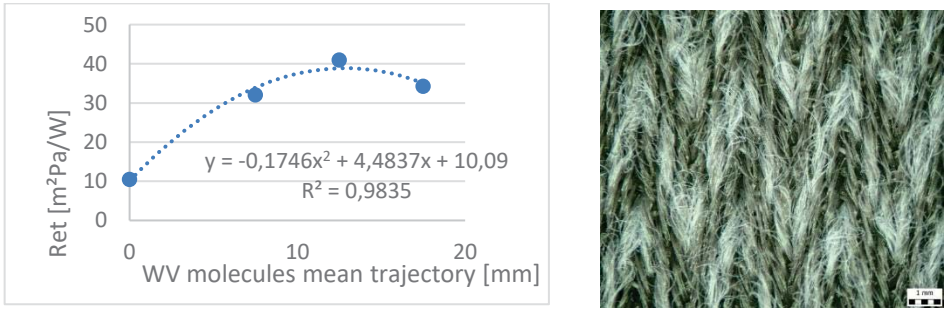


**Figure 5.** Effect of the water vapour molecules trajectory in a fabric No 10 (PES Colmax, single jersey, 138 g/m$^2$) on the experimentally determined evaporation resistance

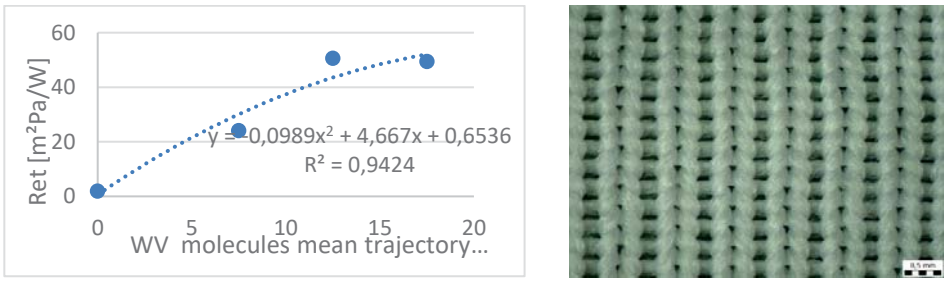


**Figure 6.** Effect of the water vapour molecules trajectory in a fabric No. 13 (Coolmax knit 178 g / m$^2$ and thickness 0,38 mm) on the experimentally determined evaporation resistance

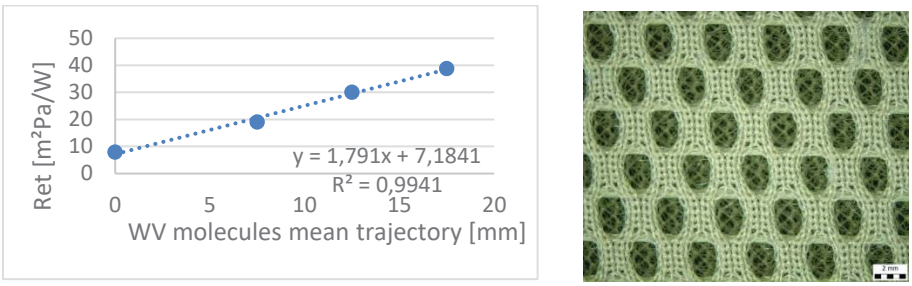


**Figure 7.** Effect of the water vapour molecules trajectory in a knitted fabric No. 14 (PES hexachannel, 250 g/m$^2$) the experimentally determined evaporation resistance

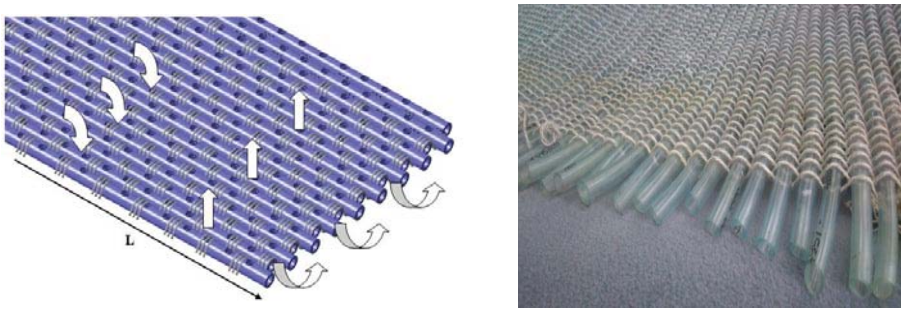


**Figure 8.** Example of a new solution of a fabric with an increased in-plane wv transfer consisting of hollow parallel thin partly perforated tubes, which should serve as a seating cover of a car seat [7]

## 4. CONCLUSIONS

In the study, a new method of determination of the in-plane evaporation resistance of textile and other fabrics was described and experimentally verified. It was based on a special application of the non-destructive PERMETEST Skin model. From the results follows, that even for very porous and relatively thick fabric, the in-plane evaporation resistance $\mathbf{R_{evap,f,\ in\text{-}pl}}$ quickly rises with the increasing distance between the source of sweat and the free edge of the studied fabric. Thus, the fabrics used for seating, furniture or fabrics partly covered by impermeable structures should be thick and very porous, in order to conduct water vapour away of the source of sweat and in this way offer higher thermophysiological comfort.

However, in this first study, the scope of the presented experiments was quite limited. Next research on larger amount of samples will follow, in order to receive the more general results.

## REFERENCES

1. Hes, L.: In - plane water vapour diffusion in fabrics (short poster).In: I -Tech Summit, Porto, April 2018
2. Hes, L., Dolezal, I.: A New Portable Computer-Controlled Skin Model for Fast Determination of Water Vapour and Thermal Resistance of Fabrics. In: Asian Textile Conf. (ATC 7), New Delhi 2003.
3. Bogusławska – Bączek M., Hes L.: The Effective Water Vapour Permeability of Wet Wool Fabric and Blended Fabrics, Fibres & Textiles in Eastern Europe, Vol 1., 2013, pp. 67-17, ISSN 1230-3666
4. Incropera, F. P., DeWitt, P. D.: Fundamentals of heat and mass transfer. Willey Digital, Cornell University, 2002.
5. Slancova, M: Knitted **f**abrics **w**ith increased cooling effect (in Czech), BSc Thesis, TU Liberec 2018
6. Machackova P.: In-plane water vapour transfer in textiles (in Czech). MSc Thesis, TU Liberec, 2017
7. Jandova, M: Evaporation nresistance of textile contact layers used for sitting (in Czech). BSc Thesis, TU Liberec, 2016

# THE EFFECT OF KNIT PATTERN ON AIR PERMEABILITY OF WEFT KNITTED RIB FABRICS FROM GLASS YARN

**Mehmet Erdem İNCE[1], Kıymet SAVCI GÜNEŞ[1], Halil İbrahim İÇOĞLU[2]**

[1] Gaziantep University, Department of Textile Engineering, Turkey
[2] Gaziantep University, Department of Metal. Mater. Engineering, Turkey

Corresponding author: eince@gantep.edu.tr

***Abstract:*** *Expandable, intermeshed, three-dimensional, porous weft-knitted fabrics*

***Abstract:*** *Expandable, intermeshed, three dimensional, porous weft-knitted fabrics manufactured on double-bed knitting machines have numerous technical application areas (comfortable protective clothing, chemical and flame resistant filter media, and impact resistant polymer matrix reinforced composite reinforcement); as they are knitted from high performance fibers such as glass, carbon and aramid. The performances of these fabrics in technical application areas depend on the fabric porosity (or fiber volume fraction) that is primarily dictated by the knit pattern (architecture), and quantified by permeability of the fabric to air. In this study, weft knitted fabrics with 1x1, 2x2, English, and fisherman rib patterns from 3-ply E-glass yarn with a nominal single-end yarn count of 133 tex were manufactured. A manual, flat, double-bed weft knitting machine with a fineness of 5E was used to knit the fabrics. Thickness, areal density, course-density, wale-density, loop length, and air permeability of the fabrics were measured. Tuck loops of English and fisherman rib architectures shortened the fabrics in wale direction that enriched fiber content and loop density; while lowering loop length. On the other hand; evolution of the knit architecture from 1x1 rib to 2x2 increased the contraction of the fabrics in course direction that improved again fiber volume percent, and loop density; while lowering loop length. Fabrics with higher fiber content and loop density; while shorter loop length possessed tight and compact structures those are less permeable to air. Therefore, 2x2 rib fabrics exhibited the lowest air permeability that was linked to their extreme course-wise contraction after removal from the machine. On the other side, presence of tuck loops shortened the fabric in wale-wise direction that lowered air permeability for English and fisherman rib fabric architectures.*

***Key Words****: weft-knitted fabrics, rib fabrics, glass yarn, physical properties, air permeability*

## 1. INTRODUCTION

Weft knitting is a low-cost, fast, and versatile technique among textile fabrics manufacturing methods; and fabric structures created by this technique offers unique properties as compared to other (woven and nonwoven) fabrics. Interlocked structures of weft knitted fabrics surpass woven and non-woven

fabrics in view of deformability, stretch ability, and drape ability. Weft knitted fabrics from high performance fibers find many application areas. Porous 3D architectures of weft knitted fabrics render them advantageous in comfortable clothing, filter media, and permeable preform for liquid composite molding [1].

Due to their low-price, high mechanical properties, flame resistance, and inertness to chemicals; glass fibers find many use areas among technical applications in the form of unidirectional fiber, random mat, woven, non-woven, and knitted fabrics. Weft-knitted rib fabrics from glass yarn can protect the bodies against hazardous chemicals, and flames; filter the hot and dangerous filtrates; and absorb the impact energy in the form of polymer composite reinforcement [2]. Additionally, weft knitted rib fabrics produced by double-bed knitting machine have more voluminous and curl-free-edge structures as compared with single-bed knitted fabrics that enhance their process ability in multi-layer clothing, filter, and liquid composite molding applications.

Once the type of raw material and the specification of the knitting machine are fixed; the most influential process parameters on the structure of weft knitted fabrics are cam setting and knit pattern. While cam setting determine size and the shape of the loops; knit architecture locate the position of the different loop types such as plain, tuck and skip loops within the knit repeat. Previous studies indicated that knit pattern created significant effect on physical properties and correspondingly air permeability and bursting strength of weft knitted fabrics [3, 4]. Similarly, the mechanical properties of layered composites from weft knitted fabrics were also dictated by knit architectures [5].

The aim of this study is to reveal the effect of knit architecture on air permeability of weft knitted fabrics from glass yarn to increase their use in technical applications.

## 2. MATERIAL AND METHOD

We manufactured weft knitted fabrics with 1x1, 2x2, English, and Fisherman rib patterns from 3-ply E-glass multi-filament yarn with a nominal single-end yarn count of 133 tex on Brother KH-864 manual, flat weft knitting machine with a fineness of 5E. Figure 1 shows technical notations, 2D hand-draft drawings, simulations, and the images taken while the fabrics were on the machine under tension, on the table in relaxed state. Thickness, areal density, course-density, wale-density, loop length; and air permeability of the fabrics were measured. Dry fabric fiber volume percent was calculated by Equation 1 given below where density of glass fiber was assumed as 2,5 g/cm$^3$. Loop density was calculated as the product of course and wale densities of the related fabric.

$$Fiber\ volume\ percent, \% = \frac{\left(\frac{fabric\ areal\ density, g/m^2}{2,5}\right)}{\left(100*100*\left(\frac{fabric\ thickness, mm}{10}\right)\right)} * 100 \quad \text{.....(1)}$$

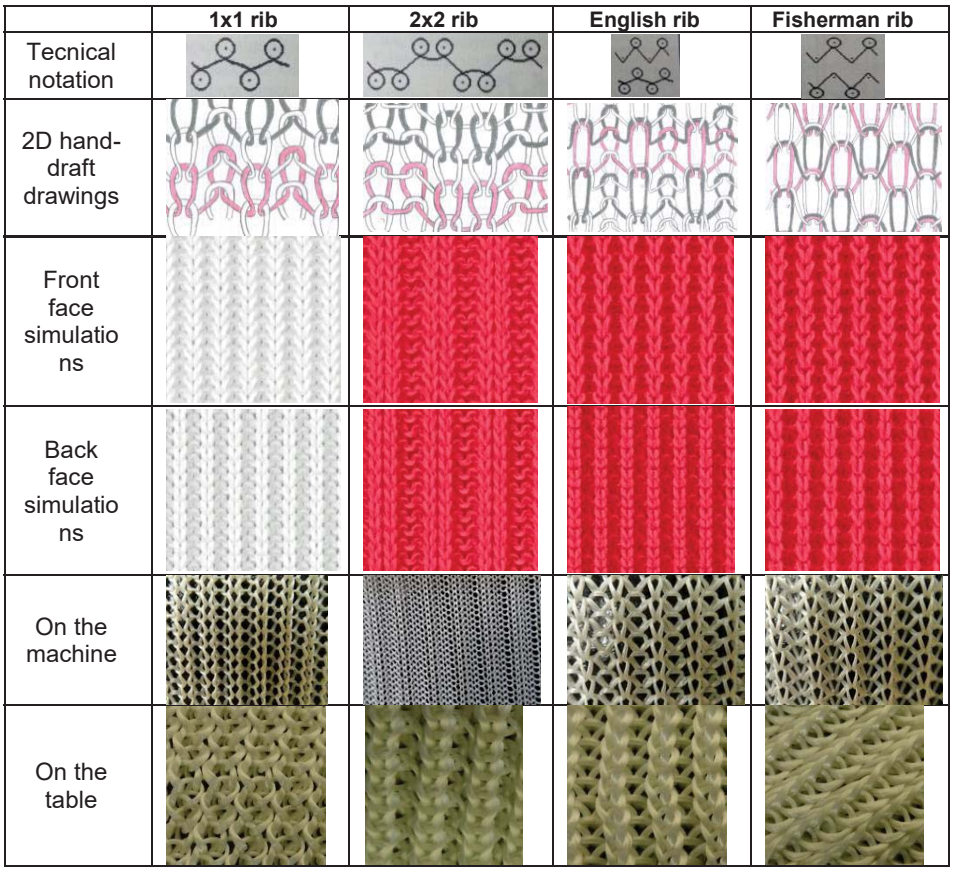


**Figure 1.** Knitted fabric architectures [1]

SDL ATLAS M021A test device was used to assess air permeability of weft knitted fabrics according to ASTM D737 [6]. At least 10 measurements per knit pattern were performed with a test head area of 20 $cm^2$ and across a pressure drop of 200 Pa. Fabric was placed under the arm and pressed down to begin test. Air was passed through the test area and air flow rate measured once a steady state air-flow was achieved at 200 Pa pressure drop. Air permeability was measured in $cm^3/(cm^2 \times s)$ unit.

## 3. RESULTS AND DISCUSSION

### 3.1. The Effect of Knit Architecture on Physical Properties of Fabrics

Figure 2 and Table 1 illustrated the effects of knit architectures on fabric thickness, areal density and fiber volume percent. Fabrics with fisherman and 2x2 rib architectures exhibited greater thickness than those with English and 1x1 rib ones at statistically significant level ($\alpha = 0,05$). Tuck loops on both sides of the

fabrics of fisherman ribs shortened the fabric length that increased thickness of the fabric. Two adjacent face loops followed by two adjacent back loops periodically in the case of 2x2 rib architectures contracted the fabrics in course direction that also increased thickness. The same trend was also observed between knit architecture and fabric areal density. While no statistically significant differences were observed among the fiber volume percents of English, 2x2, and fisherman rib architectures; fabric with 1x1 architecture exhibited the lowest fiber content at statistically significant level that was linked to its loose fabric structure.

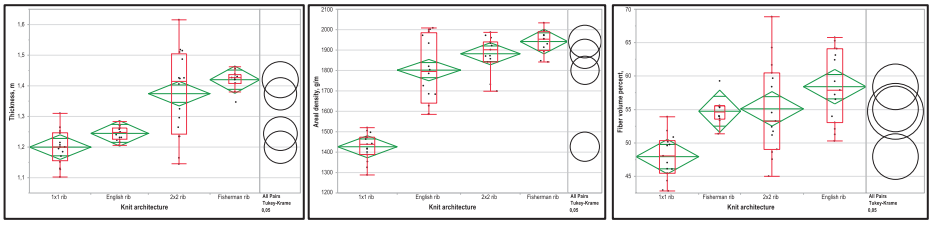

**Figure 2.** The effects on knit architecture on thickness (left), areal density (middle) and fiber volume percent (right)

**Note:** The distance between top and bottom ends of each green diamond represent the 95% confidence interval for each knit architecture level. The height of red box - a quantitative indication of variation that is similar to standard deviation - is called interquartile range of mean. Comparison circles (given on the right column) for means those are significantly different either do not intersect, or intersect slightly.

**Table 1.** Knit architecture versus thickness, areal density, and fiber volume percent report

| | Knit pattern | | | | n | mean | sd | LL | UL |
|---|---|---|---|---|---|---|---|---|---|
| **Thickness**, mm | Fisherman rib | A | | | 13 | 1,42 | 0,03 | 1,40 | 1,44 |
| | 2x2 rib | A | | | 16 | 1,37 | 0,14 | 1,30 | 1,45 |
| | English rib | | B | | 15 | 1,24 | 0,02 | 1,23 | 1,26 |
| | 1x1 rib | | B | | 16 | 1,20 | 0,06 | 1,17 | 1,23 |
| **Areal density**, g/m$^2$ | Fisherman rib | A | | | 12 | 1941,78 | 59,18 | 1904,2 | 1979,4 |
| | 2x2 rib | A | B | | 15 | 1881,99 | 82,08 | 1836,5 | 1927,4 |
| | English rib | | B | | 16 | 1801,83 | 161,47 | 1715,8 | 1887,9 |
| | 1x1 rib | | | C | 15 | 1426,46 | 66,99 | 1389,4 | 1463,6 |
| **Fiber volume percent**, % | English rib | A | | | 15 | 58,41 | 5,45 | 55,40 | 61,43 |
| | 2x2 rib | A | | | 15 | 55,10 | 6,84 | 51,31 | 58,88 |
| | Fisherman rib | A | | | 10 | 54,74 | 2,05 | 53,27 | 56,21 |
| | 1x1 rib | | B | | 15 | 47,94 | 3,31 | 46,11 | 49,78 |

**Note:** Levels not connected by the same capital letter are significantly different (α = 0,05). n: number of measurements, sd: standard deviation, LL: lower limit, UL: upper limit. Limits are based on 95% confidence level.

Figure 3 and Table 2 show the effects of knit architecture on loop density and loop length. 2x2 rib fabrics exhibited the highest loop density followed by fisherman, English and 1x1 rib fabrics, respectively. No statistically significant difference was observed between the loop densities of English and 1x1 rib fabrics. The reverse trend was observed for the association between knit architecture and loop length. Due to its loose fabric structure; 1x1 rib fabrics

exhibited the longest loop length. On the other hand; fisherman rib fabrics exhibited the smallest loop length that improved their compactness. Fabrics with tuck loops (English and fisherman rib architectures) possessed more loops with smaller size per unit area where wale-wise contraction enabled to accommodate more loops per unit area via shortening the length of the loops.

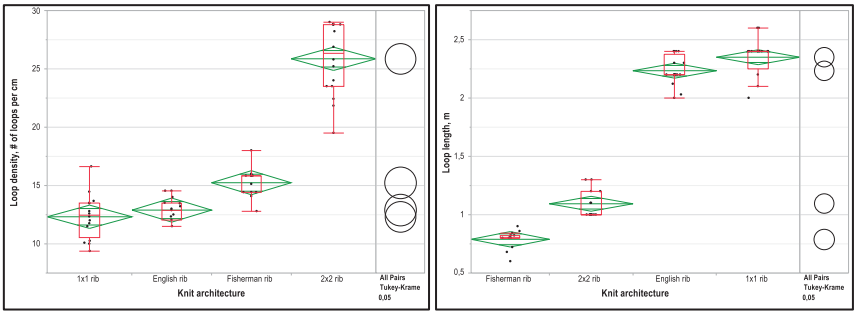


**Figure 3.** The effects of knit architecture on loop density (left), and loop length (right)

**Table 2.** Knit architecture versus loop density and loop length report

| | Knit pattern | | | | n | mean | sd | LL | UL |
|---|---|---|---|---|---|---|---|---|---|
| **Loop density**, number of loops per $cm^2$ | 2x2 rib | A | | | 16 | 25,86 | 3,09 | 24,22 | 27,51 |
| | Fisherman rib | | B | | 15 | 15,24 | 1,21 | 14,57 | 15,91 |
| | English rib | | | C | 15 | 12,90 | 1,02 | 12,33 | 13,46 |
| | 1x1 rib | | | C | 16 | 12,32 | 1,88 | 11,32 | 13,32 |
| **Loop length**, mm | 1x1 rib | A | | | 16 | 2,35 | 0,17 | 2,26 | 2,44 |
| | English rib | A | | | 16 | 2,23 | 0,13 | 2,17 | 2,30 |
| | 2x2 rib | | B | | 16 | 1,09 | 0,12 | 1,03 | 1,16 |
| | Fisherman rib | | | C | 15 | 0,79 | 0,07 | 0,75 | 0,83 |

### 3.2. The Effect of Knit Architecture on Air Permeabilities of Fabrics

Knit pattern affected the air permeability of the fabrics at statistically significant level ($\alpha = 0.05$). As the knit architectures were varied; clear statistically significant changes – quantified by fairly low p-values – were observed. While 1x1 rib fabrics exhibited the highest air permeability; 2x2 rib fabrics showed the lowest air permeability (Figure 4 and Table 3). Due to consecutive formation of two adjacent loops on front, and then on back needle beds; 2x2 rib fabrics shortened in course direction more than the other patterns that created tight fabric structure with the higher fiber volume percent, and loop density that lowered their permeability to air. On the other hand, fabrics with 1x1 rib pattern exhibited the lowest fiber volume percent, and loop density that created a loose fabric structure with the highest permeability to air. Statistically significant air permeability decrease from English to fisherman rib architectures proved that tuck loops lowered air permeability by creating tighter knit architectures.

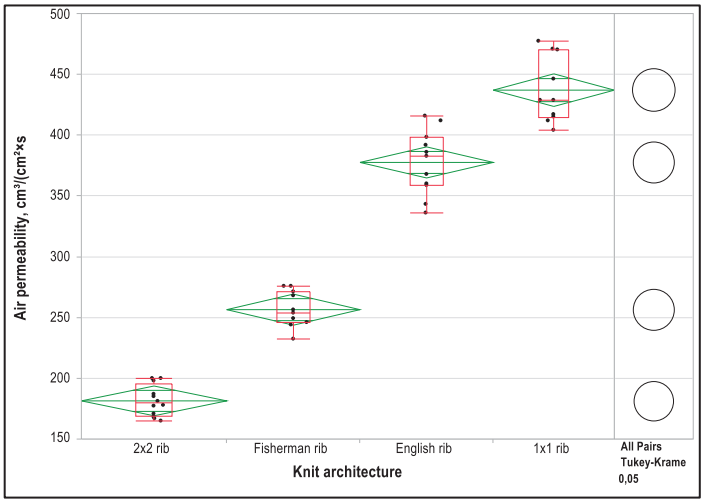


**Figure 4**. The effect of knit architecture on air permeability

**Table 3.** Knit architecture versus air permeability report

| | Knit pattern | | | | | n | mean | sd | LL | UL |
|---|---|---|---|---|---|---|---|---|---|---|
| **Air permeability** cm³/(cm²×s) | 1x1 rib | A | | | | 10 | 437,00 | 27,19 | 417,55 | 456,45 |
| | English rib | | B | | | 11 | 377,54 | 26,56 | 359,70 | 395,39 |
| | Fisherman rib | | | C | | 11 | 256,46 | 14,45 | 246,75 | 266,16 |
| | 2x2 rib | | | | D | 12 | 181,42 | 12,82 | 173,27 | 189,56 |

## 4. CONCLUSIONS

This study revealed the effect of knit pattern on air permeability of the fabrics from glass yarn. We measured thickness, areal density, structural parameters (course density, wale density, and loop length), and air permeability of double-bed weft knitted rib fabrics from 3-ply E-glass yarn. Due to extreme shortening of the fabric in course direction; fabrics with 2x2 rib architecture showed the lowest air permeability that was attributed to its compact structure with higher fiber content and loop density. Incorporation of tuck loops into the knit architectures also increased the compactness of the fabric and lowered air permeability. This study pointed that 2x2 rib pattern or the patterns with tuck stitches should be utilized where high fiber content or low porosity are requirements such as in composite, and filter applications, respectively.

## ACKNOWLEDGMENTS

This work has been supported by BAP Unit of Gaziantep University under the project code of MF.YLT.18.02.

## REFERENCES

1. Marmaralı A. B.: Atkı Örmeciliğine Giriş, 2004. E.Ü. Tekstil ve Konfeksiyon Araştırma - Uygulama Merkezi, İzmir.
2. Khondker O. A., Leong K. H., Herszberg I., Hamada H.: Impact and compression-after-impact performance of weft-knitted glass textile composites. 2005. Composites Part A: applied science and manufacturing v. 36(5), 638-648.
3. Kane C. D., Patil, U. J., Sudhakar, P.: Studies on the influence of knit structure and stitch length on ring and compact yarn single jersey fabric properties. 2007. Textile Research Journal v. 77(8), 572-582.
4. Mikučionienė D., Milašiūtė L., Milašius R.: Influence of knits structure on flammability and comfortability. 2014. AUTEX Research Journal v. 14, No. 4, 226-232.
5. Alpyildiz T., Icten B.M., Karakuzu R., Kurbak A.: The effect of tuck stitches on the mechanical performance of knitted fabric reinforced composites. 2009. Composite Structures v.89, No. 3, 391-398.
6. ASTM D737, Standard Test Method for Air Permeability of Textile Fabrics, 2018.

# EFFECT OF PROCESS PARAMETERS ON AIR PERMEABILITY AND HYDROSTATIC PRESSURE OF POLYPROPYLENE NONWOVENS PRODUCED BY MELT BLOWING

**Numan HODA[1], Firdevs MERT[2], Fatma KARA[2], Gajanan S. BHAT[3], Hande Gül ATASAGUN[4], Partha P. SIKDAR[3]**

[1] Akdeniz University, Department of Material Science and Engineering, Turkey
[2] Akdeniz University, Department of Chemistry, Turkey
[3] The University of Georgia, Department of Textiles, USA
[4] Dokuz Eylül University, İzmir Vocational School, Turkey

Corresponding author: nhoda@akdeniz.edu.tr

**Abstract:** A detailed experimental investigation was done to understand the effect of Biax melt blowing process on the structure and properties of the produced nonwovens. Process parameters such as polymer flow rate, air pressure were varied for a commercial meltblown grade polypropylene (PP) using a 38cm wide Biax pilot line, and the webs were characterized. Air permeability and hydrohead of the nonwovens were determined according to standard test methods. One-way ANOVA test was used to analyze the effects of the process parameters on these properties. This study showed that as the air pressure increased, the air permeability of nonwovens generally decreased. Moreover, both air temperature and polymer flow rate had statistically significant effects on barrier properties of the melt blown fabrics.

**Keywords**: air permeability, hydrohead, melt-blowing, microfibers, polypropylene

## 1. INTRODUCTION

Melt blowing is a spunlaid process that is used to produce finer fibers, generally 2-5 microns in average fiber diameter [1]. Nonwovens composed of these microfibers have high surface area per unit weight, high insulation value, self-bonding ability, and high barrier properties. Due to these desirable properties, they are widely used to produce high-quality filtration materials, thermal insulation materials, liquid absorption applications, medical supplies, and clothes [2]. In the melt blowing process, the extruder melts the thermoplastic resin, and the molten resin is forced through the special melt-blowing die. The die consists of a row (or multiple rows) of orifices in which molten resin flows out forming fibers and hot air jets that thin down fibers. The formed continuous fibers collect as a nonwoven web on a moving collector.

The current commercially used melt blowing processes can be categorized as Exxon and Biax/Schwarz designs according to spinneret used. The Exxon design is single-row-hole type consisting of holes with two air knives at both sides. The Biax/Schwarz design, which has multiple-row nozzles, provides a uniform stream of attenuating gas around each spinning nozzle by centering the nozzles in round

holes of gas cover plates to achieve an even gas flow around the circumference of each nozzle [3]. The structure and properties of nonwovens produced by melt blowing depend on process parameters that affect fiber diameter, which in turn influences their performance such as permeability, porosity, and absorbency [4]. In the melt blowing process, as well as nozzle designs some parameters such as polymer flow rate, air pressure, extruder temperature affect the fiber properties and the properties of nonwovens produced. So, by changing the parameters during melt processing, it is possible to manufacture nonwovens or microfibers with desired properties. It is a challenge to investigate the degree of effect of parameters on the properties of microfiber to produce nonwovens with the controllable properties.

Majority of the reported studies have been done on the melt blowing process used the Exxon type dies, which consist of holes arranged in a linear fashion [5-7]. There are a limited number of studies using the Biax process that uses multiple rows of holes in the die and is considered more efficient [8]. Also, whereas the Biax die offers advantages to the process with relatively lower air consumption, there is no data available in the literature on the effect of key process conditions on web structure. The aim of this study is to investigate the effects of process parameters such as flow rate and air pressure on the final fiber diameter and web properties.

## 2. MATERIAL AND METHODS

### 2.1. Melt Blown Processing

38cm Biax Melt Blown Pilot Line System was used in these experiments. The spinneret assembled on the line has 720 nozzles with the diameter of 150 µm (0.006") ID in 4 rows with air curtains. Polypropylene (LG Chem, South Korea), which has a relative density of 0.9 (20°C) and MFR of 1200g/10min, was used for melt blowing. During the production, melt flow rate and air pressure were varied, and other process conditions remained the same.

**Table 1.** The process parameters of PP melt blown nonwovens produced in the study

| Air pressure (Psi) | Flow rate (m/min) | Zone 1 (°C) | Zone 2 (°C) | Zone 3 (°C) | Die (°C) | Clamp (°C) | Air temperature (°C) |
|---|---|---|---|---|---|---|---|
| 5, 10, 15 | 20, 30, 40, 50, 60 | 165 | 175 | 190 | 190 | 190 | 170 |

### 2.2 Web Characterization

The fiber diameter of nonwoven webs was measured for each condition in the melt blowing process by sizing the fibers in the images taken by Leica DM750P microscope. Diameters of a total of 100 fibers were measured and averaged. Basis weight and thickness of nonwovens were measured in accordance with related standards. The air permeability was measured using TEXTEST FX 3300

equipment according to ASTM D737-96 standard. The hydrostatic head was measured in compliance with AATCC 127 by using a TEXTEST FX 3000 tester.

### 2.3. Statistical Analyses

Raw data were converted by dividing the fabric density for statistical analyses. The reason for taking into account the fabric density in the analysis is that the fabric weight and thickness differ for different process parameters due to process condition interactions, although the plan was to achieve a specific basis weight. Before the statistical analyses, normal distribution and homogeneity of variance assumptions were tested to determine the eligibility of data for parametric tests. One-way ANOVA test was used to analyze the effects of the process parameters on the measured properties at the 95% confidence level. For non-homogeneous data, the Brown-Forsythe robust ANOVA test was utilized to evaluate their effects.

## 3. RESULTS AND DISCUSSION

This research was conducted to carefully investigate the effects of process parameters on the structure and properties of nonwoven webs produced using a Biax die consisting of concentric holes. SEM pictures of two PP nonwoven webs produced are given in Figure 1. These pictures show typical fiber diameters of the melt blown webs with expected changes with a difference in process conditions.

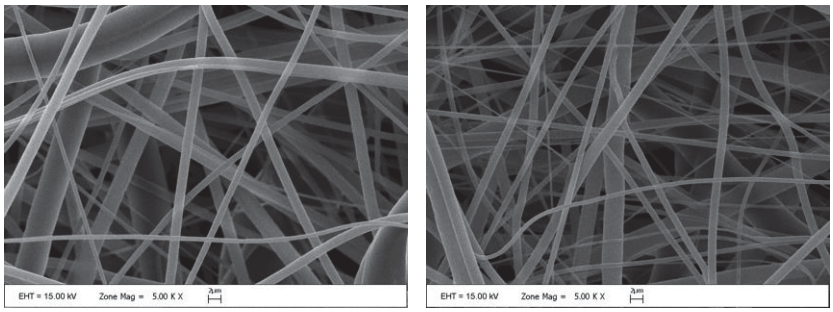


**Figure 1.** SEM pictures of some nonwovens produced

Figure 2 shows the relationships between the process parameters and structural properties of PP melt blown nonwoven fabrics. The increase in the air pressure decreased the fiber diameter in all flow rates. This finding is consistent with the study of Han et al. [9]. When the air pressure was 5 Psi, a positive linear relationship between the fiber diameter and flow rate was observed. However, this relationship changed with the rise of air pressure. Fabric density is associated with the basis weight and thickness of the nonwovens. The increase in the air pressure did not have a significant effect on the density of the webs at the flow rate of 20 and 30 m/min. On the other hand, when the flow rate was beyond the

40 m/min, the fabric density increased with the rise in the air pressure. Also, web thickness and basis weight generally showed increases with the increment in the flow rate.

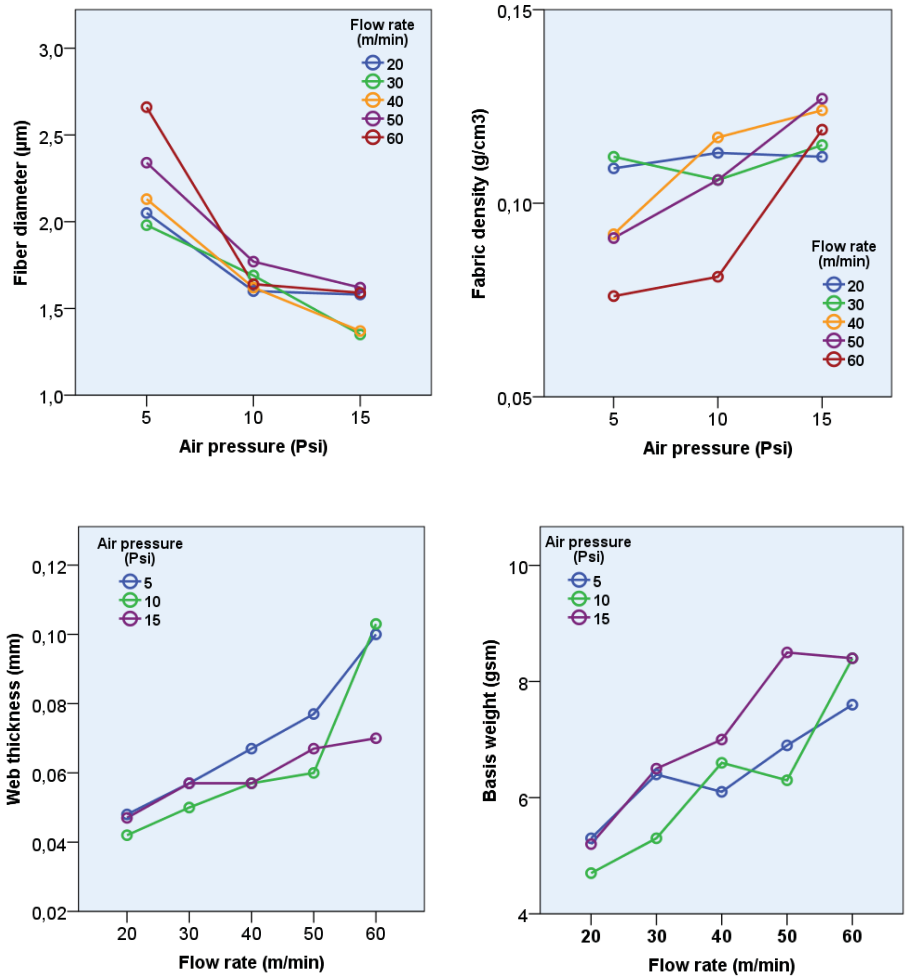


**Figure 2.** Relatioships between the process parameters and structural properties of the nonwovens

The data were grouped based on different combination of process conditions to be able to understand the effect of a particular variable. The relationship between process parameters (i.e., air pressure and flow rate) and the air permeability and hydrohead of the webs are given in Figure 3. As can be seen from Figure 3(a), as air pressure increased, air permeability generally decreased. Both air pressure and flow rate had a statistically significant effect on the air permeability of nonwovens ($p<0.05$). The findings of post-hoc tests showed that all pressure groups were different from each other and the flow rate of 60 m/min was

statistically different from other flow rate groups. Examining the statistical analyses of the hydrostatic head of nonwovens, it was observed that there was no significant effect of air pressure on the hydrostatic pressure. On the other hand, the flow rate had a statistically significant impact on this property ($p<0.05$). The results in the flow rate of 20 and 30 m/min were statistically different from the flow rate groups of 50 and 60 m/min.

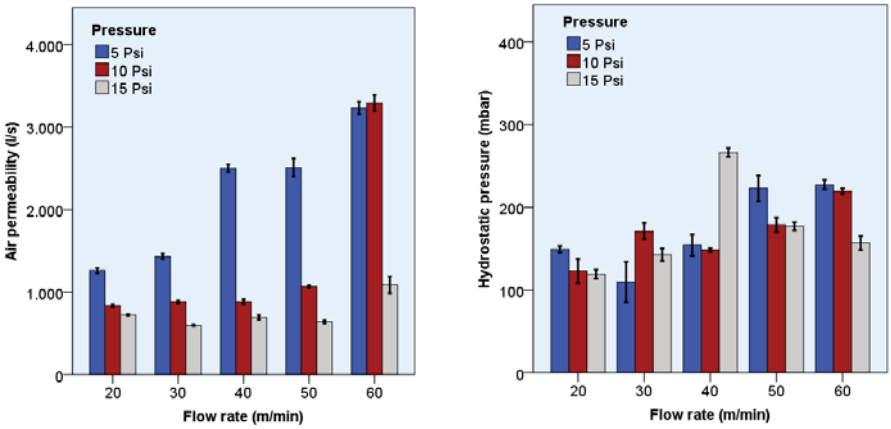


**Figure 3.** The results of the **(a)** air permeability and **(b)** hydrostatic pressure of nonwovens produced in the study. Data are shown as mean values with error bars indicating "1" standard error

## 4. CONCLUSIONS

The melt blown webs produced had fiber diameters in the ranges between 1.35-2.66 µm. Considering the fact that the Biax process uses a relatively lower amount of air as compared to the Exxon-type die, the ability to achieve fiber diameters less than 2 microns was a positive result. In all the cases, with an increase in process air pressure, fiber diameter decreased, and correspondingly, there was a tendency to decrease in air permeability of the webs. Hydrohead, which is another indication of barrier properties of the melt blown webs, were not affected by process air pressure as much as air permeability according to the findings of statistical analyses. This study will help to understand the effects of various process parameters on the structure and performance properties of webs produced using a meltblown process with multiple rows of concentric holes.

## REFERENCES

1. Bhat G.S., Malkan, S.R.: Extruded Continuous Filament Nonwovens: Advances in Scientific Aspects. 2001. J. App. Pol. Sci. 83(3), 572-585.
2. Bhat G.S., Rong, H.: Biodegradable Nonwovens. In: Blackburn RS (ed) Biodegradable and Sustainable Fibres. Cambridge: Woodhead Publishing, 2005, pp. 310-343.

3. Schwarz, E.C.A.: Apparatus and Process for Uniformly Melt-blowing a Fiber Forming Thermoplastic Polymer in a Spinnerette Assembly of Multiple Rows of Spinning Orifices. US Patent 5,476,616.
4. Yesil, Y., Bhat, G.S.: Porosity and Barrier Properties of Polyethylene Melt Blown Nonwovens. 2016. J. Text. Ins. 1-6. doi: 10.1080/00405000.2016.1218109.
5. Lee, Y., Wadsworth, L.C.: Effects of Melt-Blowing Process Conditions on Morphological and Mechanical Properties of Polypropylene Webs. Polymer, 1992, 33 (6), 1200-1209
6. Yesil, Y., Bhat, G.S.: Structure and Mechanical Properties of Polyethylene Melt Blown Nonwovens, 2016, Int. J. Cloth. Sci. Tech. 28(6), 780-793
7. Moore, E.M., Papavassiliou, D.V., Shambaugh, R.L.: Air Velocity, Air Temperature, Fiber Vibration and Fiber Diameter Measurements on a Practical Meltblowing Die, 2004, Int. Nonwovens J., Fall, 43-53.
8. Zhao, R.: Melt Blowing Polyoxymethylene Polymer. 2005. INDA J. Nonwovens Res. Summer issue, 19-24.
9. Han, W., Wang, X. Bhat, G.S.: Structure and Air Permeability of Melt Blown Nanofiber Webs. J. Nanomater. Mol. Nanotechnol. 2013. 2:3.

# 12 OCTOBER 2018

# ORAL PRESENTATIONS

# FIBER-BASED MATERIALS: TRENDS AND OPPORTUNITIES

**Raul FANGUEIRO**

University of Minho, Portugal

Corresponding author: rfangueiro@civil.uminho.pt

## 1. INTRODUCTION

Application of fibrous materials is now not limited to merely fulfill the basic needs of human beings (clothing); they also proved as a potential material to improve other aspects and quality of human life. Huge flexibility in terms of material selection, dimensions (micro or nano), structure and properties made it possible to employ fibrous materials in many advanced areas like aerospace industries, civil engineering, transportation, architecture, sports, medical field and even for energy harvesting and storage.

## 2. ADVANCED FIBRE REINFORCED COMPOSITES

The most common form in which fibrous materials have been explored in several high end applications is their combination with various matrices as fibre reinforced composites (FRCs). FRCs are being extensively used to design light weight, high strength and durable structures. The main advantage which FRCs offer is the possibility to achieve desired properties by combining different materials or designing different structures. Multi-scale FRCs [1], which can be fabricated by combining nanomaterials (such as graphene, nanotubes and nanofibers) with conventional composites, is a new generation of multi-functional composites (light weight, high strength, tough, good thermal stability, thermally and electrically conducting, etc.) and, is a potential candidate for aerospace industries.

## 3. APPLICATIONS

### 3.1 Civil Engineering

Civil engineering is one of the major areas, where FRCs find widespread applications for building constructions, reinforcing concrete as replacement of steel rebars and for retrofitting or reinforcing civil structures to improve their resistance under severe conditions (blast, earth quake, etc.) [2]. The dream of developing smart and durable civil structures, capable of sensing their own damage with subsequent automatic repairing, is appearing to be true with the advent of self-sensing FRCs.

### 3.2 Medical

The application of fibrous materials also extended to the medical fields starting from health care garments to implantable devices. It became possible to design sutures, artificial ligaments, tendons, skin, cartilage, bone or joints, artery and heart valves using fibrous structures. Moreover, fibrous materials and structures are one of the extensively used scaffolds for tissue engineering applications.

### 3.3 Energy Harvesting and Storage

The development of highly flexible energy storage and harvesting devices seems to be possible thorough the use of fibrous structures. The possibility of developing fibrous structure based super capacitors, electrolytes, thin-film batteries and organic solar cells have already been explored and this will lead to new directions towards energy harvesting and storage.

## 4. NANO AND NATURAL FIBRES

Recently, the interest on nano dimensional fibres (nanofibres) is rapidly growing. Nanofibres are finding potential applications in diversified areas such as filtration, medical and biomedical (prostheses, wound dressing, tissue engineering, drug delivery, etc.), sensors, electrical conductors, etc. Moreover, the use of natural plant fibres (sisal, jute, flax, hemp, etc. or natural nanofibres such as cellulose, chitin, chitosan, etc.) is being highly promoted to address the sustainability and environmental issues.

## 5. CONCLUSIONS

Due to their wide variety and flexibility, fibrous materials will most possibly be the materials of the future for numerous advanced and high end applications. In this context, the Fibrous Materials Research Group (FMRG) at University of Minho is actively involved in exploring fibrous materials in the mentioned advanced areas through development of innovative materials and structures, such as braided composite rods for reinforcement and sensing, masonry reinforcing systems, multiscale composites, natural fibre composites, artificial ligaments, fibrous electrolytes and batteries, etc. The results of these various research projects will presented and discussed.

## REFERENCES

1. S.Rana, R.Alagirusamy, R.Fangueiro, M.Joshi, *J. Appl. Polym. Sci.*, **125**, 1951-1958 (2011).
2. R.Fangueiro, Fibrous and composite materials for civil engineering applications, Woodhead Publishing Ltd. (2011).

# SUSTAINABLE DYEING AND FINISHING: ULTRA-DEEP BLACK DYEING OF COTTON AND STRUCTURE-PROPERTY RELATIONSHIP OF HALOGEN-FREE FLAME RETARDANTS

**Ahmed EL-SHAFEI**

College of Textlles, North Carollina Sate Universlty, Ralelgh, NC 27606, USA

Corresponding author: ahmed_el-shafei@ncsu.edu

***Abstract:*** *In this presentation, under the umbrella of sustainability, an overview of two different research paradigms in El-Shafei's research group in the College of Textiles at North Carolina State University will be discussed. These topics span: 1)-sustainable chemical treatment of cotton for furnishing sustainable and superior dyeability of cotton using reactive dyes, while completly eliminating the need for salt and alkali coupled with over 500% increase in dye exhaustion and 300% increase in color yield compared to conventional dyeing methods, and 2)-developments of halogen-free flame retardants based on different ratios of phosphorous-nitrogen containing monomers and nubmr of grafting sites, which achieved self-extinguishing properties when graft polymerized thermally or via atmospheric plasma on cotton, polyester and polypropylene. Structure-property relationships will be discussed in details for each topic.*

***Keywords****: sustainability, dyeing, reactive dyes, flame retardancy, halogen-free flame retardancy, structure-property relationship.*

## 1. INTRODUCTION

In presence of water, cotton fabrics generate negative charges, also known as zeta potential, on the surface and these charges repel anionic dyes e.g., reactive and direct dyes. Hence, to overcome cotton's lack of affinity for reactive or direct dyes, high concentrations of electrolytes are required. Furthermore, fixation of reactive dyes on cotton also requires alkali. Cotton's lack of affinity for reactive dyes results in high amounts of unfixed dyes on the cotton surface and poor washfastness. In addition, alkali used during cotton dyeing also produces hydrolyzed dyes (unreactive). Multiple rinsing and polymeric fixing agents are employed to remove unfixed dyes and improve washfastness, respectively. The waste water from cotton dyehouse contains significant amounts of electrolytes, alkali, dye and fixing agents which are responsible for environmental pollution [1] in textile mills. A common technique of electrolyte free dyeing is graft polymerization of cationic monomers into cotton. Due to the ionic interaction between anionic dye and cationized cotton, dye exhaustion is very high which also results higher color yield and excellent color fastness properties [2-5]. 3-chloro-2-hydroxypropyltrimethylammonium chloride (CHPTAC) is one of the most popular monomer used to cationize cotton. CHPTAC requires strong alkali to form

EPTAC, which is an epoxy compound and presents occupational hazards. EPTAC reacts with cotton through a nucleophilic substitution reaction, which forms a covalent bond with cotton and cationizes it. The second disadvantage of using CHPTAC to cationize cotton is the presence of alkali during the cationization process. The alkali hydrolyzes significant amount of EPTAC and renders it inactive. The cationization process of cotton with CHPTAC is shown below in Figure 1.

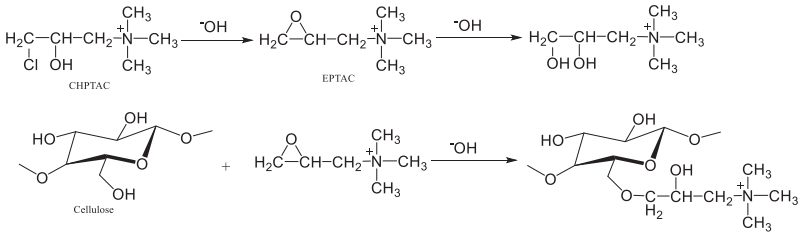


**Figure 1.** Cotton cationization using EPTAC.

Moreover, EPTAC is carcinogenic and epoxy in nature, which presents environmental hazard [6,7].

All of the aformentioned disadvantages of EPTAC can be eliminated by using our novel and sustainable chemistry, which does not require alkali to form covalent bond with cotton and does not hydrolyze.

## 2. MATERIAL AND METHOD

### 2.1. Novel and Sustainable Cationization Process

A novel and sustainable cationizaton process, proprietary, was developed and scaled up for woven cotton fabrics in the pilot plant in the College of textiles at North Carolina State University.

### 2.3. Dyeing Procedure:

Dyeing of untreated and treated cotton fabrics with our proprietary chemistry was carried out. Both untreated and treated cotton fabrics were dyed with AVITERA® BLACK SE from 2 to 6 wt.% at an increment of 0.5 wt.%. Untreated cotton fabrics were dyed following the procedure of AVITERA® BLACK SE (HUNTSMAN) 60 $^{o}$C/ 140 $^{o}$F method for dark to very deep shades. Untreated fabrics were immersed in the dyeing bath containing DI water and Glauber's salt ($Na_2SO_4$) at 27 $^{o}$C. The temperature was raised at 2.5 $^{o}$C per min to 60 $^{o}$C and dyes were added. Dyeing was continued for 40 min and soda ash was added in two installments every 20 min.

On the other hand, cotton fabrics trated with our proprietary chemistry were immersed in the dyeing bath containing only DI water at 27 $^{o}$C. The temperature

was raised at 2.5 °C per min to 60 °C and dyes were added. The dyeing cycle was completed after 2 hr with zero salt and zero alkali.

Dyed fabrics were rinsed in cold water followed by washing with a bath containing 2 g/L of nonionic detergent (Apollo Scour) in DI water at 80 °C for 10 min. Washed cotton fabrics were padded at 5 bar and 4 m/min to extract the excess water and dried at 100 °C for 5 min using Firefly conveyor oven.

### 2.4. Sustainable Flame Retardancy

Different halogen-free flame retardants based on different ratios of phosphorous-nitrogen containing monomers were developed (Figure 2) and grafted polymerized on PET, PP or cotton either thermally or using atmospheric glow discharge plasma [8-10].

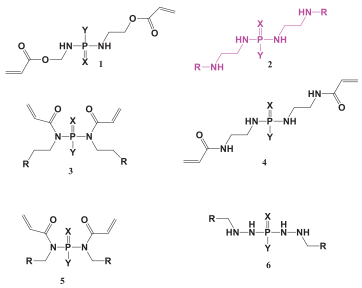

**Figure 2.** Halogen-free flame retardant monomers achieved self extinguishing properties on PET, PP and cotton.

## 3. RESULTS AND DISCUSSION

### 3.1. Sustainable Dyeing

Color yield of dyed untreated and treated cotton fabrics were compared. Figure 3 shows the color yield of untreated and treated cotton fabrics when they were dyed with AVITERA® BLACK SE.

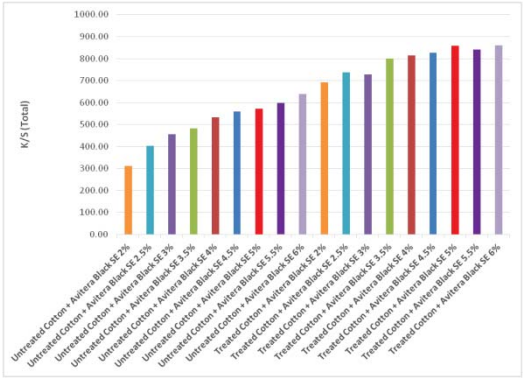


**Figure 3.** Color yield of AVITERA® BLACK SE on untreated and treated cotton fabrics.

It is evident from Figure 3 that color yield of the treated cotton fabrics is much greater than untreated cotton fabrics when dyed with AVITERA® BLACK SE. Color yield of dyed untreated and treated cotton fabrics increases with the increase of dye % shade up to 6%.

### 3.2. Sustianable Flame Retardants

Out of the six mnonomers devloped, monoers 4 and 6 showed self extiniguishing properties when graft polymerized thermally or *via* atmospheric plasma on cotton, polyester or polypropylene [8-10]. Structure-property relationship will be discussed in details.

## 4. CONCLUSION

Grafting of our proprietary chemistry into cotton completely eliminated the requirement of salt and alkali in the dyeing bath while achieving significantly high color yield with AVITERA® BLACK SE) than that of cotton fabric treated with CHPTAC. Treated cotton fabric dyed with our chemistry exhibited comparable fastness properties including crocking, washing and light when compared to dyed untreated cotton fabrics. In the case of halogen-free flame retardant monomers, the P/N ratio, % oxygen and number of grafting sites were the key in the performance of monomers for self-extinguishing properties. Monomers 4 and 6 showed self-extinguishing properties on PET and PP.

## REFERENCES


1. Bradbury, M. J., Collishaw, P. S., & Moorhouse, S. Smart rinsing: A step change in reactive dye application technology. Journal of the Society of Dyers and Colourists, 2000. 116(5), pp 144-147.
2. Cai, Y., Pailthorpe, M. T., & David, S. K. *A new method for improving the dyeability of cotton with reactive dyes. Textile Research Journal*, 1999, 69(6), pp 440-446.
3. Risti´c, N., & Risti´c, I. *Cationic modification of cotton fabrics and reactive dyeing characteristics. Journal of Engineered Fibers and Fabrics*, 2012, Vol. 7, pp 113–121.
4. Khatri, A., Peerzada, M. H., Mohsin, M., & White, M. *A review on developments in dyeing cotton fabrics with reactive dyes for reducing effluent pollution. Journal of Cleaner Production*, 2015, Vol. 87, pp 50-57.
5. Kannan, M. S. S., Gobalakrishnan, M., Kumaravel, S., Adicherala. V. T. *Influence of cationization of cotton on reactive dyeing. Journal of Textile and Apparel, Technology and Management*, 2006, 5(2), pp 23-30.
6. Hauser, P. J. and Tabba, A. H. *Improving the environmental and economic aspects of cotton dyeing using a cationised cotton. Coloration Technology*, 2001, 117 (5), pp 282-288.
7. Hebeish, A., Hashem, M., Abdel-Rahman, A.; El-Hilw, Z. *Improving easy care nonformaldehyde finishing performance using polycarboxylic acids via precationization of cotton fabric. Journal of Applied Polymer Science,* 2006, 100 (4), pp 2697-2704.
8. Brian Edwards , Stacy Rudolf , Peter Hauser and Ahmed El-Shafei*, Preparation, Polymerization, and Performance Evaluation of Halogen-Free Radiation Curable Flame Retardant Monomers for Cotton Substrates, Ind.* Eng. Chem. Res.*, 2015, 54 (2), 577–584, DOI: 10.1021/ie502915t*
9. Brian Edwards, Peter Hauser, Ahmed El-Shafei, Nonflammable Cellulosic Substrates by Application of Novel Radiation-Curable Flame Retardant Monomers Derived from Cyclotriphosphazene, *2014, Cellulose, DOI: 10.1007/s10570-014-0497-7.*
10. Stay Rudolf, Master Thesis under the direction of Ahmed El-Shafei and Peter Hauser, Durable, Self extinguishing and Halogen-free Flame Retardants for Nonwovens, 2015, NCSU library.

# BENDING PROPERTIES OF ARAMID/PHENOLIC CARBON NANOTUBE PREFORM (MWCNTs) STRUCTURES

**Kadir BİLİŞİK[1], Gulhan ERDOGAN[1], Erdal SAPANCI[2], Nesrin S. KARADUMAN[3], Sila GUNGOR[2], Gaye KAYA[4]**

[1] Erciyes University, Department of Textile Engineering, Turkey
[2] ROKETSAN Industries, Turkey
[3] Bozok University, Akdagmadeni Vocational High School, Turkey
[4] Kahramanmaras Sutcu Imam University, Department of Textile Engineering, Turkey

Corresponding author: kadirbilisik@gmail.com

***Abstract:*** *In this study, the flexural properties of nanostitched and nanoprepreg three dimensional (3D) para-aramid/phenolic composites were studied. For this reason, four types of composites were developed. They were called as stitched/nano, stitched, base/nano and base. Flexure strength and modulus of stitched/nano composites were slightly improved compared to the base composite due to addition of the stitching yarn and multiwall carbon nanotubes (MWCNTs). The flexure failure of the base and base/nano structures involved matrix peeling and large delaminated areas, whereas the stitched and stitched/nano composites had warp deformation but no visible matrix/fiber damages. In addition, the delaminated areas were severely restricted. The result showed that introducing stitching fiber and multiwall carbon nanotubes in the base structure improved its out-of-plane failure properties as a form of restricted delamination and they acted as a delamination barrier around the region. Therefore, the stitched/nano p-aramid/phenolic composites could be considered as a damage tolerance material.*

***Keywords:*** *Nano-para-aramid fiber, carbon nanotubes, PAN carbon fiber, nanoprepreg, nanostitching, bending properties*

## 1. INTRODUCTION

Fiber based material were employed in space-aerospace and industrial applications due to their high thermo-mechanical and damage tolerance properties[1-3]. However, they suffer from delamination. In order to develop a delamination free structure, Z-directional preforms were developed by three dimensional (3D) weaving[4], 3D braiding[5], and stitching techniques[6-8]. Recently, nanosphere, single wall or multiwall tubes were employed in fiber composites by dispersing the nano in the resin[9]. When nanofibers were used, they were attached, grown or grafted onto one dimensional fibers or two dimensional (2D) fabrics[10]. In another study, 3D composite was considered to have low plane properties due to Z-fiber in the thickness. The nanosphere, nanotubes or nanofibers were all randomly distributed in the fabric and they did not provide true out-of-plane reinforcement to the structure due to their discontinuous form. Fabric directional fiber ends per cm and the amount of crimp affected the flexural rigidity

of dry fabric. Multisitched layered preform showed high bending rigidity due to stitching. It decreased the inter-layer deformation in the thickness direction and was not easily formed[11].

The tensile and flexural properties of a 2D fabric composite were improved by stitching because of inter-layer stress distributions[12-13]. It was demonstrated that crack propagation in the composite was suppressed by an increase in stitching density[14]. However, several experimental studies showed that the flexural strength of stitched E-glass composite was decreased due to stress concentration[15-16]. The flexural strength in unstitched E-glass/polyester composite was influenced by yarn orientation, composite fiber volume fraction and preform packing density. It showed mode-I delamination as a form of inter-layer opening[17]. A fiber distortion model was proposed to overcome heterogeneous fiber volume fraction throughout the composite due to stitching which affected fiber misalignment during the stitching process[18]. Stitching fiber did not affect the stiffness of the stitched composite[19]. However, stitching caused weak resin-rich regions near the stitching loop section and affected the damage initiation force[20-22]. It was claimed that the flexural strength and modulus of 3D multiaxis composite were only slightly lower than that of the 3D composite because of the bias fibers[23-24].

In single wall carbon nanotubes (SWCNTs) and multiwall carbon nanotubes (MWCNTs), sampling, size, surface area/volume, density, crystallinity and purity are considered important material parameters[25-30]. The modulus of the nanocomposite decreased because of agglomeration during the consolidation process[31]. Therefore, MWCNTs were functionalized by using silanization to prevent early stage clustering and it was proven that the functionalization improved homogeneous dispersion of the nanoparticle[32-33]. Another study showed that the thermo-mechanic properties of the nanocomposite were enhanced by grafting silane to the CNT due to improved inter-layer bonding and even dispersion of the nanotubes[34-35]. In another study, amine coated SWCNTs improved the fatigue properties of the carbon/epoxy composite[36]. In addition, the inter-layer properties of E-glass composite increased with the use of coated nanotubes[37]. A carboxyl-functionalized MWCNTs (0.1-0.4%)/epoxy nanocomposite was made and it was demonstrated that its flexural properties were improved compared to those of the epoxy composite[38]. Multiscale composites improved the flexural properties of the neat composites. This was because of a better interphase between the amino coated nano particle and the resin which enhanced the load transfer mechanisms. However, it was found that the presence of minor clustering adversely influenced the load-carrying mechanism[39]. It was claimed that a naphthalene diimide and poly(dimethylsiloxane) based dispersant was synthesized to enhance the agglomeration of the SWCNTs in the matrix.[40] It was reported that the bending modulus of binary nanocomposite showed about a one-third improvement compared to the neat composite[41]. In addition, the carbon fiber surface characteristics on the bending properties of the composite were also found to be significant[42]. It was reported that nano silicon carbide affected the material

modulus but its homogeneous dispersion with the coupling agent influenced the material's strength[43]. However, the tensile strength of the E-glass composite was reduced by increasing the amount of nano silicon carbide because of the interface characteristic of the nano-resin region which caused stress concentration[44]. Another study showed that the tensile strength-modulus of E-glass/polyester was improved by increasing the amount of nanosilica[45-46]. Also, multistitching and nanosilica in E-glass composite led to an improvement in the damage resistance[45-46]. Multiwall carbon nanofibers (MWCNFs) were vertically grown on the fiber or fabric surface with chemical deposition using ethyne ($C_2H_2$) and the catalyst iron dichloride ($FeCl_2$)[47]. Spun yarn of MWCNFs (1 mm length, 50 nm diameter) was drawn from an MWCNT array by using the dry-spinning technique[48]. The MWCNF spun yarn was pultruded as a 7-ply cord/epoxy rod. It was noted that the spun nanocarbon fiber based pultruded epoxy rod had better tensile strength and modulus compared to the base epoxy, and the dominant failure mode was nanofiber breakages[49]. Hollow halloysite nanotubes (HNT, nanoclays) were employed as nanocontainer for the protection of the cellulosic materials.[50] In addition, the natural wax/HNT nano composite was introduced to repair the cellulosic archaeological materials.[51] It was also claimed that renewable polymer/HNTs composite film was made for barrier and delivery applications.[52]

A few studies were carried out on nano added stitched structures. The research was concentrated on the flexural properties of the p-aramid/phenolic composite which was developed by nano particle and multistitching. The objective of this study was to develop nanostitched and nanoprepreg p-aramid/phenolic carbon nanotube (MWCNTs) composites and to examine the flexural properties of these structures.

## 2. MATERIALS AND METHODS

### 2.1. 3D p-aramid/phenolic nanopreform and nanocomposite

Para-aramid Twaron® plain (1/1) fabric (CT 747, Teijin, JP) and basket (2/2) fabric (CT736, Teijin, JP) were employed to make the multi-stitched 3D nanopreform. The p-aramid fabric specification is provided in Table 1. P-aramid fabric was formed from 336 tex fiber for plain (1/1) weave and 168 tex fiber for basket (2/2) weave. The warp and filling densities of the plain (1/1) and basket (2/2) p-aramid fabrics were 62.5 ends per 10 cm and 127 ends per 10 cm, respectively. The p-aramid fabric unit area weight and thickness were 410 g/m$^2$ and 0.62 mm for both fabrics, respectively. The directional interlacements of the plain (1/1) and basket (2/2) fabrics are schematically represented in Fig. 1. The number of interlacements in the plain and basket fabrics was 56 and 24, respectively, and their placements in the fabrics were homogeneously distributed. The multiwall carbon nanotubes (MWCNTs, Nanothinx, GR) were selected based on better thermo-mechanical properties and commercial availability. The average sizes of MWCNTs varied from 15-35 nm in diameter, 10 μm in length and 1-2 nm in wall

thickness. The tensile strength and modulus of the MWCNTs were 200 GPa and 1 TPa, respectively, as shown in Table 2.

**Table 1.** Specifications of p-aramid fabric structures.

| Fabric label | Weave type | Fabric treatment | Yarn linear density (tex) | | Fabric density (per 10 cm) | | Fabric area weight ($g/m^2$) | Yarn crimp (%) | | Fabric thickness (mm) |
|---|---|---|---|---|---|---|---|---|---|---|
| | | | Warp | Weft | Warp | Weft | | Warp | Weft | |
| Twaron CT® 747 | Plain (1/1) | Water repellent | 336 | 336 | 62.50 | 62.50 | 410 | 5.80 | 5.90 | 0.62 |
| Twaron CT® 736 | Basket (2/2) | Water repellent | 168 | 168 | 127 | 127 | 410 | 9.40 | 11.30 | 0.62 |

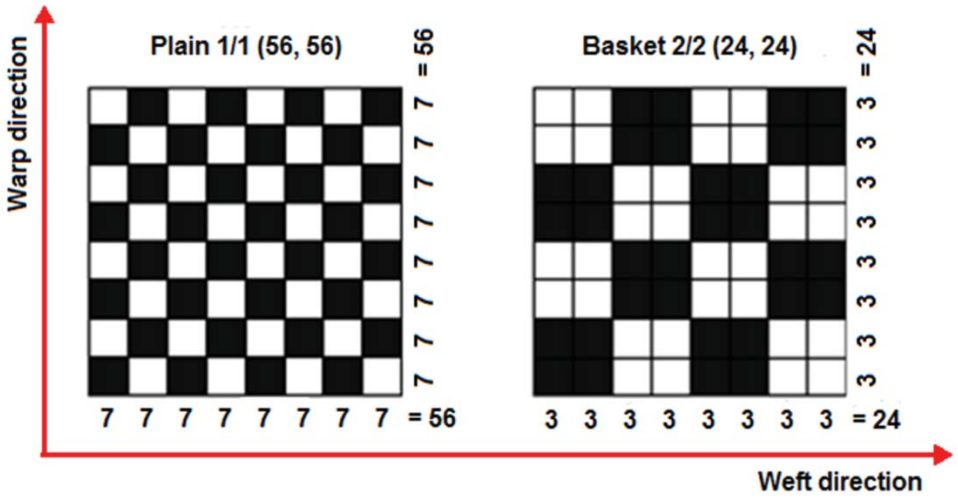


**Figure 1.** Schematic views of interlacement placement in the p-aramid fabrics (plain 1/1, basket 2/2 weaves) and number of yarn interlacements in each fabric direction.

**Table 2.** Specifications of multiwall carbon nanotubes (MWCNTs)[25,53].

| Nanomaterial | Particle dimensions (diameter x length x wall thickness) (nm x micron x nm) | Surface area ($m^2/g$) | Purity (%) | Density ($g/cm^3$) | Tensile strength (GPa) | Tensile modulus (TPa) | Melting temperature (°C) |
|---|---|---|---|---|---|---|---|
| Carbon nanotubes (MWCNTs, Nanothinx,GR) | 15-35 x 10≥ x 1-2≥ | >100 | ≥97 | 1.74 | 200 | 1.0 | 3550 |

Principally, four types of p-aramid structures were developed. These were 1) base (TPU, TBU), in that TPU was a six layer $[(0°/90°)]_6$ p-aramid plain (1/1) woven, whereas TBU was a six layer p-aramid basket (2/2) woven fabric; 2) stitched (TP-CS, TP-TS, TB-CS, TB-TS), in that TP-CS and TP-TS were six layer p-aramid plain (1/1) woven, one-directionally PAN carbon and p-aramid Twaron CT stitched in the warp (0˚), respectively, whereas TB-CS and TB-TS were six layer basket (2/2) woven, one-directionally carbon and Twaron CT stitched in the warp (0˚) structures, respectively; 3) base/nano (TPU-N, TBU-N) in that TPU-N and TBU-N were six layer p-aramid plain (1/1) and basket (2/2) woven with added MWCNTs, respectively; and 4) stitched/nano (TP-CS-N, TP-TS-N, TB-CS-N, TB-TS-N). When the MWCNTs were added to all the stitched structures which are described above, they were considered as stitched/nano structures. One-directional stitching was manually made on the layered woven structures using the PAN carbon and p-aramid Twaron CT stitching yarns as shown in Fig. 2(a-b). The stitching fiber properties are also provided in Table 3.

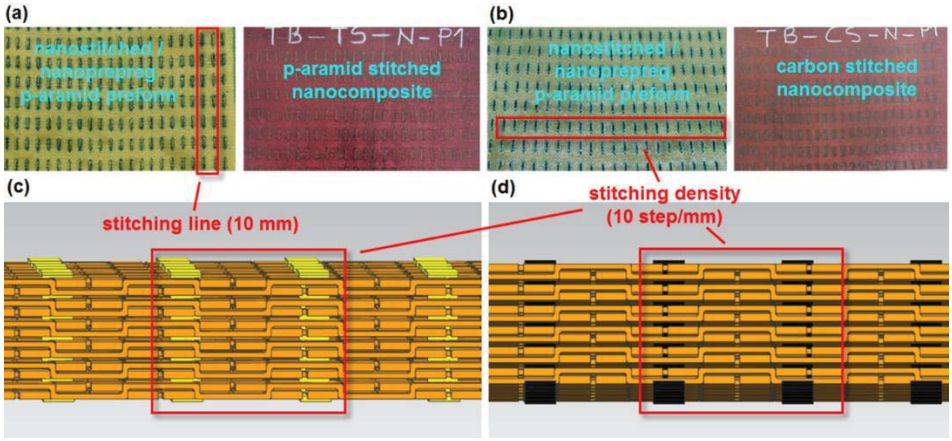


**Figure 2.** (a) Para-aramid Twaron CT multistitched 3D nanoprepreg preform (left) and p-aramid/phenolic MWCNT composite (right) (TB-TS-N); (b) PAN carbon multistitched 3D nanoprepreg preform (left) and p-aramid/phenolic MWCNT composite (right) (TB-CS-N); (c) schematic view of p-aramid stitched p-aramid structure (TB-TS); (d) schematic view of carbon stitched p-aramid structure (TB-CS).

**Table 3.** Specifications of untwisted stitching yarns

| Fiber type | Fiber diameter (μm) | Fiber density (g/cm³) | Tensile strength (GPa) | Tensile modulus (GPa) | Elongation at break (%) | Yarn linear density (dtex) |
|---|---|---|---|---|---|---|
| Twaron CT (Para-aramid fiber, Teijin, JP) | 12 | 1.45 | 3.2 | 115 | 2.9 | 3360 |
| Polyacrylonitrile (PAN) Carbon (Carbon fiber, Aksaca, TR) | 6 | 1.78 | 4.2 | 240 | 1.8 | 6 K[1] |

K[1]: 1000 filaments in the untwisted fiber TOW.

Stitched/nano multilayer p-aramid woven preforms were consolidated to make stitched/nano p-aramid composites. Figs. 3 and 4 show the processing steps for one-directionally stitched p-aramid/phenolic and stitched/nano p-aramid/phenolic composites, respectively. Initially, phenolic resin (Araldite EPN 1138, Biesterfeld Spezialchemie GmbH, DE) was put into a vacuum chamber (Metyx composites, TR) to vacuum under 0.1 MPa pressure (1 bar) for 35 minutes to remove any air bubbles. Then, the MWCNTs (0.03125, %wt.,) were added to the phenolic resin. In order to conduct pre-mixing to prevent possible heterogeneous dispersion and early agglomeration, they were stirred by a magnetic mixer (Wisestir ®, Witeg, DE) at 240 rpm for 15 minutes. Immediately after this, the phenolic/carbon nanotube solution was mixed in an ultrasonic bath (200 watt, 40 KHz, DAIHAN/WiseClean®, WUC-A03H, KR) at 25˚C for 60 minutes. In this way, a highly homogenized phenolic/nano mixture was obtained. This was further stirred by a magnetic mixer at 240 rpm for about 15 minutes to improve the homogenization and agglomeration of the mixture. After that, it was again put into a vacuum chamber to vacuum under 0.1 MPa pressure for 5 minutes to remove any remaining air bubbles. At the same time, plain (1/1) and basket (2/2) p-aramid woven fabrics, polyacrylonitrile (PAN) carbon fiber (6 K, Aksaca, TR) and para-aramid Twaron CT (3360 dtex, Teijin, JP) yarn were prepared to make the flexure test plates. We first of all made the p-aramid/phenolic carbon nanotube prepreg fabrics and yarns, and then they were consolidated for the composite.

The para-aramid fabric was heated at 40˚ C for 60 minutes to evaporate the moisture. Next, the matrix was applied to the p-aramid fabric by the hand layup method under atmospheric conditions. The resulting fabric was then put onto the shelf of an oven (Binder, DE) to pre-cure at 110 ˚C for 7 minutes in order to obtain the prepreg nanopara-aramid fabric. The same procedure was applied to the carbon and para-aramid stitching yarns to make prepreg yarns. The prepreg nanop-aramid fabric was layered as a $[0^{\circ}/90^{\circ}]_6$ sequence. The six layered prepreg nanop-aramid preform was manually stitched by carbon or p-aramid nano stitching yarn using an in-house developed apparatus to make the stitched/nano composite. The density of stitching was 1 step per cm. The space between the neighboring stitching lines was 1 cm. The stitched prepreg p-aramid/phenolic carbon nanotube preform was put in a mold, and the mold was then wrapped with Teflon film (FDM 2100, DuPont, USA) to prevent thermal shock and easy demolding after curing. The mold was cured using a hot press (Climax, TR) under 0.6 MPa pressure (6 bars) and at 170 ˚C for 120 minutes. Lastly, the mold was left in the press to cool until the temperature was gradually decreased to 40 ˚C and the stitched p-aramid/phenolic carbon nanotube composite was then removed from the mold. Some of the composites are shown in Fig. 2 (a-b).

The densities of the stitched/nano carbon composites were found by ASTM D792-91[54]. It was designated to find the density ($g/cm^3$) as the sample mass in air was divided by its volume, whereas relative density was ratio of sample density divided by water density. The composite volume fraction and void content were obtained by ASTM D3171-99[55] and ASTM D2734-91[56], respectively. In the determination of the composite fiber volume fraction, after known the sample

mass and density, the furnace was heated up to 400°C. Then, the composite sample was kept almost 5.5 hours to remove the burned matrix. The remaining residue which contains the p-aramid fiber in the fabric, was then cooled and weighed. The weight percent of the fiber in the composite was then calculated. In addition, the void content was also calculated by known parameters such as matrix and composite densities. After the flexure test, the delaminated areas and damaged surfaces of the composite sample were analyzed by an optical microscope (Olympus SZ61, JP equipped with Bs200DOC digital image analysis software-Bs200DOC, TR).

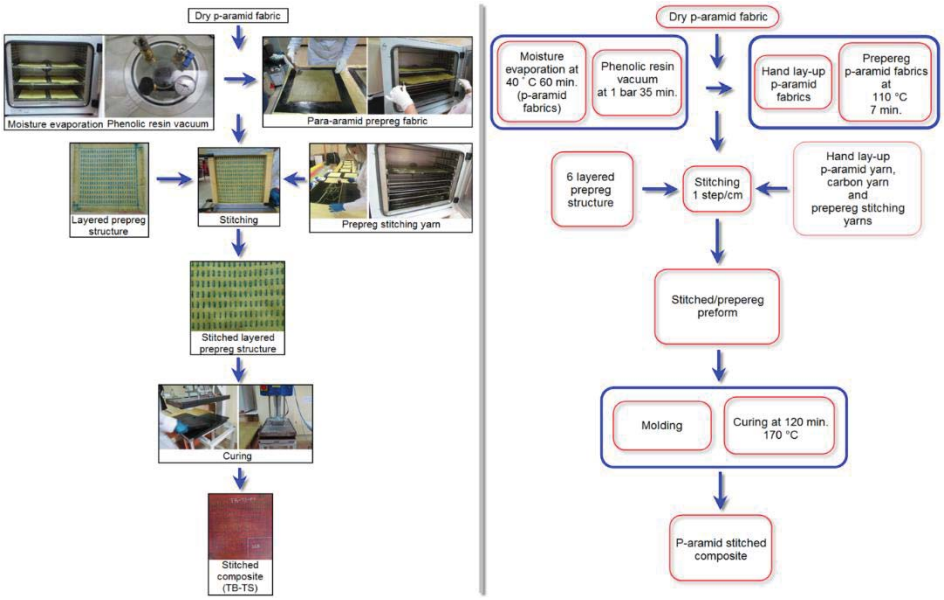


**Figure 3.** Processing steps of one-directionally stitched multilayered p-aramid/phenolic woven prepreg preforms and composites (TB-TS)

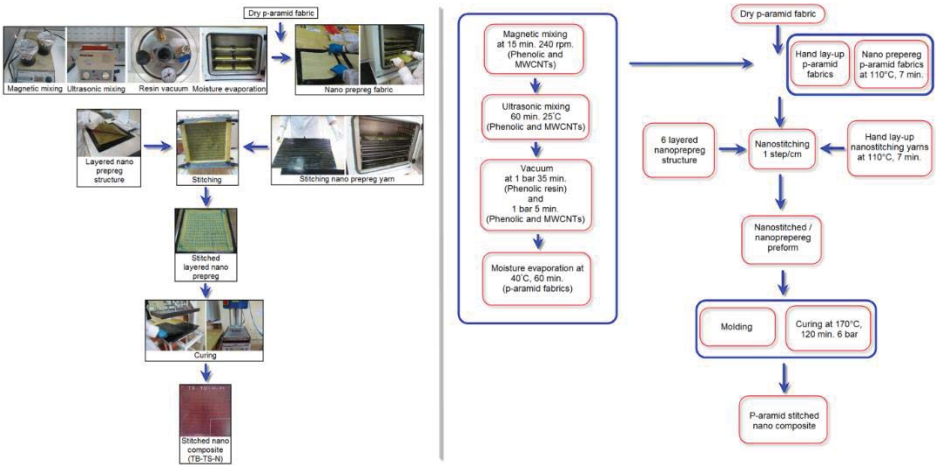


**Figure 4.** Processing steps of one-directionally stitched multilayered p-aramid/phenolic/carbon nanotube woven prepreg preforms and composites (TB-TS-N)

## 2.2. Flexural test

The three point flexural test of all composites was carried out on a Shimadzu AG-XD 50 (Japan) tester equipped with Trapezium® software with a 5kN loading cell based on ASTM D790-10[57]. The bending testing speed was 1.3653 mm/min. The test dimensions of the sample were 12.7 (width) × 130 (length) mm. The L/d (support span length/thickness) ratio was 32/1. The flexural load applied to each sample was the warp (0˚, lengthwise). Fig. 5 shows the bending test instrument and fixture with samples. Equations (1-3) for the flexural strength, modulus and strain are presented below, respectively[57]. The flexural test was conducted at the standard laboratory atmosphere having a temperature of 23˚C±2˚C and a relative humidity of 50%±10%. After the bending load was applied to the samples, they were examined by an optical microscope (Olympus SZ61, Japan).

$$\sigma_f = \frac{3PL}{2bd^2} \tag{1}$$

$$E_B = \frac{L^3 m}{4bd^3} \tag{2}$$

$$\varepsilon_f = \frac{6Dd}{L^2} \tag{3}$$

where $\sigma_f$ is the flexural strength in the outer fibers at midspan (MPa); $P$ is the load at a given point on the load-deflection curve (N); $L$ is the support span (mm); $b$ is the width of the beam tested (mm); $d$ is the depth of the beam tested (mm); $E_B$ is

the modulus of elasticity in bending (GPa); *m* is the slope of the tangent to the initial straight-line portion of the load-deflection curve; $\varepsilon_f$ is the bending strain (%); *D* is the maximum displacement of the center of the beam (mm).

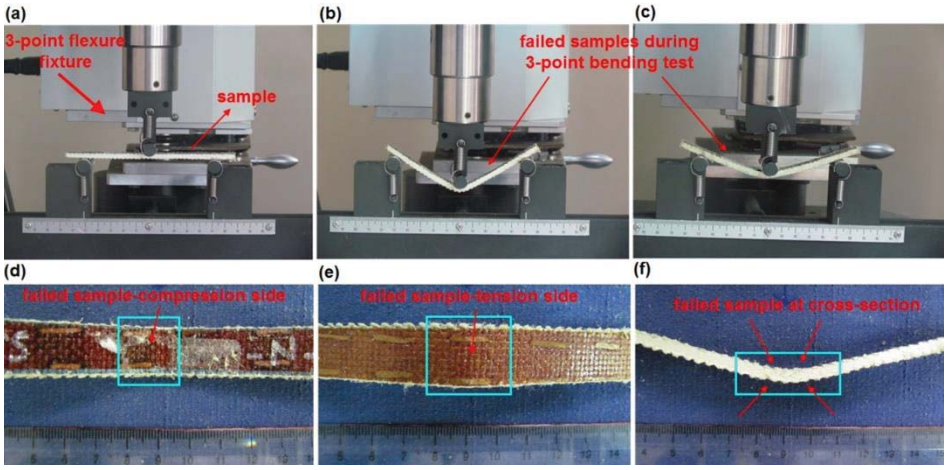


**Figure 5.** (a) Tensile tester with flexural fixture with sample at initial state; (b) base/nano sample during bending load application (TBU-N); (c) stitched/nano sample during bending load application (TB-TS-N); (d) compression side failed stitched/nano sample (TB-TS-N); (e) tension side failed stitched/nano sample (TB-TS-N); (f) failed stitched/nano sample at cross-sections (TB-TS-N, digital image)

## 3. RESULTS AND DISCUSSION

### 3.1. Density and fiber volume fraction results

The density and fiber volume fraction results of the base (TPU, TBU), stitched (TP-CS, TP-TS, TB-CS, TB-TS), base/nano (TPU-N, TBU-N) and stitched/nano (TP-CS-N, TP-TS-N, TB-CS-N, TB-TS-N) composites were evaluated. The densities of the developed structures varied from 1.30-1.33 g/cm$^3$ and the average density was 1.32 g/cm$^3$. The density differences in the structures were considered to be negligible (1%). The measured total fiber weight fractions ($V_{tfw}$) of all structures varied from 67.10-73.81% and the average total fiber weight fraction was 69.84%. The volume fraction differences between the structures were around 4-6% due to the stitching yarn weight fraction and MWCNT addition as well as to a minor stitching effect on the preforms. The measured stitching fiber weight fractions ($V_{sfw}$) of all stitched and stitched/nano structures varied from 1.47-2.13% and the average stitching fiber weight fraction was 1.81%. The void contents (weight base, $V_c$) of all structures varied from 0.71-1.83% (average 1.26%). These results were considered assuming that all structures were made in defect free processing conditions from preform preparation to consolidation.

On the other hand, the MWCNT addition and dispersion in the phenolic were analyzed during processing. We started by selecting a 0.5% (weight%) ratio for

the MWCNTs as an initial condition. Afterwards, a large agglomeration (about 200-300 microns) of nanotubes was found in the phenolic. Extensive studies were conducted to reduce the size of the agglomeration of the nanotubes. For this reason, we decreased the MNCNT ratio to 0.03125% and increased the stirring time from 60 minutes to 120 minutes in ultrasonic mixing. Therefore, the size of the agglomeration of carbon nanotubes decreased to 30-80 microns in the phenolic, as shown in Fig. 6(a). The MWCNT added phenolic was applied to the sample stitching yarn and fabric. The MWCNTs were evenly dispersed in the filament direction and intra-filament regions of the stitching yarn and in the principal directions and yarn crossing regions of the fabric, as shown in Fig. 6(b) and (c), respectively. Fig. 6(d) shows the MWCNTs distribution in the filaments of the fractured nanostitched yarn in the stitched/nano composite

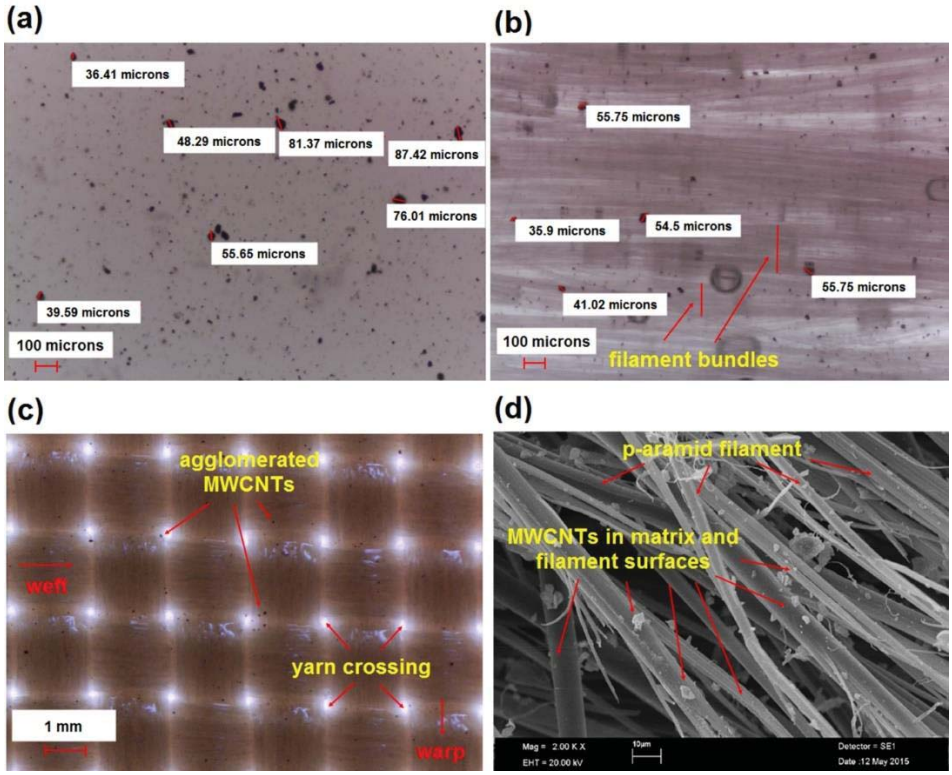


**Figure 6.** (a) MWCNT dispersion in phenolic resin; (b) phenolic/MWCNT treated uncured nanoyarn; (c) phenolic/MWCNT treated uncured nanofabric surface; (d) fractured nanostitched yarn in stitched/nano composite (TB-TS-N) (Optic photos, magnification x40, x40, x10, respectively; SEM, magnification x2000).[58]

### 3.2. Flexural results

The flexure test results of the base (TPU, TBU), stitched (TP-CS, TP-TS, TB-CS, TB-TS), base/nano (TPU-N, TBU-N) and stitched/nano (TP-CS-N, TP-TS-N, TB-

CS-N, TB-TS-N) composites are given in Table 4. The data presented in Table 4 are the average values of flexure strength, strain and modulus for each composite. Although we claimed that all structure were produced without defect, they probably microscopically involved a kind of nonlinearities at stitching piercing region of the nanoprepreg preform especially in the out-of-plane direction, heterogeneous distribution of the MWCNTs in the preform surface and intra-layer sections, and minor agglomeration of the MWCNTs in the matrix and fabric interlacement regions. Therefore, these partly affect to get reproducible data from the flexural test. The flexural test results in Table 4 also include the standard deviation (s) and the coefficient of variation (CV%) where the CVs of the flexural strength and modulus varied 1.77-9.41% and 1.80-17.12%, respectively. Fig. 7 shows the tensile stress-strain curves of some of the basket (2/2) fabric based composites. In Fig. 7, the stress-strain curves of the basket p-aramid/phenolic structure are presented together with its base, nano, carbon and para-aramid stitched, and stitched/nano forms. The p-aramid stitched and stitched/nano structures showed higher flexural strength values compared to the base and base/nano structures. In addition, the stress-strain curves almost follow the same line beginning from the initial state in the elastic region to the failure points which did not sharply drop.

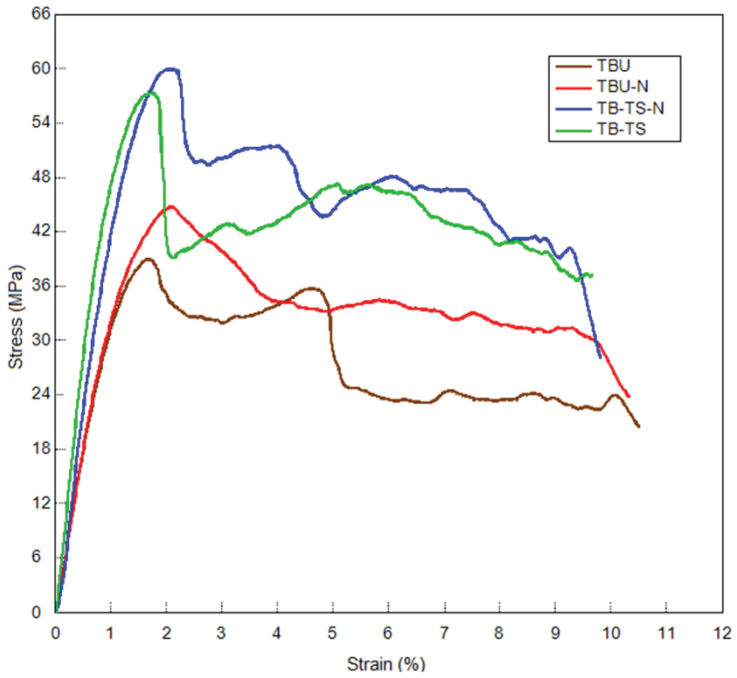


**Figure 7.** Stress-strain curves from flexure test for some of the multistitched carbon/epoxy MCNTs composites (base TBU; base/nano TBU-N, stitched TB-TS; stitched/nano TB-TS-N)

**Table 4.** Average flexural test results of various developed p-aramid/phenolic MWCNT composites

| Label | Flexural load (Max.) (N) | Flexural displacement (mm) | Flexural strain (%) | Flexural strength (MPa) | Flexural modulus (GPa) |
|---|---|---|---|---|---|
| **TPU** | 64.43 | 8.73 | 2.09 | 40.51 (s=1.98, CV%=4.89) | 3.64 (s=0.07, CV%=1.80) |
| **TBU** | 57.90 | 7.81 | 1.84 | 39.01 (s=0.69, CV%=1.77) | 3.44 (s=0.18, CV%=5.11) |
| **TP-CS** | 56.18 | 6.81 | 1.59 | 38.91 (s=3.28, CV%=8.42) | 4.21 (s=0.36, CV%=8.58) |
| **TP-TS** | 53.87 | 7.73 | 1.75 | 42.78 (s=3.15, CV%=7.35) | 4.16 (s=0.71, CV%=17.12) |
| **TB-CS** | 79.59 | 9.04 | 2.01 | 57.24 (s=3.77, CV%=6.58) | 4.90 (s=0.44, CV%=8.92) |
| **TB-TS** | 61.57 | 8.36 | 1.80 | 57.73 (s=2.53, CV%=4.38) | 5.25 (s=0.83, CV%=15.89) |
| **TPU-N** | 64.11 | 9.43 | 2.13 | 46.12 (s=1.62, CV%=3.51) | 3.86 (s=0.34, CV%=8.70) |
| **TBU-N** | 61.69 | 9.92 | 2.23 | 45.37 (s=2.83, CV%=6.24) | 3.72 (s=0.11, CV%=2.98) |
| **TP-CS-N** | 56.59 | 7.78 | 1.78 | 40.59 (s=3.82, CV%=9.41) | 3.79 (s=0.15, CV%=3.95) |
| **TP-TS-N** | 55.65 | 8.44 | 2.03 | 35.45 (s=3.11, CV%=8.76) | 2.85 (s=0.42, CV%=14.69) |
| **TB-CS-N** | 66.40 | 8.28 | 1.94 | 45.30 (s=2.82, CV%=6.21) | 3.65 (s=0.52, CV%=14.35) |
| **TB-TS-N** | 75.54 | 9.29 | 2.02 | 60.45 (s=2.78, CV%=4.60) | 4.87 (s=0.38, CV%=7.85) |

"s" represents the standard deviation and "CV%" represents the coefficient of variation.

### 3.3. Flexural strength

Fig. 8 shows the average flexural strength values of all the developed p-aramid/phenolic MWCNT composites. As shown in Fig. 8 and Table 4, the flexural strength of the base (TBU and TPU) composites varied between 39.01-40.51 MPa, whereas the flexural strength of the base/nano (TBU-N and TPU-N) composites varied between 45.37-46.12 MPa. The flexural strength of the stitched (TP-CS, TP-TS, TB-CS and TB-TS) composites varied between 38.91-57.73 MPa, whereas the flexural strength of the stitched/nano (TP-CS-N, TP-TS-N, TB-CS-N and TB-TS-N) composites varied between 35.45-60.45 MPa. The bending strength of the p-aramid stitched/nano basket 2/2 (TB-TS-N) composite was 4.50% higher for stitched (TB-TS) and 35.47% for base (TBU) composites, whereas the flexural strength of the PAN carbon stitched/nano basket 2/2 (TB-CS-N) was 20.86 % lower for stitched (TB-CS) and 13.89 % higher for base (TBU) composites. The p-aramid nanostitched composite (TB-TS-N) showed better

performance (25.06%) compared to the PAN carbon nanostitched one (CT-CS-N), whereas the p-aramid stitched structure (CT-TS) demonstrated only a slightly better performance (0.90%) compared to the stitched (CT-CS) composite. In addition, the flexural strength of the base/nano (TBU-N) composite was 14.02% higher than that of the base (TBU) composite. It was realized that stitching and the addition of MWCNTs slightly increased the bending strength of all the stitched and stitched/nano composites. The stitching fiber type also slightly affects the flexural strength of the stitched and stitched/nano composites. Also, we obtained a similar result from the p-aramid plain 1/1 composites.

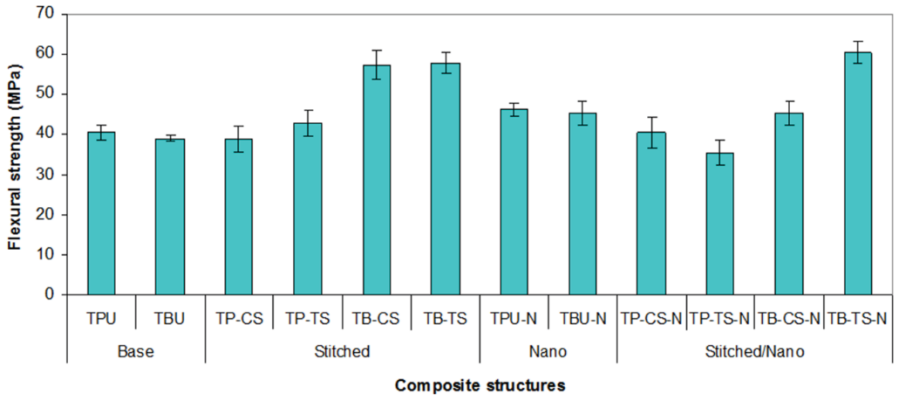


**Figure 8.** Flexural strength of various developed p-aramid/phenolic MWCNT composites

### 3.4. Flexural strain

Fig. 9 shows the average flexural strain of all the developed p-aramid/phenolic MWCNT structures. In Fig. 9 and Table 4, the flexure strain of the base (TBU and TPU) composites varied between 1.84-2.09%, whereas the flexure strain of the base/nano (TBU-N and TPU-N) composites varied between 2.13-2.23%. The flexure strain of the stitched (TP-CS, TP-TS, TB-CS and TB-TS) composites varied between 1.59-2.01%, whereas the flexure strain of the stitched/nano (TP-CS-N, TP-TS-N, TB-CS-N and TB-TS-N) composites varied between 1.78-2.03%. The flexure strain of the p-aramid stitched/nano basket 2/2 (TB-TS-N) composite was 10.90% higher than for the stitched (TB-TS) and 8.91% higher than for the base (TBU) composites, whereas the flexure strain of the PAN carbon stitched/nano basket 2/2 (TB-CS-N) was 3.48% lower than for the stitched (TB-CS) and 5.15% higher than for the base (TBU) composites. The p-aramid nanostitched structure (TB-TS-N) showed better performance (3.96%) compared to the PAN carbon nanostitched composite (TB-CS-N), whereas the p-aramid stitched structure (TB-CS) demonstrated better performance (10.44%) compared to the stitched (TB-TS) structure. In addition, the flexure strain of the base/nano (TBU-N) composite was 17.49% higher than that of the base (TBU) composite. It was realized that stitching and the addition of MWCNTs only slightly increased

the bending strain of all the stitched and stitched/nano composites. The stitching fiber type also slightly affects the bending strain of the stitched and stitched/nano composites. On the other hand, we did not obtain a consistent result from any the p-aramid plain 1/1 composites.

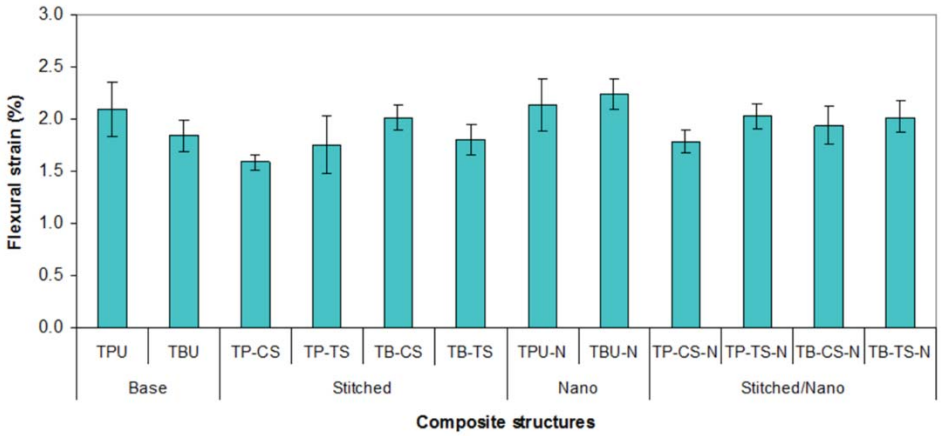


**Figure 9.** Flexure strains of various developed p-aramid/phenolic MWCNT composites

### 3.5. Flexural modulus

Fig. 10 shows the average flexural modulus values of all the developed p-aramid/phenolic MWCNT structures. In Fig. 10 and Table 4, the flexural modulus of the base (TBU and TPU) composites varied between 3.44-3.64 GPa, whereas the flexural modulus of the base/nano (TBU-N and TPU-N) composites varied between 3.72-3.86 GPa. The flexural modulus of the stitched (TP-CS, TP-TS, TB-CS and TB-TS) composites varied between 4.16-5.25 GPa, whereas the flexural modulus of the stitched/nano (TP-CS-N, TP-TS-N, TB-CS-N and TB-TS-N) composites varied between 2.85-4.87 GPa. The flexural modulus of the p-aramid stitched/nano basket 2/2 (TB-TS-N) composite was slightly (7.24%) lower than for the stitched (TB-TS) composite and 29.36% higher than for the base (TBU) composite, whereas the flexural modulus of the PAN carbon stitched/nano basket 2/2 (TB-CS-N) was 25.51% lower than for the stitched (TB-CS) composite and 5.75% higher than for the base (TBU) composite. The p-aramid nanostitched structure (TB-TS-N) showed better performance (25.05%) compared to the PAN carbon nanostitched composites (CT-CS-N), whereas the p-aramid stitched structure (TB-TS) demonstrated slightly better performance (6.67%) compared to the stitched (TB-CS) composite. In addition, the flexural modulus of the base/nano (TBU-N) composite was 7.53% higher than that of the base (TBU) composite. It was found that stitching and the addition of MWCNTs slightly affected the bending modulus of all the stitched and stitched/nano composites. The bending modulus was also somewhat affected by the stitching yarn type. In

contrast, we did not obtain a consistent result from any of the p-aramid plain 1/1 structures.

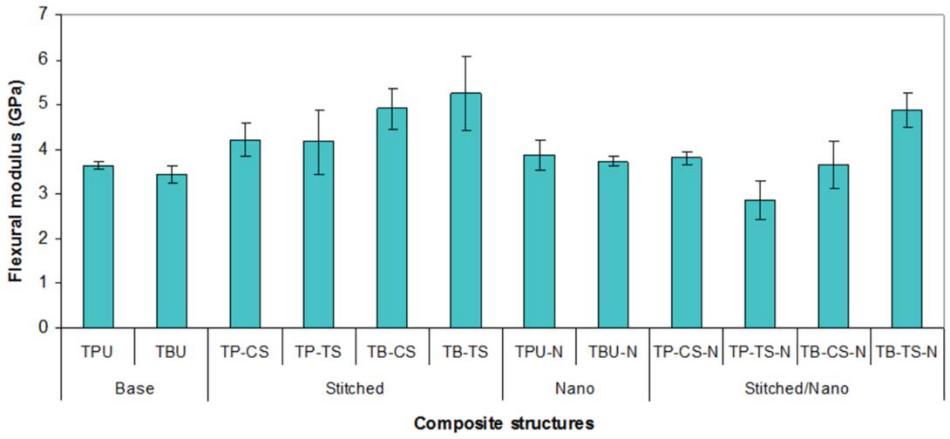


**Figure 10.** Flexure modulus of various developed p-aramid/phenolic MWCNT composites

### 3.6. Failure after flexural test results

The flexure failure of some base (TBU), base/nano (TBU-N), stitched (TB-TS) and stitched /nano (TB-TS-N and TB-CS-N) composites are presented in Figs. 11-13. The damaged areas created by bending load for each sample were barely visible. Therefore, we did not measure the damaged areas. Some of the bending failures of the base (TBU) and base/nano (TBU-N) composites are shown in Fig. 11 (a-f). The tension side of the base (TBU) and base/nano (TBU-N) structures had outward lateral multiple warp directional bending and local matrix peeling but no visible fiber breakage was observed (Fig. 11(c and f)). The compression side of the base (TBU) and base/nano (TBU-N) structure had inward warp directional bending and lateral matrix peeling but no visible fiber failure was observed (Fig. 11 (a and d)). In the cross-section of the TBU, a delaminated layer near the top surface was observed, whereas various local angular delaminated areas near the mid-surface line were found (Fig. 11 (b and e)).

Some of the bending failures of stitched (TB-TS) and stitched/nano (TB-TS-N) composites are shown in Fig. 12 (a-f). The tension side of the stitched (TB-TS) and stitched/nano (TB-TS-N) structures had outward lateral deformation on the warp but no visible matrix/fiber damage was observed (Fig. 12(c and f)). The compression side of the stitched (TB-TS) and stitched/nano (TB-TS-N) structure had an inwardly dented area around the stitching lines but no matrix/fiber damage was identified (Fig. 12 (a and d)). In the cross-section of the TB-TS composite, minor delaminated layers around the mid-plane of the structure were observed. Some local angular delaminated areas between the mid-plane line and top surface were found (Fig. 12 (b and e)). The results of bending failure showed that

all the developed p-aramid/phenolic structures were flexible and we did not find any brittle fiber breakages. Stitching and MWCNT addition to the base structure made it a delamination restricted material.

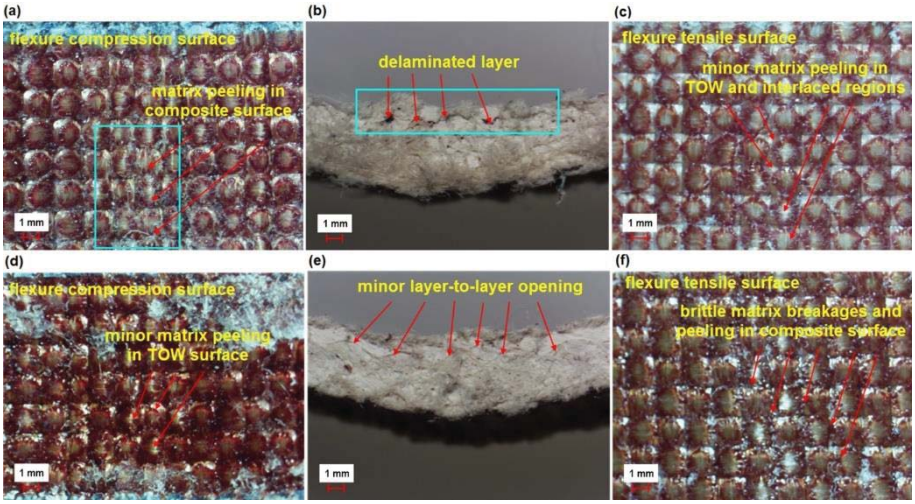


**Figure 11.** Warp directional flexure failure in various multistitched 3D p-aramid/phenolic MWCNT composites. (a) base top face (TBU); (b) base cross-section (TBU); (c) base bottom face (TBU); (d) base/nano top face (TBU-N); (e) base/nano cross-section (TBU-N) and (f) base/nano bottom face (TBU-N) (optical microscope, magnification x6.7)

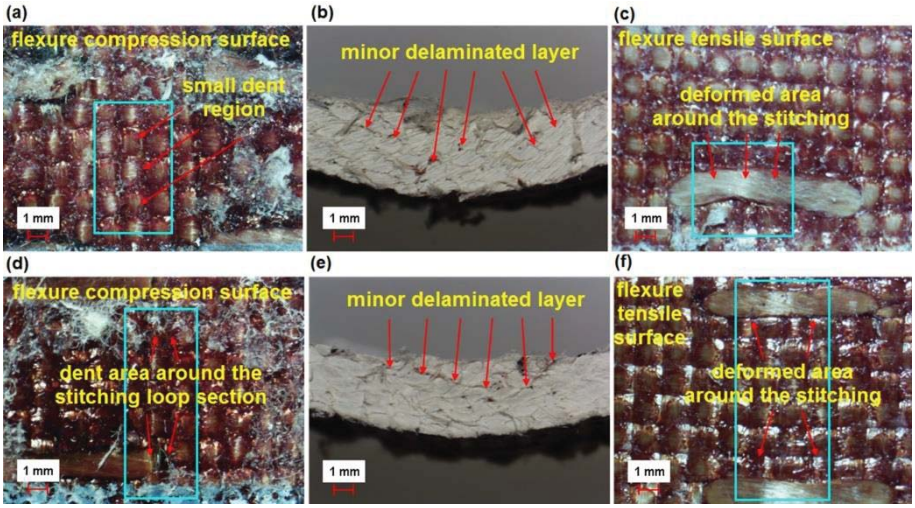


**Figure 12.** Warp directional flexure failure in various multistitched 3D p-aramid/phenolic MWCNT composites. (a) Stitched top face (TB-TS); (b) stitched cross-section (TB-TS); (c) stitched bottom face (TB-TS); (d) stitched/nano top face (TB-TS-N); (e) stitched/nano cross-section (TB-TS-N) and (f) stitched/nano bottom face (TB-TS-N) (optical microscope, magnification x6.7).

One of the bending failures of the PAN carbon stitched/nano (TB-CS-N) composite is shown in Fig. 13 (a-c). The tension side of the stitched/nano structure had a deformed area around strained stitching line (Fig. 13 (c)).

However, the compression side of the TB-CS-N had a dented area around the stitching step (Fig. 13 (a)). In the cross-section, a minor delaminated area was restricted by stitching where the stitched fiber acted as a delamination barrier around the region (Fig. 13 (b)).

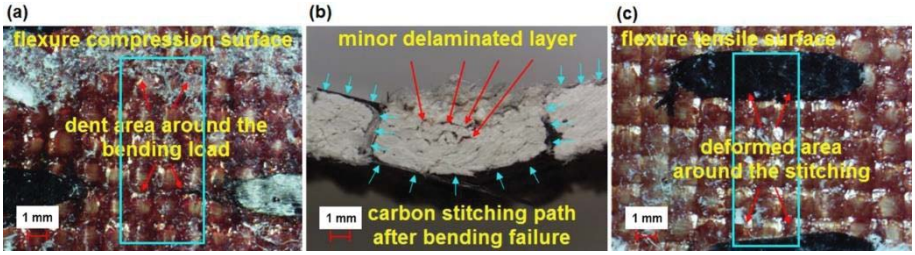


**Figure 13.** Warp directional flexure failure in PAN carbon nanostitched p-aramid/phenolic MWCNT composites. (a) stitched/nano top face (TB-CS-N); (b) stitched/nano cross-section (TB-CS-N); (c) stitched/nano bottom face (TB-CS-N) (optical microscope, magnification x6.7)

## 4. CONCLUSIONS

Stitched/nano p-aramid/phenolic composites were developed and their bending properties were studied. The flexure failure of the developed composites was also analyzed. Stitching and multiwall carbon nanotube addition to the base structures slightly increased the flexure strength, modulus and strain of all the stitched and stitched/nano composites. However, we did not generally obtain consistent results in any of the stitched, nano and stitched/nano composites, in particular plain 1/1 pattern fabric composites. It was also found that the type of stitching fiber slightly affected the flexural properties of the p-aramid/phenolic composites.

The flexural failure in the tension side of the base and base/nano structures was observed as matrix peeling and there were no visible fiber breakages and large delaminated areas near the top surface and mid-plane line, whereas the stitched and stitched/nano composites had warp deformation and no visible matrix/fiber damages and the delaminated areas were severely restricted and minor crack propagation was observed. The flexure failure in the compression side of the base and base/nano structures was lateral warp bending, lateral matrix peeling and almost no visible fiber damages, whereas the stitched and stitched/nano composites had a lateral small dented region and no visible matrix/fiber breakages. The results showed that the addition of stitching fiber and multiwall carbon nanotubes in the base structure improved the out-of-plane failure properties as a form of restricted delamination and they acted as a delamination barrier around the region. Stitched or stitched/nano p-aramid/phenolic composite could be considered as a damage tolerance material.

## ACKNOWLEDGEMENTS

This work was supported by Roketsan Industries Grant No. RS/ERCİYES DSM-76301-14-01N/R. The authors would like to thank ROKETSAN INC. for this invaluable support.

## REFERENCES


1. Kamiya R, Cheeseman B.A., Popper P, Chou T.W.: Some recent advances in the fabrication and design of three dimensional textile preforms: A review. 2000. Compos Sci Technol v. 60, 33-47.
2. Chou T.W.: Microstructural design of fibre composites, 1992. Cambridge University Press, New York, 285.
3. B. N. Cox, M. S. Dadkhah, W. L. Morris and J. G. Flintoff, ACTA Mater., 1994, 42, 3967.
4. K. Bilisik, Text. Res. J., 2012, 82, 725.
5. K. Bilisik, Text. Res. J., 2013, 83, 1414.
6. L. Tong, A. P. Mouritz and M. K. Bannister, 2002, Elsevier B.V., New York, 163.
7. K. Bilisik and G. Yolacan, J. Compos. Mater., 2014, 48, 2145.
8. G. Dell'Anno, D. D. Cartie´, I. K. Partridge, and A. Rezai, Compos. Part A-Appl. Sci. Manuf., 2007, 38, 2366.
9. E. J. Garcia, B. L. Wardle and A. J. Hart, Compos. Part A-Appl. Sci. Manuf., 2008, 39, 1065.
10. S. U. Khan and J. K. Kim, Int. J. Aeronaut. Space., 2011, 12, 115.
11. K. Bilisik, Text. Res. J., 2011, 81, 1748.
12. T. J. Kang and S. H. Lee, J. Compos. Mater, 1994, 28, 1574.
13. L. C. Dickinson, G. L. Farley and M. K. Hinders, J. Compos. Mater., 1999, 33, 1002.
14. K. T. Tan, N. Watanabe and Y. Iwahori, Int. J. Damage Mech., 2012, 21, 51.
15. A. P. Mouritz, J. Gallagher, A. A. Goodwin, Compos. Sci. Technol., 1997, 57, 509.
16. A. P. Mouritz, Compos., 1996, 27A, 525.
17. K. Bilisik and G. Yolacan, J. Reinf. Plast. Comp., 2011, 30, 1065.
18. Y. Wei and J. Zhang, Compos. Part A-Appl. Sci. and Manuf., 2008, 39, 815.
19. E. Wu and J. Wang, J. Compos. Mater., 1995, 29, 2254.
20. K. T. Tan, N. Watanabe and Y. Iwahori, Compos. Part B-Eng., 2011, 42, 874.
21. G. Chen, Z. Li, C. Kou and L. Gui, J. Reinf. Plast. Comp., 2004, 23, 987.
22. C. Xiaoquan, A. M. Al-Mansour, L. Zhengneng and K. Chenghe, J. Reinf. Plast. Comp., 2005, 24, 935.
23. K. Bilisik, J. Reinf. Plast. Comp., 2010, 29, 1173.
24. M. H. Mohamed and A. Bilisik, 1995, US Patent 5465760.
25. J. H. Lehman, M. Terrones, E. Mansfield, K. E. Hurst and V. Meunier, Carbon, 2011, 49, 2581.
26. S. Iijima, Nature, 1991, 354, 56.
27. F. Hussain, M. Hojjati, M. Okamoto and R. E. Gorga, J. Compos. Mater., 2006, 40, 1511.
28. E. T. Thostenson, Z. F. Ren and T. W. Chou, Compos. Sci. Technol., 2001, 61, 1899.
29. L. Shen and J. Li, Phys. Rev. B, 2005, 71, 035412.
30. N. Saravanan, R. Rajasekar, S.Mahalakshmi, T. P. Sathishkumar, K. S. K. Sasikumar and S. Sahoo, J. Reinf. Plast. Comp., 2014, 33, 1158.
31. H. W. Wang, H. W. Zhou, R. D. Peng, and L. Mishnaevsky, Compos. Sci. Technol., 2011, 71, 980.
32. P. C. Ma, J. K. Kim and B. Z. Tang, Carbon, 2006, 44, 3232.
33. T. Fukushima, A. Kosaka, Y. Ishimura, T. Yamamoto, T. Takigawa, N. Ishii and T. Aida, Science, 2003, 300, 2072.
34. P. C. Ma, J-K. Kim and B. Z. Tang, Compos. Sci. Technol., 2007, 67, 2965.
35. B. Yu, Z. Jiang, X. Z. Tang, C. Y. Yue and J. Yang, Compos. Sci. Technol., 2014, 99, 131.
36. D. C. Davis, J. W. Wilkerson, J. Zhu and V. G. Hadjiev, Compos. Sci. Technol., 2011, 71, 1089.
37. J. Zhu, A. Imam, R. Crane, K. Lozano, V. N. Khabashesku and E. V. Barrera, Compos. Sci. Technol., 2007, 67, 1509.
38. M. B. A. Salam, M. V. Hosur, N. Jahan, M. M. Rahman and S. Jeelani, Polym. & Polym. Compos., 2013, 21, 495.
39. M. Sánchez, M. Campo, A. Jiménez-Suárez and A. Ureña, Compos. Part B-Eng., 2013, 45, 1613.
40. L. Hong, Y. Takagaki, H. Yoshikawa and N. Nakashima, B. Chem. Soc. Jpn., 2016, 89, 183.
41. M. Hosur, T. H. Mahdi, M. E. Islam and S. Jeelani, J. Reinf. Plast. Comp., 2017, 36, 667.
42. T. Brocks, M. O. H. Cioffi and H. J. C. Voorwald, Appl. Surf. Sci., 2013, 274, 210.
43. V. Yongand and H. T. Hahn, Nanotech, 2004, 15, 1338.
44. A. Patnaik, A. Satapathy, S. S. Mahapatra and R. R. Dash, J. Reinf. Plast. Comp., 2009, 28, 1305.
45. K. Bilisik and G. Yolacan, Fiber Polym, 2014, 15, 1051.
46. K. Bilisik and G. Yolacan, Fiber Polym, 2014, 15, 614.

47. Y. Inoue, K. Kakihata, Y. Hirono, T. Horie, A. Ishida and H. Mimura, Appl. Phys. Lett., 2008, 92, 213113.
48. A. Ghemes, Y. Minami, J. Muramatsu, M. Okada, H. Mimura and Y. Inoue, Carbon, 2012, 50, 4579.
49. Y. Shimamura, K. Oshima, K. Tohgo, T. Fujii, K. Shirasu, G. Yamamoto, T. Hashida, K. Goto, T. Ogasawara, K. Naito, T. Nakano, and Y. Inoue, Compos. Part A-Appl. Sci. Manuf., 2014, 62, 32.
50. G. Cavallaro, A. A. Danilushkina, V. G. Evtugyn, G. Lazzara, S. Milioto, F. Parisi, E. V. Rozhina and R. F. Fakhrullin, Nanomaterials, 2017, 7, 199.
51. G. Cavallaro, G. Lazzara, S. Milioto, F. Parisi, V. Sparacino, Polym. Degrad. Stabil., 2015, 120, 220.
52. G. Cavallaro, D. I. Donato, G. Lazzara, S. Milioto, J Phys Chem C, 2011, 115, 20491.
53. http://www.nanothinx.com/raw-cnts-in-powder-form/; 2017 [accessed 10.01.17].
54. ASTM D792-91, 1991.
55. ASTM D3171-99, 1999.
56. ASTM D2734-91, 1991.
57. ASTM D790-10, 2010.
58. Bilisik K., Karaduman N., Erdogan G., Sapanci E., Gungor S., Fracture toughness (mode-I) of multistitched carbon/epoxy nanoprepreg composites. 2017. Proceedings of International 13th Nanoscience and Nanotechnology Conference (NANOTR-13), Antalya, Turkey.

# USE OF PVA PLAIN WEAVE TEXTILE AS REINFORCING MATERIAL IN CEMENTITIOUS COMPOSITES

**Mehmet Mustafa DASKIRAN**

Hakkari University, Department of Civil Engineering, Turkey

Corresponding author: m.mustafadaskiran@hakkari.edu.tr

***Abstract:*** *PVA fiber was produced 50 years ago as Japan's first organic fiber and since that time have been used in various applications. Especially since 1980s, it was used to reinforce cement based materials. PVA fibers have higher durability and modulus of elasticity than other organic fibers. Since PVA fibers have high bending strength and modulus of elasticity, they show multiple cracking behavior. PVA fibers show good fiber matrix adherence. Textile materials are used in cementitious composites for strengthening and producing new thin structural elements.*

*In this research, direct tension tests of in-soluble PVA plain weave technical textiles were performed. From the direct tension tests tensile strength, maksimum elongation and elastic modulus of PVA textile were obtained. PVA textile reinforced cementitious composites were prepared using 4 layers of textiles and polymer modified cement mortar. 4 point bending test were performed on cementitious composite samples. First crack load and first crack deflection, maksimum load and deflection at maximum load, maksimum deflection values were obtained from 4 point bending tests.*

*Cementitious composites cast with 4 layer of PVA textiles performed superior mechanical properties. Plain weave textile reinforced composites made very high deflection and reached high flexural load. Observed cracks, during testing, were very thin and distance between cracks were very small. After releasing the load final deflection of the samples was measured. Final deflections were smaller than maximum deflections. Deflection recovery was seen in all samples.*

***Key Words****: PVA, textile, mortar, cementitious composite, bending test*

## 1. INTRODUCTION

Textile reinforced cementitious composite is a new development in construction materials industry with superior tensile strength and high ductility [1]. They have been widely as building material for more than 10 years [3]. Textile reinforced cementitious composites are applied in various fields such as integrated formworks, the strenghtening of existing structures, permanent formworks [3-5]. These composites have two different components: matrix and textile material. Matrix materials consist of cementitous mortar with maximum grain size ≤ 2.0 mm [6].

Textile material is manufactured by knitting or weaving from natural or non-natural fiber yarns. Most commonly used textiles in cementitious composites are AR-Glass, Bazalt, PVA (Polyvinil Alcohol), PBO, Polietilen , Polipropilen, Carbon and

Aramid. However, Carbon and PBO textiles are very expensive. Recent advances in textile manufacturing for construction systems have introduced new opportunities. Woven fabric reinforced composites have been recognized as more competitive than unidirectional composites. This is due to their stability and deformation characteristics that result from coupling of reinforcement in transverse and longitudinal directions, in the load direction.

The matrices used for producing TRCC generally meet specific requirements regarding production processes, mechanical properties of the composite and durability of the reinforcement material. In most cases a small maximum grain size (<2 mm) is used so these matrix systems are called fine grained concrete. Regarding matrix composition, the essential necessity is to get full penetration into technical textiles in order to get great bonding. Production techniques, like lamination and pultrusion, requires plastic consistencies. The matrix design will always be the best adjustment between all requirements regarding fresh, mechanical and durability aspects as well as economic aspects for industrial production of TRCC elements.

Textile reinforced cementitious composites were produced using a new and patented technique called PPR (Pull pour and roll). Researchers designed a unique machine to produce high-performance textile reinforced cementitious composites. In this technique textiles are pulled first, the matrix material is poured onto the textiles and composite material is rolled onto the desired formwork. After demolding the formworks; rectangular, circular, square hollow elements or flat facade elements can be produced.

In this research, textile reinforced cementitious composites were cast using polymer modified matrix mortar and four layers of PVA textile. Before casting direct tension test procedure was applied to textiles according to EN ISO 13934-1 [7] to obtain mechanical properties of textile material. Flexural tests were performed on cementitious composites under four point bending. LVDT's were located while doing four point tests to determine midspan deflections and deflection recovery.

## 2. MATERIALS AND METHODS

### 2.1. PVA Textile and Cement Mortar

PVA textile is produced with insoluable PVA fibers and has plain weave. Direct tension test was applied to PVA textile material. 3 samples used for direct tension tests. Test results obtained from the experiment are are given in Table 1, also PVA textile material is shown in Figure 1. Direct tension test set up is shown in Figure 2.

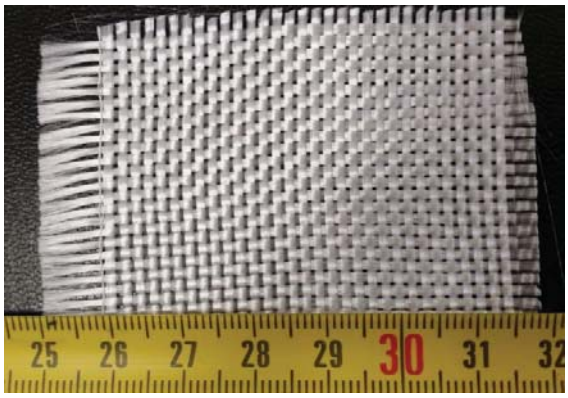


**Figure 1.** PVA Textile Material

**Figure 2.** Direct Tension of PVA textile

**Table 1.** Properties of PVA textile taken from manufacturer's technical data sheet

| PVA TEXTILE | | | | | | | |
|---|---|---|---|---|---|---|---|
| **Fibre** | **Weave** | **Thickness (mm)** | **Weight in unit area (g/m²)** | **Number of Filaments** | **Tensile Strength (N/25mm)** | **Max. Elongation Warp (%)** | **Max. Elongation Weft (%)** |
| In-soluable PVA | Plain | 0.23±0.03 | 150±8 | 200 | 900 | 13.8 | 14.4 |

Cement mortar was prepared using 0.25 mm silica sand, cement, silica fume, fly ash, defoamer and superplasticizer. Redispersible polymer powder was added to the mixture at %5 level compared to binder weigth. Water/binder ratio was 0.32. After preparing each mixture, fresh mixes were cast into 4x4x16 cm rectangular molds. Compressive strength and flexural strength of hardened mortar was

determined on 7th and 28 th day from experiments. Mixture composition is given in Table 2.

**Table 2.** Mixture composition of cement mortar

| Material | % Composition |
|---|---|
| Cement (CEM I 42.5 R) | 31 |
| Silica Fume | 4.5 |
| Fly Ash | 12.5 |
| Silica Sand (dmax≤0.25mm) | 50.8 |
| Superplasticizer | 0.8 |
| Defoamer | 0.4 |
| **TOTAL** | **100** |

### 2.2 Casting of Textile Reinforced Cementitious Composites

Textile reinforced cementitious composite samples were prepared by using a new developed PPR (Pull pour roll) technique and PPR machine. Within this technique, textiles are pulled first, the matrix material is poured onto the textiles and composite material is rolled onto the desired formwork. After demolding formworks; rectangular, circular, square hollow elements or flat facade elements can be produced. 4 layers of PVA textile material were used in the composite samples.

### 2.3. 4 point bending test of Textile Reinforced Cementitious Composites

Mechanical performance of produced composite samples was investigated using flexural test. There is no world-wide recommended standard and sample dimensions for textile cementitious composites in this test. Therefore, samples were cast and then cut using diamond-tipped blade to specific dimensions same as the sample dimensions in a previous study [8]. They were 80x400x13 mm (widthx length x thickness). Composite samples were tested on the MTS machine. Two LVDTs were used to determine deflection of midpoints. Load-deflection curves were obtained in 4 point bending tests. Effective span length was 300 mm. Four point bending test set up is shown in Figure 3.

**Figure 3.** Four point bending test set up.

## 3. RESULTS and DISCUSSION

### 3.1 Results of Cement mortar tests

Three-point flexural test results obtained from three 40x40x160 mm mortar samples in each matrix mixture series are given in Table 3. Also, the compressive strength of 40x40x40 mm mortar samples also given in Table 3. Flexural and compressive strength were obtained from average of three mortar samples.

**Table 3.** Compressive and flexural strength of cement mortar

| **Flexural Strength** | **MPa** |
|---|---|
| 7th Day | 7.3 |
| 28th Day | 13.7 |
| **Compressive Strength** | **MPa** |
| 7th Day | 45.8 |
| 28th Day | 74.2 |

Based on the flexural test results, it can be concluded that flexural strength of cement mortar was higher than conventional mortars through polymer modification.

### 3.3 Results of Direct tension tests of textile material

The mechanical properties PVA plain weave textile is given in the technical data sheet by the manufacturer company. Researcher wanted to compare these values and identify whether they are the same or distinct from each other. As it is seen from the results, the values obtained from direct tension tests within this study and the values given in the material's technical data sheet are s.

**Table 4.** Direct tension test results of PVA textile

| **Textile** | **Sample Number** | **Width (mm)** | **Length (mm)** | **Lo (mm)** | **Maximum Strength (MPa)** | **Maximum Elongation (mm)** | **Elastic Modulus (MPa)** |
|---|---|---|---|---|---|---|---|
| PVA | 1 | 43 | 17.5 | 278 | 103.1 | 9.1 | 907.8 |
| | 2 | 55 | 17.5 | 287 | 88.5 | 10.6 | 914.2 |
| | 3 | 55 | 17.5 | 300 | 119.8 | 11.7 | 1336.5 |
| | | | | **Average** | 104.0 | 10.5 | 1052.8 |

### 3.3 Results of Bending tests of composite material

In four point bending test, first crack load indicates the matrix cracking load. The first part of the Load-Deflection curve where the matrix reached its cracking load was the Region 1. After first crack composite sample passed the 2. Region. In the 2. Region formation of cracks occur in the composite sample. After reaching maximum load, the load has decrased slightly but deflection has continued to increase. Deflection recovery was seen at the end of the experiment after the sample was broken. Despite reaching service load, composite sample maintained its integrity. Almost matrix itself unable to deflect, maximum deflection

values of the composite sample was very high. This is the success of PVA textile and weaving type.

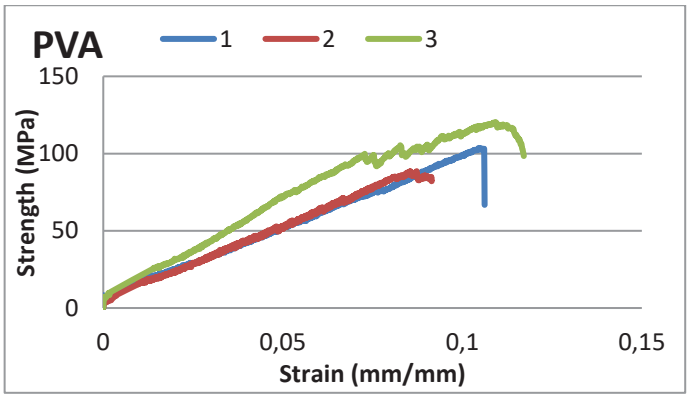


**Figure 4.** Stress strain diagram of direct tension test

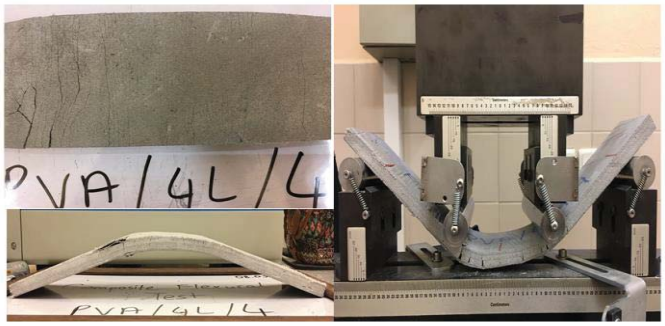


**Figure 5.** : Textile reinforced composite sample after bending test

**Table 4.** Four point bending test results of composites

| Sample Code | Sample Number | Load at first crack (N) | Deflection at first crack (mm) | Maximum Load (N) | Deflection at Maximum load (mm) | Maximum Deflection (mm) | Deflection Recovery (mm) |
|---|---|---|---|---|---|---|---|
| PVA 4Layer | 1 | 143.2 | 0.39 | 294.3 | 27.5 | 78.0 | 18.0 |
| | 2 | 247.0 | 0.54 | 321.6 | 22.6 | 71.5 | 20.5 |
| | 3 | 211.2 | 0.51 | 355.0 | 43.9 | 74.5 | 21.5 |
| | 4 | 136.7 | 0.69 | 259.3 | 38.5 | 74.6 | 24.6 |
| | **Average** | **184.5** | **0.53** | **307.6** | **33.1** | **74.7** | **21.2** |

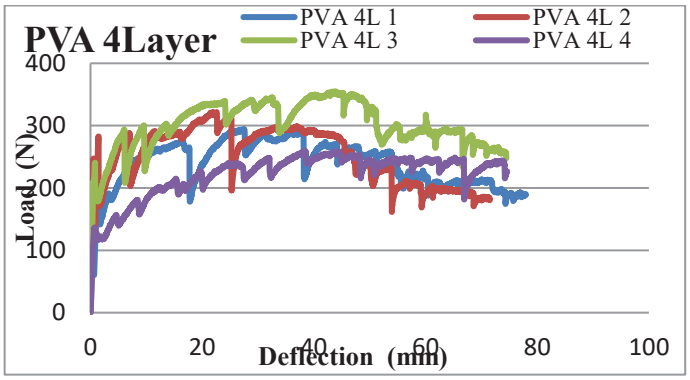


**Figure 6.** : Load deflection diagram of composite samples in bending test

## 4. CONCLUSIONS

Textile reinforced cementitious composites cast with mortar and in soluable PVA textile achieved high flexural properties. Since cementitious materials doesn't have high tensile capacity, using textile materials in cementitious composite is very effective. Adhesion between textile material and mortar has an important effect on mechanical properties. Composite samples prepared with plain weave textiles showed delemination behaviour and breaking occurs. PVA reinforced composite samples showed ductile behaviour because PVA textile material is ductile itself.

## REFERENCES

1. Soranakom, C., Mobasher B. : Flexural design of fiber-reinforced concrete. 2009. ACI Materials Journal, 106(5), 461.
2. Hartig, J., Häußler-Combe, U. ve Schicktanz, K.: Influence of bond properties on the tensile behviour of Textile Reinforced Concrete, 2008. Cement and Concrete Research, v. 30, 898-906.
3. Curbach, M. : SFB 532 ; SFB 528: Textile Reinforced Structures. 2011. Proceedings of the 2nd Colloquium, Dresden.
4. Gür, M. : Determination of shear strength of infill walls strenghtened with cement based composite plates, Master's Thesis. 2017.Istanbul Technical University.
5. Daskiran, M.M : Experimental investigation of mechanical behavior of permanent formwork elements produced with cement based composites, Doctoral Dissertation. 2018. Istanbul Technical University.
6. Brameshuber W., Brockmann T.: Development and Optimization of CementitiousMatrices for Textile Reinforced Elements. London : Concrete Society, 2001. - In:Proceedings of the 12th International Congress of the International Glassfibre Reinforced Concrete Association, Dublin, 14-16 May 2001, 237-249.
7. EN ISO 13934-1: Textiles -- Tensile properties of fabrics -- Part 1: Determination of maximum force and elongation at maximum force using the strip method, 2013.
8. Almeida, A.L.F.S, Filho, R.D.T, Filho, J.A.M. :Bending Behaviour of Cement based composites reinforced with jute textile. 2010. International RILEM Conference on Material Science-MATSCI, ICTRC, 1, 177-184.

# NANOFIBER VEIL REINFORCED COMPOSITE FOR INTERLAMINAR TOUGHENING

**Halil İbrahim İÇOĞLU[1], Mehmet Erdem İNCE[2]**

[1]Gaziantep University, Department of Metal. Mater. Engineering, Turkey
[2]Gaziantep University, Textile Engineering, Turkey

Corresponding author: icoglu@gantep.edu.tr

***Abstract:*** *Delamination is a common problem in many fiber reinforced composite applications. Electrospun nanofiber veils can be used as interleaves of laminates for a potential solution of this problem.*

*In this study, mechanical properties of polyester resin – woven glass fibers composites interleaved by polyacrylonitrile (PAN) electrospun nanofiber veils are investigated to enhance the interlaminar toughness characteristics. The composite samples are produced from seventeen layers of glass fabric reinforced by PAN nanofiber veils with polyester resin via vacuum infusion method.*

*Flexural properties and Charpy impact properties of the composite samples are tested. According to the test results, electrospun nanofiber veils improved flexural strength of composite samples about 15%. However, no significant difference between absorbed impact energy of nano reinforced and conventional composite samples was observed.*

***Key Words****: Composite, interlaminar toughening, mechanical properties, glass fiber, electrospinning*

## 1. INTRODUCTION

Fiber reinforced polymer composites have many advantages such as high stiffness and strength with low specific weight and commonly used in many areas especially automotive, aerospace, and ship-building. However, delamination strength and fracture toughness remain important problems in fiber reinforced composites [1, 2].

Enhancement delamination resistance of fiber reinforced composites means higher damage resistance, performance and in-service life. Hence, different methods have been applied to enhance delamination resistance of these materials such as modifying the matrix resin, braiding technique, interleaving of laminates [3-5].

Interleaving of composite laminates with electrospun nanofiber veils is a suitable method to mitigate delamination. Nanofiber veils can be added directly between plies or plies can be coated with electruspun nanofibers easily. Also, Nanofibers have unique characteristics such as small diameters, high porosity, and high specific surface area. Moreover, electrospinning method has advantageous properties such as low cost, repeatability, simplicity, and continuous nanofiber production [5].

Although the use of nanofiber veils has many advantages compared to traditional toughening methods, the studies are still limited. Several polymeric nanofiber veils have been investigated, e.g. polysulfone (PSU), poly(ε-caprolactone) (PCL), polyamides (PA), poly(vinylidene fluoride) (PVDF), polyacrylonitrile (PAN), polyamide-imide (PAI), poly(styrene-co-glycidyl methacrylate) P(St-coGMA), and polyvinyl butyral (PVB) [6-12].

In this study electrospun PAN nanofiber veils are used to improve delamination performance of the woven glass fiber-polyester resin composites.

## 2. MATERIAL AND METHOD

### 2.1. Materials

PAN polymer (Mw 150,000) was gently supplied from AKSA Acrylic. DMF was purchased from Sigma Aldrich. 12 wt% of PAN/DMF solution was prepared by stirring magnetically for 3 hours at a temperature of 90 $^0$C.

E-glass woven fabric (plain weave, 300 g/m$^2$, 198 tex warp and weft yarns) was used as the composite reinforcement. Unsaturated polyester (CE 92 N8, Cam Elyaf Inc., Turkey) was used as resin material. Methyl ethyl ketone peroxide and cobalt naphtanate were used as initiator and an accelerator, respectively.

### 2.2 Nanofiber production

The electrospinning setup consists of two high voltage power supplies (+50 kV and −50 kV), a syringe infusion pump, and a plate collector as indicated before (Figure1) [13]. The electrospinning apparatus is in a closed cabin. The nanofibers are collected on the aluminum foil. All air bubbles are purged prior to electrospinning. Applied voltage, tip-collector distance, solution flow rate, and needle diameter are selected as 35 kV, 15 cm, 0.5 mLh$^{-1}$, and 0.7 mm, respectively, to obtain steady-state formation. Ambient temperature and relative humidity are kept constant as 20 °C and 50%.

Six layers of glass fabric samples were directly coated with PAN nanofiber veils in this electrospinning set up for 25 minutes for the top three interlayers and bottom three interlayers of nano reinforced composite sample.

**Figure 1.** The electrospinning set up

### 2.3. Composite Production

Seventeen-layer virgin and nanofiber interleaved laminates were produced via vacuum assisted resin infusion (VARI) process [14]. Schematic representations of these two samples are given in Figure 2. Conventional composite sample was produced without using of PAN nanofiber veils. Nano reinforced composite sample was produced using of top and bottom three interlayers of PAN nanofiber veils. In this sample, no nanofiber veils were used for the other interlayers.

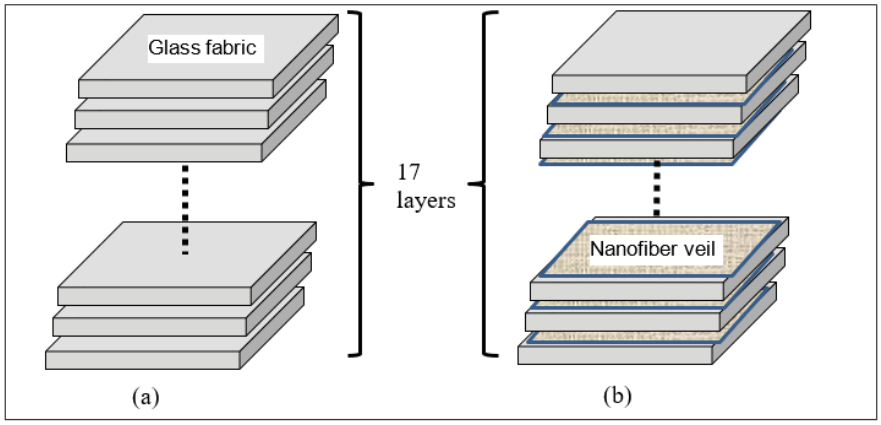


**Figure 2.** Schematic representation of composite samples:(a) Conventional composite without nanofiber veils, (b) Nano reinforced composite with top and bottom three interlayers of nanofiber veils

### 2.4. Test Methods

Before electrospinning, viscosity, conductivity, and surface tension of the solution are determined by Brookfield DV-III viscometer, Orion 4 star conductivity meter, and KSV CAM 101 surface tension meter, respectively.

The morphological appearances of the nanofibers are analyzed by using a scanning electron microscope after coating with an ion sputter. ImageJ image analysis program is used for measurement of diameters of electrospun PAN nanofiber veils.

Tripoint bending test is applied according to ASTM D790. Impact test of composites is performed according ISO 179-1 with unnotched samples and flatwise direction.

## 3. RESULT AND DISCUSSION

Viscosity, conductivity, and surface tension of the PAN/DMF solution are determined as 812 mPas, 66.8 mS/cm and 39.24 mN/m, respectively. SEM image of electrospun

PAN nanofibers is given in Figure 3. Average diameter of PAN nanofibers are determined as 257 nm ± 32 nm.

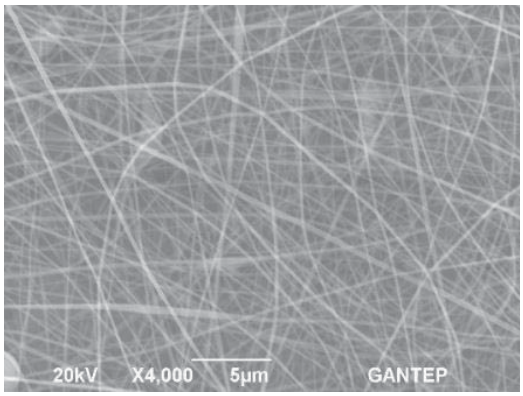


**Figure 3.**: SEM microgram of electrospun PAN nanofibers

Three point bending test and Charpy impact tests were applied for the two composite samples (nano reinforced composite and conventional composite) to evaluate delamination strength of the samples. Flexural and Charpy impact test results are given in Table 1.

**Table 1.** Flexural and Charpy impact test results

| Sample type | Max. flexural stress (MPa) | Elongation at max. flexural stress (%) | Absorbed impact energy (J) |
|---|---|---|---|
| Conventional composite | 206,54 | 1,37 | 6,58 |
| Nano reinforced composite | 244,74 | 1,63 | 6,65 |
| Percent Difference | 15,61% | 18,98% | 1,13% |

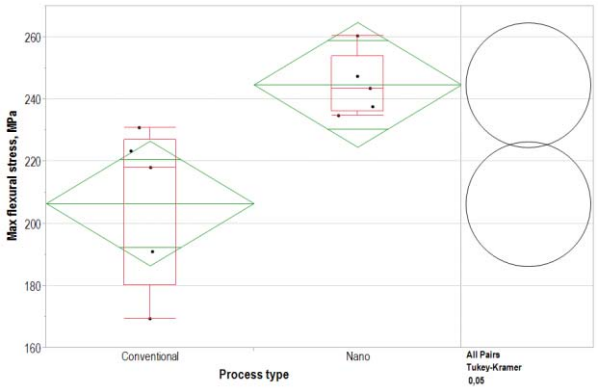


**Figure 4.** The effect of electrospun nanofiber reinforcement on flexural strength

According to Table 1, interleaving by electrospun PAN nanofiber veils improved flexural strength of the glass fiber reinforced composite about 15%. Adding nanofiber veils three top interlayers and three bottom interlayers improved flexural stress at statistically significant level (Figure 4, Table 2).

**Table 2.** The effect of electrospun nanofiber reinforcement on flexural strength

| Property | Cam setting | Mean | SD | LL | UL | p-value |
|---|---|---|---|---|---|---|
| **Max flexural stress, MPa** | Nano reinforced | 244,74 | 10,11 | 232,19 | 257,30 | 0,0073 |
| | Conventional | 206,54 | 25,61 | 174,75 | 238,34 | |

**Note: SD**: standard deviation, **LL**: lower limit, **UL**: upper limit. Limits are based on 95% confidence level. Significance level, α, was determined as 0,05. p-values were based on one-sided hypothesis testing. p-values less than 0,05 were colored in red and show statistical significance.

On the other hand, adding nanofiber veils did not improve or change absorbed impact energy of the composite samples significantly (Figure 5, Table 3).

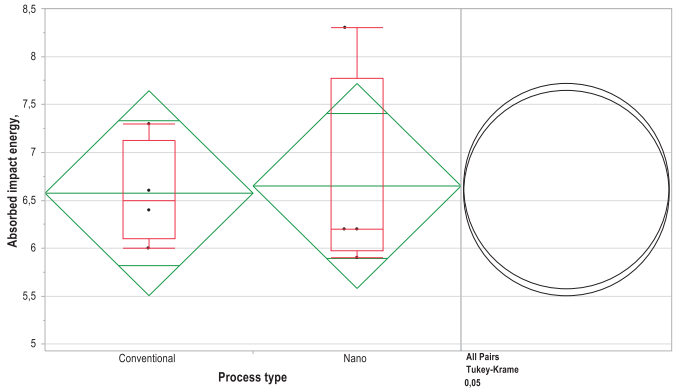


**Figure 5.** The effect of electrospun nanofiber reinforcement on absorbed impact energy

**Table 3.** The effect of electrospun nanofiber reinforcement on absorbed impact energy

| Property | Cam setting | Mean | SD | LL | UL | p-value |
|---|---|---|---|---|---|---|
| **Absorbed impact energy, J** | Nano reinforced | 6,65 | 1,11 | 4,89 | 8,42 | 0,4537 |
| | Conventional | 6,58 | 0,54 | 5,71 | 7,44 | |

## 4. CONCLUSIONS

In this study, mechanical properties of polyester resin - woven glass fiber composites interleaved by polyacrylonitrile (PAN) electrospun nanofiber veils are investigated to improve delamination properties of composites. PAN nanofiber veils are added between top three interlayers and bottom three interlayers of glass woven plain fabrics and fiber reinforced composite samples are produced by using polyester resin with vacuum assisted resin infusion (VARI) process. Among 17 layers of glass woven fabric only top and bottom three interlayers are

coated with PAN nanofiber veils. According to the test results, electrospun nanofiber veils improve flexural strength of composite samples about 15%. This is directly related to the delamination strength of composite samples. On the other hand, there is no significant difference between absorbed impact energy of electrospun veil reinforced and conventional composite samples.

## REFERENCES


1. Garg A.C.: Delamination – a damage mode in composite structures. 1988. Eng Fract Mech. 29(5):557–84.
2. Tsotsis T.K.: Interlayer toughening of composite materials. 2009. Polym. Compos. 30:70-86.
3. Mezzenga R, Boogh L, Manson JAE.: A review of dendritic hyperbranched polymer as modifiers in epoxy composites. 2001. Compos Sci Technol. 61(5):787–95.
4. Tang G, Yan Y, Chen X, Zhang J, Xu B, Feng Z.: Dynamic damage and fracture mechanism of three-dimensional braided carbon fibre epoxy resin composites.2001. Mater Des. 22(1):21–5.
5. Hojo M, Matsuda S, Tanaka M, Ochiai S, Murakami A.: Mode I delamination fatigue properties of interlayer-toughened CF/epoxy laminates. 2006. Compos Sci Technol. 66(5):665–75.
6. Li G., Li P., Zhang C., Yu Y., Liu H., Zhang S.,:Inhomogeneous toughening of carbon fiber/epoxy composite using electrospun polysulfone nanofibrous membranes by in situ phase separation. 2008. Compos. Sci. Technol. 68:987-994.
7. Van der Heijden S., Daelemans L., De Schoenmaker B., De Baere I., Rahier H., Van Paepegem W.: Interlaminar toughening of resin transfer moulded glass fibre epoxy laminates by polycaprolactone electrospun nanofibers. 2014. Compos Sci. Technol. 104:66-73.
8. Hamer S., Leibovich H., Green A., Intrater R., Avrahami R., Zussman E.: Mode I interlaminar fracture toughness of Nylon 66 nanofibrilmat interleaved carbon/epoxy laminates. 2011. Polym. Compos 32:1781-1789.
9. Kim J.S., Reneker D.H.: Mechanical properties of composites using ultrafine electrospun fibers. 1999. Polym. Compos. 20:124-131.
10. Zhang J., Yang T., Lin T., Wang C.H.: Phase morphology of nanofiber interlayers: critical factor for toughening carbon/epoxy composites, 2012. Compos Sci. Technol. 72:256-262.
11. Bilge K., Venkataraman S., Menceloglu Y.Z., Papila M.: Global and local nanofibrous interlayer toughened composites for higher in-plane strength. 2014. Compos Part A Appl. Sci. Manuf. 58:73-76.
12. Bovicelli F., Saghafi H., Brugo T.M., Belcari J., Zucchelli A., Minak G.: On consideration the mode I fracture response of CFRP composite interleaved by composite nanofibers. 2014. Procedia Mater. Sci. 3:1316-1321.
13. Kirecci A., Özkoç Ü., İçoğlu H.İ.: Determination of Optimal Production Parameters for Polyacrylonitrile Nanofibers. 2012. J. Appl. Polym. Sci. 124(6):4961-4968.
14. Matthews, F. L. and Rawlings, R. D.:Composite materials: engineering and science. 1994. Woodhead Publishing Limited, Cambridge, UK.

# PROCESS OPTIMIZATION OF GLASS FIBER REINFORCED PPS COMPOSITES PRODUCED BY AUTOMATED FIBER PLACEMENT

**Sevinç ORMAN[1], Mustafa DOĞU[2], Belma ÖZBEK[1]**

[1] Yildiz Technical University, Turkey
[2] Mir Araştırma ve Geliştirme A.Ş.

Corresponding author: sevinckaradag@gmail.com

***Abstract:*** *Polyphenylene sulfide (PPS) is a high temperature thermoplastic, which has a semi crystalline chemical structure. PPS has many applications due to its high mechanical performance, high thermal stability, magnificent chemical resistance, magnificent flame retardancy, and satisfying electrical properties. In this study, processing parameters of glass fiber reinforced PPS composites were examined by applying an experimental design and response surface methodology. A lab scale automated fiber placement machine was used for production, and the effects of temperature, pressure and speed on the performance of GF/PPS composites were observed. The optimum process conditions in which the maximum performance can be obtained by considering both the shear strength and the impact strength were found as 456 $^0$C heater temperature, 0.3 MPa roller pressure and 50.4 mm/min processing speed.*

***Keywords****: polyphenylene sulfide, mechanical properties, process optimization, automated fiber placement, experimental design*

## 1. INTRODUCTION

Polyphenylene sulfide, also known as PPS, is a semi-crystalline polymer included in the polysulfide class. The glass transition temperature of PPS is 357 K (85 $^0$C) and the melting temperature is 558 K (285 $^0$C). PPS is mainly used as high performance thermoplastic by reinforcing it with glass fiber or mineral fillers. The reinforced PPS exhibits excellent mechanical properties, high thermal stability, magnificent chemical resistance, magnificent flame retardancy, satisfying electrical-electronic properties and moulding precision [1-4]. Because of its low viscosity PPS can be loaded with fillers and reinforcement materials at high rates. Due to its self-flame retardant nature, PPS is ideal for high-temperature electrical applications [5]. It is used for automobile components (for example, air intake systems, pumps, valves, gaskets, exhaust gas recirculation systems), electrical and electronic components (for example, plugs and multiple connectors, bobbins, relays, switches, encapsulation of electronic components and etc.), and mechanical and precision engineering parts. The use of manufacturing methods such as automatic fiber placement (AFP) and automated tape laying (ATL) has become widespread to reduce material losses and human error in the production of reinforced composite materials. AFP technology is a suitable method for the production of large and complex structures, reducing material loss [6]. In this

study, glass fiber (GF) reinforced PPS composites were produced by a lab scale AFP system, and the optimum process conditions were investigated by applying Box-Behnken experimental design [7] and response surface plots, which visualize the effects of two factors on the response while the third factor is kept constant at a certain level, generally at central point [8,9].

## 2. MATERIALS AND METHOD

A lab scale automated fiber placement machine that includes of a hot-gas heater was used to produce GF/PPS composites from 5 mm towpregs purchased from Celanese. Experimental design model was utilized for determination of the process parameters effects on the performance of GF/ PPS composites. In order to optimize the main factors of the automated fiber placement (AFP) process, a 3-factor, 3 level Box-Behnken model with 15 experiments was applied.

## 3. RESULTS AND DISCUSSION

A third degree polynomial model approach was applied to the test results and the model equations were obtained according to the interlaminar shear strength (R1) and impact strength (R2). The regression coefficients of the polynomial fit are 0.9999 and 0.9986, for R1 and R2 respectively.

The response surface graphics and the model equations were examined, and it was observed that process speed has the greatest effect on the impact strength; also interaction effects of temperature play a major role in impact strength. The interaction effect of pressure on shear strength is higher than temperature and process speed. Although the direct effect of temperature appears to be lower than the other two factors, the interaction effect of temperature factor is high. According to the test results, the optimum process conditions in which the maximum performance can be obtained by considering both the shear strength and the impact strength were found as 456 $^0$C heater temperature, 0.3 MPa roller pressure and 50.4 mm/min processing speed.

## 4. CONCLUSION

A lab scale automated fiber placement machine was used to produce GF/PPS composites. In order to optimize the main factors of the automated fiber placement (AFP) process, a 3-factor, 3-level Box Behnken model with 15 experiments was applied. The effects of temperature, pressure and speed on the performance of GF/PPS composites were observed by response surface graphics and model equations. The optimum process conditions in which the maximum performance can be obtained by considering both the shear strength and the impact strength were found as 456 $^0$C, 0.3 MPa and 50.4 mm/min.

## REFERENCES


1. James E. Mark. 1999. Polymer Data Handbook, Oxford University Press, Inc, 471-478, 714-721.
2. Polyphenylene Sulphide PPS, http://www.bpf.co.uk/plastipedia/polymers/pps.aspx
3. Waghuley, Dr. Sandeep. (2013). Polyphenylene Sulfide (PPS): State of the Art and Applications.
4. Polyphenylene Sulfide (PPS) Plastic, https://plastics.ulprospector.com/generics/41/polyphenylene-sulfide-pps
5. Polyphenylene Sulfide (PPS), https://www.rtpcompany.com/products/product-guide/polyphenylene-sulfide-pps/
6. Jie Chen, Yugang Duan, 2014. Tow tension controller for robotic automated fiber placement based on fuzzy parameter self-adjusting PID. Future Mechatronics and Automation: Proceedings of the 2014 International Conference on Future Mechatronics and Automation, (ICMA 2014), 7-8 July, 2014, Beijing, China.
7. G. E. P. Box, D. W. Behnken, Some New Three Level Designs for the Study of Quantitative Variables, Technometrics 2 (1960) 455-475.
8. A. I. Khuri and S. Mukhopadhyay, Response surface methodology, WIREs Computional Statistics 2 (2010) 128–149.
9. N.Bradley, The Response Surface Methodology, Master Thesis, Applied Mathematics& Computer Science, Indiana University of South Bend, 2007.

# ANTIBACTERIAL ACTIVITY OF COPPER-BASED NANOPARTICLES SYNTHETIZED ON COTTON FABRIC PREVIOUSLY MODIFIED WITH OXALIC ACID

**Darka MARKOVİC[1], Tim NUNNEY[2], Christopher DEEKS[2], Zeljko RADOVANOVİC[1], Marija RADOİCİC[3], Maja RADETİC[4]**

[1]University of Belgrade, Inovation Center of the Faculty of Technology and Metallurgy, Serbia
[2]Thermo Fisher Scientific, UK
[3]University of Belgrade, "Vinca" Institute of Nuclear Sciences, Serbia
[4]University of Belgrade, Faculty of Technology and Metallurgy, Serbia

Corresponding author: maja@tmf.bg.ac.rs

***Abstract:*** *This study discusses the possibility of fabrication of antibacterial textile nanocomposite by in situ synthesis of Cu-based nanoparticles on cotton fabric modified with oxalic acid. The change in chemical structure of the cotton fibres was assessed by FTIR spectroscopy. The presence of Cu-based nanoparticles on the cotton fabric was proved by SEM, EDX and AAS analyses. Chemical composition of the fabricated Cu-based nanoparticles was evaluated by XPS analysis. Antibacterial activity of the textile nanocomposite was tested against Gram-negative bacterium E. coli and Gram-positive bacterium S. aureus.*

*On the basis of the XPS measurements, it was suggested that synthetized nanoparticles consisted of metallic Cu/$Cu_2O$ and $Cu_2CO_3(OH)_2$. Fabricated nanocomposite provided maximum reduction of both bacterial strains and controlled release of $Cu^{2+}$-ions in physiological saline solution which are necessary precondition for infection prevention.*

***Keywords:*** *cotton, Cu-based nanoparticles, oxalic acid, antibacterial activity*

## 1. INTRODUCTION

Recent breakthrough in nanotechnologies strongly affected a research in the field of medical, hygiene and protective textiles. Many efforts have been made to fabricate antimicrobial textile materials with immobilized metal (Ag, Cu) and metal oxide ($TiO_2$, ZnO, CuO, $Cu_2O$) nanoparticles (NPs) or their mixtures and to learn more on the mechanism of their action [1-3]. Keeping in mind that copper in various forms (ionic, copper oxides, copper complexes) is active against numerous bacterial strains as well as that precursor salts of copper are much cheaper than those of silver [4], the possible exploitation of Cu, CuO and $Cu_2O$ NPs for imparting the antibacterial protection to cotton fabrics lately became the focus of many research groups worldwide [5-6]. Although dip-coating method from the Cu-based NPs colloid/dispersion is an option, the most common method for cotton fabric impregnation with Cu-based NPs relies on *in situ* synthesis which includes three steps: the introduction of carboxyl groups to cotton fibers, the adsorption of $Cu^{2+}$-ions from salt solution and the reduction with adequate

reducing agent. In our study, desired carboxyl groups were provided by modification of cotton fabric with dicarboxylic oxalic acid prior to adsorption of $Cu^{2+}$-ions from $CuSO_4$ aqueous solution. *In situ* synthesis of Cu-based NPs was carried out by reduction of $Cu^{2+}$-ions with sodium borohydride in alkaline solution. Antibacterial activity of fabricated textile nanocomposite was tested against Gram-negative bacterium *E. coli* and Gram-positive bacterium *S. aureus*.

## 2. MATERIALS AND METHODS

### 2.1. Modification of cotton fabric

Desized and bleached cotton (Co) woven fabric (117.5 g/m$^2$, 27 picks/cm, 52 ends/cm, thickness of 0.26 mm) was used as a substrate. Co fabrics were cleaned in the bath containing 0.1% nonionic washing agent Felosan RG-N (Bezema) at liquor-to-fabric ratio of 50:1. After 15 min of washing at 50 $^oC$, the fabric was rinsed first with warm water (50 $^oC$) and then thoroughly with cold water. The samples were dried at room temperature.

Modification of Co fabric with oxalic acid was conducted by immersion of 0.50 g of the sample in 20 mL of the acid aqueous solution (10 w/v %) in the presence of 2.06 g of the catalyst sodium hypophosphite (SHP) for one hour. After drying at 80$^oC$ for 3 min the sample was cured at 170$^oC$ for 3 min. The sample was then rinsed in distilled water and dried at room temperature. 0.50 g of the Co fabric modified in described manner (Co+OX) was soaked in 25 mL of 10 mM solution of $CuSO_4$ (pH=4.63) for 2 h. In order to eliminate the excessive $Cu^{2+}$-ions, the sample was rinsed three times with deionized water. 0.050 g of $NaBH_4$ was dissolved in 25 mL of 0.1 mM NaOH solution and the sample was immediately dipped into the solution where the reduction process took place in the following 30 min at room temperature. The sample (Co+OX+Cu) was thoroughly rinsed with deionized water and left to dry at room temperature.

### 2.2. Methods

FTIR spectra of the control Co and Co+OX fabrics were recorded in the ATR mode using a Nicolet 6700 FTIR Spectrometer (Thermo Scientific) at 2 cm$^{-1}$ resolution, in the wavenumber range 500–4000 cm$^{-1}$.

Determination of carboxyl content in the Co+OX fabric was based on the calcium acetate method described by Kumar and Yang and modified by Praskalo et al [7-8].

The morphology of the control and Co+OX+Cu fibers was analysed by field emission scanning electron microscopy (FESEM, Tescan Mira3 FEG). The samples were coated with a thin layer of Au prior to analysis. Energy-dispersive X-Ray spectroscopy (EDX) of the fibers was performed using a JEOL JSM 5800 SEM with a SiLi X-Ray detector (Oxford Link Isis series 300, UK).

The amounts of adsorbed $Cu^{2+}$-ions on the Co+OX fabric from $CuSO_4$ solution was calculated on the basis of the concentration of residual $Cu^{2+}$-ions in the solution which was measured using a Spectra AA 55 B (Varian) atomic absorption

spectrometer (AAS). AAS was also used for the measurement of the total Cu content in the Co fabric after reduction process. Dry impregnated Co fabric was dissloved in the 1:1 $HNO_3$ solution. Additionaly, AAS was conducted for the assessment of the $Cu^{2+}$-ions release from samples into physiological saline solution.

X-ray photoelectron spectroscopy (XPS) measurements were performed in order to evaluate the chemistry variations of the control Co and Co+OX+Cu fabrics. The XPS analysis was performed using a K-Alpha spectrometer (Thermo Scientific, UK) utilizing a monochromated Al Kα (hv = 1486.6 eV) X-ray source. The system base pressure was less than $5 \cdot 10^{-9}$ mbar, however the pressure in the chamber during analysis was $2 \cdot 10^{-7}$ mbar due to use of the charge neutralization system which employs a combination of low energy electrons and low energy argon ions to compensate for the loss of photoelectrons from an insulating sample. First, point analysis was conducted on all samples to determine their chemical composition. Maps were then acquired of the Co+OX+Cu sample to determine the average composition of the surface.

The antibacterial activity of the Co fabrics was tested against Gram-negative bacteria *E. coli* ATCC 25922 and Gram-positive bacteria *S. aureus* ATCC 25923 using a standard test method for determination of the antimicrobial activity of immobilized antimicrobial agents under dynamic contact conditions ASTM E 2149-01 (2001). The percentage of bacterial reduction (*R*, %) was calculated by the following equation:

$$R = \frac{C_0 - C}{C_0} \cdot 100$$

where $C_0$ (CFU – colony forming units) is the number of bacteria colonies on the control fabric and *C* (CFU) is the number of bacteria colonies on the fabric with NPs.

$Cu^{2+}$-ions release was tested by immersing 0.25 g of the impregnated fabrics in 25 mL of physiological saline solution (9 g/L NaCl) at 37 ºC in static conditions. The concentration of released $Cu^{2+}$-ions was measured after 1, 3, 6 and 24 hours by Spectra AA 55 B (Varian) atomic absorption spectrometer.

## 3. RESULTS AND DISCUSSION

The intention of this study was to exploit the oxalic acid for establishing the ester bonds between its carboxyl groups and hydroxyl groups of cellulose, leaving the free carboxyl groups as potential sites for adsorption of $Cu^{2+}$-ions from solution. The modification of Co fabric with oxalic acid resulted in the appearance of the band at 1740 $cm^{-1}$ in the FTIR spectrum which confirmed the introduction of C=O groups originating from the oxalic acid (Fig. 1). In order to quantify the total content of free carboxyl groups in the Co+OX sample titrimetric measurements were conducted. One gram of Co+OX fabric contained 218±49 □mol of free carboxyl groups. A comparison of these results with our previous results where

tricarboxylic citric and tetracarboxylic 1,2,3,4-butanetetracarboxylic acids have been used [9-10] reveals that the number of free carboxyl groups on the Co fibers increases with a number of carboxyl groups in applied polycarboxylic acid. AAS measurement showed that $Cu^{2+}$-ions uptake after 2 hours long adsorption in aqueous solution of $CuSO_4$ was 173±29 □mol/g of Co+OX fabric. This is in line with previous observation i.e. larger uptake of $Cu^{2+}$-ions was obtained with mentioned acids since the larger the number of free carboxyl groups, the larger the uptake of $Cu^{2+}$-ions. Finally, the total Cu content in Co fabric modified with oxalic acid and impregnated with Cu-based NPs (Co+OX+Cu) after reduction of adsorbed $Cu^{2+}$-ions was 104±14 mol/g.

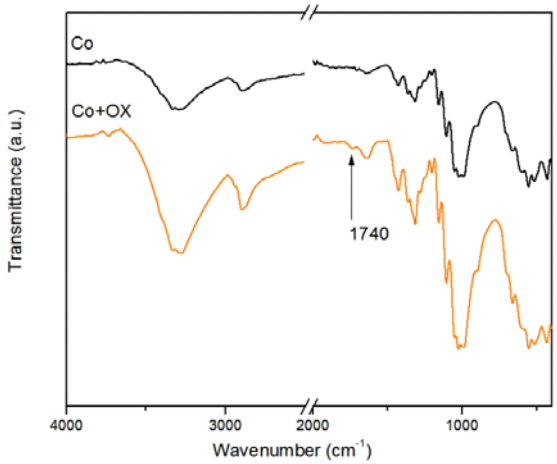


**Figure 1.** FTIR spectra of the Co and the Co+OX fabrics

The efficient reduction of $Cu^{2+}$-ions and formation of Cu-based NPs was confirmed by SEM, EDX and XPS analyses. Uniform distribution of Cu-based nanoparticles across the surface of Co fibre and characteristic peaks in EDX spectrum corresponding to Cu can be seen in Fig. 2.

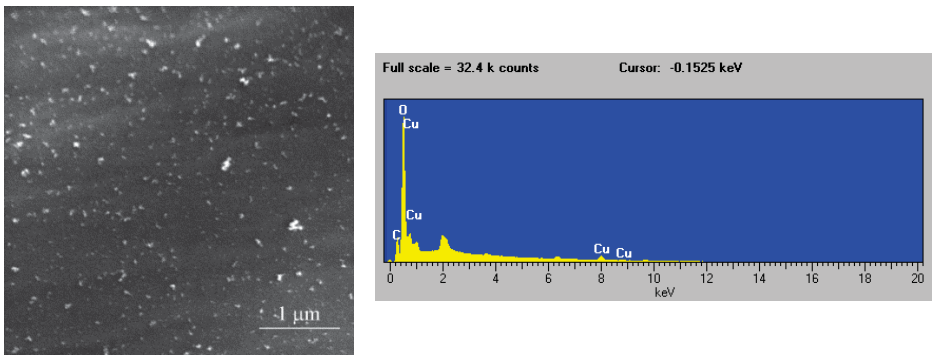


**Figure 2.** SEM image and EDX spectrum of the Co+OX+Cu fabric

To get insight into the oxidation state of the copper in synthesized NPs a single points on the surface of the Co+OX+Cu sample were analyzed by XPS. A high resolution scans of the Co+OX+Cu sample were accomplished in the C1s, O1s and Cu2p regions and they are shown in Fig. 3a, 3b and 3c, respectively. Deconvolution of the C1s spectrum of the Co+OX+Cu sample revealed the presence of three components that are assigned to C-O-, O-C-O and C-O-C groups of cellulose. Additional peak corresponding to C-C/C-H groups is attributed to residual waxes. The O1s spectrum was deconvoluted into two components attributed to organic O1s from cellulose and copper oxides.

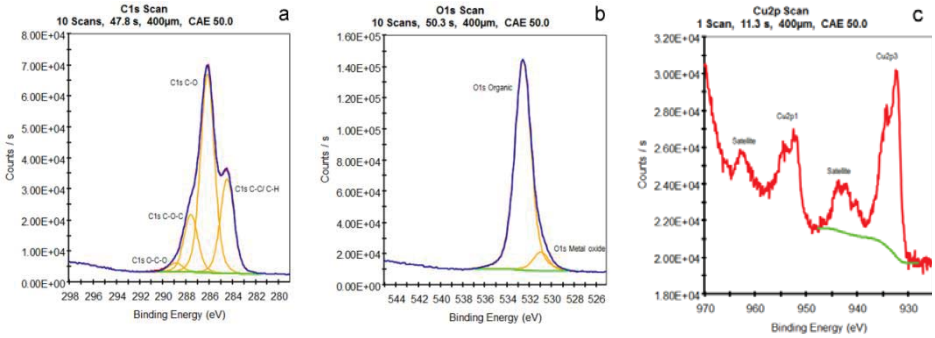


**Figure 3.** XPS high resolution spectra of the Co+OX+Cu fabric in the C1s, O1s, and Cu2p regions

The analysis of the Cu2p spectrum implied that Cu-based NPs were likely present as a mixture of different forms of copper on the Co fabrics. The deconvolution of the Cu2p high resolution XPS spectrum indicated the presence of Cu/$Cu_2O$. Obviously, the Cu2p spectrum comprises of the shakeup satellites which are absent in the case of pure Cu or $Cu_2O$ [11]. In fact, the shakeup satellites are characteristic of materials possessing a $d^9$ configuration like in a $Cu^{2+}$ [12]. Unlike in the case of modification of Co fabrics with citric acid or BTCA where CuO was detected [10], in current case likely $Cu_2CO_3(OH)_2$ has been formed during the drying of fabric in the air and further storage. Such finding is not unexpected as $Cu(OH)_2$ can be naturally stabilized by combining with $CuCO_3$ to form the azurite ($2CuCO_3 \cdot Cu(OH)_2$) or malachite ($CuCO_3 \cdot Cu(OH)_2$) [13]. In addition, it was not possible to distinguish metallic Cu from the formed $Cu_2O$ form due to their spectral overlap. The difference in binding energies of the $Cu2p_{3/2}$ signal for these two forms is only 0.1 eV (932.6 and 932.7 eV for Cu and $Cu_2O$, respectively). Taking into account the color change of the sample after reduction process from dark brown to greenish it can be assumed that initial metal form of copper was transformed into other forms due to oxidation in the air. This is in line with literature data.

The Co+OX+Cu sample was also mapped and fitted to determine the atomic concentrations across its surface and to detect the evenness of the surface. The results of the mapping of O1s, C1s and Cu2p signals are demonstrated in Fig. 4.

Though the intensity of Cu2p signal varies over the same sample, the mapping showed relatively uniform distribution of Cu-based structures across the surface of the sample.

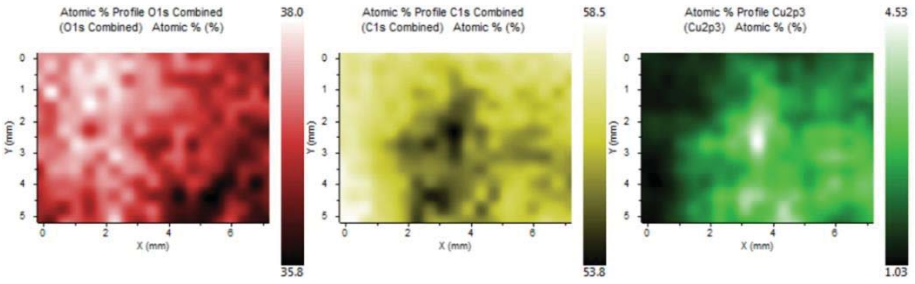


**Figure 4.** XPS maps of C1s, O1s and Cu2p signals for the Co+OX+Cu fabric

The presence of Cu-based NPs on the Co fabrics provided maximum reduction of bacteria colonies (99.9 %) in the case of both tested strains (Table 1). It is important to stress that the control Co fabric and the Co+OX fabric did not show any antibacterial activity. The mechanism of antibacterial action of Cu-based NPs is still not well understood. Antimicrobial action of Cu-based NPs is often ascribed to $Cu^{2+}$-ions release in aquatic medium in the presence of oxygen [11]. Therefore, we analyzed the release of $Cu^{2+}$-ions from the Co+OX+Cu in physiological saline solution within 24 h. Fig. 5 clearly reveals that controlled release of $Cu^{2+}$-ions occurred which is necessary precondition for infection prevention.

**Table 2.** Antibacterial activity of the Co fabric impregnated with Cu-based NPs

| Sample | Number of bacterial colonies (CFU) | R (%) | Number of bacterial colonies (CFU) | R (%) |
|---|---|---|---|---|
| | *E. coli* | | *S. aureus* | |
| Control Co | $3.5\times10^5$ | | $2.6\times10^4$ | |
| Co+OX+Cu | <10 | 99.9 | <10 | 99.9 |

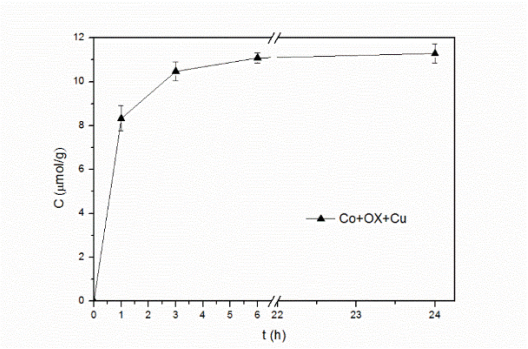


**Figure 5.** $Cu^{2+}$-ions release from the Co+OX+Cu fabric into physiological saline solution

## 4. CONCLUSIONS

Modification of cotton fabrics with oxalic acid provided the free carboxyl groups that enhanced the uptake of $Cu^{2+}$-ions. The reduction of adsorbed $Cu^{2+}$-ions resulted in the formation of Cu-based nanoparticles which were detected by FESEM analysis. Although the presence of copper was confirmed by EDX and AAS analyses, XPS analysis revealed that nanoparticles existed as a mixture of $Cu/Cu_2O$ and $Cu_2CO_3(OH)_2$. The amounts of fabricated nanoparticles on the fabric were sufficient to secure 99.9% reduction of Gram-negative bacteria *E. coli* and Gram-positive bacteria *S. aureus*. Excellent antibacterial activity and controlled release of $Cu^{2+}$-ions into physiological saline solution makes the fabricated textile nanocomposite a viable candidate for medical application.

## ACKLOWLEDGEMENT

The financial support for this study was provided by the Ministry of Education, Science and Technological Development of Republic of Serbia (projects no. 172056 and 45020).

## REFERENCES

1. Radetić M.: Functionalization of textile materials with silver nanoparticles. 2014 J Mater Sci v. 48, 95-107.
2. Simončič B., Klemenčič D. Preparation and performance of silver as an antimicrobial agent for textiles: a review. 2016. Text Res J v. 86, 210-223.
3. Yuranova T., Rincon A.G., Bozzi A., Parra S., Pulgarin C., Albers P., Kiwi J.: Antibacterial textiles prepared by RF-plasma and vacuum-UV mediated deposition of silver. 2003. J Photoch Photobio A v. 161, 27-34.
4. Eremenko A.M., Petrik I.S., Smirnova N.P., Rudenko A.V., Marikvas Y.S.: Antibacterial and antimycotic activity of cotton fabrics, impregnated with silver and binary silver/copper nanoparticles. 2016. Nanoscale Res Lett v. 11, 28.
5. Errokh A., Ferraria A.M., Conceição D.S., Vieira Ferreira L.F., Botelho de Rego A.M., Rei Vilar M., Boufi S.: Controlled growth of $Cu_2O$ nanoparticles bound to cotton fibres. 2016. Carbohyd Polym v. 141, 229-237.
6. Cady N.C., Behnke J.L., Strickland A.D.: Copper-based nanostructured coatings on natural cellulose: nanocomposites exhibiting rapid and efficient inhibition of a multi-drug resistant wound pathogen, *A. baumannii*, and mammalian cell compatibility in vitro. 2011. Adv Funct Mater v. 21, 2506-2514.
7. Kumar V., Yang T.: $HNO_3/H_3PO_4–NaNO_2$ mediated oxidation of cellulose - preparation and characterization of bioabsorbable oxidized celluloses in high yields and with different levels of oxidation. 2002. Crbohyd Polym v. 48, 403-412.
8. Praskalo J., Kostic M., Potthast A., Popov G., Pejic B., Skundric P.: Sorption properties of TEMPO-oxidized natural and man-made cellulose fibers. 2009. Carbohyd Polym v. 77, 791-798.
9. Marković D., Nunney T., Deeks C., Radovanović Ž., Radoičić M., Radetić M.: Antibacterial activity of Cu-based nanoparticles synthesized on the cotton fabrics previously modified with succinic and citric acids. 2018. Proc. of the 55th Meeting of the Serbian Chemical Society, Novi Sad, Serbia, 77-81.

10. Marković D., Nunney T., Deeks C., Radovanović Ž., Šaponjić Z., Radetić M.: The influence of 1,2,3,4-butantetracarboxylic acid on in situ synthesis of $Cu_2O$/CuO nanoparticles on the cotton fabric and its antibacterial activty. 2018. Proc. of the 55th Meeting of the Serbian Chemical Society, Novi Sad, Serbia, 82-87.

11. Ghodselahi T., Vesaghi M.A., Shafiekhani A., Baghizadeh A., Lameii M.: XPS study of the Cu@$Cu_2O$ core-shell nanoparticles. 2008. Appl. Surf. Sci. v. 255, 2730-2734.

12. Wu C.K., Yin M., O' Brien S., Koberstein T. Quantitative analysis of copper oxide nanoparticle composition and structure by X-ray photoelectron spectroscopy. 2006. Chem Mater v. 18, 6054-6058.

13. Zhu C., Osherov A., Panzer M.J.: Surface chemistry of electrodeposited $Cu_2O$ films studied by XPS. 2013. Electrochim Acta v. 111, 771-778.

# DESIGNING TEXTILE BASED SODIUM ALGINATE DRESSINGS WITH SUPER ABSORBENT POLYMERS

**Eda TUNÇ[1,2], Ezgi KÜÇÜKTOPUL[1,3], Gizem Ceylan TÜRKOĞLU[1], Sinem Yaprak KARAVANA[4], Tolga ÖNDER[5], Ayşe Merih SARIIŞIK[1]**

[1] Dokuz Eylul University, Department of Textile Engineering, Turkey
[2] Batı Basma R&D Center, Turkey
[3] Hugo Boss, İzmir, Turkey
[4] Ege University, Department Of Pharmaceutical Technology, Turkey
[5] Sağlık Bilimleri University, Gaziosmanpaşa Taksim Training and Research Hospital, Turkey

Corresponding author: gizem.turkoglu@deu.edu.tr

***Abstract:*** *In this study, textile based absorbent systems are developed to use in cyst hydatid operations caused by a parasitic infection in the liver and lung, especially in endemic regions where animal husbandry is common. The product is designed to prevent possible contamination caused by cystoma perforation in the abdominal cavity during the operation performed for cystoma removal, which will cause the formation of new cysts, and to absorb and trap the liquid to be spread into the abdominal cavity, quickly. It is aimed that the textile-based absorbent product to be designed will have a high absorbance capacity in accordance with the operation period and show a rapid absorption characteristic. Therefore, hydrogels are produced from sodium alginate solutions by ionic crosslinking. In order to enhance fluid handling capacity, super absorbent polymers were loaded to non-woven based hydrogels. Physical features (mass, thickness), absorbency characteristics and bonding properties (FT-IR) of textile based absorbent systems are examined.*

***Keywords:*** *Sodium alginate, hydrogel, super absorbent polymers, absorbency properties, medical textile*

## 1. INTRODUCTION

Although the primary duty of textile products is to protect people from environmental conditions, today textile products have gained an important place in medicine. With the developing technology, textiles can be use as materials in many different products, ranging from bandages to surgical gowns and artificial organs to vascular grafts. It is possible to use medical textiles in healthcare and hygiene products, extracorporeal devices, implantable materials, and non-implantable materials [1, 2].

Alginate is an anionic polysaccharide derived from brown seaweed, such as *Laminiaria digitata* and *L. hyperboria.* It comprises linear copolymers α-L-guluronic acid and β-D-mannuronic acid.The ratio of these copolymers determines the flexibility of the resulting cross-linked gels.Alginic acid dressings has been found to improve the rate of wound healingand cellular efficacy, such as hemostasis, adhesion and cell proliferation [3, 4].Sodium alginate can be

converted into a gel structure called the "egg box", when the sodium ion is replaced by a divalent ion such as calcium [5].

Superabsorbent polymers (SAPs) which consist of cross-linked hydrophilic structures containing anionic water-holding groups such as carboxylic acids are produced from acrylic acid (AA), its salts and acrylamide, mainly due to economic reasons, via solution polymerization or reverse-suspension polymerization techniques. The absorbency and swelling capacity of the polymer depends on the type and degree of cross-linker. SAPs with high swelling and absorption capacities are generally cross-linked at lower density whereas highly cross-link SAPs have lower absorption and swelling capacity These polymers, which have high absorption and swelling capacity, are used in water-absorbing application such as feminine hygiene products and diapers [6, 7, 8, 9].

## 2. MATERIALS AND METHODS

### 2.1. Preparation of Textile Based Absorbent Systems

In order to obtain the textile based absorbent systems, first of all optimum sodium alginate solution (1%, 2% and 4%) was prepared. Texture profile analysis (TPA) and rheological properties was examined to determine optimum sodium alginate concentration. Textile based absorbent systems was produced by two-step dipping process. In the first step, optimum sodium alginate solution with/without sodium acrylate based super absorbent polymersapplied to 100% viscose non-woven surfaces by dip-coating method. Then in the second step, the coated fabric was dipped into 0.05 M $CaCl_2$ solution for gelling.

Solubility, homogeneity, gelation properties and gel formation time of solutions prepared with sodium alginate at 20°C, were evaluated visuallyafter casting and drying.

### 2.2. Physical Properties

The mass ($g/m^2$) and thickness (mm) of the fabrics were determined in accordance with TS EN 12127 and TS EN ISO 9073-2. The thickness was determined using OMS BX1tester. The averages of five specimens were calculated.

### 2.3. Fluid Handling and Comfort Properties

Fluid handling capacity was determined according to free swell absorptive capacity, and absorption rate (s) in a specific solution containing NaCl and $CaCl_2$. Free swell absorptive capacities were determined by TS EN 13726-1. The comfort properties were evaluated according to air permeability and water vapor permeability tests.Air permeability test was performed at TEXTEST FX 3300 Air Permeability Tester III in accordance with WSP 070.1.R3.Water vapor permeability test was performed at SDL ATLAS M261 according to BS 7209: 1990.Vertical wicking test is applied to specimens cut into 15mm width and 100mm length and immersed into the solution vertically up to 10mm length and vertical wicking results were in mm after 60 seconds [10]. Rate of absorption is was evaluated with taking fully absorption time after 20 drops of specific solution

containing NaCl and $CaCl_2$ dropped onto the dressing materials. Three specimens were prepared for each test and mean values are calculated.

### 2.4. Chemical Properties

The specimens were suspended in distilledwater at a ratio of 1:100 (w/v) and kept at 20°C. The pH was measured by HANNA HI 221 after 15 min, which is designed according to operation time. The bonding between fibers and hydrogel was evaluated by Fourier Transform Infrared Spectroscopy (FT-IR).

## 3. RESULTS AND DISCUSSION

Sodium alginate solutions were casted on the petri dishes and dried at two different drying conditions (20°C: RT and 37°C: OD) to examine gel/film formation (Figure 1). The visual evaluation showed that 1% (w/v) sodium alginate solution was homogeneous but have very low viscosity, whereas 4% (w/v) solution has fragile and non-homogenous structure in the gel form. It was visually observed that the gels of 2% (w / v) sodium alginate gave the best result.The effects of drying at 37°C were darkening in color and fragility. When evaluated in terms of both casting and gel structure, studies were continued with 2% (w/v) sodium alginate solution dried at 20° C.

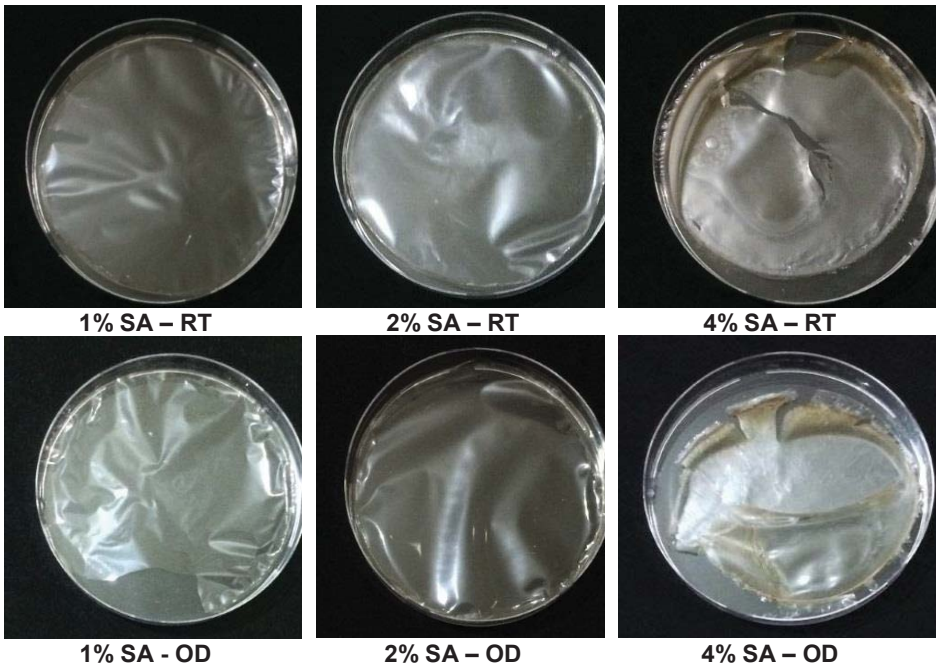


**Figure 1. S**odium alginate film formation

The solution of sodium alginate (%2) was prepared and acrylic based SAPs were added to that solution. The solutions containing SAPs at different rates (0.05%, 0.1% and 0.2% (w/v)) were applied to viscose non-woven by dip coating technique. Fabrics were immersed ina second solution composed of $CaCl_2$ right after toprovide gelation. The fabrics were named as H (%2 sodium alginate), H-SF-1 (0.01% SAP), H-SF-2 (0.1% SAP) and H-SF-3 (0.2% SAP).

Mass and thickness properties of dressings results were evaluated of hydrogel applied (H) and 0.05% (H-SF-1), 0.1% (H-SF-2) and 0.2% (H-SF-3) (w/v) super absorbent polymer containing hydrogel applied fabrics (Figure 2). When the results were examined, it was seen that the masses and thicknesses of the dressing materials increased due to the increasing amount of polymer.

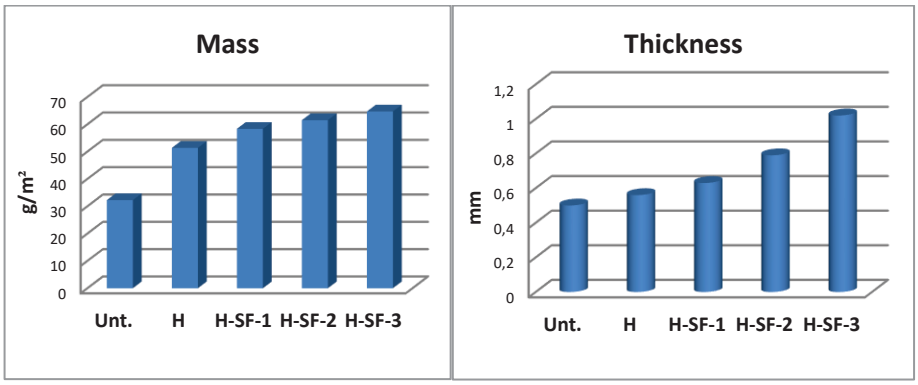


**Figure 2**. Mass and thickness properties of dressing materials

The air permeability and water vapor permeability of the non-woven surfaces were examined (Figure 3). Both air permeability and water vaporpermeability values were decrease with the hydrogel application and increase of SAP content, as expected. It also thought that the porous structure might be swollen and closed due to wet application conditions.

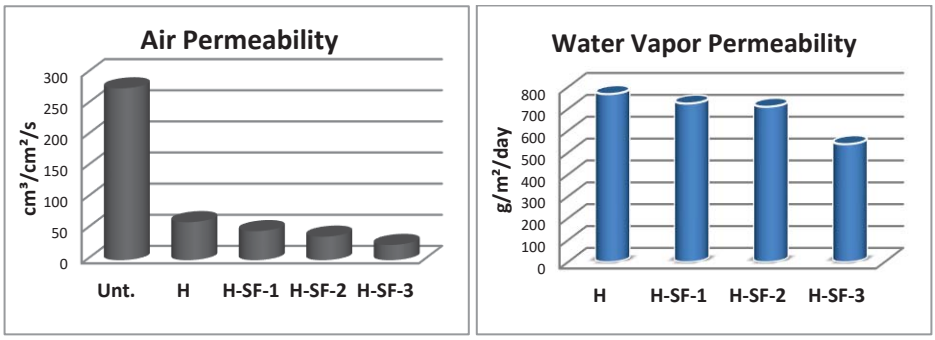


**Figure 3.** Air permeability and water vapor permeability properties

In Figure 4, fluid handling capacities and vertical wicking properties are presented. The fluid handling capacities of the samples were increased moderately with increasing SAP concentration. Vertical wicking results were examined, and it was determined that all the dressings were showed good capillary rising properties due to hydrophile nature of supporting viscose non-woven surface. With hydrogel formation and addition SAPs to the non-woven dressings, capillary rising values decreased slightly. The reason of that might cause from a rapid absorption of sodium alginate hydrogel and SAPs presented on the surface and prohibiting the water rising vertically during the one-minute test period. Therefore, dressings showed lower capillary rising features [10].

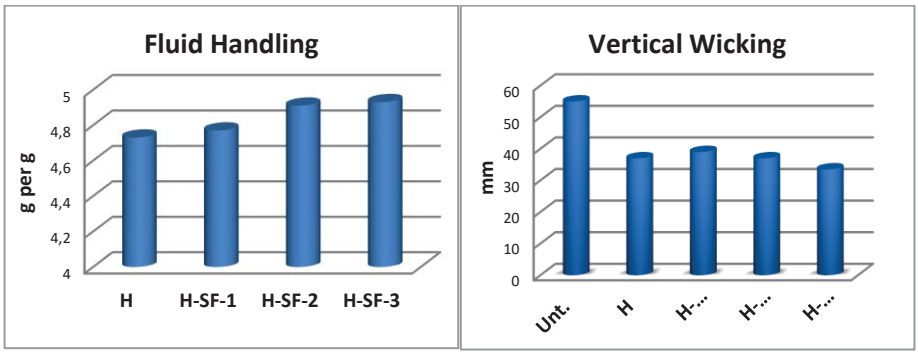


**Figure 4.** Fluid handling and vertical wicking properties

Absorption rates and pH values were determined of the dressings designed to use in operations, like cyst hydatid removal, that requiring rapid medical intervention (Table 1). Rate of absorption test showed that all the dressings have rapid absorption features. A piece of dressing was put into a distilled water (1:100 w/v) and pH was measured after 15 minutes. The results showed that solutions of all the dressings were in neutral pH range. Therefore, it would not affect adversely the operation medium.

**Table 1.** pH values and absorption rates of dressing materials

| | Untreated | H | H-SF-1 | H-SF-2 | H-SF-3 |
|---|---|---|---|---|---|
| **Rate of Absorption** | <0 s | <0 s | <0 s | <0 s | <0 s |
| **pH** | 8.22 | 7.06 | 7.56 | 7.5 | 7.43 |

FT-IR spectra (Figure 5) pointed to the hydroxyl groups on the non-woven fabric surface with the -OH peaks observed in wave lengths of 3000-3200 $cm^{-1}$. This shows the presence of moisture in the structure. It is thought that the increased depth on the hydroxyl-band is depend on the amount of super absorbent polymer.

Therefore, it may indicate that the super absorbent polymers are adhered in the sodium alginate hydrogel structure.

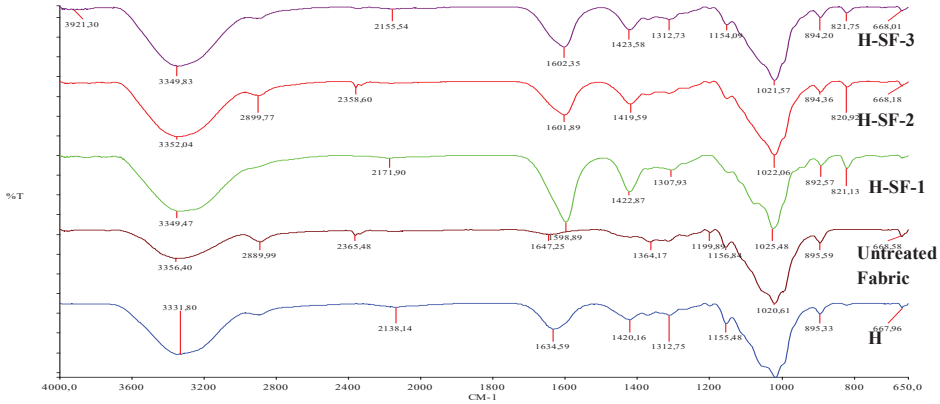


**Figure 5.** FT-IR Spectra of dressing materials

## 4. CONCLUSION

In this work, it is aimed to create textile-based hydrogel structures containing superabsorbent with sodium alginate, a natural polymer known to be biocompatible. Sodium alginate is odorless, biocompatible, cost-friendly and has high fluid handling capacity, therefore it is a suitable polymer for the developed product. When the results are evaluated, it is thought that products with rapid and high swelling properties have potential to use immediate operations as a tampon. In the later stages of the study, *in-vitro* cytotoxicity and cell proliferation properties will be examined.

## ACKNOWLEDGMENT

The authors would like to express their gratitude to Serkan KAHRAMAN from Hayat Kimya A.Ş. (Molfix) that provide super absorbent polymers to the research.

## REFERENCES

1. Horrocks A.R, Subhash C.A. (eds.): Handbook of technical textiles. Elsevier Science & Technology, Elsevier Health Sciences.2000.
2. Anand S.C., Kennedy J.F., Mirafta M., Rajendran S. (eds.): Medical textiles and biomaterials for healthcare. Elsevier Science & Technology, Elsevier Health Sciences. 2005.
3. Kamoun E.A., Kenawy E.R.S., Chen X.: A review on polymeric hydrogel membranes for wound dressing applications: PVA-based hydrogel dressings. 2017.Journal of Advanced Research, 8(3), 217-233.

4. Wang W., Liu X., Xie Y., Zhang H., Yu W., Xiong Y., Xie W., Ma, X.: Microencapsulation using natural polysaccharides for drug delivery and cell implantation. 2006. Journal of Materials Chemistry, 16, 3252–3267.
5. Yoo S.H, Song, Y.B. Chang P.S., Lee H.G.: Microencapsulation of α-tocopherol using sodium alginate and its controlled release properties. 2006. International Journal of Biological Macromolecules, 38, 25–30.
6. Yimin Q. Medical Textile Materials. 2016. Woodhead publishing Series in textile, 174, 71-87.
7. Zohuriaan-Mehr M. J.,KabiriK.: Super absorbent polymer materials: a review. 2008. Iranian Polymer Journal, 17 (6), 451-477
8. WiegandC., Abel M., Ruth P., Hipler U. C.: Super absorbent polymer-containing wound dressings have a beneficial effect on wound healing by reducing PMN elastase concentration and inhibiting microbial growth. 2011. Journal of materials science materials in medicine, 22, 2583–2590
9. AhmedR., Syed K. A.: Synthesis of süper absorbent polymer (sap) via industrially preferred route. 2016. Journal of Basic &Applied Sciences, 12, 383-387
10. Uzun, M., Anand, S.C., Shah, T.: In vitro characterization and evaluation of different types of wound dressing materials. 2013. Journal of Biomedical Engineering and Technology, 1, 1-7.

# ANTIBACTERIAL FABRIC PRODUCTION WITH PROCESS WATER OF SYNTHESIS OF NANOPARTICLE BY HYDROTHERMAL METHOD

**Burcu SANCAR BEŞEN[1], Onur BALCI[2]**

[1] Adıyaman University, Department of Textile Engineering, Turkey
[2] Kahramanmaraş Sütçü İmam University, Department of Textile Engineering, Turkey

Corresponding author: bbesen@adiyaman.edu.tr

**Abstract :**In the present study, it was aimed to produce antibacterial fabrics through using the residual water of synthesis of nanoparticles by hydrothermal process. For this purpose, zinc oxide and silver nanoparticles and zinc oxide/silver composite nanoparticles were synthesized with hydrothermal method at 98 ˚C during 120 minutes. After the process time, the synthesized nanoparticles were filtered from the process waters. The residual process waters were applied to the fabrics both padding and exhaust methods. In order to evaluate the results, the antibacterial activities of the fabrics and process waters were examined. In addition, the process waters were also investigated via TEM analysis. The results showed that whole process waters had quite high antibacterial activities and the activities changed depending on the synthesized nanoparticles. Furthermore, it was possible to save antibacterial activity to the textiles with the process water of the hydrothermal synthesis and the fabrics gained high antibacterial activity.

***Key words:*** *Antibacterial, nanoparticle, hydrothermal process, zinc oxide, silver*

## 1. INTRODUCTION

Bacterial infectious diseases are serious health problem that has drawn the public interest in worldwide as a human health danger, that causes to economic and social complications [1]. Those bacteria were found everywhere, and also on the textile fabric surfaces. The textile materials carry microorganisms such as pathogenic bacteria, odor-generating bacteria and fungi due to the adhesion of these organisms on the fabric surface [2-5]. Because of the health problems, the textile materials are wanted to be produced as having antibacterial activities and therefore numerous studies have been carried out. Development of new and effective antimicrobial agents have greatest importance [6]. Recently, nano-sized antibacterial materials draw great interest because of their effectiveness. Especially, ZnO nanoparticles have been investigated in many studies due to being a multifunctional material and non-toxic to human body [1,3].

There are many methods to produce ZnO nanoparticles. The most adopted fabrication methods include thermal evaporation, hydrothermal synthesis, sol-gel technique, simple thermal sublimation, self-combustion, polymerized complex method, vapor–liquid–solid technique, double-jet precipitation, and solution synthesis [1,3,7]. Among these methods, the hydrothermal method is promising for producing ideal material with special morphology due to the simple, fast, less

expensive, low growth temperature, high yield and controllable process conditions [3].

Although there are a lot of studies about hydrothermal method in the literature, none of them has investigated the antibacterial activity of its process water. For this reason, in the present study, we researched the possibilities of saving antibacterial activity to the textiles through using the residual water of the hydrothermal synthesis of the ZnO, Ag, and ZnO/Ag nanoparticles.

## 2. MATERIAL AND METHOD

### 2.1. Material

In this experimental study, zinc nitrate hexahydrate, zinc acetate, silver nitrate, silver acetate, hexamethylenetetramine (HMTA) and ethanol purchased from MERC were used for hydrothermal synthesis of ZnO, Ag, and ZnO/Ag nanoparticles. In the application studies, the pretreated 100% cotton plain weave fabric (warp 30/1 combed yarn-50 thread/cm; weft 20/1 combed yarn-22 thread /cm), laboratory type fulard for padding method, and laboratory type HT dyeing machine for exhaust method were used. The distilled water was also used in the processes.

### 2.2. Method

In order to obtain the process waters of the hydrothermal method, ZnO, Ag, and ZnO/Ag nanoparticles were synthesized at 98˚C during 120 minutes. In any methods, 0.01 M zinc salt, 0.01 M silver salt, 0.01 M HMTA, and 200 ml distilled water-200 ml ethanol were used. After the process time, the synthesized nanoparticles were filtered and the residual waters were used in the applications without diluting according to experimental plan given in Table 1. The residual process waters were also coded as 1W-8W, since same waters were used both in the padding and exhaust processes.

**Table 1.** The experimental plan of the application studies

| Experimental Number | Zinc Salt | Silver Salt | HMTA | Application Method |
|---|---|---|---|---|
| 1-**9** | Zinc nitrate | - | ✓ | Exhaust- **Padding** |
| 2-**10** | Zinc acetate | - | ✓ | Exhaust- **Padding** |
| 3-**11** | Zinc nitrate | Silver acetate | ✓ | Exhaust- **Padding** |
| 4-**12** | Zinc nitrate | Silver nitrate | ✓ | Exhaust- **Padding** |
| 5-**13** | Zinc acetate | Silver acetate | ✓ | Exhaust- **Padding** |
| 6-**14** | Zinc acetate | Silver nitrate | ✓ | Exhaust- **Padding** |
| 7-**15** | - | Silver acetate | ✓ | Exhaust- **Padding** |
| 8-**16** | - | Silver nitrate | ✓ | Exhaust- **Padding** |

*-: Absence ✓: Presence*

The exhaust method was carried out at 40˚C during 30 minutes with liquor ratio of 1:10 in HT dyeing machine while the fabrics were squeezed up to 80% pick up

in the padding method. After the applications, the fabric samples were dried at the room temperature.

After the applications, the antibacterial activities of the fabric samples were measured against *E.Coli* and *S. Aureus* bacteria with ASTM 2149-01 Standard. In addition, the antibacterial activities of the process waters used in the applications were examined via agar diffusion plate test against *E.Coli* bacteria and TEM analyses were also carried out to the waters.

## 3. RESULTS AND DISCUSSION

### 3.1. The Antibacterial Activities and TEM Results of the Process Waters

The inhibition zones of the process waters investigated with agar diffusion plate test were given in Table 2.

**Table 2**. The antibacterial activity results of the process water

| Process water | Inhibition zone (mm) |
|---|---|
| **1W** | 13 |
| **2W** | 13 |
| **3W** | 26 |
| **4W** | 33 |
| **5W** | 25 |
| **6W** | 32 |
| **7W** | 36 |
| **8W** | 36 |

When the inhibition zones were evaluated, the results were given as resistance (≤12), intermediate (13-15) and susceptible (≥16) according to the CLSI (Clinical and Laboratory Standards Institute) recommendations [8]. Table 2 showed that all of the process waters had high inhibition zones against *E. coli* bacteria and all of the results were higher than resistance limit. Thus, it could be possible to say that all of the process waters had antibacterial activities. When the Table 2 was investigated in detail, it could be seen that the inhibition zones had been changed depending on the combination of the salts used in the experimental. The highest antibacterial activities were achieved when the silver salts were used alone, while the lowest ones were obtained when zinc salts used alone. The results indicated that the salts used in the hydrothermal processes were crucial for the antibacterial activities of the process waters.

The TEM images of the process waters were given in Figure 1.

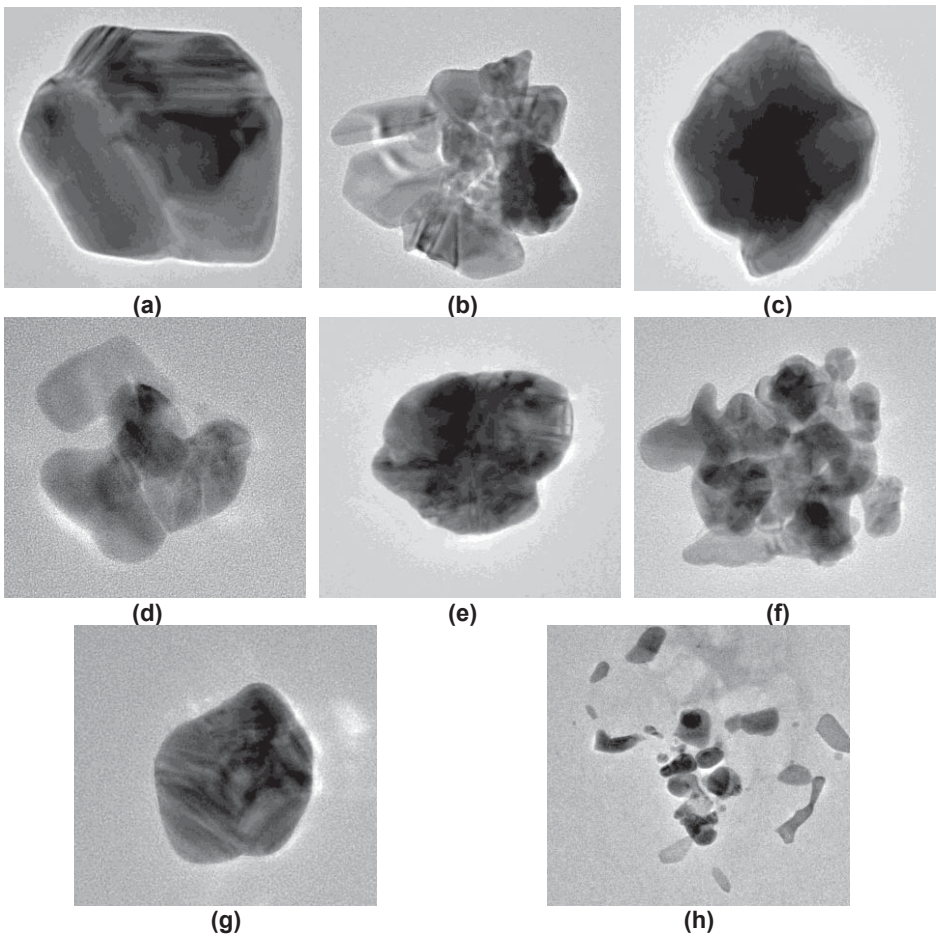


**Figure 1.** TEM images of the process waters a.1W, b.2W, c.3W, d.4W, e.5W, f.6W, g.7W, h.8W

Figure 1 demonstrated that there were Zn, Ag or Zn/Ag nanoparticles having smaller than 200 nm dimensions in the process waters which were not be able to be filtered. It was thought that the antibacterial activities of the process waters resulted from those nanoparticles in the waters.

### 3.2. The Antibacterial Activities of the Fabric Samples

The antibacterial activity results of the fabric samples applied to the process waters with exhaust process and padding method were given in Table 3 and Table 4, respectively.

**Table 3.** The antibacterial activity results of the fabric samples applied with exhaust method

| Sample Code | E.Coli | | | S.Aureus | | |
|---|---|---|---|---|---|---|
| | Number of initial bacteria/ml* | Number of bacteria after 4 hours/ml* | Reduction | Number of initial bacteria/ml* | Number of bacteria after 4 hours/ml* | Reduction |
| **1** | 4.4 | 0 | % 100 | 5.0 | 0 | % 100 |
| **2** | 3.6 | 0 | % 100 | 2.8 | 0 | % 100 |
| **3** | 3.8 | 0 | % 100 | 2.6 | 0 | % 100 |
| **4** | 5.0 | 0 | % 100 | 3.2 | 0 | % 100 |
| **5** | 4.9 | 0 | % 100 | 2.0 | 0 | % 100 |
| **6** | 2.6 | 0 | % 100 | 3.0 | 0 | % 100 |
| **7** | 6.2 | 0 | % 100 | 4.0 | 0 | % 100 |
| **8** | 5.8 | 0 | % 100 | 4.5 | 0 | % 100 |

*1.000.000

**Table 4.** The antibacterial activity results of the fabric samples applied with padding method

| Sample Code | E.Coli | | | S.Aureus | | |
|---|---|---|---|---|---|---|
| | Number of initial bacteria/ml* | Number of bacteria after 4 hours/ml* | Reduction | Number of initial bacteria/ml* | Number of bacteria after 4 hours/ml* | Reduction |
| **9** | 6.1 | 0 | % 100 | 4.1 | 0 | % 100 |
| **10** | 3.5 | 0 | % 100 | 4.0 | 0 | % 100 |
| **11** | 7.4 | 0 | % 100 | 2.6 | 0 | % 100 |
| **12** | 4.0 | 0 | % 100 | 1.9 | 0 | % 100 |
| **13** | 2.0 | 0 | % 100 | 3.5 | 0 | % 100 |
| **14** | 4.0 | 0 | %100 | 2.9 | 0 | %100 |
| **15** | 5.5 | 0 | % 100 | 6.0 | 0 | % 100 |
| **16** | 2.9 | 0 | % 100 | 4.6 | 0 | % 100 |

*1.000.000

When Table 3 and Table 4 were focused, it could be seen that all of the bacteria in the medium had killed after 4 hours for whole samples and the samples had gained 100% antibacterial activity against both *E.Coli* and *S.Aureus* after the applications with the process water. In addition, the methods of which the applications were carried out (padding or exhaust) did not affect the antibacterial activity results. Therefore, it could be possible to say that the determined application conditions were quite acceptable for applying the process waters having high antibacterial activity to the fabrics. Besides, it was possible to save antibacterial activity to the textiles through using the process water of the nanoparticle synthesis by hydrothermal method.

## 4. CONCLUSION

In the present study, the possibility of saving antibacterial activity to the textiles via using the process water of the hydrothermal synthesis were investigated. For this reason, ZnO, Ag, and ZnO/Ag nanoparticles were synthesized and the they were filtered. After the filtration, the residual process waters were used in order to save antibacterial activity to textile fabrics. The process waters were applied through padding and exhaust methods at the determined process conditions.

After the treatments, the antibacterial activities of the process waters and the fabric samples applied process waters were investigated. In addition, the TEM images of the waters were taken for researching the particles in the waters. The findings showed that the process waters had high antibacterial activities and there were the smallest nanoparticles which were not be able to be filtered in the waters. Besides, the results demonstrated that it was possible to save antibacterial activity to the textile surfaces with the process water of the synthesis of nanoparticles by hydrothermal method and the determined process conditions in this study provided quite high antibacterial activity to the fabric samples.

## REFERENCES


1. Sirelkhatim, A., Mahmud, S., Seeni, A., Kaus, N.H.M., Ann, L.C., Bakhori, S.K.M., Hasan, H., Mohamad, D.: Review on Zinc Oxide Nanoparticles: Antibacterial Activity and Toxicity Mechanism. 2015. Nano-micro Letters v.7(3), 219-242.
2. Abedi, D., Mortazavi, S.M, Mehrizi, M.K., and Feiz, M..: Antimicrobial Properties of Acrylic Fabrics Dyed with Direct Dye and a Copper Salt. 2008. Textile Research Journal v.78(4), 311-319.
3. Balcı, O., Alver, Ü., Sancar Beşen., B., Tanrıverdi, A., Tutak, M.: In-situ Generation of ZnO on the Textile Surfaces by Hydrothermal Method. 2014. Industria Textila v.65(2), 80-84.
4. Palamutcu, S., Keskin, R., Devrent, N., Sengül, M., Hasçelik, B.: Functional Textiles II: Antimicrobial Textiles. 2009. Electronic Journal of Textile Technologies, v.3(3), 95-108.
5. Ursache, M., Loghin, C., Mureşan, R., Cerempei, A., Mureşan, A.: Investigation on the Effects of Antibacterial Finishes on Dyed Cotton Knitted Fabrics. 2011. Textile and Apparel v.3, 249-256.
6. Küçük, D., Balcı, O., Tutak, M: In-situ Coated of Ag, ZnO, Ag/ZnO Composite Nano Particles to the Technical Fiber by Hydrothermal Method. 2016. International Journal of Clothing Science and Technology v.28(3), 340-67
7. Bacaksiz, E., Aksu, S., Yılmaz, S., Parlak, M., Altunbaş, M.: Structural, Optical and Electrical Properties of Al-doped ZnO Microrods Prepared by Spray Pyrolysis. 2010. Thin Solid Films v. 518(15), 4076-4080.
8. Çağan Aktaş, S., Gençer, S., Ayşe Batirel[1], Haciseyitoğlu, D., Özer, S.: Fosfomycin Susceptibility of Urinary *Escherichia coli* Isolates Producing Extended-Spectrum Beta-Lactamase According to CLSI and EUCAST Recommendations 2014. Bulletin of *Microbiology v.48(4), 545-555.*

# POROSITY MEASUREMENT OF MICROFILAMENT FABRICS BY IMAGE PROCESSING AND PREDICTION OF AIR PERMEABILTY BY REGRESSION ANALYSIS

**Elif GÜLTEKİN[1], Maher ALSAYED[1], Halil İbrahim ÇELİK[1], Hatice Kübra KAYNAK[1], Osman BABAARSLAN[2]**

[1] Gaziantep University, Department of Textile Engineering, Turkey
[2] Çukurova University, Department of Textile Engineering, Turkey

Corresponding author: tuluce@gantep.edu.tr

***Abstract:*** *Filament woven fabrics are widely used for the end uses such as parachutes, sails, wind-proof clothes, sleeping bags, tents, filters and surgical textiles. For these application areas, fabrics woven from microfilament yarns serve advantage as good barrier effect owing to low level of porosity in the yarn structure. Air permeability measurement is a widely used assessment for determination of barrier effect and is strongly related with the porosity of the fabric. On the other hand, image processing is a very effective technique for determination of the total porosity of filament woven fabrics which is composed of porosity between the yarns and between the filaments. Since, the porosity is determined by the light transmission. In this study, polyester filament woven fabrics were produced with 1/4 satin weave structure, with four different weft sett and using five different filament linear density in weft yarn. By this way 20 woven fabrics are obtained. It is intended to use image processing techniques to obtain porosity values of the fabric samples and then the regression analysis were used to predict the air permeability value of fabrics by using porosity, thickness and fabric mass parameters.*

***Key Words****: air permeability, microfilament, woven fabric, image processing, filament linear density*

## 1. INTRODUCTION

Producing microfilaments (fibers have linear density below 1 dtex) are considered as an important development in the synthetic fiber technology world, due to their high performance and their very compact structure as a result of the existence of the small pores between yarns and between the fibers of yarns. Fabrics which are produced from microfilaments have a good barrier property. In addition, the microfilaments provide light weight and durability. For these reasons, we can use high density woven fabrics produced from microfilament yarns as surgical gowns, parachutes, sails, wind proof clothes and tents, etc. [1].

Surgical gowns should provide us a barrier effect against the infection source and also should give us a comfortable sensation. Bacteria and viruses are considered as micro-organisms which are in charge of spreading the illnesses [2]. Another important parameter to demonstrate effective barrier function and ease of use is

the pore morphology of textile structures. High density woven fabrics produced from microfilament yarns are suitable for providing a good barrier effect among their small pores between filaments preventing micro-organism passage. The factors which affect the barrier function are: the surface structure of the fabrics, the number and the size of the continues pores through the fabrics, where the pores of the fabric appear between yarns and between the filaments of the yarns [3].

Surgical gown fabric should provive extremely low air permeability for a high level of barrier effectiviness. In general, air permeability relays on the substance of constitutional yarns and structural parameters of the fabric known as fabric geometry. Air permeability is affected by the pore characteristics of the fabric that is function of fabric geometry.

In the literature there are many studies focused on the influence of woven fabric construction on their porosity and air permeability [5-18]. Among these studies, some of them focused on determination of porosity by image processing techniques. Previous investigations have been conducted to relieve the evaluation of the barrier effect on surgical gowns, as well as on its relaxation properties. For this reasons it is necessary to known the influences of the fabric's constructional parameters, such as the linear density of the filament yarns, type of weave and fabric density on the pore structure. These studies show the pore structure of commercially available woven fabrics by using the image processing technique viewing the fabric cross-sections with different constructions. These studies were predicted to facilitate the usage of suitable choice with filament fineness, yarns and fabric weave parameters which improved barrier performance [15-18]. But, in the literature there is a lack of information about determination of porosity of high density woven fabrics and correlation between porosity and air permeability. Apart from the literature, in this study it is aimed to study the porosity of high density woven fabrics produced from microfilament yarns for a usage area of surgical gowns. For this aim, polyester filament woven fabrics were produced with 1/4 satin weave structure, with four different weft sett and using five different filament linear density in weft yarn. By this way 20 woven fabrics are obtained. It is intended to use image processing techniques to obtain porosity values of the fabric samples and then the regression analysis were used to predict the air permeability value of fabrics by using porosity, thickness and fabric mass parameters.

## 2. MATERIALS AND METHOD

The air permeability of a fabric is defined as the amount of air passed over a surface under a certain pressure difference in a unit time. The value of the air permeability determines significantly the end-use performance of the fabrics [4].

In this study, polyester filament woven fabrics were used, it was aimed to investigate the effects of filament linear density and weft sett on porosity and air permeability properties of them.

The chosen filament linear densities in weft direction were polyester microfilament textured yarns of 110 dtex with 0.33, 0.57 and 0.76 dtex filament linear densities and conventional polyester textured yarns of 110 dtex with 1.14 and 3.05 dtex filament linear densities. On the other hand, for warp yarn 83 dtex polyester yarn with 1.14 dtex filament linear density was used.

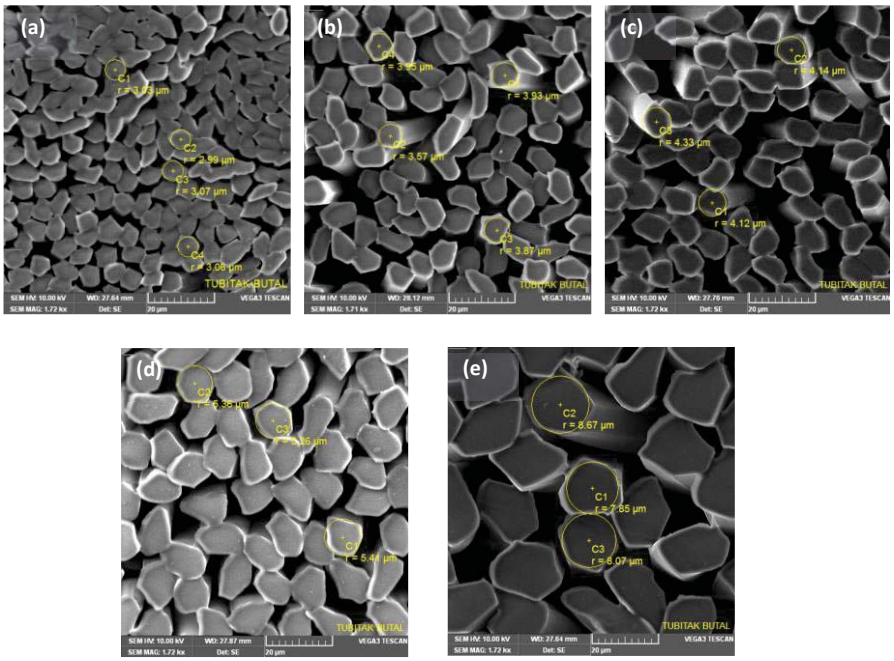


**Figure 1.** Cross-sectional SEM views of weft yarns with (a) 0.33 dtex, (b) 0.57 dtex, (c) 0.76 dtex, (d) 1.14 dtex, (e) 3.05 dtex filament linear density with 1720 times magnification

It can be inferred from Figure 1 that the higher filament linear density means having lower number of filaments in yarn cross section. The texturizing process was applied to the yarns in order to increase the bulkiness of the yarns. After this process, it seen from SEM views that the cross section geometry of the filaments changed from round shape to the cornered one due to the applied heat and mechanical forces. In order to investigate the influence of filament fineness on fabric performance, the yarn samples were used for woven fabric production with the same weave type of 4/1 Satin. Each fabric sample was woven with four different weft setts; 43 wefts/cm, 45 wefts/cm, 47 wefts/cm and 49 wefts/cm. Our 20 woven fabric samples were produced with warp sett of 85 warps/cm. Thermal fixation process was applied to samples at 195ºC with 25m/min process speed. Structural properties namely, weft sett, fabric weight, fabric thickness and yarn crimp of sample fabrics were determined according to TS 250 EN 1049-2 (1996),

TS EN 12127(1999), TS 7128 EN ISO 5084 (1998) and TS 254(1989), respectively. Structural properties of the sample fabrics are given in Table 1.

**Table 1.** Structural properties of sample fabrics

| Weft yarn filament linear density, dtex | Weft sett, wefts/cm | Fabric weight, g/m² | Fabric thickness, mm | Weft crimp, % | Warp crimp, % |
|---|---|---|---|---|---|
| **0.33** | 43 | 130 | 0.22 | 6 | 5 |
| **0.57** | 43 | 130 | 0.22 | 6 | 5 |
| **0.76** | 43 | 128 | 0.22 | 6 | 5 |
| **1.14** | 43 | 129 | 0.22 | 6 | 5 |
| **3.05** | 43 | 129 | 0.23 | 6 | 5 |
| **0.33** | 45 | 133 | 0.23 | 6 | 5 |
| **0.57** | 45 | 133 | 0.22 | 6 | 5 |
| **0.76** | 45 | 132 | 0.22 | 6 | 5 |
| **1.14** | 45 | 131 | 0.22 | 6 | 5 |
| **3.05** | 45 | 132 | 0.23 | 6 | 5 |
| **0.33** | 47 | 136 | 0.23 | 6 | 5 |
| **0.57** | 47 | 136 | 0.22 | 6 | 5 |
| **0.76** | 47 | 134 | 0.23 | 6 | 5 |
| **1.14** | 47 | 132 | 0.23 | 6 | 5 |
| **3.05** | 47 | 133 | 0.23 | 6 | 5 |
| **0.33** | 49 | 138 | 0.23 | 6 | 5 |
| **0.57** | 49 | 140 | 0.23 | 6 | 5 |
| **0.76** | 49 | 138 | 0.23 | 6 | 5 |
| **1.14** | 49 | 139 | 0.22 | 6 | 5 |
| **3.05** | 49 | 136 | 0.23 | 6 | 5 |

To get knowledge about barrier effectiveness of polyester filament woven fabrics and analyze them to reveal the effects of filament fineness and weft sett, air permeability test was conducted. All fabric samples were conditioned according to TS EN ISO 139 (2008) before the tests and the tests were performed in the standard atmosphere of 20±2ºC and 65±4% relative humidity. Air permeability was determined according TS 391 EN ISO 9237 (1999) with ten measurements from each sample, by a digital air permeability test device at 200 Pa pressure drop and 20 $cm^2$ test area.

The porosity is one of the most important parameter that affects the air permeability behavior of the fabrics [20]. So, the porosity properties of the fabric samples were determined to deduce the relationship between air permeability and porosity. In this study, image processing technique was used to measure the porosity values. Some different approaches were offered for porosity measurement with image processing method [15-18]. Generally there are two different lightening systems; the back lightening and the front one in the literature [21]. For this study, the back lightening system was used and was installed under the fabric samples. The camera was placed on the top of sample so that the amount of light intensity that passes through the fabric structure could be detected. The image processing method is based on measurement of the light

intensity transmitted through the fabric structure. The pixel values of the image frame are assigned according to the light transmission level so that pore regions are seen bright while the regions covered by fibers are seen dark. In this study, the porosity of the fabric samples was determined by using image processing algorithm. The image frames were acquired by using a digital microscope camera. Ten image frames were acquired from different place of each sample in order to obtain an average porosity value. So, totally 200 sample image frames were processed. The porosity ratio is determined as average of ten measurements of each sample. The image frames get in RGB format were convert to 8 bit gray level images. The image frames were applied the low pass Gaussian filter. The Gaussian filter makes the image frame smoother and removes certain types of noise [11]. The filtered image is then applied binarization process. Each pixel of the image frame is converted to black or white color according to being below or above threshold level. The threshold level is calculated by using Otsu method [12]. If the pixel value of the image frame is below threshold level, the gray level value of that pixel is allocated as “0”. Otherwise, it is set as “1”. The pixel value “1” corresponds to white and “0” corresponds to black. In the binary image frame, the white regions indicate the pores and the black regions indicate the fibers. In order to clear the area of pores, morphological operations; opening and erosion are applied in sequence. Opening is a morphological operation of erosion followed by dilation with the same structuring element. The opening operation removes small, isolated objects from the foreground of an image, place them in the background. It smoothes the contour of a binary object, breaks the narrow joining regions and eliminates the thin protrusions. In the erosion operation, the center pixel of the structuring element is placed on each foreground pixel value 1. If any of the neighborhood pixels are background pixels value 0, then the foreground pixel is switched to background. Finally, the pore areas (white regions) of the binary are labeled as seen in Figure 2. The porosity value of the sample was calculated as the percentage of white regions to whole image frame size.

## 3. RESULTS AND DISCUSSION

### 3.1 Porosity Results

The general accepted knowledge about the relationship between the porosity and fabric density is that when weft or warp setts of fabric structure increases, the yarns get closer to each other and so the porosity of the fabric decreases. But these results are obtained with the fabric types with low or medium density. Theoretical or experimental porosity measurement methods are not valid for high density fabrics which are woven from microfilament yarns. Since, there is high number of filaments in yarn cross-section with microfilaments than conventional filaments. Microfilaments occupy higher area and provide less spaces between each other. The higher compactness and small pores between fibers and yarns in the high density fabric structure leads to lower liquid or gas flow and less light transmittance. Therefore, it is very difficult to study on the porosity measurement

of high density microfilament fabrics. The porosity values of the samples obtained by image processing technique is given in Figure 3. As given in Figure 3, there is no significant change between the porosity values of the fabric samples with 0.33 and 0.57 dtex filaments at different weft sett values. It is considered that the lower filament linear density in yarn cross-section cause very small pores in fabric structure and this situation compensates the effect of weft sett change on fabric porosity. When the filament linear density is increased to 0.76 dtex, the porosity difference is observed in accordance with weft sett change. The effect of the weft sett on fabric porosity can be evaluated for the samples with 1.14 and 3.05 dtex filament linear density. However, there is no regular relationship between different weft sett values. Except for the fabrics which produced with 0.33, 0.57 and 0,76 dtex microfilament yarns, the effect of weft sett was obviously seen on the fabrics which produced with 1.14 and 3.05 dtex microfilament yarns. After the filament fineness of 0.76 dtex, for each weft sett the porosity values of the fabric increases when the filament linear density increases.

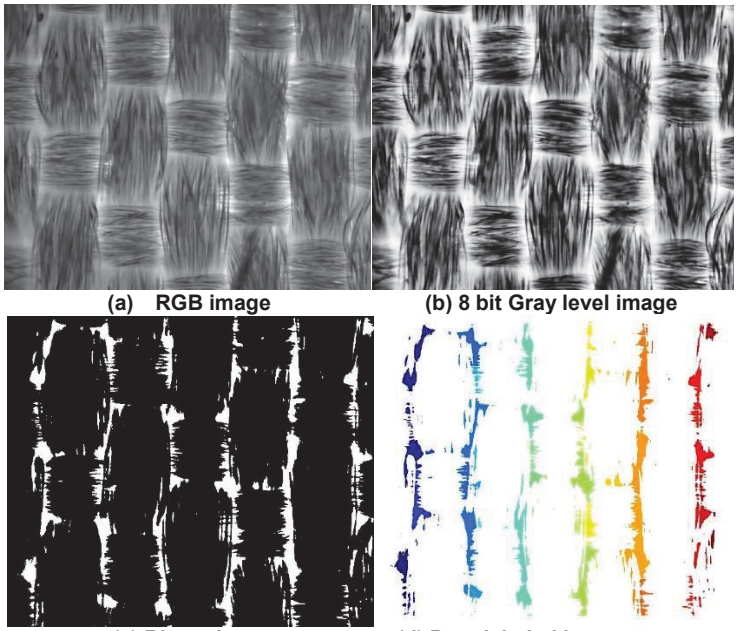


**Figure 2.** Porosity algorithm application

### 3.2 Air Permeability Results

The target of this study is to find out the effects of filament linear density on air permeability of microfilament (0.33 dtex, 0.57 dtex and 0.76 dtex) and conventional filament (1.14 dtex and 3.05 dtex) ranges. In addition, this issue was stated by satin structure by applying different weft setts. In this study, to get reliable samples we obtained our 20 woven fabrics systematically.

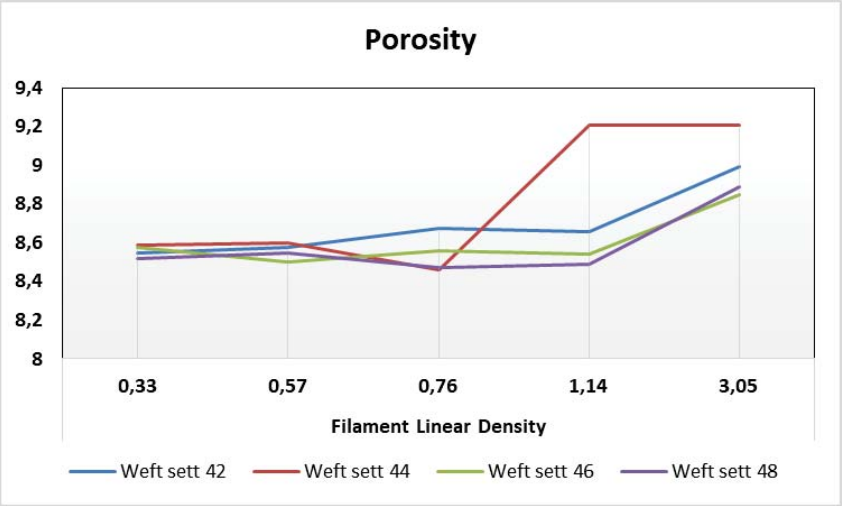


**Figure 3.** Porosity of satin fabric

It is clear from Figure 4 that the weft sett values cause an obvious decrease of air permeability as a result of that, the lower weft sett provide higher air permeability. On the other hand, the higher filament linear density results in higher air permeability. As mentioned above, as the filament becomes coarser, air permeability becomes higher because more spaces in the cross section are obtained. On the other hand, air permeability gets decreased with finer filaments because there is less space within the yarns.

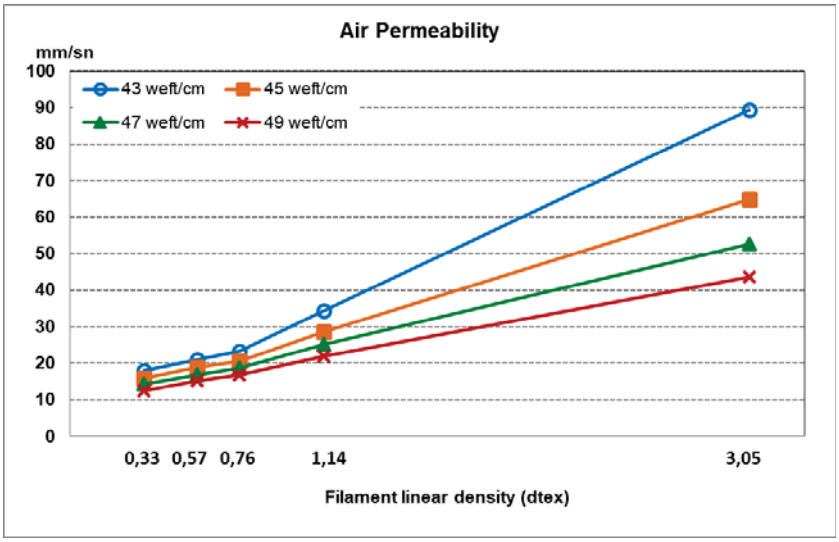


**Figure 4.** Air permeability of samples

For statistical analyses SPSS 21.0 statistical package program was used. For this issue correlation analyses were applied to air permeability, porosity, fabric weight and fabric thickness. The results are given in Table 2. According to correlation analysis, it is seen that there is a strong and positive correlation (r = 0.877) between fabric porosity and air permeability, at 1% significance level. In the view of thickness effect, it can also be said that there is a low and positive correlation (r = 0.377) between fabric thickness and air permeability. The analysis indicates low and positive correlation between fabric thickness and air permeability. The correlation between the fabric weight and air permeability is determined as low and the relationship is negative (r=-0.314). That means when the fabric weight increases, the air permeability of fabric decreases.

**Table 2.** Correlation analysis between air permeability and fabric structural features

| | | Porosity | Air permebility | Fabric thickness | Fabric weight |
|---|---|---|---|---|---|
| **Porosity** | **Pearson Correlation** | 1 | 0.877** | 0.377 | -0.314 |
| | **Sig. (2-tailed)** | | 0.000 | 0.102 | 0.177 |
| | **N** | 20 | 20 | 20 | 20 |
| **Air permebility** | **Pearson Correlation** | 0.877** | 1 | 0.283 | -0.391 |
| | **Sig. (2-tailed)** | 0.000 | | 0.226 | 0.088 |
| | **N** | 20 | 20 | 20 | 20 |
| **Fabric thickness** | **Pearson Correlation** | 0.377 | 0.283 | 1 | 0.378 |
| | **Sig. (2-tailed)** | 0.102 | 0.226 | | 0.100 |
| | **N** | 20 | 20 | 20 | 20 |
| **Fabric weight** | **Pearson Correlation** | -0.314 | -0.391 | 0.378 | 1 |
| | **Sig. (2-tailed)** | 0.177 | 0.088 | 0.100 | |
| | **N** | 20 | 20 | 20 | 20 |
| **. Correlation is significant at the 0.01 level (2-tailed). | | | | | |
| b. Cannot be computed because at least one of the variables is constant. | | | | | |

**Table 3.** Multiple linear regression analysis for fabric structural features affecting air permeability

| **Coefficients[a]** | | | | | | |
|---|---|---|---|---|---|---|
| Model | | Unstandardized Coefficients | | Standardized Coefficients | t | Sig. |
| | | B | Std. Error | Beta | | |
| 1 | (Constant) | -605.069 | 160.449 | | -3.771 | 0.002 |
| | Porosity | 82.850 | 14.966 | 0.820 | 5.536 | 0.000 |
| | Fabricthickness | 112.567 | 588.941 | 0.029 | 0.191 | 0.851 |
| | Fabricweight | -.804 | 0.824 | -0.145 | -0.977 | 0.343 |
| a. Dependent Variable: AirPermebility | | | | | | |

According to linear regression analysis (Table 3), the regression equation is obtained as below. When the fabric structural parameters; fabric weight, thickness and porosity are evaluated together in multiple linear regression analysis in terms of effect on the air permeability performance, it can be

concluded that the porosity has the most significant effect. The effect of the thickness on air permeability performance is obviously less than porosity. The fabric weight has negative effect on air permeability performance of fabric samples.

The regression analysis was used to predict the air permeability value of fabrics by using porosity, thickness and fabric mass. Obtained regression equation is given below.

$$Air\ permeability\ \left(\frac{mm}{s}\right) = -605.069 + 82.850\ \ porosity\ + 112.567\ thickness - 0.804\ \ fabric\ mass$$

## 4. CONCLUSION

Microfilament fabrics are exposed to various environmental conditions according to their usage area. Barrier effect parameter which is crucial for surgical gowns produced from high density microfilament fabrics is the uppermost characteristic. Since this characteristic property defines the ability of protecting the user from various bacteria and microorganisms. Pore morphology of textile structure is a very important parameter for high density fabrics.

There is a strong relationship between air permeability and porosity. We clearly observed that filament linear density and weft sett of fabrics have considerable effects on air permeability of fabrics. Higher porosity in fabric structure provides an easier passage of air through the fabric and air permeability increase. In other words, higher barrier effect or lower air permeability is possible with lower porosity which can be obtained by low amount of pores between the yarns and also between the filaments in yarn structure.

According to the results of our study, image processing is a very effective technique for determination of the total porosity of filament woven fabrics which is composed of porosity between the yarns and between the filaments.

## REFERENCES

1. O. Babaarslan & H.K. Kaynak, (2011)“Air Permeability of Windproof Polyester Microfilament Fabrics at Different Pressure Drop Values” .
2. Aibibu D., Lehmann B., and Offermann P., “Image Analysis for Testing and Evaluation of the Barrier Effect of Surgical Gowns Dilibaier,” vol. 3, no. 2, pp. 1–8, 2003.
3. Aibibu D., Lehmann B., and Offermann P., “Barrier effect of woven fabrics used for surgical gowns,” *Autex Res. J.*, vol. 3, no. 4, pp. 186–193, 2003.
4. Ogulata R.T. and Mavruz S., “Investigation of porosity and air permeability values of plain knitted fabrics,” *Fibres Text. East. Eur.*, vol. 82, no. 5, pp. 71–75, 2010.
5. Ogulata R.T. and Mezarcioz S., “Total porosity, theoretical analysis, and prediction of the air permeability of woven fabrics,” *J. Text. Inst.*, vol. 103, no. 6, pp. 654–661, 2012.
6. Ogulata R.T., “Air Permeability of Woven Fabrics,” *J. Text. Apparel, Technol. Manag.*, vol. 5, no. 2, pp. 1–10, 2006.
7. Zupin Z., Hladnik A., and Dimitrovski K., D.(2012)“Prediction of one-layer woven fabrics air permeability using porosity parameters,” *Text. Res. J.*, vol. 82, no. 2, pp. 117–128, 2012.

8. Militky J., Vik M., Vikova M., and Kremenakova D., "Influence of fabric construction on their porosity and air permeability," *Proc. 2nd Sci. Conf. "International Symp. Text. Eng.*, pp. 1–18, 2004.

9. Dubrovski D.P.and Brezocnik M., "The Usage of Genetic Methods for Prediction of Fabric Porosity," *Genet. Program. - New Approaches Success. Appl.*, pp. 171–198, 2012.

10. Atmaca M, Dal V., Yılmaz A. and Kurtulus A.B., D. (2015) Investigation of the effects of fabric parameters on air permeability of woolen fabrics Textile Research Journal 2015, Vol. 85(20) 2099–2107

11. Havlová M. Air Permeability and Costructional Parameters of Woven Fabrics. FIBRES & TEXTILES in Eastern Europe 2013; 21, 2(98): 84-89.

12. Guocheng Z. , Fang Y. , Zhao Li , Wang J. and Chen W., D.( 2017) Prediction of structural parameters and air permeability of cotton woven fabric Textile Research Journal ! The Author(s) 2017

13. Afzal, A., Hussain, T., Malik, M. H., and Javed, Z. (2015). Predıctıon And Correlatıon Of Aır Permeabılıty And Lıght Transmıssıon Propertıes Of Woven Cotton Fabrıcs Autex Research Journal, Vol. 17, No 1

14. Gadah Ali Abou Nassif. Effect of Weave Structure and Weft Density on the Physical and Mechanical Properties of Micro polyester Woven Fabrics. *Life Sci J* 2012; 9(3):1326-1331]. (ISSN: 1097-8135). http://www.lifesciencesite.com. 191

15. Regab A, Fouda A, El-Deeb H, Abou-Taleb H (2017) Determination of Pore Size, Porosity and Pore Size Distrubition of Woven Structures by Image Analysis Techniques. J Textile Sci Eng 7: 314. Doi: 10.4172/2165-8064.1000314

16. Turan R.B., Okur A., Deveci R. and Açıkel M. (2011) Predicting the Intra-yarn Porosity by Image Analysis Method. Textile Research Journal 85(16) 1720-1728

17. Çay A., Vassiliadis S., Rangoussi M., and Tarakçıoğlu I. (2005) On the Use of Image Processing Techniques fort he Estimation of the Porosity of Textile Fabrics. Word Academy of Science, Engineering and Technology 2 2005

18. Aibibu D., Lehmann B., Offermann P. (2003) Image Analysis for Testing and Evaluation of the Barrier Effect of Surgical Gowns. Journal of Textile and Apparel, Technology and Management Volume 3, Issue 2, Fall 2003

19. Vassiliadis S., Matsouka D., Inogamdjanov D., Beart F., Çay A. and Priniotakis G., (2018) Effect of Weaving Patterns on The Porosity of Woven Fabrics. AUTEX World Textile Conference, June 20-22,2018. ID No M 02.

20. Çelik H.İ, D. (2017) Determination of Air Permeability Property of Air-Laid Nonwoven Fabrics Using Regression Analyses. Periodicals of Engineering and Natural Sciences Vol.5, No.2, June 2017, pp. 210~216

21. Hanbay K., Talu M.F., Özgüven O.F., D. (2016) Fabric defect detection systems and methods—A systematic literature review. Optik 127 (2016) 11960–11973

# MOISTURE MANAGEMENT PROPERTIES OF THERMALLY ENHANCED DENIM FABRICS BY CHENILLE YARN

**Sibel KAPLAN[1], Sümeyye ÜSTÜNDAĞ[2], Sinem YÜCEL[2], Hüseyin Gazi TÜRKSOY[2]**

[1] Süleyman Demirel University, Turkey
[2] Erciyes University, Turkey

Corresponding author: sibelkaplan@sdu.edu.tr

***Abstract:*** *In this study, chenille weft yarns having different pile materials (PET having different counts, viloft/PET and acrylic) were used for denim fabric to enhance its insulation, thermal feelings and moisture management properties for end uses such as sports and work activities in cold environments. Moisture management performances of the inner sides of fabrics covered with pile structure consisting of different materials were investigated and results were put forward about the material and structure of the functional denim fabrics. According to the results, MMT measurements gave quite high variations for fabrics having a rough surface. Synthetic and cellulosic based materials (PET, viloft and acrylic) had different performances in pile form of a woven fabric from their performances within knitted and woven fabrics because of the different fabric geometry. Denim fabric including PET/viloft pile have good moisture management parameters according to their liquid absorption and transfer capabilities among the selected materials for functional denim fabrics.*

***Keywords:*** *denim fabric, chenille yarn, moisture management.*

## 1. INTRODUCTION

Denim is a durable warp faced twill or satin fabric which can be considered among the most popular fabrics for clothing. It has been preferred by people at any age, social/professional group and country because of its style and comfort properties. Denim garments have a long history that it was first used by Italian sailors in 1600's and after 1930's, it has become very popular among young people and it became a symbol of rebel with the help of media and films [1]. Its usage has always an increase trend and it is thought that different designs, appearances and colors obtained by various washing and fading processes support the mentioned trend after 1990's. Different finishing techniques are applied to create the approved worn look and apart from the fashion appeal; thermal, pressure [2] and skin sensorial comfort properties [3] are now becoming more important for denim garment users

Because of the great demand for denim comfort besides aesthetic properties, there are many attempts to enhance thermal comfort of denim fabrics. Cooler sensations, insufficient insulation and liquid transfer during summer and winter uses are the thermal comfort problems of denim sourced from its material and

fabric structure. The most established way to develop denim garments with better thermal comfort is to manufacture denim with different fiber contents which are lighter in weight, can dry rapidly and provide a warm feeling to wearers under cold and humid conditions [4]. Cotton can be engineered to transfer moisture or can be blended with lycra, polyester, lyocell, wool, silk, flax, hemp, etc. for developing special types of denim. Moisture management finishes are other solutions to enhance drying periods by increasing transfer capability and reducing absorption capacity of the fabric [3]. Moisture management is crucial for both summer and winter uses but in the worst winter conditions, for a warm feeling, dryness is the first condition. For this, the clothing must transport the body moisture away from the skin, keep dry and warm air close to the body [5]. Effects of different materials (cotton, polyester and core spun lycra weft), structural parameters and finishing/washing treatments on thermal feeling of denim fabrics and some thermal comfort parameters (air permeability, thermal conductivity, absorptivity, moisture vapor permeability, moisture management and drying rate) were investigated in different studies [6-8].

Chenille yarn is generally used in home textiles applications and as far as we know, there are no studies investigating effects of chenille yarn on clothing thermal comfort, mainly insulation. This study reports moisture management (MMT) results of a wider project investigating thermal comfort performance of denim fabrics modified by chenille yarn including different pile materials as warp. The produced fabrics were intended to be used for cold environments as sports or protective clothing.

## 2. MATERIAL AND METHOD

### 2.1. Production of Chenille Yarn Filled Denim Fabrics

Different denim fabrics including chenille yarns having identical core yarns (Ne 40 compact cotton) and pile yarns of different materials (polyester having different counts, viloft/polyester [PET] and acrylic), were woven on a Picanol GT-Max projectile weaving machine. Final count of chenille yarns is Nm 9, twist number is 850 Tpm and pile length is 1 mm. An elastic commingling (EC) yarn (78 dtex elastane and 200D/72F polyester) was also used as weft yarn besides chenille yarns. Microscopic images of the chenille yarns obtained with an Olympus SZ61 stereo microscope, weight and thickness values of the fabrics can be seen in Table 1. The warp and weft densities were 35 ends/cm and 22 pics/cm in turn. The weave construction was selected according to the target appearance that, chenille yarn can be seen from the inner side of the fabric (given in last column of Table 1). Fabric samples were exposed to a basic finishing process including rinse washing.

**Table 1.** Physical properties of chenille yarns and produced denim fabrics

| Code | Pile Yarn | Fabric Weight (g/m²) [S.D.] | Fabric Thickness (mm) [S.D.] | Microscopic images | Weave Structure/ Fabric photos in trousers form |
|---|---|---|---|---|---|
| **D36PET** | 100d/36F PET Filament | 380.53 [1.82] | 1.57 [1.6] |  | 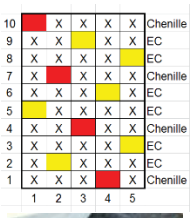   |
| **D96PET** | 100d/96F PET Filament | 377.33 [1.75] | 1.38 [1.4] |  | |
| **DVIL/PET** | Ne 30 50/50% Viloft/PET | 388.75 [19.3] | 1.41 [1.4] |  | |
| **DACRY** | Ne 40/1 Acrylic | 403.91 [2.5] | 1.48 [1.5] |  | |

## 2.2. Physical and MMT Measurements

Weight and thickness tests were carried out according to TS 251 and ASTM D 1777 with 5 g/cm2 pressure by James Heal R&B Cloth Thickness Tester (James Heal Corp., UK) respectively. Moisture Management Tester (MMT) (SDL Atlas Textile Testing Solutions Co.) tests were conducted on the inner sides of the fabrics including pile structure according to AATCC 195-2012 [9]. Variation of the MMT parameters were quite high because of the heterogeneous surface energy of the fabric covered with pile, therefore, test replications were more than necessary for the standard. Wetting time, absorption rate and spreading speed parameters giving consistent results were selected for investigation. IBM SPSS Statistics 21 was used for variance analyses of the results.

## 3. RESULTS AND DISCUSSION

Thickness values of the denim fabric including different chenille yarns ranged between 1.38-1.57 mm having statistically significant differences ($p < 0.05$). According to statistical analysis results, while 100d/36F PET filament including fabric (D36PET) have statistically identical thickness values with fabric including acrylic (DACRY) ($p > 0.05$), their thickness values are significantly higher than other fabrics including finer polyester (D96PET) and polyester/viloft blend (DVIL/PET) as chenille pile material.

According to MMT results, denim fabrics including PET or PET/viloft pile yarns (D36PET, D96PET, DVIL/PET) have statistically identical wetting time values (Figure 1). Fabric including acrylic pile (DACRY) had significantly ($p<0.05$) higher wetting time values. Cellulosic component of DVIL/PET and PET filament count (D36PET and D96PET) did not have any influence on absorption behavior as a

pile material of the denim fabric. It is thought that, acrylic pile decreased surface energy of the fabric and had a poor performance in liquid absorption.

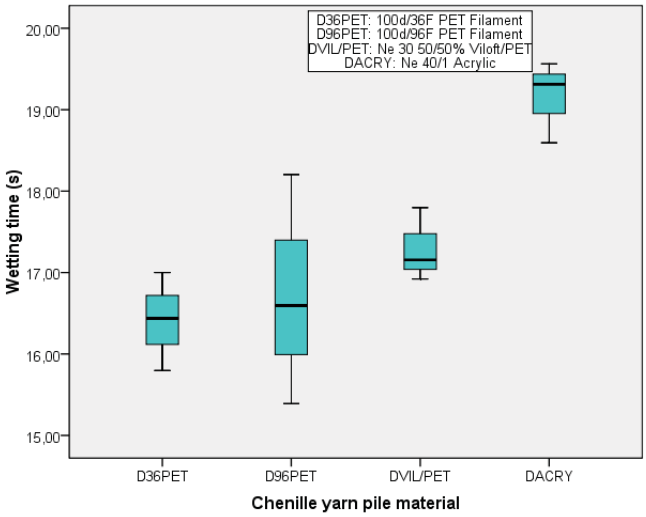


**Figure 1.** Wetting time (top) results of denim fabrics including different chenille yarn pile materials

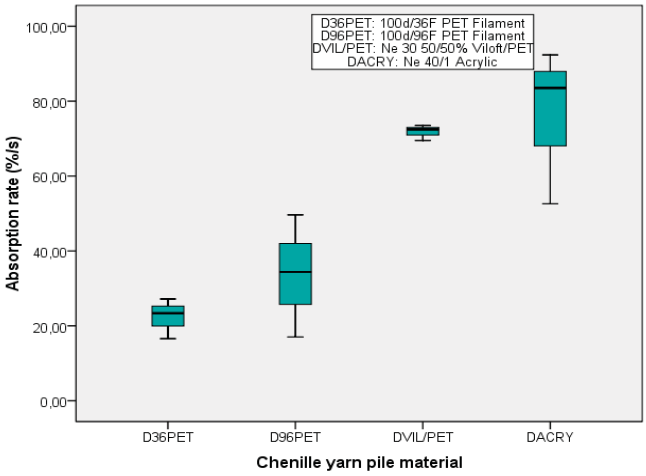


**Figure 2.** Absorption rate (top) results of denim fabrics including different chenille yarn pile materials

According to absorption rate results, denim fabrics having PET pile (D36PET and D96PET) had significantly lower results and other fabrics have statistically identical and higher transfer capabilities within the fabric. The better transfer

performance of PET, especially fibers having lower counts, could not be observed as pile form. Besides its lower absorption capacity, DACRY fabric transferred liquid sufficiently but performance of DVIL/PET is more consistent that its both absorption and transfer performances are acceptable.

Spreading speed values are better for D96PET and DVIL/PET fabrics including finer PET and PET/viloft blend in turn and the only significant statistical difference is between DACRYL and D96PET which has the highest spreading speed. DVIL/PET had also better performance in spreading the liquid faster than the other fabrics including different pile materials. This performance enables larger fabric area where the liquid is transferred, hence, quicker drying periods.

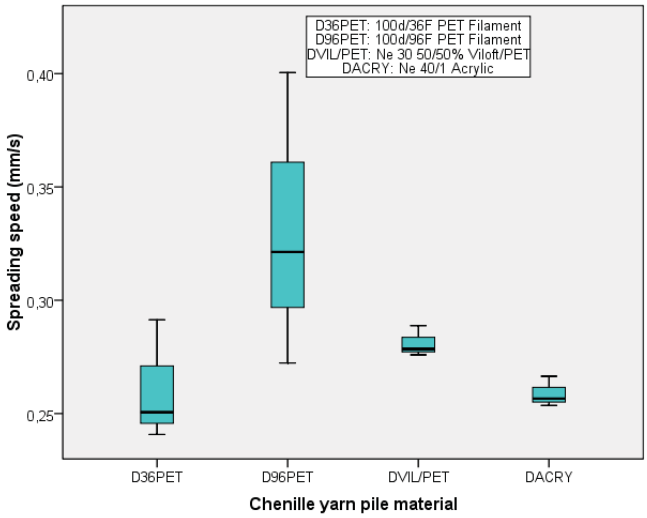


**Figure 3.** Spreading speed (top) results of denim fabrics including different chenille yarn pile materials

## 4. CONCLUSION

Chenille yarns including different pile materials were used as weft yarns of denim fabric to enhance its thermal comfort parameters in cold environments. MMT results show that PET/viloft giving acceptable liquid absorption and transfer parameters can be suggested for pile material of chenille yarn used for denim fabrics. It can be concluded that, besides functionality for insulation and thermal feelings, pile materials of chenille yarns may play a role in sweat transfer from the body for enabling thermal comfort. For sufficient moisture management performance, chenille yarns should include cellulosic components within their pile structures to remove liquid from the body. Such kind of material and fabric geometry modifications may enhance thermal comfort, hence, end use areas of denim products.

## ACKNOWLEDGEMENTS

This work was supported by Turkish Ministry of Industry and Technology by the project having number 0624.STZ.2014.

## REFERENCES

1. http://www.designboom.com/eng/education/denim2.html
2. Ertaş, O. G., Zervent Ünal, B., & Çelik, N. (2016). Analyzing the effect of the elastane-containing dual-core weft yarn density on the denim fabric performance properties. The Journal of The Textile Institute, 107(1), 116-126.
3. Paul, R. (Ed.). 2015.*Denim: manufacture, finishing and applications*. Elsevier.
4. Bliss, R. M., Flax fiber offers cotton cool comfort, 2005. *Agricultural Research Magazine, Nov*, *53*(11).
5. Matusiak, M. (2006). Investigation of the thermal insulation properties of multilayer textiles. Fibres & Textiles in Eastern Europe, 14(5), 98-102.
6. Hes, L., Mangat, M.M., The effect of industrial washing on thermal comfort properties of denim fabrics. 7th International TEXSCI Conference, 6-8 Sept., 2010, Liberec.
7. Vivekanadan, M. V., Raj, S., Sreenivasan, S., Nachane, R. P., Parameters affecting warm-cool feeling in cotton denim fabrics, 2011. Indian Journal of Fiber and Textile Research, 36, 117-121.
8. Midha, V., Suresh Kumar, S., & Nivas Kumar, M., Investigation on permeability and moisture management properties of different denim fabrics after repeated laundering, 2017. *The Journal of The Textile Institute*, *108*(1), 71-77.
9. MMT Operation Manual, Version 3.06, SDL Atlas Corp., UK, 2005.

# SINGLE BATH DYEING OF POLYAMIDE/COTTON BLENDS WHICH ARE USED IN SPORTIVE TEXTILES

**Rıza ATAV[1], Selma SOYSAL[2], Erkan ÇAĞLAR[2], Fatma YILDIZ[2]**

[1] Namık Kemal University, Turkey
[2] Gülle Entegre Tekstil İşletmeleri

Corresponding author: ratav@nku.edu.tr

***Abstract:*** *The aim of this work is to examine the single-bath dyeability of nylon/cotton blends which are used in sportive textiles in order to reduce water consumption and thus waste water consumption at the same time within the clean production concept of textile. For this purpose, 50%/50 Nylon/Cotton blend fabrics containing elastane were dyed in two separate baths using the conventional 2 bath method using 1:2 metal complex / reactive dye combination. The color and fastness properties of the samples were then compared to those dyed according to the single-bath method. The results show that water consumption can be reduced by about 1/3 when Nylon/Cotton blend fabrics are dyed according to the single bath method and the total dyeing time can be shortened by about 9%.*

***Key words:*** *Nylon/Cotton, sportive textile, dyeing, color, fastness, single bath dyeing*

## 1. INTRODUCTION

Mixture refers to the population possibilities that can be formed by many fiber polymers that differ in their physical or chemical properties [1]. Mixtures may be needed for a variety of reasons. Blends have become a key word to meet the increasing demands of consumers in order to optimize the clothing comfort and at the same time to bring innovative trends to the fashion industry [2]. Nylon / Cotton blends are fabrics produced on a very large scale. While the nylon part of the nylon / cotton blend provides quick drying and form stability properties, the cotton part adds value to the fabric in terms of sweat and water absorbency and attitude. It is necessary to take into account that dyeing technology of dye technicians is a complex subject [3, 4]. PA / CO blends are used in the fields of shirts, light suit fabrics and dress fabrics, sportswear containing PA in warp, CV in weft, CO-based and PA pile upholstery woven fabrics and so on. [5]. The aim of this work is to examine the single-bath dyeability of nylon/cotton blends in order to reduce water consumption and thus waste water consumption at the same time within the clean production concept of textile. For this aim, 50%/50 Nylon/Cotton blend fabrics containing elastane were dyed in two separate baths using the conventional 2 bath method using 1:2 metal complex / reactive dye combination. The color and fastness properties of the samples were then compared to those dyed according to the single-bath method.

## 2. MATERIAL AND METHOD

50% / 50% Nylon / Cotton knitted fabric (produced from 150 denier Nylon yarn and Ne 24/1 cotton yarn containng 40 denier elastane) ready for dyeing (pre-treated with caustic-peroxide) was used in experiments. Experiments were carried out using 1: 2 metal complex dye for the nylon component, reactive dye for the cotton component. The experiments were carried out with the single bath two step dyeing method with reference to the conventional method of two bath dyeings, Dyeing methods are explained below in detail.

**Two bath dyeing:** First cotton was dyed with reactive dye and then nylon part was dyed with 1: 2 metal complex dye. For this, dyeing was started with liquor containing 0.4 g/L sequestering agent and 1.5 g/L anti-creasing agent at 40˚C, then reactive dye dosage was carried out. Afterwards within 15 minutes salt (50 g/L) was dosed. Temperature was raised to 80°C and after 10 min. of migration, it was decreased to 60°C. After 5 min. the soda dosage was made in 2 portions within 50 minutes. It was continued for 45 min. and then liquor was drained. Afterwards the following washing steps were applied: over rinsing (at 50˚C for 5 min.) → neutralization with acid (at 50˚C for 6 min.) → soaping (0.4 g/L) (at 90˚C for 8 min.) → soaping (0.4 g/L) (at 80˚C for 8 min.)→ rinsing (at 60˚C for 6 min.) → cold rinsing (for 6 min.)

In the second step, dyeing was started with liquor containing 1 g/L levelling agent at 40˚C and after 5 minutes 1:2 metal complex dye dosage was carried out within 10 min., after processing at this temperature for 5 min., temperature was raised (1°C/min.) to 98˚C. After dyeing at this temperature for 20 min. temperature was decreased (1°C/min.) to 75°C. 1 g/L acid donor was added and after 5 min. the temperature was raised (1°C/min.) to 110˚C. Dyeing was continued for 45 min. and then temperature was decreased (1°C/min.) to 75°C and the liquor was drained. Afterwards the following washing steps were applied: over rinsing (at 40˚C for 10 min.) → rinsing (at 40˚C for 10 min.) → aftertreatment (for this aim it was started with liquor containing 2% fixing agent and acetic acid (pH 4.5) at 40˚C, then temperature was raised to 75˚C and fabric was treated for 20 min.)

**Single-bath two-step dyeing:** After the cotton part is dyed, the temperature of the dyebath was decreased to 40°C and the pH of the liquor was adjusted to 7 with acetic acid. Then the nylon part was dyed and it was passed on to aftertreatments. over rinse (5 min. at 50˚C) → soaping (0.4 g/L) (5 min. at 90˚C) → soaping (0.4 g/L) (5 min. at 80˚C) → rinsing (5 min. at 60˚C) → rinsing (10 min. at 40˚C) → aftertreatment (for this aim it was started with liquor containing 2% fixing agent and acetic acid (pH 4.5) at 40˚C, then temperature was raised to 75˚C and fabric was treated for 20 min.)

✓ ***Color measurements:*** CIE L*a*b* color values and reflectance (R%) values of dyed samples were measured with spectrophotometer (D 65/10°) and color yields (K/S) of dyed samples were calculated by Kubelka Munk equation:

$$K/S = (1-R)^2/2R$$

R=Reflectance value in maximum absorption wave length (nm)

K=Absorption coefficient

S=Scattering coefficient

✓ ***Fastness tests:*** Washing (at 60˚C) and rubbing (dry and wet) fastness values of dyed samples were assessed according to ISO 105 C06 and ISO 105-X12 standards respectively.

## 3. RESULTS AND DISCUSSIONS

Table 1 shows the color measurement results of the fabric samples which were dyed according to the conventional two bath dyeing and the newly developed single bath two-step dyeing method.

**Table 1.** CIEL*a*b* and color yield (K/S) values of fabrics dyed with two bath and single bath dyeing methods

| Color | Dyeing | L* | a* | b* | c | h | K/S |
|---|---|---|---|---|---|---|---|
| **Fuchsia** | Two bath | 47,23 | 47,38 | -7,44 | 47,96 | 351,08 | 5,66 |
| | Single bath | 48,85 | 43,30 | -5,70 | 43,67 | 352,51 | 4,53 |
| **Red** | Two bath | 42,98 | 51,98 | 25,33 | 57,83 | 25,97 | 14,59 |
| | Single bath | 41,75 | 50,23 | 23,25 | 55,35 | 24,84 | 14,69 |

When Table 1 is examined, it is seen that there is no significant difference in h values that refers to color hue between the samples dyed with one and two baths, that is, the colors are the same. Furthermore, when the c values expressing the chroma are taken into consideration, it can be said that the color saturation of the samples dyed with two bath method is slightly lower than that of the samples dyed with single bath dyeing method.

On the other hand, the a * values of samples dyed with single baths are smaller, ie the nuances of the two bath dyeings are redder. When we evaluate from the point of color yield, it is seen that there is not a significant difference between single and two bath dyeings in red color. In case of the fuchsia color, it can be said that the single bath dyeings are lighter. However, it should be noted that the two bath dyeings were made in mill conditions and the single baths are made in laboratory scale. It is possible to say that the differences are not important if it is taken into account that these kind of color differences are already encountered between the laboratory and the mill scale dyeings.

Washing and rubbing fastness values of dyed samples are given Table 2.

**Table 2.** Washing and rubbing fastness values of fabrics dyed with two bath and single bath dyeing methods

| Color | Dyeing | Washing | | | | | | Rubbing | |
|---|---|---|---|---|---|---|---|---|---|
| | | CA | CO | PA | PES | PAN | WO | Dry | Wet |
| **Fuchsia** | Two bath | 5 | 4-5 | 4-5 | 5 | 5 | 5 | 4-5 | 4 |
| | Single bath | 5 | 4-5 | 4 | 5 | 5 | 5 | 4-5 | 4 |
| **Red** | Two bath | 4-5 | 4 | 3-4 | 5 | 5 | 5 | 4-5 | 4 |
| | Single bath | 4-5 | 4 | 3 | 5 | 5 | 5 | 4-5 | 3-4 |

When fastness values of single bath dyeings are evaluated, it can be said that washing and rubbing fastness values are generally the same or half points lower than those of two bath dyeings. However, it can be said that the fastness values obtained in single bath dyeings are very good in general.

## 4. CONCLUSION

As a result of the study, 50% / 50% Nylon / Cotton blended fabrics containing elastane can be dyed as a single bath instead of two bath method using 1: 2 metal complex / reactive dye combination. When the color and fastness properties of the samples are examined, it can be said that the single-bath dyeings do not make a significant difference compared to the two-bath dyeings. In the case of single-bath dyeing, it is saved from one dye-bath. Furthermore washing processes of cotton and nylon are combined. Thus, instead of totally 9 steps of washing procedure (6 for cotton and 3 for nylon), a washing process consisting of 6 steps are carried out, by the way it is saved from 3 washing baths. As a result total bath number is decreased from 11 to 7 and water consumption is reduced approximately by about 1/3. On the other hand, the total dyeing time including dyeing, washing and aftertreatments, is 550 minutes in the two bath dyeing method. When it is done with single-bath dyeing, it decreases to 500 minutes. This situation shows that 9% savings in time will be achieved.

In the light of these results, it can be said that the single-bath dyeing of 50% / 50 Nylon / Cotton blend fabrics containing elastane is promising in order to reduce water consumption and thus waste water and also to decrease dyeing time. It is worth noting, however, that it may be possible to make more precise judgments after working on a larger number of colors and in production-scale experiments.

## REFERENCES

1. Aniş P., Eren H.A.: Poliester/Pamuk Karışımlarının Boyanması: Uygulamalar ve Yeni Yaklaşımlar. 2003. Uludağ Üniversitesi Mühendislik-Mimarlık Fakültesi Dergisi, 8(1): 131-139.
2. Shore J., Blends Dyeing. 1998. Society of Dyers & Colourists.
3. Kazan C., Liflerin Kimyasal Modifikasyonu Yoluyla Poliester/Pamuk Karışımlarının Tek Banyoda Boyanabilirliğini Sağlayacak Yeni Bir Yöntem Geliştirilmesi, Namık Kemal Üniversitesi Fen Bilimleri Enstiitüsü, Yüksek Lisans Tezi, Haziran 2015
4. http://textileinfo.com/en/dyes/sumitomo/kyujin/page03-03.html, 28.10.2005
5. Nunnn D.M., The Dyeing of Synthetic-Polymer and Acetate Fibers. 1979. Dyers Co. Publications Trust, 433-437.

# STUDY OF COMFORT PROPERTIES OF THREE-DIMENSIONAL WARP KNITTED SPACER AND NEOPRENE LAMINATED FABRIC STRUCTURES

**Bekir BOYACI[1], Güneş SAYIT[1], Servet GÜL[1], Gökberk DEVRİM[1]**

[1] Sun Tekstil San. ve Tic. A.Ş. Research and Development Center

Corresponding author: gunes.sayit@suntekstil.com.tr

***Abstract:*** *The basic construction of spacer fabrics is formed of two textile layers held by*

***Abstract:*** *To produce different kinds of orthopedic support materials, neoprene and polyurethane foam laminated knitted fabrics have been traditionally used. These flexible foams have impact resistance properties, but they are not comfortable enough and might cause problems for the consumer.*

*In addition to these foam structures, three dimensional spacer fabrics having comfort properties can be used for production of medical textiles. The basic construction of spacer fabrics is formed of two textile layers held by spacer threads in a defined spacing. Thanks to spacer fabric is highly breathable, thus creating a moisture free environment, which reduces the chances of skin maceration. These lead to an increased level of comfort when compared to materials like foam, neoprene and laminate fabrics.*

*The moisture vapor transfer of textile is important in comfort properties in conditions that involve sweating. The moisture transfer properties of clothing materials contribute to determining the thermal and sensorial comfort of garments. In this study, the influence of spacer fabric and neoprene laminated knitted fabric structures on air (TS 391 EN ISO 9237) and water vapor permeability (ISO 11092) and moisture management properties were measured, and the results were discussed.*

***Key Words****: 3-D spacer fabric, neoprene, thermal comfort properties, moisture management characteristics*

## 1. INTRODUCTION

Spacer fabric is a three-dimensional knitted fabric consisting of two separate knitted substrates which are joined together or kept apart by spacer yarns. There are two types of spacer fabrics: warp knitted spacer fabric and weft-knitted spacer fabric. The first type is knitted on a rib raschel machine having two needle bars, while the second is knitted on a double jersey circular machine having a rotatable needle cylinder and needle dial.

The basic construction of three dimensional spacer fabrics is formed of two textile layers held by spacer threads in a defined spacing. This structure provides tortuous spaces which let heat and moisture to be transferred through the fabric with air easily. These characteristics of the spacer fabrics make them suitable for

medical purpose such as beds, supporting pillows, bandages, shoes, operation tables and so on [2].

One of the textile properties that has steadily gained importance among increasingly well-informed consumers is the breathability of the material, because this property seems to be directly linked to comfort of functional fabric materials [3]. To be comfortable and to maintain the state of comfort, cushioning material must be designed to allow the body's heat balance to be maintained under a wide range of environmental conditions and body activity.

The main problem associated with thermal comfort is the incompatibility between the requirement of heat conservation during low metabolic activity and heat dissipation at high energy level. Air permeability being a biophysical feature of textiles, determines the ability of the air flow through the fabric. Airflow through textiles is mainly affected by the pore characteristics of fabrics [4]. The pore characteristics of the fabric are mainly determined by their structure and density [5]. Water vapor permeability determines breathability of the cushion material, i.e. the ability to transmit vapor away from the body. The mechanism involved in water vapor transmission through fabric from the body to the outer surface is by diffusion and absorption–desorption method. The ability of fabric to transport water vapor is an important determinant of physiological comfort [6].

In case of orthopedis support structures, the thermo-physiological properties may be very specific requirements because these properties make the users feel comfortable. Generally, neoprene and polyurethane foam laminated knitted fabrics are used for different kinds of orthopedic materials. Thanks to spacer fabric is highly breathable, thus creating a moisture free environment, which in turn reduces the chances of skin maceration. These lead to an increased level of comfort when compared to materials such as foam, neoprene and laminate fabrics. Spacer fabrics are regarded as environmentally friendly textile materials (unlike polyurethane foam), since they can be recycled [1].

The heat and moisture vapor transport capability of fabrics, produced by human body, with high water vapor permeability is one of the most important factors allowing the human body to provide cooling due to evaporation [7]. Air permeability has a great influence on comfort because an air permeable material is also vapor or liquid permeable. A very porous or open structure will allow wind penetration through the material, resulting in the body cooling and also presents difficulties in maintaining product [4].

The moisture vapor transfer of textile is important in comfort properties especially in conditions that involve sweating. The moisture transfer properties of clothing materials contribute to determining the thermal and sensorial comfort of garments made from them. In fact, an important purpose for clothing designers is keeping the skin dry after physical activity by rapid transport of liquid perspiration away from the skin, because of the role of humidity next to the skin in determining comfort levels [7].

## 2. MATERIAL AND METHOD

### 2.1. Materials

In the experimental study, three warp spacer knitted fabrics consisting polyester fibres having similar structural parameters (Table 1) were used. The fabric characteristics of interest include the fabric density, spacer yarn type, thickness of the spacer fabric, spacer yarn diameter and arrangement. All the experiments were carried out under standard conditions at 20 0C and 65% relative humidity. No finishing and dyeing treatment were applied to the fabrics before tests.

**Table 1.** Warp Knitted Spacer Fabrics Characteristics

| Sample | Areal mass ($g/m^2$) | Fabric thickness (mm) | Course (per cm) | Wales (per cm) | Compression (kPa) | Tensile Strength (N) | Elongation at Break (%) |
|---|---|---|---|---|---|---|---|
| Spacer Fabric 1 | 349.67 | 4.17 | 12.5 | 9 | 14.87 | 316.67 | 84.79 |
| Spacer Fabric 2 | 319 | 4 | 11.5 | 9 | 15.02 | 347.70 | 99.43 |
| Spacer Fabric 3 | 324.67 | 4.30 | 18.5 | 10 | 13.74 | 267.52 | 134.38 |

Generally, the velour fabrics are laminated to neoprene to provide the hook and loop structure in the orthopedic support materials. To achieve this structure, %86 polyamide-%14 elasthane 220 $g/m^2$ velour fabric was laminated to spacer fabric and neoprene with the thickness of 4 mm in this study.

### 2.2. Methods

In this study, the influence of different spacer fabrics and neoprene laminated knitted fabric structures on comfort properties such as air and water vapor permeability, moisture management properties and thermal behaviour of spacer fabric were measured and the results of these parameters will be discussed. For determination of these comfort properties and characteristics of three different warp knitted spacer fabrics and one neoprene laminated knitted fabric were experimented.

The fabric characteristics of interest include fabric density, spacer yarn type, thickness of the spacer fabric, spacer yarn diameter and arrangement. All the experiments were carried out under standard atmospheric conditions at 20 $^0$C and 65% relative humidity. The air permeability of the samples was studied with the Airtronic 3240C air permeability tester device according to TS 391 EN ISO 9237 [7]. Its principle is depending on the measurement of the air flow passing through the fabric at certain pressure gradient. Thermal resistance and water vapor resistance properties were measured on Atlas Sweating Guarded Hotplate, which works on similar skin model principle, as stated in ISO 11092 [4,8].

### 2.2.1 Thickness Test

The thickness of spacer fabrics were measured using digital thickness gauge according to DIN EN ISO 5084. Essentially the determination of fabric thickness consists of the precise measurement of the distance between two plain parallel plates when they are separated by the cloth, a known arbitrary pressure between the plates being applied and maintained. It is convenient to regard one of the two plates as the pressure foot and the other as anvil. The thickness tester has such two parallel plates. The upper plate serves as a collar and supports for the additional load which produce pressure.

### 2.2.2 Air Permeability Test

Air permeability of fabric samples were measured using Airtronic 3240C air permeability tester according to TS 391 EN ISO 9237. The principle of air permeability is depending on the measurement of the air flow passing through the fabric at certain pressure gradient. The measurements were done in controlled laboratory conditions. Ten specimens were tested for each sample and the average value was reported. All measurement were experimented on the 200 Pa and 20 cm2 measurement area.

**Figure 1.** Airtronic 3240C Air Permeability Tester

### 2.2.3 Water Vapor Permeability Test

Thermal resistance and water vapor resistance properties were measured on Atlas Sweating Guarded Hotplate according to ISO 11092. This device comprising has the ability to simulate the possible body condition comprising a controlled environmental chamber, sweating guarded hot plate, and data acquisition system. The instrument used for the experiments is shown schematically in Figure 2. The sweating guarded hot plate was placed in a chamber with ambient conditions of 25°C, and 65% relative humidity (RH). This guarded hot plate comprised of different components including a 37°C hot plate as a heat source, a water container, a piece of animal skin for simulating human skin and the sensors for humidity and temperature determination. One side of the sample faces the sweating skin but not in contact, whereas the other side is exposed to the controlled environment. Five humidity and temperature sensors

were located above and below the sample. The driving forces for the movement of moisture vapor are the temperature and vapor gradients maintained between the points where the moisture vapor emerges from the simulated skin (37°C, 90% RH) and the ambient environment controlled at 25°C and 65% RH.

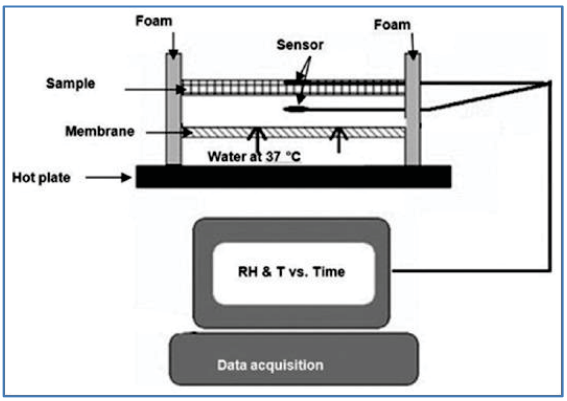


**Figure 2.** Schematic design of the instrument for measurement of moisture transfer

### 2.2.4 Moisture Management Test

The liquid moisture transport capabilities of the fabrics were measured the SDL Moisture Management Tester (MMT) according to AATCC 195 standard. This test is used to measure the liquid management properties of any technical fabric with great precision such us every parameter related the wicking behaviour instead of only vertical wicking test behaviour by traditional wicking test.

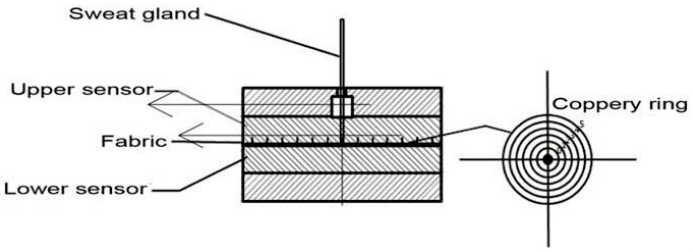


**Figure 3.** Schematic diagram of the instrument for moisture transfer tester

## 3. RESULTS AND DISCUSSION

According to the air permeability results Sample 2 were selected to laminate with velour fabric due to superior features which are compression, elongation and tensile strength.

The air permeability of the velour laminated spacer fabric and velour laminated neoprene fabric structures are shown in Table 3.

**Table 3.** The Air Permeability Results of Velour Laminated Spacer and Neoprene

| Sample | Air permeability (l/dm²/min) |
|---|---|
| Velour Laminated Spacer Fabric | 2124.50 |
| Velour Laminated Neoprene | 0 |

The thermal resistance and water vapor resistance properties of the velour laminated spacer fabric and velour laminated neoprene fabric structures are shown in Table 4.

**Table 4.** The Thermal Resistance And Water Vapor Resistance Properties Results of Velour Laminated Spacer and Neoprene

| Sample | RET (m².Pa/W) | RCT (m².K/W) |
|---|---|---|
| Velour Laminated Spacer Fabric | 10.78 | 0,0528 |
| Velour Laminated Neoprene | 11.83 | 0,0587 |

The moisture management properties of the velour laminated spacer fabric and velour laminated neoprene fabric structures are shown in Table 5.

**Table 5.** The Moisture Managemet Results of Velour Laminated Spacer and Neoprene

| Sample | OMMC |
|---|---|
| Velour Laminated Spacer Fabric | 0,30 |
| Velour Laminated Neoprene | 0.11 |

An analysis of Table 3 and Tablo 4 shows that velour laminated spacer sample has the lowest air resistance and thermal conductivity, while velour laminated neoprene sample has the highest values for thermal conductivity and it has no air permeability.

Table 5 indicates the moisture management properties of velour laminated spacer and neoprene fabrics. According to OMMC results, velour laminated neoprene has lower moisture management properties than velour laminated spacer fabric for the production of orthopedic support material.

## 4. CONCLUSIONS

In conclusion, this study performs a quantitative investigation of various fabric characteristics, such as air permeability, thermal and mechanical properties of warp knitted spacer fabrics and neoprene laminated knitted fabrics. It is found that both air permeability and thermal properties are related to the fabric characteristics.

After an analysis on the structure characteristics and knitting process, three different spacer fabrics were produced on a warp knitting machine. Comfort properties, such as air permeability, and thermal resistance were evaluated and compared with velour laminated selected spacer fabric and velour laminated neoprene structure. The results have shown that developed spacer fabric have better properties than neoprene foam structure. The spacer fabric also have very good air permeability and lower heat resistance, so that they can offer much better comfort than neoprene.

In addition, the results show that spacer fabric have a capability to transport the moisture and water vapor produced by sweating can be easily and quickly transferred from close to the skin to the outer surface of spacer fabrics to keep the skin dry and they give excellent wear comfort to wearer. In addition, because of undesirable comfort characteristics of neoprene structure, moisture transport and air permeability of neoprene integrated knitted fabric results show a very low value.

## ACKNOWLEDGMENTS

The authors wish to express their gratitude to Ames Europe Textile for providing warp knitted spacer fabric samples.

## REFERENCES

1. Yip J., Ng S., Study Of Three-Dimensional Spacer Fabrics: Physical And Mechanical Properties. 2008. Journal Of Materials Processing Technology, 206, 359–364
2. Bagherzadeh R., Montazer M., Latifi M., Sheikhzadeh M., Sattari M., Evaluation of Comfort Properties of Polyester Knitted Spacer Fabrics Finished with Water Repellent and Antimicrobial Agents. 2007. Fibers and Polymers, Vol.8, No.4, 386-392
3. Corberan, J., Verde, M., Gil, M., & Martinez, N. Study of adsorption materials for their application as perspiration-absorbing textiles. 2010. Textile Research Journal, 80, 1160–1171.
4. Crina B., Blaga M., Luminita V., Mishra R., Comfort Properties Of Functional Weft Knitted Spacer Fabrics. 2013. Tekstil Ve Konfeksiyon, 23(2)
5. Abramaviciute, J., Mikucioninene, D., & Ciukas, R. Structureproperties of knits from natural yarns and their combination with elastane and polyamide threads. 2011. Material Science, 17, 43–46.
6. Bagherzadeh, R., Gorji, M., Latifi, M., Payvandy, P., & Kong, L. X. Evolution of moisture management behavior of high wicking 3D warp knitted spacer fabrics. 2012. Fibers and Polymers, 13, 529–534.
7. Borhani S., Seirafianpour S., Ravandi S. A. H., Sheikhzadeh M., Mokhtari R., Computational and Experimental Investigation of Moisture Transport of Spacer Fabrics. 2010. Journal of Engineered Fibers and Fabrics, Volume 5, Issue 3
8. Sampath M.B., Aruputharaj A., Senthilkumar M., Nalankilli G., Analysis of thermal comfort characteristics of moisture management finished knitted fabrics made from different yarns. 2011. Journal of Industrial Textiles, 42(1) 19–33

# DESIGN OF A TENS KNEE PAD WITH INTEGRATED TEXTILE ELECTRODES

**Duygu ERDEM[1], Sevil YEŞİLPINAR[2], Yavuz ŞENOL[2]**

[1]Selçuk University, Turkey
[2]Dokuz Eylül University, Turkey

Corresponding author: duygu.erdem@selcuk.edu.tr

***Abstract:*** *Transcutaneous electrical nerve stimulation (TENS) is defined as the application of electrical current to the skin for pain control by the American Physical Therapy Association (APTA). The TENS treatment is extensively preferred since it is safe, not expensive and has no side effects when compared to drug therapy. TENS therapy is applied using clinical or portable type TENS devices and TENS electrodes. However, conventional electrodes are not hygienic because they are not washable and their sticky structure makes patients uncomfortable. Furthermore, they are not suitable to be integrated into a smart garment. In this study, a knee pad with integrated electrodes and textile transmission lines have been designed and developed to be used for TENS therapy. Electrical resistance values of textile electrodes and transmission lines which is integrated into the knee pad was measured. The developed knee pad was connected to a commercially available TENS device and electrical current transmission on subjects was tested. Furthermore, washing tests were conducted on knee pad.*

***Keywords:*** *electronic textiles, smart garment, conductive yarns, conductive materials.*

## 1. INTRODUCTION

Transcutaneous electrical nerve stimulation (TENS), one of the electrical pain treatments, is defined as the application of electrical current to the skin for pain control by the American Physical Therapy Association (APTA) [1]. In TENS treatment, all or some of the sensory, motor, sensory-motor-nociceptive nerve fibers are stimulated using electrodes to influence the neuro-hormonal, neuro-physiological and cognitive system. Thus, the central system is affected as much as the peripheral system and thereby the pain is reduced. TENS treatments are based on different action mechanisms however the most commonly used one is the “Gate Control Theory” which was introduced by Melzack and Wall in 1965 [2]. According to this theory, substantia gelatinosa acts a gate control system that modulates the synaptic transmission of nerve impulses from peripheral fibers to central cells. A schematic diagram of the gate control theory in pain mechanisms is given in Figure 1 [3].

The fundamental indications of TENS treatment are acute and chronic pain syndromes. It is known that TENS therapy, which was tested and still being tested by many researchers, is used in cases such as rheumatoid arthritis, osteoarthritis, low back pain, neck pain, neuropathic pain, labor pain, dysmenorrhea, after multiple rib fractures and so on [2]. The effect of TENS

treatment varies depending on the source of the pain, the pain threshold of the individual, the electrode location, the intensity of stimulation and the electrical characteristics of the stimulation applied [4]. The TENS treatment is extensively preferred since it is safe, not expensive and has no side effects when compared to drug therapy [5].

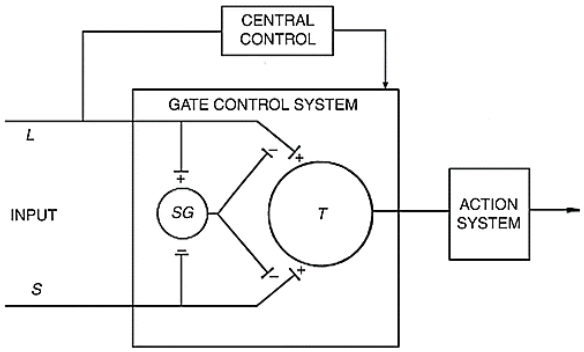


**Figure 1.** A schematic diagram of the gate control theory in pain mechanisms: L, the large-diameter fibers; S, the small-diameter fibers; SG, substantia gelatinosa; T, transmission cells; +, excitation; -, inhibition [3]

TENS therapy is applied using clinical or portable type TENS devices and TENS electrodes. Metal plate electrodes covered by fabric tissue, carbon electrodes, and self-adhesive hydrogel electrodes are used as TENS electrodes up to this point [6]. The performance of these electrodes is very good. However, they are not hygienic because they are not washable and their sticky structure makes patients uncomfortable [7]. Furthermore, they are not suitable to be integrated into a smart garment. For these reasons, many researches about textile electrodes is performing by researchers from all over the world recently.

Most of the studies on textile electrodes focused on physiological monitoring and ECG, EMG and EEG measurements [8, 9, 10, 11, 12, 13, 14, 15]. However, some of them concentrate on other fields such as electrical stimulation [16, 17, 18, 19, 20, 21]. Studies on electrical stimulation have not only been limited by electrodes, electrotherapy garments were also studied, too. When papers about electrotherapy garments were examined, it is seen that in some studies only commercial electrodes were tried to be incorporated into the garments, while structures with fully integrated textile electrodes were developed in others.

Prochazka et al. (1997) developed a functional electrical stimulation (FES) glove that improves hand function in people with spinal cord injury. The glove has conductive areas which contact self-adhesive electrodes previously placed on the skin. Signals from a sensor in the glove detect voluntary wrist movement and control FES of muscles [22]. Lee et al. (2009) designed a smart wear with built-in thermotherapy and TENS device for relief of dysmenorrhea. They used a silicon stimulating pad [23]. Nisar et al. (2016) developed a rechargeable

therapeutic wearable for the prevention of pressure ulcers. The wearable consists of an embedded electrical stimulation device and skin adhesive electrodes and delivers electrical stimulation to the pressured points in gluteal muscles [24]. Keller et al. (2006) presented a transcutaneous electrical stimulation (TES) system consisted of a garment sleeve holding 60 textile embedded electrode pads and other electronic equipment. Developed system allows dynamic real-time adjustments of the electrode size and location for multiple regions on a single garment [25]. Li et al. (2010) designed and developed an intelligent garment with TENS function based on intarsia knitting technique. Silver conductive yarn was knitted into the garment to be used as electrodes and conducting wires [7]. Kim and Cho (2013) developed an e-textile-based smart glove with embedded textile electrodes. One side of the electrodes is a conductive snap which was used to combine with one end of a transmission line [17]. Goncu Berk (2018) presented the design process of a wearable pain management system with embroidered textile electrodes [26].

In this study, a knee pad with integrated electrodes and textile transmission lines have been designed and developed to be used for TENS therapy. Optimum electrode connections and electrode locations on knee pad have been investigated. Electrical resistance values of textile electrodes and transmission lines which is integrated into the knee pad was measured. The developed knee pad was connected to a commercially available TENS device and electrical current transmission on subjects was tested. Furthermore, washing tests were conducted on knee pad and washing effect on textile electrodes and transmission lines were examined.

## 2. MATERIAL AND METHOD

### 2.1. Sample Production

Knee pad is produced from two layers of a laminated fabric. Electrodes and transmission lines were machine embroidered on one layer. The second fabric layer was used for providing a more aesthetical look. In this way, the sides of the electrodes which are not in contact with the skin and the transmission lines were concealed between two fabric layers. An empty area with 5 cm in diameter was formed on the patella to be used as a reference point for patients. The fabric layers were assembled using piping. Front and back views of knee pad can be seen in Figure 2.

**(a)** **(b)**

**Figure 2.** (a) Front and (b) back views of knee pad

Totally four textile electrodes were embroidered on the knee pad. Electrode locations were chosen according to expert opinions and previous studies about this subject. In TENS therapy, three different electrode localization methods are determined. The first one is to position the electrode on pain region or its surrounding. The second one is to position the electrode on dermatome regions which are related to pain and the last one is to position the electrode on some special points on human body like acupuncture or trigger points [2]. Based on this localization methods, patella was chosen as the center of knee pad and electrodes were positioned on lower and upper corners. Electrodes, in size of 5 cm × 5 cm, and transmission lines, in sizes of 16 cm x 0.5 cm and 3 cm x 0.5 cm, were directly machine embroidered on the fabric with Tajima TFGN embroidery machine. For a better conductivity, conductive yarns were preferred as both top thread and bobbin thread. A technical drawing of knee pad is presented in Figure 3.

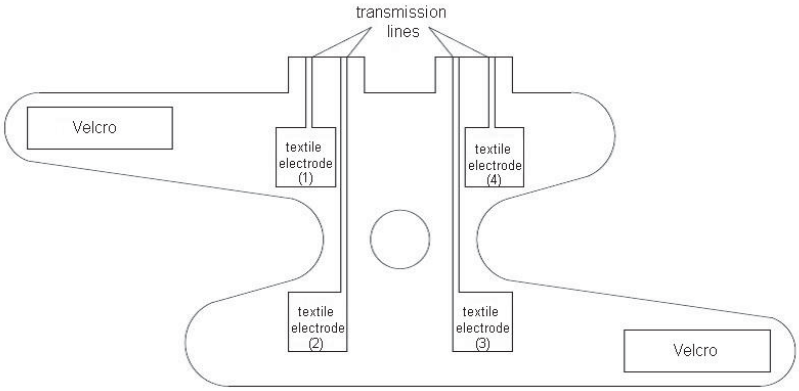


**Figure 3.** Technical drawing of knee pad

Two different conductive yarns (X-Silver and X-Static) were used for the production of conductive parts. Overlapped high-density patterns were used for the production of electrode regions and transmission lines based on previous studies [27, 28]. Transmission lines and electrodes were embroidered at once to prevent disconnections between electrodes and TENS device. Female banana plug connectors were used by being fastened to the one end of textile transmission lines. Connectors were 2.54 cm in diameter, noncorrosive, and commercially available products. Totally 2 knee pad samples were produced and tested.

### 2.1. Testing of Samples

Since one of the main aims of this study is to develop an integrated and washable product, washing tests were applied to the knee pads for ten times. Washing tests were carried out using 4 g/lt household detergents at 30°C main washing temperature in a domestic washing machine with reference to TS 5720 EN ISO

6330-2002 6A standard. After washing processes, samples were dried flat at room temperatures.

In order to evaluate the performance of textile electrodes and textile transmission lines, two different tests were applied. Firstly, electrical resistance values were measured before washing and after 1st, 5th and 10th washing cycles with a Thurlby 1503 digital multimeter. Before the measurements, knee pad samples were conditioned for 24 hours in laboratory conditions with a relative humidity of 20 ± 2 °C and 65 ± 2%. Then, knee pad samples were connected to a Stimtec 2 model commercially available TENS device and current transmission were tested subjectively. Subjective trials were performed on 3 subjects (2 females, 1 male) which vary in ages from 28 to 52, from 165 to 187 cm in length and from 60 to 88 kg in body weight. Volunteers do not have any health problems. Subjective trials were repeated before washing and after 1st, 5th and 10th washings.

## 3. RESULTS AND DISCUSSION

The measured resistance values were evaluated with IBM SPSS Statistics 22 software and presented in Figure 4 and Figure 5 for knee pads produced using X-Silver and X-Static yarn, respectively. Electrical resistance values of electrodes and transmission lines were measured together and entitled as electrode number.

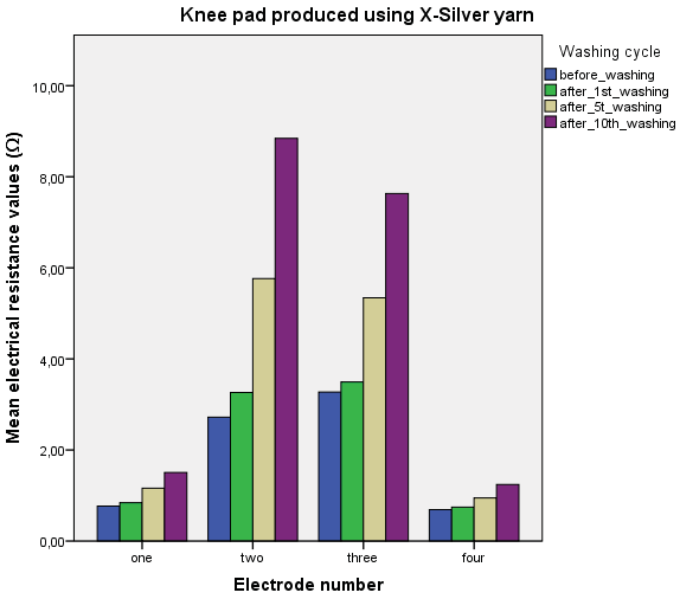


**Figure 4.** Electrical resistance measurement results of knee pad produced using X-Silver yarn

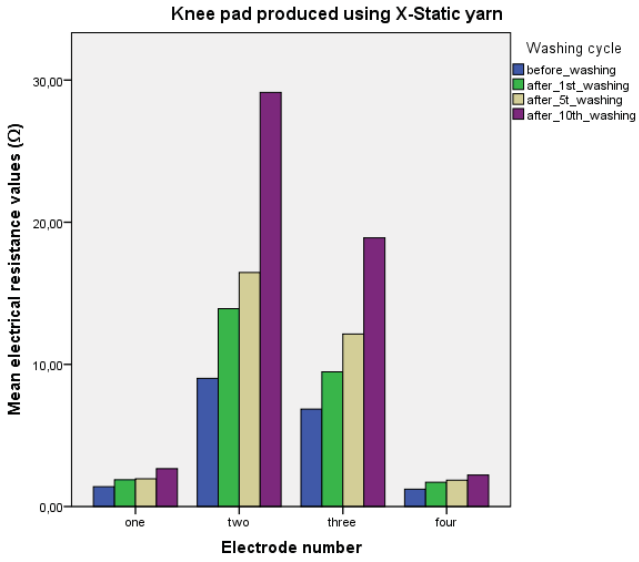


**Figure 5.** Electrical resistance measurement results of knee pad produced using X-Static yarn

When Figure 4 and Figure 5 were examined, it is seen that electrical resistance values of first and fourth electrodes are quite smaller when compared to second and third electrodes for both knee pads. The reason is that the first and fourth electrodes are located at the upper part of the knee pad and has shorter transmission lines, while other electrodes are located at the lower part and has longer transmission lines. All electrodes have same dimensions and theoretically have same electrical resistance values. Under these circumstances, it can be said that the difference between electrodes arise from the length of the transmission lines. Increase in the length of transmission lines causes increase of electrical resistance values. When the figures are evaluated separately, it is observed that the electrical resistance values for the knee pad produced using X-Static yarn are higher especially for electrodes with longer transmission lines.

When Figure 4 and Figure 5 were taken into consideration in the way of electrical resistance values before and after washing, it is observed that washing cycles give similar results for both knee pads. After washing processes, the electrical resistance values of electrodes and transmission lines are slightly increased. This increase is followed by an increasing trend in direct proportion to the washing processes. It is concluded that after washing processes, the increase of electrical resistance values of longer lines is bigger than shorter lines. The increase of resistivity is caused by the deformed transmission lines effected by number of washings. However, it can be said that the change of electrical resistivity is not significant with increased number of washing.

In addition to electrical resistance measurements, subjective tests were also performed on the developed knee pads. The knee pads were connected to the

StimTec brand TENS device and experiments were carried out while subjects were in standing and sitting positions. Subjective trials were repeated before washing and after 1st, 5th and 10th washings. Mean current transmission results of subjective trials were presented in Table 1 and Table 2, general results were presented in Figure 6.

**Table 1.** Mean current transmission results of knee pad using X-Silver yarn

| | Sitting position | | Standing position | |
|---|---|---|---|---|
| | **Upper electrodes** | **Lower electrodes** | **Upper electrodes** | **Lower electrodes** |
| **Before washing** | 4,8 mA | 5,2 mA | 3,2 mA | 3,6 mA |
| **After 1st washing** | 3,8 mA | 5,0 mA | 3,2 mA | 5,0 mA |
| **After 5th washing** | 6,0 mA | 2,8 mA | 2,8 mA | 4,2 mA |
| **After 10th washing** | 6,8 mA | 3,8 mA | 4,0 mA | 3,4 mA |

**Table 2**. Mean current transmission results of knee pad using X-Static yarn

| | Sitting position | | Standing position | |
|---|---|---|---|---|
| | **Upper electrodes** | **Lower electrodes** | **Upper electrodes** | **Lower electrodes** |
| **Before washing** | 3,2 mA | 3,2 mA | 4,2 mA | 4,0 mA |
| **After 1st washing** | 3,0 mA | 3,2 mA | 2,6 mA | 2,6 mA |
| **After 5th washing** | 2,2 mA | 3,2 mA | 2,8 mA | 2,6 mA |
| **After 10th washing** | 3,0 mA | 3,8 mA | 2,2 mA | 2,6 mA |

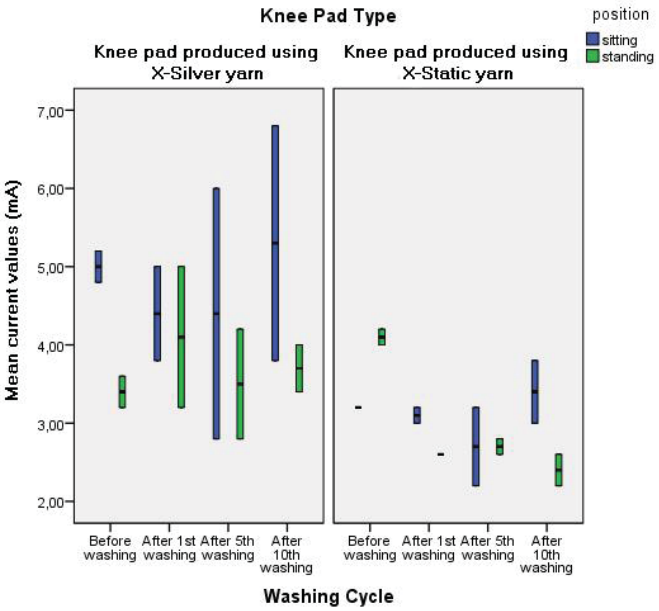


**Figure 6.** Subjective trial results of knee pads

## 4. CONLCUSION

In this paper, knee pads with integrated textile electrodes and textile transmission lines have been designed and produced for use in TENS therapy and effectiveness of the knee pads have been investigated by preliminary tests. These preliminary tests were washing test, electrical resistance measurement and subjective trials. In preliminary work cables were used for electrical transmission, however, cables were broken especially after washing processes. In this study, textile transmission lines and banana plug connectors were used to solve this problem and products that are more resistant to washing processes were developed.

When electrical resistance measurements were taken into consideration, it is observed that different yarns cause different electrical resistance values. In our example, electrodes and transmission lines of knee pad produced using X-Static yarn have higher electrical resistance values than knee pad produced using X-Silver yarn. Washing cycles give similar results for both knee pads. After washing processes, the electrical resistance values of electrodes and transmission lines are slightly increased.

In trials with TENS device and designed knee pads on the subjects, it is noted that subjects had electrical stimulation from knee pads. Also, according to these subjects' feedback there is not any discomfort feeling.

In consequence of first trials, it is concluded that produced knee pads can be used for pain relief and it is planned to test the effectiveness of knee pads on knee osteoarthritis patients after taking ethical committee permission. Furthermore, in this study, only the effect of 10 washing cycles to electrical resistance values was examined. In further studies, it is planned to investigate the effect of more washing cycles and laundry processes.

## REFERENCES

1. Sluka, K. A., Walsh, D.: Transcutaneous electrical nerve stimulation: basic science mechanisms and clinical effectiveness. 2003. The Journal of Pain, 4 (3), 109-121.
2. Bélanger, A. Y.: Kanıta dayalı elektroterapi. 2008. E. Yakut (ed.), Pelikan Yayınevi, Ankara, 43-76.
3. Melzack, R., Wall, P. D.: Pain mechanisms: a new theory. 1965. Science, 150 (3699), 971-979.
4. Jette, D. U.: Effect of different forms of transcutaneous electrical nerve stimulation on experimental pain. 1986. Physical Therapy. 66 (2), 187-190.
5. Jones, I., Johnson, M. I.: Transcutaneous electrical nerve stimulation. 2009. Continuing Education in Anaesthesia, Critical Care & Pain. 9 (4), 130-135.
6. Keller, T., Kuhn, A.: Electrodes for transcutaneous (surface) electrical stimulation. 2008. Journal of Automatic Control. 18 (2), 35-45.
7. Li, L., Au, W. M., Li, Y., Wan, K. M., Wan, S. H., Wong, K. S.: Design of intelligent garment with transcutaneous electrical nerve stimulation function based on the intarsia knitting technique. 2010. Textile Research Journal. 80(3), 279-286.
8. Guo, L., Berglin, L., Wiklund, U., Mattila, H.: Design of a garment-based sensing system for breathing monitoring. 2013. Textile Research Journal, 83 (5), 499-509.
9. Kannaian, T., Neelaveni, R., Thilagavathi, G.: Design and development of embroidered textile electrodes for continuous measurement of electrocardiogram signals. 2013. Journal of Industrial Textiles. 42 (3), 303-318.

10. Löfhede, J., Seoane, F., Thordstein, M.: Textile electrodes for EEG recording-a pilot study.2012. Sensors. 12 (12), 16907-16919.
11. Mestrovic, M. A., Helmer, R. J., Kyratzis, L., Kumar, D.: Preliminary study of dry knitted fabric electrodes for physiological monitoring. 2007. Proceedings of 3rd International Conference on Intelligent Sensors Sensor Networks Information, Melbourne, Australia.
12. Paradiso, R., Loriga, G., Taccini, N., Gemignani, A., Ghelarducci, B.: WEALTHY-a wearable healthcare system: new frontier on e-textile. 2005. Journal of Telecommunications and Information Technology, 4, 105-113.
13. Pola, T., Vanhala, J.: Textile electrodes in ECG measurement.2007. Proceedings of the 3rd International Conference on Intelligent Sensors, Sensor Networks and Information, Melbourne, Australia.
14. Rattfält, L., Lindén, M., Hult, P., Berglin, L., Ask, P.: Electrical characteristics of conductive yarns and textile electrodes for medical applications. 2007. Medical & Biological Engineering & Computing, 45 (12), 1251-1257.
15. Song, H. Y., Lee, J. H., Kang, D., Cho, H., Cho, H. S., Lee, J. W., et.al: Textile electrodes of jacquard woven fabrics for biosignal measurement. 2010. The Journal of the Textile Institute. 101 (8), 758-770.
16. Malešević, N. M., Maneski, L. Z. P., Ilić, V., Jorgovanović, N., Bijelić, G., Keller, T., Popović, D. B.: A multi-pad electrode based functional electrical stimulation system for restoration of grasp. 2012. Journal of Neuroengineering and Rehabilitation. 9(1), 66.
17. Kim, R. H., Cho, G.: Effectiveness of the smart healthcare glove system for elderly persons with hypertension. 2013. Human Factors and Ergonomics in Manufacturing & Service Industries, 23(3), 198-212.
18. Zięba, J., Frydrysiak, M., Tokarska, M.: Research of textile electrodes for electrotheraphy. 2011. Fibres & Textiles in Eastern Europe. 5(88), 70-74.
19. Gniotek, K., Frydrysiak, M., Zieba, J., Tokarska, M., Stempien, Z.: Innovative textile electrodes for muscles electrostimulation. 2011. Proceedings of the 6th IEEE International Symposium on Medical Measurement and Applications, IEEE MeMeA, Bari, Italy.
20. Frydrysiak, M., Zięba, J., Tęsiorowski, L., Tokarska, M.: Textronic system to muscle electrostimulation. 2012. International Scholarly and Scientific Research & Innovation. 6(11), 1311-1317.
21. Papaiordanidou, M., Takamatsu, S., Rezaei-Mazinani, S., Lonjaret, T., Martin, A., Ismailova, E.: Cutaneous recording and stimulation of muscles using organic electronic textiles. 2016. Advanced Healthcare Materials. 5(16), 2001-2006.
22. Prochazka, A., Gauthier, M., Wieler, M., Kenwell, Z.: The bionic glove: an electrical stimulator garment that provides controlled grasp and hand opening in quadriplegia. 1997. Archives of physical medicine and rehabilitation, 78(6), 608-614.
23. Lee, W. J., Um, S. H.: R & D of Smartwear built-in TENS device for relief of dysmenorrhea. 2009. The Research Journal of the Costume Culture, 17(2), 320-329.
24. Nisar, H., Malik, A. R., Asawal, M., Cheema, H. M.: An electrical stimulation based therapeutic wearable for pressure ulcer prevention. Proceedings of the IEEE EMBS Conference in Biomedical Engineering & Sciences (IECBES), Kuala Lumpur, Malaysia.
25. Keller, T., Lawrence, M., Kuhn, A., Morari, M.: New multi-channel transcutaneous electrical stimulation technology for rehabilitation. 2006. Proceedings of the International Conference of the IEEE Engineering in Medicine and Biology Society, New York, USA.
26. Goncu Berk, G.: Design of a wearable pain management system with embroidered TENS electrodes. 2018. International Journal of Clothing Science and Technology, 30(1), 38-48.
27. Erdem, D., Yesilpinar, S., Senol, Y., Karadibak, D., Akkan, T.: Design of TENS electrodes using conductive yarn. 2016. International Journal of Clothing Science and Technology, 28(3), 311-318.
28. Erdem, D., Yeşilpinar, S., Şenol, Y., Akkan, T., Karadibak, D.: Design of TENS electrodes using different production techniques. 2016. Tekstilec, 59(2), 132-136.

# TRANSFERRING OF THE PVA MICROCAPSULES CONTAINING OZONIZED OILS ONTO TEXTILE SURFACES AND EVALUATION OF THEIR ANTI-BACTERIAL ACTIVITY

**Koray PEKTAŞ[1], Onur BALCI[1], Burcu SANCAR BEŞEN[2], Cem GÜNEŞOĞLU[3], Mehmet ORHAN[4]**

[1] Kahramanmaraş Sütçü İmam University, Department of Textile Engineering, Turkey
[2] Adıyaman University, Department of Textile Engineering, Turkey
[3] Gaziantep University, Department of Textile Engineering, Turkey
[4] Uludağ University, Department of Textile Engineering, Turkey

Corresponding author: koraypektas@ksu.edu.tr

***Abstract:*** *In this study, the vegetable oils were ozonized and then used as a core material for the PVA Poly (vinyl alcohol) microcapsules. PVA microcapsules containing ozonized oils were transferred onto textile surfaces for gaining antibacterial activity. With this aim, the Gas Chromatography (GC), the Scanning Electron Microscope (SEM), Fourier Transform Infrared Spectroscopy (FTIR), optical microscope and antibacterial activity test against to E. coli and S. aureus were employed for characterization both ozonized oils and textile surfaces loaded PVA microcapsules. According to data from characterization tests, it was seen that ozonized vegetable oils showed antibacterial activity.*

***Key Words****: Ozonized oil, microencapsulation, pva, antibacterial activity, textile surface*

## 1. INTRODUCTION

The ozone ($O_3$) has been known as one of the best bactericidal, antiviral and antifungal agents and it has been used to treat many illnesses such as cellulite, burnt, ulcer, chronic wounds, immune system illnesses [1,2]. The beneficial effects of $O_3$ wound healing could be thanks to decreasing bacterial infection, increasing oxygen tension from $O_3$ exposure in the wound area [3]. The vegetable oils containing 97-98 % triglycerides have many compositions of saturated and unsaturated fatty acids depending on their specific structures [1,4]. The reaction between ozone and vegetable oils occur C=C double bounds in the unsaturated fatty acids. With this reaction, several oxygenated compounds come to exist such as hydroperoxides, ozonides, aldehydes, peroxides, diperoxides and polyperoxides [4]. Antibacterial, antifungal and antiviral properties of the oils are obtained by the ozonation process and these properties are interested in cosmetic and pharmaceutical industries. [5]. The microencapsulation is a caging method that liquid or solid particles, which are located small droplets, are hindered in a thin film. The microencapsulation is formed by many methods such

as in-situ polymerization, interfacial polymerization, coacervation, spray drying etc. [6].

In this study, the vegetable oils were ozonized and then used as a core material for the PVA Poly (vinyl alcohol) microcapsules. The PVA microcapsules containing ozonized oils were transferred onto textile surfaces for gaining antibacterial activity by coating method. With this aim, GC, SEM, FTIR, optical microscope and antibacterial activity test against to E. coli and S. aureus were employed for characterization both ozonized oils and textile surfaces loaded PVA microcapsules.

## 2. OBTAINING ANTIBACTERIAL TEXTILE SURFACES

### 2.1. Ozonotaion of Vegetable Oils

The olive oil, the common st john's wort oil were ozonized by the ozone generator, which generates 25g ozone gas in an hour. Each oil sample (100 ml) were ozonized for two hours to improve anti-bacterial activity of them.

### 2.2 Microencapsulation of Ozonated Oils

In the microencapsulation process, the Poly (vinyl alcohol), PVA which is Mw:63,000 and 88% hydrolysis degree, was used as a shell material, while raw and ozonated oils were used as core materials. The oil containing microcapsules were prepared by coacervation/crosslinking method which consist of three steps: (I) dispersion of the oil phase into PVA solution with the aid of a high-speed stirrer, (II) addition of the phase inducer such as sodium sulphate and (III) cross-linking of the coacervated membrane with a cross-linking agent [7]. 5% PVA solution (%w/v) were used and shell: core ratio was determined as 1:2. Besides, for the phase inducing, 20% (w/v) sodium sulphate solution was prepared.

### 2.3. Transferring of PVA Microcapsules Containing Vegetable Oils

The obtained PVA microcapsules containing vegetable and ozonated vegetables oils were transferred by knife on air coating application onto 100% viscose hydrophilic non-woven textile surfaces.

### 2.4. Tests and Analyses

During this study, from ozonation process to medical textile surfaces, a set of tests were employed. GC (Gas Chromotography) analysis was employed to determine amount of unsaturated fatty acids in oils before and after ozonation process, FTIR (Fourier Transform Infrared Spectroscopy) analysis was employed to observe the difference of the peaks having oils before and after ozonation process. SEM (Scanning Electrone Microscopy) images were taken for seeing microcapsules on the fabric after coating process and anti-bacterial activity test was done against to *E. coli and S. aureus* to evaluate antibacterial activity of the oils before and after ozonation process and the fabrics loaded microcapsules containing oils.

## 3. RESULTS AND DISCUSSIONS

It is no doubt that mono and polyunsaturated fatty acids in the oils tend to vanish after ozonizing process. The GC analysis were done for observing of the decrease of the unsaturated fatty acids amount in these ozonized oils. The amount of the oleic acid and linoleic acid in the olive oil sharply decreased after ozonation process. In additional, the percentage changes of the unsaturated fatty acid in these oils were given in Table 1.

**Table 1.** Unsaturated fatty acid amount of the olive oil before and after ozonation process

| Oil type | Oleic acid (%) | Linoleic acid (%) | Total (%) |
|---|---|---|---|
| Olive oil | 71.263 | 10.835 | 82,098 |
| Ozonated olive oil | 0,849 | 1,684 | 2,533 |
| Common st john's wort oil | 75,282 | 7,874 | 83,156 |
| Ozonated common st john's wort oil | 1,499 | 0,137 | 1,636 |

It was explicitly seen that FT-IR data of the ozonized oils supported GC analysis of the ozonated olive oil and common st john's wort oil. In comparison with the raw oils, FT-IR analyses showed that =C-H stretching (ca. 3000 $cm^{-1}$) of the mono and polyunsaturated fatty acid faded away while C-O stretching (ca.1100 $cm^{-1}$) of the ozonides came to exist (Figure 1). ıt could be said that vegetable oils were exposed to ozone gas sufficiently.

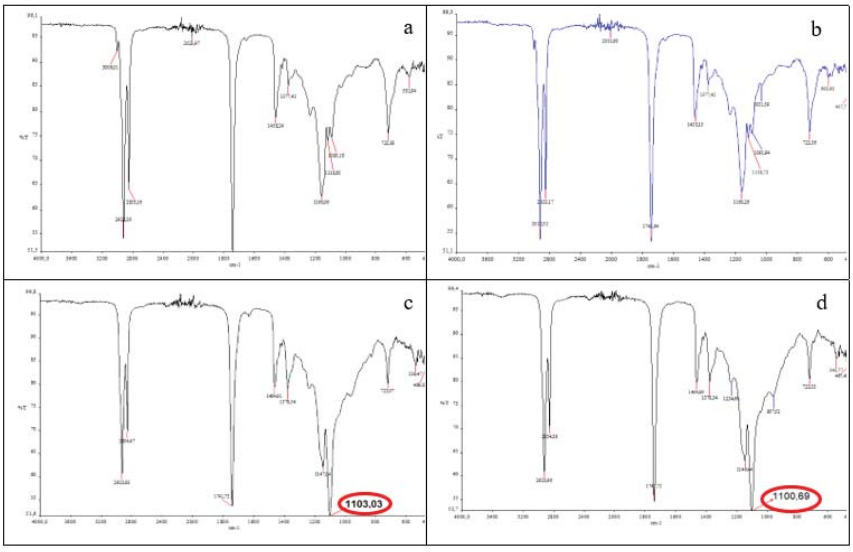


**Figure 1.** FTIR data of the vegetable oils a. olive oil, b. ozonated olive oil, c. common st john's wort oil, d. ozonated common st john's wort oil

On considering antibacterial activity of the raw olive oil, the common st john's wort oil and ozonized oils, ıt was seen that antibacterial activity of the oils increased after ozonizing process of the raw oils. It was obviously seen that ozonized oils showed much more antibacterial activity then the raw ones (Table.2).

**Table 2.** Anti-bacterial activity of the the vegetable oils a. olive oil, b. ozonated olive oil, c. common st john's wort oil, d. ozonated common st john's wort oil

| **Sample** | **Zone Diameter (mm)** | |
|---|---|---|
| | *E. Coli* | *S. aureus* |
| Olive Oil | 76 | 80 |
| Ozonated olive oil | 90 | 90 |
| Common st john's wort oil | 88 | 86 |
| Ozonated common st john's wort oil | 147 | 89 |

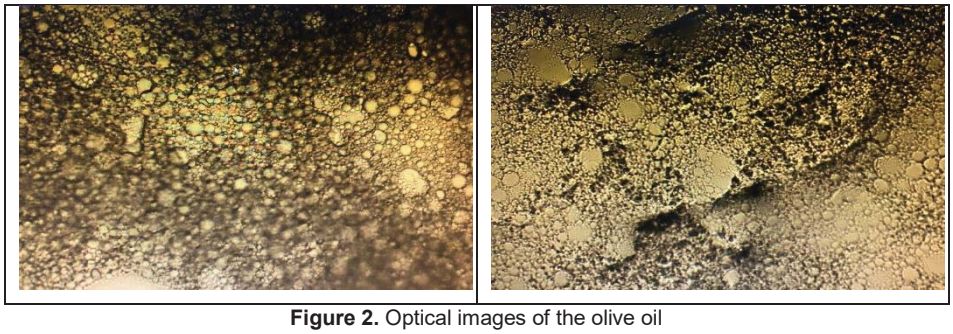

**Figure 2.** Optical images of the olive oil

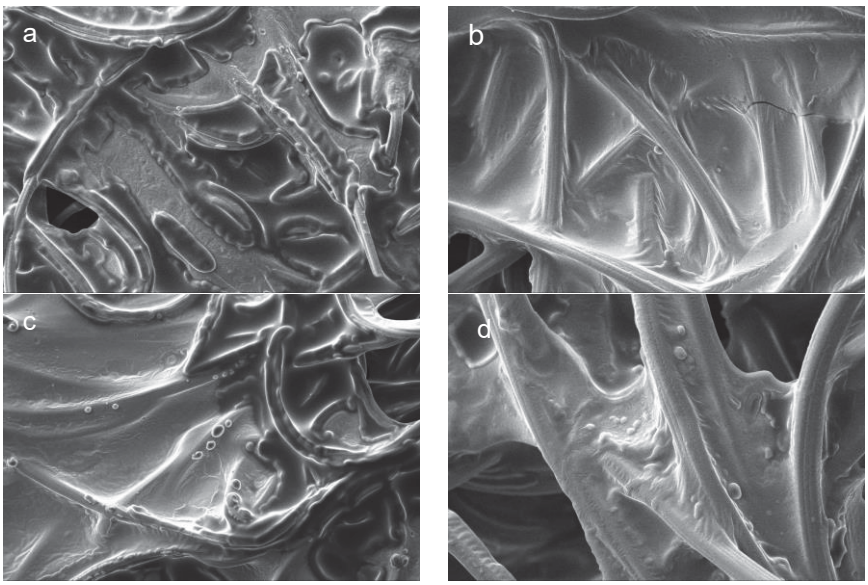


**Figure 3.** SEM images of the non-woven textile surfaces containing a. olive oil, b. ozonated olive oil, c. common st john's wort oil, d. ozonated common st john's wort oil microcapsule and hydrogel

Optical microscope images of the raw olive oil showed that microencapsulation process was successful (Figure 2). After transferring of the PVA microcapsules containing vegetable oils onto non-woven textile surfaces by coating method, SEM images showed that existence of the vegetable oil onto textile surfaces both microcapsule shape and coated by PVA (Figure 3).

FTIR analyses of the non-woven textile surfaces indicated that along with existence of specific peaks of PVA (≈1085 -1150 $cm^{-1}$ which indicates C-O-C bound), it was obviously observed specific FTIR peaks of raw and the ozonated oils, which were ≈1100 cm-1, ≈1742 cm-1, were disappeared after successful microencapsulation process by coacervation (Figure 4).

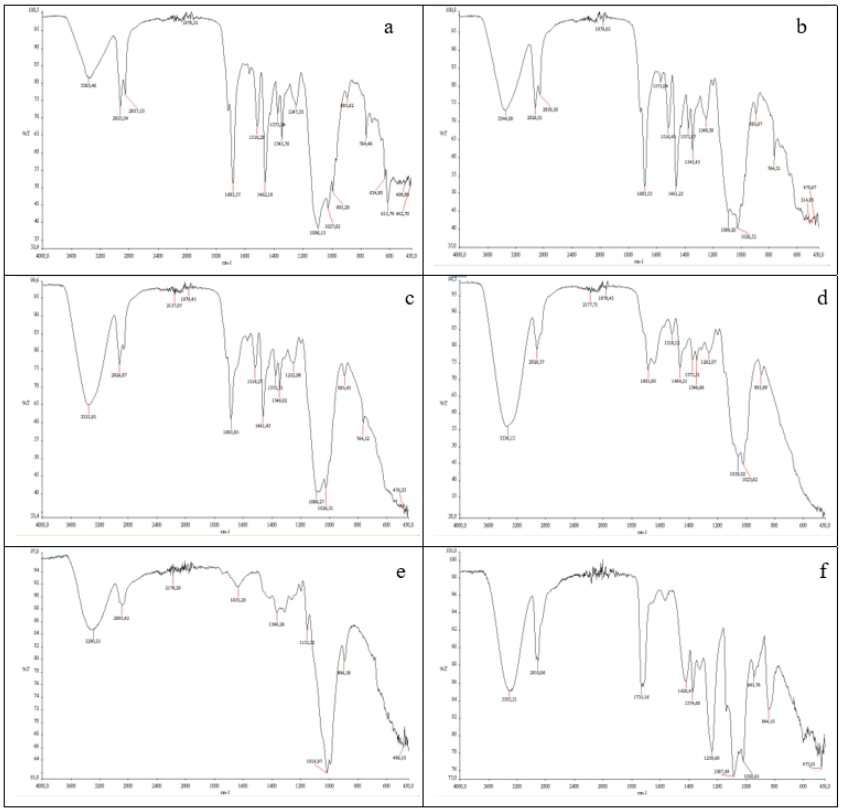


**Figure 4.** FTIR spectrum of the non-woven textile surfaces containing a. olive oil, b. ozonated olive oil, c. common st john's wort oil, d. ozonated common st john's wort oil microcapsule e. untreated non-woven textile surface f. neat PVA powder

According to ASTM E 2149-01, Antibacterial activity test on the non-woven textile surfaces loaded PVA microcapsules containing vegetable oils indicated that these textile surfaces have antibacterial activity against to *S. aureus* and *E. coli*. Moreover, *S. aureus* was vulnerable to both raw and ozonized oils. In addition,

reduction of bacteria proliferation on fabric loaded ozonized oils were better than raw oils.

**Table 3**. Anti-bacterial activity of the non-woven textile surfaces coated PVA microcapsules with vegetable oils

| Sample | % Change on bacteria proliferation (24h) | |
|---|---|---|
| | *E. coli* | *S. aureus* |
| Untreated non-woven textile surface | +307,77 | +113 |
| Olive oil | -55,18 | -100 |
| Ozonated olive oil | -85,12 | -100 |
| Common st john's wort oil | -62.14 | -100 |
| Ozonated common st john's wort oil | -93,59 | -100 |

## 4. CONCLUSIONS

In the scope of this study, upon considering GC, FTIR and antibacterial activity test of both raw and ozonized oils, it was seen that olive and the common st john's wort oil were ozonized accomplishly. Besides, after ozonation process of these oils, they were trapped into PVA by coacervation method. PVA microcapsules were transferred onto non-woven textile surfaces by coating method. In addition, SEM images showed that entrapped vegetable oils into PVA were found onto textile surfaces as microcapsules. Antibacterial activity test indicated that antibacterial activity of the vegetable oils was increased after ozonation process of these oils. Moreover, non-woven textile surfaces containing ozonized oils microcapsules and coating showed antibacterial activity better than untreated vegetable oils by ozone gas. It was thought that textile surfaces loaded ozonized oil could be used for wound care.

## REFERENCES

1. Beşen BS, Güneşoğlu C, Balci O,: Antibacterial Finishing of 100% Cotton Fabric with with β-Cyclodextrin-Ozonated Olive OilInclusion Complex. 2016. AATCC J.3(6):12–8.
2. Valacchi G, Lim Y, Belmonte G, Miracco C, Zanardi I, Bocci V, et al. Ozonated sesame oil enhances cutaneous wound healing in SKH1 mice. 2011. Wound Repair Regen.19(1):107–15.
3. Valacchi G, Zanardi I, Sticozzi C, Bocci V, Travagli V. Emerging topics in cutaneous wound repair. 2012. Ann. N.Y. Acad. Sci 1259:136–44.
4. Díaz MF, Hernández R, Martínez G, Vidal G, Gómez M, Fernández H, et al. Comparative Study of Ozonized Olive Oil and Ozonized Sunflower Oil. 2006;17(2):403–7.
5. Cirlini M, Caligiani A, Palla G, Ascentiis A De, Tortini P, Cirlini M, et al. Stability Studies of Ozonized Sunflower Oil and Enriched Cosmetics with a Dedicated Peroxide Value Determination. 2012. Ozone : Science & Engineering The Journal of the International Ozone Association. 9512.
6. Karthikeyan M, Ramachandran T, Shanmugasundaram OL. Synthesis , characterization , and development of thermally enhanced cotton fabric using nanoencapsulated phase change materials containing paraffin wax. 2014. J Text Inst 105(12):1279-1286.
7. Bachtsi A, Boutris C, Kiparissides C. Production of Oil-Containing Crosslinked Poly(vinyl alcohol) Microcapsules by Phase Separation: Effect of Process Parameters on the Capsule Size Distribution.1996. Journal of Applied Polymer Science, Vol. 60, 9-20.

# DEVELOPMENT OF NOVEL SANITARY NAPKIN AIRLAID ABSORBENT CORE MATERIAL WITH IMPROVED LIQUID ACQUISITION PERFORMANCE

**Suna KARAKURD ELMA[1], İsmaiL KAYNAK[1], Serkan NOHUT[2], Mehmet DAŞDEMİR[3]**

[1] Selçuk İplik San. ve Tic. A.Ş. Ar-Ge Merkezi
[2] İstanbul Gedik University, Turkey
[3] Gaziantep University, Turkey

Corresponding author: suna.karakurd@kholding.com.tr

***Abstract:*** *In this study, an air laid nonwoven composite composed of three layers to be used as liquid acquisition core material in sanitary napkins is developed. This study investigates the effects of using different ratios of SAP particles in different layers and layer thicknesses on liquid acquisition time and liquid acquisition capacities of composite core material. In addition, the effect of the thermal calendaring on liquid acquisition performance is also examined. As a result of the study, a new air laid sanitary napkin liquid acquisition core material is developed with the thermal modification of the surface and the optimization of the SAP quantities at different layers. In this new material, the liquid acquisition time and thickness are decreased without decreasing the liquid acquisition capacity.*

***Key Words****: Sanitary pad, absorbent core, nonwoven, technical textiles, airlaid*

## 1. INTRODUCTION

The term air laid nonwoven refers to a manufacturing technology that produces a web from short fibers, most often softwood pulp. While the principal fiber used to produce air laid nonwovens is fluff pulp other natural and synthetic fibers can be used [1].

Absorbent layers in sanitary napkins are mostly composed of three layers. The uppermost layer is liquid acquisition layer, the middle layer is preferably a liquid storage layer comprising Super Absorbent Polymer (SAP) particles and a subsequent liquid dispersant layer. Important parameters which determine the performance of liquid acquisition core material are liquid acquisition time, liquid acquisition capacity and thickness.

In the literature, there are very limited studies on the properties and performance of the absorbent layers in sanitary napkins [2, 3]. Waksmundzki et al. [2] claimed that using two or more superabsorbent polymer having different absorbing properties at different layers of the air laid not only improved absorbency of the core layer but also decreased rewet and the time for overall absorption. Conio and Mantovani [3] pointed out that multi-layer structures comprising super

absorbent polymer in between cellulosic fiber layer can enhance wicking action, thereby increasing the absorption rate.

In this study, we investigated the influences of using different ratios of SAP particles in different layers and layer thicknesses on acquisition time and liquid acquisition capacities of composite core material.

## 2. MATERIALS AND METHODS

Air laid nonwoven composite fabric samples for the absorbent core material of feminine sanitary napkin were produced using Oerlikon Neumag air laid nonwoven manufacturing line (see Fig. 1). Tissue paper, wood pulp, polyacrylate based super absorbent polymer (SAP), latex and PP/PE bicomponent fiber were used in the formation of air laid nonwoven composites. List of the applied tests and their standards are given in Table 1.

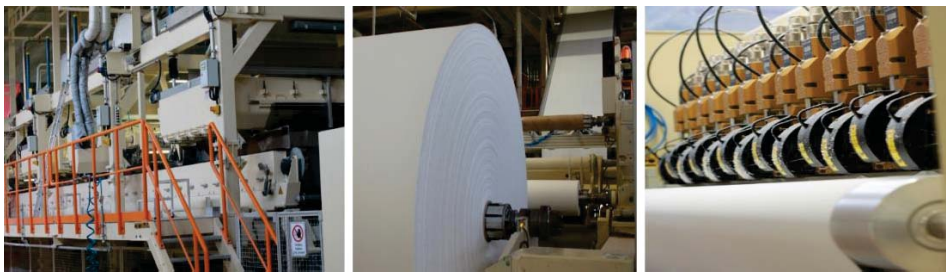

**Figure** 1. Oerlikon Neumag air laid nonwoven manufacturing line

**Table 1.** List of the applied tests and their standards

| Test Name | Standard No |
|---|---|
| **Mass per Unit Area** | NWSP 130.1 R0 (15) |
| **Nonwoven Thickness** | NWSP 120.6 R0 (15) |
| **Breaking Force and Elongation of Nonwoven Materials (Strip Method)** | NWSP 110.4 R0 (15) |
| **Three Standard Test Methods for Nonwoven Absorption** | NWSP 010.1 R0 (15) |
| **Coverstock Wetback for Nonwovens** | ISO 9073-14: 2006 |
| **Repeated Liquid Strike-Through Time for Nonwovens** | ISO 9073-13: 2006 |
| **Determination of Liquid Strike-Through Time (Simulated Urine) for Nonwovens** | ISO 9073-8: 1995 |
| **Superabsorbent Materials — Polyacrylate Superabsorbent Powders — Gravimetric Determination of Fluid Retention Capacity in Saline Solution After Centrifugation** | NWSP 243.0 R2 (15) |

## 3. RESULTS AND DISCUSSION

The most critical parameters of the absorbent core used in feminine hygiene are liquid absorbency capacity and rate (i.e. 3rd liquid absorbency time) using both

water and artificial blood as test fluid, retention and thickness. Thickness is important for the producers and consumers due to comfort properties.

In all samples, air laid core samples with basis weight of 200 gsm (g/m$^2$) and SAP ratio of 30 % were manufactured. The SAP particles were used only on the Layer-1 (under paper tissue) and Layer-2 with different ratios. Without changing the SAP ratio between layers, a decrease of thickness around 15-20 % decreased the retention ratio and increased the 3rd liquid absorbency time with water.

However, the change of the 3rd liquid absorbency time with artificial blood and absorbency capacity was ignorable. When the SAP ratio in Layer-2 increases, the retention ratio increases since the wetback of the liquid is prevented due to the SAP particles in Layer-2. In addition, the 3rd liquid absorbency time with water and artificial blood decreases as the SAP particles in Layer-2 increases. On the other hand, the absorbency capacity decreases since this parameter is strongly affected by the SAP particle rate in Layer-1.

These results show that, the thickness and the rates of SAP particles in each layer determine the liquid absorbency capacity of Air laid core materials in feminine hygiene.

## 4. CONCLUSIONS

In this study, we have developed a novel air laid sanitary napkin liquid acquisition core material and achieved lower liquid acquisition time and thickness without comprising the liquid acquisition capacity in the final product. We also revealed that the liquid absorbency capacity of air laid core materials in feminine hygiene product can be determined by adjusting the thickness and the rates of SAP particles in each layer of the core structure.

## REFERENCES

1. Wilson, A.: 1 – The formation of dry, wet, spunlaid and other types of nonwovens. 2010. Applications of Nonwovens in Technical Textiles. 3-17.
2. Waksmundzki, A., Litvay, J. and Glaug, F.: Absorbent core having two or more types of superabsorbent. 2006. US Patent Application No: 20060069367A1.
3. Conio, G. and Mantovani, G.: Slight-incontinence sanitary napkin structure, 2011. European Patent Application No: 2301497 A1.

# READY-TO-PRINT & WEAR: 3D PRINTING APPLICATIONS IN FASHION

**Elif TEKCAN[1], Arzu VURUŞKAN[1], Ender YAZGAN BULGUN[1], Mert KALAYCI[1]**

[1] Izmir University of Economics, Turkey

Corresponding author: elif.tekcan@ieu.edu.tr

***Abstract:*** *3D printing and digital manufacturing technologies are expected to change the future of fashion industry by creating alternatives for the existing production and consumption patterns. In addition to bringing ease to small-scale productions and DIY projects, 3D printing technology defines a common manufacturing method that will facilitate the co-production of different industries and design disciplines. Considering this advantage, this study investigates how 3D printing technologies can be integrated with illuminative fashion applications with the help of electronics. Following a short review of related examples in this field, the paper presents the design process of a garment prototype. In this prototype, 3D printed surfaces were combined with optical fibers, which can change color by the user controlled software application.*

***Keywords:*** *3D printing technologies, fashion, innovation, future trends, digital manufacturing*

## 1. INTRODUCTION

3D printing and digital manufacturing technologies are revolutionizing fashion industry by introducing a new production model which affects all the phases of supply chain starting from material sourcing to design, manufacturing, inventory, warehousing and distribution. This system reduces production costs by eliminating some steps in the supply chain; and diminishes waste by replacing traditional (subtractive) production methods that generate textile cut-offs, with an alternative method (additive) using only the necessary amount of material for the production [1,2]. 3D printing technology takes further attention in the field of sustainable fashion by offering durable and self-mending materials, which extend the product's life-span; and eco-friendly materials which bring less harm to the environment [1,3]. The technology is also compatible with current marketing trends, such as online shopping and mass customization, since designers can work with digital files enabling them to make customized and quick design variations [1]. Although 3D printing technology already provides many advantages for the companies seeking for innovation, it is still new and needs further explorations for fashion applications.

Within this context, we aimed to develop the design process of a 3D printed garment integrated with optical fibers. The first part of this paper introduces the design research phase. A short review of 3D printed fashion applications are included, which are produced with various manufacturing methods such as selective laser sintering (SLS), stereolithography (SL), polyjet, and fused deposition

modeling (FDM). Following this, research for printing techniques and design development phases were conducted.

## 2. DESIGN RESEARCH

3D printing technology has begun to be used in the fashion industry in the last decade, and enabled designers to take the advantage of digital design methods for the creation of more complex garment structures which cannot be produced with textiles. Dutch designer Iris van Herpen became one of the first fashion designers who experimented this technology. In SS 2011 “Crystallization” RTW collection, she integrated selective laser sintering (SLS) method in collaboration with architect Daniel Widrig and MGX Company [4]. Since that year, Herpen teamed up with renowned professionals including Julia Koerner, Neri Oxman [5], Niccolò Casas [6] and Philip Beesley [7] for 3D printed projects. Especially the cape and skirt ensemble that she designed with Neri Oxman, became one of the early and the most successful examples produced with polyjet technology. An example from this SS 2013 “Voltage” haute couture collection is given in Figure 1 [1, 5]. Also, fall 2013 “Wilderness Embodied” haute couture collection included a dress made of semi-transparent pieces. These bone-like structures were produced with Mammoth’s stereolithography (SL) printers using liquid resin, and coated with silicon to achieve a soft and flexible look [1, 8].

In addition to fashion designers, the technology inspired artists and architects who want to create wearable structures. The first fully articulated 3D printed dress was designed in 2013 with the collaborations of architect Francis Bitonti and designer Michael Schmidt for Dita Von Teese. The long futuristic black gown was manufactured with selective laser sintering (SLS) method [9].

Noa Raviv and Danit Peleg integrated 3D printing technology to their graduate collections. In “Hardcopy” collection, Raviv used Objet Connex multi-material 3D printer to construct voluminous pieces creating optical illusion (Figure 2) [10]; and Peleg’s “Liberty Leading the People” collection was produced with Witbox FDM desktop 3D printers, by using FilaFlex material and became the first 3D printed collection produced at home environment (Figure 3) [11].



**Figure 1 (Left):** The cape and skirt ensemble designed with the collaborations of Iris van Herpen and Neri Oxman. **Figure 2 (Center):** An outfit from Noa Raviv’s “Hardcopy” collection. **Figure 3 (Right):** An outfit from Danit Peleg’s “Liberty Leading the People” collection.

## 3. MATERIALS AND METHODS

For design development of the prototype, we conducted extensive research on four 3D printing methods including stereolithography (SL), selective laser sintering (SLS), fused deposition modeling (FDM), and polyjet, which are frequently used in fashion applications.

SL printers include a tank filled with UV-sensitive liquid resin. UV lasers selectively hardens the material in the tank where the structure is built starting from bottom layer to top. The technique which is suitable for the creation of sculpture-like structures, is preferred for high-end finishes. However, it requires raft removal and sanding which increase production time, and reduce product quality. The printers work with liquid resin, which is an expensive material with limited color option [1], [12]. SLS printers selectively sinter polymer powders in a powder bed where the form is constructed layer by layer from bottom to top. The technique enables the production of delicate, yet strong forms with a wide range of materials such as plastic, glass, metal and ceramics. It does not produce support rafts, therefore it eliminates the additional manual task of raft removal, and requires less sanding. Despite all these advantages, the quality of the structure produced with SLS is lower compared to SL [1], [13]. FDM is a frequently used method because of its affordability. As material, FDM printers uses thermoplastic polymers which are available in filament form. In addition to polylactic acid (PLA) and acrylonitrile butadiene styrene (ABS) which are frequently used, the companies offer special filaments made of wax, metals, woods and ceramics. Especially flexible filament options are much preferred by fashion designers who would like to create delicate structures. However, since the filaments are heated during the printing process, the temperature changes can result in visible seam lines. Also it produces rafts that need to be removed after printing [1].Polyjet technology provides a significant advantage for fashion designers who want to print wearable structures using multiple materials. Photopolymer resin is used as material, which selectively drop on building platform. The technique is also preferred for its high speed and high-quality surface finish [1].

Among these methods, FDM was preferred for the prototype development since it is already an available facility in the university, therefore provides practicality and cost efficiency. As material, PLA, ABS and eFlex filaments were preferred as frequently used materials for this type of printers. Methods of integrating light elements (LEDs and optical fibers), 3D printed surface thicknesses, dimensions of single units to be printed in the 3D printer, pattern design of these single units and their connections were some of the investigation issues in order to finalize the designs. We also experimented how 3D printed surfaces can be combined to create a garment form. For example, different joint options were designed and tested on the samples in relation to the body. Attachable/detachable elements (collar, cuff etc.) were developed as accessories for practical purposes and are suggested as design solutions for combining fashion and technology. Another significant stage in the process was the integration of appropriate software in order to support light control by the user and communication with other smart objects.

## 4. RESULTS

The design development project achieved its primary targets by integrating 3D printed surfaces with optical fibers and LEDs on a wearable structure. On the prototype, the integration of 3D printed units were created with the use of interlocking parts. With the available FDM 3D printer in the university, maximum possible printing dimensions were 20 cm x 20 cm. This was a limiting factor for the design of single 3D printed units. Figures 4 and 5 illustrate the 3D drawing of one of these units.

On these test pieces, different joint alternatives were applied based on the characteristics of materials. One joint option was more appropriate with flexible material, such as eFlex filament (Figure 7 and 8), whereas another joint design could work for both flexible (softer) and harder materials, such as standard ABS or PLA (Figure 4 and 5). This latter joint includes tunnels as seen in Figure 5, where optical fibers are lined up to support connection points. This is accepted as an innovative approach since optical fibers are used not only as connections (joints), but also for decorating 3D printed units. These optical fibers are illuminated with LEDs hidden in 3D printed structures.

Before garment construction phase, these design units were printed to determine the most appropriate size / thickness. By using FDM method, alternative design units were produced in thickness ranging between 0.3 - 3.5 mm with PLA, ABS and eFlex filaments. These units were combined with interlocking parts giving the surfaces a puzzle-like structure. This structure enabled the integration of attachable/detachable design components and brought an advantage for users who want to wear the garment in different forms, and who prefer to use some pieces as accessories on regular garments.

The project received positive feedback at the initial demonstration, where the design alternatives are introduced to the audience in the University[1]. Based on collected experiences, alternative printing methods such as stereolithography will be tried as a follow up of this research, which is a much-preferred method in fashion applications for its high end finishes.

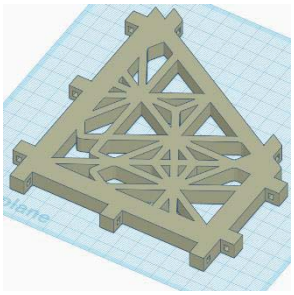

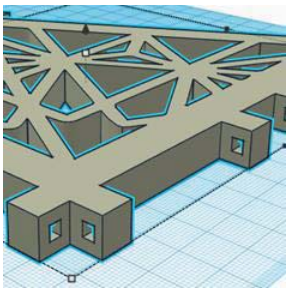

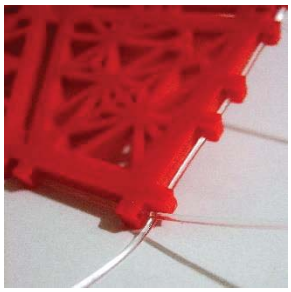

**Figure 4 (Left):** One of the units modeled with 3D modeling software. **Figure 5 (Center Left):** A tunnel system designed for the integration of units and transition of optical fibers. **Figure 6 (Right):** 3D printed version of the tunnel system

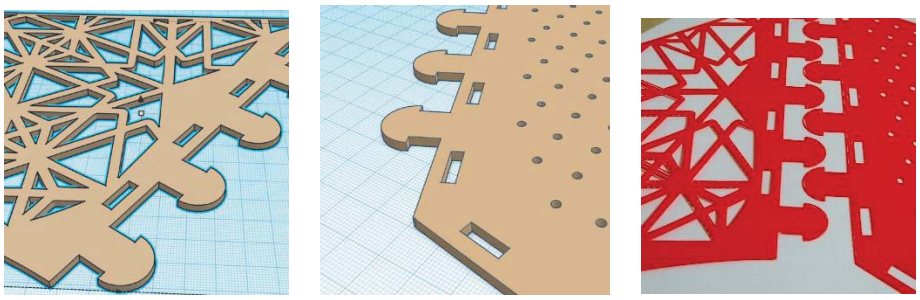

**Figure 7 and 8 (Left and Center):** A joint system which is applicable for units printed with eFlex.
**Figure 9 (Right):** 3D printed version of the joint system

## 5. CONCLUSIONS

3D printing technology has already been used by many designers in fashion collections. This technology which is constantly updated with the development of new printers and materials, is expected to be used more frequently in the fashion industry. This project contributes to the field, by adding smart features to a 3D printed garment with the help of electronics and software applications. The project is also connected to the most recent innovations of the Internet of things (IOT), which is a driving source for Industry 4.0. In addition to luxurious couture 3D printed dresses, it is expected that such digital manufacturing technologies will provide customizable and ready-made clothing in an affordable way.

## REFERENCES


1. Vanderploeg, A., Lee, S.-E. & Mamp, M., 2017. The application of 3D printing technology in the fashion industry. *International Journal of Fashion Design, Technology and Education,* 10(2), pp. 170-179.
2. Minshall, T., 2016. "How 3D printing is enabling the '4th Industrial Revolution." TED. June 2016. Lecture. [Online] Available at: https://www.youtube.com/watch?v=lsJLZ1UYxGc [Accessed 02 July 2018].
3. Siegle, L., 2018. Ten ways to make fashion greener. [Online] Available at: https://www.theguardian.com/fashion/2018/jun/24/ten-ways-to-make-fashion-greener [Accessed 02 July 2018].
4. Anon., 2010. *Mind-blowing 3D printed fashion.* [Online] Available at: https://i.materialise.com/blog/en/mind-blowing-3d-printed-fashion/ [Accessed 01 July 2018].
5. Thilmany, J., 2013. Fashion that's print a porter. Mechanical Engineering-CIME, 135(4), p. 10.
6. Mau, D., 2014. *How Iris Van Herpen's Ice-Like 3-D Printed Dress Was Created.* [Online] Available at: https://fashionista.com/2014/10/iris-van-herpen-3-d-printing [Accessed 02 July 2018].
7. Benesh, C. L. E., 2018. Iris van Herpen: Transforming Fashion. Ornament, 40(3), pp. 26-29.
8. Anon., 2013. *Iris van Herpen presents her Wilderness Embodied Collection.* [Online] Available at: https://i.materialise.com/blog/en/iris-van-herpen-presents-her-wilderness-embodied-collection/ [Accessed 02 July 2018].

9. Howarth, D., 2013. *3D-printed dress for Dita Von Teese by Michael Schmidt and Francis Bitonti.* [Online] Available at*:* https://www.dezeen.com/2013/03/07/3d-printed-dress-dita-von-teese-michael-schmidt-francis-bitonti/ [Accessed 02 July 2018].

10. Howarth, D., 2014. *Noa Raviv combines grid patterns and 3D printing for Hard Copy fashion collection.* [Online] Available at: https://www.dezeen.com/2014/08/21/noa-raviv-hard-copy-fashion-collection-grid-patterns-3d-printing/ [Accessed 02 July 2018].

11. Bonime, W., 2017. *Danit Peleg's Beautiful Fashion Tech Must-Haves for Fall 2017.* [Online] Available at: https://www.forbes.com/sites/westernbonime/2017/09/10/danit-pelegs-beautiful-fashion-tech-must-haves-for-fall-2017/#4c5cde753a9b [Accessed 02 July 2018].

12. Anon., 2018. *How Does Stereolithography Work?.* [Online] Available at: https://www.materialise.com/en/manufacturing/3d-printing-technology/stereolithography [Accessed 02 July 2018].

13. Anon., 2018. *What is SLS?* [Online] Available at: https://www.3dhubs.com/knowledge-base/introduction-sls-3d-printing#what [Accessed 02 July 2018].

## FIGURES

1. Figure 1: Topbaş, H., 2017. *Futurism Genius: Iris Van Herpen. [Online] Available at: http://www.architectureoflife.net/en/futurism-genius-iris-van-herper/* [Accessed 02 July 2018].

2. Figure 2: Anon., 2015.*Grid Patterns and 3D Printing.* [Online] Available at: *http://www.ishandchi.com/2015/01/* [Accessed 02 July 2018].

3. Figure 3: Anon., 2018. *3D Printed Fashion by Danit Peleg*. [Online] Available at: https://www.radissonred.com/blog/fashion/3d-printed-fashion-by-danit-peleg/ [Accessed 02 July 2018].

# THE FUTURE OF TEXTILE AND FASHION DESIGN IN VIRTUAL REALITY

**Faik KARTELLİ[1], Markus BERGER[1], Selda KOZBEKÇİ AYRANPINAR[2], Nesrin ÖNLÜ[2]**

[1] Dokuz Eylül University, Department of Film Design, Turkey
[2] Dokuz Eylül University, Department of Textile and Fashion Design Department, Turkey

Corresponding author: onlunesrin@gmail.com

***Abstract:*** *Virtual Reality is a technology that gives the user the experience of being surrounded by a computer-generated environment. With the recent upcoming of affordable VR technology a boom can be seen in a variety of areas. The fast paced progress made in this technology makes it important to also think of ways to connect it with fashion design. Possibilities to transfer the designing process into a virtual environment using drawing applications like Tilt Brush already exist. By placing a digital dummy puppet into the virtual environment the designer is able to intuitively paint clothes onto it. The created designs can then be exported and directly transferred to other 3D software packages for further processing or turned into plastic print-outs by a 3D printer. Transferring the whole prototyping process of clothes into a virtual environment will make it more intuitive, flexible and time saving.*

***Key Words****: Virtual Reality, Immersion, Textile, Fabric, Fashion, Design*

## 1. INTRODUCTION

Computer technology, used in the field of fashion design, ensures fast and error-free production. This means designing and creating production reports in a digital environment without using paper, pencil, dyestuff, etc.. At the same time, for example in weaving fabrics, production reports can be transferred via computer directly to the weaving machines which then turn the designs into fabrics . Computer technology allows us to apply different patterns, models, colors etc. onto the designs very quickly. Limitless numbers of color variations or completely new patterns can be generated from one single existing pattern without effort. Quickly accomplished calculations can be sent online to the weaving or printing machines. After selecting the fabrics for the garment, molds can be prepared. Even the entire garment creation process can be produced in a digital environment, using computer aided design (CAD) and computer aided manufacturing (CAM). The invention of digital cameras has accelerated this process even further. By using a digital camera combined with a computer, in the scope of digital design and production, for example, a photograph can turned into a pattern which can then be directly printed, woven, knitted or embroidered. Animation, the way the design looks on the podium as well as body fit and mobility of the 3D virtual garment design, dressed onto the previously scanned and

imported body model, can be viewed in real time (For detailed information look at: Magnenat-Thalmann, Nadia, 2010).

The emergence of broadly available, affordable high-quality virtual reality (VR) technology, however, brings a whole new perspective to the designing process. But before getting closer into the subject it is important to clarify the terminology:

Virtual Reality is a term that is being used for quite a variety of things. For the sake of clarity a more specific definition of how the term will be used in the following is needed. Steve Bryson suggests following definition: “Virtual Reality is the use of computer technology to create the effect of an interactive three-dimensional world in which the objects have a sense of spatial Presence” (Bryson, 2013, p. 4).

In other words, the user finds him/herself surrounded by an artificial, computer generated, three-dimensional environment, which is achieved in most cases by replacing the sense of vision with a head-mounted display (HMD), and the sense of sound with headphones. In turn, the term HMD refers to a type of equipment, that strapped to the head of the user places small computer displays directly in front of his/her eyes.

Since the introduction of consumer VR headsets, like the Oculus Rift or the HTC Vive, a constant development of new applications can be observed in a great variety of different areas. Beside the gaming and entertainment industry we see uses in engineering, education or medicine. It is therefore reasonable to assume that VR will play a big part in the field of designing. Fabric and garment design will surely not stand back in this progress.

Creating designs and patterns in VR can offer interesting possibilities. By immersing themselves into a virtual environment designers are able to examine and interact with the design as if it had materialized in front of them. Not being bound to a two dimensional surface, like paper or a graphics tablet, a whole new experience arises by drawing directly onto 3D space (figure 1).

**Figure 1.** Interaction with Google’s Tilt Brush application [8]

Instead of having to look at a screen the user finds him/herself in a virtual surrounding and can design, assuming the whole space as if it was the fabric or garment itself. Unlike handling a conventional computer user interface the use of

tools is much more intuitive because the designer is basically holding them in his/her own hands. Feeling a part of the garment the designer can transfer all emotions and thoughts into the design. Designing in a virtual environment combines the hands-on-feeling of working in a traditional tailor workshop with all the advantages and flexibility a computer aided system brings to the process (figure 2). Therefore, through the use of virtual reality technology very different designs can be created in much shorter time and later directly be transferred to production machines. In the light of this information the aim of the paper is to show examples of works done in fabric and garment design with the use of virtual reality technology until now, to explain and demonstrate how textile and garment designs can be created in a virtual reality environment, and to predict how development and innovation in the field can be achieved.


**Figure 2.** By use of a virtual draping dummy the design can be drawn directly onto it [9]

## 2. MATERIAL AND METHOD

The setup for this attempt requires a head-mounted display (HMD) and two VR hand controllers. For this setup the Oculus Rift HMD is used in combination with Oculus Touch controllers (Figure 3). Two sensors placed diagonally in front of the user track the position of the headset and the controllers and send this data to the software, making sure that the movement the user does in the physical space is transferred to the virtual environment. The controller feature more or less the same buttons a regular gamepad does. But in combination with the position and rotation tracking they become representations of the user's hands in the virtual world.

**Figure 3.** : Oculus HMD, Position Tracking Sensor and Hand Controllers [10]

In order for the Oculus Rift HMD to display high quality images with great detail smoothly, it has to be connected to a powerful gaming computer via cables. The PC used in the setup features an 8GB graphics card, an Intel i7 Processor with a speed of 3.60GHz and 16GB of RAM memory. This computer is used both to run the VR equipment and to process all the data, that is peripheral to the designing process.

For the actual designing in virtual reality Google's Tilt Brush software is being used. The tools featured in the application are quite similar to those of any simple computer-based drawing program, with a few additions. The main difference, however is, that the users find themselves in a virtual environment, by using the hand controllers is able to draw lines directly into the air and can then walk around the drawings to look at them from any desired angle. The simple user interface makes it possible to intuitively change parameters like bush style, brush size, line color or line opacity. The user can scale up or down the drawn as he/she desires. One of the available environments features the 3D model of a regular draping dummy (Figure 4). But any kind of 3D model can be imported into the program (figure 4).

**Figure 4.** View through VR headset. Custom 3D models can be imported [7]

For the designing process the user moves freely around the draping dummy, intuitively drawing the clothing onto it (figure 5). This can be done in a very rough a sketchy manner but by scaling up the the drawings also very detailed designs can be created. At any point the design can be exported as a 3D model and further modified in any kind of 3D application or even sent to a 3D printer to create a 3D plastic print-out of it.

Along with commonly used body scanners and the development of standards in fashion, every passing day new advances in digital garment modeling and simulation applications are being introduced to the fashion industry. Both 2D and 3D CAD / CAM systems are broadly used. 2D CAD systems allow the creation of two-dimensional molds of the designed garment. Using a 3D CAD system, the molded parts can then be placed according to earlier taken body measurements or onto a digital human avatar created through body scanning (Vitali & Rizzi, 2018, pp. 131-135). This digital workflow makes it possible to rehearse virtual

clothing on an individual. Thanks to the 3D imagery, the fit on the body and the way the fabric falls can be observed. These methods are common practice in the clothing sector today. The concept communicated here, with the use of virtual reality, however, combines the designing of the garment, the creation of 2D molds, the rehearsal and control of the clothing's fit on the individual and by doing so makes improvement of the garment development process, a decrease of time and cost and the attaining of results in shorter time foreseeable.

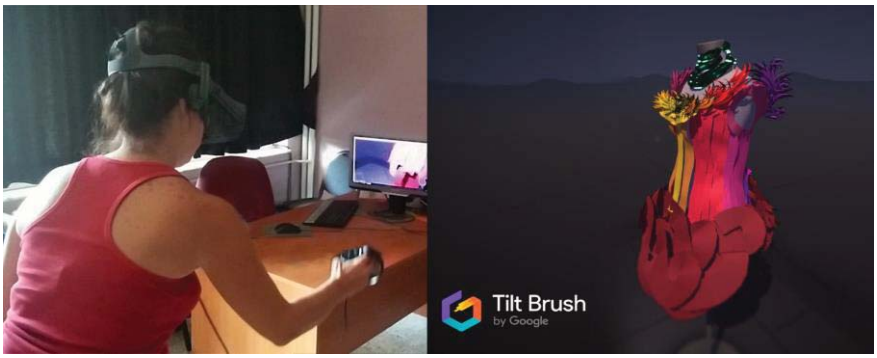


**Figure 5.** Use of VR headset and hand controllers (left). Finished design (right) [performer S. Kozbekçi Ayranpınar]

## 3. DISCUSSION

As can be understood from the information above, with VR technology it is possible to design fabrics and clothes as well as make quick changes to them in a virtual 3D environment, send them to other programs or print them out using a 3D printer.
VR drawing applications like Google's Tilt Brush are great tools, especially for sketching out ideas, however, they are limited and designed to be intuitive and easy to use. The next step has to be to design tools created with the fashion and fabric designer in mind. With the right applications a full integration of virtual reality into the design and production process is thinkable and will quite possibly open doors for completely new workflows and areas of application. If VR can be used for designing clothes or patterns then it will also be possible to design the characteristics of different fabric structures like texture, the volumetric structure depending on production technology and material characteristics, like woven, knitted or non-woven surfaces. Production reports of the fabric designs can be prepared and then transferred directly to the production machine online.

There are two approaches towards clothing design. Designing clothes according to the fabric or designing the fabric according to the apparel model. Ensuring that the desired effect of the fabric texture or pattern is achieved when applied to the designed clothes is what makes a successful design.

The designing of clothes is a long process including work steps like the production of the fabric, draping, cutting, sewing or fitting the clothes on the costumer. It requires the right use of time and immediate action. Transferring that process to a virtual environment will make it much more flexible and lead to results in much shorter time.

Additionally, more than one textile and fashion designer could work together on the same virtual design at the same time without having to be present at the same physical location.Developing new software will make it possible to transform three-dimensional fashion designs prepared in a virtual environment into two dimensional garment molds. The design created on the virtual draping dummy can be divided into mold sections on the same draping dummy making it possible to directly obtain the necessary parts. This way, extracting a mold for each section of the clothing and rehearsing each module separately is not necessary anymore. Thus, it is possible to obtain the clothing molds fitting the body in much shorter time. At this point, the production can directly be started without needing a sample garment.
Another possible scenario for the employment of VR technology into the production process is in creating highly customized clothing. Customers could send 3D scans of their own body online to the tailor, which could be done from their home. The 3D scanned body model is than placed into a virtual working environment, where the tailor, wearing a VR headset and VR hand controls, takes the measurements (Vitali, A., & Rizzi, C. (2017)). The designing process can start at the same time by drawing and fitting the garment directly onto the customers body. For feedback the customer can be invited into the virtual environment online to discuss the design without having to be in the same physical space with the designer.

After the design process is finished the virtual environment can be turned into a professional photo studio. By placing spotlights and adjusting the background as well as camera settings, professional pictures of the design can be taken, even before the production process has started. Within the same application a finished three dimensional design could then be transformed into two dimensional garment molds. The design created on the scanned 3D model of the customer's body can be divided into the mold sections needed for the production for the garment. The garment molds are then directly transferred to the production machines which output the finished product. So almost like regularly ordering clothes online Virtual Reality could open up the possibility to shop for custom created clothes without having to leave their home.

Additionally, it is important to note that VR technology is still pretty much at the beginning of its possibilities. The technology has been available to the broad public only for a little more than two years and it has continued being in a state of constant development since. For example powerful, untethered headsets are starting to be released enabling the user to move around in the virtual environment more freely, without having to worry about cables. In the close future VR gloves and suits will make the feeling of being part of the virtual world much more vivid and will make it possible to feel virtual objects. It will be possible to

touch surfaces and feel its textures and thereby feel different fabrics. Around the globe engineers, designers and artists are keen to discover the possibilities of the medium, where many of the rules are still to be written. Also in the field of fashion and fabric design it is of important to stay curious, keep the eyes open for new developments and an open mind.

## 4. CONCLUSIONS

When designing in a virtual environment the designer has the possibility to easily try out different textures, patterns, colors and shapes and is able to examine the results in real time. This new dimension to the designing process will reflect in the products and will leave an innovative visual impact. Being immersed into this three-dimensional environment creates a whole new experience for designers and is sure to inspire new approaches to the creative process.

Virtual Reality (VR) is an important development for the conceptual design process, which allows designers to visualize their imagined designs as real-life appearances, rather than present them as two-dimensional sketches. 3D garment design will make it possible to adjust clothing so it fits regular sized customers as well as those who have the potential to not fit the norm. It will enable to make designs directly on uploaded human avatars given the desired measurements. Designing in a virtual environment, by simulating the effect of the garment on the human body replace repeatedly manual changes on the life model as is common practice in a traditional designing process. But the most important advantages that this system brings to product development are the need for less samples, faster prototyping and easier decision-making.

Making fabric and garment designs in a virtual environment can be an effective way of bringing clear results in tailoring molds according to the individual's ergonomics and body type. It is fair to consider that better results in creating molds especially for drop size and anatomical defects like scoliosis (Hong, Y., Bruniaux, P., Zeng, X., Liu, K., Curteza, A., & Chen, Y., 2018, p. 35-45), hip protrusion, rounded shoulders can be achieved.

Through virtual reality taking measurements and rehearsal process by a professional can lead to healthy result even over long distances. Designer and Customer don't have to find themselves at the same place. In this case, the designer will be able to evaluate body type, body size and anatomical structure in the virtual environment and make accurate determinations and measurements. Instead of verbalizing the results, he/she may present the results to the customer visually.

The three-dimensional garment design created in the virtual environment can, again, be transformed into two-dimensional garment molds. The appropriately partitioned garment mold pieces can be obtained from the same draping dummy on which it was designed. This way the process of extracting every module of the garment individually to rehearse it can be abolished and it will be possible to obtain plainly fitting garment molds.

## REFERENCES


1. Makryniotis, Thomas, (2015). 3D Fashion Design: Technique, design and visualization. Pavilion Books. ISBN 1849942935, 9781849942935
2. Editor; Magnenat-Thalmann, Nadia (2010). Modeling and Simulating Bodies and Garment. London: Springer. ISBN 978-1-84996-262-9. e-ISBN 978-1-84996-263-6. DOI 10.1007/978-1-84996-263-6
3. Vitali, A., & Rizzi, C. (2017). A virtual environment to emulate tailor's work. Computer-Aided Design And Applications, 14(5), 671-679. doi:10.1080/16864360.2016.1273584
4. Bryson, S. (2013). Virtual Reality: A Definition History - A Personal Essay.
5. Hong, Y., Bruniaux, P., Zeng, X., Liu, K., Curteza, A., & Chen, Y. (2018). Visual-Simulation-Based Personalized Garment Block Design Method for Physically Disabled People with Scoliosis (PDPS). Autex Research Journal, Vol 18, Iss 1, Pp 35-45 (2018), (1), 35. doi:10.1515/aut-2017-0001
6. Vitali, A., & Rizzi, C. (2018). Acquisition of customer's tailor measurements for 3D clothing design using virtual reality devices. Virtual And Physical Prototyping, 13(3), 131-145. doi:10.1080/17452759.2018.1474082.
7. prototypeD TEAM Inc. [Screen name]. (2017, April 08). Virtual Fashion - Tiltbrush VR to Blender [Video file]. Retrieved from https://www.youtube.com/watch?v=pyZmIX1KP5E&t=397s
8. VRScout [Screen name]. (2016, August 22). Tilt Brush Fashion - Dress Form HTC Vive Mixed Reality [Video file]. Retrieved from https://www.youtube.com/watch?v=pyZmIX1KP5E&t=397s
9. [Digital image]. (n.d.). Retrieved from https://www.boomer.fr/wp-content/uploads/tilt-brush.png
10. Wikipedia (2018, January 29). The tale of two Flaccos. Retrieved from Wikipedia (2018, August 29). Oculus Rift,. Retrieved from https://en.wikipedia.org/wiki/Oculus_Rift

# BENDING PROPERTY OF SEAMS SEALED WITH ADHESIVE TAPE

**Ayşe ŞEVKAN MACİT[1], Bahar TİBER[1]**

[1] Uşak University, Turkey

Corresponding author: ayse.sevkan@usak.edu.tr

***Abstract:*** *There are many different products in technical textiles according to various application areas. Waterproof fabrics have widespread use among these products that show functional features in this field. In seaming of waterproof products, conventional seaming methods can be used if the stitched part is covered with adhesive tape to close the holes formed by needle. In our study, both conventional seams and conventional seams sealed with adhesive tape were compared before and after washing process in terms of bending properties using different fabrics. The results were evaluated statistically in terms of fabric type, seam type and washing process. It is determined that the bending length values are higher in the fabrics sealed with adhesive tape than those the fabrics only sewn with conventional seaming and the difference is statistically significant. In the study, the effects of sealing process on the other parameters were evaluated.*

***Key Words:*** *Bending property, adhesive tape, conventional seam, sealing, waterproof fabric*

## 1. INTRODUCTION

There are many products that have functional properties in technical textiles. Among these products, waterproof textile products have a lot of usage areas. The holes formed during the conventional sewing process of waterproofing products are undesirable. This is why alternative seaming methods are preferred for sewing waterproof fabrics. In cases where alternative seaming methods are not available, these products are sewn by conventional seaming methods, and then the stitched area is covered with the adhesive tape to close the needle holes formed during conventional seaming [1-4]. The effects of this extra process on the stitched area and how it affects the stitch characteristics have a great importance. From this point of view; the effect of the adhesive tape process on bending property, which is closely related to fabric stiffness, must be taken into consideration. The increase in bending rigidity means that the fabric has a stiffer handle [5]. This study is important to determine how this process which applied to maintain the waterproofing property affects the fabric stiffness and whether it is statistically significant.

There are some studies on adhesive tape. In these studies, it has been demonstrated that how adhesive tape processing affects the fabric properties such as seam strength [6, 7], thickness [7], tear strength [8], water permeability [7, 8] and stiffness [7, 9]. Among these studies investigating the stiffness of adhesive sealed seams [7, 9], there are comparisons with only ultrasonic seam

stiffness but no conventional seam stiffness. Our study aims to compare conventional seams and conventional seams sealed with adhesive tape in terms of bending property by using woven fabrics coated with polyurethane membrane which are used as blouson. Bending property of the sewn fabrics was compared before and after washing process and the results were evaluated statistically.

## 2. MATERIAL AND METHOD

In this study, polyurethane membrane coated woven fabrics which have waterproofing property were used. The fabrics were in plain and twill structures with two different weights. Fabric samples were prepared along the warp directions. Conventional seam process was performed to woven fabrics by using Brother S-7200C-403 electronic lock stitch sewing machine. Stitch density was 2.6 stitches/cm. Teksmak 7705 seam sealing machine was used to seal polyurethane adhesive tape having 2 cm width. Six types of sewn fabrics were gained. The properties of fabrics and the seams are characterized in Table 1.

**Table 1.** Properties of the fabrics and seam parameters

| Fabric code | Weaving structure | Weight in grams (g/m²) | Thickness (mm) | Raw material | Seam type |
|---|---|---|---|---|---|
| $F_1$ | Plain | 105 | 0.366 | Polyester | Conventional seam |
| $F_1$ | Plain | 105 | 0.366 | Polyester | Conventional seam sealed with adhesive tape |
| $F_2$ | Plain | 170 | 0.432 | Polyester | Conventional seam |
| $F_2$ | Plain | 170 | 0.432 | Polyester | Conventional seam sealed with adhesive tape |
| $F_3$ | Twill | 170 | 0.540 | Polyester | Conventional seam |
| $F_3$ | Twill | 170 | 0.540 | Polyester | Conventional seam sealed with adhesive tape |

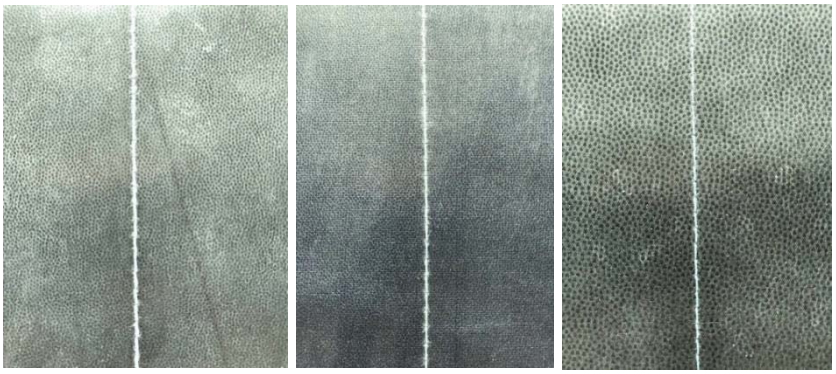

**Figure 1.** Fabrics sewn with conventional seam

The images of the fabrics sewn with conventional seam and the fabrics sewn with conventional seam and sealed with adhesive tape are given in Figure 1 and Figure 2, respectively.

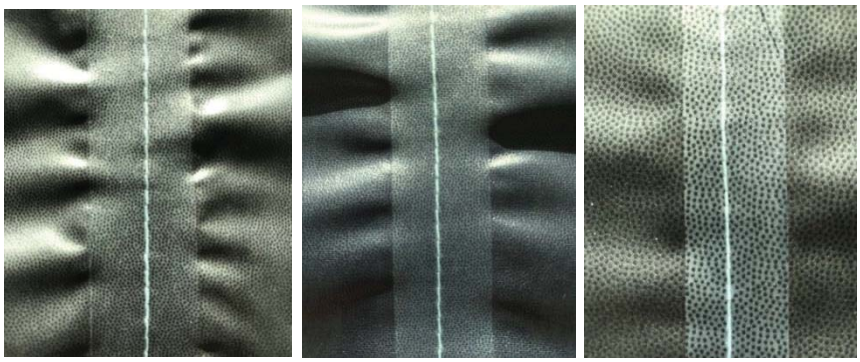

**Figure 2.** Fabrics sewn with conventional seam and sealed with adhesive tape

All of the sewn fabrics were washed at 30°C with synthetic washing programme without prewashing according to TS EN ISO 6330:2012 test standard [10]. 4 g/l ECE non-phosphate reference detergent without optical brightening agent was used for washing processes. Washing process was repeated for five times.

Bending tests were performed to fabrics before and after washing processes with the instrument designed for bending rigidity test method according to TS 1409:1973 [11]. Five samples were prepared from each sewn fabric having dimensions 2.5x15 cm. The samples were conditioned for 24 hours in standard atmospheric conditions (temperature 20±2 °C and relative humidity 65±2%). The conditioned samples were then tested for both faces and both sides. Twenty falling length values were read on the instrument and the average of these twenty values was divided into two to obtain the bending length value for each sewn fabric type. Bending rigidity is formulated in TS 1409:1973 as follows:

$G = 0.1\ W\ C^3$

where:

X= Falling length (cm)

C= X/2 =Bending length (cm)

W= Fabric mass per unit area ($g/m^2$)

G= Bending rigidity (mg.cm)

In the standard TS 1409:1973, bending rigidity is calculated according to above equation for a single layer fabric without any seam. However we used two-layered

sewn fabrics in our study so we have compared the fabrics in terms of bending length values. Test results were evaluated statistically considering fabric type, seam type and washing process.

## 3. RESULTS AND DISCUSSION

Bending length values of the fabrics sewn with conventional seam and the fabrics sewn with conventional seam and sealed with adhesive tape before and after washing processes are given in Table 2 and Graph 1.

**Table 2.** Bending length values of the sewn fabrics before and after washing processes (cm).

| Fabric Code | Conventional Seam | | Conventional Seam and Adhesive Tape | |
|---|---|---|---|---|
| | Before Washing | After Washing | Before Washing | After Washing |
| **F1** | 3,03 | 2,92 | 3,47 | 3,22 |
| **F2** | 3,28 | 3,2 | 3,96 | 4,29 |
| **F3** | 3,72 | 3,62 | 4,03 | 3,75 |

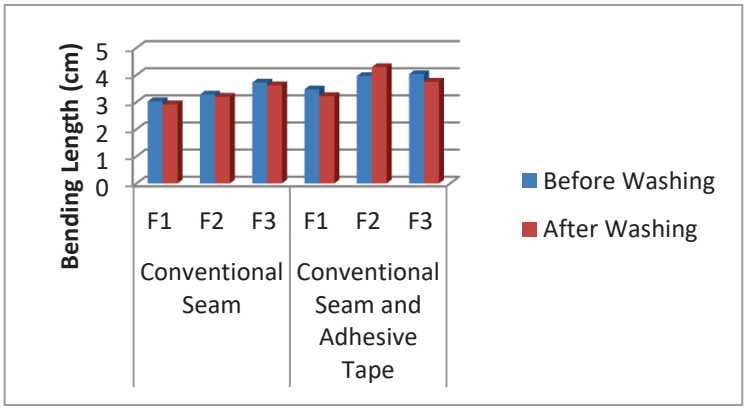


**Graph 1.** Bending length values of the sewn fabrics before and after washing processes (cm)

As a result; our study demonstrated that the bending length values of the fabrics sewn with conventional seam and sealed with adhesive tape are higher than the fabrics only sewn with conventional seam (Table 2 and Graph 1). The difference is found to be statistically significant. It is also clear from the results that the bending length values decreased with reducing weight in grams and thickness. The difference between F1 fabric with the other fabrics is statistically significant according to multiple comparisons. On the other hand, these values are higher in twill structure than in plain structure at equivalent weight in grams except for fabrics sealed with adhesive tape after washing processes. In addition, generally the bending length values decreased after washing processes for both conventional seams and conventional seams sealed with adhesive tape.

Table 3 shows that the effects of the fabric type and seam type on the bending length values are statistically significant. On the other hand, the effects of washing process on the bending length values are statistically insignificant (Table 3).

**Table 3.** The analysis of variance table for bending length values of the sewn fabrics

| Variable | Factor | F | Significance |
|---|---|---|---|
| Bending length | Fabric type | 20,987 | ,000* |
| | Seam type | 30,567 | ,000* |
| | Washing process | ,537 | ,467 |

*:Statistically significant for α =0.05.

## 4. CONCLUSION

In this study, conventional seaming and adhesive tape sealing were performed to polyester woven fabrics coated with polyurethane membrane which are used as blouson. The effect of seams sealed with adhesive tape and fabric structure on bending property were investigated considering fabric type and seam type before and after washing processes. Consequently, our study demonstrated that;

- The bending length values of the fabrics sewn with conventional seam and then sealed with adhesive tape are higher than the fabrics only sewn with conventional seam. The difference between them is statistically significant.
- The bending length values decreased with reducing weight in grams and thickness. The difference between the fabrics is statistically significant.
- The bending length values are generally higher in twill structure than in plain structure at equivalent weight in grams.
- Generally; the bending length values decreased after washing processes for both conventional seams and sealed with adhesive tape ones. But the effects of washing process on the bending length values are statistically insignificant.

Where alternative seaming methods are not available, sealing adhesive tape process is preferred in order to preserve the waterproofing properties of waterproof fabrics after conventional seaming process. When the results of the study are examined; it was determined that this method has an increasing effect on the bending property which is important in terms of stiffness of fabric, and the difference between them is statistically significant. It is thought that this process can be used to keep the waterproofing properties of products which are considered as not a disadvantage by increasing the fabric stiffness. It should be kept in mind that sealing adhesive tape process is an additional process to conventional seaming and this method should be compared in terms of investment costs with alternative seaming methods which provide a waterproofing effect by a single process.

## ACKNOWLEDGMENTS

This study has been supported by Uşak University Scientific Research Project under grant [2015/MF005].

## REFERENCES

1. Bulut, Y., Sülar, V., Kaplama veya Laminasyon Teknikleri ile Üretilen Kumaşların Genel Özellikleri ve Performans Testleri, 2008, Tekstil ve Mühendis, 15 (70-71): 5-16.
2. Sivri, Ç., 2008, Membranla Lamine Edilmiş Nefes Alabilir Kumaşların Konfor Özelliklerinin İncelenmesi, Yüksek Lisans Tezi, Süleyman Demirel Üniversitesi Fen Bilimleri Enstitüsü, Isparta.
3. Kaynak Bantı Yapıştırma Makineleri, http://www.uppa.com.tr/tr/index.php?option=com_content&view=article&id=101&Itemid=450, [Erişim tarihi: 03.09.2017].
4. Laing, R. M., Webster, J., 1998, Joining Materials, Stitches and seams, Textile Institute, 37-50.
5. AK, F. N., Belirli Doku Konstrüksiyonlarının Kumaş Performans Özelliklerine Etkisi, 2006, Master Thesis, Çukurova Üniversitesi Fen Bilimleri Enstitüsü, Adana.
6. Ghosh, S., Reddy, R. K., 2009, Ultrasonic Sealing of Polyester and Spectra Fabrics Using Thermo Plastic Properties, Journal of Applied Polymer Science, Vol. 113: 1082–1089.
7. Jevšnik, S., Eryürük, S. H., Kalaoğlu, F., Karagüzel Kayaoğlu, B., Komarkova, P., Golombikova, V., Stjepanovič, Z., 2017, Seam properties of ultrasonic welded multilayered textile materials, Journal of Industrial Textiles, 46(5): 1193-1211.
8. Shi, H., Zhang, L. X., Wang, J. P., Luo, S. H., 2016, Application of Ultrasonic Welding Technology in Flexible Waterproof Composites, AATCC Review, 16(5): 45-49.
9. Reddy, R. K., 2007, Ultrasonic Seaming of Pet, Pet/Cotton Blend And Spectra Fabrics, Yüksek Lisans Tezi, Eastern Michigan University, Michigan.
10. TS EN ISO 6330, Textiles - Domestic washing and drying procedures for textile testing, 2012.
11. TS 1409, Stiffness determination of woven textiles, 1973.

# DEVELOPMENT AND CHARACTERISATION OF NONWOVEN FABRICS FOR APPAREL APPLICATIONS

**Muhammad S. CHEEMA[1], Tahir H. SHAH[2], Subhash C. ANAND[1], Navneet Soin[1]**

[1] University of Bolton, Institute of Materials Research and Innovation (IMRI), UK
[2] National Textile University, Pakistan

Corresponding author: chscheema@gmail.com

***Abstract:*** *The cost of making apparel fabrics for garment manufacturing is very high because of their conventional manufacturing processes and new methods/processes are being constantly developed for making fabrics by unconventional methods. With the advancements in technology and the availability of the innovative fibres, durable nonwoven fabrics by using the hydroentanglement process that can compete with the woven fabrics in terms of their aesthetic and tensile properties are being developed. In the work reported here, the hydroentangled nonwoven fabrics were developed through a hybrid nonwoven manufacturing processes by using fibrillated Tencel® and bi-component (sheath/core) polyethylene/polyester (PE/PET) fibres, in which the initial nonwoven fabrics were prepared by the needle-punching method followed by hydroentanglement process carried out at optimal pressures of 50 to 250bars. The prepared fabrics were characterised according to the British Standards (BS 3356:1990, BS 9237:1995, BS 13934-1:1999) and the attained results were compared with those for a standard plain-weave cotton, polyester woven fabric and commercially available nonwoven fabric (Evolon®). The developed hydroentangled fabrics showed better drape properties owing to their flexural rigidity of 252 mg.cm in the MD, while the corresponding commercial hydroentangled fabric displayed a value of 1340 mg.cm in the MD. Tensile strength of the developed hydroentangled fabrics showed an approximately 200% increase than the commercial hydroentangled fabrics. Similarly, the developed hydroentangled fabrics showed higher properties in term of air permeability, such as the developed hydroentangled fabric exhibited 448 mm/sec and Evolon fabric exhibited 69 mm/sec at 100 Pa pressure. Thus for apparel fabrics, the work combining the existing methods of nonwoven production, provides additional benefits in terms of cost, time and also helps in reducing the carbon footprint for the apparel fabric manufacture.*

***Keywords:*** *hydroentanglement; nonwoven apparel; durable nonwovens; Tencel®; Evolon®*

## 1. INTRODUCTION

Traditionally, it is being assumed that garments are made through woven and knitted fabrics. Because of their acceptable aesthetical and mechanical properties, these conventional methods of making fabrics for garments, captured a big market. From the literature review, it was found that there was very limited penetration of nonwoven fabrics in outerwear owing to their inherent limitations

in term of strength, appearance and workability. In 1960, for the first time nonwoven fabric was developed as an outer wear, but could not succeed came as outer fabric but could not success because of its limitations. Nonwoven fabrics are thus being used as supporting materials in garment manufacturing industry, such as garment lining, insulation, and fusing etc. Recently, there has been a great deal of interest in the area of research and innovation activities in nonwoven fabrics for apparel applications, such as Evolon (Evolon.com) and Miratech. Traditionally, it was assumed that nonwoven fabrics can only perform in wipes, scaffolds, geo textiles, filters and disposable articles (Luki, 2004) and only 1 percent of nonwoven fabrics are utilised in apparel sector (Lee, 2006). Now, because of the new advancements in the nonwoven technologies, especially in the hydroentanglement process, the applications of hydroentangled nonwoven fabrics have diversified into many fields and apparel fabrics application is one of them. The key area of research is to develop the nonwoven fabrics that can withstand the external forces in the use and provide comfort to the wearer in terms of softness, moisture management, appearance and also exhibit enough strength that can withstand the laundry process (Vaibhav, 2012) etc.

Nonwoven fabrics are made directly from the fibres without making any yarn and without the use of weaving or knitting processes. A nonwoven fabric is defined by INDA as follows: “Sheet or web structure bonded together by entangling fibres or filament, by various mechanical, thermal and/or chemical processes. These are made directly from the separate fibres or from molten plastic or plastic film”. The unique advantage of the nonwoven fabric manufacture is that it is a continuously linked process, in which at the first stage raw materials (fibres) are converted into webs via the carding process and at the second stage these fibrous webs are bonded into finished products. The first nonwoven apparel fabric was the disposable paper clothing that was launched in early 1966 by an American company Scott Paper, however, the fabric could not capture any significant part of the apparel market because of its ill fit and uncomfortable nature. In the same era, Mars Manufacturing Company invented different types of nonwoven dresses that were used as evening wear and wedding gowns. However, these all-paper-clothing were short-lived and became obsolete in 1968 (Andrew, 2008). The breakthrough in the nonwoven apparel fabrics came in 1970, when DuPont invented the hydroentanglement technique for the nonwoven fabrics, known as spunlace technology (Andrew, 2008). This new technique gave a competitive edge to nonwovens, as the nonwoven fabrics produced by the hydroentanglement process possessed much superior aesthetical properties than the conventional nonwovens. The company also developed the foam bonded spunlaced fabric (polyester spunlaced fabric), wherein 30% soft acrylic latex was used to strengthen the spunlaced fabric that withstood five laundering cycles (Zheng, 2003).

In this study, functional hydroentangled fabrics have been developed through a hybrid process of needling and hydroentanglement, by utilising innovative Tencel and bi-component sheath/core (PE/PET) staple fibres. The resultant fabrics, when compared against the industry standard commercially available Evolon®

and woven plain-weave cotton/polyester fabric exhibited acceptable test values related to the aesthetical and mechanical properties of the garments such as flexural rigidity, air permeability and tensile strength etc. The resultant fabrics can be used in different applications such as in the hospital for patients' uniforms. Owing to its comfortability, it can be used in the processing industry as uniforms such as in the meat industry, printing industry and in the chemical industry. Further research work is being carried out in order to enhance the quality of the fabrics especially in relation to laundering and washing.

## 2. EXPERIMENTAL

### 2.1. Materials

The fabrics were produced in collaboration with the Nonwovens Research Institute, University of Leeds by utilising two different types of fibres: Tencel® and bi-component sheath/core (PE/PET) staple fibres. Tencel® fibres were 1.4 dtex, 38mm in length with a smooth surface, while the PE/PET bi-component fibres were 2.2 dtex and 40mm in length with a crimped surface. The required amount of each fibre was separately weighed and initially hand blended in preparation of the next process. These hand-mixed fibres were manually opened into small tufts and further mixed in order to obtain a smooth web. After manually opening the fibres, the fibres were then carded through the pilot carding machine and a parallel-laid web produced was used in the next process. Before going into the hydroentanglement process, the carded web was lightly needled by using 8mm penetration and 100 strokes per min, after which the needled substrate was rolled and packed for the next process of hydroentanglement.

### 2.2. Hydroentanglement process

The needled fibrous webs were uniformly hydroentangled by using pilot hydroentanglement system, as illustrated in Figure 1.

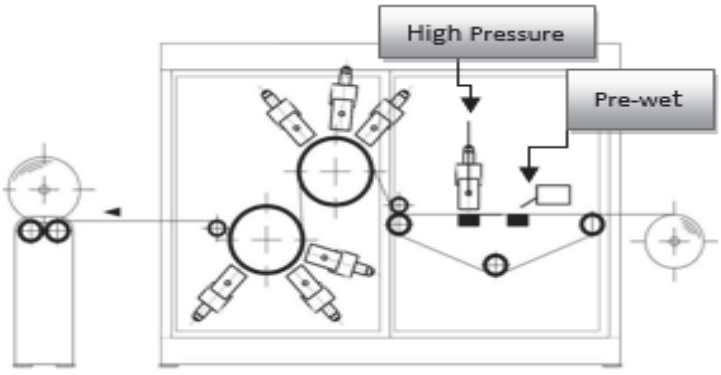


**Figure 1.** Action View of Hydroentanglement Process

Before going under the high pressure area of the hydroentanglement process, the fibrous web was pre–wetted to minimise the dispersion ratio of the fibres in high pressure zone. After pre-wetting, the material is passed through the high water pressure jet head for bonding of the fibres as shown in Figure 1. The Fabrics were prepared at varying hydroentanglement pressures of 100 and 125 bars with two passes, at the line speed of 3m/min. The orifice of jet strip was 150µm and the density of the jet orifice was 5.56/cm. All the fabrics were manufactured from the same web with 120±5 $gm^{-2}$ nominal weight. It was observed that for these specific blends, at lower pressures (50-75 bars), the fibres were not consolidated to the required level, which negatively affected the mechanical properties by reducing the tensile strength of the obtained fabric. On the other hand, at higher pressures (150-250 bars), the fibres were easily dispersed and consequently very limited number of fibres per unit area of the fabric was observed, which reduced the GSM as well as the tensile properties to below the acceptable values. The two hydroentangled nonwoven fabrics denoted as fabric 1 and fabric 2, were prepared at 100 and 125 bars, respectively, at the same constituent levels of 70% Tencel and 30% PE/PET bicomponent fibres. The properties of developed fabrics are shown in Table 1.

**Table 1.** Details & characteristics of the hydroentangled nonwoven fabrics prepared in this study

| Fabric Number | Hydroentanglement Pressure (bars) | Contents | Area Density ($gm^{-2}$) | Thickness (mm) | Bulk Density ($gcm^{-3}$) |
|---|---|---|---|---|---|
| **Fabric 1** | 100 | Tencel (70%) and Sheath core PE/PET (30%) | 150 ± 2.5 | 0.99 ± 0.05 | 0.15 ± 0.01 |
| **Fabric 2** | 125 | Tencel (70%) and Sheath core PE/PET (30%) | 145 ± 2.5 | 0.88 ± 0.05 | 0.17 ± 0.01 |

## 2.3. Mechanical and aesthetical testing

The prepared fabrics were tested according to the British Standards (BS 3356: 1990, BS 9073-6: 2003, BS 13934-1: 1999) in order to determine their mechanical and aesthetical properties. For flexural rigidity, Shirley flexometer apparatus was used, where a 25 ±1 mm x 100±1 mm strips were cut and the flexural rigidity values were determined according to the standard procedures. The tensile tests were performed by the Instron apparatus according to the appropriate standard methods. The cross-head speed was 200mm±1/min and the fabric size was 200±1 x 50±1 mm. Three specimens of each fabric were tested. The wicking test was performed by strip test method and absorption test was carried out by dipping (10 cm x10 cm) fabric specimens into water for 20min at 20$^{o}$ C and 65±2 relative humidity.

The results obtained were then compared with the commercially available nonwoven fabric “Evolon” and with the reference fabric of a plain weave of woven fabric to ascertain the suitability of our developed fabrics for use as apparel fabrics.

## 3. RESULTS AND DISCUSSION

### 3.1. Dimensional properties

The results presented in Figure 2 show that fabrics 1 and 2, produced at 100 and 125 bars hydro pressure had thickness values of 0.99±0.05 mm and 0.88± 0.05 mm, respectively. This indicates that when the hydroentanglement pressure was increased, a small reduction in the fabric thickness was observed due to a higher compaction and alignment of the fibres, which is expected to influence the tensile properties and bending rigidity of the produced fabric. In a study by Zheng et al (2003), it was shown that by increasing the specific energy (hydro pressure), the fabric area density decreased due to the fabric stretching caused by the impact of the water jets.

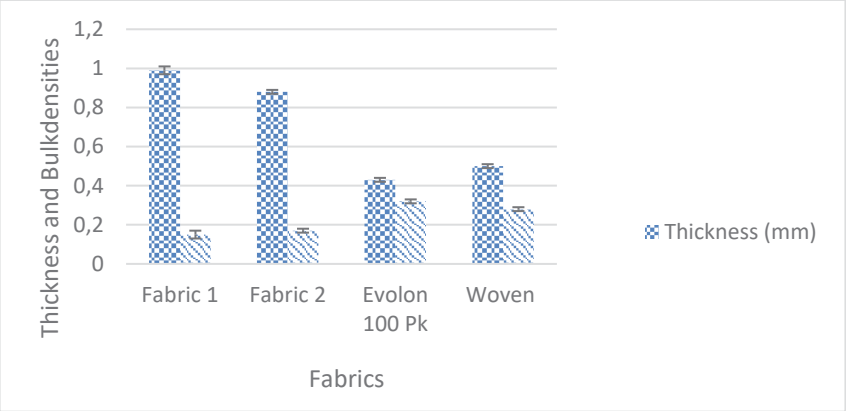


**Figure 2.** Thickness and Bulk density of developed fabrics 1 (100 bars) and 2 (125 bars)

Moreover, it was observed that both the fabrics exhibited almost very similar bulk density values, which is an indication that the number of fibres per unit area in these fabrics were similar to each other. When compared to the values for the commercial nonwoven fabric and a typical woven fabric, these comparative results clearly show that the dimensional properties such as thicknesses of the hydroentangled nonwoven fabrics (1 and 2) were higher, because fabric 1 exhibited 0.99 ± 0.05 mm and fabric 2 exhibited 0.88 ± 0.05 mm thickness and Evolon and woven fabrics showed 0.43 and 0.50 mm thickness values respectively. The bulk densities of both fabrics were lower than Evolon® and

woven fabrics. Woven and Evolon fabrics' higher bulk density values were because of their compact structures as shown in Table 2.

**Table 2.** Details of reference fabrics

| Fabrics | Processes | Contents | Area Density ($gm^{-2}$) | Thickness (mm) | Bulk Density ($gcm^{-3}$) |
|---|---|---|---|---|---|
| Evolon® | Hydroentanglement | PET and PA | 140 | 0.43 | 0.32 |
| Woven | Plain weave | Cotton and PET | 144 | 0.50 | 0.29 |

### 3.2. Flexural rigidity

The flexural rigidity of the fabrics is a pivotal property for apparel applications. The fabric stiffness is related to its inherent properties, such as fibre material and the structure itself of the fabric (Mehmet, 2008). The flexural rigidity results in the machine (MD) and cross (CD) directions for the fabrics produced during this resarch are presented in Figure 3.

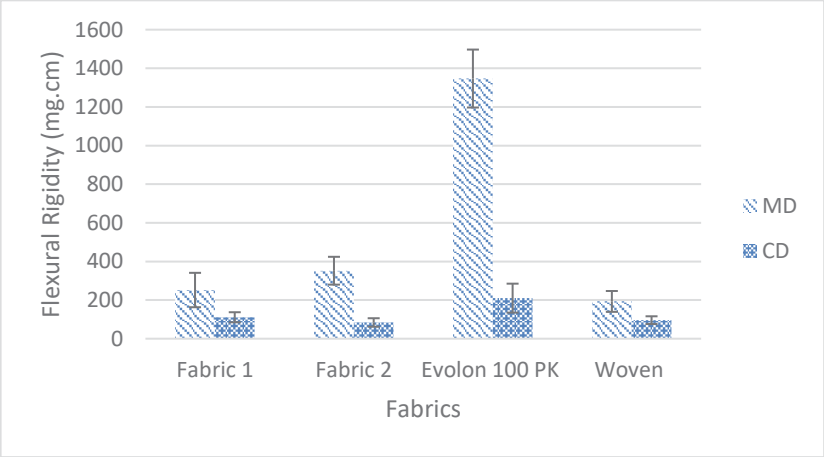


**Figure 3.** Flexural Rigidity comparison of developed fabrics 1 and 2 with Evolon 100PK and Woven fabric

It was observed that the flexural rigidity values for the nonwoven fabrics prepared in this study were much lower than the commercial nonwoven fabrics (Evolon®) in both the MD and CD. Furthermore, these values were very similar to those observed for the woven fabric (Figure 4). These results clearly show that the flexural behaviour of fabrics 1 and 2 was very similar to that of the woven fabric and it can be further enhanced through the finishing processes.

The bending rigidity of the fabrics depends on the movement of the fibres within the fabric structure. It seems that the Evolon fabrics exhibit higher bending rigidity as the fibres are highly intertwined with its neighbouring fibres due to the nature

of the spun-laid process and the inherent fine filaments of the bi-component PA6/PET “island in the sea” filament structure. Additionally, due to the high hydroentanglement pressure, the fine filaments form a tight structure with little or no space for fibre movement to occur within the fabric. On the other hand, the prepared fabrics showed lower flexural rigidity as compared to the commercial nonwoven fabric due to the more open structure of these experimental nonwoven fabrics. In their study, Smith et al (2003) have reported that if the fibres are able to act independently in the fabric structure, a reduction in the flexural rigidity of the fabric is observed. Hence, it is evident that bending rigidity does not depend on the thickness of the fabric and rather is directly proportional to the movement of the fibres within the structure of the fabric. Evolon® exhibited higher flexural rigidity in both the machine and cross directions, even though it had a lower thickness value. On the other hand, the developed hydroentangled nonwoven fabrics exhibited lower flexural rigidity in the machine and cross directions, as compared with the Evolon, while showing higher thickness values than the Evolon® fabric. Woven fabric had similar thickness as compared with the Evolon® but exhibited much lower values’ of flexural rigidity in the machine and cross direction. Ancutiene et al (2010), found in their studies that the fabric structure has a more significant effect on the flexural rigidity of the fabric. Emin et al (2008) too have endorsed this principle that the fabric parameters affect the stiffness of the fabric.

Figure 4 represents the microscopic images of the three different types of fabrics studied during the course of the work.

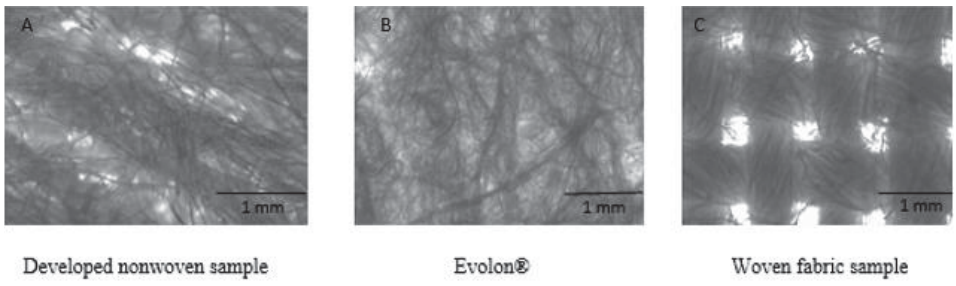


**Figure 4.** Microscopic Views of (a) developed hydroentangled, (b) Evolon® and (c) woven

These images show that the nonwoven fabrics developed in this study and the woven fabric have similar open structures and the fibres appear to be better aligned than the commercially available Evolon, wherein the fibres appear to be randomly placed. (Komori, 1997) found that the arrangement of the fibres in the fabric structure has a major influence on the mechanical properties of the fabric. Thus, the experimental nonwoven and woven fabrics exhibit similar flexural behaviour and have significantly lower flexural rigidity values as compared to the commercial nonwoven fabric. In the developed hydroentangled fabrics, the fibres are largely aligned in a single direction and the open spaces between the fibres

can lead to the lowering of the flexural rigidity. Similar results have been obtained by (Bahari, 2015) and (Smith, 2003), wherein it was observed that the fibre's independent movement within the fabric structure led to a lower fabric flexural rigidity.

### 3.3. Absorption and wicking tests

The moisture transportation in a fabric determines its cooling effect and thus provides comfort to the wearer. The wear comfort of clothing is continually gaining importance owing to the consumer demand and therefore considerable efforts have been made to study the wicking characteristics of apparel fabrics (Berrfelder, 2013). During exercise or working conditions, the human body produces sweat and if it does not evaporate from the skin to the atmosphere, because of the clothing, then the wearer feels uncomfortable and this may give rise to a loss in working efficiency of the wearer. Therefore moisture management by the fabric is very important in order to optimise the wearer's comfort. The fibre types (natural or synthetic), blending ratio of fibres, the fabric structure and fabric characteristics (densities of yarns, thickness) etc. are the parameters that affect the moisture management and the thermal properties of the fabrics (Hassan, 2012).

The prepared nonwoven and woven fabrics were characterised for their absorption and wicking properties and the results are presented in Table 3 and illustrated in Figure 5.

**Table 3.** Absorption and wicking properties of nonwoven fabrics

| Fabrics | Area Density $gm^{-2}$ | Absorption $gg^{-1}$ | Wicking (g.cm) | |
|---|---|---|---|---|
| | | | MD | CD |
| **Fabric 1** | 150 | 6.78 | 9.61 | 9.26 |
| **Fabric 2** | 145 | 4.96 | 12.44 | 8.21 |
| **Evolon®** | 140 | 0.7 | 1.4 | 0.6 |
| **Woven** | 144 | 1.5 | 1.4 | 0.6 |

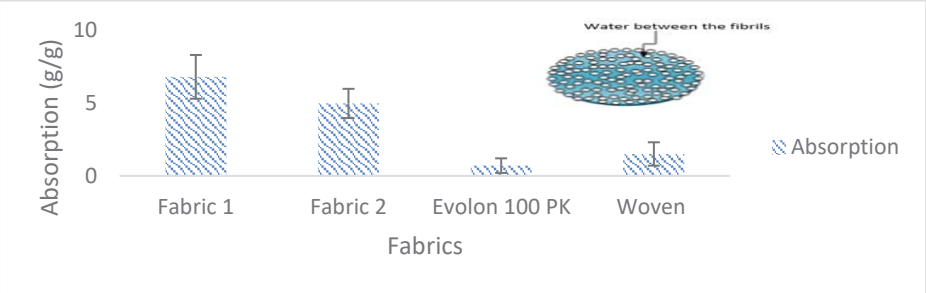


**Figure 5.** Absorption properties of nonwoven fabrics

The results show that the experimental fabrics 1 and 2 exhibit better absorption and wicking behaviour than Evolon 100PK and the woven fabric. The absorption value of fabric 1 was ~78% higher than the woven fabric and about 90% higher than Evolon® 100PK. Similarly, fabric 2 exhibited 70% and 86% higher absorption values than woven and Evolon® fabrics, respectively. This enhanced absorption is mainly due to the fact that the experimental nonwoven fabrics have a more porous structure and the fibres are well oriented within the fabric structure. Moreover, owing to the Tencel fibres' hygroscopic nature, it absorbs the water molecules readily, thus providing higher absorption values. Furthermore, the Tencel® fibres used have a higher wet and dry strength than the other cellulosic fibres, viscose fibres show 22-26 cN/tex tenacity in dry state and 10-15 cN/tex in wet state and on the other hand Tencel fibres show 34-38 cN/tex and 38-42 cN/tex in dry and wet states respectively and have higher moisture regain properties than the polyamide and polyester fibres used in the commercial nonwoven fabric (Evolon). Additionally, the fibril structure of Tencel fibres provides superior capillary action within the fabric structure (Firgo, 2006). Woven fabric displayed restricted absorption properties owing to its fabric structure, wherein, due to the high number of crimps per unit area, along with the highly twisted yarns, did not allow the fibres to act as capillaries, unlike the exhibited properties of the nonwoven fabrics.

The results presented in Table 3 also show that the wicking values obtained for fabrics 1 and 2 were considerably higher than the woven fabric and Evolon 100PK nonwoven fabrics, both in the MD and CD. The wicking properties mainly depend on the fibre fineness and the fabric structure. Fabric 1 and 2 showed 9.61 and 12.44 g.cm wicking values in MD where as Evolon and woven exhibited wicking values of 1.4 and 1.4 g.cm in MD. The higher wicking values of the developed fabrics were because of the Tencel fibres consist of countless hydrophilic and crystalline nano fibrils which act as tubes and absorb the water through the capillary action between the fibrils (Firgo, 2006). On the other hand, Evolon, composed of polyester and polyamide fibres, show lower absorption, as the synthetic fibres like polyester are hydrophobic in nature. The fibre orientation also contributes in the absorption values of the fabric, Miller, 2000 has studied the pore size effects on the capillary behaviour of the material. For the developed hydroentangled fabrics, the smaller pore size along with the higher capillary action from Tencel fibres led to the enhanced wicking properties, as compared to the other fabrics.

### 3.4. Tensile properties

The tensile properties of fabrics 1 and 2 in MD and CD are shown in Figure 6 (a, b), respectively.

The results show that the tensile strength of fabrics 1 and 2 are higher than the Evolon 100 PK and woven fabric in MD (Figure 6a). It also appears that the tensile behaviour of the fabrics 1 and 2 is significantly different from both the woven and the commercial nonwoven fabrics. As mentioned earlier, the developed fabrics were prepared at 100 and 125 bars, respectively. In their study Cannoly, 1993, have observed that an increase in the hydroentanglement pressure results in an

increase in the tensile strength due to the higher degree of entanglement of the fibres. The tensile strength also depends on other factors, such as the fibre and web properties. As discussed previously by Ghassemieh, 2001, to prepare a hydroentangled fabric, a sufficient amount of energy is essential to get an optimal product with suitable dispersion and sufficient tensile strength, which itself depends on the web making parameters and fibre properties such as modulus, stiffness, length and friction between the fibres. Mao 2000, found in his research that less stiff fibres consumed less energy for attaining the maximum fibre entanglement within the fabric structure. Moreover, because of the staple fibres in the developed fabrics, during hydroentanglement process, more fibres were twisted around with surrounding fibres, because of the rebound of the water after hitting the plate underneath the web, resulted in intensive entangling behaviour of the fibres that caused the higher tensile strength of the developed fabrics as compared with other fabrics. The experimental nonwoven fabrics have breaking extension values that are similar to the Evolon fabrics, however their failure mechanism is quite different as these fabrics tend to yield before they fail. Due to its rigid structure, the woven fabric exhibited higher modulus and lower breaking extension values as compared to the nonwoven fabrics.

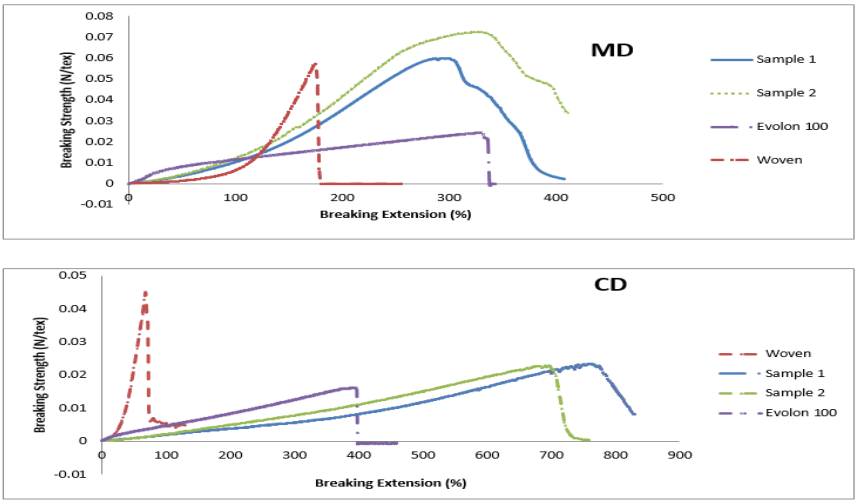


**Figure 6.** Tensile tests of nonwoven fabrics in MD and CD

The tensile properties of the various fabrics in CD are illustrated in Figure 6b. The results show that the ultimate strength values of these experimental nonwovens are slightly lower than the woven fabric but higher than Evolon 100PK. The breaking extension values of all the nonwovens are in excess of 80% and these are considerably higher than the woven fabric. The Evolon fabric is composed of continuous filaments of bi-component Island in the sea that can impart higher strength to the fabric, whereas the woven fabric is composed of twisted yarns

with a compact weave that give additional strength to the fabric. On the other hand, fabrics 1 and 2 are composed of fine staple fibres and the fibres were aligned in machine direction so because of less number of fibres in the cross direction region, the developed fabric exhibited lower tensile strength in CD. Evolon fabric is also based on synthetic fibres and is produced by using split able bi-component fibres which are finer in diameter than those used for preparation of the experimental fabrics and are therefore able to entangle more intensely in the fabric structure and also the filaments were in different directions that caused higher tensile strength in CD than the developed fabrics as shown in Figure 7.

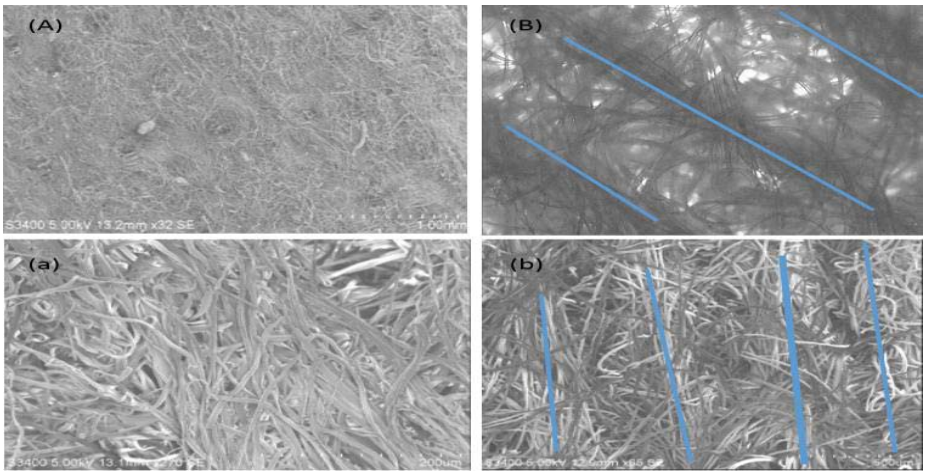


**Figure 7.** Optical and SEM views of Evolon 100 PK (A,a) and developed hydroentangled fabric (B,b)

## 4. CONCLUSIONS

In this study, an attempt has been made to develop nonwoven fabrics that are suitable for apparel applications. A hybrid nonwoven approach has been adopted where the fibres are first converted into a parallel-laid web followed by needlepunching of the web. The needlepunched fabric is then subjected to the hydroentanglement process at optimal values of 100 and 125 bars. The results demonstrate that the nonwoven fabrics produced in our study have superior moisture management properties such as developed fabric gave 6.78 g/g values of absorption and Evolon and woven gave 0.7 and 1.5 g/g, respectively. The bending flexural rigidity characteristics of the developed fabrics were also lower than the Evolon fabrics, wherein the developed fabrics exhibited 252 mg.cm in MD while the Evolon fabrics showed a value of 1347 mg.cm in MD. The tensile properties of the experimental nonwoven fabrics are higher than the commercially available nonwoven fabrics, especially the breaking extension values. The developed fabric exhibited a value of 0.07 N/tex in MD and Evolon exhibited value of 0.02 N/tex in MD. The tensile strength of the woven fabric is somewhat higher in CD than the nonwoven fabrics, but the bending rigidity values are very similar

to the experimental nonwovens. The absorption and wicking properties of the developed fabrics were higher than the Evolon and woven fabric in both the machine and cross directions because of the hygroscopic and fibril structure of the Tencel fibres. The developed fabric exhibited an absorption value of 6.78 g/g and Evolon fabric exhibited 0.7 g/g absorption value. This prove that the developed fabrics quickly absorb the sweat from the body and because of their strong wicking action, the sweat disperses in the fabric structure that assists in the evaporation into the environment. The wicking values of developed fabric fabrics were 9.61 and 12.44 g.cm and the wicking values of Evolon and woven fabrics were 1.4 and 1.4 g.cm, respectively. It is strongly believed that with further optimisation of the hybrid process parameters and the fabric finishing techniques, nonwoven textile structures can be developed that are suitable for many apparel applications, including patients' uniforms, uniforms for processing industries, outer wear etc.

## ACKNOWLEDGEMENTS

The authors wish to thank Dr S. Rathore at NRI, University of Leeds, for his help with the processing of experimental fabrics.

## REFERENCES

1. https://store.extension.iastate.edu/Product/pm1663d-pdf, Accessed on June. 2013.
2. www.Evolon.com
3. Russell S. J. (2007) , Handbook of Nonwoven, Woodhead Publishing Limited, Vol. 1, First edition, 286-287
4. Vaibhav K., Webster L., Govekar A., (2012): Nonwoven in fashion apparel applications, International Journal of Fibre and Textile Research, 2(2), 12-20
5. Shawver S. E., Collier L. W., Estey P.W., Paul S.C., (1997) Elastic Breathable Barrier Fabric, US Patent 5,695,849, Dec.
6. www.paperdressvintage.co.uk/livintage-boutique/history
7. Andrew D. H., (2008): Colouration of Hydroentangled Nonwoven Fabrics, Phd Theses, University of Leeds, 30
8. Zheng H., Seyam A. M., D. Stiffler, (2003) The Impact of Input Energy on the Performance of Hydroentangled Nonwoven Fabrics, INJ
9. Mehmet Y., Thomas H., Sabit A., (2008) Influence of the fabric properties on fabric stiffness for the industrial fabrics, TEKSTIL ve KONFEKSIYON, 4, 263-267
10. Smith K., Ogale A. A., Maugans R., Walash L.K., Patel R. M., (2003) Effect of bond roll pattern and temperature on the micro structure and properties of polyethylene nonwoven, Textile Res. J. 70, 845-853,
11. Kristina A., Eugenija S., Anastasija N., ( 2010), The Relationship between Fabrics Bending Rigidity Parameters Defined by KES-F and FAST Equipment, Materials Science, 16, 346-352
12. Emin M., Howard T., Adanur S., (2008) Influence of the Fabric Properties on Fbaric stiffness for the industrial fabrics, TEKSTIL ve KONFEKSiYON, 4,263-267

13. Komori T., Itoh M., Takaku A., (1997), Analysising the compressibility of a random fibre mass based on modified theory of fibre contact, Textile Res. J., 67, 204-210

14. Bahari N., Hasani H., Zarrebini M., Hassanzadeh S., (2015), Investigating the effects of material and process variables on the mechanical properties of low-density thermally bonded nonwoven produced from estabragh (milkweed) natural fibers, Journal of Industrial Textiles, 1-18

15. Birrfelder P., Dorrestijn, Roth C., ( 2013), Effect of fibre count and knit structure on intra and inter-yarn transport of liquid water, Textile research Journal, 83, 1477-1488

16. Hassan M., Qashqary K., Hassan H.A., Shady E., Alansary M., (2012) Influence of Sportswear Fabric Properties on the Health and Performance of Athletes, FIBRES & TEXTILE in Eastern Europe, 20, 82-88

17. Firgo H., Schustera K. C., Suchomela F., Männera J., Burrowa T., Abu-Rousb M., (2006), THE FUNCTIONAL PROPERTIES OF TENCEL® - A CURRENT UPDATE, Lenzinger Berichte, 85, 22-30

18. Miller B., (2000), Critical Evaluation of Upward Wicking Tests, International Nonwoven Journal, 9

19. Connolly T.J., Parent L.R., (1993) Influence of specific energy on the properties of hydroentangled nonwoven fabrics, Tappi Journal, 76,135-141

20. Ghassemieh E., Acar M., Versteeg K., (2001), Improvement of the efficiency of energy transfer in the hydroentanglement process, Compos. Sci. Technology, 62, 1681-1694

21. Lee H. J., Cassill N., (2006): Analysis of World Nonwoven Market, Journal of Textile and Apparel, Technology and Management, 5.10-18

22. Luki S., Jovani P., (2004), Structural analysis of abrasive composite material with nonwoven textile matrix. Material Letters, 58, 439-443

23. Mao N., (2000) effect of fabric structure on the liquid transport characteristics of nonwoven wound dressing, PhD thesis, University of Leeds, UK,

# PROVIDING THE WASHABLE FEATURE TO WORSTED FABRICS BY LBL METHOD

**Şule Sultan UĞUR[1], Nazlı ÇAĞLAR CİNPERİ[2], Ayşe Merih SARIIŞIK[3]**

[1]Süleyman Demirel University, Department of Textile Engineering, Turkey
[2]YÜNSA-R&D Center
[3] Dokuz Eylül University, Department of Textile Engineering, Turkey

Corresponding author: suleugur@sdu.edu.tr

***Abstract:*** *There are many different methods used in the industry to improve the antifelting and shrinkproof properties of woven wool fabrics. In the study, Layer by Layer (LBL) method which is one of the most effective and new methods was applied on woven wool fabrics by using nano polyurethane. After the application on suit fabrics, relaxation and felting shrinkage, breaking and tear strength, alkali solubility tests were performed. It is ensured that the relaxation and felting shrinkage values are within ± 3%. It has been observed that soft handle fabrics are obtained after coating without any negative effect on the fabric key. In addition, SEM-EDX analysis was performed to examine the surface properties of the fabrics and to perform elementary analyses, and FTIR-ATR analysis was performed to determine bond characterization of the resulting films.*

***Key Words****: washable woven wool fabrics, LBL method, felting shrinkage, relaxation shrinkage, nano polyurethane*

## 1. INTRODUCTION

During production or use, the effect of temperature, mechanical effect, alkali or acid solutions and fleece on the wool fibers are intertwined with each other to gray out the resulting woolen fabric. The felting garments lose air permeability, soft and airy grip, and the fabric becomes hard and thick in a period of time that has not changed in size. The woolen fabrics can not be washed and the cleaning is done with organic solvents. In terms of ease of maintenance, the ability to wash woolen fabrics on the machine has always been a demand feature. In order to increase the washability of woven wool fabrics, many methods such as removing, adding and combining methods are used in the industry. Even though different methods are used to improve the antifelting and shrinkproof properties of woven wool fabrics in the industry, desired values (<± 3%) can not be obtained as a result of felting shrinkage test even if good values are obtained in size change as a result of relaxation shrinkage test using more than one method. Another drawback is that a hard handle is achieved. Extra processes have to be applied in order to soften the fabric. These additional operations result in extra cost for both energy and chemical and labor costs. With the studies made, nano polyurethane (PU) is used to achieve a felting shrinkage value of ± 3% in suit and uniform fabrics with multi-layer coating method. It has been found that the nano

polyurethane based multilayer coating has soft handle fabrics that do not have a negative effect on the fabric [1,2]. There are many applications in the literature which are made by textile coating with multi layer coating method. Chen and his colleagues conducted a multi-layered construction on a cotton surface with a self-repairing ability, which was a flammable feature in 2015 [3]. Ahmed and Emam worked on multi-layer coating of nano silver for high performance cotton fabric in 2016 [4]. Truong-Phuoc et al. have worked on multilayer photocatalytic devices for textile products that have become self-cleaning with sunlight in 2016 [5]. Junthip et al. have studied the coating of textile products for extended drug release by multi-layer coating with two oppositely loaded cyclodextrinpolyelectrodes in 2016 [6]. Tian et al. have worked on the ultraviolet protective cotton fabric obtained by self-assembled graphene oxide and chitosan method and electrostatic multi-layer coating method in 2016 [7]. Uğur et al. worked on the multilayer coating system of antibacterial inclusion complexes in 2016 [8]. Forsman et al. have worked on multi-layered hydrophobic coatings for cellulose nanofibril films and textile products, polylysine and natural-derived particles in 2017 [9]. In the project, it is aimed to acquire shrinkage properties in woven wool fabrics by multi-layer coating method using nano polyurethane. For this purpose, layer by layer (LBL) method which is one of the most effective and new methods was applied on woven wool fabrics by using nano polyurethane.

## 2. MATERIAL AND METHOD

Experiments on 4 different cationic polyelectrolyte types, 3 different solution application temperatures, 2 different layers with 100% ecru wool fabric were made. Optimum pH, concentration, number of layers in the preliminary experiments were taken into consideration. Two cationic dye fixatives (CDF-1, CDF-2) were used besides cationic poly (diallyl dimethyl ammonium chloride) (PDDA) and Poly(acrylamide-co-diallyldimethylammonium chloride) (P(AAm-co-DADMAC)) as cationic polyelectrolyte. Polyelectrolyte and polyurethane solutions were prepared at the concentrations determined in the experimental design and mixed with the magnetic stirrer heater. Prepared solutions were adjusted to optimum pH values with the aid of dilute hydrochloric acid and sodium hydroxide.

One of the selected polyelectrolytes for the experiments is PDDA which is a colorless liquid completely soluble in water, having a density of 1.04 g/cm$^3$. The other type of polyelectrolyte is P(AAm-co-DADMAC), a viscous, colorless liquid with a pH of 5-8. One of the commercial cationic dye fixatives was selected as CDF-1. The aqueous solutions of this product are used as an enhancer for fastness (especially rubbing and water fastness) for polyester fabrics in the textile industry; at the same time, it increases the washing strength without changing the handle of pigment printed fabrics. It is a clear yellow liquid with a pH of around 3, which can dry at 130-140 ° C. Another commercial polyelectrolyte used is CDF-2. It is an anionic, water-soluble yellow liquid with a pH of 6, is a product used for post-staining cleaning of polyester and blends in the textile industry. These

polyelectrolytes and nano polyurethane solutions were prepared at specified ratios at Table 1.

**Table 1.** Application conditions

| Fabric Blend | 100% wool |
|---|---|
| PU Concentration (g/l) | 50 |
| Polyelectrolyte Concentration (g/l) | 10 |
| Squeezing Roller Pressure (bar) | 3 |
| Squeezing Roller Velocity (m/min) | 3 |
| Drying Temperature ($^0$C) | 130 |
| Fixation Temperature ($^0$C) | 180 |
| Fixation Velocity (m/min) | 1 |
| Decatising Pressure (bar) | 1 |

At coating process, a horizontal foulard with a Cr-Ni Stainless steel body that can be adjusted to a cylinder speed of 550 mm wide and 70 Shore rigid, adjustable roller pressure of 1-6 bar, and cylinder speed of 0.5-7 m/min was used. The process was initiated by the application of a polyelectrolyte solution loaded opposite to the fabric surface charge. The excess polymer solution on the fabric surface was removed with the help of foulard using softened water. The fabric was then covered with a nano-polyurethane solution containing oppositely charged polyion, the surface charge was reversed again and the excess polymer solution was removed by washing with softened water. Each polymer solution applied to the surface was evaluated as a layer and the operations were continued until the total number of layers were reached. The nano-layered fabrics obtained after coatings were dried and fixed in the mini stenter machine located in the finishing area in the plant; followed by a decatising machine. The application conditions can be followed from Table 2. We obtained 24 different coating with different temperature values (25, 50 and 65 C) and layer numbers (12 and 16).

Breaking strength (TS EN ISO 13934 standard), tear strength (TS EN ISO 13937), 7A (relaxation shrinkage) and 5A (felting shrinkage) dimensional change in washing (TS 5720 EN ISO 6330 standard) and alkali solubilitiy tests (ASTM D-1283 standart) were carried out to examine the effect of the multilayer coating method on the fabric. Also, whiteness indexes were measured in the CIE L* a * b system with D65-10 measurements in the spectrophotometer. Optimum conditions for cationic polyelectrolyte type, solution application temperature, number of coating layers were determined by comparing test results.

The surface properties of multi-layer film coated fabrics were examined by SEM-EDX analysis and elementary analyzes were performed. FTIR-ATR analysis of the filmin binding characterization was determined. Also, alkali solubilities were tested on the selected optimum resulted fabrics.

## 3. RESULTS AND DISCUSSION

When the test results were evaluated, it was seen that the values of relaxation and felting shrinkage values were improved and the standards of quality test values were provided (Table 2). After the multilayer coating applications on 100% wool fabric using P(AAm-co-DADMAC) polyelectrolyte, it has been observed that the increase in solution temperature value and the number of coating layers showed a little improvement on the washing shrinkage values. In experiments with thePDDA polyelectrolyte, the effect of temperature changes and number of layers on washing shrinkage was seen not significant; but it has been found that hot applications reduce the tear strength of the fabric to some extent. It is used in textile industry as an enhancer for fastness (especially rubbing and water fastness) for polyester fabrics; when the commercial cationic dye fixture (CDF-1), which also increases the washing resistance without changing the soft handle of the fabrics, increases the tear strength as the temperature and the number of layers increase; It has also been observed that the increase in temperature improves the washing shrinkage values. It has been observed that when a commercial polyelectrolyte (CDF-2) used in post-staining cleaning of polyester and blends in the textile industry reduces the tear strength of the solution temperature increase, the increase in the number of layers increases the tear strength. If a general evaluation is made, it can be said that the CDF-1 solution, a commercial product, gives the best values for 100% woolen fabrics. In addition, significant improvement in the washing shrinkage of nano-film coated fabrics obtained using PDDA polyelectrolyte has been observed. The whiteness indexes were measured and compared for examining the color change caused by the fabric in the fabric. After application, it was seen the fabrics tend to be yellowing in certain amounts.

**Table 2:** Relaxation, felting shrinkage test results and Whiteness indexes of the samples

| Sample Number | Warp (% change) | | | | Weft (% change) | | | | Breaking Strength (daN) | | Tear Strength (cN) | | CIE Whiteness Index | Whiteness Change (Delta) |
|---|---|---|---|---|---|---|---|---|---|---|---|---|---|---|
| | 7A Fabric | 7A Cuff | 5A Fabric | 5A Cuff | 7A Fabric | 7A Cuff | 5A Fabric | 5A Cuff | Warp | Weft | Warp | Weft | | |
| **1** | -1,60 | -3,25 | -6,50 | -7,50 | -2,30 | -3,50 | -3,00 | -4,00 | 37 | 21 | 2011 | 987 | 19,90 | - |
| **2** | -1,50 | -2,25 | -3,50 | -6,50 | -1,25 | -1,50 | -2,00 | -2,00 | 33 | 19 | 1386 | 651 | -4,11 | -24,01 |
| **3** | -1,80 | -2,00 | -3,10 | -4,25 | -1,60 | -2,50 | -2,60 | -2,50 | 31 | 21 | 1652 | 887 | 5,91 | -13,99 |
| **4** | -1,50 | -2,00 | -2,90 | -4,25 | -1,30 | -2,50 | -1,50 | -2,00 | 32 | 21 | 1508 | 805 | 4,23 | 16,67 |
| **5** | -1,80 | -2,00 | -3,60 | -3,25 | -1,30 | -2,00 | -2,10 | -2,25 | 32 | 20 | 1508 | 832 | 3,71 | 16,18 |
| **6** | -1,60 | -2,00 | -3,00 | -3,50 | -1,30 | -2,50 | -1,60 | -2,00 | 32 | 20 | 1746 | 832 | 4,96 | 14,93 |
| **7** | -1,30 | -2,00 | -2,50 | -4,25 | -1,00 | -1,50 | -1,80 | -2,50 | 30 | 20 | 1605 | 860 | 4,31 | 15,60 |
| **8** | -1,80 | -2,00 | -3,10 | -3,00 | -1,10 | -2,00 | -2,00 | -3,00 | 31 | 19 | 1928 | 832 | 4,23 | 15,70 |
| **9** | -1,30 | -1,50 | -3,00 | -3,50 | -1,00 | -1,25 | -1,80 | -2,00 | 32 | 20 | 1563 | 736 | 7,42 | 12,48 |
| **10** | -1,50 | -2,50 | -3,00 | -5,00 | -1,00 | -1,50 | -2,00 | -2,00 | 48 | 20 | 1662 | 736 | 7,08 | 12,82 |
| **11** | -1,25 | -1,75 | -2,80 | -4,50 | -0,90 | -1,75 | -2,00 | -1,75 | 33 | 20 | 1710 | 849 | 2,86 | 17,03 |
| **12** | -1,25 | -1,75 | -2,50 | -3,00 | -0,80 | -1,50 | -1,60 | -2,00 | 33 | 20 | 1539 | 793 | 2,68 | 17,22 |
| **13** | -1,80 | -2,00 | -2,75 | -3,25 | -1,30 | -2,00 | -1,45 | -2,00 | 34 | 21 | 1386 | 679 | 4,72 | 16,18 |
| **14** | -2,00 | -2,75 | -2,75 | -4,00 | -0,80 | -2,00 | -2,08 | -4,25 | 32 | 20 | 1463 | 708 | 1,92 | 17,98 |
| **15** | -1,30 | -2,00 | -2,50 | -3,00 | -1,40 | -1,50 | -1,80 | -1,75 | 29 | 21 | 1412 | 821 | 2,06 | 17,84 |
| **16** | -0,50 | -1,25 | -1,75 | -2,50 | -0,40 | -0,75 | -1,00 | -1,75 | 32 | 20 | 1563 | 849 | 0,83 | 20,72 |
| **17** | -1,00 | -1,25 | -2,10 | -3,75 | 0,00 | -1,00 | -1,00 | -1,50 | 32 | 21 | 1412 | 765 | 6,08 | 13,82 |
| **18** | -1,00 | -1,50 | -2,50 | -4,50 | -0,30 | -1,00 | -1,10 | -2,00 | 32 | 20 | 1488 | 765 | 7,89 | 12,00 |
| **19** | -1,25 | -2,00 | -2,00 | -4,50 | -0,40 | -1,00 | -1,00 | -1,50 | 33 | 21 | 1613 | 821 | 8,16 | 11,74 |
| **20** | -0,75 | -2,00 | -1,50 | -3,75 | -0,25 | -0,50 | -1,00 | -1,00 | 33 | 21 | 1734 | 793 | 6,78 | 14,12 |
| **21** | -1,30 | -2,25 | -3,00 | -3,50 | -1,10 | -2,25 | -1,60 | -2,50 | 31 | 21 | 1710 | 849 | 8,04 | 11,96 |
| **22** | -1,33 | -2,00 | -4,00 | -5,75 | -1,16 | -2,25 | -2,50 | -4,00 | 36 | 22 | 2347 | 1048 | 6,86 | 13,06 |
| **23** | -1,60 | -2,00 | -2,60 | -4,00 | -1,30 | -2,50 | -1,60 | -2,50 | 30 | 20 | 1358 | 665 | 4,76 | 24,66 |
| **24** | -1,00 | -1,50 | -1,75 | -2,00 | -0,30 | -0,50 | -0,50 | -0,75 | 29 | 19 | 1539 | 736 | 2,28 | 17,62 |
| **25** | -2,30 | -2,50 | -5,00 | -6,50 | -0,80 | -1,50 | -3,00 | -3,50 | 30 | 20 | 1361 | 622 | 6,76 | 14,14 |
| **26** | -1,00 | -1,50 | -2,50 | -2,25 | -0,50 | -0,75 | -1,00 | -1,00 | 30 | 20 | 1386 | 651 | 8,86 | 11,04 |

SEM-EDX analysis was performed to examine the surface properties of the samples with good results and to perform elementary analyzes, and FTIR-ATR analysis was performed to determine the bond characterization of the resulting films. In the SEM images, it was seen that the flake edges of the Nano PU multi-layer film-coated fibers were clearly covered and the sharp edges were blunted (Figure 1).

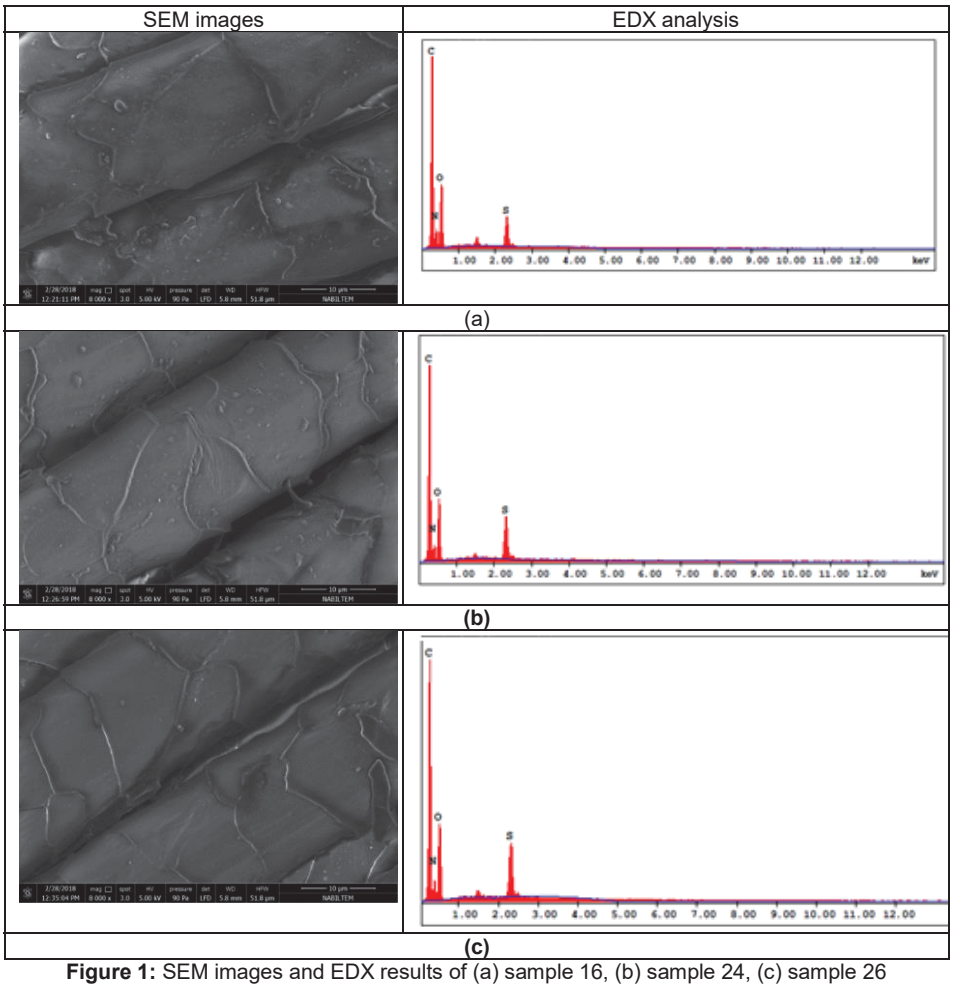


**Figure 1:** SEM images and EDX results of (a) sample 16, (b) sample 24, (c) sample 26

The results of the alkaline solubility tests based on the choosen samples results are shown in Table 4.

Alkaline solubility is a good indicator of fibers life damage after various chemical treatments. The higher the solubility of wool in alkaline shows the right proportion with the loss in the fibers [10]. For the choosen samples, there is no big difference

between the number of layers. The LBL method does not increase the alkaline solubility of woolen fabrics, so it was determined that it did not damage the product.

**Table4:** Alkali solubility values of the samples

| Sample numbers | Alkaline solubility (%) |
|---|---|
| 1 | 14,1 |
| 16 | 12,7 |
| 24 | 12,9 |
| 26 | 12,5 |

## 4. CONCLUSIONS

The optimum conditions for the experiments were obtained by coating the CDF-1 solution and the nano polyurethane solution 16 times at 25 °C. In the experiments using CDF-2, 16 times at 50 °C and 12 times at 65 °C gave the ideally results. 5A and 7A wash shrinkage were obtained under ± 3% values in weft and warp direction. The application caused the breaking strengths to decrease by 4,8-9,5% in the weft and 13,5-21,6% in the warp. In tear strengths, it decreased by 14-34% in the weft direction and by 22.3-31.1% in the warp direction. As a result of the project work, a sustainable method has been developed for the first time in the world by using multi-layer coating method using nano-polyurethane, ensuring that suits, uniforms and upholstery woolen fabrics are washable in the washing machine. In this way, the need for dry cleaning will be removed, so energy resources will be used more efficiently.

## ACKNOWLEDGMENTS

This study was conducted as a part of the project ‘‘Providing the Washable Feature to Worsted Fabrics by LBL Method’’ Funded by The Scientific and Technological Research Council of Turkey (TUBİTAK), TUBİTAK-TEYDEB Project No. 3160094.

## REFERENCES

1. Mori, M., Matsudaira, M., Comparison of Woolen Anti-felting Treatment with Classic Anti-felting Procedures, Textile Research Journal, 2012, doi: 10.1177/0040517512458343.
2. Shahidi, S., Rashidi, M., Ghoranneviss, M., Anvari, A.; Wiener, J.: Plasma Effects on Anti-felting Properties of Wool Fabrics, Surface & Coatings Technology, 2010, vol. 205, pp. 349-354.
3. Chen, S., Li, X., Li, Y., Sun, J., Intumescent Flame-Retardant and Self-Healing Superhydrophobic Coatings on Cotton Fabric, ACS Nano, 2015, vol. 9, (4), pp. 4070–4076.
4. Ahmed, H.B., Emam, H.E., Layer by Layer Assembly of Nanosilver for High Performance Cotton Fabrics, 2016, 17, 3, 418-426.
5. Truong-Phuoc, L., Christoforidis, K.C., Vigneron, F., Papaefthimiou, V., Decher, G., Keller, N., Keller, V., Layer-by-layer Protocatalytic Assembly for Solar Light-Activated Self-Decontaminating Textiles, ACS Appl. Mater. Interfaces, 2016, 8, 34438-34445.

6. Junthip, J., Tabary, N., Chai, F., Leclercq, L., Maton, M., Cazaux, F., Neut, C.., Paccou, L., Guinet, Y., Staelens, J.N., Bria, M., Landy, D., Hedoux, A., Blanchemain, N., Martel, B., Layer-by-layer coating of textile with two oppositely charged cyclodextrin polyelectrolytes for extended drug delivery, Journal of Biomedical Materials Research A, 2016,104A, 6, 1408-1424.
7. Tian, M., Hu, X., Qu, L., Du, M., Zhu, S., Sun, Y., Han, G., Ultraviolet protection cotton fabric achieved via layer-by-layer self-assembly of graphene oxide and chitosan, Applied Surface Science, 2016, 377, 141-148.
8. Ugur, S., Sarıışık, M., Türkoğlu, G., Erkan, G., Erden, E., Layer by layer assembly of antibacterial inclusion complexes, International Journal of Clothing Science and Technology, 2016, 28, 3, 368-377.
9. Forsman, N., Lozhechnikova, A., Khakalo, A., Johansson, L.S., Vartiainen, J., Österberg, M., (2017), Layer-by-layer assembled hydrophobic coatings for cellulose nanofibril films and textiles, made of polylysine and natural wax particles, Carbohydrate Polymers, 173, 392-402.
10. Bahtiyari, M. I., (2009), Investigation of some usage areas of environmentally friendly novel methods in textile pretreatment, PhD Thesis, Ege University Textile Engineering Department, 206.

# CARBON NANOTUBE COVERED HIERARCHICALLY STRUCTURED TECHNICAL TEXTILES' PREPARATION VIA MICROWAVE ENERGY-BASED APPROACH

**Selcuk POYRAZ**

Adıyaman University, Department of Textile Engineering, Turkey

Corresponding author: spoyraz@adiyaman.edu.tr

**Abstract:** Through a facile, simple, yet efficient, affordable and ultrafast (30 s) microwave (MW) energy-based approach, hierarchically structured technical textiles made up of carbon fibers (CFs) decorated with multi-walled carbon nanotube (MWCNT) forest were produced at ambient conditions in one-step. Morphological features of the as-produced textiles were characterized in details by using scanning and transmission electron microscopy (SEM, TEM) and the elemental analysis (EDX) techniques. Both the composite material characterization results and the versatile and easily controllable nature of the above mentioned process strongly support its promising success for the fabrication of such products that could be effectively used as a building material for a wide variety of advanced engineering applications including aerospace ships, communication satellites, passenger and war planes, vehicles in transportation, wind turbine blades, sports equipment and prosthetic limbs.

**Key Words**: microwave energy, carbon nanotube, carbon fiber, hierarchical structure, technical textiles

## 1. INTRODUCTION

Not only because of its excellent mechanical strength but also its thermal and electrical conductivity, light weight and high processability, CF and its products have been extensively utilized as a building material in various advanced engineering systems such as aerospace ships, communication satellites, planes, hybrid vehicles, wind turbine blades, sports equipment, prosthetic limbs and so on [1]. As an expected result of its unique fibrous structure, CF usually serves as a reinforcing component to enhance the multi-scale properties of the above mentioned bulk composite materials made up of both thermoset and thermoplastic polymers, metals and concrete, as well [2]. A great deal of research effort has been devoted to enhance the reinforcing performance of CFs, in order to; (i) reduce or even eliminate the problems that are often caused by phase separation and also shearing upon excessive and repeating stress, and (ii) to achieve strong, light-weight, durable and high performance composite materials that can be used for a wide variety of real-life engineering applications [3-5].

In recent years, CNT growth on CF surface has been proposed as a promising solution in order to address the needs and tackle the challenges in the above

mentioned matters, since a nanostructured, 3D CNT forest surrounding the CF surface can both provide sufficient number of anchoring points and can significantly increase the effective specific surface area to reach a better adhesion performance between CFs and the bulk material matrix [6-8]. Moreover, with the addition of distinct mechanical, thermal, and electrical features of the CNTs into the structure, enhanced transverse and shear resistance can also be expected from the as-produced CNT/CF hierarchical composites, as a result of the intense interfacial interactions that exist between the as-grown CNT forest and CFs. In general, the CNT forest is grown on the CFs' surface by following either a bottom-up method such as chemical vapor deposition (CVD) or a top-down method such as lithography [9, 10]. Although these methods can provide highly precise and uniform products, they usually suffer from their complex production process and from their need of harsh process conditions, i.e. high vacuum, high temperature, high pressure and hazardous chemicals' use. Additionally, these methods' overall fabrication processes are not easily scalable and are very time consuming, as well. Thus, the as-obtained sample amounts are usually limited and this restricts the common uses of such methods for the applications at industrial level. In order to eliminate these obstacles and to realize a practical application for the CNT/CF composites preparation, in this study, a well-established MW energy-assisted fabrication technique, which can rapidly grow a homogenous MWCNT forest decoration on CFs surface, is proposed [11]. The as-prepared CNT/CF composites from this method offer promising and wide range application potential for various advanced engineering and scientific fields including fiber reinforced composites' preparation for wind energy harvesting, super-capacitance, microelectronics, telecommunication, transportation, sports equipment and medical applications.

## 2. MATERIALS AND METHODS

### 2.1 Materials Used

Plain weave CF fabric, acetone (JT Baker), toluene (JT Baker) and ferrocene (AlfaAesar) were all used as purchased without further purification, unless otherwise specified.

### 2.2 Pre-treatment and Preparation of CF Mesh Samples

Prior to the MW energy-assisted rapid CNT forest growth process, several 1"×1" CF fabric samples were continuously heated in a conventional kitchen MW oven (Panasonic Inverter) at full power (1250 W) for 60 s, in order to; (i) remove the protective thin sizing layer, and (ii) to reveal as much reactive sites as possible on CFs' surface for the following process steps (Figure 1). Next, 0.2 M ferrocene solution was prepared by dissolving 0.11 moles of ferrocene in 550 mL of toluene, for the homogenous deposition of the carbon and catalyst source precursor chemical on the as-treated CF samples. After that, CF fabrics were individually soaked into this solution for 10 min under continuous gentle shaking. Eventually, all the samples were drip dried on a nylon string before the ultrafast MW heating process (Figure 2).

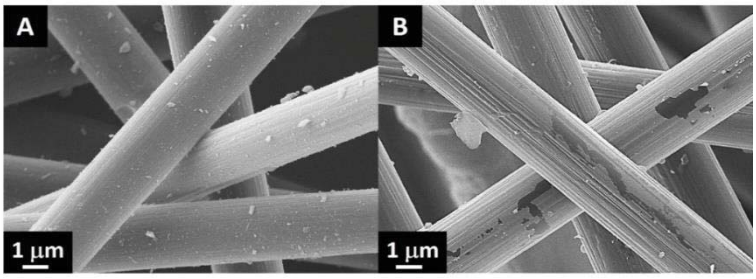


**Figure 1.** Scanning electron microscopy (SEM) images of CFs; A. before and B. after MW pre-treatment

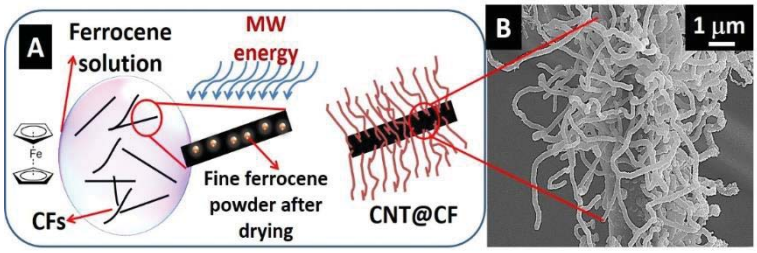


**Figure 2.** A. Schematic representation of the MW energy-assisted ultrafast CNT forest growth process on CFs, B. SEM image of a single CF covered by CNT forest on its surface

### 2.3 MW Energy-assisted Ultrafast CNT Forest Growth Process on CFs

The as-prepared CF fabric sample was tightened vertically between a pair of glass rods on a handmade PVC stand, and then it was placed on the glass MW tray. Here, the evenly deposited thin ferrocene layer was clearly observed on the CF fabric with an orange tint. The glass tray was then placed into the MW oven chamber. The CF fabric on the PVC stand was irradiated at the maximum power level, while intensive reactions were observed inside, as indicated by the sparking flames and dense chemical vapor emission. After getting heated by MWs for 30 s, the CF fabric sample with the as-grown CNT forest decoration on its surface was taken out and then gently rinsed with acetone to remove any impurities and unreacted chemicals (Figure 3).

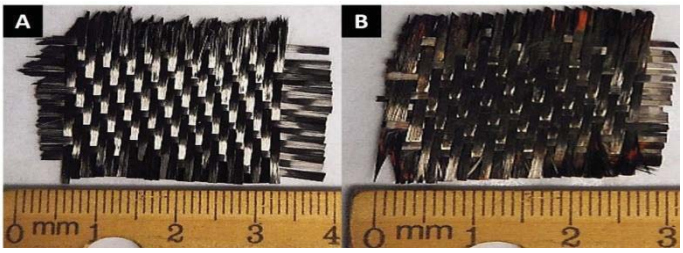


**Figure 3.** Digital images of a CF fabric sample; A. before and B. after the MW energy-assisted ultrafast CNT forest growth process

### 2.4 Characterization of the As-prepared Composite Material

Morphological and elemental analyses of the as-obtained composite materials were done by using a JEOL JSM-7000F scanning electron microscope (SEM) equipped with an energy dispersive X-ray (EDX) detector. An EMS 550X auto sputter coating device was also utilized for surface Au sputter coating of composite samples, which were readily prepared on carbon tape mounted sample holders, prior to their analysis. The in-depth morphological property analysis of the as-prepared composites was performed on a JEOL 2100F transmission electron microscope (TEM), operated at 200 kV. Here, CF strands from the as-treated fabric sample were carefully removed and dispersed in ethyl alcohol by ultrasonication for 10 min. in order to separate the as-grown CNTs from the CFs. Next, droplets (~5µL) from the supernatant surface were collected with a pipette and then transferred onto a carbon coated copper Formvar grid and left to get dried at ambient conditions before TEM testing.

## 3. RESULTS AND DISCUSSION

After the MW heating process, a dense CNT forest layer was intensively grown on the CF fabric surface and covered almost the entire fiber surface with a radially aligned and entangled assembly look, which is clearly exhibited in the SEM images shown in Figures 4A and 4B. At higher magnifications, the nano/micro interface between CNTs and CF can be clearly observed, as the dense CNT forest was grown perpendicularly from the CF surface (Figure 4C).

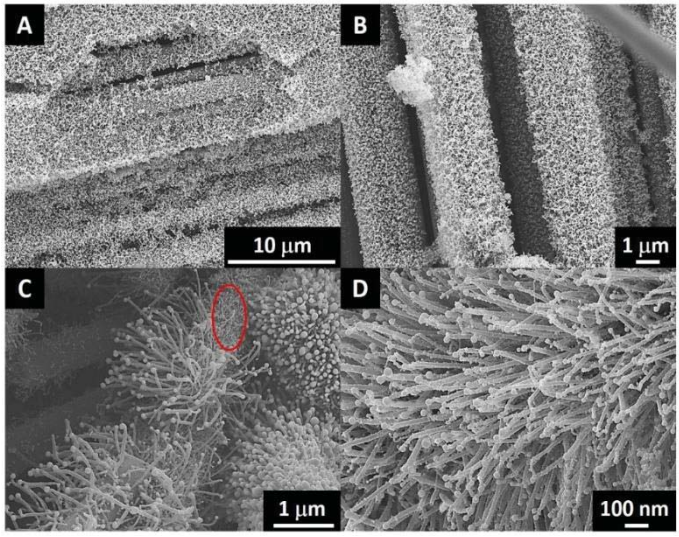


**Figure 4.** SEM images of; A.-B. hierarchically structured CNT/CF composites, C. CFs covered by the as-grown CNT forest on their surfaces, D. zoomed-in view of the marked area in Figure 4C

After proving the as-proposed MW-energy based ultrafast CNT growth technique's success on generating CNT/CF hierarchical composites via SEM characterization, the in-depth morphological and elemental features of these structures were further characterized by both TEM microscopy and EDX analysis. Collected results from these analyses are shown in Figure 5. The TEM image in Figure 5A provides more detailed information about the as-grown CNTs by showing their hollow stems that encapsulate catalyst iron NPs. This morphological structure was obtained during the tip-growth process, whose working mechanism would be explained along the following paragraphs. As it also can be seen from the TEM image in Figure 5C, a single ~25 nm × 5 nm iron catalyst NP was encapsulated within the as-grown MWCNTs' wall, which was made up of ultrathin graphene layers. The EDX analysis results of both the as-grown MWCNTs and the encapsulated catalyst iron NPs are shown in Figures 5B and 5D. These diffractograms provide more evidence for the presence of the as-grown MWCNTs and iron NPs that are made up of C and Fe elements, respectively. Also, there are two sharp peaks with Cu indicators in these diffractograms, both of which were caused by the copper grid used for the TEM imaging process as the sample holder.

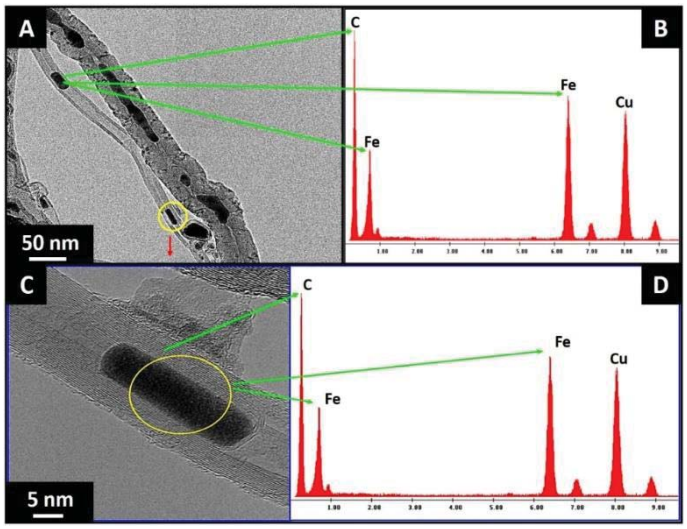


**Figure 5.** A. TEM image of the catalyst iron NPs encapsulated within the as-grown MWCNTs, B. the EDX diffractogram of the catalyst iron NP and the as-grown MWCNT, C. HR-TEM image of the marked area in Figure 5A, and D. the EDX diffractogram of the marked area in Figure 5C.

The CNT forest's coverage on the CF fabric surface was high, since the growth was observed to span along the full fiber axis length. Both long-winding and short-rigid CNT types were grown in this forest, indicating the heterogeneous nature of the catalytic growth process induced by MWs [11]. Morphological property details of the as-obtained CNTs were also investigated, and their average diameter was

calculated to be ~50 nm while their length could extend up to couple of microns (Figure 4D). The high aspect ratio of these CNTs thus provide an ultra-high surface area, which enables enhanced interfacial interactions and enable multi-scale functions for the composite, through the formation of new interfaces. In good agreement with the relevant previous literature results [12-14], the tip-growth mechanism was also effective on the current CNT forest's growth on CF fabric samples. The characteristic matchstick-like morphology, which is composed of hollow and multi-walled stem with oxidized iron nanoparticle (NP) tip, of the as-grown CNTs in this forest (Figure 4D) clearly indicates the effective tip-growth mechanism, as well.

It is thus revealed that the MW-energy assisted ultrafast heating technique was successful on generating CNT/CF nano-micro hierarchical composite structures with high yield and density and within a short period of time. It is strongly believed that the ultrafast CNT growth mechanism on the CF fabric sample surface majorly depends on the high reaction temperature between ferrocene particles and CFs upon MW irradiation. That is to say, as soon as absorbing the MW energy; (i) highly conducting CF fabric sample started sparking and arcing, (ii) then it's surface temperature was rapidly increased above 1000 °C, and (iii) this caused a large amount of heat release within a few seconds. As a result, the fine ferrocene particles on the sample fabric surface got decomposed into its iron and cyclopentadienyl ligands through an instant chain reaction, in gas form. At this point, the iron NPs served as catalysts while the cyclopentadienyl groups were realigned and served as the carbon source for the formation of MWCNTs, respectively [11-14]. After all, the dense CNT forest was grown on the CF fabric surface through this liquid-solid-vapor transition mechanism.

## 4. CONCLUSIONS

Hierarchical CNT/CF composites with aligned nano-micro interfacial structure were fabricated within seconds by applying MW irradiation. Homogenously grown CNT forest was obtained on the CF fabric surface with high yield, high aspect ratio, and high coverage density. The as-produced hierarchically structured CNT/CF composites offer promising potential for widespread advanced applications including medical applications, supercapacitors, transportation, and microelectronics and so on. The as-proposed highly efficient and cost-effective MW energy-assisted fabrication technique also secures the industrial scale production of relevant next generation composites, as well.

## REFERENCES

1. Chand, S. (2000) Carbon fibers for composites, Journal of Materials Science, 35(6), 1303-1313.
2. Chen, H., Roy, A., Baek, J. B., Zhu, L., Qu, J., Dai, L. (2010) Controlled growth and modification of vertically-aligned carbon nanotubes for multifunctional applications, Materials Science & Engineering R-Reports, 70, 63-91.

3. Delamar, M., Desarmot, G., Fagebaume, O., Hitmi, R., Pinsonc, J., Saveant, J. M. (1997) Modification of carbon fiber surfaces by electrochemical reduction of aryl diazonium salts: Application to carbon epoxy composites, Carbon, 35(6), 801-807.
4. Liu, Z., Wang, J., Kushvaha, V., Poyraz, S., Tippur, H., Park, S., Kim, M., Liu, Y., Bar, J., Chen, H., Zhang, X. (2011) Poptube approach for ultrafast nanotube growth, Chemical Communications, 47, 9912-9914.
5. Poyraz, S., Liu, Z., Liu, Y., Zhang, X. (2013) Devulcanization of scrap ground tire rubber and successive carbon nanotube growth by microwave irradiation, Current Organic Chemistry, 17, 2243-2248.
6. Poyraz, S., Zhang, L., Schroder, A., Zhang, X. (2015) Ultrafast microwave welding/reinforcing approach at the interface of thermoplastic materials, ACS Applied Materials & Interfaces, 7, 22469-22477.
7. Samsur, R., Rangari, V. K., Jeelani, S., Zhang, L., Cheng, Z. Y. (2013) Fabrication of carbon nanotubes grown woven carbon fiber/epoxy composites and their electrical and mechanical properties, Journal of Applied Physics, 113(21), 214903-214908.
8. Thostenson, E., Ren, Z., Chou, T. (2001) Advances in the science and technology of carbon nanotubes and their composites: a review, Composites Science and Technology, 61(13), 1899-1912.
9. Thostenson, E. T., Li, W. Z., Wang, D. Z., Ren, Z. F., Chou, T. W. (2002) Carbon nanotube/carbon fiber hybrid multiscale composites, Journal of Applied Physics, 91(9), 6034-6037.
10. Xie, H., Poyraz, S., Thu, M., Liu, Y., Snyder, E. Y., Smith, J. W., Zhang, X. (2014) Microwave-assisted fabrication of carbon nanotubes decorated polymeric nano-medical platforms for simultaneous drug delivery and magnetic resonance imaging, Rsc Advances, 4, 5649-5662.
11. Xu, B., Wang, X., Lu, Y. (2006) Surface modification of polyacrylonitrile-based carbon fiber and its interaction with imide, Applied Surface Science, 253(5), 2695-2701.
12. Yu, B., Jiang, Z., Tang, X. Z., Yue, C. Y., Yang, J. (2014) Enhanced interphase between epoxy matrix and carbon fiber with carbon nanotube-modified silane coating, Composites Science and Technology, 99, 131-140.
13. Yuan, H., Wang, C., Zhang, S., Lin, X. (2012) Effect of surface modification on carbon fiber and its reinforced phenolic matrix composite, Applied Surface Science, 259, 288-293.
14. Zhao, Z. G., Ci, L. J., Cheng, H. M., Bai, J. B. (2005) The growth of multi-walled carbon nanotubes with different morphologies on carbon fibers, Carbon, 43, 651-673.

# POSTER PRESENTATIONS

# TRAILER FABRIC (TARPAULIN) WHICH IS DEVELOPED FOR ELIMINATING THE ADDITIONAL REINFORCEMENT PROCESS

**Habibe Gülben SELVİ[1], Şafak KARAGENÇ[1], Murat YILDIRIM[1]**

[1]Zorluteks Tekstil Tic ve San. A.Ş.

Corresponding author: gulben.ulgen@zorlu.com

**Abstract:** The aim of the project is to improve strength and cut resistance properties by designing fabric constructions with an innovative approach for Trailers. In this direction, different fabric designs and optimum production process conditions is determined by the influence of acting force on fabric will be analyzed. The tarpaulin which has improved performance, will be produced with an innovative method for the first time in Turkey.

**Keyword:** Cut Resistance Tarpaulin, Reinforced Tarpaulin, Trailer, PVC Coating, Tensile Strength

## 1. INTRODUCTION

In the direction of the researches, trailer vehicles are mostly used in the road haulage sector. As is known, there are deformations in the charge and tarpaulin that are carried due to accidents and bad weather conditions when charge transport with the trailer [1]. Nowadays it has been seen that safety enhancing works have to carry out for trailer when trailer cover (tarpaulin) is cutted by theft or people who want to escape by illegal means. In this case, trucks producers need to cover truck with reinforcement and cut resistance tarpaulin. These tarpaulin are reinforced by applying strips horizontally, vertically and diagonally on the tarpaulin at regular intervals [2,3,4]. These additional operations cause extra cost, labor and loss of time for the trucks companies. For these reasons, the main objectives of the project are to secure the materials transported from the road, remove the extra labor cost and increase the tensile strength of the tarpaulin against the impact. The project aims to increase the resistance against the forces acting on fabrics that will be developed using high-performance yarns with improved technical specifications. The fabric will be resistant to UV rays, water repellent and flammable functional properties. In this direction, optimum working conditions of the weaving and coating(PU, PVC) processes will be determined. As a result, using this innovative method developed by fabric structures and manufacturing processes for tarpaulin will be produced for the first time in Turkey that increased the performance.

## 2. MATERIAL AND METHOD

### 2.1. Analysis of Impact Forces on Trailer Fabric

The forces acting on Tarpaulin will be analyzed. Code XL dynamic and static standards will be applied for analysis. The European Standard DIN EN 12642 describes the minimum requirements for the strength of vehicle bodies. It applies to all structural elements (side walls, front and back walls) of trucks and trailers with a maximum permitted gross vehicle weight exceeding 3.500 kg. Testing of a trailer for compliance to the normal (Code: L) and reinforced structures (code: XL, higher test loads), can be performed by static or dynamic tests. Vehicles, whose structure has been approved for the EN 12642 XL regulation, require less or no additional lashing of their loads. To statically test a trailers' body for compliance to the EN 12642 XL regulation, following test loads (absolute values) are required for the determination of the structure firmness with a payload of 27.000 kg [6]:

**Table 6.** Static Test Parameter

| | DC 9.5 | EN 12642 L | EN 12642 XL |
|---|---|---|---|
| Front wall (0,5 x payload) | 13.500 daN | 5.000 daN | 13.500 daN |
| Side wall (0,4 x payload) | 8.100 daN | 8.100 daN | 10.800 daN |
| Rear wall (0,3 x payload) | 8.100 daN | 3.100 daN | 8.100 daN |

To perform a static test, a wall needs to be installed in the trailer. A balloon is then inflated between the wall and the side-curtains, to simulate a lateral pressure of 10.800 kg. The EN 12642 XL regulation stipulates that the maximum body deformation must be less than 30 cm.

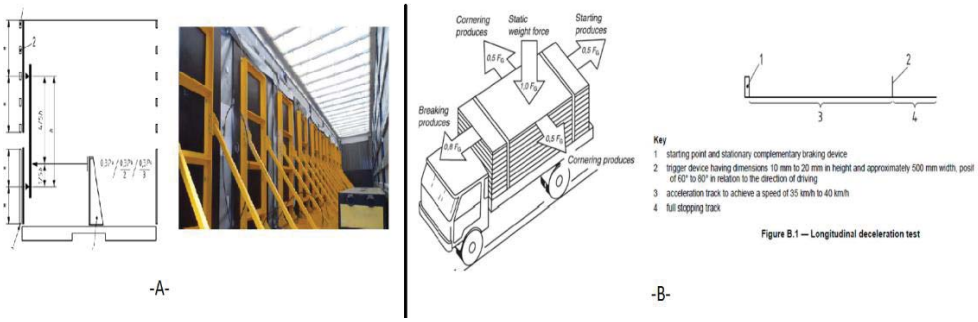


**Figure 2.** A) Static Test; B) Dinamic Test

A dynamic test is performed by driving with a fully loaded trailer on an airfield. The EN 12642 XL regulation stipulates that 2 different driving tests are to be

performed 3 times one after another. During these tests, following forces are to be obtained at each driving test[6]:

- Deceleration of 0.8 g in the driving direction
- Lateral acceleration of 0.5 g
- Lane change test with 0.5 g
- Backward acceleration of 0.5

### 2.2. Development of Fabric Constructions

First of all, the analysis of the force distribution acting on the fabric while the trailer is moving will be carried out with the EN12642 specifications. In the direction of the obtained results, composite fabric constructions will be improved by using 1000 dtex/288F Polyester, 1000 dtex/288F high strength Polyester and 1100 dtex KEVLAR cut resistant yarns. Standard Curtainsider tarpaulins are reinforced by vertical and horizontal belts (Figure 2). The belts have been secured the tarpaulin. The belts have to meet the following requirements:

• vertical belts: tensile strength ≥ 23 kN;

• horizontal belts: tensile strength ≥ 12 kN.

Commonly used method of securing the belt to the tarpaulin is by welding. This process will be removed from the trailer production stages when the reinforced tarpaulin is developed. Fabric construction designs will be developed using the EAT program. Weaving and coating process will be optimized for the developed constructions.

**Figure 3.** Standard Reinforced Tarpaulin and Reinforcement Process

The quality of the fabric used will be such that the resulting product will conform to the requirements of Table 2 and ensure uniformity of the performance.

**Table 7.** Fabric Requirements

| Characteristic | Requirements | Test method according to |
|---|---|---|
| Breaking strength in warp and weft<br>• at 23 °C ± 5 °C [a]<br>• at – 25 °C [b] | <br>≥ 4 000 N / 5 cm<br>≥ 2 700 N / 5 cm | EN ISO 1421 |
| Resistance to tear propagation in warp and weft<br>• at 23 °C ± 5 °C [a]<br>• at – 25 °C [b] | <br>≥ 300 N<br>≥ 130 N | EN 1875-3 |
| Adhesion [c] | ≥ 100 N / 5 cm | EN ISO 2411 |
| Dimensional stability | ≤ 1 % | 24 h at 70 °C |
| Buckling strength | No cracks after 100 000 bending operations | EN ISO 7854/B |
| Reaction to fire | Burning rate < 100 mm/min | ISO 3795 |
| Total mass per area | > 850 g/m² | EN ISO 2286-2 |

[a] i.e. room temperature.

[b] For special applications, a test temperature of –40°C may be applied, if agreed between user and supplier.

[c] EN ISO 2411 specifies the requirement for attaching a separate piece of fabric, using glue, to facilitate the test. For purposes of EN 12641-2, this attachment should be effected by the use of a welding process.

## 3. RESULTS AND DISCUSSION

First time in Turkey, it will be produced reinforced tarpaulin which has been developed for the additional reinforcement process. The reinforcement tarpaulin will be also help to reduce extra cost, labor and time. The following results are expected with these developments;

- Additional tarpaulin reinforcement process will be removed,
- Reinforced tarpaulin production without additional processing in the weaving process using different yarns such as high strength and cut resistance,
- Increase resistance to cutting to the tarpaulin that may come from outside impact,
- Ensuring the safety of the carried cargo with trailer,
- Development of fabric constructions providing weft and warp tensile strength according to EN 12642 standard,
- Development of UV strength, water repellency and FR tarpaulin fabrics,
- Determination of optimal production weaving and coating parameters for the new approach reinforcement tarpaulin.

## 4. CONCLUSION

The aim of the project is to improve tensile strength and cut resistance properties by designing fabric constructions with an innovative approach for Trailers. In this direction, different fabric designs and optimum production process conditions is determined by the influence of acting force on fabric will be analyzed. The tarpaulin which has improved performance, will be produced with an innovative method for the first time in Turkey.

## ACKNOWLEDGMENTS

This work has been partly supported by the The Scientific and Technological Research Council of Turkey (TUBITAK) in frame of the 1501 - Industrial R&D Projects Grant Programme.

## REFERENCES

1. Ünal L., Terzioğlu Y., Akkaş U., İlhan B., Özdek N.,2011 Karayolarında Ağır Taşıt Trafiğinin ve Yük Taşımacılığının Özellikleri ve Eğilimleri
2. James M. McKinney, North Augusta, John G. Hodson, Graniteville, 1986, Coated Fabrıc, US Patent, Patent No: 4,594,286.
3. Allan M. Dellinger, Waxhaw N.C., Michelle C. Carter, Madison, NJ.,1995, Cut-Resistant Tarpaulin, US Patent, Patent No: 5,431,979.
4. Callens Christophe, Dynatex S.A.,2007, Reınforcement Materıal And Roof Stabılısatıon System To Prevent Deformatıon Of Chargers, Traılers And/Or Lorrıes, European Patent, Patent No: EP 2 001 694 B1.
5. Bulut Y. Sular V.,2015, Kaplama veya Laminasyon Teknikleri İle Üretilen Kumaşların Genel Özellikleri Ve Performans Testleri, Tekstil ve Mühendis, Yıl: 15, Sayı: 70-71, Sayfa: 6-16.
6. European Standart, 2005, Swap Bodies and Commercial Vehicles – Tarpaulins EN12641, European Committee for Standardization, Brussels

# THE OBJECTIVE EVALUATION OF PILLING TENDENCY OF KNITTED FABRICS THROUGH DIGITAL IMAGE PROCESSING

**Abdurrahman TELLİ[1], İlkan ÖZKAN[1]**

[1]Cukurova University, Department of Textile Engineering, Turkey

Corresponding author: atelli@cu.edu.tr

***Abstract:*** *Pilling of knitted fabrics is a serious problem in terms of fabric appearance and product usage life. There are different methods and devices developed for the determination of the pilling of fabrics under laboratory conditions (Martindale, ICI, Random tumble and etc.). However, subjective methods are still using to evaluate the pilling characteristics of the fabric such as comparison of samples with standard photographs. In the literature, several objective methods were proposed for pilling assessment. But, these methods have not found a common use in textile industry for now. In this study, the degrees of pilling on fabric surface were measured objectively by texture analysis using Gray Level Co-occurrence Matrix from image processing techniques in MATLAB package program. Statistical measures were extracted from matrices obtained from images taken in digital scanners. These statistics provide information about the effects of pilling on the texture. This study contributes to applications of computer vision in fashion, conventional and technical textiles.*

***Key Words****: pilling, digital image processing, GLCM, texture analysis, MATLAB*

## 1. INTRODUCTION

The pilling of knitted fabrics is a serious problem for the textile industry. The pills are formed protruding from the fabric surface during wearing or washing under the rubbing actions. The development of pills on a fabric surface initiates the attrition of the garment. Furthermore, this condition brings along an irritating appearance. This appearance, which does not belong to the product when purchased, causes dissatisfaction from the manufacturer. For this reason, the pilling of the fabrics is tested before the customer is presented. Apparel suppliers make an effort to predict and minimize the tendency of pilling on the fabric surface using various material and methods.

There is a large volume of published studies describing definition of pilling, mechanism of pill formation, measurement of pills, factors affecting pill formation and control of pilling [1]. There are different methods and devices developed for the determination of the pilling of fabrics under laboratory conditions. However, subjective methods are still using to evaluate the pilling characteristics of the fabric such as comparison of samples with standard photographs. Numerous studies have attempted to evaluation fabric pilling as objective with the applications of the image processing technology. Image-processing technology, which has rapidly developed since the 1960s, is used in textile manufacturing and

inspections, including determination of textile-surface characteristics. Image-processing is basically the technique of manipulating and improving gray-scale images by using mathematical functions. Image analysis involves calculations on an ultimate image to produce numerical results [2]. Image analysis as a method for evaluating the fabric pilling started in the late 1980s as a try to replace the applied subjective evaluation methods [3]. In recent years, there has been an increasing interest in machine vision-based pilling assessment [4]. But, these methods have not found a common use in textile industry for now. Evaluation of fabric pilling passes through four main stages in the mentioned studies. Stages of quantitative fabric pilling evaluation are surface digitization, pills segmentation, pills quantization and pills classification [3]. In this study, the levels of pilling on fabric surface were measured objectively by texture analysis using Gray Level Co-occurrence Matrix from image processing techniques in MATLAB package program.

## 2. MATERIAL AND METHOD

Single jersey and double jersey knitting fabrics containing 100% cotton fibers were used in this study. “Martindale Pilling and Abrasion Test Instrument developed by Atac Machine” was chosen to evaluate pilling resistance of the fabrics in compliance with ASTM D 4970. The images of fabrics were obtained by digital scanner before the process of placing in the rubbing area. Brother DCP-7055 preferred in standard offices was used as digital scanners without install a special image acquisition system. The tests were carried out at 5000 turns. After this procedure, fabric surfaces containing pills were scanned again. Taken images before and after in pilling were resized as 900x900 pixels at the same size.

The RGB color images of fabrics are loaded to MATLAB package program. These images are three-dimensional matrices in "900x900x3 uint8" format. After that, matrices must be two-dimensional (900x900 uint8) in order to be able to operate on them. Thus, matrices expressing the different tone of the gray consisted values ranging from 0 to 256 were generated. These matrices are transformed into a form (900 x 900 double) that will have a value between 0 and 1. These forms of matrices were ready for texture analysis using GLCM from image processing techniques. Standard deviation filter was implemented on these matrices in the context of texture analysis. Standard deviation filtered images were segmented using Otsu's global thresholding algorithm. Thus, the pills in the image were separated from the image background. Values below the specified radius were masked using close mask. This application removes pills smaller than the determined element. In this study, fabric images before pilling were used to determine the reference radius. The radius was increased until there is one pill in the image. The radius was measured as 4 pixels for both fabrics. The same radius was also used to mask fabric images after pilling to provide the possibility of comparing the fabrics. Furthermore, the fabric's own fuzz and structure are not regarded as discomfort. After this phase, the negative of images were obtained applying "invert mask" to matrices. Image processing was finished by clearing the

borders of the image. And so, matrices of images have reached to "900x900 logical" format. Several statistics were derived with feature extraction from these matrices.

## 3. RESULTS AND DISCUSSION

Figure 1 provides images of single jersey fabric obtained from image processing. The results obtained from the image processing of rib fabric are presented in Figure 2. Table 1 shows the summary statistics of images. These statistics provide information about the texture of images.

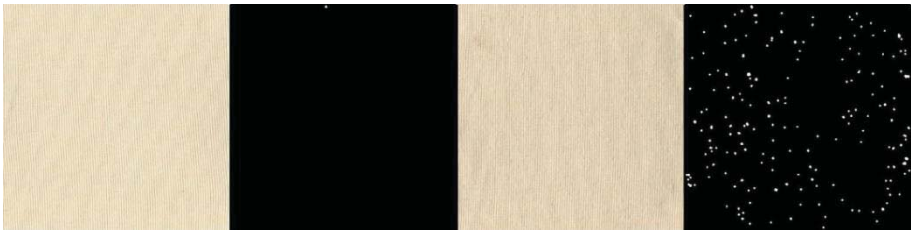

**Figure 1.** Single Jersey fabric (a), SJ fabric after image processing (b), SJ fabric after pilling (c), Pills in SJ fabric after IP (d)

**Figure 2.** Rib fabric (e), Rib fabric after image processing (f), Rib fabric after pilling (g), Pills in rib fabric after IP (h)

**Table 1.** Statistics obtained from binary images with feature extraction

| Type | Std. Dev. | Entropy | Number of pills | Area of pills | Mean Area | Contrast | Correlation | Energy | Homogeneity |
|---|---|---|---|---|---|---|---|---|---|
| **b** | 0,009 | 0,0013 | 1 | 70 | 70,00 | 0,00002 | 0,8428 | 0,9998 | 1 |
| **d** | 0,120 | 0,1093 | 176 | 11739 | 66,70 | 0,00460 | 0,8405 | 0,9669 | 0,9977 |
| **f** | 0,011 | 0,0017 | 2 | 98 | 49,00 | 0,00004 | 0,8163 | 0,9997 | 1 |
| **h** | 0,084 | 0,0604 | 80 | 5695 | 71,19 | 0,00210 | 0,8470 | 0,9839 | 0,9989 |

Pilling on the fabric surface could be detected from images taken in digital scanners without install a special image acquisition system. According to the findings, there was a decrease in energy and homogeneity after pilling for both fabrics. The increase in standard deviation, entropy, number of pills, area of pills and contrast was observed. No trend was detected in the results of mean area and correlation. However, these variables may be related to others. For instance, subjective evaluations are affected largely from mean pill size. This data can be an important coefficient or variable in the objective measurement of pilling. Statistics measures obtained from binary images with feature extraction in Table 1 will provide important benefits to assess pilling grades. These data can be used

for correlation, regression, cluster analysis or ANN applications. The results show that the degree of pilling can be predicted by more detailed studies.

## 4. CONCLUSION

Researchers have investigated image analysis of pilling in four stages as surface digitization, pills segmentation, pills quantization and pills classification. Surface digitization is a process converting of fabric surface to a digital format which can be processed on a computer. For this purpose, various camera systems and laser sensors are used by researchers in image acquisition. Different techniques have been put forward by researchers for the detection of piling, the separation from the background and image segmentation. Edge detection algorithms and filters are used. Pills quantization is determined using statistics values obtained from the fabric images. The ultimate aim of all these operations is to classify the images [4, 5].

In this study, it is seen that the three stages were carried out successfully by using above mentioned techniques differently from previous studies. In this way, quantitative values of the pills were obtained. Furthermore, trends for the various properties were determined in which direction. Thus, this research has thrown out new techniques in need of further investigation about the objective evaluation of pilling tendency. However, it is clear that the classification process of images as a final stage are be in need of more experimental sets.

In future studies, test plans should be produced to give different levels of pilling. In addition to this, the results of classical method that evaluates with standard photographs by the expert operator should be measured subjectively. It is recommended that the relationship between subjective assessments and the characteristics properties of the matrix structures to be produced from this test plan were investigated by using clustering analysis. It is suggested that statistical analysis of the obtained results and generating equations in which these pills quantitative values are variable.

## ACKNOWLEDGMENTS

This work was financial supported by the Cukurova University BAP Unit (Project No: FBA-2017-9938).

## REFERENCES

1. Ukponmwan, J. O., Mukhopadhyay, A., & Chatterjee, K. N. (1998). Pilling. *Textile progress*, 28(3), 1-57.
2. Behera, B. K. (2004). Image-processing in textiles. *Textile Progress*, 35(2-4), 1-193.
3. Eldessouki, M. (2018). Evaluation of fabric pilling as an end-use quality and a performance measure for the fabrics. *In Applications of Computer Vision in Fashion and Textiles* (pp. 147-187).
4. Furferi, R., Governi, L., & Volpe, Y. (2015). Machine Vision-Based Pilling Assessment: A Review. *Journal of Engineered Fabrics & Fibers (JEFF)*, 10(3).
5. Eldessouki, M., & Hassan, M. (2015). Adaptive neuro-fuzzy system for quantitative evaluation of woven fabrics' pilling resistance. Expert Systems with Applications, 42(4), 2098-2113.

# EFFECTS OF CALENDERING AND FLUOROCARBON TREATMENT ON WATERPROOFNESS OF COATED POLYPROPYLENE FABRICS

**Sukran KARA[1], Sevil YEŞİLPINAR[1]**

[1]Dokuz Eylul University, Department of Textile Engineering, Turkey

Corresponding author: sukran.kara@deu.edu.tr

***Abstract:*** *Polypropylene (PP) fiber is a good candidate to be used in technical areas with its advantageous properties such as high hydrophobicity, high wicking property, lightweight, low cost and easy processability. Recently, use of PP fiber is limited in protective garment industry. Within the context of this study, it was aimed to expand the usage of PP fiber by combining its properties with breathable-waterproof coatings. Individually in this study, effects of calendering and FC pre- and post- treatments were investigated on the waterproofness property of coated polypropylene fabrics.*

***Keywords:*** *calendering, fluorocarbon treatment, coating, water-based polyurethane, polypropylene.*

## 1. INTRODUCTION

Coating is an advanced finishing method in which a thin polymer layer is applied to one or both sides of a base fabric. By coating, advantages of coating polymer and base fabric are combined to enhance the performance, appearance or functional properties of the end product. One of the most important properties provided by coating is waterproofness. Waterproofness makes a coated fabric impermeable to pressurized water, rain and most of the hazardous liquids. Waterproof fabrics can be generally classified as impermeable fabrics and breathable-waterproof fabrics. Breathable–waterproof fabrics are preferred for garment production as they are more comfortable [1, 2]. Breathable-waterproof coatings may be prepared by solvent based polymers or water-based polymers. Water-based polymers are more eco-friendly and sensitive to human health during production [3, 4].

In our previous studies effects of polyurethane (PU) type, curing temperature, curing time, cross-linker amount and fluorocarbon (FC) pre-treatment were investigated on the properties of coated polypropylene, polyester, polyamide and cotton fabrics [5-7]. In this study, effects of calendering and FC pre- and post-treatment on the waterproofness property of coated polypropylene fabrics were investigated. Polypropylene base fabric was coated with water-based breathable-waterproof polyurethane blend. It was expected to expand the usage of polypropylene fabrics in coated textiles area and create a base fabric alternative for new applications.

## 2. MATERIALS AND METHODS

### 2.1. Materials

Materials of the study were PP base fabric, FC, aliphatic polyether type PU coating polymers and auxiliary materials. Auxiliary materials consisted of polyacrylic and PU based thickeners, blocked isocyanate type cross-linker, defoamer and deaerating agent.

Samples were diversified according to the processes they were exposed. Experimental design and sample codes are given in Table 1. Samples were coated with three layers of polymer. After coating each layer, samples were dried at 100ºC for 2 min. Finally, all samples were cured at 135ºC for 2 min.

**Table 1.** Samples of the study

| Schematics of experiments | Sample Code | FC pre-treated (PT) | Coated (C) | Calendered (CL) | FC post-treated (PS) |
|---|---|---|---|---|---|
| FC pre-treatment → blade coating process → FC post-treatment (1st layer coating, Calendering (20 tons), 2nd layer coating, 3rd layer coating) | PP | No | No | No | No |
| | PPC | No | Yes | No | No |
| | PPC-PS | No | Yes | No | Yes |
| | PPC-CL-PS | No | Yes | Yes | Yes |
| | PPC-PT-PS | Yes | Yes | No | Yes |
| | PPC-PT-CL-PS | Yes | Yes | Yes | Yes |

### 2.2. Methods

Waterproofness of the samples were tested before and after washing. In addition, mass changes after washing and add-on values were determined. Waterproofness test was performed according to TSE 257 EN 20811 standard [8] by using Textest FX 3000 Hydrostatic Head Tester III. Test was repeated 3 times for each sample type. Samples were subjected to domestic washing cycles according to TS 5720 EN ISO 6330-2002 6A standard [9].

## 3. RESULTS AND DISCUSSION

Add-on and mass change results are given in Figure 1 a. Add-on values were between 8 % and 16 % for coated samples. Mass decrements after washing were detected between 1.5 % and 2.5 % for coated fabrics. Any relationship between calendering, FC treatment and mass changes were not detected.

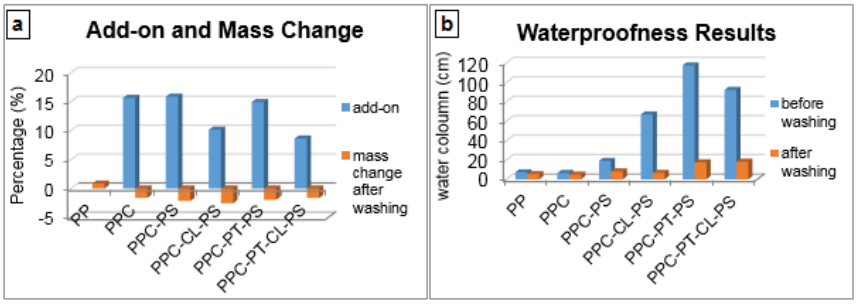


**Figure 1. a)** Add-on and mass change values **b)** waterproofness results

Waterproofness results are given in Figure 1 b. PP base fabric and only coated sample (PPC) exhibited very low waterproofness. FC post-treatment after coating increased the waterproofness up to 18.9 cm water coloumn (w.c.) (PPC-PS). Calendering and FC pre-treatment contributed to waterproofness of samples. FC pre-treated PPC-PT-PS and PPC-PT-CL-PS samples showed higher waterproofness when compared to equivalent samples which were not FC pre-treated, namely PPC-PS and PPC-CL-PS. Highest waterproofness was obtained from PPC-PT-PS sample which was coated, FC pre-treated and FC post-treated (117 cm w.c.). Lowest level of waterproofness was admitted as 130 cm w.c. by Sen and Damewood [1] and 100 cm w.c. by Fung [2]. PPC-PT-PS was the only sample which provided the lowest level of waterproofness, before washing. After washing, waterproofness of all coated samples decreased dramatically. It was thought to be a result of relatively lower used curing temperature (135˚C) and FC effect. Relatively low curing temperature was used because of low melting point of PP (160-170˚C) [10]. Also, delamination of coating layer was observed for some of the samples after washing.

## 4. CONCLUSION

Calendering and FC pre-treatment enhanced the waterproofness of coated PP fabrics. After washing, waterproofness decreased dramatically and some delamination was observed. FC treatment contributed to waterproofness before washing but inhibited the adhesion between fabric and coating polymer and resulted with lower waterproofness after washing. Curing at 135˚C may lead to lower cross-linking. In further studies, new cross-linking agents having lower curing temperatures will be explored.

## REFERENCES

1. Sen, A. K. ve Damewood, J. (2005). Coated textiles: Principles and applications. Boca Raton: CRC Press.
2. Fung, W. (2002). Coated and laminated textiles. Boca Raton: CRC Press.
3. Nicholson, J. W., Prosser, H. J., & Wilson, A. D. (Eds.). (1988). Surface Coatings-2. Elsevier.
4. Jassal, M., Khungar, A., Bajaj, P. ve Sinha, T. J. M. (2004). Waterproof breathable polymeric coatings based on polyurethanes. Journal of Industrial Textiles, 33 (4), 269-280.
5. Kara, S., Yeşilpınar, M.S. (2014). Poliüretan kaplanmış pamuk ve poliester kumaşların su geçirmezlik özelliklerinin incelenmesi. 2. Uluslararası Tekstil Zirvesi, October 22-24, 2014, Kahramanmaras, Turkey.
7. Kara, S., Yeşilpınar, S., Akşit, A. Comparison of waterproofness and air permeabilities of coated and laminated polyester and polyamide fabrics. 16th AUTEX World Textile Conference 2016, June 8–10, 2016, Ljubljana, SLOVENIA, p. 153, Book of Abstracts.
8. Kara, S., Yeşilpınar, S., Akşit, A. Permeability properties and abrasion resistance of coated polypropylene fabrics. 9th Central European Conference, September 11-13, 2017, Liberec, Czech Republic, pp. 84-85, Book of Abstracts.
9. TSE 257 EN 20811: 1996. Textiles-Fabrics-Determination of Resistance to Water Penetration-Hydrostatic Pressure Test.
10. TS 5720 EN ISO 6330- 6A: 2002. Textiles- Domestic washing and drying procedures for textile testing.
11. Mclntyre J.E. (2005). Synthetic fibers: Nylon, polyester, acrylic, polyolefin. Woodhead Publishing: Cambridge.

# PROVIDES THERMAL INSULATION, BREATHABLE, ANTIBACTERIAL TOWEL LAMINATED DENIM FABRIC DESIGN

**Eyüphan YENER[1], Sevil TÜRKÇEN[1], Saliha Büşra AVŞAR[1], Oğuzhan USLU[1]**

[1]Bursalı Tekstil San. ve Tic. A.Ş.

Corresponding author: eyuphan.yener@bursalitekstil.com

***Abstract:*** *It is aimed to develop a breathable fabric with high strength resistance, which provides thermal comfort with towel lamination denim fabric which will be run by our R & D center. The fabric to be developed will be subjected to a lamination process to form a thermal layer. In practice, the denim fabric will be laminated with a special application towel using a PU (polyurethane) based adhesive. Thus a denim thermal layer will come into play in the fabric. Towel lamination denim fabric is pre-plated for use in cold geography and has a serious market potential. As a result of the work to be done, thanks to the obtained fabric will not need to use an extra type of thermal jacket. With the project to be realized, it is aimed to design and develop a thermal layered denim fabric by applying a different process to the towel fabric for the first time. With the lamination to be applied, it is possible to obtain textile surfaces that are superior to the existing technical textiles and can be used in everyday life with thinner, lighter and more comfortable.*

***Key Words****: lamination towel, applications based on polyurethane, denim fabric, heat-proofing, technical textiles.*

## 1. INTRODUCTION

The importance of technical textiles is increasing day by day in today's textile industry. Technical textile is an expensive high value added product group which has durability to chemicals, weather conditions, microorganisms also it has superior performance and functional characteristics. The scope of the project is to design and develop breathable and high strenght products to provide thermal comfort for cold regions. In the first step, application of the towel fabric to denim cloth will be realized with the HOT MELT METHOD of polyurethane based adhesive material. A single layer structure will be obtained on this count. As a gain of this lamination application, the textile surface will obtain lightweighted and comfortable, thinner, superior of the existing technical textile and suitable for daily usage.

## 2. MATERIAL AND METHOD

Our project will emerge as a result of material denim and towels will occur in a different application model in the industry. Designed for use in cold climatic

conditions towel laminated denim fabric do not sweat, with warm, breathable and thus provided a structure to minimize heat loss reduction will be created. According to other air permeability adhesive substance with a high and low amounts of polyurethane based adhesive material due to their use will be used. Denim fabric material obtained in air permeability values, towels can be caught in the laminated denim fabric spot lamination applications will be done. Towels and jeans fabric structures considering the most appropriate method of laminating a hot solution method has been decided.

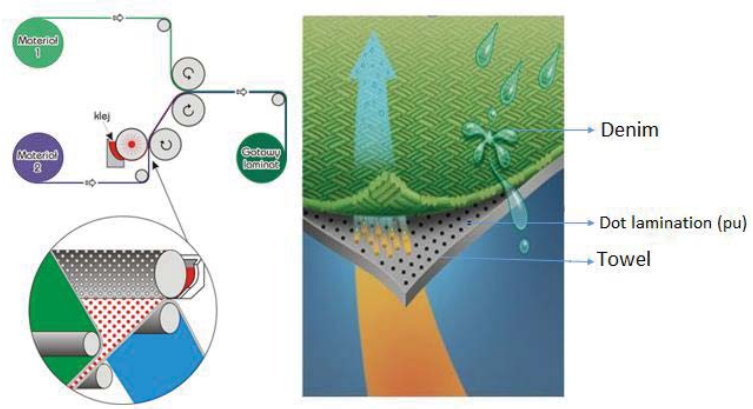


**Figure 1.** Hot Melt Method

The characteristics of the machine we laminate are given in Table 1:

**Table 1.** Capacity Specifications

| | |
|---|---|
| **Model** | Taytex Hotmelt Mach,ne |
| **Maximum Product Width** | 1700 mm |
| **machine cylinder length** | 1800 mm |
| **Cylinder Pore Bonding Ratio** | 25 g |
| **machine speed** | 10-60 m/min |
| **Power** | 55.0 KW |
| **Dimensions** | 11800 x 2900 x 3600 mm |

✓ The adhesive is transferred equally to the material surface with the patterned (point) cylinder. For this reason, laminating materials, soft waterproof and breathable products will be obtained.

✓ Hot Melt Adhesive; are in the form of a thermoplastic adhesive which is pushed into rigid cylindrical rods of various diameters. Thanks to these rods, the electric hot glue is heated in the gun and the adhesive is melted. The plastic is used with a continuous melting heating system which either pushes the adhesive

into the gun or a mechanical trigger is used. It is transferred to the adhesive fabric by point transfer technology.

✓ During the lamination process; blood pressure control, edge alignment adjustments are possible.

✓ After the lamination process is finished, the fabric adhered to each other is wrapped and left to stand for 24 hours.

✓ The high temperature resistant teflon coating on the drying cylinder surface, the contamination of the cylinder adhesive is prevented and the quality of the lamination process is increased.

**Table 2.** Construction characteristics of the ground (denim) fabrics

| Specification | Denim 1 | Denim 2 |
|---|---|---|
| **Raw Material** | 98% COTTON - 2% Elastane | 100% COTTON |
| **Warp** | Az Bükülmüş Karde | Az Bükülmüş Karde |
| **Weft** | Core Spun Yarn | Carded |
| **Pattern Design** | 3/1 Z Dimity | 3/1 Z Dimity |
| **Dye** | İndigo | İndigo |
| **Colour** | Pure/ İndigo-2 | Pure / İndigo-2 |
| **Weight/ASTM D 3776-09** | 407 g/m² | 407 g/m² |
| **Vehicle Width /ASTM D 3774-96** | 153 cm | 169 cm |
| **Warp /cm / ASTM D 3775-08** | 30 | 27 |
| **Weft /cm / ASTM D 3775-08** | 20,5 | 20 |
| **Dimensional Stability After Washing / Warp** | %-1,5 | %-1,5 |
| **Dimensional Stability After Washing / Weft** | %-14 | %-1 |
| **Elasticity** | %30 | %0 |

The construction characteristics of the ground (denim) fabrics subjected to the lamination process are given in Table 2.

The construction properties of the laminated towel fabrics are given in Table 3.

**Table 3.** Construction characteristics of the laminated towel fabrics

| Specification | Towel 1 | Towel 2 |
|---|---|---|
| **Ground Yarn** | Nm 20/2 Ring | Nm 20/2 Ring |
| **Weft Yarn** | Nm 16/1 | Nm 16/1 |
| **Pile Yarn** | Nm 16/1 Ring | Nm 20/1 Ring |
| **Product** | Boucle Towel | Velvet Towel |
| **Weight g/m²** | 340 | 330 |
| **Floor Density** | 11 warp/cm | 11 warp/cm |
| **Weft density** | 17,93 weft/cm | 22,76 weft/cm |
| **Pile Density** | 11 warp/cm | 11 warp/cm |
| **Pile Length** | 6,967 | 8,3 |
| **Colour** | Blue | Salmon |

## 3. RESULTS

In the light of the work done, the useful technical value and the resistance of the technical textile samples are improved by avoiding the performance of the existing technical textile samples. The results of the first experiments are described in the graphs below and studies to improve the functional properties of the product continue.

**Figure 2.** Thermal layer denim fabric

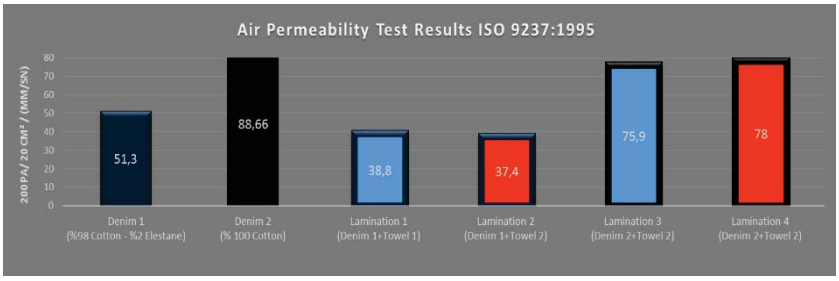


**Figure 3.** Air permeability test results

Ten repeat measurements were made for each sample. According to the data obtained in the structure of two different denim air permeability values, this denim fabric laminated structure consisting in close results have been achieved.

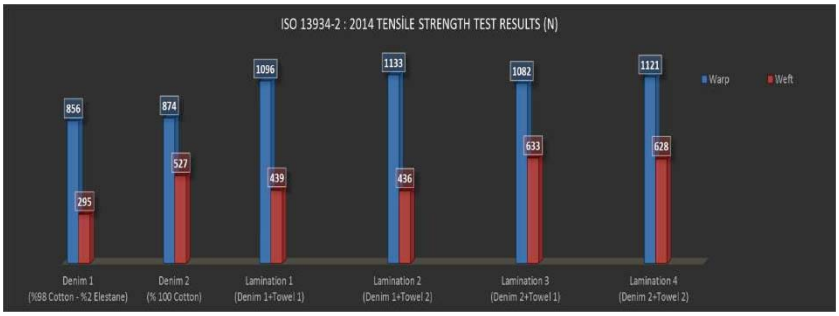


**Figure 4.** Tensile strength test results

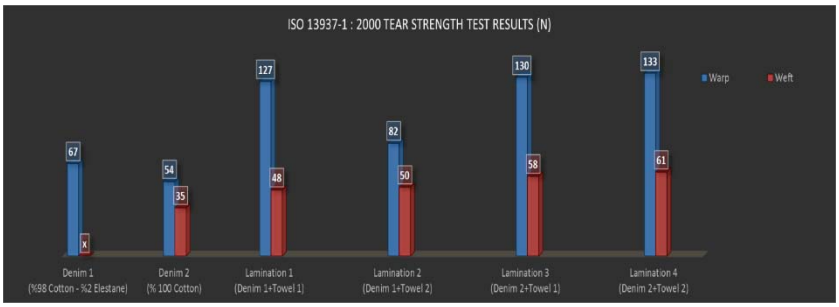


**Figure 5.** Tear strength test results

The tear and tensile strength tests were repeated 3 times. The tearing and breaking values in the weft and warp direction of the lamination structures composed of three different constructions were examined and the results were close to the desired values.

## 4. CONCLUSIONS

Towels can be used in cold laminated denim fabric is at the forefront of its geography, has the potential to have a serious market. As a result of the studies is obtained thanks to an extra thermal underwear fabric type you need to use a garment will not be heard. Applied to lamination method with will gain features, superior of the existing technical textile, thinner, lightweight and can be used in everyday life has been getting comfortable textile surfaces. These works, breaking the first mukavemetii tear strength and air permeability is the targeted level. Will continue its efforts to develop the structure of the fabric.

## REFERENCES

1. Marmarali A., Kretzschmar S., Özdil N., Oğlakcioğlu N., Affecting Thermal Comfort Parameters İn Clothes. 2006. Tekstil Ve Konfeksiyon.
2. Kadem F., Ergen A., Different Membrane Laminated Fabrics A Study On Comfort Properties. 2015. Teskon / Isil Konfor Sempozyumu.
3. Arsoy R., Üçgül İ., The Theory of Textile Materials Pasted. 2015. Sdu Technical Sciences Journal V. 5, 1-18.
4. Bulut Y., Sülar V., Coating or Lamination Techniques With General Properties Of Fabrics Produced. 2015. The Journal of Textiles And Engineer.

# INVESTIGATION OF THE PERFORMANCE CHARACTERISTICS OF OUTDOOR WORKERS CLOTHES

**Burcu USLU[1], Şeyma ÇAKMAK[1], Merih SARIIŞIK[1], Gülşah Ekin KARTAL[1]**

[1]Dokuz Eylül University, Department of Textile Engineering, Turkey

Corresponding author: gulsah.kartal@deu.edu.tr

***Abstract:*** *The working clothes are very important issue for the outdoor workers due to the severe working conditions. Workers spend at least eight hours in a day in the same clothes. Therefore, the worker clothes have to be comfortable, easy to use and suitable for the body features to be protective of the health and safety of workers. In this study, structural analysis of the some kind of workers' clothes was conducted, usage properties were examined and a survey which is workers' thoughts about these work clothes was analyzed. In this study, workwear which is used by workers in different sectors, were analyzed and colour and usage properties of workers' clothing were investigated.*

***Key Words****: Worker clothes, performance properties, structural analysis, survey*

## 1. INTRODUCTION

Work clothes prevents human according to the risk of exposure to adverse environmental conditions or reduce this risk. The worker clothes have to be comfortable, easy to use and suitable for the body features to be protective of the health and safety of workers. Exactly the clothes wear over the human is in constant contact with person and these clothes have a direct effect on the human psychology. So it needs to be designed depending on an accurate anthropometric measurement. In addition, work clothes have to protect the health of the workers and should not reduce the person's comfort and work performance [1, 3-5].

According to the place and working area, the work wear offer comfort and it should be considered at the design stage. Fabric which carries the features required for the respective lines of works, clothing appearance and clothing comfort are the criteria that should be in work clothes. The raw materials used in production of work clothes must have high quality. The result of the investigations clothes which wear in the sector, usually cotton and cotton / polyester fabrics are being used.

Nowadays, work conditions are very heavy, so clothes which workers wear while working have great importance. Workers wear the same clothes at least 8 hours in one day. In this reason, it is necessary that these clothes either protect workers health and safety or comfort, and suitable for body motions. Especially, it has great importance that work clothes don't prevent the body motions. If they limit

body motions, this situation will either disturb workers or influence work speed, unit time, and productivity [1-8].

In this study, colour and usage properties of worker clothes were examined. For this purpose, different work clothes were chosen and fastness analyzes, UV aging and color strength values were analyzed. On the other hand, survey studies were carried out on the 50 employees who work related to the work clothes and contentment levels related to the existing clothes were determined.

## 2. MATERIAL AND METHOD

### 2.1. Materials

Six different types of outdoor worker groups have been supplied work clothes and analyzes were performed. The worker clothes were shown in Figure 1. Commercial detergent was used for washing process. Histidine monohydrochloride monohydrate ($C_6H_9O_2N_3$ 2HCI $H_2O$), sodyum klorit (NaOH), sodyum di-hidrojen phosphatedihydrate ($NaH_2PO_4.2H_2O$), disodyum hidrojen orthophosphatedihydrate ($Na_2HPO_4.2H_2O$), were supplied by Merck for fastness analysis.


**Figure 1.** Work clothes, a: Gardener's Work Suit, b: Municipal Worker's T-Shirt, c: Outerwear of Workers, d: Municipal Worker Trousers, e: Electrician's Trousers, f: Construction Worker Vest

## 2.2. Methods

A variety of tests and methods to examine and evaluate the properties of the clothing fabrics were applied. The fastness to washing, fastness to perspiration, fastness to light, fastness to rubbing, UV aging, dimension change and water repellency analysis were done according to the standards which are TS EN ISO 105-C06, TS EN ISO 105-E04, TS 1008 EN ISO 105-B02, TS EN ISO 105 X12, ASTM G 154 UVB-313, TS EN ISO 50-77, TS EN ISO 4920, respectively. On the other hand, each sample were washed 10 times, separately at 30°C, 65 min in domestic type washing machines with commercial detergent and color strength values were evaluated with Minolta CM 3600D spectrophotometer.

## 3. RESULTS AND DISCUSSION

Within the scope of this study, the results of the questionnaires on workers and workers' clothes were evaluated. 50 people were administered a survey to assess their work clothes which about performance characteristics of the garments used by outdoor workers. Some questions like "Are you satisfied with your work clothes from the viewpoint of health and safety? Do you wear sweaty work clothes? Do you wear the same work clothes all the seasons? How long does your workplace give you new clothes? During the washing do color changes come to fruition, do you want your work clothes to be improved? “were asked on survey. The charts for some of the questions are below (Figure 2). The colors in the charts represent the following answers: “Blue: Yes, Red: No and Green: Often”.

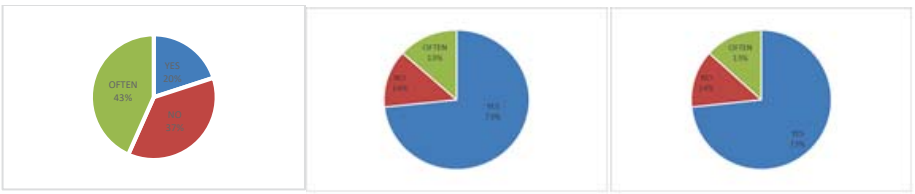


a b c

**Figure 2.** Charts of some survey questions a: “Are you satisfied with your work clothes from the viewpoint of health and safety?”, b: “Do you wear sweaty work clothes?”, c: “Do you wear the same work clothes all the seasons?”

As a result of the survey, workers have come to the conclusion that they are not sufficiently satisfied with their work clothes. It is desirable that work clothes have to be healthier and more comfortable. It is also requested that workplaces provide workwear more often. It has been determined that there is a problem of quick pollution and perspiration in working clothes. So all participants in the survey wanted to improve their work clothes.

In the light of the survey results, some of the workers' clothes used in the sector were analyzed.

The raw materials of the fabrics and their ratios were evaluated with optic microscope and quantitative analysis. The following data on analysis results which are, construction worker vest and outerwear of workers are polyester, municipal worker's t-shirt and municipal worker trousers are cotton, gardener's work suit and electrician's trousers are cotton/polyester blend were obtained. The cotton / polyester blending ratios have been determined as 35/65% according to quantitative analysis.

Fastness and color measurement results after UV aging analyses which are carried out in this study, are indicated in Table 1 and Table 2.

**Table 1.** Fastness Results of Work Clothes

| Sample | Fastness to Light | Fastness to Rubbing | | Fastness to Washing | | | | | | Fastness to Perspiration | | | | | | | | | | | |
|---|---|---|---|---|---|---|---|---|---|---|---|---|---|---|---|---|---|---|---|---|---|
| | | Dry | Wet | | | | | | | Alkali | | | | | | Acid | | | | | |
| | | | | CA | CO | PET | PA | PAC | Wool | CA | CO | PET | PA | PAC | Wool | CA | CO | PET | PA | PAC | Wool |
| Gardener's Work Suit, | 2/3 | 5 | 2 | 4/5 | 4 | 4 | 3/4 | 4/ 5 | 4/5 | 2/3 | 1/2 | 2/3 | 3 | 2/3 | 2/3 | 3 | 1 | 2 | 1/2 | 2 | 2 |
| Municipal Worker's T-Shirt | 4 | 5 | 3 | 4 | 3 | 4/5 | 4/5 | 5 | 4/5 | 3/4 | 3/4 | 3/4 | 3 | 4 | 3 | 4 | 4 | 3 | 3/4 | 4 | 3 |
| Outerwear of Workers | 4 | 5 | 4/5 | 4/5 | 4/5 | 4/5 | 4/5 | 4/5 | 4/5 | 4 | 4 | 3/4 | 3/4 | 3/4 | 3 | 4 | 4/5 | 4 | 3/4 | 4 | 4 |
| Municipal Worker Trousers | 3 | 4 | 1/2 | 4 | 3 | 3/4 | 3 | 4 | 4 | 3/4 | 2/3 | 3/4 | 3 | 4 | 3/4 | 3/4 | 2/3 | 3/4 | 3 | 3/4 | 3 |
| Electrician's Trousers | 6 | 4/5 | 4 | 4/5 | 4 | 4 | 3 | 4/5 | 4 | 1/2 | 1/2 | 2/3 | 1/2 | 2/3 | 3 | 2 | 2 | 3 | 1/2 | 3 | 2/3 |
| Construction Worker Vest | 3 | 5 | 4/5 | 4/5 | 4/5 | 4/5 | 4 | 4/5 | 4/5 | 4 | 4 | 4 | 3/4 | 4 | 3/4 | 4 | 3/4 | 3/4 | 3/4 | 3/4 | 3 |

According to the fastness analyses results, it is observed that the usage properties of worker clothes are not very suitable for the working areas. It was observed a decrease up 1 point in the fastness results after washing.

UV aging test results showed that, workwear fabrics have color differences when comparing the pre-treatment and this change was particularly observed in dark color workwear samples as expected.

Dimension change and water repellency analyses which are carried out in this study, are indicated in Table 3 and Table 4.

When the results on the table are evaluated, the largest dimension change were analyzed in municipal worker’s t-shirt. On the other hand, all values are within acceptable limits.

The water repellent feature for work clothes is a desirable feature for electrician's trousers, construction worker vest or outerwear of workers but it is not a desirable feature for t-shirts. According to the spray test analysis, water repellency of

outwear of workers and work clothes are better from the other clothes. On the other hand, t-shirt does not have the water repellent feature as expected.

**Table 2.** Color Measurement Results after UV Aging

| | UV Aging | L | a | b | C | H | ΔE |
|---|---|---|---|---|---|---|---|
| Construction Worker Vest (440 nm) | Untreated | 66,720 | -29.679 | 55.506 | 62.942 | 28.133 | 1.160 |
| | Treated | 93.721 | -36.232 | 92.142 | 99.010 | 21.466 | |
| Outerwear of Workers (610 nm) | Untreated | 59.617 | 1.055 | -1.304 | 1.678 | 308.980 | 1.780 |
| | Treated | 59.464 | 1.021 | -1.388 | 1.723 | 306.338 | |
| Electrician's Trousers (600 nm) | Untreated | 25.572 | 7.835 | -33.952 | 34.844 | 282.995 | 0.469 |
| | Treated | 23.148 | 7.585 | -33.975 | 34.811 | 282.584 | |
| Municipal Worker's T-Shirt (670 nm) | Untreated | 51.918 | -29.108 | -26.544 | 39.394 | 222.362 | 5.741 |
| | Treated | 55.942 | -31.049 | -28.532 | 42.168 | 222.561 | |
| Gardener's Work Suit (590 nm) | Untreated | 15.931 | 0.974 | -9.282 | 9.333 | 275.989 | 0.635 |
| | Treated | 15.333 | 1.049 | -9.083 | 9.143 | 276.565 | |
| Municipal Worker Trousers (590 nm) | Untreated | 14.163 | 0.826 | -6.767 | 6.818 | 276.958 | 1.855 |
| | Treated | 15.950 | 0.948 | -6.317 | 6.388 | 278.538 | |

**Table 3.** Dimension Change Results of Work Clothes

| | In the direction of weft Dimension Change | In the direction of warp Dimension Change |
|---|---|---|
| **Construction Worker Vest** | 0 % | 0 % |
| **Outerwear of Workers** | 0 % | 0 % |
| **Electrician's Trousers** | -2 % | -2 % |
| **Municipal Worker's T-Shirt** | -3,2 % | %1 |
| **Work clothes** | -2 % | -2 % |
| **Municipal Worker Trousers** | -1,6 % | 0 % |

**Tablo 4.** Water Repellency Test Results

| | AATCC |
|---|---|
| **Construction Worker Vest** | ISO 0 |
| **Outerwear of Workers** | ISO 3 |
| **Electrician's Trousers** | ISO 0 |
| **Municipal Worker's T-Shirt** | ISO 0 |
| **Work clothes** | ISO 2 |
| **Municipal Worker Trousers** | ISO 0 |

## 4. CONCLUSIONS

Work clothes should be designed according to workplace, work environment and made in accordance with the act in the intense pace of working life. Considering that used for at least 8 hours a day of work clothing, properties of worker clothes have a major importance.

In our study, structural and usage properties of worker clothes were examined. According to the fastness analyses and survey about the clothes showed that, work clothes is required to be healthier and more comfortable. On the other hand, in usage time contamination and perspiration problems were obtained in worker clothes. According to analysis and implementation of the survey results it concluded that the work clothes should be developed considering the requests of workers.

## REFERENCES

1. Acar H.,Topalak Ö. , Eroğlu H. (2002), Ormancılığımızda Kullanılması Gereken Koruyucu Elbise ve Ekipmanların Uluslararası Çalışma Örgütü(ILO) Standartlar Açısından Değerlendirilmesi, SDU Faculty of Forestry Journal, A(1),121-133.
2. Çivitçi Ş., Dengin S., (2014). Koşu Giysileri Konforunun Kullanıcılar Tarafından Değerlendirilmesi Üzerine Bir Araştırma, International Journal of Science Culture and Sport, 16(1), 553-569.
3. Konsoy O., Dirgar E., Kirtay E. (2008). Sanayide Çalışanlar İçin Uygun İş Kıyafetlerinin Geliştirilmesi, Journal of Textile and Apparel, 18(4), 306-309.
4. Marmarali A., Özdil N., Kretzschmar S., Oğlakcioğlu G. (2006). Giysilerde Isıl Konforu Etkileyen Parametreler, Journal of Textile and Apparel, 16(4) ,241-246
5. Okur A., Öner E., (2010). Materyal, Üretim Teknolojisi ve Kumaş Yapısının Termal Konfora Etkileri, Journal of Textiles and Engineer, 17(80), 20.
6. Uludağ K., (2010). Kadın Posta Dağıtıcıların Yazlık Üniformalarına İlişkin Memnuniyet Durumlarının İncelenmesi ve Bir Örnek Tasarım, Master's Thesis, Gazi University Institute of Educational Sciences.
7. Yoo S., Barker R. (2005), Comfort Properties of Heat-Resistant Protective Workwear in Varying Conditions of Physical Activity and Environment. Part I: Thermophysical and Sensorial Properties of Fabrics, Comfort Response to Garments and its Relationship to Fabric Properties, Textile Res. J, 75(7), 523-530.
8. Yoo S. , Barker R.(2005), Comfort Properties of Heat Resistant Protective Workwear in Varying Conditions of Physical Activity and Environment. Part II: Perceived Comfort Response to Garments and its Relationship to Fabric Properties, Textile Res. J, 75(7), 531-539

# KINETIC MODELING ON ROSEMARY ESSENTIAL OIL RELEASE FROM BEESWAX MATRIX

**Angela DANILA[1], Emil Ioan MURESAN[2], Cezar Doru RADU[1], Augustin MURESAN[1], Alina POPESCU[3], Laura CHIRILA[3], Lenuta Irina COSTAN[1]**

[1] Gheorghe Asachi Technical University of Iasi, Department of Chemical Engineering in Textiles and Leather, Romania
[2] Gheorghe Asachi Technical University of Iasi, Department of Environmental Engineering and Management, Romania
[3] The National Research-Development Institute for Textiles and Leather Research

Corresponding author: rcezar2010@yahoo.com

***Abstract:*** *The aim of the present study was to design the controlled release of rosemary essential oil from beeswax matrix by emulsion method. Essential oil was entrapped into biodegradable beeswax matrix which were prepared at different essential oil/beeswax ratios 2:1, 1:1, 2.6:1 and 1:2.25 using gelatin and Tween 80 as emulsifying agents. The effect of amount of core and shell materials were studied on in vitro essential oil release at pH 5-6 for 4 h. The in vitro essential oil release data of beeswax formulations was fitted to various mathematical models (zero-order, first-order, Higuchi, Korsmeyer–Peppas and Hixon and Crowell models).*

***Key Words****: rosemary essential oil, controlled release, beeswax*

## 1. INTRODUCTION

At present, the application of aromatherapy in textiles is commonly concentrated on skin care benefits and stress management. When different active substances for body care or health are loaded/embedded into textiles, they are then later releasing them systematically (that means they interact with the body) being gradually transferred to the skin by natural movement, pressure or the effect of the skin's natural warmth and enzymes. Transdermal drug delivery is a form of medicinal administration wherein active ingredients are delivered across the skin for systemic distribution, such us transdermal patches. Many chemical compounds extracted from natural sources (vegetable or animal origin) show potential as skin penetrating agents [1].

In the last years essential oils have gained their importance in therapeutic, cosmetic, aromatic and fragrant fields. Essential oils are colorless pleasant smelling liquids that consist from saturated and unsaturated hydrocarbons, alcohol, aldehydes, esters, ethers, ketones, oxides phenols and terpenes [2].

In this study rosemary essential oil (*Rosmarinus officinalis L*.) was used as the active compound. It is known for its effects such as antioxidant, antibacterial and antifungal effect [3]. The challenge for using essential oils in textile field is to

captures the fragrance in its original form with minimal change and protects the fragrance from interaction with environment and from premature release during storage [4].

Many studies have demonstrated the ways to protect active compounds from adverse environmental conditions by entrapping them into a carrier [5].

Waxes have been used extensively as carriers for various types of active compounds in pharmaceutical applications [6].

Beeswax is a complex mixture of hydrocarbons (12%–16%), free fatty acids (12%–14%), esters of fatty acids and fatty alcohol (15%–27%), diesters and exogenous substances [7].

To better exploit the properties of the rosemary essential oil applied to textile materials this study presents the obtaining beeswax/rosemary essential oil system and kinetic modeling on essential oil release from beeswax matrix.

## 2. MATERIAL AND METHOD

### 2.1. Materials

Beeswax was used as shell material for entrapping the rosemary essential oil in the core and was purchased from a private apiary in the Northeast region of Romania. Rosemary essential oil (extract of Rosmarinus officinalis) was purchased from Fares SA Romania. Tween 80 was supplied by Merck - Germany. 99.5 % pure vegetable glycerine was purchased from SC Elemental SRL, Romania. Scoured and bleached 100 % cotton knitted fabrics were used in the experiments.

**Table 1.** The main compounds of rosemary essential oil

| **Chemical Families** | **Compounds** | **%** |
|---|---|---|
| Monoterpenoids | α-pinene | 12 |
| | β-pinene, Camphene | 22 |
| | Myrcene | 1.5 |
| | α - phellandrene<br>β - phellandrene<br>limonene | 0.5-2 |
| | γ -terpinene<br>p-Cymene | 2 |
| Sesquiterpenoids | β-caryophyllene | 3 |
| Monoterpenols | linalool | 0.5-1 |
| | Terpinen-4-ol<br>α -terpineol | 1.5 |
| | borneol | 3-5 |
| Terpenic acids | 1,8-cineole<br>Caryophyllene oxide<br>Humulene epoxide I and II | 30 |
| Monoterpenoids | Camphor | 30 |
| | Verbenone<br>carvone | 0,4 |

## 2.2 Emulsion preparation

To remove impurities, the beeswax has been cleaned and subjected to a conditioning process. Clarification and washing were done by repeatedly melting the beeswax chips in softened water at a temperature of 90°C. Finally, the purified beeswax was poured and allowed to solidify in a crystallizer.

Beeswax/rosemary essential oil system was prepared by emulsion method. The beeswax was melted at 63 °C and a 600 rpm speed over which distilled water was added at 63°C. The Tween 80 emulsifier was added to the wax / water system. The system was kept under stirring for 10 minutes at 63°C, after which vegetable glycerol was added. After complete homogenization, the system was cooled to 40°C, over which the rosemary essential oil was added dropwise.

**Table 2.** Treatment variants

| Treatment variant codes | Essential oil, % (w/v) | Beeswax, % (w/v) | Tween 80*, % (w/v) | Glycerine, %(w/v) | Water %(w/v) |
|---|---|---|---|---|---|
| $V_1$ | 4.2 | 2.1 | 20 | 10 | 63.7 |
| $V_2$ | 4.2 | 4.2 | 20 | 10 | 61.6 |
| $V_3$ | 7.2 | 2.7 | 20 | 10 | 60.1 |
| $V_4$ | 1.2 | 2.7 | 20 | 10 | 66.1 |
| $V_5$ | 1.2 | 0.6 | 20 | 10 | 68.2 |

*An initial solution of 30% Tween 80 was used in experiment

## 2.3. Coating of knitted fabrics with emulsion

Cotton knitted fabrics (1g) were padded twice with prepared emulsions ($V_1$-$V_5$) to a wet pick-up of 100%. The padded fabrics were dried at $57^0$C for 30 minutes.

## 2.4. *In-vitro* release study

Samples of cotton fabric, treated with prepared emulsions, were introduced into a well-known volume of phosphate buffer solution and were maintained under stirring (100rpm) at 32˚C.

Aliquots of 5 mL were withdrawn from the release medium at each hour (1-4h) and replaced with equivalent amount of buffer solution. The amount of rosemary essential oil release was determined spectrophotometrically on a UV-VIS Camspec M 501 Single beam Scanning spectrophotometer and calculated using the calibration curve.

## 2.5. Release kinetics

Skin is a very effective barrier that limits the penetration of molecules into the body [8]. However, essential oils having a molecular weight less than 800 amu can penetrate this barrier.

In order to predict the kinetics of the rosemary essential oil release from the beeswax formulations, various mathematical models were used:

Zero-order (data obtained from in vitro drug release studies were plotted as cumulative amount of essential oil released versus time), first-order (data were plotted as log cumulative amount of essential oil remaining versus time), Higuchi (the data obtained were plotted as cumulative amount of essential oil release versus square root of time), Korsmeyer–Peppas (the data were plotted as log cumulative amount of essential oil release versus log time) and Hixon and Crowell (data obtained from in vitro drug release studies were plotted as cube root of drug amount remaining in matrix versus time) [9,10].

In order to determine which of these kinetic models is optimal and to quantify the more appropriate it is, one used Akaike criterion (AIC) that combines probability theory, information theory and concept of information entropy.

Akaike criterion is defined by the equation below:

$$AIC = n \cdot \ln WSS + 2p \tag{1}$$

where:

- n is the number of experimental points;
- p is the number of parameters;
- WSS is the sum of squared distances from experimental points to curve, measured vertically.

## 3. RESULT AND DISCUSSION

The effects of beeswax/essential oil concentrations on the release profile were evaluated with the aid of MS Excel by fitting the cumulative mathematical model distribution function to the release results employing the linearized form [11].

The amount of rosemary essential oil released at different preset periods of time (1-4h) was calculated by means of equation given by standard curve (y = 0.5094x; where x is the concentration of biologically active compound solution and y is the absorbance obtained from UV spectral analyses).

Kinetic profiles for controlled release of rosemary essential oil according to Higuchi model is shown in Figure 1.

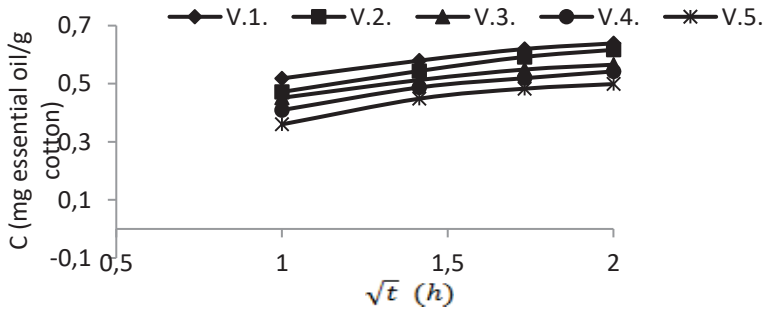


**Figure 1.** Kinetic profiles for controlled release according to Higuchi model

Kinetic profiles for controlled release of rosemary essential oil according to the 0 order model is shown in Figure 2.

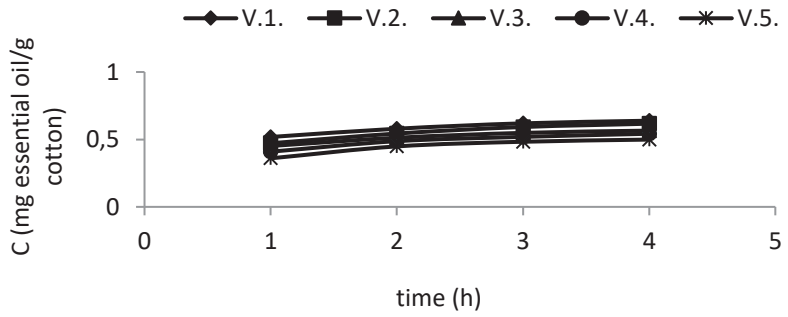


**Figure 2.** Kinetic profiles for controlled release according to the zero order model

Kinetic profiles for controlled release of rosemary essential oil according to the first order model is shown in Figure 3.

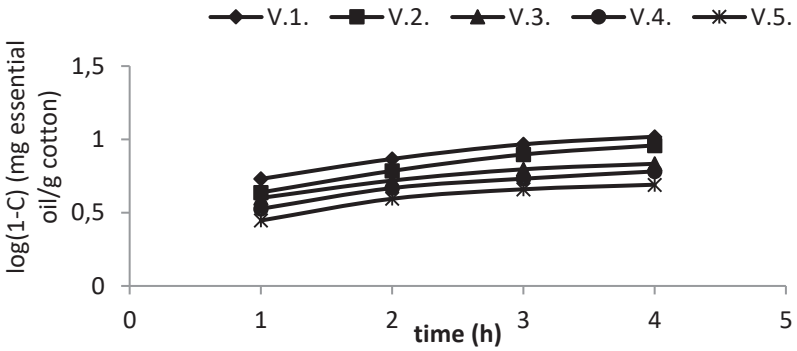


**Figure 3.** Kinetic profiles for controlled release according to the first order model

Kinetic profiles for controlled release of rosemary essential oil according to Hixson–Crowell model is shown in Figure 4.

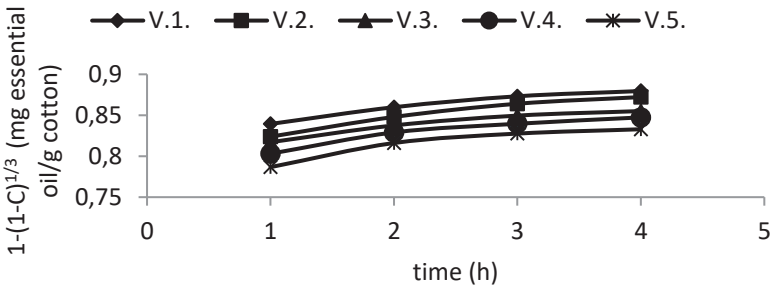


**Figure 4.** Kinetic profiles for controlled release according to Hixson–Crowell model

Criteria for choosing the most appropriate model was based on best goodness of fit, coefficient of determination ($r^2$) and Akaike Information Criteria (AIC). The release rate constant (k values) as well as $r^2$ obtained from the curve fitting were summarized in Table 3.

**Table 3.** Parameters obtained from each model for the different concentrations of beeswax

| Treatment variant codes | Higuchi Model | | The zero order model | | The first Order model | | Hixson–Crowell model | |
|---|---|---|---|---|---|---|---|---|
| | $r^2$ | $k_H$ | $r^2$ | $k_o$ | $r^2$ | $k_1$ | $r^2$ | $k_{HC}$ |
| $V_1$ | 0.9826 | 0.1226 | 0.9481 | 0.0402 | 0.9632 | 0.0419 | 0.9481 | 0.0134 |
| $V_2$ | 0.9857 | 0.1474 | 0.9536 | 0.0483 | 0.9695 | 0.0467 | 0.9536 | 0.0161 |
| $V_3$ | 0.9747 | 0.1158 | 0.9347 | 0.0378 | 0.9485 | 0.0370 | 0.9347 | 0.0126 |
| $V_4$ | 0.9640 | 0.1322 | 0.9192 | 0.0430 | 0.9372 | 0.0360 | 0.9192 | 0.0143 |
| $V_5$ | 0.9612 | 0.1211 | 0.8808 | 0.0430 | 0.8991 | 0.0346 | 0.8808 | 0.0150 |

Akaike values were calculated for each experimental data using the sum of square deviations of experimental data from the data calculated according to matematical models, also called the sum of errors (WSS). Treatment variant that has the lowest value for AIC criterion is the best variant.

**Table 4.** The WSS values for each model

| Treatment variant codes | Higuchi model | zero order model | first order model | Hixson–Crowell model |
|---|---|---|---|---|
| $V_1$ | 0.309704 | 0.409979 | 0.382031 | 1.676072 |
| $V_2$ | 0.322389 | 1.143510 | 0.383950 | 1.617359 |
| $V_3$ | 0.332350 | 0.422297 | 0.374745 | 1.554701 |
| $V_4$ | 0.366513 | 0.461409 | 0.394173 | 1.490629 |
| $V_5$ | 0.434733 | 0.796398 | 0.449340 | 1.378340 |

From the above tables results that Higuchi model best represent the data that describe the controlled release of rosemary essential oil from beeswax matrix. Regression coefficient $R^2$ were found to be 0.9826, 0.9857, 0.9747, 0.964 and

0.9612 respectively. The results agreed with the studies previously reported [12]. It can be observed that the k values increased with the decreasing amount of rosemary essential oil in the matrix formulations. The incorporation of hydrophobic essential oil can decrease the drug release from hydrophobic matrix. All treatment variantes have the lowest value for AIC criterion for Higuchi model, that also confirm that Higuchi model best represents the release experimental data.

**Table 5.** The Akaike values for each kinetic model

| Treatment variant codes | Akaike values | | | | Optimum model |
|---|---|---|---|---|---|
| | Higuchi model | Zero order model | First Order model | Hixson–Crowell model | |
| $V_1$ | -2.68855 | -1.5666 | -1.84902 | 4.065811 | Higuchi model |
| $V_2$ | -2.52798 | 2.536408 | -1.82898 | 3.923179 | Higuchi model |
| $V_3$ | -2.40626 | -1.44819 | -1.92604 | 3.765132 | Higuchi model |
| $V_4$ | -2.01489 | -1.09388 | -1.72386 | 3.596793 | Higuchi model |
| $V_5$ | -1.33208 | 1.089376 | -1.1999 | 3.283519 | Higuchi model |

From the above tables results that Higuchi model best represent the data that describe the controlled release of rosemary essential oil from beeswax matrix. Regression coefficient $R^2$ were found to be 0.9826, 0.9857, 0.9747, 0.964 and 0.9612 respectively. The results agreed with the studies previously reported [12]. It can be observed that the k values increased with the decreasing amount of rosemary essential oil in the matrix formulations. The incorporation of hydrophobic essential oil can decrease the drug release from hydrophobic matrix. All treatment variantes have the lowest value for AIC criterion for Higuchi model, that also confirm that Higuchi model best represents the release experimental data.

## 4. CONCLUSION

Akaike Criterion allows to determine which kinetic model is more appropriate and quantify with how is more appropriate; combines probability theory, information theory and concept of information entropy. The kinetics of the drug release from wax matrix fit well with Higuchi's diffusion model. The results of this study could be helpful to give an idea for selecting suitable released-controlling agent in hydrophobic release formulation.

## ACKNOWLEDGMENTS

This work was supported by a grant of the Romanian National Authority for Scientific Research and Innovation, CCCDI – UEFISCDI, project number 29/2018 COFUND-MANUNET III-AromaTex, project title "Manufacturing of value-added textiles for aromatherapy and skin care benefits ", within PNCDI III.

## REFERENCES


1. Fox L.T., Gerber M., Du Plessis J., Hamman J.H.: Transdermal drug delivery enhancement by compounds of natural origin. 2011. Molecules, v. 16, 10507-10540.
2. Babar A., Naser A. A.-W., Saiba S., Aftab A., Shah A. K., Firoz Anwar: Essential oils used in aromatherapy: A systemic review. 2015. Asian Pac J Trop Biomed, v.5(8), 601–611.
3. Socaci S. A., Tofana M., Socaciu C., Varban D., Muste S.: Comparative study of different rosemary essential oil. 2007. Bulletin USAMV-CN, v. 63, 591-595.
4. Rossi W., Bonet-Aracil M., Bou-Belda E., Gisbert-Payá J., Wilson K. and Roldo L.: Characterization of orange oil microcapsules for application in textiles. 2017. 17th World Textile Conference AUTEX 2017- Textiles - Shaping the Future, 1-6.
5. Prasertmanakit S., Praphairaksit N., Chiangthong W., and Muangsin N.: Ethyl Cellulose Microcapsules for Protecting and Controlled Release of Folic Acid. 2009. AAPS PharmSciTech. v. 10, 1104-1112.
6. Milanovic J., Manojlovic V., Levic S., Rajic N., Nedovic V. and Bugarski B.: Microencapsulation of Flavors in Carnauba Wax. 2010. Sensors. v. 10, 901-912.
7. Fratini F., Cilia G., Turchi B., Felicioli A.: Beeswax: A minireview of its antimicrobial activity and its application in medicine. 2016. Asian Pacific Journal of Tropical Medicine, v. 9, 839–843.
8. Vîlceanu N., Popescu M.: Transdermal patches – allternative drug delivery systems for therapeutic areas of interest, 2015, v. 8 , 29-43.
9. Thakur G., Singh A., and Singh I.: Formulation and evaluation of transdermal composite films of chitosanmontmorillonite for the delivery of curcumin. 2016. Int J Pharm Investig, v. 6(1), 23–31.
10. Azadi S., Ashrafi H., Azadi A.: Mathematical modeling of drug release from swellable polymeric nanoparticles. 2017. Journal of Applied Pharmaceutical Science, v. 7 (04), 125-133.
11. Al-Zoubi N., Malamataris S.: Three-layer matrix tablets and simple approach of drug release programming. 2008. J. DRUG DEL. SCI. TECH, v. 18 (6), 431-437.
12. Charumanee S., Yotsawimonwat S., Wongpayapkul L., Piyamongkol S.: The roles of channeling agents on the drug release from wax matrix tablet prepared by melt granulation. 2016. Journal of Drug Delivery & Therapeutics, v. 6(3), 51-58.

# DEVELOPING OF SAILCLOTH TO BENEFIT FROM WINDS DEFINED AS LOW INTENSITY ON BEAUFORT SCALE WITH THE HIGHEST EFFICIENCY

**Şafak KARAGENÇ[1], Murat YILDIRIM[1]**

[1] Zorluteks

Corresponding author: safak.karagenc@zorlu.com

***Abstract:*** *In the development of sails sail clothes have a big importance. Present applications on sail clothes include techniques based on yarn, finishing and lamination. In this project a sail cloth has special construction can benefit from acting effect of winds even at low speed will be developed as a woven fabric. The surface of fabric which clutch the wind successfully will be designed inspiring by the tubercle structure of humpback whale fin. Wavy surface is the aim of design. In this way the frictional area increased and the wind gains a suitable precession. With this precession the suction effect of flow for movement increases. Herewith the minimum spacing on Beaufort Scale for the acting of sails can be reduced to 3.5-4 knots from 4-6 knots. The project aims to provide the basic properties of sailcloth such as UV resistance and sea water resistance using high tenacity polyester yarn as well.*

***Keywords:*** *wind flow, construction, humpback whale fin, sailcloth, Beaufort Scale*

## 1. INTRODUCTION

Sailcloth is the part of sail which convert the wind energy to kinetic energy. The main principal of motion of sails is explained with Bernoulli's rule. According to Bernoulli's rule low and high pressure sections occurs on the different surfaces of body under effect of fluid. The pressure difference creates a suction effect and due to this effect the sail starts to move. Tubercle structure increases the frictional area and makes the surface more available for precession. In different areas of industry such as energy and aeronautics used the same approach of biomimicry for designing of propellers and turbines considering humpback whale fin to use wind energy efficiently according same principal. Success of this fabric construction developed for sail clothes also can be measured getting reference the decreasing of minimum values on Beaufort Scale for the motion of sails.

## 2. MATERIAL AND METHOD

### 2.1. Fabric Design

High tenacity polyester is the raw material of developed fabric has the tenacity 8.80-9.00 grams for per denier. Weave type will be arranged to obtain the wavy structure of surface using different combinations of warp and weft positions. For

the structures have ability to reach the aimed results computational designs are prepared on EAT design software.

### 2.2. Main Properties of Fabric

Sailcloth is exposed many dynamical fluid effects during motion. In the other hand sea water effect is very important parameter as well. When we consider these situations several strengths and handle properties sorted as follows gain importance;

- Lightness
- Dimensional stability
- Bursting resistance
- Tear resistance
- Air permeability
- Coverage
- Waterproof
- UV Resistance
- Resistance to saltwater
- Handle

According to these parameters we will be produced fabric for sailcloth as plain weave. Appreciations of tests are controlling by below standards;

- TS EN ISO 105-E02 Resistance to saltwater
- AATCC TM 186 Aging resistance under effect of UV
- TS EN ISO 6330 Dimensional stability
- TS EN ISO 9237 Air permeability
- AATCC 22 Waterproof
- TS EN ISO 13937-4 Tear resistance
- TS EN ISO 13938-2 Bursting resistance

### 2.3. CFD Analysis

Structures obtained from EAT are simulated with fluid effects on Computational Fluid Dynamics Software to calculate the efficiencies of designs. In this method cage structures must be created for fabric geometries of each design. After this process the fluid effects simulated on surface with different angles and values.

### 2.4. Wind Tunnel Experiments

The samples obtained considering designs and analysis are tested in laboratories include wind tunnel embodiments. In this way CFD and experimental results can

be correlated. According to results of correlations analyses or designs can be renovated.

## 3. RESULT AND DISCUSSION

Fabric construction designed using parameters weaving method, high tenacity polyester yarn and wavy surface inspiring tubercle structure of humpback whale fin gives successful results in terms of acting sails in conditions also include low intensity of wind speed.

## 4. CONCLUSION

Owing to developed structural design of fabric minimum acting values of sails marked on Beaufort Scale could be decreased in proportion as 12 %. Through the high tenacity polyester yarn the basic performance properties have provided also tenacity and UV resistance could be increased in proportion as 10%.

## REFERENCES

1. Polat A., Kurban M. : Kambur Balina Yüzgecinden Esinlenerek Tasarlanan Rüzgar Türbin Kanatlarının Karşılaştırmalı Analizi. 2015. http://www.emo.org.tr/ekler/8b1d2b75b2a76d8_ek.pdf

2. Lasher W., Sonnenmeier J., Forsman D., Tomcho J. : The aerodynamics of symmetric spinnakers. 2005. The Pennsylvania State University at Erie, The Behrend College

3. Öksüz M. : Gemi seyir verileri kullanılarak güç marjininin belirlenmesi. 2008. İstanbul Teknik Üniversitesi Fen Bilimleri Enstitüsü

# THE USE OF COMMERCIAL PHOTOCHROMIC DYES IN PREVENTION OF COUNTERFEITING

**A. Merih SARIISIK[1], Özlem TOPBAS[2], Gökhan ERKAN[1], Orhun EK[3]**

[1] Dokuz Eylul University, Department of Textile Engineering, Turkey
[2] Dokuz Eylul University, The Graduate School of Natural and Applied Sciences, Turkey
[3] Soktas Weaving Industry Company

Corresponding author: merih.sariisik@deu.edu.tr

**Abstract:** In this sudy, three different colour commercial photochromic dyes (violet, blue and orange) which include microcapsules that are available on the market were applied to the 100% cotton fabric by printing method and 100% cotton yarn by conventional exhaust process. The scanning electron microscope (SEM) were utilized to characterize the structure, morphology, size and size distribution of commercial photochromic dyes. Then, the activities of commercial photochromic dyes on the fabric were analyzed by colour analysis under different light sources, washing and rubbing fastness tests. At the same time, in order to investigate the colour formation of the yarn which are carried out by a portable spectrophotometer. The main purpose of this study was to investigate the use of commercial photochromic dyes in preventing counterfeiting.

**Key Words**: Commercial photochromic dye, prevention of imitation, printing, yarn dyeing

## 1. INTRODUCTION

Chromic materials make available to together using facilities fashion technology and design with smart and controlled solutions, especially clothing industry, in textile. At this point, the researchers in textile as the other industry fields focus on the wide range of products. Recently, there has been some interest in developing photochromic smart textiles [1-3].

Photochromism is a reversible transformation of a chemical species included in one or both directions by absorption of electromagnetic radiation, between two states having observable light absorptions in different regions of spectrum:

$$A \text{ (colourless)} + h\nu_1 \rightarrow B \text{ (colourful)}$$

$$B \text{ (colourful)} + h\nu_2 \rightarrow A \text{ (colourless)}$$

Reversibility is the main criterion for photochromism [4-7].

The colours of photochromic dyes (colour changing dyes with UV or visible light), change with the changing in the colour intensity by reversing the change. And then they return to their original colours with the disappearance of the radiation. Usually they are colourless in the dark, but the molecular structure of the material changes when exposed to sunlight or UV radiation and the colour formation exhibited. When the light source is removed, the colour which exists is lost (Figure 1) [8]. Utilizing these features of photochromic materials, depending on fashion

trends in the textile industry as well as the prevention of imitation, also benefits from protectionism.

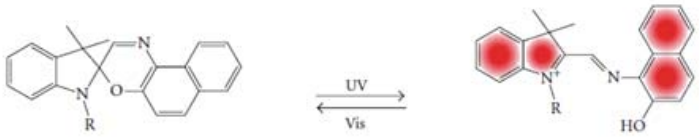


**Figure 1.** Schematic representation of photochromism mechanism

The aim of this study was to investigate the colour formation of commercial photochromic dyes which include microcapsules on the fabric and yarn. Then, the application of commercial photochromic dye was realized to fabric by printing methods and to yarn by conventional exhaust process. The activities of dyes on the fabric and yarn were analyzed by colour analysis under different light sources and rubbing fastness tests.

## 2. MATERIAL AND METHOD

### 2.1. Materials

The commercial photochromic dyes that include microcapsules were obtained from Nanorenk Incorporated Company, Turkey. Securon DC (complexing agent, Pulcra Chemical), Lava® Con LDA P (DyStar), Lava® Fast S (laundry auxiliary, DyStar) and Sera® Gal C-RFX (low-foaming special product for the dyeing of cotton, DyStar) were used in yarn dyeing process. All chemicals were used without any purification.

### 2.2. Application to Fabric and Yarn

In this study, photochromic microcapsules were applied to fabric by printing method. Firstly, the photochromic microcapsules (10 g) were added into a 100 mL beaker containing printing paste (90 g) which is consist of binder, thickener, antifoaming agent, fixer, ammonia, cross linker and water. After they were homogeneous mixed under stirring was continued for 5 min to make photochromic microcapsules and printing paste matrix mixed completely. Then, the photochromic printing paste was applied to 100% cotton fabric in the printing machine (Atac, Turkey) through pigment printing and dried naturally in the dark place. The properties of used fabric are shown in Table 1.

Also, these commercial photochromic dyes were implemented to 100% cotton yarn according to the conventional exhaust process. The yarns were pretreated as follows before process.

**Table 1.** Properties of Fabric

| Fabric Type | 100% Cotton | |
|---|---|---|
| **Weaving Type** | 1x1 Plain | |
| **Yarn Number (Ne)** | Warp | 60 |
| | Weft | 60 |
| **Weaving Frequency (wire/cm)** | Warp | 62 |
| | Weft | 42 |
| **Weight (g/m²)** | 107 | |

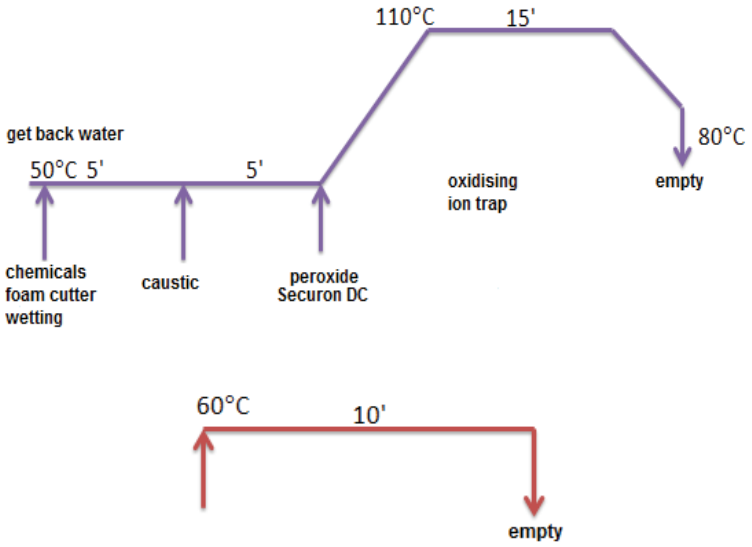


**Figure 2.** Preatment process

After pretreatment, dyeing was done according to conventional exhaust method.

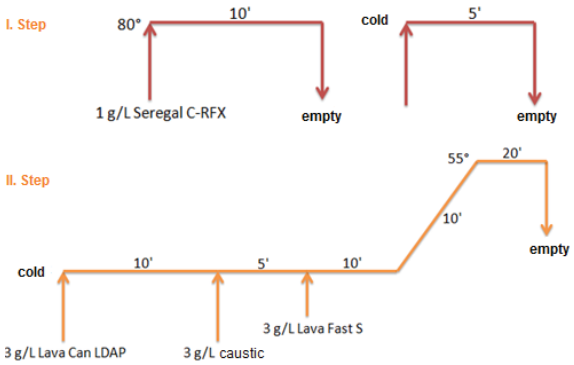


**Figure 3.** Dyeing conditions

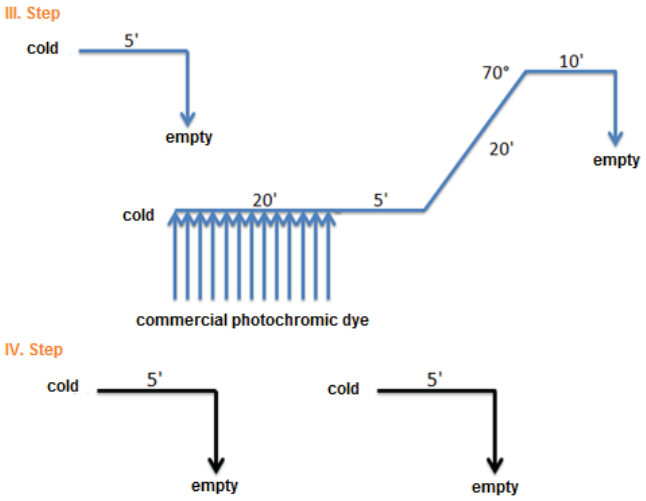


**Figure 3.** Dyeing conditions (continiued)

The properties of used yarn are shown in Table 2.

**Table 2.** Properties of Yarn

| Number of Yarn | 90/1 Ne |
|---|---|
| Elong (%) | 4,64 |
| RKM | 20,72 |
| % U | 11,63 |
| % Cvm | 14,66 |
| Hairness | 2,43 |

### 2.3. Colour Analysis

The discolouration of the fabrics was observed under different light sources in the light cabinet. At the same time, in order to investigate the colour formation of the fabric and yarn; colour measurements of these fabrics and yarns were carried out by a portable spectrophotometer (ColourLite Sph870, Germany) in a UV cabinet (UVP- UV2/PCR) under UV light exposure.

### 2.4. Laundering Test and Rubbing Fastness Analysis

To test laundering durability specimens were treated on a short time program in a Atlas Linitest or 30 min at 40˚C, in accordance with ISO 105-C06:2010 Textiles-Tests for colour fastness-Part C06: Colour fastness to domestic and commercial laundering (ISO 105-Textiles-Part C06:2010). At the end of the cycle samples were dried at room conditions. All samples were examined after 1 cycles. The value of the colour fastness of the sample with the value of colour fastness by straining of multifiber is determined by grey-scales.

At the same time, strength of specimens to rubbing were performed by using Atlas Crockmeter rubbing device, according to ISO 105-X16:2001 Textiles-Tests for colour fastness-Part X16: Colour fastness to rubbing-small areas (ISO 105-Textiles-Part X16:2001). It was measured according to the standard wet and dry rubbing fastness. Colour flows to rubbing pieces are evaluated with grey-scale.

## 3. RESULTS AND DISCUSSION

Typical photomicrographs obtained by scanning electronic microscopy of commercial photochromic dye (violet, blue and orange coloured) are shown in Figure 4. It can be seemed in figure that the commerical photochromic dyes in the fabrics are composed mainly by spherical-shape capsules.

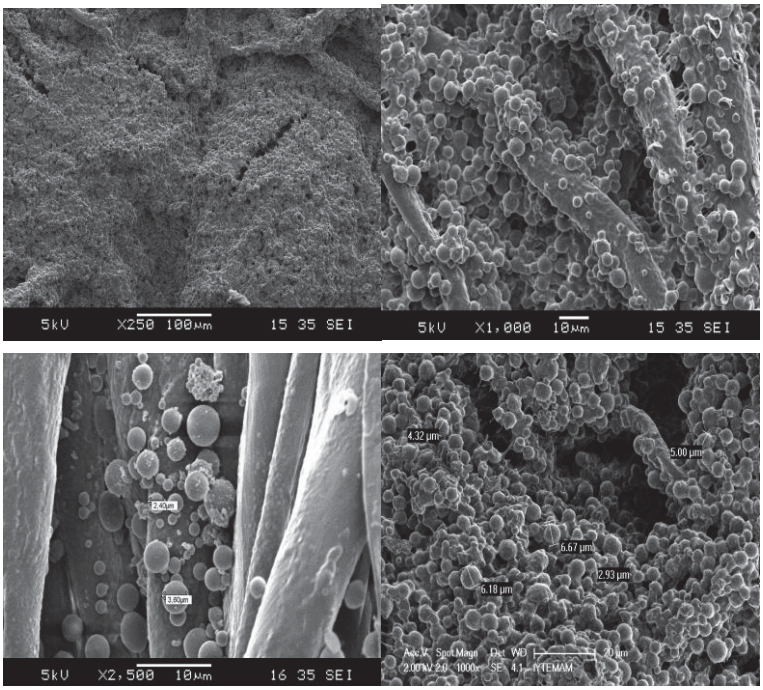


**Figure 4.** SEM photomicrographs of commercial photochromic dyes in the fabrics

Figure 5-7 depicts colour changes of the fabrics under different light sources in the light cabine. At the same time; L*, a*, b*, h, C and ΔE values of the fabrics are illustrated in Figure 8-10. It was observed that colour changes and colour values of the fabrics showed the discolouration of the fabrics.

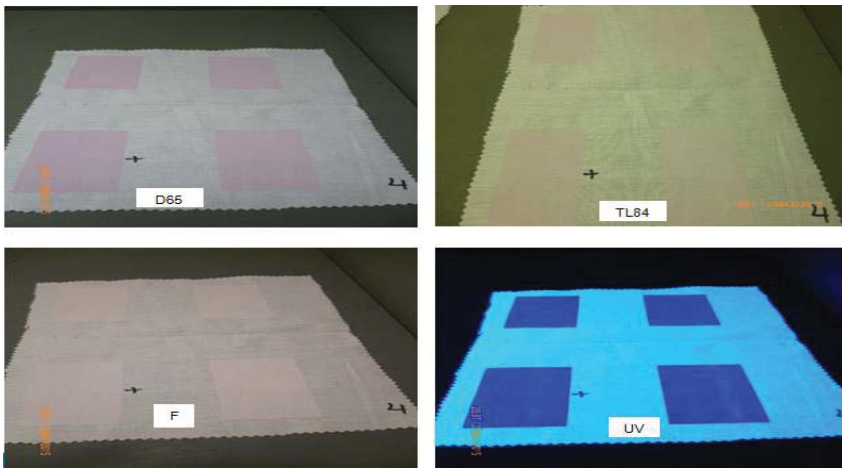


**Figure 5.** Images of at different light sources of fabric which applied violet coloured commercial photochromic dye by printing method

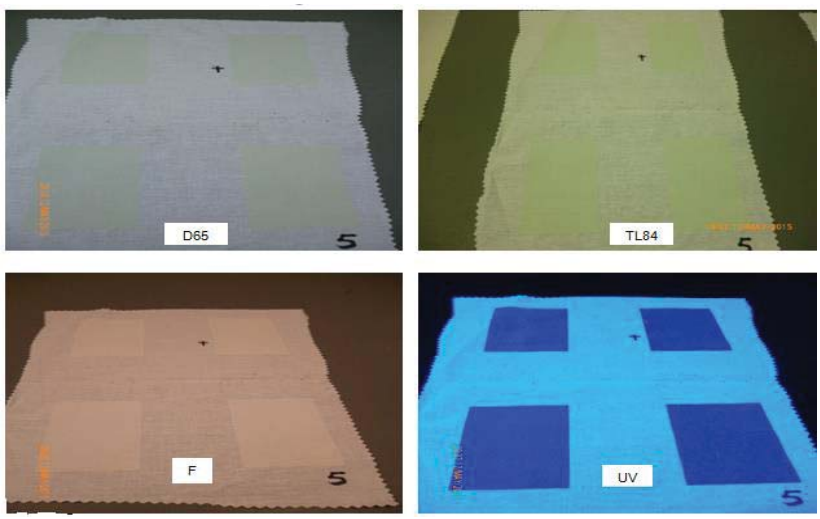


**Figure 6.** Images of at different light sources of fabric which applied blue coloured commercial photochromic dye by printing method

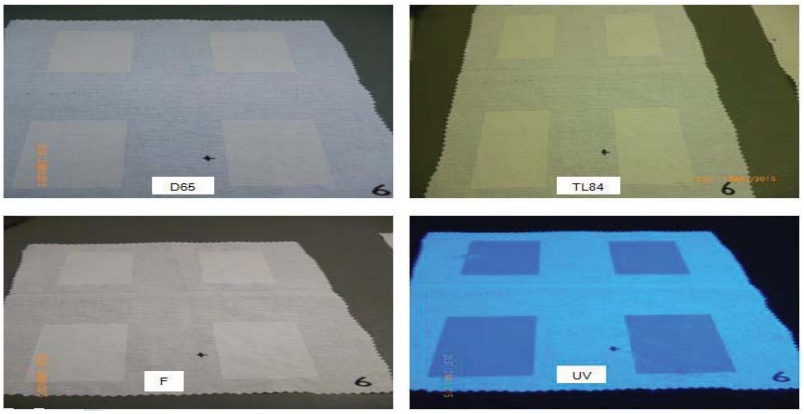


**Figure 7.** Images of at different light sources of fabric which applied orange coloured commercial photochromic dye by printing method

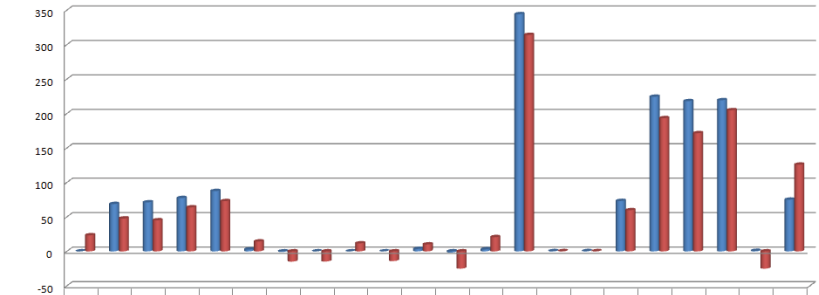


| | dE | X | Y | Z | L* | a* | b* | dL* | da* | db* | u* | v* | C* | h* | x | y | R457 | R | G | B | YI | WI |
|---|---|---|---|---|---|---|---|---|---|---|---|---|---|---|---|---|---|---|---|---|---|---|
| under daylight | 0 | 68,72 | 71,15 | 77,37 | 87,56 | 2,77 | -0,79 | -0 | -0 | -0 | 3,5 | -1,68 | 2,8812 | 344,17 | 0,316 | 0,328 | 73,13 | 224,29 | 217,97 | 219,35 | 0,7 | 75,019 |
| under UV light source | 23,36 | 47,71 | 45,07 | 63,83 | 72,94 | 14,36 | -14,85 | -14,62 | 11,59 | -14,06 | 10,12 | -24,98 | 20,654 | 314,04 | 0,305 | 0,288 | 59,75 | 193,32 | 171,45 | 204,82 | -24,99 | 125,81 |

**Figure 8.** Colour values of fabric which applied violet coloured commercial photochromic dye by printing method

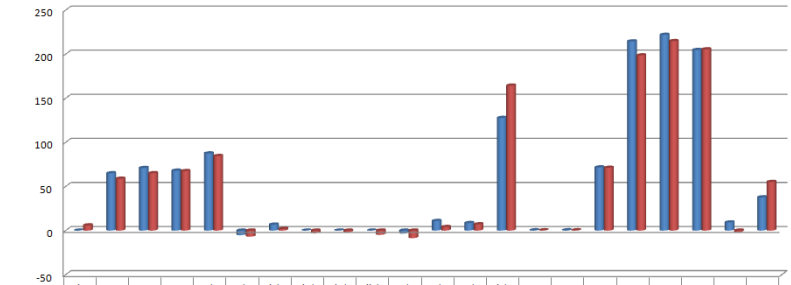


| | dE | X | Y | Z | L* | a* | b* | dL* | da* | db* | u* | v* | C* | h* | x | y | R457 | R | G | B | YI | WI |
|---|---|---|---|---|---|---|---|---|---|---|---|---|---|---|---|---|---|---|---|---|---|---|
| under daylight | 0 | 64,98 | 70,99 | 67,88 | 87,48 | -5,21 | 6,74 | -0 | -0 | -0 | -3,35 | 10,92 | 8,516 | 127,7 | 0,319 | 0,348 | 71,64 | 214,5 | 222 | 204,8 | 9,21 | 37,66 |
| under UV light source | 5,89 | 58,81 | 65,05 | 67,54 | 84,51 | -6,83 | 1,91 | -2,97 | -1,62 | -4,83 | -8,48 | 4,06 | 7,089 | 164,3 | 0,307 | 0,34 | 71,2 | 198,7 | 214,9 | 205,5 | -1,68 | 55,13 |

**Figure 9.** Colour values of fabric which applied blue coloured commercial photochromic dye by printing method

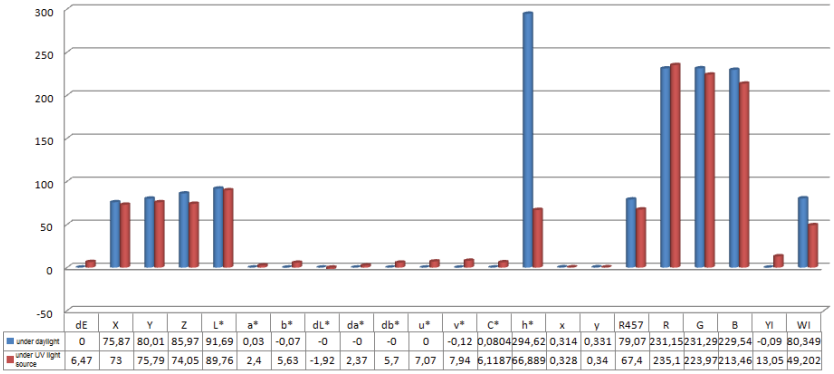


| | dE | X | Y | Z | L* | a* | b* | dL* | da* | db* | u* | v* | C* | h* | x | y | R457 | R | G | B | YI | WI |
|---|---|---|---|---|---|---|---|---|---|---|---|---|---|---|---|---|---|---|---|---|---|---|
| under daylight | 0 | 75,87 | 80,01 | 85,97 | 91,69 | 0,03 | -0,07 | -0 | -0 | -0 | 0 | -0,12 | 0,0804 | 294,62 | 0,314 | 0,331 | 79,07 | 231,15 | 231,29 | 229,54 | -0,09 | 80,349 |
| under UV light source | 6,47 | 73 | 75,79 | 74,05 | 89,76 | 2,4 | 5,63 | -1,92 | 2,37 | 5,7 | 7,07 | 7,94 | 6,1187 | 66,889 | 0,328 | 0,34 | 67,4 | 235,1 | 223,97 | 213,46 | 13,05 | 49,202 |

**Figure 10.** Colour values of fabric which applied orange coloured commercial photochromic dye by printing method

Figure 11 depicts colour changes of the yarns under UV light source. At the same time; L*, a*, b*, h, C and ΔE values of the yarns are illustrated in Figure 12-14. It was observed that colour changes and colour values of the yarns showed the discolouration of the yarns.


**Figure 11.** Colour changes of the yarns which containing violet, blue and orange coloured commercial photochromic dye (a, b,c): without UV light source (d,e,f): under UV light source, respectively

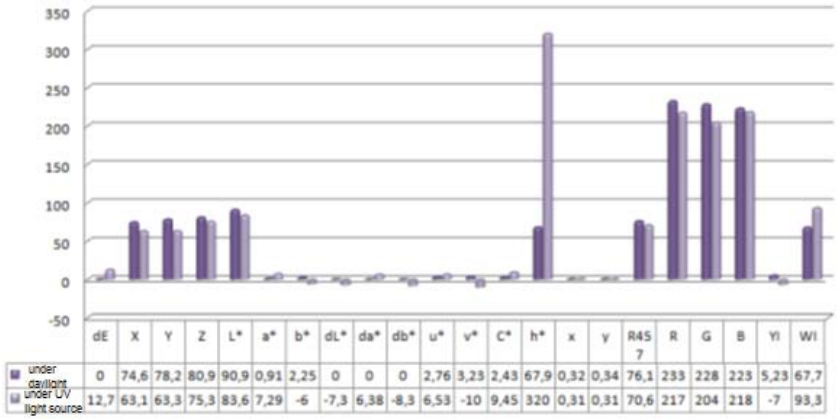


| | dE | X | Y | Z | L* | a* | b* | dL* | da* | db* | u* | v* | C* | h* | x | y | R457 | R | G | B | YI | WI |
|---|---|---|---|---|---|---|---|---|---|---|---|---|---|---|---|---|---|---|---|---|---|---|
| under daylight | 0 | 74,6 | 78,2 | 80,9 | 90,9 | 0,91 | 2,25 | 0 | 0 | 0 | 2,76 | 3,23 | 2,43 | 67,9 | 0,32 | 0,34 | 76,1 | 233 | 228 | 223 | 5,23 | 67,7 |
| under UV light source | 12,7 | 63,1 | 63,3 | 75,3 | 83,6 | 7,29 | -6 | -7,3 | 6,38 | -8,3 | 6,53 | -10 | 9,45 | 320 | 0,31 | 0,31 | 70,6 | 217 | 204 | 218 | -7 | 93,3 |

**Figure 12.** Colour values of the yarn which containing violet coloured commercial photochromic dye

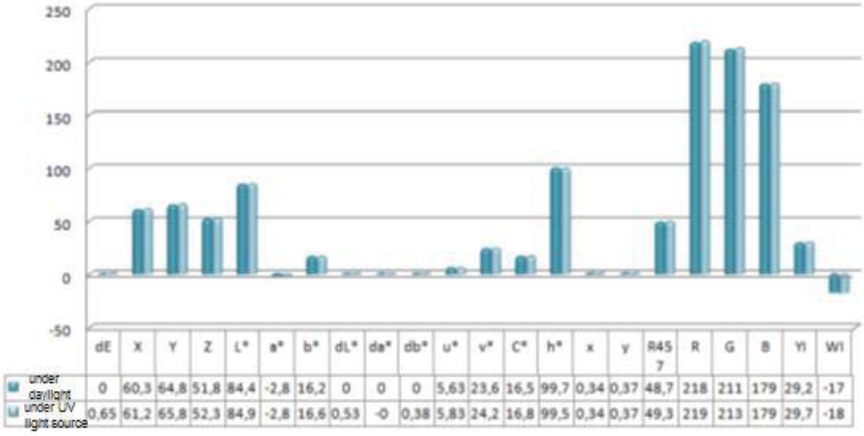


| | dE | X | Y | Z | L* | a* | b* | dL* | da* | db* | u* | v* | C* | h* | x | y | R457 | R | G | B | YI | WI |
|---|---|---|---|---|---|---|---|---|---|---|---|---|---|---|---|---|---|---|---|---|---|---|
| under daylight | 0 | 60,3 | 64,8 | 51,8 | 84,4 | -2,8 | 16,2 | 0 | 0 | 0 | 5,63 | 23,6 | 16,5 | 99,7 | 0,34 | 0,37 | 48,7 | 218 | 211 | 179 | 29,2 | -17 |
| under UV light source | 0,65 | 61,2 | 65,8 | 52,3 | 84,9 | -2,8 | 16,6 | 0,53 | -0 | 0,38 | 5,83 | 24,2 | 16,8 | 99,5 | 0,34 | 0,37 | 49,3 | 219 | 213 | 179 | 29,7 | -18 |

**Figure 13.** Colour values of the yarn which containing blue coloured commercial photochromic dye

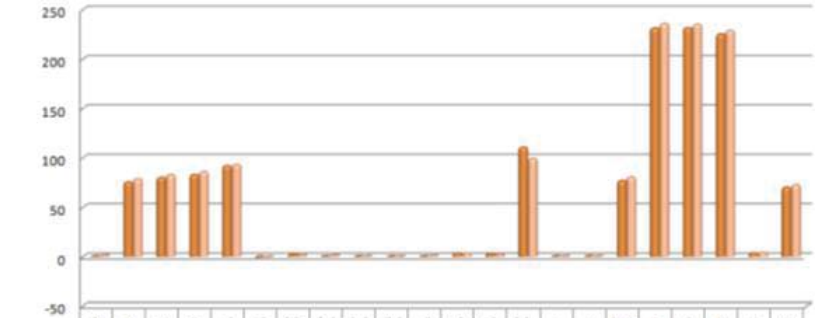


| | dE | X | Y | Z | L* | a* | b* | dL* | da* | db* | u* | v* | C* | h* | x | y | R457 | R | G | B | YI | WI |
|---|---|---|---|---|---|---|---|---|---|---|---|---|---|---|---|---|---|---|---|---|---|---|
| under daylight | 0 | 75,3 | 79,8 | 82,8 | 91,6 | -0,8 | 2,09 | 0 | 0 | 0 | 0,2 | 3,29 | 2,23 | 110 | 0,32 | 0,34 | 76,6 | 231 | 231 | 225 | 3,52 | 70 |
| under UV light source | 1,36 | 78,3 | 82,7 | 85,7 | 92,9 | -0,4 | 2,24 | 1,28 | 0,42 | 0,15 | 0,9 | 3,45 | 2,26 | 99,2 | 0,32 | 0,34 | 80,3 | 236 | 235 | 229 | 4,09 | 72,4 |

**Figure 14.** Colour values of the yarn which containing orange coloured commercial photochromic dye

The colour changes and staining degrees of fabrics for multi fibers were evaluated with grey scale under $D_{65}$ light (standard sun light). Table 3 shows colour fastness to laundering of the fabrics. It was observed that colour change and staining value were very good.

**Table 3.** Colour fastness to washing

| Fabric | Colour Change Value | Staining Value |
|---|---|---|
| **Fabric applied commercial photochromic dye in violet colour** | 5 | 5 |
| **Fabric applied commercial photochromic dye in blue colour** | 5 | 4 |
| **Fabric applied commercial photochromic dye in orange colour** | 5 | 5 |

The staining degrees of rubbing fabrics were evaluated with appropriate grey scale according to wet and dry rubbing test results. Change in colour was assessed using the standard grey scale, where a rating of 5 is considered as excellent and 1 is poor. Fastness results of the fabrics are given in Table 4. It was observed that dry and wet rubbing fastness seemed to be same value.

**Table 4.** The fastness values of the fabrics

| Fabric | Dry Rubbing Fastness | Wet Rubbing Fastness |
|---|---|---|
| **Fabric applied commercial photochromic dye in violet colour** | 4 | 4 |
| **Fabric applied commercial photochromic dye in blue colour** | 4 | 4 |
| **Fabric applied commercial photochromic dye in orange colour** | 4/5 | 4/5 |

## 4. CONCLUSION

In this study, commercial photochromic dyes were successfully applied to cotton fabric and yarn. The colour of fabric and yarn was observed to change very quickly under different light source. It has proven to be used to prevent counterfeiting of photochromic dyes applied fabric and yarn.

## ACKNOWLEDGEMENTS

We are grateful to the financial support from Republic of Turkey, Ministry of Science, Industry and Technology (Project No: 0547.STZ.2013-2), The Scientific Research Department of Dokuz Eylul University (Project No: 2014.KB.FEN.010) and Soktas Weaving Industry Company.

## REFERENCES

1. Billah S. M. R., Christie R. M., Shamey R.: Direct colouration of textiles with photochromic dyes. Part 1: Application of spiroindolinonaphthoxazines as disperse dyes to polyester, nylon and acrylic fabrics. 2008. Colouration Technology, 124, 4, 223-228.
2. Billah S. M. R., Christie R. M., Morgan K. M.: Direct colouration of textiles with photochromic dyes. Part 2: The effect of solvents on the colour change of photochromic textiles. 2008. Colouration Technology, 124, 4, 229-233.
3. Mattila, H. R.: Introduction to Chromic Materials. 2006. Intelligent Textiles and Clothing, Section 11, Woodhead Publishing.
4. Brown G. H.: Photochromism. 1971. 853.
5. Crano J. C., Gugliemetti R. J.: Organic photochromic and thermochromic compounds. 1999. New York: Kluwer Academic/Plenum Publishers, Vol.1&2, 400.
6. Bamfield P.: Chromic phenomena: Technological applications of colour chemistry. 2001. 394.
7. Dürr H., Bouas-Laurent H.: Photochromism: Molecules and systems. 2003. Elsevier Science, p.1218.
8. El-Shishtawy R.: Functional dyes and some hi-tech applications. 2009. International Journal of Photoenergy, 1-21.

# DEVELOPMENT OF OZONE EFFECTING SYSTEM WITHOUT USING HARMFUL CHEMICALS

**Ali KESKIN[1], Ozgur BULUT[1], Ugur YILMAZ[1], Ibrahim YILDIZ[1]**

[1] Wiserwash Konfeksiyon Tekstil Sanayi Dış Ticaret Anonim Şirketi

Corresponding author: ali.keskin@wiserwash.com.tr

***Abstract:*** *Recently, some alternative bleaching methods as well as conventional bleaching chemicals have begun to be used [1]. Conventional bleach chemistries used in bleaching include sodium hypochlorite, potassium persulfate, potassium permanganate, hydrogen peroxide, sodium perborate, sodium percarbonate, and benzoyl peroxide [1]. Scientific studies have been carried out according to the known saate of the art. However, it has been determined as a result of research that it is not industrial. In this study, an alternative bleach ozone effect was applied. only the ozone can be used with different techniques without the use of any harmful chemicals, and the textile washing and effect giving process has been achieved. With the system developed within the scope of the project, Technical specifications and visual designs of products between conventional bleaching and ozone bleaching were compared. In terms of both technical and visual aspects, successful results have been obtained in comparison with the conventional method in ozone technology. It has also been observed when no chemicals are used in the washing process and water consuption has reduced the rate of 60-90%.*

**Keywords:** *Ozone, give effect,* washing, *bleaching*

## 1. INTRODUCTION

Denim fabric is a kind of woven fabric which has been produced mostly from cotton fiber and also used fibers such as polyester, elastane, linen and viskon in recent years and has a wide range of patterns that can be touched with various grades, dyed with horse dyeing, warp indigo dyestuff in classic types [2]. Waste waters containing metals, phenols, toxic compounds and phosphates can be found in waste water due to fibers, chemicals and auxiliary substances used in textile production processes. These components, which are often resistant to conventional biological treatment, can be treated without purification in conventional wastewater treatment systems. Therefore, chemical oxidation methods are much more effective in the treatment. Chemical oxidation with ozone is the most suitable process for color removal in textile wastes. Oxidation is more effective when mineralization is not efficient and economical [3].

## 2. MATERIAL AND METHOD

### 2.1. Reaction with ozone indigo and preparation of ozone device.

Firstly the conditions of the ozone generator are adjusted to give effect to the fabric with ozone. Then are put the fabrics to be applied into the washing machine. The formation and breakdown reaction of ozone is given in Figure 1.

The properties of the fabric used in the study are given in Table 1.

**Table 1** The properties of the fabric used in the study

**SHARABATI DENIM**

**Fabric Specification Sheet**

Denim

| | | | |
|---|---|---|---|
| **Date:** | 01.08.2016 | **Status:** | Under Development |
| **Code:** | DRS500062 | **Weave:** | 3/1 Z |
| **Type:** | Denim Dual-Force | **Color:** | Ocean Blue /7.5 |
| **Fabric Name:** | **ULTRA JET 0401** | **Finishing:** | Pre Shrunk |
| **Composition:** | 94CO + 4PES + 2EL | | |

| Physical Properties | | Actual | Unit | Tolerance | | Standards | Remarks |
|---|---|---|---|---|---|---|---|
| **Weight *Dry*** | | 9.5 | oz/y² | ±5% | | ASTM D3776 (2013) | un-washed |
| **Weight *Washed*** | | 11 | oz/y² | ±5% | | - | washed (AATCC 135-2004) |
| **Width *Overall*** | | 142 | cm | ±2 | | ASTM D3774 (2012) | un-washed |
| **Width *Cuttable*** | | 139 | cm | ±2 | | ASTM D3774 (2012) | un-washed |
| **Shrinkage *Warp*** | | 2.5 | % | min. 2.5 | max. 4 | AATCC 135 (2004) | washed |
| **Shrinkage *Weft*** | | 16 | % | ±2 | | AATCC 135 (2004) | washed |
| **Movement** | | 0 | % | ±3 | | AATCC 179 (2004) | washed |
| **Tear *Warp*** | ELMENDORF | 15 | lbf | -30% | | ASTM D1424 (2013) | washed |
| **Tear *Weft*** | ELMENDORF | 8.8 | lbf | -30% | | ASTM D1424 (2013) | washed |
| **Tensile Strength *Warp*** | | 175 | lbf | -30% | | ASTM D5034 (2013) | washed |
| **Tensile Strength *Weft*** | | 55 | lbf | -30% | | ASTM D5034 (2013) | washed |
| **Stiffness** | | | KGF | ±0.2 | | ASTM D4032 (2012) | un-washed |
| **Elasticity** | | 65 | % | min. 61 | max. 69 | ASTM D3107 - Modified | washed (AATCC 135-2004) |
| **Growth** | | 3.5 | % | min. 0.5 | max. 6.5 | ASTM D3107 - Modified | washed (AATCC 135-2004) |
| **Recovery** | | 94 | % | | | ASTM D3107 - Modified | washed (AATCC 135-2004) |
| **Abrasion Resistance** | MARTINDALE | | rubs | - | | ISO 12947-2 (1998) | max. 20.000 Rubs<br>2 Thread Breaks |
| **Seam Slippage** | | | - | | | ISO 13936-1 | |
| **Pilling Tendency** | MARTINDALE | | - | | | ISO 12945-2 (2000) | |
| **pH** | | 6.5 | - | min. 5 | max. 7.5 | AATCC 81 (2012) | |
| **Crocking *Dry* (Rubbing)** | | 4-5 | - | | | ISO 105-X12 (2001) | |
| **Crocking *Wet*** | | 1-2 | - | | | ISO 105-X12 (2001) | |
| **Wash Fastness Grey Scale (A 03)** | | | - | | | | |
| **Color Change** | | 4 | - | | | ISO 105-C06 - C1S (2010) | |
| **Staining** | Cotton | 4 | - | | | ISO 105-C06 - C1S (2010) | |
| | Diacetate | 4 | - | | | ISO 105-C06 - C1S (2010) | |
| | Polyamide | 4 | - | | | ISO 105-C06 - C1S (2010) | |
| | Polyester | 4-5 | - | | | ISO 105-C06 - C1S (2010) | |
| | Acrylic | 4 | - | | | ISO 105-C06 - C1S (2010) | |
| | Wool | 4-5 | - | | | ISO 105-C06 - C1S (2010) | |

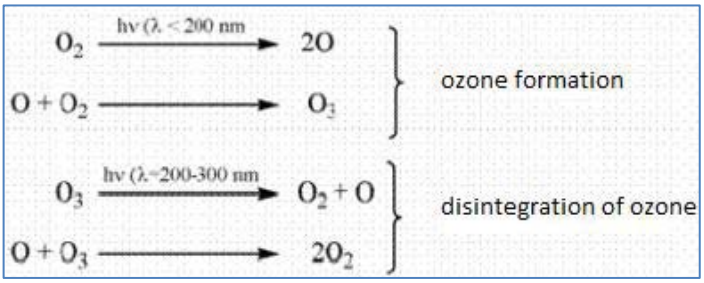


**Figure 1.** Ozone Reaction

### 2.2. Preparation of fabric sample

Test such as color fastness, elastic recovery, shrinkage test have been maken to fabrics that has been applied onone.. 25 cm for the weft, 7.5 cm for the warp. 50*50 cm for shrinkage test.

The characteristics of the ozone gas are given in Table 2.

**Table 2.** Properties of ozone gas

| | |
|---|---|
| Molecular formula | $O_3$ |
| Molecular mass | 47.984743866 g $mol^{-1}$ |
| View | Pale blue gas |
| Density | 2.144 mg $cm^{-3}$ (0 °C) |
| Melting point | −192.2 °C; −313.9 °F; 81.0 K |
| Boiling point | −112 °C; −170 °F; 161 K |
| Resolution (in water) | 1.05 g $L^{-1}$ (0 °C) |

## 3. RESULTS AND DISCUSSION

Technical specifications and visual designs of products between conventional bleaching and ozone bleaching were compared. In terms of both technical and visual aspects, successful results have been obtained according to the conventional method in ozone technology. It has also been observed when no chemicals are used in the washing process and water consuption has reduced the rate of 60-90%. The technical properties of the fabrics are given in Table 3.

**Table 3.** Technical results of average fabric

| ELASTICITY (EXTENSION) | RECOVERY | EXPLANATION |
|---|---|---|
| 31,5% | 7,0% | Bleaching with ozone |
| 29,0% | 4,0% | Convertional bleaching |

## REFERENCES

1. Ege, V., Denim Yıkama Oryantasyon Sunumu 2008.
2. Bağiran, İ.C., problems occuring in denim laundry, their preventive solutions and correction possibilities Ege Üniversitesi Fen Bilimleri Enstitüsü, 2011. (Yüksek Lisans Tezi) p. 80-83.
3. Kaan Morali, N.U., Utku Yetiş, Ozonation pre and post-treatment of denim textile mill effluents: Effect of cleaner production measures. Journal of Cleaner Production, 2016. 137: p. 1-9.

# MONOFILAMENT FIBER PRODUCTION WITH POLYMER FOAMS

**Rumeysa CELEN[1], Yusuf ULCAY[1]**

[1] Uludag University, Turkey

Corresponding author: rumeysa@uludag.edu.tr

***Abstract:*** *The aim of the study is to produce monofilament bicomponent yarns for use in insulation applications (for example; thermal insulation, acoustic insulation etc.) Therefore, polymer foam material is used for insulator material. Sheath and core bicomponent spinning method was used. Different ratios (%1 and %3) of LDPE foam was used in monofilament yarn. Longitudinal section and cross section of the fibers were investigated. Tenacity and elongation tests were made by Shimadzu test instrument.*

***Key Words****: Bicomponent spinning, monofilament yarn, polypropylene, polymer foam, insulation.*

## 1. INTRODUCTION

Throughout history, humanity has worked to improve our quality of life. Following that goal, we have been changing and improving the places we live in. One important point in order to improve quality of life is isolating ourselves from the vibration and electricity from all that equipment that makes our life easier, weather tail, external temperature and noise. Therefore, insulation techniques are continuously on the rise [1].

Polymeric foams, such as polystyrene (PS), polyethylene (PE) and polyurethane (PU), are widely used because of their lower cost, low thermal conductivity, high specific strength, excellent heat and sound insulation performance, great energy absorption property, compared to conventional plastic materials [2, 3].

Textile materials often use at thermal and acoustic insulation applications due to their porous structure and low cost [4, 5, 6 etc.]

## 2. MATERIAL AND METHOD

### 2.1. Material

Properties of polypropylene chips which used at the sheath section of fiber were given in Table1. It was supplied by Petkim Petrokimya Holding A.Ş.

Low Density Polyethylene (LDPE) foam was used at core section of fiber. It was supplied by Durfoam Insulation & Packaging Co.

**Table 1.** Properties of polypropylene chips

| Description | Value |
|---|---|
| Melting flow rate (MFR), (2160 g, 230°C) | 20-28 g/10m |
| Tensile strength | 350 kg/cm$^2$ |

**Table 2. Properties of LDPE foam**

| Description | Value |
|---|---|
| Blowing agent | Azo dicarbon amide |
| Density | 25-250 kg/m$^3$ |
| Decomposition Temperature | >300 °C |

## 2.2. Method

Sheath and core bicomponent spinning method was used. Low density polyethylene foam was used as an insulator material. LDPE foam was used at core section, polypropylene (PP) was used at sheath section.

%1 and %3 adding ratios of LDPE foam was used in monofilament yarn. Production parameters were given in Table 3.

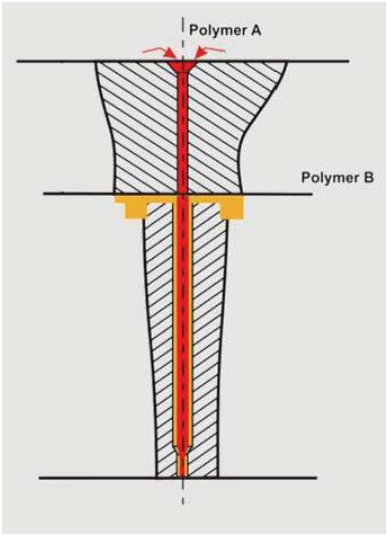


**Figure 1.** Schematic view of sheath/core bicomponent spinning

Longitudinal section and cross section of the fibers were investigated. Tenacity and elongation tests were made by Shimadzu test instrument. In tenacity and elongation tests three measurements were performed and average values were given.

**Table 3.** Production Parameters

| Additive | Yarn Codes | Extruder Speed Ratios (Sheath/Core) | Drawing / Winding Ratio |
|---|---|---|---|
| **1 % LDPE** | 1.5.1 | 5/1 | 1/ 0,5 |
| **1 % LDPE** | 1.4.1 | 4/1 | 1/ 0,5 |
| **1 % LDPE** | 1.2.1 | 2/1 | 1/ 0,5 |
| **3 % LDPE** | 3.5.1 | 5/1 | 1/ 0,5 |
| **3 % LDPE** | 3.4.1 | 4/1 | 1/ 0,5 |
| **3 % LDPE** | 3.2.1 | 2/1 | 1/ 0,5 |

## 3. RESULTS and DISCUSSION

Yarn number, tenacity and elongation test results were given in Table 4. Compared to the reference yarn tenacity was increased, elongation was decreased. PE foam additive effected yarn's mechanical properties positively.

**Table 4.** Test results of monofilament yarns

| Yarn Codes | Yarn Number [tex] | Tenacity [N] | Elongation [%] |
|---|---|---|---|
| 1.5.1 | 350 | 8.19 | 32.87 |
| 1.4.1 | 400 | 9.36 | 43.5 |
| 1.2.1 | 305 | 11.24 | 60.84 |
| 3.5.1 | 460 | 11.19 | 48.80 |
| 3.4.1 | 270 | 12.38 | 58.84 |
| 3.2.1 | 280 | 14.29 | 60.45 |

**Reference PP yarn Tenacity [N]: 2.62 Elongation[%] :290.56*

**Figure 2.** Cross section of **(left)** 1.4.1 **(center)**1.2.1 **(right)** 3.5.1

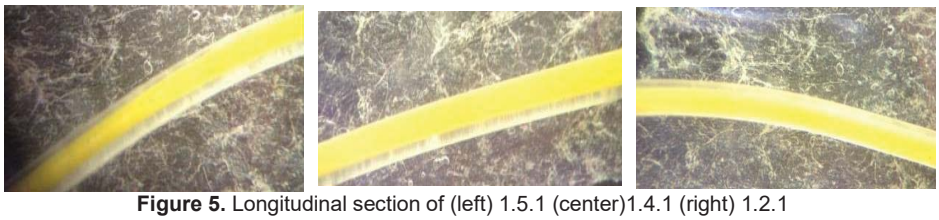

**Figure 5.** Longitudinal section of (left) 1.5.1 (center)1.4.1 (right) 1.2.1

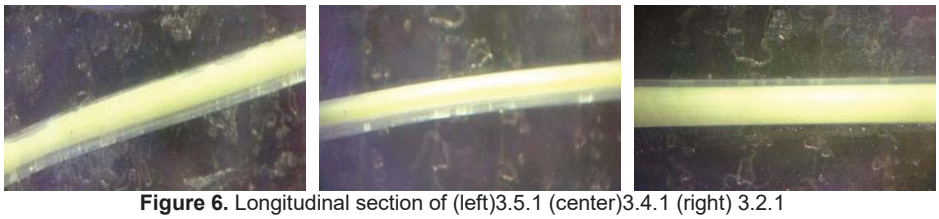

**Figure 6.** Longitudinal section of (left)3.5.1 (center)3.4.1 (right) 3.2.1

## 4. CONCLUSION

- The foam polymer improved yarn properties as expected.
- For both additive ratios (1% and 3%), increased with sheath's speed ratio, tenacity values of monofilaments were decreased.
- In future work; different polymer foams will be studied.
- Maximum polymer foam additive ratio will be determined.
- Thermal and acoustic insulation properties of yarns will be measured.

## REFERENCES


1. Thermal and Noise Insulation Technologies https://www.ennomotive.com/thermal-noise-insulation-technologies/ Latest Access Date: 25.03.2017.
2. Sauceau, Martial, et al. New challenges in polymer foaming: A review of extrusion processes assisted by supercritical carbon dioxide. *Progress in Polymer Science*, 2011, 36.6: 749-766.
3. Gautam, R.; Bassi, A. S.; Yanful, E. K. A review of biodegradation of synthetic plastic and foams. *Applied Biochemistry and Biotechnology*, 2007, 141.1: 85-108.
4. Abdelfattah, A., Ghalia, E., & Eman, R.. Using nonwoven hollow fibers to improve cars interior acoustic properties 2011, *Life Sci J*, *8*, 344-351.
5. Frydrych, I., Dziworska, G., & Bilska, J. Comparative analysis of the thermal insulation properties of fabrics made of natural and man-made cellulose fibres 2002, *Fibres and Textiles in Eastern Europe*, *10*(4), 40-44.
6. Büyükakıncı B., Sökmen N. Küçük H. Doğal elyaf karışımlı poliüretan kompozitlerin ses ve ısı yalıtım özelliklerinin incelenmesi, 2011, *Tekstil ve Konfeksiyon,*21(2): 124-132.

# EVALUATION OF THERMAL PROPERTIES OF SEAMLESS THERMAL FABRICS

**Fatma Filiz YILDIRIM[1], Sultan ARAS[1], Mustafa ÇÖREKCİOĞLU[1], A. YILMAZ**

[1] Ozanteks Tekstil San ve Tic A.Ş. Ar-Ge Merkezi

Corresponding author: filiz@ozanteks.com.tr

**Abstract:** Comfort is a mixed concept involved various factors such as fiber and fabric properties, human factors and environment. Thermal comfort is stated as satisfaction of the person's thermal conditions. The garments must have high thermal resistance against cold to provide thermal comfort. In this study, 3 different types of thermal fabrics were evaluated by their thermal resistance values and their thermal camera measurements. Wool/polyamide fabrics exhibited highest thermal resistance values. Additionally this sample exhibited different curve in the thermal camera measurements.

**Key Words**: thermal fabrics, thermal camera, thermal resistance, seamless

## 1. INTRODUCTION

Garments play a protective role as a buffer between the human and the living environment and play an important role in a healthy life. Comfort is a complex concept involving many physical and psychological factors and is influenced by fiber properties, fabric factors, human factors and environment. The comfort of the person is determined by the air layer between human skin and clothing, also called microclimate (Figure 1). Microclimate is influenced by environmental factors, activity level of the person and clothing characteristics [1 - 4, 10].

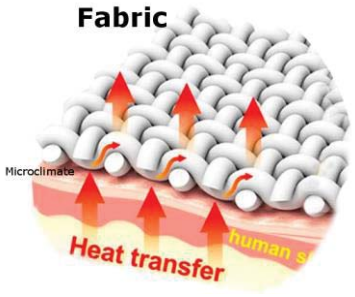


**Figure 1.** Microclimate between human skin and fabric [11]

Thermal comfort is a type of thermoregulation system consisting of a combination of signals from the thermo receptors on the deep surface and the lower layers of skin. According to the standards of ASHRAE (The American Society of Heating, Refrigerating and Air Conditioning Engineers), thermal comfort is expressed as satisfaction with the thermal conditions of the environment [1, 4].

An ideal garment fabric should have three important features in terms of thermal comfort (Figure 2) [1]:

- High thermal resistance to protect from cold,
- Low water vapor resistance for effective heat transfer in climatic conditions
- Liquid handling capability to prevent discomfort due to sweating.

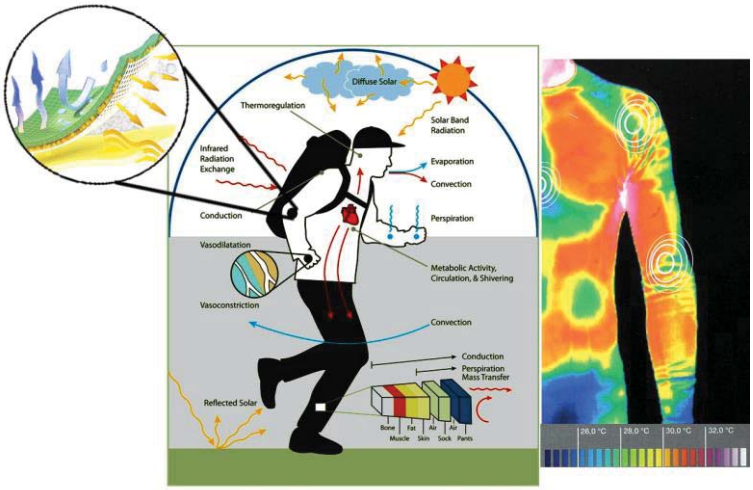


**Figure 2.** Thermoregulation system in human and garment [12-14]

The metabolic heat generated to stay in the thermal balance is balanced through the transmission of heat through the skin, the radiation and also by perspiration. Direct heat transfers are achieved by the temperature difference between the body and the environment. The more heat flow causes bigger difference. This heat flow also depends on the thermal resistance property [1]. Many researches were made many studies for determining thermal comfort of the fabrics. In these studies, various parameters such as thermal conductivity, thermal resistance, air permeability and relative water-vapour permeability were investigated [1, 4- 30].

The thermal cameras make apparent an infrared imaging and measurement system to visualize and measure the thermal energy emitted from objects in the environment [31]. In this study, 3 different types of thermal fabrics were evaluated by their thermal resistance values and their thermal camera measurements. It is possible to observe features such as camouflage (thermal concealing) or thermoregulating properties of fabrics thanks to thermal cameras [32, 33]. However, in this study, thermal resistance characteristics of garments having high thermal resistance were compared using thermal camera measurements.

## 2. MATERIALS AND METHOD

### 2.1. Materials

In this study, three different seamless thermal fabrics were used. %40 wool - %60 polyamide seamless knitted fabric, %76 polyamide-%18 poyester-%6 elastane seamless knitted fabric and %30 polyester-%63 polyamide-%7 elastane seamless knitted fabric were used in this study.

### 2.2. Mechanical Properties

Thermal resistance properties of the fabrics were also evaluated. Thermal resistance measurements of the samples were performed according to (sweating guarded hot plate) TS EN ISO 11092 11-2014 test. The thermal resistance Rct (m2K/W) value is evaluated from the supplied steady-state heating power (Q), the temperature difference between the air in the wind channel and the skin model (Ts) and the size of the measuring surface (A). The equation of Rct Eq. (1) is given below [34]:

$$R_{ct} = A \cdot \frac{T_s - T_a}{Q} \tag{1}$$

Other thermal measurements were made for evaluating surface temperatures of the samples at different times using thermal camera (Fluke-Visual IR Thermometer). The distance between thermal camera ans samples was 30 cm. the samples were observed using the thermal camera at specific time intervals (such as 1, 10, 20, 30, and 40 min).

## 3. RESULTS AND DISCUSSION

The thermal resistance results of three fabrics are given on Table 1. It is known from the literature, it is important that the fabrics show high thermal resistance in order to provide high insulation.

Thermal camera results are given on Table 2 and Figure 3-7.

**Table 1.** Thermal Resistance Values of Samples

| Samples | | Weight ($g/m^2$) | Knit | Thermal Resistance Rct ($m^2$Kelvin/Watt) | |
|---|---|---|---|---|---|
| Sample 1 | %40 wool %60 polyamide | 190 | Rib | 0,042 |  |
| Sample 2 | %76 polyamide %18 polyester %6 elastane | 240 | Rib | 0,021 | 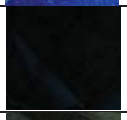 |
| Sample 3 | %63 polyamide %30 polyester- %7 elastane | 225 | Rib | 0,015 | 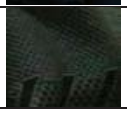 |

**Table 2.** Thermal camera measurements of Samples

| Measurements | Stages | Sample 1 | Sample 2 | Sample 3 |
|---|---|---|---|---|
| 1. measurement | First measurement from fabric surface | 52,7 °C | 46,1 °C | 58,4 °C |
| 2. measurement | After 1 minute | 53,7 °C | 49,2 °C | 54,3 °C |
| 3. measurement | After 10 minutes | 58,1 °C | 54,8 °C | 50,9 °C |
| 4. measurement | After 20 minutes | 54,3 °C | 51 °C | 50,3 °C |
| 5. measurement | After 30 minutes | 52,6 °C | 45,5 °C | 48,8 °C |
| 6. measurement | After 40 minutes | 49,5 °C | 44,3 °C | 48,3 °C |

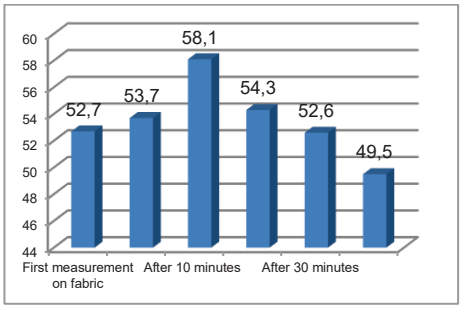


**Figure 3.** Thermal camera measurements of sample 1 (°C)

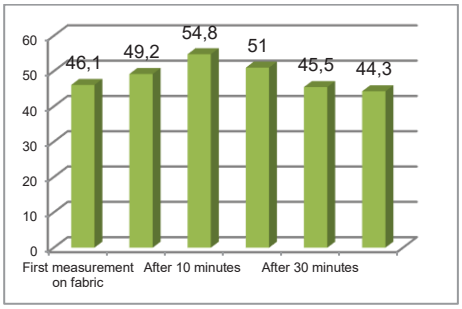


**Figure 4.** Thermal camera measurements of sample 2 (°C)

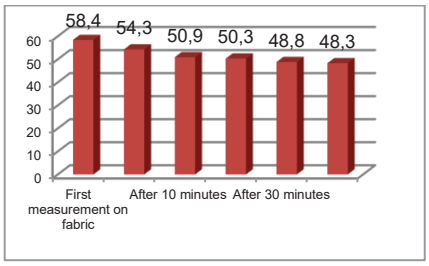


**Figure 5.** Thermal camera measurements of sample 3 (°C)

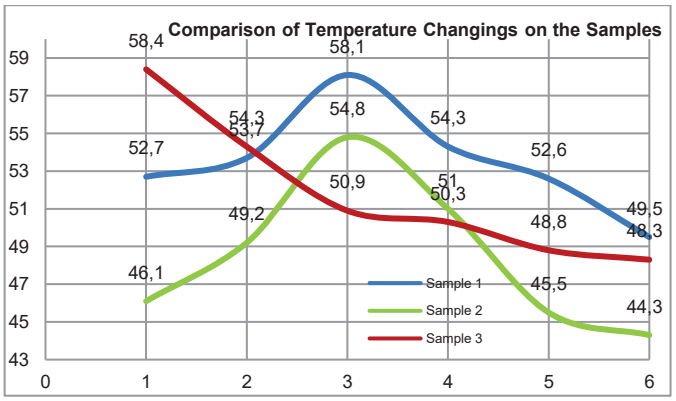


**Figure 6.** Comparison of temperature changings on the samples

As seen on table 2 and figures, the fabric (sample 1) with the highest thermal resistance value exhibited a different curve from the other fabrics in the thermal camera measurements. In addition, the highest temperature after 40 minutes belongs to this sample. As seen on Figure 4, the temperature changing curves of the sample 1 and sample 2 exhibited quite similar trends. Their thermal resistance values are range from 0,020 to 0,042 ($m^2K/W$). However sample 3 has different temperature changing trend and thermal resistance value of Samples 3 is 0,015 ($m^2K/W$). Thermal conductivity of various fibers used in garments is comparable has been known for years. Fiber type and conductivity can be given as follow (W/m.K); Cotton : 0.226, polyester: 0.141, polyamide: 0.243 and wool: 0,193. The air contained in the fabric dominates the thermal resistance value. If all other variables are constant, air contained in wool yarns may be expected greater than that of other yarns [35]. This may explain why the thermal resistance values of the wool fibers are high.

Some researchers noted that weight of the fabric has a little direct influence upon the fabric's thermal insulation [36]. Although samples 1 has lower weight, it exhibit higher thermal insulation value. There are other factors that influence thermal insulation such as fiber type, density, air content. The amount of the temperature changes on the surface of the fabrics is given in Figure 7.

The temperature changing rates of the fabrics show that sample 1 has the lowest temperature changing rate. The thermal resistance value of the sample 1 is the higher than the others.

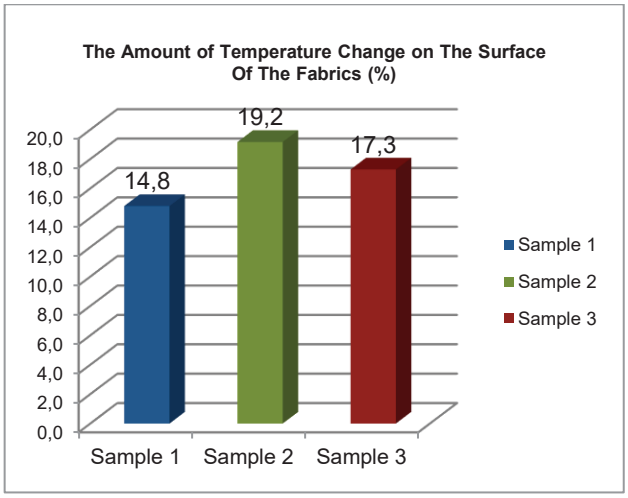


**Figure 7.** The amount of the temperature changes on the surface of the fabrics

## 4. CONCLUSIONS

The thermal resistance represents the temperature difference between the two sides of the material and expresses in Kelvin square meters / Watt. This is one of the significant features of thermal comfort. In this study, three different fabrics

were evaluated for their thermal resistance values. Wool/polyamide fabrics exhibited highest thermal resistance values. Additionally this sample exhibited different curve in the thermal camera measurements and also lowest temperature changing rates on the fabric surface.

## ACKNOWLEDGMENTS

This work has been partly supported by Ozanteks R&D center in frame of the Project 18U01.

## REFERENCES

1. Eren, Ö. N. E. R. (2010). Materyal, Üretim Teknolojisi Ve Kumaş Yapısının Termal Konfora Etkileri. *2010 (Cilt: 17)*,
2. Hatch, K. L., (1993) , MN: West Publishing Co., Minneapolis
3. Yoo, H. S., Hu, Y. S., (2000), Effects of Heat and Moisture Transport in Fabrics and Garments Determined with a Vertical Plate Sweating Skin Model, Textile Research Journal, 70(6): 542-549
4. TÜRKSOY, H. G., ÜSTÜNTAĞ, S., & ÇARKIT, G. (2017). Thermal Comfort Properties of Fabrics Knitted from Bamboo/Cotton Blended Yarns. *Journal of Science and Engineering*, *19*(56).
5. Wang, Z., W., (2002), Heat and Moisture Transfer and Clothing Thermal Comfort, Phd Thesis, The Hong Kong Polytechnic University, Institute of Textiles and Clothing, Hong Kong, 324s.
6. Das, B., Das, A., Kothari, V., Fanguiero, R. ve Araújo, M. 2007. Moisture transmission through textiles Part I: Processes involved in moisture transmission and the factors at play, AUTEX Research Journal, vol. 7 (2), p. 100-110.
7. Onofrei, E., Rocha, A. ve Catarino, A. 2011. The influence of knitted fabrics' structure on the thermal and moisture management properties, Journal of Engineered Fibers and Fabrics, vol. 6 (4), p. 10-22.
8. Oğlakçıoğlu, N. ve Marmaralı, A. 2007. Thermal comfort properties of some knitted structures, Fibres & Textiles in Eastern Europe, vol. 15 (5-6), p. 64-65.
9. Verdu, P., Rego, J. M., Nieto, J., Blanes, M., (2009) Comfort Analyses of Woven Cotton/Poliester Fabrics Modified With A New Elastic Fiber, Part 1 Preliminary Analyses of Comfort and Mechanical Properties, Textile Research Journal, Vol 79(1): 14-23
10. Nayak, R., Punj, S., Chatterjee, K. ve Behera, B., 2009. Comfort properties of suiting fabrics, Indian Journal of Fibre ve Textile Research, vol. 34, p. 122-128.
11. https://phys.org/news/2017-11-fabric-cool.html
12. http://www.marsan.com.tr/en/product;
13. https://www.earthslab.com/physiology/thermoregulation-human-body/;
14. https://www.ebay.com/itm/X-Bionic-Invent-Shortsleeve-Technical-Shirt-Compression-Ski-Biking-Gym-Base-NEW-/312046960763
15. Cimilli, S., Nergis, B. U., Candan, C., Özdemir, M., (2009) A Comparative Study of Some Comfort-related Properties of Socks of Different Fiber Types, Textile Research Journal, Vol 0 (0): 1-10
16. Troynikov, O. ve Wardiningsih, W. 2011. Moisture management properties of wool/polyester and wool/bamboo knitted fabrics for the sportswear base layer, Textile Research Journal, vol. 81 (6), p. 621-631.
17. Namligoz, E. S., Coban, S. ve Bahtiyari, M. I., 2010. Comparison of moisture transport properties of the various woven fabrics, Tekstil ve Konfeksiyon, vol. 20, p. 93–100.

18. Prakash, C., Ramakrishnan, G., & Koushik, C. V., 2012. A study of the thermal properties of single jersey fabrics of cotton, bamboo and cotton/bamboo blended yarn vis-a-vis bamboo fibre presence and yarn count, Journal of Thermal Analysis and Calorimetry, vol. 110, p. 1173–1177.
19. Atasağun, H., Öner, E., Okur, A. ve Beden, A., 2015. A comprehensive study on the general performance properties of Viloft-blended knitted fabrics, The Journal of The Textile Institute, vol. 106 (5), p. 523-535.
20. Guanxiong, Q., Yuan, Z., Zhongwei, W., Jianli, L., and Jie, Z., (1991) , International Man-Made Fibres Congress Proceeding, Dornbirn, s112-124
21. Weder, M., (2004) , International Textile Congress Proceeding, Portugal, s34-38
22. Gülsevin, N., (2005), Spor Giysilerin Konfor Özellikleri Üzerine Bir Araştırma, Yüksek Lisans Tezi, Ege Üniversitesi Fen Bilimleri Enstitüsü, İzmir, 80s
23. Güneşoğlu, S., Meriç, B., and Güneşoğlu, C., (2005) , Thermal Contact Properties of 2-Yarn Fleece Knitted Fabrics, 2nd International Technical Textiles Congress, İstanbul, s46-50
24. Üte, B. T., Oğlakçıoğlu, N., Çelik, P., Marmaralı, A., ve Kadoğlu, H., (2008 , Doğal Renkli Pamuk ve Angora Tavşan Lifi Karışımından Üretilen İpliklerin Özellikleri ve Örgü Kumaşların Isıl Konforuna Etkileri Üzerine Bir Araştırma Tekstil ve Konfeksiyon, 3/2008: s191-19
25. Stankovic, S.B., Popovic, D. and Poparic, G. B., (2008) Thermal Properties of Textile Fabrics Made of Natural and Regenerated Cellulose Fibers, Polymer Testing, 27/2008: 41-48
26. Verdu, P., Rego, J. M., Nieto, J., Blanes, M., (2010) Comfort Analyses of Woven Cotton/Poliester Fabrics Modified With A New Elastic Fiber, Part 2 Detailed Study of Mechanica, ThermoPhysiological and Skin Sensorial Properties, Textile Research Journal, Vol 80(3): 206-215
27. Kaplan, S., (2009) Kumaşların Mekanik Özelliklerinden ve Geçirgenlik Özelliklerinden Yararlanılarak Giysi Konforunun Tahminlenmesi, Doktora Tezi, Dokuz Eylül Üniversitesi Fen Bilimleri Enstitüsü, İzmir, 236 s
28. Shim, M. H., Park, C. H., Shim, H. S., (2009) Effect of Ceramics on the Physical and Thermo-Physiological Performance of Warmup Suit, Textile Research Journal, Vol 79(17): 1557-1564
29. Majumdar, A., Mukhopadhyay, S., Yadav, R., (2010) Thermal Properties of Knitted Fabrics Made From Cotton and Regenerated Bamboo Cellulosic Fibres, International Journal of Thermal Sciences, Vol 49: 2042-2048
30. Małgorzata Matusiak & Wioletta Sybilska (2016) Thermal resistance of fabrics vs. thermal insulation of clothing made of the fabrics, The Journal of The Textile Institute, 107:7,
31. Domina, T., Kinnicutt, P., & MacGillivray, M. (2011). Thermal pattern variations analyzed using 2D/3D mapping techniques among females. *Journal of Textile and Apparel, Technology and Management*, *7*(1).
32. RUBEŽIENĖ, V., PADLECKIENĖ, I., ŽURAVLIOVA, S. V., & BALTUŠNIKAITĖ, J. (2013). Reduction of thermal signature using fabrics with conductive additives. *Materials Science*, *19*(4), 409-414.
33. Zin, J. J. N., San Yee, O., & Htay, S. S. Investigation on the Concealing Effect of Polyester/Stainless Steel Blended Fabrics in Far Infrared Spectral Rane
34. Scott, R. A. (Ed.). (2005). *Textiles for protection*. Elsevier.
35. Williams, J. T. (Ed.). (2009). *Textiles for cold weather apparel*. Elsevier.
36. Rohde, R. O. (1963). Thermal insulation values of wool and acrylic blankets before and after laundering.

# THERMAL COMFORT EFFECT OF KNITTED FABRIC USED IN TEXTILES

**Sultan ARAS[1], Fatma Filiz YILDIRIM[1], Mustafa ÇÖREKCİOĞLU[1]**

[1] Ozanteks Tekstil San ve Tic A.Ş. Ar-Ge Merkezi

Corresponding author: saras@ozanteks.com.tr

***Abstract:*** *In many industrial applications, a wide range of textile materials have been used for thermal comfort purposes. The thermal insulation properties of textile fabrics depend on their thermal conductivity, density, thickness and thermal emission properties. Experiments have been carried out to study heat transfer through different types of fabrics used for thermal comfort. In this study, the thermal comfort effects of different fabric types used in the textile industry are examined in the light of studies in the literature and the basic concept equations are given and the criterias and importance of these criteria are mentioned for the thermal comfort tests to be done in Ozanteks.*

***Keywords:*** *knitted fabrics, heat transfer, thermal comfort, basic concept, equations*

## 1. INTRODUCTION

Clothing is one of the most intimate objects associated with our daily life [1]. Therefore Thermal properties of textile fabrics are of great interest and relevance for textile researchers, since they determine several of the major characteristics related to the wearer's overall comfort perception having significant effects on the skin mean temperature also [2].

Thermal comfort, protection of body heat balance at various activity levels is a concept related to the heat and moisture transfer properties of the garment that is required for the garment. According to ISO 7730, thermal comfort is defined as a condition that describes satisfaction with the thermal environment. According to the standards of ASHRAE (The American Society of Heating, Refrigerating and Air Conditioning Engineers), thermal comfort is expressed as satisfaction with the thermal conditions of the environment [3-4].

Marmaralı et al. (2006), study measured the thermal comfort properties of fabrics knitted in different weaves and at different frequencies, from yarns of different properties produced from different materials. In the study, 100% wool, cotton and acrylic knitted fabrics as well as cotton / polyester and wool / PAC knitted fabrics with different mixing ratios were examined. According to the findings obtained, cotton has the highest thermal conductivity in the fabrics made from different raw materials and it is followed by acrylic and wool fibers. For both cotton and polyester materials, the thermal conductivity values of the fabrics decrease as the yarn becomes finer. For both cotton and polyester yarns, it is seen that the thermal conductivity of the supple fabrics is lowest, followed by 1X1 ribs and interlock fabrics, respectively. Supreme fabrics made from cotton and polyester

yarns have the highest relative water vapor permeability value, followed by 1x1 rib and interlock fabrics. As the mesh density decreases and the fabric becomes less frequent, it is seen that there is generally an increase in the relative water vapor permeability value [5].

Onofrei et al. (2011), study, was to compare, in dry and wet states, the thermal comfort properties of elastic knitted fabrics with thermo-regulating yarns, namely Viscose Outlast and Polyester Coolmax to better understand thermal behavioral changes due to moisture content of the fabrics. Surface moisture transfer between the fabrics and a wet skin was also assessed and enabled to evaluate the level of the unpleasant contact feeling. Air permeability that is related to the thermal behavior was also investigated. The results obtained showed that at 22% moisture content, which simulates a sweating sensation, the change in thermal properties is similar for both fabrics. Above the 'sweating sensation' moisture, significant differences on the thermal properties with the moisture content were registered between fabrics, Outlast fabric being more prone to thermal properties changes due to moisture uptake than the Coolmax one. When worn in conditions of wet skin, the unpleasant cool feeling increased for both fabrics, but the effect is more pronounced for Outlast fabric [6].

Chidambaram et al. (2012), study presents the thermal comfort properties of single jersey knitted fabric structures made from cotton, regenerated bamboo and cotton-bamboo blended yarns. Cotton, bamboo fiber and blends of the two fibers (100% cotton, 100% bamboo, 50:50 cotton: bamboo, 67:33 cotton: bamboo, 33:67 cotton: bamboo) were spun into yarns of identical linear density (20 tex). Each of the yarns so produced was converted to single jersey knitted fabrics with loose, medium and tight structures. The thermal conductivity of the fabrics was generally found to decrease with increase in the proportion of bamboo fiber. The water vapour permeability and air permeability of the fabrics were observed to increase with increase in bamboo fiber content. Statistical analysis also indicates that the results are significant for air permeability, thermal resistance, thermal conductivity and water vapour permeability of the fabrics [6].

Ouzzahra et al. (2012), studies have compared thermal sensitivity between body segments, little is known on regional variations within body segments. Furthermore, the effects of exercise on the thermal sensation resulting from a cold stimulus remain unclear. The current experiment therefore aimed to explore inter- and intra-segmental differences in thermal sensitivity to cold, at rest and during light exercise.

## 2. BASIC CONCEPT EQUATIONS

The heat energy can be transferred through the textile fabrics by conduction, convection and radiation, as well as easily explainable phenomena such as heat exchange in porous media. The basic concepts of heat transfer through fabrics are explained as follows in table 1 [3].

**Table 1.** Basic Concept Equations

| Basic Concept | Equations | Referances |
|---|---|---|
| Conductivity Factor (λ) | $\lambda = \frac{Q.L}{A.t.(T_1 - T_2)}$ | [4], [9], [10], [13], [14], [15] |
| Heat Transfer Coefficient (K) | $K = \frac{Q}{A.t.(T_1 - T_2)}$ | [4], [12] |
| Specific Heat Resistance, (r) | $r = {}^{1}/_{\lambda} = \frac{A.t.(T_1 - T_2)}{Q.L}$ | [4], |
| Heat Resistance, (R) | $R = {}^{1}/_{K} = \frac{Q}{A.t.(T_1 - T_2)}$ | [4], [13], [15] |
| Thermal Resistance, ($R_{th}$ ) | $R_{th} = L/k$ | [4], [8], [9], [10], [13], [15] |
| Thermal Absorbency (b) | $b = \sqrt{\lambda.\rho.c}$ | [9], [11], [13], [15] |
| Heat Flow, (Q) | $Q = -k.A.\frac{(T_1 - T_2)}{L}$ | [4], [12] |
| Heat Flux by Radiation, ($q_r$) | $q_r\,(x) = 4.\sigma.T_0^3.(T_1 - T_2)$ at $0 \le X \le L$ | [4], [12] |
| Energy equation | $k\frac{\partial^2 T}{\partial X^2} = \rho.C_p.\frac{\partial T}{\partial t} + \frac{\partial q_r}{\partial X}$ | [4] |
| Thermal Insulating Value (TIV) | $(TIV)\% = 100.\left[1 - \left(\frac{K_t}{\varepsilon_0}\right) \Big/ L + \left(\frac{K_t}{\varepsilon_1}\right)\right]$ | [4] |
| Conversion of TIV to the Tog | $(TIV)\% = 100.\left[1 - \left(\frac{I_0}{I_1}\right)\right]$ | [4] |

## 3. PRELIMINARY FEASIBILITY STUDY IN OZANTEKS ON THERMAL COMFORT

Fabrics with different blends for preliminary work, thermal resistance according to different knitting structures TS EN ISO 11092: 2014 test standards;

Air temperature: 20˚C

Airspeed: 1 m/s

The humidity of the air: %65

Measuring unit temperature: 35˚C tests will be performed.

Preliminary feasibility studies have shown that the results of different thermal properties of selected sample fabrics for different yarn contents and different types of knitting are different and do not show adequate thermal resistance.

From this observation, it was decided to conduct tests with different yarn types and different knitting structures and thermal comfort parameters in the other phases of the research in our company meetings. variance analysis will be done

by measuring thermal resistance with five samples from sample fabrics to be made.


**Figure 1.** Sample fabrics to be tested

In this context, the most suitable knitting type and fabric content will be determined for optimum thermal comfort for Ozanteks Textile R & D Center, as well as test methods to be applied and heat transfer calculations and analyzes to be performed for thermal comfort.

## 4. CONCLUSIONS

Increased consumer expectations for textiles and comfort in clothing preferences have led researchers, textile and apparel manufacturers to produce more comfortable garment systems. In recent years, the development of subjective and objective comfort measurement and evaluation methods and the development of new materials, sportswear, protective clothing, Development. It is possible to produce highly sophisticated designs and products for the convenience of the fields. This thermal comfort study will be a linear method of numerical solution to support subjective test methods.

## REFERENCES

1. J.Y.Hu Lubos Hes Y.Li K.W. Yeung B.G.Yao,2006. Fabric Touch Tester: Integrated evaluation of thermal–mechanical sensory properties of polymeric materials. Polymer Testing, 25, 8, 1081-1090.
2. Romeli, D., Barigozzi, G., Esposito, S., Rosace, G., Salesi, G., 2013. High sensitivity measurements of thermal properties
1. of textile fabrics. Polymer Testing, 32, 1029-1036.
2. Oner, E., Okur, A., 2010. Materyal, Üretim Teknolojisi Ve Kumaş Yapısının Termal Konfora Etkileri. Tekstil ve Mühendis, 17(80), 20-29.
3. 4.Oner, E., 2015. Çeşitli Liflerden Üretilen Kumaşlardan Yapılan Spor Giysilerinin Termal Konforunun Değerlendirilmesi ve Geliştirilmesi. Dokuz Eylül Üniversitesi, Fen Bilimleri Enstitüsü, Doktora Tezi, s.,228, İzmir.
4. Abdel-Rehim, Z.S., Saad, M.M., El-Shakankery, M., Hanafy, I., 2006. Textile Fabrics as Thermal Insulators. AUTEX Research Journal, 6(3), 148-161.

5. Marmaralı, A., Kretzschmar, S.D., Özdil, N., 2006. Örme Kumaşların Isıl Özellikleri Üzerine Bir Araştırma. TUBİTAK Proje No: MİSAG-218
6. Onofrei, E., Rocha, A.M., Catarino, A., 2011. Investigating The Effect of Moisture on the Thermal Comfort Properties of Functional Elastic Fabrics. Journal of Industrial Textiles, 42(1), 34-51.
7. Chidambaram, P., Govindan, R., Venkatraman, K.C., 2012. Study of Thermal Comfort Properties of Cotton/Regenerated Bamboo Knitted Fabrics. African Journal of Basic & Applied Sciences, 4(2), 60-66
8. Ertekin, G., Marmaralı, A., 2011. Askı ve Atlamanın Düz Örgü Kumaşların Isıl Konfor Özelliklerine Etkisi. Tekstil ve Mühendis, 18(83), 21-26.
9. Marmaralı, A., Kretzschmar, S.D., Özdil, N., Oğlakcıoğlu, N.G., 2006. Giysilerde Isıl Konforu Etkileyen Parametreler. Tekstil ve Konfeksiyon, 4, 241-246.
10. Uzun, M., 2013. Konvansiyonel ve Kompakt Ring İplik Eğirme Yöntemlerinin Dokuma Kumaş Mukavemet ve Termal Özelliklerine Etkilerinin İncelenmesi. Marmara Üniversitesi, Fen Bilimleri Dergisi, 25(3), 91-99.
11. Güneşoğlu, S., Meriç B., 2006. Giysi ve Kumaşlarda Termal Temas Hissi. Tekstil ve Mühendis, 13(64), 33-37.
12. Kaplan, S., Okur, A., 2006. Tekstil Materyallerinde Meydana Gelen Isı ve Kütle Transferi Mekanizmalarinin Giysi Termal Konforu Üzerindeki Etkileri. Tekstil ve Mühendis, 13(62-63), 28-36.
13. Uzun, M., 2012. Ultrasonik ve Klasik Yıkama Yöntemlerinin Dokuma Kumaş Termal Özelliklerine Etkisinin İncelenmesi. Tekstil ve Mühendis, 19(86), 1-6.
14. Matusiak, M., 2006. Investigation of The Thermal Insulation Properties of Multilayer Textiles. Fibers&Textiles, 14(5), 98-102.
15. Rosace, G., Guido, E., Colleoni, C., Barigozzi, G., 2016. Influence of Textile Structure and Silica Based Finishing on Thermal Insulation Properties of Cotton Fabrics. International Jo0urnal of Polymer Science, Article ID 1726475, 1-10.

# A SUSTAINABLE APPROACH OF USING PRE-CONSUMER DENIM FABRIC WASTAGE AND RECYCLING PROCESS

**İsmail İVEDİ[1], Bahadır GÜNEŞOĞLU[1], Harri YAFFE[1], Sibel TOPBASAN[1]**

[1] Roteks Tekstil İhr. San. ve Tic. A.Ş.

Corresponding author: ismailivedi@roteks.com.tr

***Abstract:*** *The purpose of this study is to make the preliminary work to investigate potential of pre-consumer textile waste and recycling/reusing possibilities. For this purpose the waste points from fabric to final product in denim garment production process were determined. Then the fabric wastes arose from these points were collected.*

*The pre-consumer waste denim fabrics were then send to yarn mill and deconstructed into scraps and shredded into raw cotton again. This cotton fibre is then blended with recycled and virgin polyester to ensure good tensile strength. This yarn used as the weft while virgin polyester used as the warp yarn in the weaving process. Produced fabric with indigo shade used as pocket fabric in denim cloths and compared with the conventional pocket fabric. The effect of fiber types on yarn or fabric characteristics were investigated in accordance with planning design and construction.*

*There is no significant affect was observed in the resultant tenacity properties between the recycled yarn and conventional yarn. The results of this investigation show that the washing conditions have significant affect on the resultant fabric tear strength and shrinkage properties in all samples. These results shows the fabric include recycled materials can be used as pocket fabric of denim cloths.*

***Keywords****: Sustainable, recycling, denim, pocket, denim wastage*

## 1. INTRODUCTION

Every year million tons of textile waste is being sent to landfills. It is estimated that approximately half of the disposed textile waste is consisted of pre-consumer textile waste. Although the amount of pre-consumer textile waste is as high as post-consumer textile waste, recovering opportunities for pre-consumer textile waste is substantially disregarded. Pre-consumer textile waste is easier to reuse than post-consumer waste because it does not have the same hygiene and collection challenges (Lau, 2015).

Denim garments are made mostly of the seemingly pure and all natural plant based fibre that is cotton. Cotton is a crop plant which is grown world wide with 75% of it being cultivated in China, USA, India, Pakistan and Brazil. This thirsty plant depends on fertile land, intensive irrigation, pesticide spraying and a sunny climate in order to thrive. Cotton is often referred to as “White Gold” because of the high demand for this valuable natural fibre. Cotton agriculture is often

subjected to corruption and capitalism, which not only devastates the environment but suppresses farmers to work with hazardous chemicals and often for unfair pay. An average pair of jeans uses up to 3.781 litres of water in its full lifecycle with 70% of this precious water being used in cotton farming alone. Most of the worlds cotton is grown in arid regions where it depends on the limited supply of groundwater for irrigation. Water is the most precious natural resource on our planet and we depend on it for survival, yet 663 million people (1 in 10) lack access to safe water (unwater.org, 2017)

Denim jeans are normally hard wearing trousers traditionally made from cotton, with more modern versions using other fibres such as polyester and elastane, in twill weave structure. The classic Levi 501 jeans takes 33.4 kg of $CO_2$, 3.781 litres of water and 400,1 mJ of energy to produce, this is the equivalent of driving 69 miles, 246 hours of watching TV on plasma big screen (Levi's Co., 2015)

The purpose of this study is to make the preliminary work to investigate potential of pre-consumer textile waste and recycling/reusing possibilities. For this purpose the waste points from fabric to final product in denim garment production process were determined. Then the fabric wastes arose from these points were collected. The pre-consumer waste denim fabrics were then send to yarn mill and deconstructed into scraps and shredded into raw cotton again. This cotton fibre is then blended with recycled polyester to ensure good tensile strength. This yarn used as the weft while virgin polyester used as the warp yarn in the weaving process. Produced fabric with indigo shade used as pocket fabric in denim cloths and compared with the conventional pocket fabric. The breaking tenacity of recycled yarn was measured as 10 cN/tex according to ISO 7211-5:1984 standard while conventional weft yarn used in the pocket fabric composition was measured as 12 cN/tex. There is no significant affect was observed in the resultant tenacity properties between the recycled yarn and conventional yarn. Therefore the fabric include recycled materials can be used as pocket fabric of denim cloths.

The effect of fiber types on yarn or fabric characteristics were investigated in accordance with planning design and construction.

The results of this investigation show that the amount of recycled material have significant affect on the resultant fabric tear strength and shrinkage properties.

## 2. MATERIAL AND METHOD

9363V1 is the code name of fabric that used in the denim pockets constantly. This fabric used as control fabric for comparing the results between recycled fabrics and conventional fabric. Wlow refers to low degree washing conditions. Whigh refers to high degree washing conditions. P1 and P2 is the code name of fabric that were developed with recycled materials. Details are shown on the table below.

Waste of denim fabric containing different amount of raw materials such as polyester, cotton and lycra which were arose during the cutting process were

collected. Then pre-consumer denim fabric wastes are deconstructed into scraps and shredded into raw material again. These fibres are then blended with recycled polyester to ensure good tensile strength by recovery mill in Turkey, and woven into new denim pocket fabric by weaving factory in Turkey. At weaving process virgin polyester used as warp yarn.

Table 1 on the below, provides the properties of recycled yarns.

**Table 1.** Properties of recycled yarns

| Desing Code | Blending Composition (w/w) | Blending Type | Yarn Count | Breaking Tenacity (Rkm) | Yarn Twist (twist/m) |
|---|---|---|---|---|---|
| 9363V1 | %70 virgin CO %30 recycled CO | OE | 30/1 Nm | 12.2 | 580 |
| P1 | %50 recycle PET %50 recycle CO | Ring | 24/1 Nm | 10.5 | 870 |
| P2 | %50 recycle PET %50 recycle CO | OE | 24/1 Nm | 9.5 | 870 |

Sustainable denim fabrics were produced from these yarns used in weft according to fabric details from Table 2. After that, 25x25 cm pieces drawn from the fabric produced. Followed by two different washes were carried out for measuring the tear strength and shrinkage properties of fabric. Tear strength of the fabrics were carried out by using TITAN tensile testing device in conformity with ISO 13937-2. All of performance the tests were carried out after conditioning in standard atmospheric conditions according to TS EN ISO 139. Shrinkage properties of fabrics were measured according to ISO 3759 standard. Composition of fabrics are tested according to ISO 1833:2006, mechanical and chemical composition method. Abrasion resistance of fabric samples were measured according to BS EN ISO 12947-2:1999. The pressure value used in analysis was 595 g – 9kPa.

**Table 2**. Fabric properties

| Weft Yarn | Warp Yarn | Fabric Width | Warp End | Weft End | Mass per unit area (g/m2) |
|---|---|---|---|---|---|
| 30/1 Nm, OE | 100 Denier PES | 150 cm | 58 | 23 | 90 |
| 24/1 Nm, Ring | 70 Denier PES | 150 cm | 36 | 25 | 114 |
| 24/1 Nm, OE | 70 Denier PES | 150 cm | 36 | 25 | 115 |

## 3. RESULTS AND DISCUSSION

Table 3 shows the average shrinkage and tear strength of fabrics obtained from the results of two repeated washings, respectively, Wlow and Whigh. Furthermore, the relationships of shrinkage values between preferred fabrics and washing conditions were investigated.

**Table 3.** Average shrinkage and tear strength of fabrics

| Material | Mass per unit g/m2 (before wash) | Mass per unit g/m2 (after wash) | Washing Conditions | Shrinkage(%) | | Tear Strength (N) | |
|---|---|---|---|---|---|---|---|
| | | | | Mean Width | Mean Length | Warp | Weft |
| (P1)363670 | 114 | 115 | Wlow | 0 | 1.6 | 19.09 | 16.54 |
| (P2)363671 | 115 | 117 | Wlow | 0 | 1.2 | 16.46 | 10.66 |
| 9363V1 | 86 | 88 | Wlow | 0 | 1.8 | 21.35 | 16.26 |
| 9363V1-H | 86 | 83 | Whigh | 1 | 2.6 | 6.91 | 12.09 |
| (P1)363670-H | 114 | 108 | Whigh | 1 | 2.8 | 5.72 | 9.02 |
| (P2)363671-H | 115 | 112 | Whigh | 1 | 2 | 4.28 | 6.55 |

Composition test results are shown in Figure 1. According to figure there is no significant difference between 363670 and 363671. As it can be seen both 363670 and 363671 fabric samples include more cotton than 9363 fabric sample.

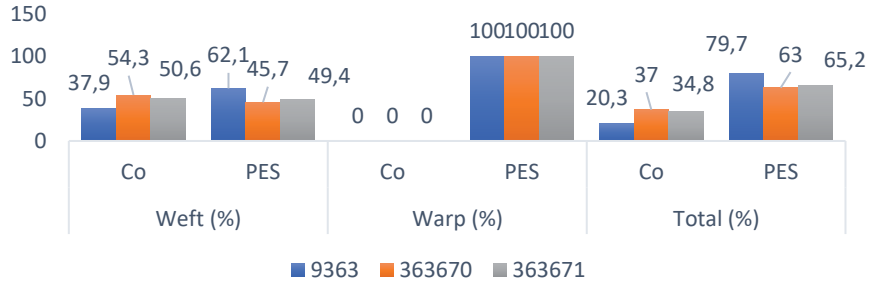


**Figure 1.** Composition analysis of fabric samples

Abrasion resistance of fabric samples are shown in Figure 2. According to results, abrasion resistance of samples directly related with washing conditions. As it can be seen on the Figure 2, the abrasion resistance value of samples decreases under high degree washing conditions. It can also be considered from the Figure 2 that as the amount of cotton increases, the abrasion resistance value increases.

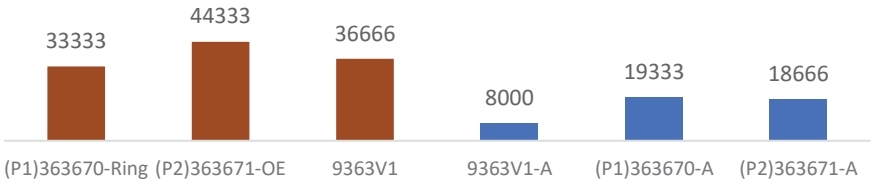


**Figure 2**. Abrasion resistance values of fabric samples

According to Figure 3 there is a significant difference between washing conditions on the shrinkage values. It can be seen on the table, washing conditions affect the resultant tear strength values. Also, it can be seen from the Figure 3, composition of samples affect the resultant tear strength values.

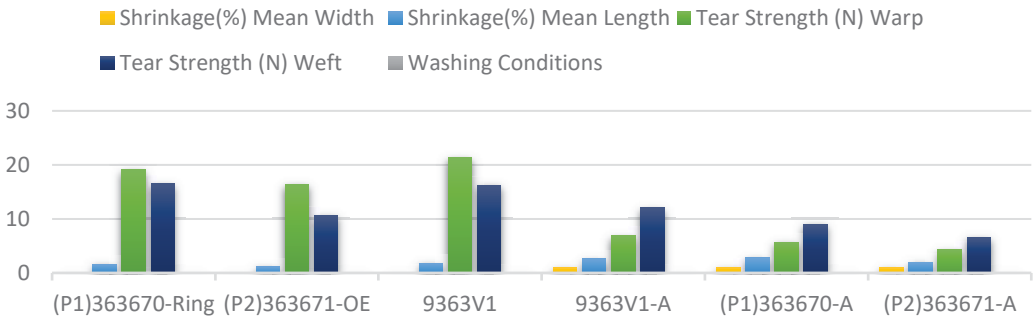


**Figure 3**. The relationship between fabric strength and shrinkage values

## 4. CONCLUSION

In this study, the recycle possibilities of pre-consumer denim waste fabrics as pocket fabric in denim garments were investigated. The results shows that there is no significant difference was observed in the resultant tenacity properties between the recycled yarn and conventional yarn. Also when tear strength and shrinkage values of samples were examined there is no significant difference was observed according to fabric and yarn properties. Washing conditions affect the resultant tear strength and shrinkage values as expected. This study shows that recycle material can be used in denim products as a pocket fabric. Abrasion resistance of samples are directly related with washing conditions. High degree of washing conditions are cause that decrease of abrasion resistance values.

## REFERENCES

1. Altun, Ş.:Prediction of Textile Waste Profile and Recycling Opportunities in Turkey. 2012. FIBRES & TEXTILES in Eastern Europe; 20, 5(94): 16-20.
2. Lau, Yuk-lan.: Reusing pre-consumer textile waste, 2015. Practical Social and Industrial Research (PSIR) Symposium. Wan Chai, Hong Kong
3. Levi Strauss & Co (2015). The lifecycle of a jean. San Francisco, USA.
4. WHO/UNICEF (2017). Joint Monitoring Programme for Water Supply, Sanitation and Hygiene (JMP)

# USING OF KNITTED FABRICS CONTAINING CHITOSAN FIBER AS HAEMOSTATIC EFFECT

**Kevser GÜNAL[1], Fatma KARAKADILAR[1]**

[1]Arıkan Mensucat San. Tic. A.Ş.

Corresponding author: fatma.inan@arikan.com.tr

***Abstract:*** *As a consequences of globalization, it is certain that human demand has been changing rapidly due to impact of economic and technological improvements since early 19th centry. Those changes have caused to face strict vital conditions such as war, traffic accident, industrial accident etc. Starting from this point, it is necessary to pay attention to use of textile products that helps rapid healing of disease and prevent bleeding in order to leave more beautiful and healthy world to next generations. In this context, it is very important to give the necessary importance biomedical textiles.*

*This study aims to determine how to stop bleeding easily and quickly by accelerating the clotting of open bleeding wounds. In order to do so, chitosan fiber reinforced cotton and viscose fibers were developed with supple woven fabrics and the blood-stopping activities of the developed knitted fabrics were investigated. It is believed that our new stop - bleeding fabric will be widely used in textile industry, particularly, in the field of military use.*

***Key Words****: Chitosan Fiber Effect, Antibacterial, Haemostatic Effect, Biomedical Textile, Technical Textile.*

## 1. INTRODUCTION

For years the development of techniques and products that have been able to prevent or stop the flow of the bleeding in first aid intervention has been a broad research topic in haemostatic (bleeding control) technology [1]. Despite significant progress in haemostatic technology over recent years, hemorrhages that can not be controlled, especially during wartime injuries, are among the leading causes of death [2,3]. In the most common method used to control blood loss, a gauze or direct continuous pressure is applied to the wound. However, this technique may be in adequate in the first intervention of serious injuries. Therefore, innovative strategies and methods continue to be the most important factor in the improvement and development of new generation haemostatic windings in the biomedical supplies market. In this context, the use of chitosan fiber is being used effectively. Chitin is widely found in the world from chitosan, resulting in the deacetylation of chitin, which is the main component of natural shell, crustacean shells [2,4].

## 2. AIM OF THE PROJECT

To provide consumer demands, products are obtained with methods that will not harm the ecological system. That means, natural and recyclable materials play

an active role. Antibacterial, anti – inflammatory and haemostatic products are important in terms of protecting human health, personal hygiene and comfort in textile products with functional properties. The production of textile products from renewable sources at low cost is an important feature which increases the added value of products that can be easily broken down in nature after completing the usage life. In this study, production of antibacterial, antiinflammatory and haemostatic properties of cotton fabrics alone and in different concentrations of chitosan will be of great benefit both economically and environmentally.

## 3. MATERIAL & METHOD

### 3.1. Haemostatic Effect

Because of chitosan is positively charged, it interacts with blood cells with reactive amino groups [7]. Since the outer membranes of the erythrocytes and thrombocytes are negatively charged, they are attracted by the positive charge of chitosan, leading to thrombocyte activation and thrombus formation[6]. Furthermore, in applications where chitosan is blood – stained, the positively charged chitosan attracts circulating plasma proteins and adsorbs to the material surface, resulting in platelet adhesion, activation of the material surface, and thrombus formation. With this feature, chitosan has been reported to be used for bleeding control purposes for therapeutic purposes. Chitosan increases the intracellular Ca2 + level of thrombocytes, depending on the dose. The increase in Ca2 + mobilization is one of the important mechanisms that cause chitosan to activate the platelet function.

### 3.2. Effect on Wound Healing

Chitosan adheres uniformly to the fresh wound area, and if adhesion does not occur, it is shown that infiltration fluid can accumulate and small air gaps that bacteria may proliferate. Chitosan has been shown to stimulate granule tissue formation by angiogenesis and wound healing by stimulating the release of growth factors from platelets. It has been also shown to stimulate haemostatic action, macrophage activation and cell proliferation during wound healing [8].

### 3.3. Chitin and Chitosan in Textile Industry

Although, the chrysanthemums are widely used in various countries, the rate is lower in our country. Textile industry is also used for many purposes [5].

For instance: to provide antimicrobial properties, reducing the amount of salt in reactive dye, dyeability of cotton with acid colors, to provide antistatic properties, use as deodorant material and medical textile applications can be counted.

## 4. CONCLUSION

In this study, various tests were applied to cotton fabrics made with chitosan and the blood – stopping properties of chitosan were investigated. Although, test results can not be explained at this stage in the light of commercial interests.

However, it has become clear that the fabric accelerates blood clotting. When the ongoing project of optimization is completed, the cost of biochemical products and medical textile products, which have no side effects to human health, will be obtained by providing haemostatic properties to the knitted fabrics that can be used as underwear and also the sea shells forming the waste loads in the nature will be prevented. In addition to that, the national economy benefit will be provided. Antibacterial and antiinflammatory properties of chitosan will also be examined in the later stages of the study.

## REFERENCES


1. Snow C.,Olson C., Melcer T.: TheNavyMedicalTechnologyWhatch: HemostaticDressingProductsforthe Battlefield. Naval HealthResearch Center.: Technical Document No.07-1A.
2. Champion H.R.,Bellamy R.F., Roberts C.P., Leppaniemi A.: A Profile of Combat Injury. J Trauma. 2003;54:S13-S19.
3. Stewart R.M.,Myers J.G., Dent D.L., et al. Seven HundredFifty-Three ConsecutiveDeaths in a Level TraumaCenter:theArgumentforİnjuryPrevention.J. Trauma.2003;54:66-70.
4. M.W.WAN, C.C.KAN.B.D.Rogel, M.L.P.Dalida, Carbonhydrate Polymers 2010, 80 sf.
5. Şahin, U.K., Gürsoy N.Ç., 2005, Tekstil Teknrisinde kitin ve kitosanaklar, Tekstil Teknik, Ağustos, s.176, 245
6. Rao SB., Sharma CP (1997): Use of chitosan as a biomaterial: Studies on its safety and hemostatic potential, J. Biomed. Mater. Res., 34, 21-28.
7. No HK, Park NY, Lee SH, Meyers SP, 2002. Antibacterial activity of chitosans and chitosan oligomers with different molecular weights. International Journal of Food Microbiology 74, 65 – 72.
8. Azad AK, Sermsintham N, Chandrkrachang S, Stevens WF. Chitosan membrane as a wound-healing dressing: characterization and clinical application. J Biomed Mater Res B Appl Biomater 2004;69:216–22.

# AIR PERMEABILITY AND BURSTING STRENGTH OF WEFT KNITTED FABRICS FROM GLASS YARN

**Mehmet Erdem İNCE[1], Hilal YILDIRIM[1]**

[1]Gaziantep University, Department of Textile Engineering, Turkey

Corresponding author: eince@gantep.edu.tr

***Abstract:*** *Technical textiles - designed according to the needs of use area - have penetrated many segments of our lives in the form of medicine, transportation, protection, agriculture, sports, packaging, and civil engineering products. The targets for technical textiles can be achieved by combining different basic textile skills of fibers, fabrics and finishing techniques with an accurate understanding the properties of raw materials. Transformation of glass fiber into fabrics offers unique properties for technical applications such as flame resistant protective clothing, impact resistant polymer composite. In recent years glass fiber is enormously used in composite applications as reinforcement because of its low cost and other characteristic properties. Weft knitting is a rapid and low-cost manufacturing technique that creates stretchable interlocked fabric architectures. The use of knitted technical textiles has been rising due to design of complex patterns, near-net-shape preforming, drape vability and easy-to-shape capability. In this study, the effect of cam setting (that create loose or tight fabric) and number of yarn ply (2-, or 3-ply yarn) on air permeability and bursting strength of weft knitted fabrics from glass yarn were tested. Tight cam setting increased fiber content, and stitch density that formed fabrics with shorter loop lengths. Fabrics from 3-ply yarn exhibited higher fiber volume percent; lower stitch density; and longer loop length than fabrics from 2-ply yarn. Fabrics knitted thru tight cam setting exhibited less air permeability, and higher bursting strength than those knitted thru loose setting. Fabrics from 3-ply yarn showed less air permeability and higher bursting strength than those from 2-ply.*

***Key Words****: glass yarn, weft knitted fabrics, bursting strength, air permeability*

## 1. INTRODUCTION

Weft knitting is low-cost, rapid, and versatile manufacturing technique that creates stretchable, porous, 3D, and interlocked fabric architecture. On the other hand, glass fibers have good mechanical properties in addition to flame and chemical resistance. Therefore, conversion of glass fibers into weft knitted fabrics leads to new avenues in technical textile applications: impact resistance composites, comfortable protective clothing, and flexible filter media.

Structure of knitted fabrics is affected from machine settings, yarn count and knit design parameters; and their performances are designed according to use area thru physical properties such as thickness, areal density, knit architecture, and loop length. Studies about the structure – property relationships of weft knitted fabrics from glass yarn are limited. This study is about the effects of cam setting

and number of yarn ply on air permeability and bursting strength of weft knitted fabric, and the literature review within this context is given below.

Mikučionienė et. al [1, 2, 3] investigated flammability and comfort properties of weft knitted single jersey fabrics by varying loop length, and number of yarn ply in a loop. They tested knit fabrics from Nomex Delta TA 18 tex×2 yarns with different yarn linear densities. Increase in loop length, or decrease in yarn linear density increased air permeability. Fabrics from high yarn linear density exhibited compact fabric structure with less air permeability and longer burning time.

Kane et. al [4] studied on dimensional stability, comfort, mechanical and other properties of tuck-knit and plain fabrics that were produced from ring and compact yarns with different loop length. Fabric properties such as dimensional stability, comfort, mechanical and handle were affected by loop length. Tuck-knit stitch fabrics had better performance in abrasion resistance, air permeability, water absorbency, thermal insulation, and mechanical properties. Air permeability and bursting strength properties of single jersey fabric were better than other structures.

Uyanık et. al [5] investigated effect of number and location of tuck stitches in knitted fabric produced by circular knitting machine on fabric properties. Knitted fabrics with tuck stitches possessed greater thickness, width and areal weight, and tuck stitches made the fabric more porous as compared with loop stitches. Strength and elongation of yarn and fabric structural parameters influenced bursting strength of knitted fabrics. When loop length increased, bursting strength decreased. The study indicated that location of tuck stitches are more decisive parameter than number of tuck stitches in view of bursting strength property.

Literature review indicated that generally synthetic and natural fibers were used in knitted technical textiles fabrics. The study on weft-knitted fabrics from glass yarn is limited. Literature review also indicated that loop length and knit architecture affected properties of the knitted fabrics significantly. In this study glass yarn and weft knitting process are preferred because glass fiber is cheaper than other fibers which are commonly used in technical textiles, and weft knitting process is low-cost. The aim of this paper is to reveal the effect of cam setting and number of yarn ply on physical properties, air permeability, and bursting strength of weft knitted fabrics from glass yarn.

## 2. MATERIALS AND METHODS

In this study: single-end yarn count of 133 tex, E-glass multi-filament yarn was consumed to manufacture fabrics on Brother KH-864 manual, flat weft knitting machine that has a fineness of 5E. Table 1 indicates the experimental plan of our study. Two input variables; cam setting and number of yarn ply were taken into consideration.

**Table 1.** Experimental plan of the study

| Variables: | Cam setting | Yarn ply number |
|---|---|---|
| Levels: | Loose fabric | 2-ply |
| | Tight fabric | 3-ply |

Tension dial (Figure 1-left) that is scaled from 0 to 10, and each scale being subdivided into three parts is rotated to adjust cam setting of the machine. This dial changes the size and correspondingly tension of the loops. 0 corresponds to the tightest tension (i.e. the smallest stitch) in which the needles go downhill to a specified level on the needle bed, once they passed the hooked yarn through the former loop; and 10 corresponds to the loosest tension (i.e. the largest stitch) in which the needles goes downhill to the lowest position on the bed, once the hooked yarn is passed through former loop. Figure 2-right demonstrates two fabric structures produced by lower and higher number of tension dial adjustments. In this study; two different tension dial settings were used; number 3 and 8, where number 3 formed a taut fabric structure (with smaller stitches), and number 8 formed a slack fabric structure (with larger stitches).

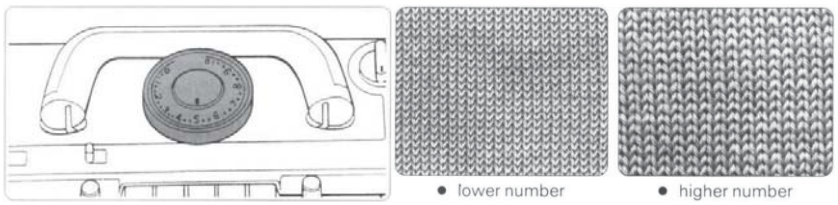


**Figure 1.** Tension dial of the knitting machine
(left) and fabric structures produced by different tension dial adjustments (right)

The second input variable was number of yarn ply as 2- and 3-ply. Thickness, areal density, course-density, wale-density, loop length, air permeability and bursting strength of the weft knitted fabrics from glass yarn were measured. Thicknesses of weft knitted fabrics were measured by digital thickness gauge with a pressure foot diameter of 21.15 mm. Areal density of weft knitted fabrics was measured according to ASTM D3776 [6]. A custom design die cutter with a surface area of 25 (5x5) cm² were used to cut 6 specimens from each sample for areal density and other physical properties analyses. Fiber volume percent was calculated using Equation 1. Glass fiber density was taken as 2,5 g/cm³.

$$\text{Fiber volume percent}, \% = \frac{\left(\frac{\text{fabric arealdensity,g/m}^2}{2{,}5}\right)}{\left(100*100*\left(\frac{\text{fabric thickness,mm}}{10}\right)\right)} * 100 \quad \ldots\ldots\ldots\ldots\ldots\ldots\ldots\ldots 1$$

Course and wale densities were measured according to ASTM D8007 [7]. Stitch density (number of stitches per centimeter square) was calculated from the multiplication of course and wale densities of the related sample. BS 5441 [8] was followed to measure loop length.

SDL ATLAS M021A test device was used to assess air permeability of weft knitted fabrics according to ASTM D737 [9] with a test area of 20 cm² and a pressure drop of 200 Pa. Air permeability was measured in cm³/(cm²×s) unit. Bursting strength was measured by James H. Heal TruBurst² Bursting Strength Tester according to ASTM D3786 [10]. Test area was chosen as 50 cm² (79,8 mm diameter). Pressure and distension units were selected as kPa, and mm respectively. Time to burst was adjusted as 20±5 seconds. Clamp pressure was set to 800 kPa to prevent slippage.

## 3. RESULTS AND DISCUSSION

### 3.1. The Effects of Cam Setting and Number of Yarn Ply on Physical Properties

Changing the cam setting from loose to tight fabric increased both thickness and areal density; and areal density increase rate (29,48 %) exceeded thickness one (15,28 %) that resulted in statistically significant increase in fiber volume percent which is roughly the ratio between areal density and thickness (Figure 2 and Table 2). In a similar vein, changing number of yarn ply from 2 to 3 increased fiber volume percent; however this change did not reach to statistically significant level due to very close increase rates of areal density and thickness; 34,84 and 31,34 % respectively.

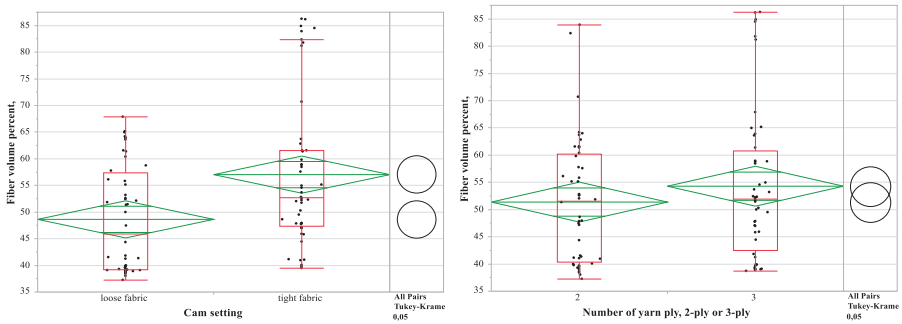


**Figure 2.** The effects of cam setting (left) and number of yarn ply (right) on fiber volume percent

**Note:** The distance between top and bottom ends of green diamond represents the 95% confidence interval. Comparison circles (given on the right column) for means those are significantly different either do not intersect, or intersect slightly. The height of red box (known as interquartile range) is a quantitative indication of variation.

**Table 2.** The effects of cam setting and number of yarn ply on fiber volume percent (%)

| Variable | Level | Mean | SD | LL | UL | p-value |
|---|---|---|---|---|---|---|
| Cam setting | loose fabric | 48,64 | 10,01 | 45,73 | 51,54 | 0,0005 |
| | tight fabric | 57,03 | 13,97 | 52,97 | 61,09 | |
| # of yarn ply | 2-ply | 51,37 | 11,46 | 48,05 | 54,70 | 0,2670 |
| | 3-ply | 54,29 | 13,99 | 50,23 | 58,35 | |

**Note:** Significance level (α) was determined as 0,05. p-values greater than 0,05 were colored in black and show lack of statistical significance.

Due to accommodation of more small-size loops per unit fabric area; cam setting change from loose to tight fabric enhanced course and wale densities that improved stitch density at statistically significant level (Figure 3 and Table 3). Due to greater size of 3-ply yarn than 2-ply one; fabrics from 3-ply yarn exhibited less course and wale densities than fabrics from 2-ply ones; therefore, number of yarn ply lowered stitch density at statistically significant level. Due to smaller p-value of cam setting change; cam setting exhibited more pronounced effect on stitch density than number of yarn ply.

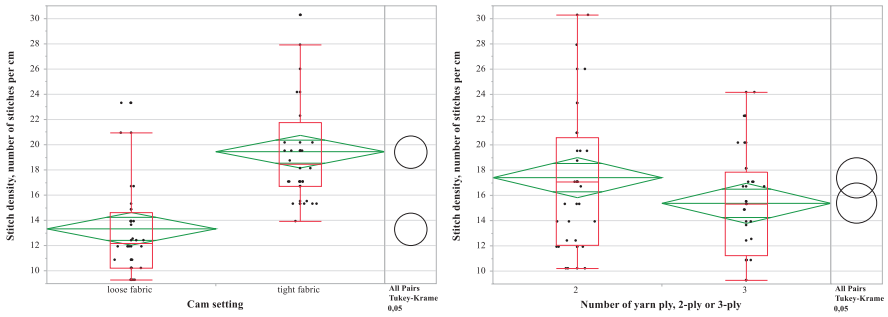


**Figure 3.** The effects of cam setting and number of yarn ply on stitch density

**Table 3.** The effects of cam setting and number of yarn ply on stitch density (number of stitches per $cm^2$)

| Variable | Level | Mean | SD | LL | UL | p-value |
|---|---|---|---|---|---|---|
| Cam setting | loose fabric | 13,34 | 4,02 | 12,05 | 14,62 | < 0,0001 |
| | tight fabric | 19,45 | 4,19 | 18,11 | 20,79 | |
| # of yarn ply | 2-ply | 17,41 | 5,67 | 15,60 | 19,22 | 0,0375 |
| | 3-ply | 15,38 | 4,31 | 14,00 | 16,76 | |

While cam setting lowered loop length via creating smaller size loops at statistically significant level; number of yarn ply increased loop length at statistically non-significant level due to spread of higher-ply loops over a larger area (Figure 4 and Table 4).

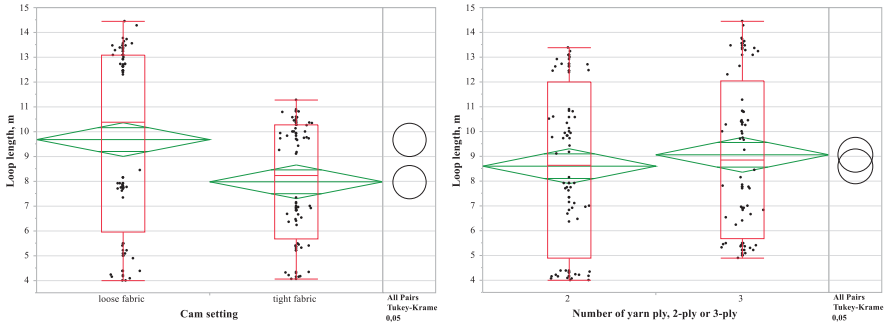


**Figure 4.** The effects of cam setting and number of yarn ply on loop length

**Table 4.** The effects of cam setting and number of yarn ply on loop length (mm)

| Variable | Level | Mean | SD | LL | UL | p-value |
|---|---|---|---|---|---|---|
| Cam setting | loose fabric | 9,68 | 3,65 | 8,87 | 10,49 | 0,0003 |
| | tight fabric | 7,98 | 2,37 | 7,45 | 8,50 | |
| # of yarn ply | 2-ply | 8,60 | 3,23 | 7,88 | 9,32 | 0,1813 |
| | 3-ply | 9,06 | 3,13 | 8,36 | 9,75 | |

### 3.2. The Effects of Cam Setting and Number of Yarn Ply on Air Permeability and Bursting Strength

Changing cam setting from loose to tight fabric created tight fabrics with higher fiber content, and higher stitch density with shorter loop lengths that decreased the permeability of the fabrics against air at statistically significant level (Figure 5 and Table 5). Number of yarn ply enhanced fiber volume percent, lowered stitch density, and increased loop length; combination of all these effects lowered air permeability of fabrics with 3-ply yarn as compared with those with 2-ply yarns at statistically non-significant level (Figure 5 and Table 5).

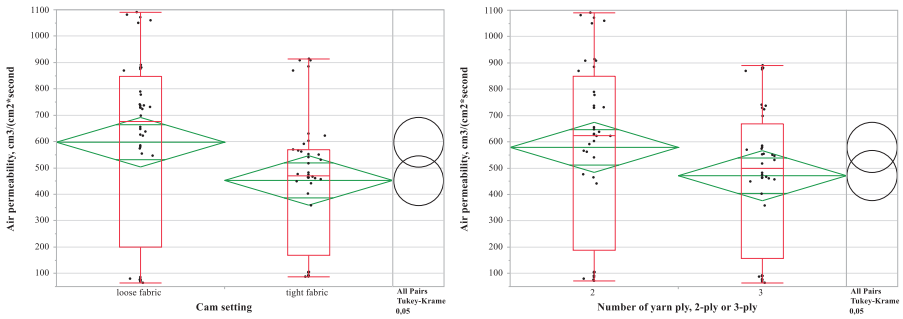


**Figure 5.** The effects of cam setting and number of yarn ply on air permeability

**Table 5.** The effects of cam setting and number of yarn ply on air permeability ($cm^3/(cm^2*s)$)

| Variable | Level | Mean | SD | LL | UL | p-value |
|---|---|---|---|---|---|---|
| Cam setting | loose fabric | 597,59 | 338,36 | 489,38 | 705,81 | 0,0165 |
| | tight fabric | 452,68 | 251,54 | 372,24 | 533,13 | |
| # of yarn ply | 2-ply | 578,97 | 333,67 | 472,26 | 685,89 | 0,0576 |
| | 3-ply | 471,30 | 266,92 | 385,94 | 556,67 | |

Due to their higher fiber volume percent, higher loop density with shorter loops as compared with loose fabrics; fabrics knitted via tight cam setting displayed higher bursting strength than fabrics knitted via loose cam setting (Figure 6 and Table 6). Number of yarn ply increased fiber volume percent, and loop length at

statistically non-significant level; lowered stitch density at statistically significant level; however it improved bursting strength at statistically significant level. This behaviour of fabrics from 3-ply yarns can be explained through greater load bearing capability of 3-ply yarns than 2-ply ones.

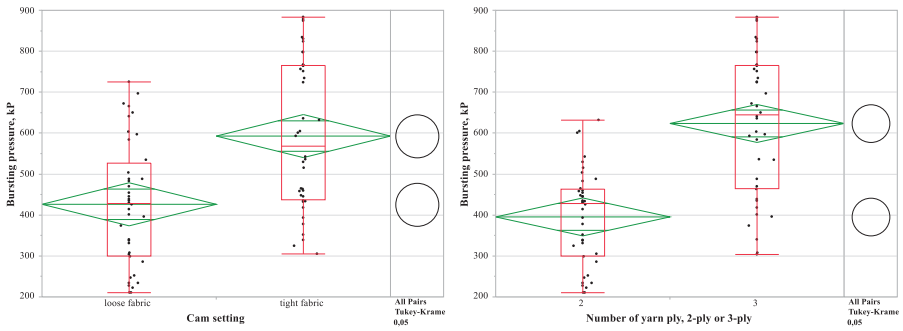


**Figure 6.** The effects of cam setting and number of yarn ply on bursting strength (kPa)

**Table 6.** The effects of cam setting and number of yarn ply on bursting strength (kPa)

| Variable | Level | Mean | SD | LL | UL | p-value |
|---|---|---|---|---|---|---|
| Cam setting | loose fabric | 426,19 | 151,70 | 377,67 | 474,70 | <0,0001 |
| | tight fabric | 592,80 | 181,07 | 534,89 | 650,71 | |
| # of yarn ply | 2-ply | 395,39 | 115,88 | 358,33 | 432,35 | <0,0001 |
| | 3-ply | 623,60 | 172,92 | 568,30 | 678,90 | |

## 4. CONCLUSIONS

Weft knitted fabrics from glass yarn were produced while varying cam setting and number of yarn ply within the full factorial experimental study design perspective of this study. While cam setting was as loose and tight fabric; number of yarn ply was varied as 2-, and 3-ply. Cam setting change from loose fabric with long loops to tight fabric with short loops increased fiber volume percent and stitch density that lowered air permeability and increased bursting strength at statistically significant level. On the other hand, number of yarn ply increase from 2 to 3 increased fiber volume percent and loop length at statistically non-significant level, and lowered stitch density at statistically significant level that improved bursting strength at statistically significant level. This study clearly indicated response of glass yarn in the form of weft knitted fabrics against cam setting and number of yarn ply change in view of air permeability and bursting strength.

## REFERENCES

1. Mikučionienė D., Baltušnikaitė J., Milašius R.: Influence of the number of yarns in a loop on the flammability of knits. 2011. FIBRES & TEXTILES in Eastern Europe v. 19, No. 6 (89), 71-74.
2. Mikučionienė D., Milašiūtė L., Baltušnikaitė J., Milašius R.: Influence of plain knits structure on

flammability and air permeability. 2012. FIBRES & TEXTILES in Eastern Europe v. 20, No. 5 (94), 66-69.

3. Mikučionienė D., Milašiūtė L., Milašius R.: Influence of knits structure on flammability and comfortability. 2014. AUTEX Research Journal v. 14, No. 4, 226-232.
4. Kane CD, Patil UJ, Sudhakar P.: Studies on the influence of knit structure and stitch length on ring and compact yarn single jersey fabric properties. 2007. Textile Research Journal v.77, No. 8, 572-582.
5. Uyanık S., Değirmenci Z., Topalbekiroğlu M., Geyik F.: Examining the Relation Between the Number and Location of Tuck Stitches and Bursting Strength in Circular Knitted Fabrics. 2016. FIBRES & TEXTILES in Eastern Europe. v. 24, No. 1(115), 114-119.
6. ASTM D3776M, Standard Test Methods for Mass Per Unit Area (Weight) of Fabric, 2017
7. ASTM D8007, Standard Test Method for Wale and Course Count of Weft Knitted Fabrics, 2015
8. BS 5441, Methods of test for knitted fabrics 1988.
9. ASTM D737, Standard Test Method for Air Permeability of Textile Fabrics, 2018.
10. ASTM D3786, Standard Test Method for Bursting Strength of Textile Fabrics – Diaphragm Bursting Strength Tester Method, 2018

# ANTI-STATIC KNITTED FABRIC

**Alaaddin AKKÜNCÜ[1], Ali Uğur PABUÇÇU[1]**

[1]ÇMS Tekstil Ar-Ge Merkezi

Corresponding author: aakkuncu@balsuyu.com

***Abstract:*** *Interest of the technical textile have increased day by day from consumers. With the help of the developing technology, the importance of the protective textile structures have taken attention among the technical textiles. In the technical textiles, Protective textiles are one of the application area having the lowest production ratio. On the other hand, especially in the developing countries, as the industrial development escalades, and new standards and the sanctions impose on the health, security and hygiene, the demands towards protective cloths have been soaring. In this study, it was aimed at obtaining anti-static knitted fabric by using carbon fiber in knitting as an anti-static electric material. Carbon fibers were given into yarn while blending. After yarn producing, was knitted double pique and dyed. Conductivity of the fabric was tested according to both TS EN 1149-2: 2000 standard and UNE-EN 1149-3:2004 standard. Data from conductivity tests were showed that carbon fiber could be used as a static charger in protective clothing. This provides comfortable and effective working area for workers.*

***Keywords****: Carbon fiber, anti-static, protective clothing, knitting fabric, technical textile.*

## 1. INTRODUCTION

In daily life, expectations from textiles have increased. Consumers expect from textile not only wearing, but also some functions. With the usage of technical textiles, such spesific functions could be gained. Technical textiles almost fall into every aspect of our lives. Moreover, technical textile uses for the comfort. This comfort is protecting workers from static electric. Carbon fiber has the excellent conductivity, so it can be used for anti-static material.

Usage area with the development and applicability of carbon fibers it expanded. Its main areas of use are defense apparel, space vehicles, the automobile industry, medical uses (especially in orthopedic operations) and so on. [1]

Static charge usually builds up in synthetic fibres such as nylon and polyester because they absorb little water. Cellulosic fibres have higher moisture content to carry away static charges, so that no static charge will accumulate. As synthetic fibres provide poor anti-static properties, research work concerning the improvement of the anti-static properties of textiles by using nanotechnology were conducted. [5]

Static electricity poses a real threat to human life, health and material resources. This risk is presented in many spheres of human activity, especially in dangerous working environments where electrostatic fields and discharges may cause fire or explosions, as well as disturbances in the production process [6].

An antistatic agent is a compound used for treatment of materials or their surfaces in order to reduce or eliminate buildup of static electricity generally caused by the triboelectric effect. The molecules of an antistatic agent often have both hydrophilic and hydrophobic areas, similar to those of a surfactant; the hydrophobic side interacts with the surface of the material, while the hydrophilic side interacts with the air moisture and binds the water molecules [7].

Antistatic fabric is a type of technical textile which is sought by manufacturers of work uniforms. These fabrics are used in the construction of work uniforms for hospitals, electronic industry firms, electrostatically affected dye house, pharmaceutical and medical equipment manufacturers and research laboratories, and are also needed for the use of military personnel, fuel and gas handling personel. When it is desired to give antistatic properties to fabrics, electrical conductivity is increased by adding additives such as conductors (carbon, metal dust or conductive polymer) to yarns and fibers. [2]

In the production of carbon fibers, as a result of the heating of organic raw materials other atoms get away except carbon so that filaments made of carbon atoms are obtained. After crystallization of these filaments, high strength fibers are obtained.[3]

Carbon fiber has each crystallite consists of multiple layers. Each layer consists of carbon atoms arranged in a hexagonal structure called the graphene layer. While strong C-C bonds in the layer give high strength and stiffness to fiber, weak van der Waals bonds between the layers lead to an increase in shear resistance, resulting in excellent heat and electrical conductivity [3].

Static charges generally occur on the surface of synthetic polymers such as polyester and nylon fibers because they provide a low moisture content when compared to more hydrophilic cellulosic fibers [4].

In this study, it was aimed at obtaining anti-static knitted fabric by using carbon fiber in knitting as an anti-static electric material. Carbon fibers were given into yarn while blending. After yarn producing, was knitted double pique and dyed. Conductivity of the fabric was tested according to both TS EN 1149-2: 2000 standard and UNE-EN 1149-3:2004 standart. Data from conductivity tests were showed that carbon fiber could be used as an static charger in protective clothing.

## 2. MATERIAL AND METHOD

### 2.1. Material

Carbon fiber was added into yarn while blending. Mixing ratio was %65 cotton, % 34 poliester and %1 carbon fiber. Yarn number was 24/1 Ne Combed spinning. Containing carbon fiber yarn was knitted in 30 inch 28 fein kemyong knitting machine as a double pique after spinning. Raw fabric was dyed by reactive and dispers dyestuff.

### 2.2 Method

With the aim of determining antistatic properties of the fabric containing carbon

fibers, samples were measured by two different test methods (TS EN 1149-2: 2000 standard, UNE-EN 1149-3:2004 standard).

TS EN 1149-2: 2000 standard, a test method for measuring the vertical electrical resistance of protective clothing materials. In this standard, the test samples were tested after 24 hours of conditioning at 23 ± 1 $^0$C temperature and 25 ± 5% relative humidity.

UNE-EN 1149-3:2004 standart, a test method for measuring the electrostatic properties of protective clothing. Before this method is applied, the washing process is carried out according to ISO 6330: 2012 standard. The samples in the study were subjected to 5 washes at 40 $^0$C and applied flat drying procedure in this standard. Test samples were tested after 24 hours of conditioning at 23 ± 1 $^0$C temperature and 25 ± 5% relative humidity. Ambient conditions test was at 23,0 $^0$C temperature and 26,2 % relative humidity. In this test method induction charge, (1200 ± 50) V in 30 µs potential was applied throughout 30s.

## 3. RESULTS AND DISCUSSION

The test was repeated 10 times and the average was taken. Knitted fabric tested according to TS EN 1149-2:2000 Vertical Resistance and result was 4,2*107 ohm (Ω) (Table 1.), this average value is range from min: 2,2*107 Ω to max: 7,5*107 Ω). It was seen that the fabric containing carbon fiber showed anti-static properties.

**Table 1.** According to TS EN 1149-2:2000 test result

| TYPE OF FABRIC | ANTISTATIC FEATURE |
|---|---|
| 24/1 Combed Cotton –Pes Double Pique | 4,2 x 107 ohm (Ω) |

According to the standart UNE-EN 1149-3:2004 for the induction charge method result was $t_{50}$ < 4 s or S > 0,2 ($t_{50}$=Decay half time, S=Shielding factor). Data from the fabric containing carbon fiber showed that shielding factor avarage of the fabrics were 0.24, decay half time avarage were 1.23 seconds. (Table 2). On considering of these taken results from both standards, it could be said that adding of the carbon fibers in the yarn could be gained anti-static properties of the fabric.

**Table 2.** According to UNE-EN 1149-3:2004 test result

| **Reference** | **SET OF JACKET AND TROUSERS BTS GMN 2000PLUS** | |
|---|---|---|
| Specimen | Shielding factor (units) | Decay half time (s) |
| 1 | 0,23 | 1,54 |
| 2 | 0,27 | 1,05 |
| 3 | 0,23 | 1,11 |
| **Average** | **0,24** | **1,23** |

## 4. CONCLUSION

Technical textile are everywhere in our lives. They make life easy, comfort and effective. Carbon fiber has the most important place in technical textiles. Carbon fiber has many usage area and one of the area is using as a protective material. People need to be comfort while working so carbon fiber was used for antistatic material. In this study, carbon fiber were used for obtaining anti-static knitted fabric. Taken results from employed different standarts showed that carbon fiber could help fabrics to gain anti-static properties.

## REFERENCES

1. Yaman E., Öktem T., Seventekin N.: Karbon liflerinin üretimi. 2006. Tekstil ve Konfeksiyon Dergisi.
2. Özyüzer L., Meriç Z., Selamet Y., Kutlu B., Cireli A.: Mıknatıssal saçtırma sistemi ile metal kaplanan polipropilen liflerinin antistatik ve antibakteriyel özellikleri. 2010. Tekstil ve Mühendis Dergisi.
3. Yaman E., Öktem T., Seventekin N.: Karbon liflerinin özellikleri ve kullanım olnakları üretimi. 2007. Tekstil ve Konfeksiyon Dergisi.
4. Abdel-Halim S.A., Abdel-Mohdy F.A., Al-Deyab S.S., El-Newehy M.H: 2010. Chitosan and monochlorotriazinyl-β-cyclodextrin finishes improve antistatic properties of cotton/polyester blend and polyester fabrics. Carbohydrate Polymers 82 (2010) 202-208.
5. Wong Y. W. H., Yuen C. W. M., Leung M. Y. S., Ku S. K. A., Lam H. L. I.: Selected applications of nanotechnology in textiles. 2006. Autex Research Journal, Vol. 6.
6. Kowalski J.M., Wroblewska M.: Premises for practical evaluation of the anti-electrostatic properties of protective garments. Fibres & Textiles in Eastern Europe. Vol. 14, No.5(59).
7. Patra J. K., Gouda S.: Application of nanotechnology in textile engineering. 2013. Academic Journals. Vol. 5(5), PP 104-111.

# IMPROVING OF THERMOREGULATION PROPERTIES OF DENIM GARMENT WITH THE HEAT STORING MICROCAPSULE APPLIED

**Sevda KÖKSAL DABAN[1], Sercan YAZ[1]**

[1] ERAK Giyim Ar-Ge Merkezi

Corresponding author: sevda.daban@erak.com

***Abstract:*** *The aim of this study is to improve thermal regulation property in denim garment. Phase change materials are the textile chemicals which can stabilize the temperature of a material by absorbing or releasing heat. Microencapsulated PCM chemical was applied experimentally 150 g/Land 300 g/L different rate with dipping and spraying method when 1 g/L polymer cross linker is used and not used. Thermoregulation property of denim garments were analyzed by DSC test method. The best result was obtained in 300 g/L PCM and 1g/L polymer cross linker by with ΔH of 9,809 J/g.*

***Keywords****: Phase Change Material (PCM), Denim, Thermoregulation properties*.

## 1. INTRODUCTION

Thermal equilibrium between body and environment is vital necessity for humans due to keep health. With this consciousness, textile industry is developing innovative methods to improve thermal capacity of the clothing. For the thermal management in clothes, innovative agents as phase change materials (PCMs) have been used intensively. PCMs are preferred due to their thermal energy storage properties. It's use in textiles is based on a research program initiated by NASA (National Aeronautics and Space Administration) with the aim of heat protection of astronaut wears at the beginning of the 1980's [1].In the last years many researchers intensified their research on the subject ([5]; [3]; [6]; [7]; [8]). Due to absorb, store and release of heat capability pf PCM's, they can be used in textiles as heat exchanger units. While physical state of PCM's changing, it can absorb energy and delay chilling when physical conditions become reversed. They have positive effect on textiles as heat bariier agents witout changing temperature themselves while environmental conditions changing. In textile ındustry, lots of phase changing chemicals like Octadecane, Nanodecane, Eicosane, Heptodecane uses, however they are usually known with their trading names in scientific papers as PCM28, PCM15. Due to has strong properties as chemical and thermal stability, paraffinic hydrocarbon PCM's are more useful than fatty acid PCM's in textiles [4]. Due to their liquid phase, PCMs are microencapsulated to prevent it's stem. Denim garment microencapsulated PCM chemical has been applied experimentally in various process and recipes in industrial laundry at finishing stage and PCM application has been tested whether

thermal regulation is achieved at working temperature of PCM material, in these different process conditions[2].For these purpose heat storage properties of the denim garment were evaluated following an encapsulation of PCM with dipping and spraying method when polymer cross linker is used and not used, with PCM usage in different rate.

## 2. MATERIAL AND METHOD

### 2.1 Material

Denim woven fabrics with 99% cotton and 1% elastane suitability were used for the application of heat-setting microcapsules. The particle size is approximately 20µm, microcapsules (Rudolf Durener, Bursa) containing paraffin with a melting temperature of 28°C, melting enthalpy of 195-205J/g, density of 0.78g/ml were used. Cross-linker was used (Lava Protect XL,DyStar ) as an auxiliary product.

**Table 1.** Properties of fabric used in trials

| Structure | Composition | Warp density (threads/cm) | Weft density (threads/cm) | Weight in grams ( $g/m^2$ ) |
|---|---|---|---|---|
| Weave | %99 cotton+%1 elastane | 28 | 21 | 387 |

### 2.2 Method

For using trials, 8 trousers were sewn with finished fabric. Before the application of PCMs to the denim pants, stone washing and stone enzyme washing were carried out with the aim of giving vintage effect and clean the fabric surface. Microcapsules were applied at different concentrations using the dipping and spray methods (Table 3). Thus, the variation in heat storage capacities of denim garments containing microcapsule PCM at different rates was investigated.

**Table 2.** Denim garment washing receipt of PCM application

| Process No. | Process | Process Detail |
|---|---|---|
| 1 | Dry Process | Laser Scrabing |
| 2 | Prewash | Rinsing(50°C, 3min) |
| 3 | Stonewash | Stone +stone enzyme (45°C, 20min)<br>Rinsing (20°C, 2 min)x2<br>Extracting,<br>Dryig (70°C, 30min) |
| 4 | PCM Application | Dipping<br>Spray |
| 5 | Finishing | Drying(100°C,15 min)<br>Fixation (160°C, 10min) |

**Table 3.** The process properties of PCM applications.

| Recipe | PCM Application Method | Concentration of The PCM. | Drying and Fixation |
|---|---|---|---|
| R1 | Dipping | 150 g/L | Drying-100°C 15 min. Fixation-160°C 10 min. |
| R2 | Spray | 150 g/L | |
| R3 | Spray | 300 g/L | |
| R4 | Spray | 150 g/L | |

***Dipping Method***

The inverse surface of denim garment was dipped into PCM solution prepared with duration 2 min. 300g/L concentration of Microcapsulated PCM was applied on the denim garment by dipping method (as shown in Table 3). After the dipping process, the denim garment was dried and fixation (Table 3).

***Spray Method***

Different concentration is 150g/L and 300g/L of PCM solutions were applied on inverse surface of denim garment by spray process. After the spray process, the denim garment was dried and fixation (Table 2). In R1 and R2 receipts, cross linker was not used in PCM solution. In R3 and R4 receipts, 1g/L cross linker was used in PCM solutions.

### 2.2.1 Optical Microscopy Analysis

Microcapsul existence was observed with optical microscope analysis. For this purpose Olympus BX-51 microscope and Q-Capture digital imaging programme were used.

### 2.2.2 Differential Scanning Calorimeter (DSC) Analysis

A differential-scanning calorimeter (DSC) is used to measure the heat capacity or enthalpy of the microcapsules and the fibre containing the microcapsules. The heating and cooling rates of the DSC run were both 10°C/min in the nitrogen atmosphere. Latent heat accumulation of PCM was viewed on DSC graph curve with unit of $\Delta H$ (Joule/g). Perkin Elmer-Jade DSC 'instrument was used in DSC analysis.

## 3. RESULTS AND DISCUSSION

In this study, the application of microencapsulated PCM chemicals to denim garments at different methods and concentrations has been examined to improve the thermal regulation of denim garment.

### 3.1 Optical Microscopy Analysis

Microscopic images of microcapsules were examined to explain the presence of microcapsules in the fabric structure of the microcapsulated PCM applied denim garment. Figure 1 shows microscope images of microcapsules which were seen at 40x magnification. When the images obtained from the optical microscope are

examined, microcapsules are seen in the form of particles on the fiber surface (Show in Figure1)

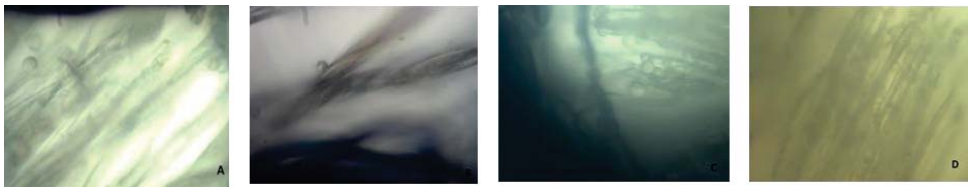

**Figure 1.**Optical Microscope images of fabric tread with microencapsuled PCM using A)150g/LPCM by dipping**,** B)150g/LPCM by spray, C)300g/L PCM with 1 g/L cross-linker by spray, D)150g/L PCM with 1 g/L cross-linker by spray

### 3.2 Differential Scannin Calorimeter (DSC) Analysis

The DSC analysis was performed to get the samples' phase change temperature range and enthalpy. The testing temperature range was −20 to 50°C, and the scanning speed was 10°C/min with liquid nitrogen protection. ΔH (J / g) value on the graph shows the amount of latent heat stored by the PCM. As this value increased, the phase change performance on the surface of the chemical also increased.

The melting temperatures and solidification temperatures and enthalpies of different amounts of microencapsuled PCM treated denim fabric samples were measured using a DSC instrument.

**Table 4.** Δ*H* (J/g) values of PCM applications

| Receipt Number | PCM Application Method | ∆H (Joule/g) |
|---|---|---|
| **R1** | Dipping | 2.855 |
| **R2** | Spray | 1.122 |
| **R3** | Spray | 9.809 |
| **R4** | Spray | 3.919 |

R1 and R2 are the recipes with the same concentration of PCM but with different application method. No crosslinkers were used in solution in the R1(150 g/L PCM) spray and R2(150g/L PCM) dipping method. As seen the table 4, when the value of ∆H is taken into consideration, the dipping method gave better result was obtained in R1(150 g/L PCM by dipping) with ∆H of 2.855j/g than the spray method. There are two DSC graphs are figure 2 and figure 3, belonging to recipe 1 and recipe 2 which were given as R1 and R2.

However, white spots are formed on denim pants in R1 method(Show in Figure4). Thus, the spray method was used in the R3 and R4 experiments.

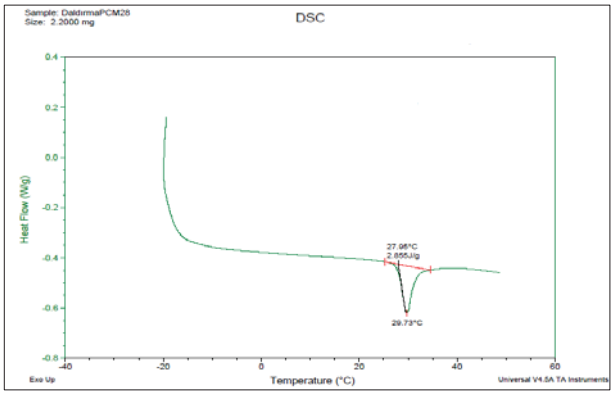


**Figure 2.** DSC graph of R1 (15Og/L PCM by dipping)

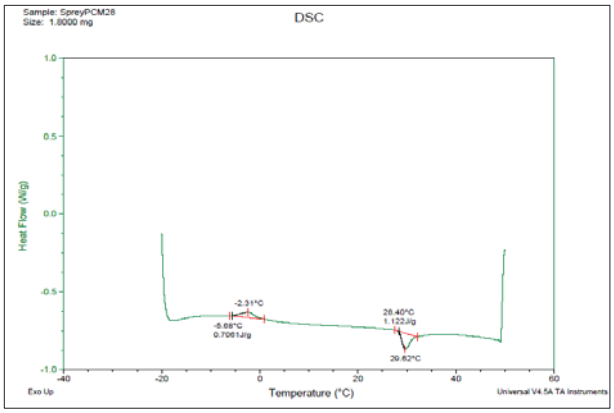


**Figure 3.** DSC graph of R2 (150g/L PCM by spray)

**Figure 4.** White spots are on denim garment

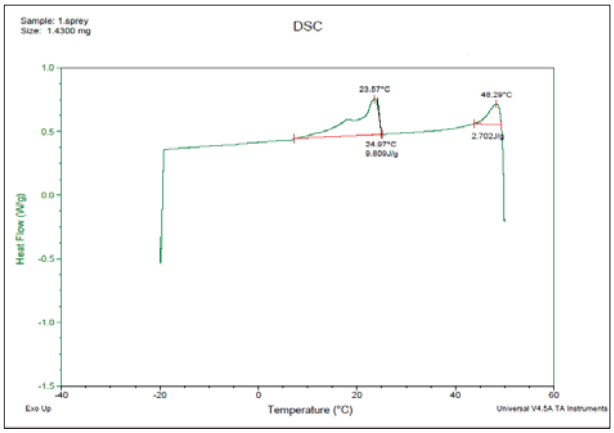


**Figure 5.** DSC graph of R3 (300g/L PCM with 1 g/L cross-linker by spray)

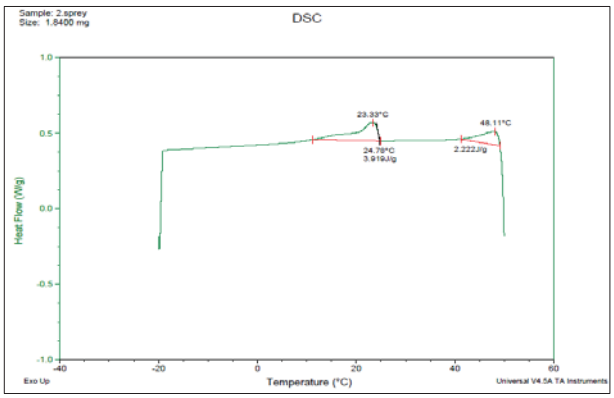


**Figure 6.** DSC graph of R3 (150 g/L PCM with 1 g/L cross-linker by spray)

300 g/L PCM in the R3 and 150 g /L PCM in the R4 method and 1 g/l cross linker in both methods were used. It has been observed that when the PCM concentration increased the ΔH value of the fabric increased. Despite the use of 150 g/L PCM in the R2 and R4 methods, the use of a 1 g/L cross-linker indicated that the amount of capsule adhering to the fiber surface and the ΔH value increased as a result of DSC analysis.

## 4. CONCLUSION

In this study, microencapsulated PCM was applied on denim garment various concentration by dipping and spray method. Thermo-regulating properties of the denim garments were compared as a result of DSC analysis measurements. Microscopic images of microencaplused were examined to explain the presence

of microcapsules in the fabric structure of the microencaplused PCM applied denim garment. Although the dipping method was showed better results than the spray method, application is not preferred due to causes white spots on the clothing. It has been observed that both PCM capsules increase the concentration in solution in the spray method and the use of 1g/L crosslinkers improves the heat regulation property. As PCM concentration increases, the heat storage or release capacity increases in terms of J/g. Consequently, it is possible to conclude from the preliminary results of PCM application that phase change material improve the thermoregulation properties of denim garments.

## REFERENCES

1. Tözüm M.S., Demirbağ S., Aksoy S.A., 2011. Isı Depolayan Mikrokapsül Uygulanmiş Kumaşların Isi Düzenleme Özelliklerinin Araştırılması., Tekstil ve Mühendis, 18(84):1-14.
2. Saraç G.Ö. 2015. Denim Giyside Isıl Düzenleme Özelliğinin Geliştirilmesi (Yüksek Lisans Tezi). Çukurova Üniversitesi Fen Bilimleri Enstitüsü, 81 s.
3. Karthikeyan M., Ramachandran T., Shanmuga Sundaram OL. 2014. Nanoencapsulated phase change materials based on polyethylene glycol for creating thermoregulating cotton. Journal of Industrial Textiles 44(1): 130-146.
4. Arjun D. and Hayavadana J. 2014. Thermal Energy Storage Materials (PCM's) for Textile Applications. Journal of Textile and Apparel, Technology and Management, 8(4): 1-11.
5. Tomaszewski W., Twarowska-Schmidt K., Moraczewski A., Kudra M., Szadkowski M., Palys B. 2012. Nonwovens with Thermal Storage Properties Based on Paraffin-Modified Polypropylene Fibres. FIBRES&TEXTILES in Eastern Europe, 20, 6B(96):64-69.
6. Liu X, Lou Y. 2015. Preparation of Microencapsulated Phase Change Materials by the Sol-gel Process and Its Application on Textiles. FIBRES&TEXTILES in Eastern Europe, 2(110):63-67.
7. Aksoy A.S., Alkan C., Tözüm M.S., Demirbağ S., Anayurt A.R., Ulcay Y. 2017. Preparation and textile application of poly(methyl methacrylate co-methacrylic acid)/n-octadecane and n-eicosane microcapsules. The Journal of the Textile Institute, 108(1): 30-41.
8. Kadem F.D., Saraç E.G. 2017. An experimental Application on Denim Garment to Give Thermal Regulation Property. The Journal of the Textile Institute, 108(3):353-360.

# OPTIMIZATION OF ANTISTATIC AGENT CONTENT AND TYPE FOR CARBON FIBER PRECURSOR FINISH OIL

**Serdar ASMAOĞLU[1], Bahar SEZGİN[2], Ümmihan EKER[1]**

[1] Dowaksa İleri Kompozit Malzemeler San. Ltd. Şti, Yalova, Turkey

[2] Akkim Kimya Sanayi ve Tic. A.Ş., Yalova, Turkey

***Abstract:*** *The precursor fibre should possess the required properties to be heat treated to form carbon fibres. The polyacrylonitrile (PAN) precursor fibre properties are hugely dependent on wet-spinning and post wet-spinning finishes. The temperature and stretch conditions affect the orientation and resultant mechanical properties. The spin finish oil applied gives an ease of operation and better performance [1]. A spin finish or lubricant is applied to synthetic fibres for ease of processing during manufacturing. Synthetic fibres easily generate electrostatic charge while they rub against each other or different machine parts[2]. This charge can cause major problems in processing. Electrostatic charge build-up can cause fibres to repel or attract each other. They can also stick to the machine parts they come in contact with. This can disrupt yarn formation and lead to non-uniform PAN precursor tows. The primary function of a spin finish is to eliminate the build-up of static electric charges on fibres during processing. A spin finish can reduce the amount of friction to a level which avoids problems such as end-breaks in fibres [3]. Ensuring a continuous filament tow is necessary to obtain optimum yield of carbon fibres. [4] At the same time, the spin finish should be compatible with the fibre. The layer of spin finish should not hamper any of heat treatment processes for the final carbon fibre production [5]*

***Key Words****: carbon fiber, finish oil, spin finish, precursor, PAN*

## 1. INTRODUCTION

Finish oil is one of the key raw materials for carbon fiber precursor production which protects filaments during stabilization against sudden temperature increase, uncontrolled reaction rate and fusing. Stabilization is treating precursor fiber with controlled heating process to transform linear molecular chains to ladder structure to prepare fiber for next carbonization stage. Besides this protection, it is expected form a superior spin finish to provide processability such as; lubrication effect for low fuzz level, lower static charge generation and lower residual chemical content on machine rollers. Charging on fiber during processing creates fuzzy fibers, wraps and breakages. Similarly, residual chemical content on rollers increases wraps and change over times due to cleaning. In this study; Dowaksa and Akkim created a cooperation in 2016 to develop a finish oil for carbon fiber production having superior processability and tensile strength performance.

## 2. MATERIALS AND METHODS

Studies were concentrated on Dowaksa's A42 type poly(acrylonitrile) base fiber which has tow size of 24000 filaments, linear density of 1.6 g/m, and tensile strength of 4600 MPa at average. Finish oil's were formulated and manufactured by Akkim. Polyethylene glycol (PEG) type surface active agents, PEG 1500 and PEG 2000 with average molecular weights (Mw) of 1500 g/mol and 2000 g/mol, respectively, were tested. This ingredient was also used to enhance antistatic property of finish oils. The influence of Mw and amount of PEG type active agent on static charge and residual chemical content on rollers were investigated by conducting a design of experiments study. A full factorial design was used with two factors, 2 center points and 6 runs. Levels of content and type were 0%, 0.2%, 0.5% (w/w) and PEG 1500, PEG2000, respectively. Static charge on fiber was measured from drying section of precursor machine by using Kasuga KSD-0120 static meter. Residual chemical content on rollers was visually observed and evaluated with ranking from 0: non to 10: high level.

## 3. RESULTS AND DISCUSSION

List of trials, static charge measurement results and overall comparison are given in Table 1, Figure 1. and Figure 2, respectively. Statistical analysis for static charge measurements of precursor fibers indicated that molecular weight of PEG has no significant effect. On the other hand, the amount of this active agent in finish oil dramatically influences static charging. As the content increases, charging level decreases proportionally.

**Table 8.** Factors and Levels of Design of experiment

| Finish Oil | PEG_Type | Agent Content (% w/w) |
|---|---|---|
| A | PEG 2000 | 0 |
| B | PEG 1500 | 0,25 |
| C | PEG 1500 | 0,5 |
| D | PEG 2000 | 0,25 |
| E | PEG 2000 | 0,5 |
| F | PEG 1500 | 0 |

Although, PEG type active agent content enhances charging properties, excess amount increases residual chemical content on rollers regarding to visual observations. Minimum level of residuals were observed for finish oils A and F with active agent content of % 0, and maximum residual chemical level was observed for C which has 0.5 % agent content.

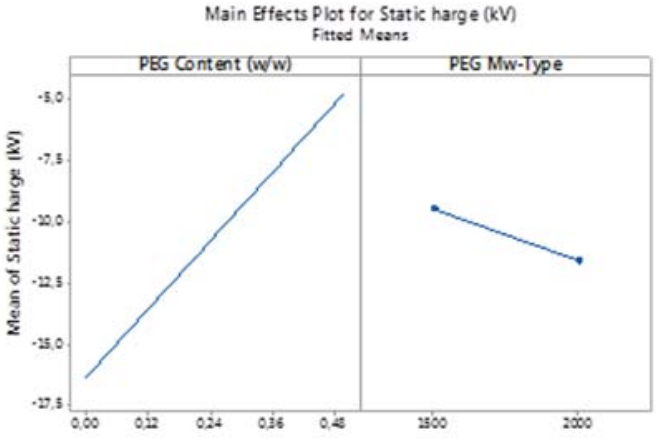


**Figure 1.** Static Charge Measurement Results of Trials

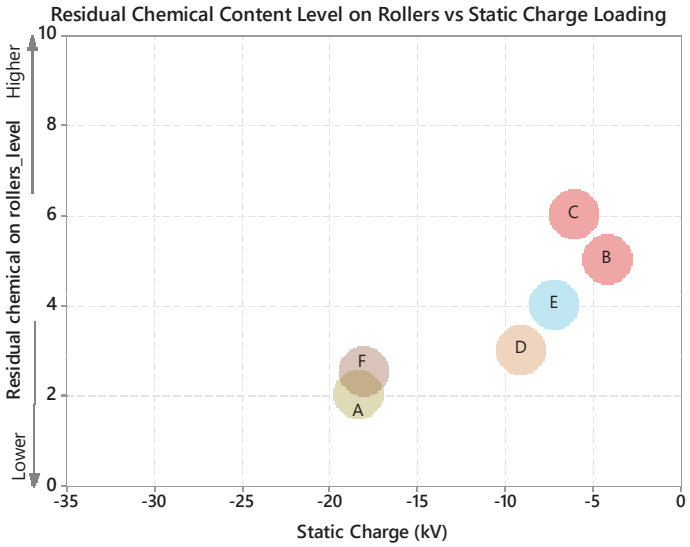


**Figure 4.** Residual-static charge relations

## 4. CONCLUSIONS

Ingredients in finish oil formulation have fundamental influences on fiber production processability from fuzz formation to change over time point of views. Hence, it is needed to optimize ingredients' contents and types for a finish oil composition. In this study, optimum conditions for antistatic active agent were predicted for the amount as 0.25 % and type as PEG 2000.

## REFERENCES

1. Effect of Wet-Spinning Parameters and Spin-Finish Application on Production of Polyacrylonitrile Precursor for Carbon Fibre Production. Available from: https://www.researchgate.net/publication/311821812_Effect_of_Wet-Spinning_Parameters_and_Spin-Finish_Application_on_Production_of_Polyacrylonitrile_Precursor_for_Carbon_Fibre_Production [accessed Sep 22 2018
2. E. Ashley Morris, Matthew C. Weisenberger, Stephanie B. Bradley, Mohamed G. Abdallah, Sue J. Mecham, Priya Pisipati, James E. McGrath, 2014. Synthesis, spinning, and properties of very high molecular weight poly(acrylonitrile-co-methyl acrylate) for high performance precursors for carbon fiber, Polymer, 55, pp. 6471-6482.
3. M.C. Paiva, C.A. Bernardo, M. Nardin, 2000. Mechanical, surface and interfacial characterisation of pitch and PAN-based carbon fibres, Carbon, 38 (9), pp. 1323-1337.
4. http://zoltek.com/carbonfiber/how-is-it-made/
5. http://www.compositesworld.com/blog/post/the-making-of-carbon-fiber

# DEVELOPMENT OF CUSTOM-MADE SIZING FORMULATIONS FOR CARBON FIBERS

**Ümmihan EKER[1], Bahar SEZGİN[2]**

[1] Dowaksa İleri Kompozit Malzemeler San. Ltd. Şti , Yalova, Türkiye

[2] Akkim Kimya Sanayi ve Tic. A.Ş., Yalova, Türkiye

***Abstract:*** *Carbon fibers, which are a new breed of high-strength materials, are mainly used as reinforcements in composite materials such as carbon fiber reinforced plastics, carbon-carbon composite, carbon fiber reinforced materials, and carbon fiber reinforced cement. Carbon fibers offer the highest specific modulus and highest specific strength of all reinforcing fibers [1]. Carbon fibers are generally fragile and subject to abrasion during handling. It has now been discovered that sizing compositions based on certain epoxy compounds protect carbon fibers against such damage. When carbon fibers are to be used in preparing composite structures with resin matrix systems, they are frequently subjected to a surface pretreatment to improve the adhesion between the carbon fibers and the resin matrix [2]. In this study, different type of water-borne sizing agent formulation is prepared. Epoxy resins improve interfacial adhesion between fiber and epoxy matrix of composite resin. Similarly, other resins are required to improve compatibility and adhesion between similar resin types. This study opens the window of opportunities to improve all physical characteristics of composite materials.*

***Key Words****: carbon fiber, sizing, resin, composite*

## 1. INTRODUCTION

Carbon fiber is a lightweight material and excellent in strength and modulus that can be combined with various materials such as epoxies and polyurethanes to produce composite materials. Physical characteristics such as tensile strength and modulus is affected by sizing agent on carbon fiber surface. Sizing agent is applied to carbon fibers before winding process to minimize fiber breakage and make fibers more appealing. Sizing agent formulation is so critical. It needs to be glossy, however, should not behave as an impurity on carbon fiber surface that could be detrimental to final composite properties. So far, we have imported sizing agents. These sizing agents were not able meet our requirements. These imported sizing agents showed very poor winding characteristics and led to severe fiber breakage. In this study, we develop a custom-made sizing formulation for carbon fiber that can surpass drawbacks of current sizing agents and meet all desired characteristics for composite materials.

## 2. MATERIALS AND METHODS

### 2.1. Carbon Fiber Production Process

The Polyacrylonitrile (PAN)-based carbon fiber is obtained by PAN-precursors. PAN-precursor is prepared from PAN polymer dissolved in DMAC solvent. This solution is spinned and coagulated in the mixture of DMAC-water solution. After coagulation, PAN-precursors are stretched and dried. PAN-precursor is stabilized in air at temperature between 200-300°C. During this process, cyclization and oxidation reaction of PAN occurs. After stabilization, carbonization and graphitization process starts. Stabilized PAN is gradually heated to higher temperatures from 400 to 1200°C in an inert atmosphere to produce carbon fibers. After carbon fiber is produced, sizing agent is applied to carbon fiber. This application is performed in the sizing bath shown in Figure 1.

**Figure 1.** Sizing bath set-up

### 2.2 Sizing Agent Formulation

A series of water-borne sizing agent formulation is prepared. Water-borne systems are preferred due to minimized health and safety risks in work environment. Sizing formulation might consist of either epoxy, polyester, phenolic or polyurethanes. Each of the polymeric materials might be useful for different purposes. Epoxy resins improve interfacial adhesion between fiber and epoxy matrix of composite resin. Similarly, other resins are required to improve compatibility and adhesion between similar resin types. For instance, polyester resins in sizing formulation are used to improve compatibility between sizing agent and polyester resin in composite resin. This study opens the window of opportunities to improve all physical characteristics of composite materials. After the study is finalized, we aim to have various sizing agent formulations that are compatible with various resin systems.

## 3. RESULTS AND DISCUSSION

List of trials, band-width, stiffness results and coefficient of friction are given in Table 1, Figure 2,3,4, respectively. Analysis for band-width and stiffness of carbon fibers indicated that polyurethane resin narrow down the band width and decreases stiffness. As the PU content increases, coefficient of friction decreases.

**Table 9.** Factors and Levels of Design of Experiment

| Sizing Agent | PU Content (%) |
|---|---|
| A | 20 |
| B | 50 |
| C | 70 |

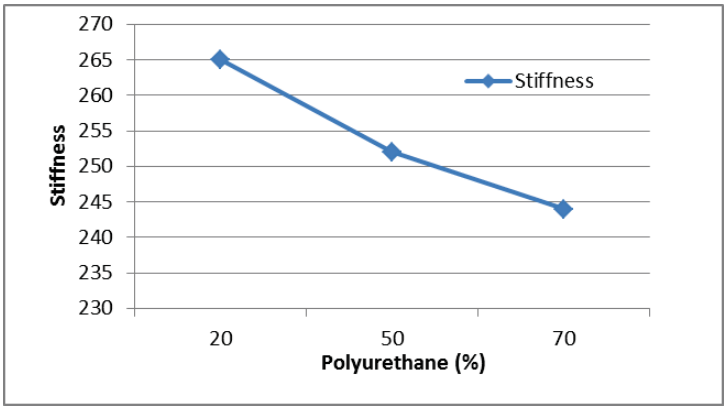


**Figure 2.** Stiffness-PU (%) comparison

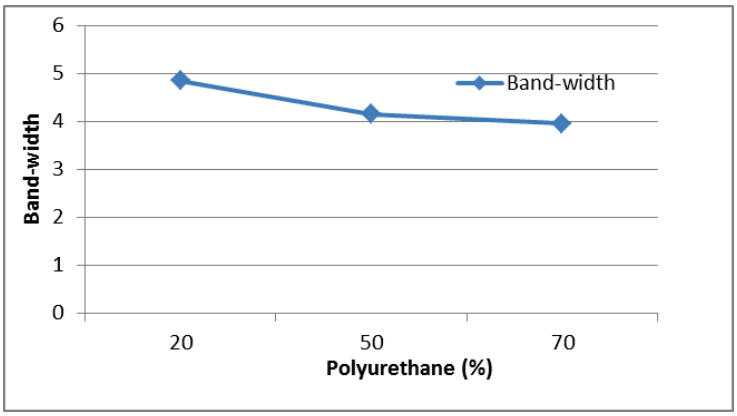


**Figure 3.** Bandwidth-PU (%) comparison

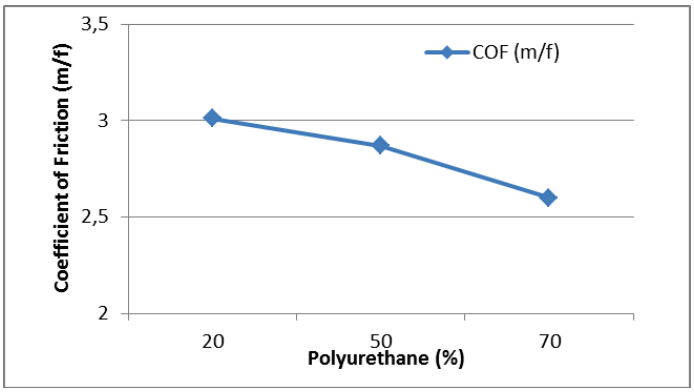


**Figure 4.** COF-PU (%) comparison

## 4. CONCLUSIONS

Sizing formulation ingredients have fundamental effects on properties of carbon fiber from stiffness to coefficient of friction. In this study, polyurethane content of sizing agents were investigated in carbon fiber applications and it has been found that the band-width, stiffness and coefficient of friction decrease as the polyurethane content increases. According to these results, it is necessary to continue working on the correct polyurethane type and quantity to reach optimum carbon fiber performance values.

## REFERENCES

1. Chand, S.:Review carbon fibers for composites. 2000. Journal of Materials Science, 35:1303.
2. Winfred E. Weldy.:Sized carbon fibers. 1975. United States Patent, no:3919504.